EQL Report No. 16-2

# METHODS FOR SULFATE AIR QUALITY MANAGEMENT

## Volume 2

## — Main Text —

by

GLEN R. CASS

EQL REPORT NO. 16-2
May 1980

Environmental Quality Laboratory
CALIFORNIA INSTITUTE OF TECHNOLOGY
Pasadena, California 91125

# METHODS FOR SULFATE AIR QUALITY MANAGEMENT

Volume 2

Main Text

by

Glen R. Cass

EQL Report No. 16-2

First Printing December, 1977
Second Printing May, 1980

Environmental Quality Laboratory
California Institute of Technology
Pasadena, California 91125

Final Report to the

STATE OF CALIFORNIA
AIR RESOURCES BOARD

in

completion of research under
ARB Contract No. A6-061-87



Disclaimer

The statements and conclusions in this report are those of the Contractor and not necessarily those of the State Air Resources Board. The mention of commercial products, their source, or their use in connection with material reported herein is not to be construed as either an actual or implied endorsement of such products.

to Jeanie

# ACKNOWLEDGMENTS

In early 1973, discussions with Professor Lester Lees led us to conclude that a "clean fuel" shortage would develop in the Los Angeles area in the late 1970's. Increased sulfur oxides emissions from increased fuel oil combustion were expected to eventually provoke a change in sulfur oxides emission control policy in Southern California. From Professor Sheldon Friedlander's instruction in the dynamics of aerosol formation, it was concluded that the sulfate air quality impact of these increasing sulfur oxides emissions would provide the most pressing questions for scientific research and for emission control strategy engineering. Professor Norman H. Brooks provided advice and encouragement throughout this project, and was indispensable in arranging for the substantial financial resources needed to complete this research. Professor Roger Noll's insight into the economics of regulation helped to frame questions for emission control strategy analysis. Professor Joel Franklin's instruction in stochastic processes led me to attempt the approach to air quality modeling employed in Chapter 3 of this study, while discussion with Professor Fredrick Shair helped to sharpen the physical assumptions built into that modeling effort. These faculty members have served as the advisory committee for this project. I am especially grateful to my principal advisor, Lester Lees, for giving me the liberty to pursue this research task by the methods which I felt would be necessary in order to cope with a complex air quality

problem over a period of many years within the context of one of the world's most extensively industrialized urban areas.

Without the advice on computing provided by Dr. Robert C. Y. Koh, completion of this research project within a reasonable length of time would have been impossible. Nearly all of the computations performed in this study were expedited by use of Bob Koh's universal data handling system called MAGIC. The computer-generated graphs in this thesis are examples of the excellent results which were quickly attainable by use of MAGIC.

Many members of the staff of Caltech's Environmental Quality Laboratory contributed to this project's success. The energy and sulfur balance study of Appendix A3 was co-authored by Pamela S. McMurry, while the crude oil characterization of Appendix A1 was co-authored by James Houseworth. David Sarokin edited the graphics. Anna Pechanec persisted through three consecutive attempts to reproduce previously published traffic count data for Los Angeles until we got the emissions inventory grid aligned properly. Gregory J. McRae read and commented on drafts of this work, and (believe it or not) succeeded in shortening the final version by several hundred pages. Charles Hales, Betsy Krieg, Tom Lawler and Lewis Hashimoto helped me to acquire the raw data for this study, almost all of which had to be transcribed by hand onto computer load sheets, followed by keypunching. They also helped with literature searches and preliminary data analysis tasks.

Margo Huffman, Pat Hofmann, Diane Davis, Jeanie Cass and Dana Leimbach typed this manuscript. Pat Rankin organized the flow of work during the typing phase. Jeanie Cass prepared the index to contents, figures and tables. Their patience with many revisions is gratefully acknowledged.

Work in this study has benefited from discussions with technical staff of the Environmental Quality Laboratory, Dr. John Seinfeld's research group in Chemical Engineering, and Dr. Sheldon Friedlander's group in Environmental Health Engineering. In particular, thanks are due to Dr. Robert G. Lamb, who took the time to comment on the air quality model derived in Chapter 3. While not all of the improvements that he suggested could be incorporated within our computing budget, the model validation effort of Chapter 5 benefited greatly from a few last-minute changes, particularly from his challenge that horizontal diffusion could not be neglected. Conversations with Drs. Paul T. Roberts, Warren H. White, Susanne Hering, Cliff Davidson, Peter H. McMurry, William Goodin and John Trijonis have been useful in hammering out approaches to specific problems as they arose in the course of this work.

The South Coast Air Quality Management District (and its predecessor agencies) went to considerable effort to cooperate in providing data for this study. Special thanks are due to Eric Lemke, Janet Dickinson, John Nevitt, Arthur Davidson, Margaret Brunelle,

Margil Wadley, Wayne Zwiacher, Ken Overturf, Julian Foon, Paul Chu, Sanford Weiss, Robert Murray, Herbert Whitehead, Martin Kaye, and Steve Menkus for answering an endless number of questions or for making staff available to provide answers when information was needed that went beyond that normally required to complete the District's mission. Joseph Stuart and Robert Lunche directed the District during the period that this work was performed.[1]

Staff of the Southern California Edison Company, Chevron Research Corporation, Union Oil Company, the Southern California Gas Company, Kaiser Steel, and KVB Incorporated have cooperated by providing data for this analysis, or by commenting on work in progeess. The librarians at Union Oil and at ARCO have been helpful in obtaining documents not normally collected by a university library.

---

[1] During the period of the research project, the Los Angeles Air Pollution Control District, the Orange County Air Pollution Control District, the Riverside County Air Pollution Control District and the San Bernardino County Air Pollution Control District were first consolidated into the Southern California Air Pollution Control District and then reorganized into the South Coast Air Quality Management District. Throughout this thesis, the attempt has been made to cite the organizational name prevailing at the time that a particular piece of referenced information was collected. The abbreviation APCD when used refers to the work of the above organizations.

This work was carried out within the academic program of the Environmental Engineering Science Department of the California Institute of Technology. The Environmental Quality Laboratory at Caltech provided a financial foothold for the project and much staff assistance. The author's support was provided by the Joseph Warren Barker Fellowship in Engineering, given by the Research Corporation; by a Rockwell International Graduate Fellowship, and by Graduate Research Assistanships financed by research grants and by private gifts to the Environmental Quality Laboratory. The bulk of the cost of this project was met by a grant from the Ford Foundation (No. 740-0469) and by the California Air Resources Board (Contract No. A6-061-87).

The California Air Resources Board and their Research Department headed by Dr. John Holmes have cooperated by giving us free rein to approach this problem without constraint or preconditions. Jack Suder has been the contract monitor. All findings and conclusions are solely the responsibility of the authors and the Caltech advisory committee.

Glen R. Cass

Pasadena, California

# ABSTRACT

Particulate sulfate air pollutants contribute to visibility deterioration and are of current public health concern. This study develops the technical understanding needed for sulfate air quality control strategy design. Methods which link sulfate air quality and air quality impacts on visibility to the cost of controlling sulfur oxides air pollutant emissions are presented. These techniques are tested by application to the Los Angeles Basin over the years 1972 through 1974.

An air quality simulation model is developed which directly calculates long-term average sulfate concentrations under unsteady meteorological conditions. Pollutant concentrations are estimated from Lagrangian marked-particle statistics based on the time sequence of historical measured wind speed, wind direction and inversion base height motion. First order chemical reactions and ground level pollutant dry deposition are incorporated within a computational scheme which conserves pollutant mass.

Techniques are demonstrated for performing both mass balance and energy balance calculations on flows of energy resources containing sulfur throughout the economy of an air quality control region. The energy and sulfur balance approach is used to check the consistency of a spatially and temporally resolved air quality modeling emission inventory for the South Coast Air Basin.

Next the air quality model is validated against sulfur oxides emissions and sulfate air quality patterns observed in the Los Angeles Basin over each month of the years 1972 through 1974. A seasonal variation in the rate of $SO_2$ oxidation to form sulfates is inferred. Overall average $SO_2$ oxidation rates of about 6% per hour prevail during late spring, summer and early fall, while mean $SO_2$ oxidation rates of between 0.5% per hour and 3% per hour prevail from October through February of our test years. From the model results, it is concluded that three to five major $SO_x$ source classes plus background sulfates must be considered simultaneously at most monitoring sites in order to come close to explaining observed sulfate levels. The implication is that a mixed strategy aimed simultaneously at a number of specified source types will be needed if substantial sulfate air quality improvements are to be achieved within this particular airshed.

Techniques are developed for analysis of the *long-run* impact of pollutant concentrations on visibility. Existing statistical models for light scattering by aerosols which use particle chemical composition as a key to particle size and solubility are modified so that the relative humidity dependence of light-scattering by hygroscopic aerosols could be represented in a more physically realistic manner. Coefficients are fitted to the model based on ten years of air pollution control agency routine air monitoring data taken at downtown Los Angeles. Sulfates are found to be the most effective light scatterers in the Los Angeles atmosphere. It is estimated that the

visibility impact of reducing sulfates to a half or to a quarter of their measured historic values on each past day of record would be manifested most clearly in a reduction in the number of days per year of less than three-mile visibility. The number of days of average visibility less than ten miles would be little affected.

Two retrospective examples are worked to show how the results of the air quality simulation models may be used to define a variety of sulfate air quality control strategy options. It is suggested that a package of technological emissions control measures and institutional changes (including natural gas price deregulation) may provide greater improvements in both sulfate air quality and visibility at less cost than can be obtained from a purely technological solution to the Los Angeles sulfate problem.

TABLE OF CONTENTS

TABLE OF CONTENTS (Continued)

TABLE OF CONTENTS (Continued)

TABLE OF CONTENTS (Continued)

TABLE OF CONTENTS (Continued)

TABLE OF CONTENTS (Continued)

TABLE OF CONTENTS (Continued)

VOLUME 3 APPENDICES

TABLE OF CONTENTS (Continued)

TABLE OF CONTENTS (Continued)

TABLE OF CONTENTS (Continued)

TABLE OF CONTENTS (Continued)

TABLE OF CONTENTS (Continued)

TABLE OF CONTENTS (Continued)

TABLE OF CONTENTS (Continued)

LIST OF FIGURES

LIST OF FIGURES (Continued)

LIST OF FIGURES (Continued)

LIST OF FIGURES (Continued)

LIST OF FIGURES (Continued)

LIST OF FIGURES (Continued)

LIST OF FIGURES (Continued)

LIST OF FIGURES (Continued)

LIST OF FIGURES (Continued)

LIST OF FIGURES (Continued)

LIST OF FIGURES (Continued)

LIST OF FIGURES (Continued)

LIST OF FIGURES (Continued)

LIST OF FIGURES (Continued)

LIST OF FIGURES (Continued)

LIST OF FIGURES (Continued)

LIST OF FIGURES (Continued)

LIST OF FIGURES (Continued)

LIST OF FIGURES (Continued)

LIST OF FIGURES (Continued)

LIST OF TABLES

LIST OF TABLES (Continued)

LIST OF TABLES (Continued)

LIST OF TABLES (Continued)

LIST OF TABLES (Continued)

LIST OF TABLES (Continued)

LIST OF TABLES (Continued)

LIST OF TABLES (Continued)

# CHAPTER 1

# INTRODUCTION

## 1.1 Objective

The objective of this research is to create a policy-responsive mathematical description of an urban sulfate air pollution problem. The study is placed in the context of the Los Angeles Basin, but methods of analysis are developed which have general application to air pollution control strategy design.

The nature and origin of sulfate pollution in an urban airshed first will be described. Existing air quality and meteorological data bases will be assembled into an organized picture of the pollution problem at hand. Sulfur balance and energy balance techniques will be developed which tie sulfur oxides air pollutant emissions to their origin in a regional energy economy. Then mathematical models will be derived and tested which simulate emissions/air quality relationships, and air quality impacts on local visibility. A technical foundation thus will be laid for future studies of the impact of alternative emissions control strategies on sulfate air quality.

## 1.2 The Importance of Understanding Sulfate Air Quality Management Options

Control of sulfur oxides air pollutant levels is one of the most persistent air quality problems facing industrialized societies. On a global basis, combustion and processing of sulfur-bearing fossil

fuels and smelting of sulfur-bearing ores leads to the release of $65 \times 10^6$ metric tons of sulfur into the atmosphere yearly (Friend, 1973). While naturally occurring sulfur sources exceed this man-made pollution burden on a global-average basis, the fuel-burning origin of man's sulfur oxides emissions often means that pollutants are generated in close proximity to population centers. When an urban atmosphere becomes overloaded with sulfur oxides and particulate matter, well publicized public health disasters occasionally have occurred: the Meuse Valley, Belgium (1930); Donora, Pennsylvania (1948), and London, England (1952). Other far less dramatic consequences of sulfur oxides pollution are present on a more or less continuous basis in many urban areas, as will be discussed shortly.

Most of man's sulfur oxides emissions to the atmosphere are in the form of sulfur dioxide gas. Sulfur dioxide is known to be a mild respiratory irritant at elevated concentrations and is capable of inflicting damage to vegetation (National Research Council, 1975). Because of the predominance of $SO_2$ as the primary pollutant being emitted, and perhaps because it has been readily measurable for many years, current National Ambient Air Quality Standards for sulfur oxides in the United States (and the standards of most other nations) are stated solely in terms of limits on sulfur dioxide concentrations. As a result of this attention, extensive progress has been made in designing emissions control strategies aimed at achieving legally mandated limits on $SO_2$ concentrations.

In accordance with the requirements of the Clean Air Act (42 U.S.C.

§§ 1857 et seq.) in the United States, nearly every state has adopted an Implementation Plan containing a sulfur dioxide abatement strategy. Over the decade 1975 through 1985, it has been projected (Temple, Barker and Sloan, 1976) that the electric utility industry alone will incur capital expenditures of 11.6 billion dollars in order to comply with existing Federal $SO_2$ emission control policies. Sulfur dioxide abatement is thus one of the most expensive large scale environmental control programs undertaken in the United States. In view of the large fixed costs involved, it is important that sulfur oxides control strategies once adopted continue to serve long-run needs.

Unfortunately, control strategies aimed at reduction of sulfur dioxide levels alone may not address themselves to some of the most important consequences of burning sulfur-bearing fuels. Sulfur dioxide gas has been shown to undergo atmospheric oxidation to form suspended particulate sulfates.[1] These sulfate particles tend to accumulate in a size range around 0.5 microns in diameter (Hidy et al., 1975). Particles of this size are extremely effective scatterers of light (Middleton, 1952) and are also capable of deep penetration into the lung (Task Group on Lung Dynamics, 1966). In addition, there is a body of toxicological and epidemiological evidence suggesting that sulfate particulates are

---

[1] As used in this study, the definition of "sulfates" is an operational one: particulate sulfur oxides collected on glass fiber filters by high volume sampling and measured as $SO_4^=$ ion by wet chemical methods such as those described later in this study. The term "sulfates" thus denotes a broad class of particulate sulfur oxides in the atmosphere, including sulfuric acid mist, ammonium sulfate and bisulfate, and metallic sulfate salts, to name but a few of the more prominant components of this particulate complex.

much more irritating to the respiratory system per unit mass concentration than an equivalent amount of sulfur present as $SO_2$ alone (National Research Council, 1975). Sulfate air pollutants are thought to play an important role in the acidification of rain water (Committee on Mineral Resources and the Environment, 1975), and can be associated with chemical attack on materials and visibility deterioration (Middleton, et al., 1970).

Concern for these known or anticipated adverse effects of particulate sulfur oxides has prompted an extensive review of current knowledge in this area by the National Academy of Sciences (National Research Council, 1975). They note that air pollution control efforts during the past decade have generally led to a substantial reduction in urban sulfur dioxide concentrations. In contrast, suspended sulfates levels have remained largely unchanged in urban areas and may have increased in rural areas. *In short, apparently effective strategies currently employed for reducing $SO_2$ concentrations do not appear to lead to corresponding reductions in sulfate levels.*

If one were to accept that both ambient $SO_2$ and regionally enriched sulfate levels have a common source in man's sulfur oxides air pollutant emissions, a paradox would seem to arise from the failure to control both jointly. One fairly straightforward explanation for this situation, however, has been offered (National Research Council, 1975) as follows. In spite of the reduced $SO_2$ concentrations in urban areas, total sulfur oxides emissions from man's activities in the United States have been increasing at about 4 percent annually over the past decade.

Urban $SO_2$ reductions have been achieved by localized use of low sulfur fuels and by separating $SO_2$ emissions spatially from the immediate vicinity of population centers. Growth in fuel burning for electric power generation has been shifted to rural areas, and tall stacks have been used to inject pollutants higher into the atmosphere. Population exposures to sulfur dioxide associated with close proximity to a primary emission source thus have been reduced.

Man-made sulfates are largely a decay product of sulfur dioxide emissions. Sulfates are formed in the atmosphere over intermediate to long travel distances downwind from a sulfur dioxide emissions source. Widespread dispersion of pollutants would occur over long travel times regardless of steps taken to separate initial emissions from local receptor populations. Therefore the National Research Council study suggests that regional sulfates levels depend on total regional sulfur oxides emissions more than they depend on close proximity to a given emission source.

The widespread regional nature of sulfate air pollution problems is illustrated in Figure 1.1. Two areas of the United States are seen to be affected: the entire eastern United States, and the South Coast Air Basin of Southern California which contains metropolitan Los Angeles.

Large uncertainties presently frustrate formulation of sulfur oxides emissions control plans which <u>will</u> achieve control over sulfate levels. In a recent position paper, the U.S. Environmental Protection Agency (1975) stated that a National Ambient Air Quality Standard for

FIGURE 1.1

Geographical Distribution of Typical Urban Sulfate Levels in the United States (Annual Means)

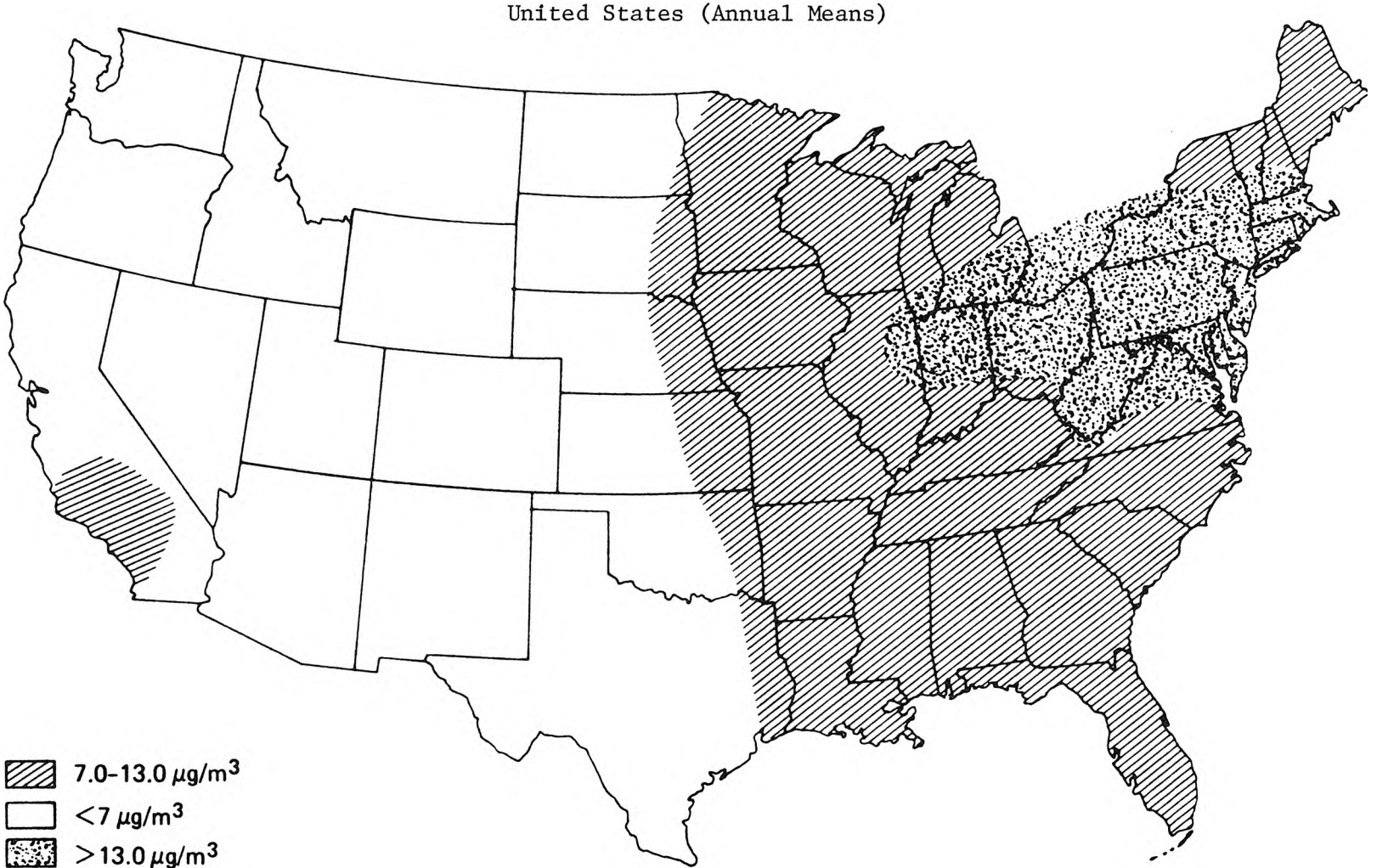


Reference: National Research Council (1975).

particulate sulfates would not be proposed for at least three to five years due to a lack of clear understanding of several fundamental aspects of the sulfate pollution syndrome. More complete information is wanted to characterize atmospheric sulfate concentrations, health and welfare effects, chemical transformation/transport interactions, and emissions control options.

There is, in our opinion, a danger that if this additional information needed to formulate sulfate air quality control strategies is sought piecemeal, an improved decision-making capability may not result. Health and welfare effects research may be conducted in geographic regions for which emissions and air quality information are either lacking or poorly organized. Emissions control strategy design might be confined to regions with coal combustion problems that are not representative of the petroleum dominated fuel use in many of the nation's coastal population centers. Air quality models may be developed in the absence of an appreciation that they are needed to clarify a choice between long-run commitments of resources to possible emission control alternatives. Perhaps the most fundamental uncertainties in control strategy development lie in the dilemmas that will arise if small pieces of the problem analyzed separately fail to integrate into a comprehensive picture of control strategy costs and effects prior to the time when public pressure to make some costly choices becomes overwhelming.

For that reason, this research project will concentrate on developing the tools needed for sulfate air quality control strategy design

within the context of a single well chosen case study. Emphasis is placed wherever possible on development of techniques which utilize only that information commonly available from air pollution control agency historic data bases and other existing public records. This is done in recognition of the fact that a truly useful air quality control strategy design procedure must not only lead to economically efficient control strategy options; the design procedure itself must be economical or it will not be used. Expensive new field measurement programs needed to acquire specialized data bases are probably beyond the means of most state and local regulatory agencies.

The need for this approach to an improved understanding of sulfate air quality management options is apparent. In the words of the National Academy of Sciences Committee:

> Decisions to be made on sulfur oxide emissions from power plants will involve tens of billions of dollars in electrical generation costs in the next decade and massive effects on human health and welfare. Greatly expanded efforts should be made to develop improved models and data for use on a case by case basis to improve decisionmaking on emission control strategy alternatives. [National Research Council, 1975].

## 1.3 The Approach Used in This Work

An air pollution control strategy is a systematic means of restricting air pollutant emissions in order to achieve a desired level of ambient air quality or some limited measure of air pollution damage. Air pollution control strategy development is a design process in which the objective is to define a variety of possibly acceptable courses of action. Each alternative should be an efficient one, that is to say, a set of control possibilities which contains some desirable

properties which cannot be attained at any lower economic cost. From among this large variety of possibly acceptable courses of action, decision-makers are free to choose with the knowledge that they are not wasting resources in order to attain the result selected.

Figure 1.2 outlines an approach to sulfate air quality control strategy design. That process naturally divides into two phases. A flexible physical description of the air pollution problem first is constructed, then alternative courses of action may be evaluated by perturbing the current emissions control strategy and observing the airshed's response.

The first of these tasks is chosen as the subject for this project. A policy-responsive mathematical description of an urban sulfate air pollution problem will be constructed. The most prominent features of that air quality problem first will be identified by analysis of historical air monitoring data. Sulfur oxides pollutant emissions next will be linked to their origin in regional energy use patterns. Then mathematical models will be developed which describe emissions/air quality relationships and air quality impacts on local visibility. It is important to note at the outset that these mathematical models themselves no more constitute an air pollution control strategy design procedure than having a hammer constitutes building a chair. Unless a prototype procedure is demonstrated for bringing these tools to bear on a real problem, the tools' existence is of very superficial importance. For that reason, the application of analytical tools to the Los Angeles sulfate problem will form the core around which this discourse is organized.

FIGURE 1.2

Research Plan

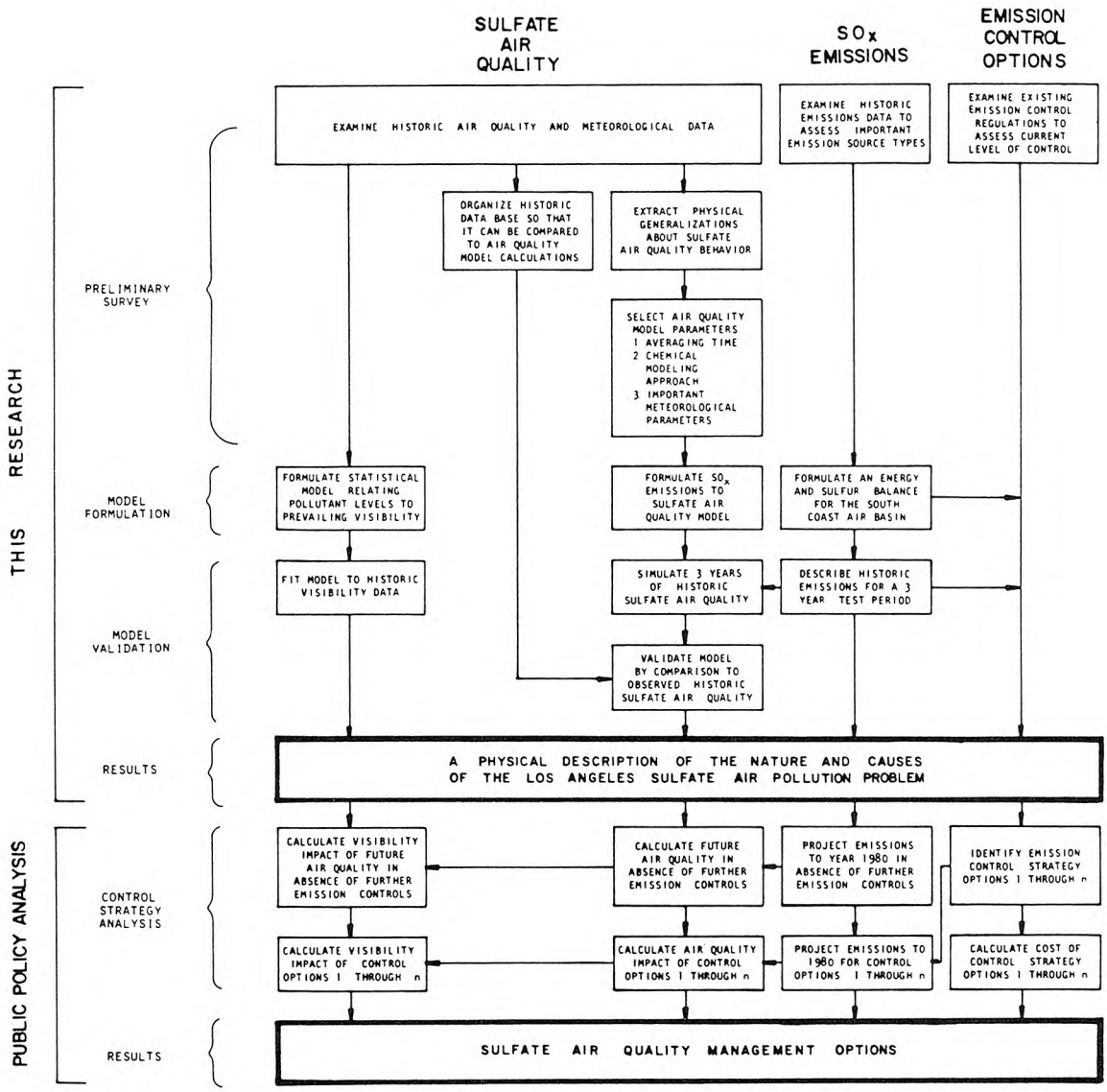

The first step in this air quality control strategy design procedure is to define the nature of the air quality problem at hand. From statistical analysis of existing air quality data one can draw important generalizations about the physical processes most directly influencing sulfate concentration changes. These physical assumptions will later be used to reduce the complexity of a deterministic emissions to air quality model to manageable proportions.

At the outset, only a huge mass of disorganized ambient air quality measurements will be available. An orderly picture of sulfate air quality behavior will be shown to exist. Spatial gradients in sulfate air quality are explored to verify an enrichment in atmospheric sulfate levels above natural background in the Los Angeles area. Day-to-day fluctuations in sulfate concentrations will be used to show that sulfate pollutant levels rise and fall in a closely coupled fashion over a large region of Southern California. The causes of these day-to-day concentration changes are explored in terms of specific meteorological and co-pollutant variations. Sulfate concentration changes are shown to depend on daily mixing depth in the Los Angeles Basin, and on factors such as relative humidity plus suspended particulate and oxidant concentrations which would be expected to affect the rate of oxidation of $SO_2$ to form sulfates. Then a selection is made of the important features of sulfate air quality behavior in Los Angeles which could be used to construct and validate a deterministic emissions to air quality simulation model.

Existing models relating emissions to long-term average air quality are reviewed and found to lack the ability to even approximately model several of the features most important to Los Angeles sulfate air quality such as air parcel retention time or strong temporal changes in emission source strength. A new type of long-run average air quality model for slowly reacting air pollutants is then developed based on long-run average Lagrangian marked particle statistics.

A spatially resolved inventory of sulfur oxides emissions is assembled for each month of three test years, 1972 through 1974. This inventory is actually constructed in the form of a fuel switching simulation model such that emissions may be projected to future years in which natural gas curtailment will have altered the spatial distribution of sulfur-bearing fuel oil combustion. The emissions generation model is linked to the air quality model, and predicted sulfate air quality for the test years 1972 through 1974 is compared to actual historical measurements.

One tangible benefit from lowered future sulfate levels would be an improvement in visibility in the Los Angeles Basin. A statistical model is formulated which explains the long-term distribution of prevailing visibilities at Los Angeles in terms of changes in pollutant levels and relative humidity. The model is tested against a decade of atmospheric observations at Los Angeles, then projections are made of the future distribution of visibilities which would be expected if sulfate concentrations in the Los Angeles Basin were significantly reduced.

## 1.4 Relationship of This Research to Future Work

The analytical techniques developed in this study are designed to be applied to a public policy analysis of sulfate control strategy options in the central portion of the South Coast Air Basin of California, as outlined in Figure 1.2. That emissions control strategy study could be pursued as follows.

Emissions projections for the early 1980's could be made on the basis of anticipated natural gas curtailment and electric generation levels in those years. The effect of sulfuric acid mist emissions from catalyst-equipped cars should be introduced into the model. Then air quality levels resulting from this 1980's emissions pattern could be projected using the previously validated air quality model.

An emissions control study then could be conducted to establish the cost of altering future sulfur oxides emissions levels. Specific options within three general classes of emissions control techniques should be explored: purchased naturally occurring low sulfur fuels, fuel desulfurization, and stack gas cleaning. Costs imposed on an acceptable emissions control program by institutional barriers, such as Federal Power Commission gas price regulation, should be discussed. Then the least-cost means of achieving a variety of altered future sulfate air quality patterns could be established.

An estimate could be made of the impact of each sulfate control strategy on visibility at downtown Los Angeles. Benefits to visibility could be arrayed against the air quality levels and the cost of each control strategy option. Decision-makers then would have a tool for

selecting an air quality control strategy from a set of options, each of which is an economically efficient means of attaining the air quality levels and distribution of control costs described.

## 1.5 Relationship of This Study to Previous Work and Ongoing Research

The only previous sulfate air quality control strategy study for a multiple source urban setting was conducted by Trijonis et al. (1975). The present study provides the foundation for improving upon such previous efforts by statistically exploring the underlying physical causes of sulfate air quality fluctuations in order to improve modeling capability, by developing a unique deterministic spatially resolved diffusion model to suit this application, by illustrating the importance of both mass balance and energy balance calculations when dealing with a sulfur oxides pollution problem, and by examining benefits to visibility from sulfate air quality control. Sulfate air quality control strategies in the comprehensive economic and technical sense used here have also been approached by the previously mentioned National Research Council (1975) committee, but only for hypothetical cases most directly related to siting of single coal-fired power plants in the eastern United States.

Other sulfate air quality modeling or control strategy studies are underway at the present time. The Sulfate Regional Experiment (SURE) project is proceeding under sponsorship by the Electric Power Research Institute. The Multi-State Atmospheric Power Production Pollution Study (MAP3S) is being conducted by the U.S. Energy Research and Development Administration. Both of these projects have as an objective the

identification of the contribution of the electric utility industry to sulfate levels observed in the Northeastern United States. The Midwest Interstate Sulfur Transformation and Transport (MISTT) project is being conducted by the U.S. Environmental Protection Agency to determine sulfate formation mechanisms in sufficient detail that they may be incorporated explicitly within air quality simulation models. Economic evaluation of sulfate air quality control strategies involving the electric utility industry is being pursued by the U.S. Environmental Protection Agency and Teknekron Inc. as part of the Integrated Technology Assessment of Electric Utility Energy Systems project. The Long Range Transport of Air Pollutants (LRTAP) study is being conducted by the Organization for Economic Cooperation and Development (OECD) to determine the relationship between sulfur oxides emissions and sulfate deposition in Western Europe.

## 1.6 An Introduction to Los Angeles Sulfur Oxides Air Pollution

When the smog problem in the Los Angeles Basin was first investigated, attention was focused on sulfur oxides emissions from industrial sources. Most of these emissions to the atmosphere were in the form of sulfur dioxide gas. Additional atmospheric measurements also identified particulate sulfur compounds, often referred to in the early literature as sulfuric acid mist or its gaseous precursor, sulfur trioxide. These particulate sulfur compounds were initially believed to be responsible for "thirty to sixty percent of the total reduction in visibility" at Los Angeles (Los Angeles Air Pollution Control District, 1950). It was also soon recognized that there was something unusual about Los Angeles sulfate air quality. The Los Angeles

atmosphere exhibited sulfate concentrations comparable to those of cities in the industrial northeastern United States despite the fact that sulfur dioxide emissions in Southern California were modest by comparison. At the conclusion of an extensive aerometric survey of the Los Angeles area (Renzetti, et al., 1955), the question was posed, "Why are the sulfate and nitrate concentrations in the particulate loading in smog higher in Los Angeles than in other cities?" Twenty years later that question is only partially answered.

As the sulfur dioxide emission control program succeeded in reducing ambient $SO_2$ concentrations, and as the extremely complex chemical nature of photochemical smog became better understood, public attention was directed at the control of emissions from the automobile which dominated other aspects of local air quality. Recently, two things have happened which suggest that current control strategies for sulfur oxides should be reviewed.

The first of these is a rekindling of scientific interest in the role of particulate sulfates in the Los Angeles atmosphere. In 1969 an academically organized study of aerosol behavior (Whitby et al., 1971; Hidy et al., 1972) noted that man's contribution to the aerosol loading in Los Angeles was concentrated in submicron particles which were easily respirable. Many of these submicron aerosols were found to be the result of gas to particle conversion processes occurring in the atmosphere. Sulfates were identified as a major fraction of this "secondary" particulate burden. A large-scale Aerosol Characterization Study sponsored by the California Air Resources Board followed

(Hidy, et al., 1975). This study concluded, as had early investigation in the 1950's, that sulfates were largely responsible for the well-known visibility deterioration at downtown Los Angeles. A concurrent study by Roberts (1975) examined Los Angeles sulfate air quality and measured the rate of conversion of $SO_2$ to form sulfates in the atmosphere. Translation of these findings into design of an improved sulfur oxides air pollution control strategy for Los Angeles remains to be accomplished.

A second compelling reason for focusing on Los Angeles is a potential increase in basin-wide sulfur dioxide emissions due to curtailment of natural gas deliveries to Southern California. Figure 1.3 shows the Pacific Lighting Corporation's (1974) estimated gas supplies from existing sources in contrast to projected requests for service at current prices. It had been estimated by the Los Angeles Air Pollution Control District (1975a) that substitution of sulfur-bearing fuel oil for natural gas combustion over the next few years could increase $SO_2$ emissions in Los Angeles County from a low of 257 tons per day in 1970 to a level of about 470 tons per day by 1979 in the absence of any further emission controls beyond those existing in 1974. On the same basis, the California Air Resources Board estimated that $SO_2$ emissions in the entire South Coast Air Basin (which contains Los Angeles County) could increase from a 1973 level of 515 tons per day to a level of between 720 and 920 tons per day by 1983 (California Air Resources Board, 1975). Control of the impact of this potential increase in sulfur oxides emissions is a matter of current public policy importance.

FIGURE 1.3

PACIFIC LIGHTING CORPORATION
NATURAL GAS SUPPLY VS. EXPECTED REQUESTS
FOR SERVICE AT CURRENT PRICES

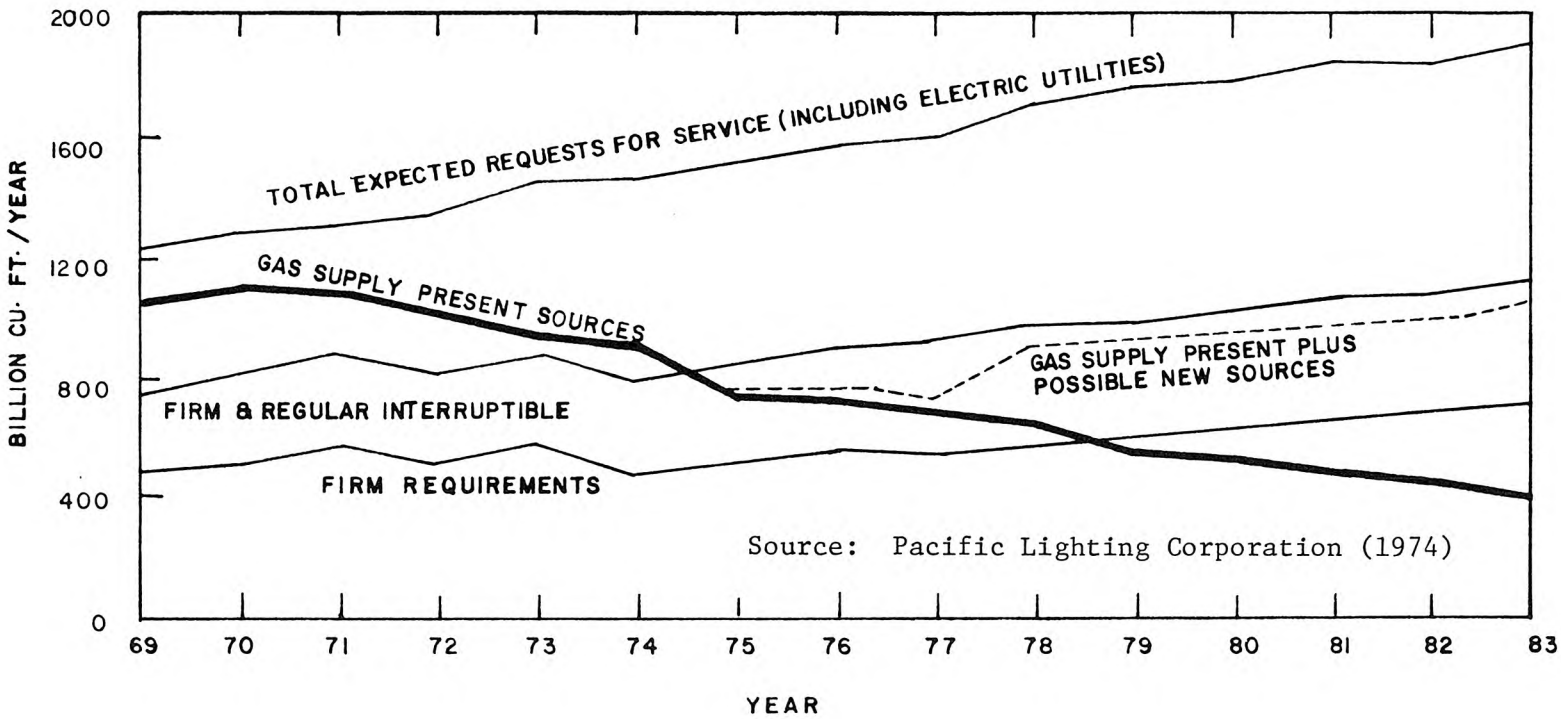


Source: Pacific Lighting Corporation (1974)

Prompted by the impending emissions increase, the local findings concerning visibility, and the previously mentioned national debate over the health consequences of sulfate air quality, the California Air Resources Board recently adopted an air quality goal for total suspended particulate sulfates. A 24-hour average sulfate concentration of 25 micrograms per cubic meter is not to be exceeded.[2] Some initial steps also have been taken to blunt the expected $SO_x$ emissions increase by decreasing the sulfur content of fuel burned in the Los Angeles Basin. As yet, no comprehensive emission control strategy has been adopted for meeting the state sulfate air quality goal in Los Angeles over the long term. If such actions are proposed, they undoubtedly will be quite expensive. Substantial savings might be achieved by better understanding the options available for managing sulfate air quality in this particular air basin in an economically efficient manner.

### 1.6.1 Sulfur Dioxide Emission Trends

A brief historical account (Los Angeles Air Pollution Control District, 1975b) of past sulfur oxides management policy in the Los Angeles area will help put many of these issues into perspective. When the nature of the Los Angeles smog problem was first investigated in the late 1940's, considerable attention was focused on the need for sulfur dioxide emission controls. In 1947, prior to the imposition of any discharge limitations, sulfur dioxide emissions in Los Angeles

[2] In recent years, that sulfate air quality standard would have been exceeded about one seventh of the time in Los Angeles.

County totaled about 680 tons per day, distributed among source categories as shown in Table 1.1 (Lemke, et al., 1969).

In 1947, the Los Angeles Air Pollution Control District (LAAPCD) adopted Rule 53 which limited sulfur compounds in exhaust gases from any source to 0.2 percent by volume (calculated as $SO_2$). By 1958, enforcement of this regulation had resulted in a lowering of total $SO_2$ emissions within the County to a level of 453 tons per day. The bulk of this initial reduction was achieved by removal of hydrogen sulfide from refinery gases prior to their combustion. Other refinery process operations were also affected. As shown in Figure 1.4, non-fuel-burning refinery process $SO_2$ emissions dropped sharply in 1957 and remained relatively unchanged thereafter over the next eighteen years.[3] Changes in sulfur dioxide emissions from refinery fuel burning are reflected in the "other" category of Figure 1.5.

In 1958, Rule 62 was adopted by the LAAPCD. The regulation prohibited the burning of any solid or liquid fuel containing over 0.5 percent sulfur by weight from May through November of the year, *provided that natural gas was otherwise available*. Rule 62 first went into effect in the summer of 1959. Referring to Figure 1.5, we note a steady drop in $SO_2$ emissions from fuel burning following adoption of Rule 62, reaching a relative minimum in about 1963.

---

[3] Data on emission trends and projections used in Figures 1.4 through 1.7 were obtained from the Los Angeles Air Pollution Control District (1975b), and reflect historic records and forecasts through the close of 1974. Missing data were estimated by linear interpolation.

TABLE 1.1

Sulfur Dioxide Emissions in Los Angeles County for 1947
(Prior to Initial Emission Control Regulations)

| Source Class | $SO_2$ Emission Rate (Tons/Day) |
|---|---|
| (1) Combustion of Fuels<br>Including: utility boilers<br>refinery fuel<br>industrial fuel | 575 |
| (2) Refinery Processes Operations | 30 |
| (3) Motor Vehicles | 40 |
| (4) Remaining Sources<br>Including: chemical plants<br>other stationary sources | 35 |
| TOTAL | 680 |

Note: Emission values are taken from a graph presented by Lemke, et al. (1969). This graph could be read no more closely than ±5 tons/day.

FIGURE 1.4

SO2 EMISSIONS FROM PETROLEUM REFINING, PRODUCING AND MARKETING (SHADED)

VS. TOTAL SO2 EMISSIONS IN LA COUNTY, WITH LAAPCD FUTURE PROJECTION

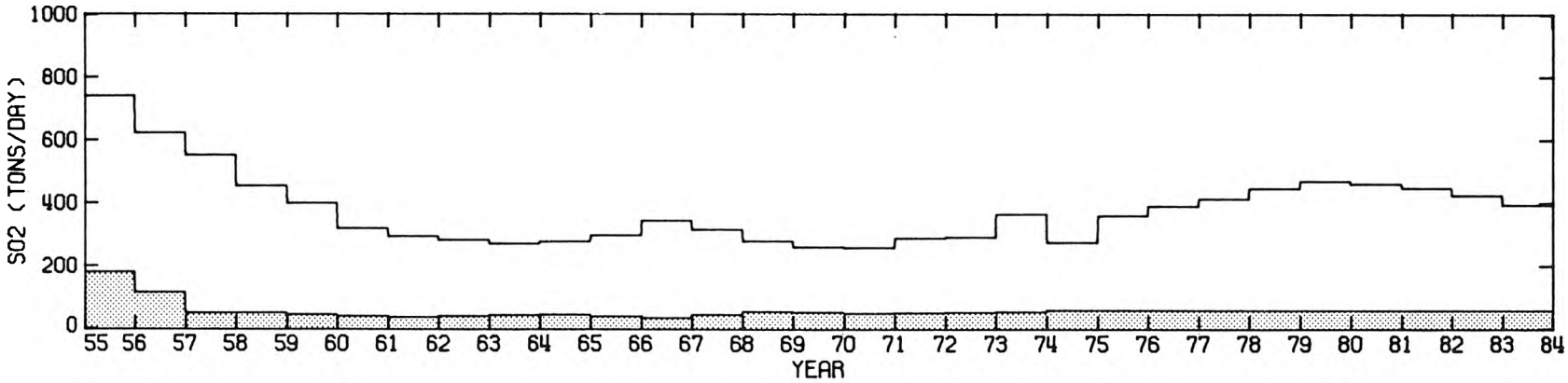


Reflects all $SO_2$ emissions from refinery processes except for fuel burning and sulfur recovery operations. Includes activities such as catalyst regeneration, waste water treatment, distillation losses, plus asphalt and coking operations.

FIGURE 1.5

SO2 EMISSIONS FROM FUEL BURNING SOURCES (SHADED) VS.

TOTAL SO2 EMISSIONS IN LA COUNTY, WITH LAAPCD FUTURE PROJECTION

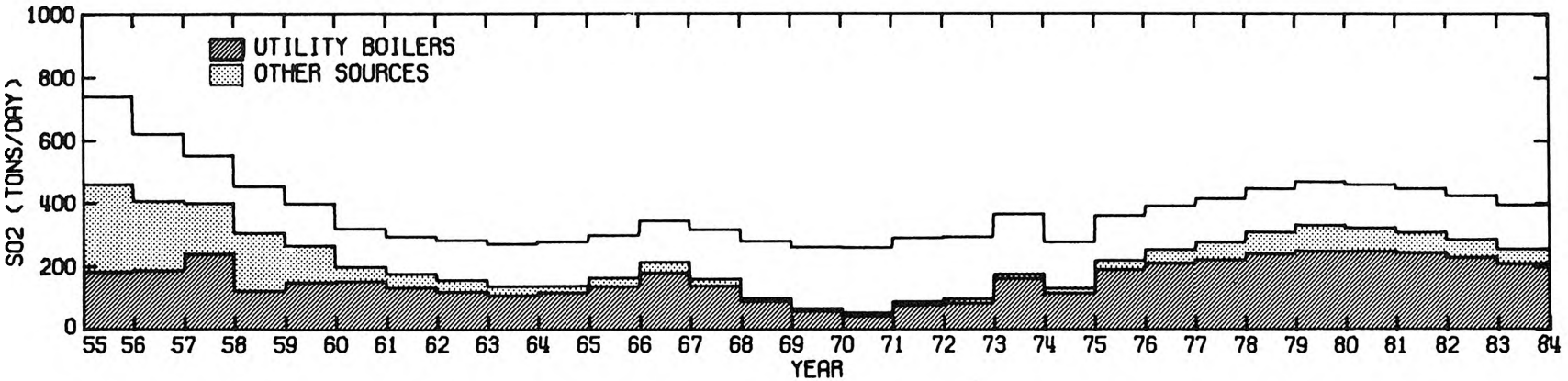


The Other Sources category includes $SO_2$ emissions from fuel combustion by industrial, commercial, institutional, and residential sources. The projections shown above were based on emission control regulations in effect in 1975 which limited the sulfur content of fuel oil to 0.5% sulfur by weight. Emission control regulations have since been tightened to blunt some of the expected emissions increase indicated in this graph.

In spite of continued restrictions on the sulfur content of fuel, expansion of electric generating capacity in the Basin caused an increase in total $SO_2$ emissions beginning in about 1963. In January of 1964, Rule 62 was amended (by adoption of Rule 62.1) to make the sulfur content of fuel provisions applicable *year-round*. A limited supply of natural gas during the winter months rendered that change ineffective at slowing the growth in total emissions. These increasing emissions from stationary source fuel burning were eventually reversed in the late 1960's by importation of low sulfur fuel oil from Indonesia and southern Alaska, and by increased deliveries of natural gas. By October of 1968, Rule 62 was again amended to prohibit the burning of high sulfur fuel oil, *irrespective of natural gas supply conditions*. Shortly thereafter, natural gas deliveries began to diminish, with attendant substitution of low sulfur fuel oil leading to the upward trend in $SO_2$ emissions from fuel burning projected for Los Angeles County in the decade of the 1970's in Figure 1.5.

As a result of concern over increased sulfur oxides emissions from fuel burning activities, a further tightening of the sulfur content of fuel oil limitations became effective in early 1977. A fuel oil sulfur content of 0.25% by weight is not to be exceeded provided that such low sulfur oils are sufficiently available. That regulation is being reviewed at the present time, and may be modified within the next year. Fuel oil sulfur content limitations are in such a state of flux at the present time that this study will not attempt to anticipate the exact course of future events. The 0.5% sulfur content of fuel oil

limitation prevailing over the past two decades will be viewed as the baseline for our study, and further tightening of that standard will be considered to be a proper subject for control strategy analysis.

Another long-term feature of the $SO_2$ emission inventory for Los Angeles County is the emergence and subsequent control of substantial pollutant emissions from chemical process industries. In order to reduce emissions from refinery operations, sulfur-bearing refinery gases and acid sludge often were transported to adjacent plants which recovered elemental sulfur or sulfuric acid from the refinery effluent. These sulfur recovery operations were not one hundred percent efficient, and in time became major $SO_2$ sources in their own right. By 1970, Figure 1.6 shows that chemical processes accounted for 115 tons per day of $SO_2$ emissions, or nearly half of the total $SO_2$ emission inventory at that time. In 1971, Rule 53 was amended (effective 1973) to repeal certain exemptions previously granted to scavenger plants and to limit effluent streams from these plants to not more than 500 ppm of sulfur compounds calculated as $SO_2$. A maximum emission rate of not more than 200 pounds per hour of sulfur-bearing gases calculated as $SO_2$ was also imposed at that time. Figure 1.6 clearly shows the effect of these regulations on 1974 and subsequent $SO_2$ emission rates.

Automotive exhaust contains sulfur oxides derived from trace amounts of sulfur initially present in gasoline. California gasolines have traditionally been higher in sulfur content than the national average (Bureau of Mines, 1972 through 1975). As shown in Figure 1.7, $SO_2$ emissions from automobiles totaled about 35 tons per day in Los

FIGURE 1.6

SO2 EMISSIONS FROM CHEMICAL PLANTS INCLUDING SULFUR SCAVENGER PLANTS (SHADED)

VS. TOTAL SO2 EMISSIONS IN LA COUNTY, WITH LAAPCD FUTURE PROJECTION

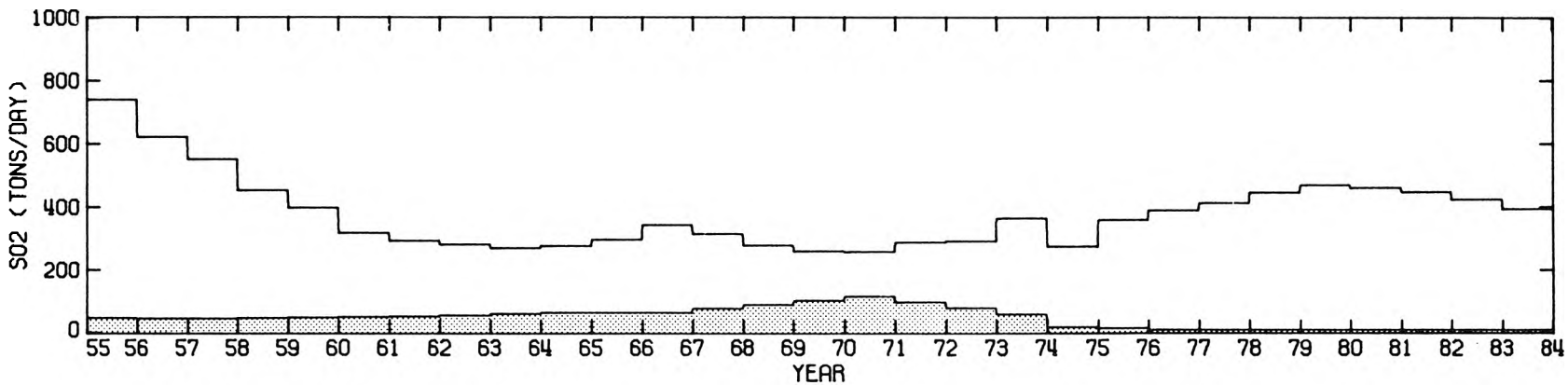


Includes sulfur recovery and sulfuric acid operations associated with petroleum refining.

FIGURE 1.7

SO2 EMISSIONS FROM MISCELLANEOUS SOURCES (SHADED) VS.

TOTAL SO2 EMISSIONS IN LA COUNTY, WITH LAAPCD FUTURE PROJECTION

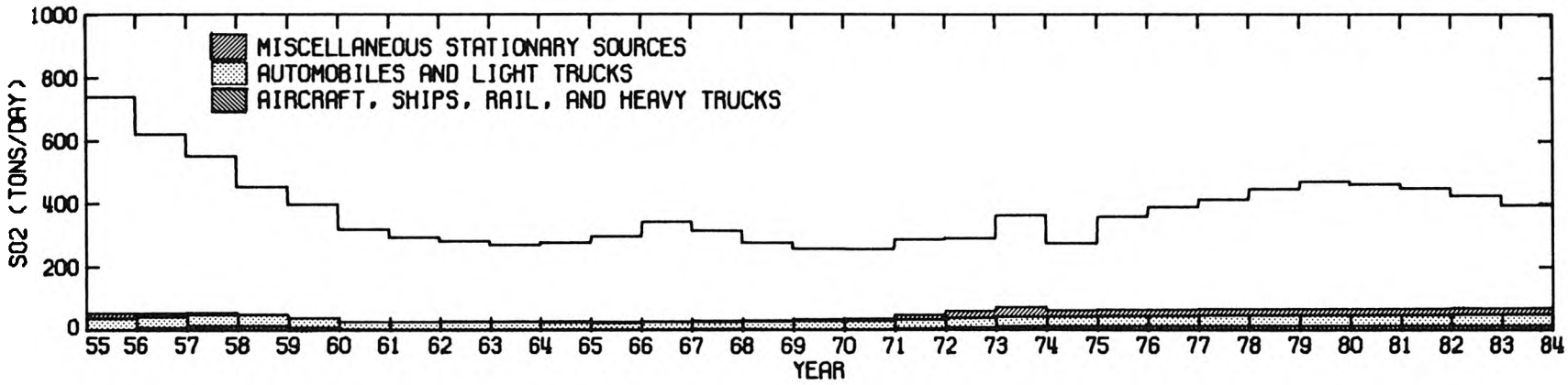

Angeles County in the mid 1950's. Increased sophistication of refining operations permitted a decline in the sulfur content of local gasolines in the following decade. In spite of progressive increases in vehicle miles traveled yearly, automotive $SO_2$ emissions in Los Angeles County declined, reaching a minimum of 23 tons per day in 1965. By the early 1970's, increased gasoline consumption had returned sulfur dioxide emissions from automobiles to the vicinity of 30 tons per day. Although automotive $SO_2$ emissions represent only about 10 percent of the total $SO_2$ emission inventory, they are important to an understanding of Los Angeles sulfur oxides air quality for at least two reasons. First, automotive emissions occur at ground level where atmospheric dispersion is least effective at diluting the effluent prior to reaching receptor populations (and local air monitoring stations). Secondly, as automobile exhaust is passed over an oxidizing catalyst intended for hydrocarbon and carbon monoxide control, a fraction of the exhaust $SO_2$ is converted to sulfuric acid mist. The basin-wide air quality impact of incremental increases in primary sulfate emissions from automobiles is poorly quantified at present and can only be placed in perspective if viewed in the context of the local sulfate air quality problems arising from other sources.

Emissions from miscellaneous mobile and stationary sources in Los Angeles County are also shown in Figure 1.7. Miscellaneous stationary source $SO_x$ emissions are presently dominated by calcining of petroleum coke produced by local refineries. Non-automotive mobile source emissions are dominated by highway use of diesel fuel and by combustion of high sulfur fuel oil by ships.

### 1.6.2 Sulfur Dioxide Air Quality Trends

Sulfur dioxide emissions undergo atmospheric transport, dilution, and removal processes resulting in the $SO_2$ concentrations measured at receptor air monitoring stations. Figure 1.8 displays the seasonal trends in $SO_2$ measurements over the past two decades at two such LAAPCD monitoring stations, Long Beach and downtown Los Angeles. Long Beach is chosen because it represents a location in the vicinity of major $SO_2$ sources in the harbor area. On the other hand, downtown Los Angeles is a commercial center located about 15 miles inland from the major coastal point sources of $SO_2$.

These ambient air quality graphs were generated by passing the time sequence of the LAAPCD's 24-hour average $SO_2$ readings over the period of interest through a linear digital filter.[4] The effect of this processing is to reveal long-term air quality trends by smoothing out fluctuations with frequency greater than four cycles per year, leaving the seasonal variations intact.

Referring to Figure 1.8, the following observations can be drawn. $SO_2$ air quality has improved since the mid 1950's at both Los Angeles and Long Beach. A sharp drop in $SO_2$ concentration occurred at both locations in 1959, at about the same time as the imposition of the initial controls on the sulfur content of fuel oil. From 1959 to 1963,

---

[4] The filter's characteristics are such that it returns the low frequency signal with unit gain, half power cutoff set to remove disturbances with period shorter than three months, and roll-off at the half power point of 20 db per octave. For a discussion of digital filtering methods, see Bendat and Piersol (1971), Chapter 9.2.

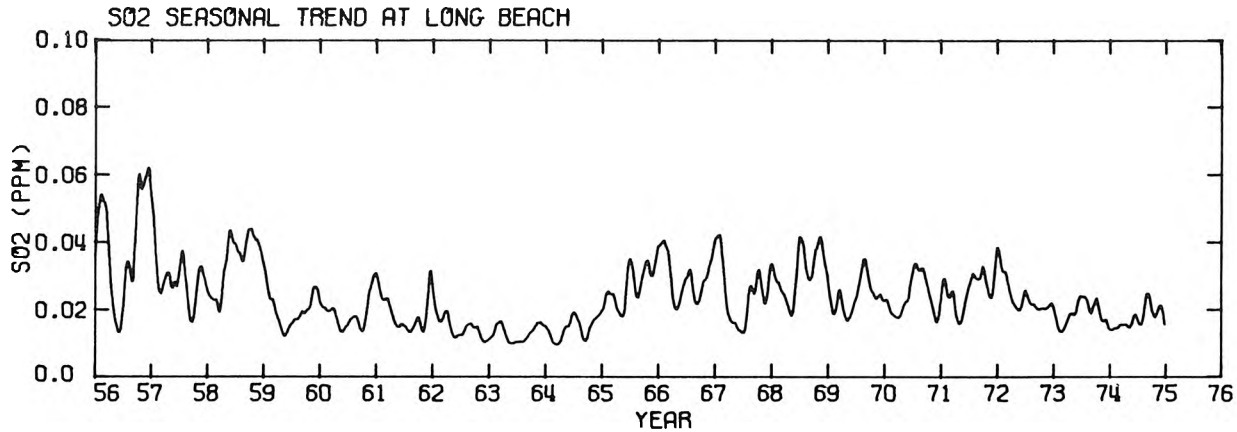


FIGURE 1.8(a)



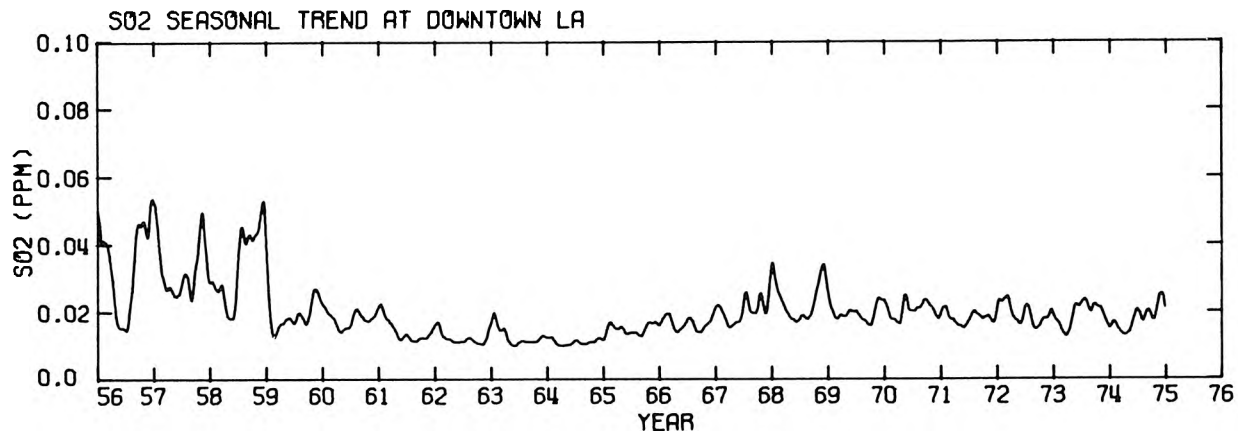


FIGURE 1.8(b)

air quality improved slightly at both locations, reaching a relative minimum in 1963 at the same time as the 1963 relative minimum in $SO_2$ emissions. $SO_2$ levels then rose, accompanying the subsequent late 1960's emission increases from chemical plants and automobiles. Since 1970, $SO_2$ concentrations at downtown Los Angeles have remained relatively constant, while at Long Beach a declining trend is apparent over the period 1972 through 1974 as nearby chemical plants installed new emission control equipment. Sulfur dioxide air quality is thus known to respond to changes in emission control regulations in a fairly predictable manner.

Successful past sulfur dioxide air quality control policies can be seen to have resulted from a sequential decision-making process. Growth in emissions from a single source class was observed. Emission control measures capable of containing the most pressing single problem at the moment were devised. Rapid feedback from atmospheric measurements confirmed that control strategies were working.

In the case of sulfate air quality, it would be hard to proceed with any degree of confidence to manage air resources by this traditional approach. The relative importance of various source classes to observed sulfate concentrations is a complex function of source location, meteorological conditions, atmospheric chemical reactions and long distance pollutant transport. Air monitoring data sufficient to deduce sulfate source-receptor relationships on the basis of response to past sulfur oxides control strategy changes probably do not exist. Analytical methods needed for an alternate approach to sulfate air quality management will be developed by this research.

# CHAPTER 2

# BASELINE AIR QUALITY CHARACTERIZATION: SULFATE AIR QUALITY IN THE SOUTH COAST AIR BASIN

## 2.1 Introduction

In preparation for an air quality control strategy study, we wish to characterize the readily observable features of sulfate air quality in the Los Angeles area. Design of a practical sulfate air quality modeling procedure requires that informed physical assumptions be made about the nature of the problem at hand. From this characterization, we hope to choose a modeling region which provides maximum opportunity to compare model calculations to historic observed air quality. The sulfate concentrations in air entering that modeling region will be specified, and an averaging time for the air quality model calculations will be selected. From spatial and temporal gradients in pollutant concentrations within the study region, generalizations will be drawn which impact the spatial and temporal resolution required of meteorological inputs to the modeling process. The evidence for chemical transformation of sulfur oxides within the Los Angeles atmosphere will be explored, and an approach to modeling the chemical conversion of sulfur dioxide to form sulfate will be selected.

Since historic sulfate and sulfur dioxide air quality data must be acquired and processed in order to address these issues, these data will be organized in passing so that they may be easily compared to future model calculations. Quality control checks will be applied to

the ambient data, and confidence intervals will be estimated for important parameters of the atmospheric measurements.

A rather comprehensive survey of the observed behavior of sulfur oxide air quality in the Los Angeles Basin thus will be undertaken. The objective is to select the bounds within which an air quality model relating sulfur oxides emissions to long-term average sulfate air quality might be specified with a reasonable chance for verifying its predictions.

## 2.2 Sulfate Air Quality in the South Coast Air Basin

### 2.2.1 Estimation of Sulfate Background Air Quality

On a global basis, over seventy percent of the emissions of sulfur compounds to the atmosphere arise from natural sources (Friend, 1973). These natural sources include sulfates from windblown sea salt, reduced sulfur compounds from biological decay, and emissions from volcanic activity. As a result of these natural sulfur sources, plus enrichment from man-made emissions, the global atmosphere contains low level "background" concentrations of sulfates, even at sites remote from major pollution sources.

The air entering the South Coast Air Basin thus contains non-zero levels of sulfate particulates which are not subject to further reduction by installation of controls on local emission sources. We wish to estimate these background concentrations so that they may be taken into account in our modeling exercise. The problem of estimating

South Coast Air Basin sulfate background levels has been treated by Hidy, et al., (1975) and by Trijonis, et al., (1975). Our discussion is built on much of the data used by these previous investigators.

The prevailing winds along the Southern California coast indicate that most new air masses entering the South Coast Air Basin are of marine origin. Early studies by Junge (1957) indicate that mid-Pacific marine air masses contain sulfate concentrations of the order of one microgram per cubic meter. "Giant particles" of a radius greater than 0.8μ were shown to contain the bulk of the sulfates at sea level in the Hawaiian Islands. Most of the sulfur content of these marine aerosols was traced back to the sulfate content of sea salt, although some ammonium sulfate of non-marine origin was also present. Sulfate concentrations due to sea salt were shown to decrease substantially with distance inland from the shore and with increasing altitude. More recent samples taken by Gillette and Blifford (1971) at a location about 250 km west of Santa Barbara, California showed particulate sulfur concentrations equivalent to about 0.72 $\mu gm/m^3$ of sulfate near the ocean's surface. A declining concentration with increasing altitude was also noted.

Moving closer to the South Coast Air Basin, there are indications that sulfate concentrations increase above the levels present in mid-ocean. Holzworth (1959) measured rather high total suspended particulate as well as sulfate concentrations at San Nicolas Island, the most remote of the Channel Islands off the Southern California coast (see Figure 2.1 or 2.3). More recent studies by Hidy, et al.,

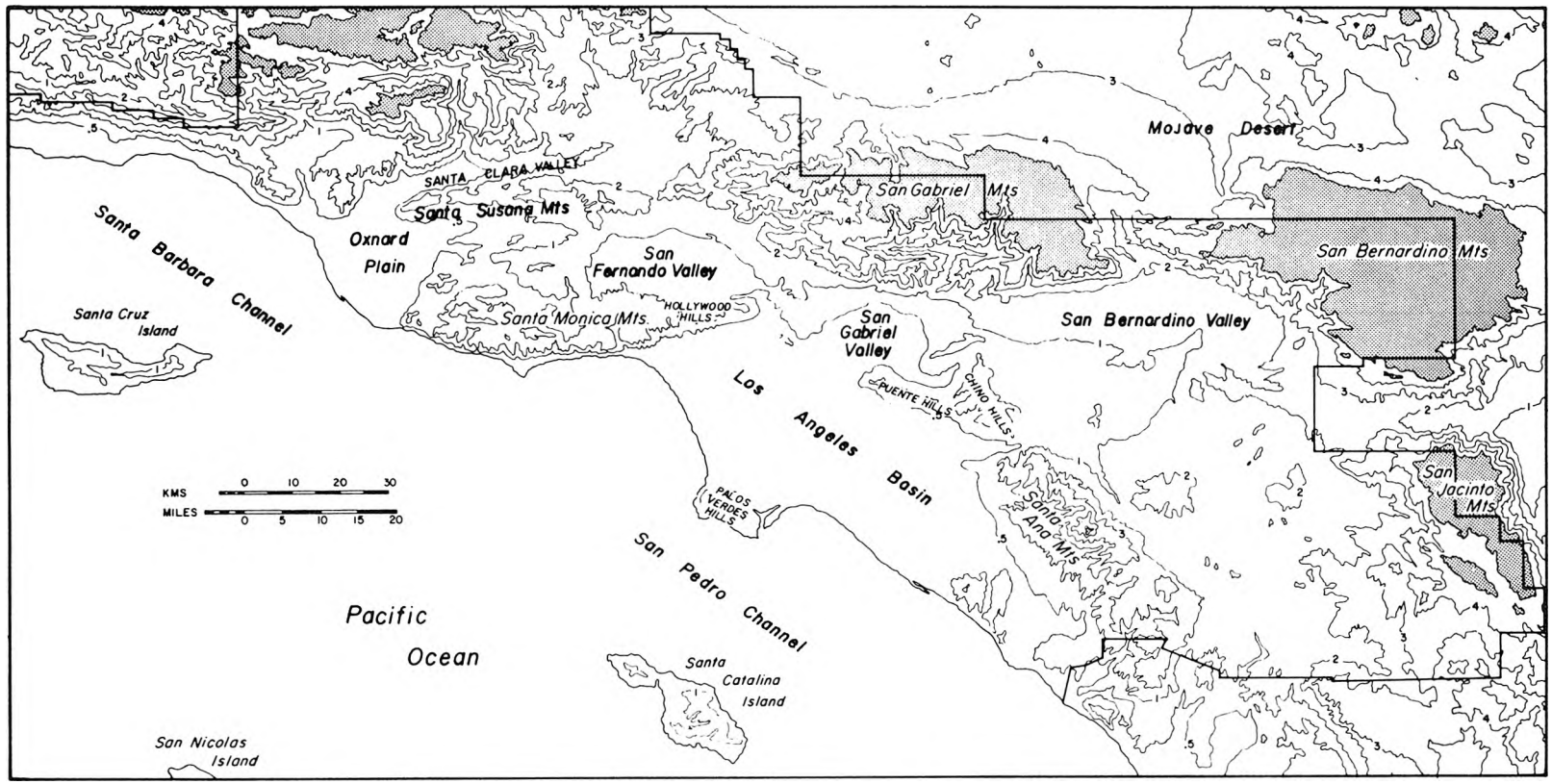


FIGURE 2.1

Topographic Map of Southern California
Showing the South Coast Air Basin in 1974

(1974), also measured air quality at San Nicolas Island but found sulfate concentrations more in line with what one would expect on the basis of the mid-ocean studies.

Hidy's group took thirteen sulfate samples on San Nicolas Island at an elevation of 200 meters above sea level. In Figure 2.2, the data of Hidy, et al., (1974) are plotted on log-probability paper along with all of the sulfate data of record taken by the Los Angeles Air Pollution Control District (LAAPCD) at downtown Los Angeles during the same time period, late July through early October 1970. A comparison of the statistics of these two data sets are given in Table 2.1. Methods used to estimate the parameters and confidence intervals shown in Table 2.1 are outlined in Appendix B4.

Geometric mean sulfate concentrations in incoming marine air averaged about a factor of four lower than those observed at downtown Los Angeles during the same season of 1970. The geometric standard deviation of the San Nicolas Island data is about the same as that of the inland observations. Thus while the air over the Channel Islands is noticeably less polluted than that at Los Angeles, extrapolation of the San Nicolas Island data would indicate that sulfate concentrations at remote locations exceeding the current California 24-hour average sulfate standard of 25 $\mu gm/m^3$ might be expected roughly one half of one percent of the time during the summer and fall seasons. In the absence of any more extensive marine air monitoring data, our modeling study will use the description of San Nicolas Island sulfate

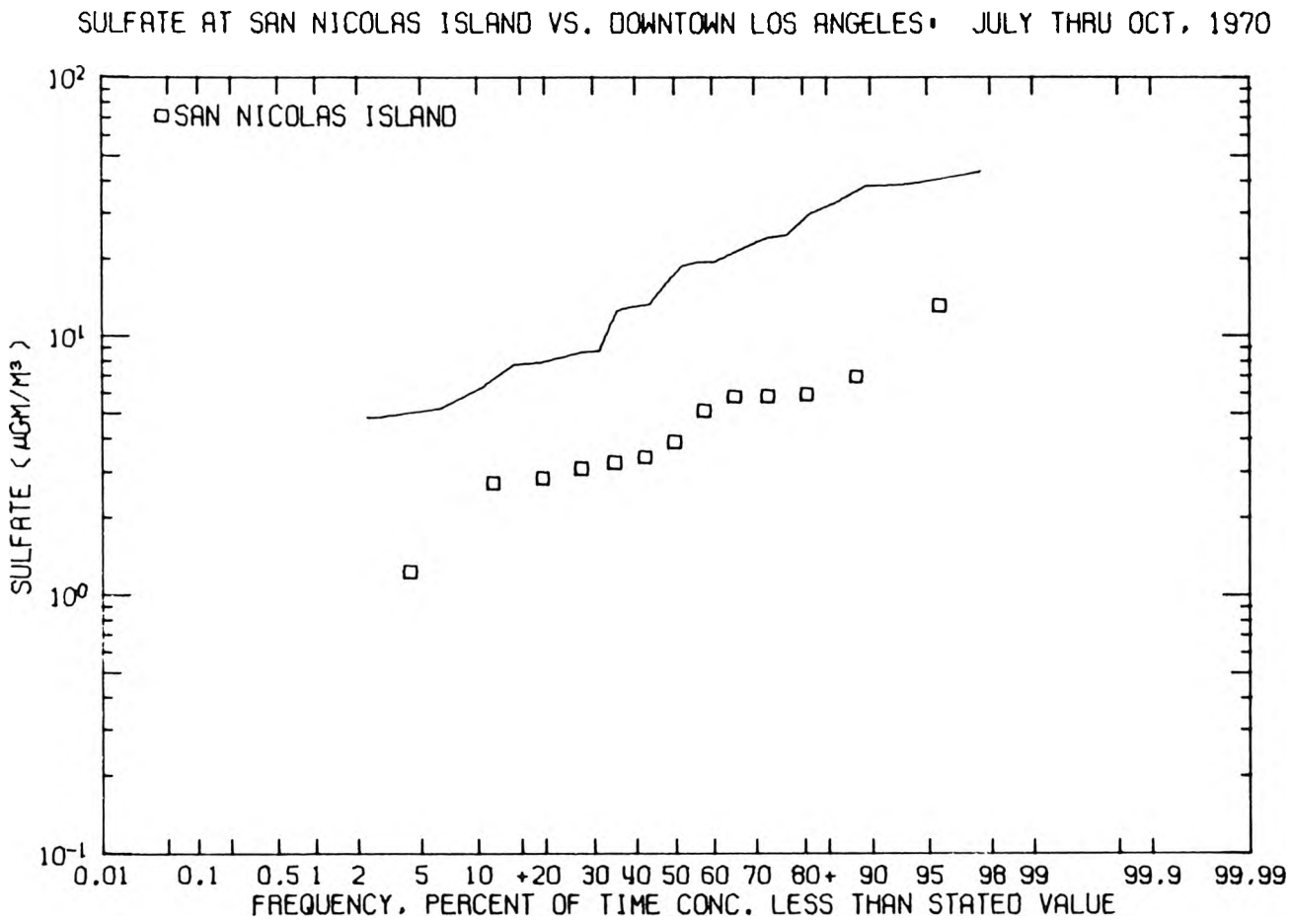
SULFATE AT SAN NICOLAS ISLAND VS. DOWNTOWN LOS ANGELES, JULY THRU OCT, 1970
SAN NICOLAS ISLAND
SULFATE (μGM/M³)
10²
10¹
10⁰
10⁻¹
0.01 0.1 0.5 1 2 5 10 +20 30 40 50 60 70 80+ 90 95 98 99 99.9 99.99
FREQUENCY, PERCENT OF TIME CONC. LESS THAN STATED VALUE

FIGURE 2.2

TABLE 2.1

Statistical Comparison of Sulfate Concentrations at San Nicolas Island vs. those at Downtown Los Angeles: Late July Through Early October, 1970

| | ARITHMETIC STATISTICS | | | | | GEOMETRIC STATISTICS | | | | |
|---|---|---|---|---|---|---|---|---|---|---|
| | SAMPLE ARITHMETIC MEAN $\bar{y}$ | SAMPLE ARITHMETIC STANDARD DEVIATION $\sigma$ | NUMBER OF SAMPLES $n$ | LOWER CONFIDENCE LIMIT ON $\bar{y}$ (2.5 %ile) | UPPER CONFIDENCE LIMIT ON $\bar{y}$ (97.5 %ile) | ESTIMATED MEAN LOG $\alpha$ | ESTIMATED VARIANCE OF LOGS $\beta^2$ | ESTIMATED GEOMETRIC MEAN $\mu_g$ | ESTIMATED GEOMETRIC STANDARD DEVIATION $\sigma_g$ | ARITHMETIC MEAN ESTIMATED FROM $\alpha$ and $\beta^2$ |
| Downtown Los Angeles | 18.7 | 11.5 | 24 | 14.7 | 22.6 | 2.73 | 0.43 | 15.4 | 1.93 | 19.0 |
| San Nicolas Island | 4.9 | 3.0 | 13 | 3.4 | 6.4 | 1.44 | 0.33 | 4.2 | 1.78 | 5.0 |

(Units on arithmetic statistics are $\mu gm/m^3$)

air quality as given in Table 2.1 as one basis for estimation of sulfate concentrations in air entering the South Coast Air Basin.

While most new air masses entering the South Coast Air Basin are of marine origin, it is reassuring to note that even under desert breeze conditions, sulfate background concentrations will not deviate greatly from the background levels at San Nicolas Island. A number of monitoring programs have examined air quality in the Mojave Desert. The LAAPCD routine air monitoring station at Lancaster reported arithmetic mean sulfate levels of 3.1 $\mu gm/m^3$ for the last half of 1973 and 3.2 $\mu gm/m^3$ for calendar year 1974 (MacPhee and Wadley, 1975a, 1975b). At greater distances from the South Coast Air Basin, Gillette and Blifford (1971) measured particulate sulfur concentrations in Death Valley equivalent to about one microgram per cubic meter of sulfate.

The picture emerging from this analysis is as follows. At great distances from the South Coast Air Basin, either out to sea or well into the desert, sulfate concentrations appear to be about one microgram per cubic meter. Immediately adjacent to the air basin at San Nicolas Island or Lancaster, average sulfate concentrations are in the 3 to 5 $\mu gm/m^3$ range. We have seen that sulfate levels at downtown Los Angeles are substantially elevated above background. But what do the gradients in sulfate concentration look like within the Los Angeles Basin?

---

Note: As used throughout this study, the word "background" denotes pollutants present in air upwind of a source area of interest upon which the effect of emissions from within the source area will be superimposed. This regional background aerosol includes both natural emissions plus manmade material from distant sources.

### 2.2.2 Previous Surveys of Sulfate Air Quality Data in the Los Angeles Area

Within the past few years, a number of investigators (Tokiwa, et al., 1974; Trijonis, et al., 1975; Kurosaka, 1976) have surveyed the availability of sulfur dioxide and sulfate air quality data in the South Coast Air Basin. A composite listing of the data sources cited in these references plus some pioneer studies of historical interest are shown in Table 2.2, classified according to the purpose for which the sulfate air monitoring program was conducted.

Ideally, to define pollutant patterns over an air basin, one would like to have simultaneous observations on pollutant concentration at a large number of well spaced air monitoring locations. A high degree of temporal resolution in the data base would be desired. Sample analysis would be by comparable methods. Unfortunately, no single sulfate data base is available which provides long-term simultaneous sampling, basin-wide geographic coverage and high temporal resolution. The special studies mentioned in Table 2.2 often contain the most detailed information on diurnal sulfate concentration patterns. However, they do not attempt to provide a long-term continuous record over a wide-enough geographic area to allow one to draw many firm conclusions about spatial concentration gradients or seasonal pollutant trends. On the other hand, the routine 24-hour average sulfate air monitoring data gathered by local, state and federal agencies possibly satisfy at least two of our criteria. A large number of widely spaced monitoring sites exist and the sampling histories at these sites stretch over long periods of time. The 24-hour average temporal resolution of

# TABLE 2.2

SOURCES OF SULFATE AIR QUALITY DATA IN THE SOUTH COAST AIR BASIN
(through 1974)

A. Routine Air Monitoring Programs in Operation in 1974 (List Compiled by Kurosaka, 1976)

| Agency | Number of Stations in South Coast Air Basin(1974) | Sulfate Sampling/ and Analysis Method (1974)*** | Sulfate Data Averaging Time | $SO_2$ Sampling Method | $SO_2$ Data Averaging Time | Sampling History |
|---|---|---|---|---|---|---|
| Los Angeles Air Pollution Control District (LAAPCD)* | 7 | Hi-Vol/Turbidimetric | 24 hour | conductometric | 1 hour | 1965-Present |
| San Bernardino Air Pollution Control District* | 8 | Hi-Vol/Turbidimetric | Quarter Year Composite | conductometric | 1 hour | 1965-Present |
| Riverside Air Pollution Control District* | 1 | Hi-Vol/Turbidimetric | 24 hour | conductometric | 1 hour | 1974-Present |
| National Air Surveillance Network (NASN) | 11 | Hi-Vol/Methylthymol Blue | 24 hour | West-Gaeke | 24 hour | Mid 1950's-Present |
| Community Health and Environmental Surveillance System (CHESS) | 6 | Hi-Vol/Methylthymol Blue | 24 hour | West-Gaeke | 24 hour | 1972-Present |

B. Recent Special Studies (List compiled by Kurosaka, 1976)

| Study Title and Investigators' Affiliation | | | | | | |
|---|---|---|---|---|---|---|
| Aerosol Characterization Experiment (ACHEX) | Rockwell International Science Center* | Variety of methods compared | 2 hour and 24 hour | flame photometric | | several days during 1972-1973 |
| California Air Resources Board Monitoring Program | California Air Resources Board | Low-Vol filter/X-Ray fluorescence | 2 hour | | | 1973 to present |
| Regional Monitoring of Smog Aerosols | U.C. Davis** | Lundgren Impactor ion-excited X-Ray emission | | NONE | | 1973 to present |
| Sulfur Dioxide Conversion Study | Caltech | flash vaporization | 1 hour | flame photometric | | several days, 1973 |

C. Recent Studies of Freeway Air Quality (List Compiled by Kurosaka, 1976)

| | | | | | | |
|---|---|---|---|---|---|---|
| Impact of Motor Vehicle Exhaust catalysts on Air Quality | Rockwell International AIHL, U.S. Navy ** | Variety of methods compared | 2 hour | | | 1974 to present |
| Los Angeles Catalyst Study | U.S. EPA | Hi-Vol/? | 4 hour and 24 hour | | | 1974 to present |
| Air Resources Board Freeway Monitoring Study | California Air Resources Board | Low-Vol filter/X-Ray fluorescence | 2 hour | | | 1975 to present |
| | | Hi-Vol? | 24 hour | | | |

D. Additional Sources of Sulfate Data in or near the South Coast Air Basin (Data taken prior to 1972)

| Reference | | | | | |
|---|---|---|---|---|---|
| Renzetti et.al, (1955) (Air Pollution Foundation) | Hi-Vol/Turbidimetric | 24 hour | conductometric | | Aug. thru Nov. 1954 |
| Holzworth, (1959) (U.S. Weather Bureau) | Hi-Vol/Turbidimetric | 24 hour | NONE | | May, 1956 - Jan. 1957 |
| Thomas, (1962) | Conductometric | 30 minutes | conductometric | | several weeks 1961 |
| Los Angeles APCD "Sulfur Trioxide" Monitoring Program | Conductometric | 1 hour | conductometric | 1 hour | 1963-1969 |
| Gillette and Blifford, (1971) | Impactor/X Ray fluorescence | 1 hour | NONE | | 1967 |
| Lundgren, (1970) | Impactor & Filters/ Turbidimetric | 4 hour and 24 hour | NONE | | Nov, 1968 |
| Hidy, et.al, (1974) | Hi-Vol & Low-Vol/ Turbidimetric | 24 hour | NONE | | Jul- Oct. 1970 |

* Now part of the Southern California Air Pollution Control District

** Sponsored by the California Air Resources Board

*** While X-Ray fluorescence is listed as a mean of sulfate determination, the actual measurement made in that case is for total particulate sulfur.

these monitoring programs, while not as refined as some special studies, is still short when compared to our objective of defining seasonal trends. This baseline air quality characterization will first focus on the nature of the available sulfur oxides routine air monitoring data.

### 2.2.3 Routine Air Monitoring Programs for Sulfates and Sulfur Dioxide in the South Coast Air Basin

During the period 1972 through 1974, the APCD, CHESS and NASN air monitoring programs listed in Table 2.2 operated concurrently. Each agency sampled for both sulfur dioxide and suspended particulate sulfates. If these data bases could be pooled, measurements at over two dozen monitoring sites would be available against which to compare air quality model calculations. Thus the years 1972 through 1974 will be chosen as the base years for our study.

But the question remains, "To what extent were the sampling methods used by these agencies comparable?" In Appendix B1 to this report, each of these air monitoring programs has been described in an attempt to isolate differences in experimental design. It is found that ideally the sulfate air quality monitoring methods used by each of these agencies should be comparable. However, the CHESS network encountered some analytical problems in practice and a correction factor must be applied to some of their data. Sulfur dioxide monitoring methods used by the LAAPCD are judged to be significantly different from those of CHESS and NASN. Some important implications of these

differences in sulfur dioxide sampling methodology will become apparent as our investigation proceeds.

Figure 2.3 indicates the location of sulfate air quality monitoring stations operated in or near the South Coast Air Basin during the period 1972 through 1974. Since the validity of the San Bernardino County APCD sulfate data during those years has been questioned (Kurosaka, 1976), only stations operated by the Los Angeles Air Pollution Control District, EPA's CHESS program, and the National Air Surveillance Network are shown. Steps taken to acquire and prepare data from these air monitoring stations for comparative analysis are outlined in Appendix B2.

### 2.2.4 Long-Term Average Sulfate Air Quality

Concentration averages given in Figure 2.4 represent the arithmetic mean of sulfate concentrations for all days of record at the CHESS, LAAPCD and NASN monitoring stations during the years 1972 through 1974. It is seen that long-term average sulfate levels are of the same order of magnitude over most portions of the South Coast Air Basin. Concentrations appear higher than average in the San Fernando Valley and lower than average at the western-most and southern-most monitoring sites. These deviations from the basin-wide mean of 11.7 $\mu gm/m^3$ are still small, perhaps $\pm$ 3 $\mu gm/m^3$. But how much uncertainty is associated with these concentration averages? Is that uncertainty larger than the differences in average sulfate concentration computed at separate monitoring sites? How many samples must one average in

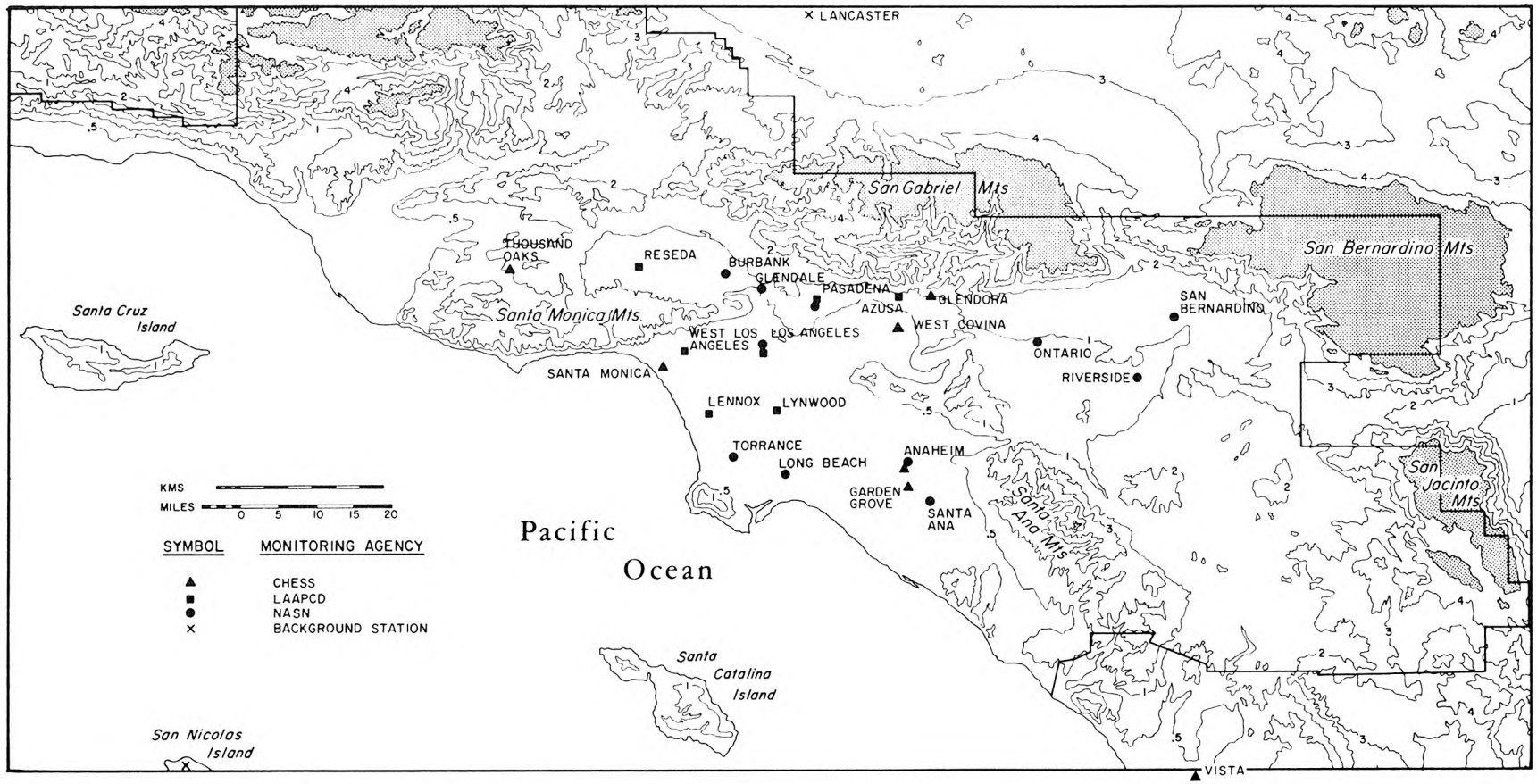


FIGURE 2.3

Sulfate Air Quality Monitoring Sites in or near the South Coast Air Basin

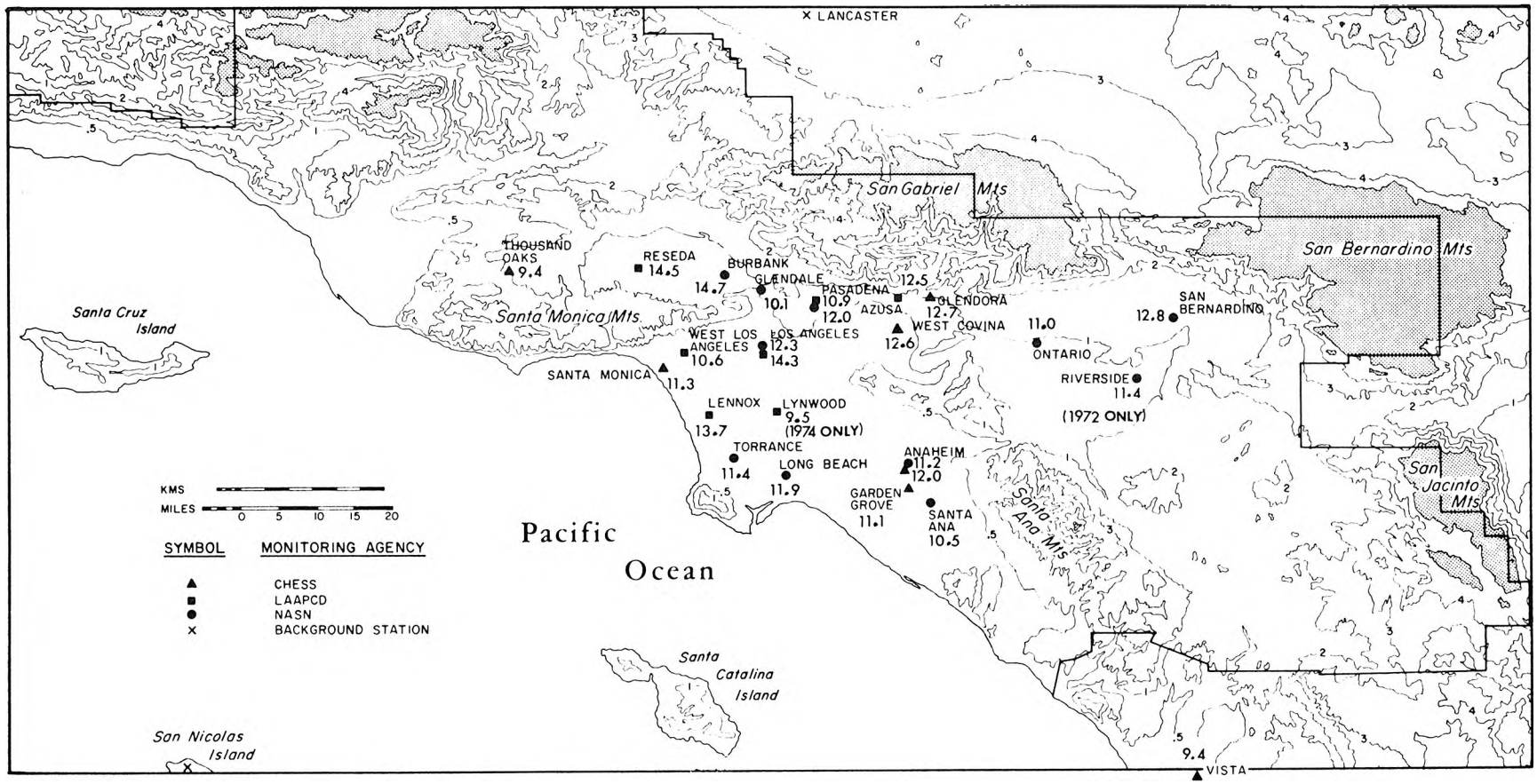


FIGURE 2.4

Arithmetic Mean Sulfate Air Quality: 1972 through 1974
Concentrations Shown Adjacent to Monitoring Site Location in $\mu gm/m^3$

order to make useful statements about differences in sulfate levels from one time period to the next? The complexity and averaging time chosen for our air quality model will depend on the outcome of those inquiries.

One way to approach answering these questions is to examine the statistical sampling distribution of the air quality measurements made at individual air monitoring stations. Empirical work pioneered by Larsen (1971) suggests that air quality measurements approximately follow a simple two parameter log-normal distribution for all pollutants and all averaging times. An exception to this rule of thumb often occurs when minimum detection limit problems distort pollutant measurements made at low concentrations. A quick visual check on the log-normality assumption as it applies to our sulfate air quality data is provided in Figures 2.5, 2.6, and 2.7. These three figures represent log-probability plots of sulfate concentration measurements made over the period 1972 through 1974 at typical NASN, LAAPCD, and CHESS air monitoring stations, respectively. It can be seen that the cumulative distribution of the sulfate data plots as a nearly straight line at sulfate concentrations above 2 $\mu gm/m^3$, indicating that the data indeed approximately fit a two parameter log-normal distribution in that range. At the CHESS and LAAPCD stations, the lower tails of the distribution sag noticeably at concentrations below 2 $\mu gm/m^3$, while values in that range are unavailable at the NASN station. The departure from two parameter log-normality by the LAAPCD data at very low sulfate concentrations could well be due to the measurement problems at low

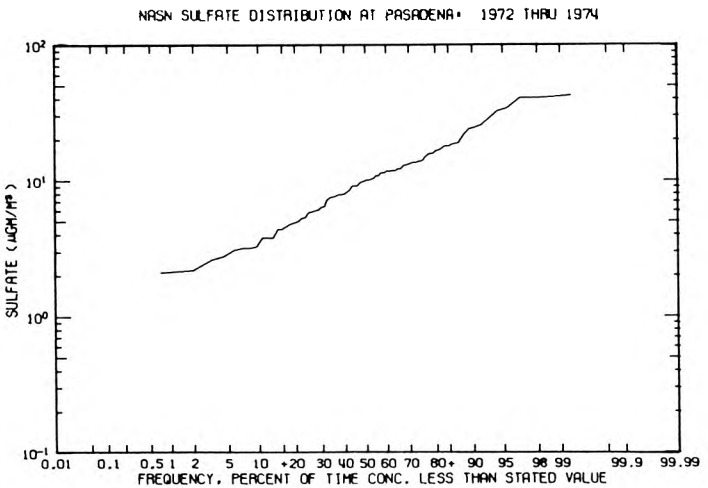


FIGURE 2.5

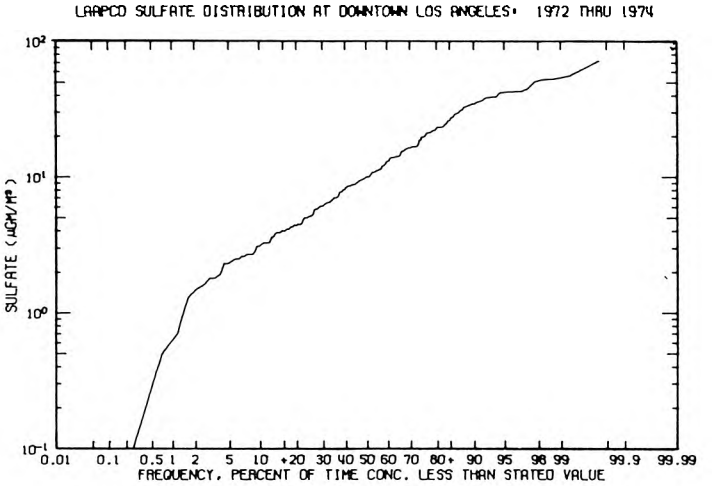


FIGURE 2.6

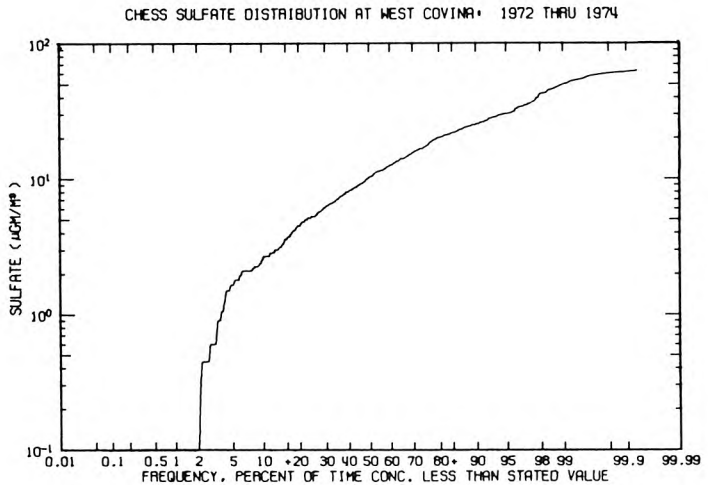


FIGURE 2.7

concentrations reported by Porter, et al. (1976). A similar but previously unreported problem may have affected the CHESS monitoring program. *In any case, the absolute magnitude of the sulfate concentration by which these samples deviate from a simple two parameter log-normal distribution at low concentrations is extremely small.* A complete set of graphs showing the cumulative distribution of the sulfate data at each of the monitoring stations under consideration is given in Appendix B3. In general, the smoothest, straightest lines on log-probability paper occur at stations with the greatest number of observations. Cumulative distributions at NASN stations with relatively few observations (e.g. Riverside with 18 samples) would seem to be a bit lumpy. This is to be expected at small sample sizes.

Table 2.3 shows some pertinent statistics of the observations at sulfate air monitoring stations over the period 1972 through 1974. Estimates of the mean natural log, $\alpha$, and variance, $\beta^2$, of the natural logs of the sulfate observations are given in that table. Parameter estimation procedures are outlined in Appendix B4.

Our intended air quality modeling effort will later result in calculation of arithmetic mean sulfate concentration patterns over portions of the South Coast Air Basin. If we are to compare model results to field observations, it becomes important to be able to place confidence intervals around the arithmetic mean calculated from a given set of sulfate air quality data. Approximate 95% confidence

# TABLE 2.3

## Statistical Description of Sulfate Air Quality Data in the South Coast Air Basin: 1972-1974

| | | ARITHMETIC STATISTICS | | | | | GEOMETRIC STATISTICS | | | | |
|---|---|---|---|---|---|---|---|---|---|---|---|
| | | SAMPLE ARITHMETIC MEAN $\bar{y}$ | SAMPLE ARITHMETIC STANDARD DEVIATION $\sigma$ | NUMBER OF SAMPLES $n$ | LOWER CONFIDENCE LIMIT ON $\bar{y}$ (2.5 %ile) | UPPER CONFIDENCE LIMIT ON $\bar{y}$ (97.5 %ile) | ESTIMATED MEAN LOG $\alpha$ | ESTIMATED VARIANCE OF LOGS $\beta^2$ | ESTIMATED GEOMETRIC MEAN $\mu_g$ | ESTIMATED GEOMETRIC STANDARD DEVIATION $\sigma_g$ | ARITHMETIC MEAN ESTIMATED FROM $\alpha$ and $\beta^2$ |
| THOUSAND OAKS | CHESS | 9.41 | 9.08 | 890.00 | 9.08 | 9.73 | 1.87 | 0.83 | 6.48 | 2.48 | 9.80 |
| RESEDA | LAAPCD | 14.53 | 16.59 | 214.00 | 12.53 | 16.53 | 2.09 | 1.31 | 8.11 | 3.14 | 15.62 |
| SANTA MONICA | CHESS | 11.27 | 8.82 | 840.00 | 10.91 | 11.62 | 2.16 | 0.57 | 8.64 | 2.13 | 11.50 |
| WEST LA | LAAPCD | 10.64 | 9.51 | 215.00 | 9.49 | 11.78 | 1.97 | 0.86 | 7.19 | 2.53 | 11.04 |
| LENNOX | LAAPCD | 13.71 | 10.76 | 219.00 | 12.43 | 14.99 | 2.32 | 0.64 | 10.19 | 2.22 | 14.00 |
| TORRANCE | NASN | 11.40 | 6.59 | 83.00 | 10.04 | 12.77 | 2.29 | 0.29 | 9.84 | 1.72 | 11.40 |
| LONG BEACH | NASN | 11.94 | 7.65 | 79.00 | 10.31 | 13.57 | 2.33 | 0.27 | 10.28 | 1.68 | 11.78 |
| LYNWOOD | LAAPCD | 9.47 | 8.55 | 68.00 | 7.50 | 11.44 | 1.87 | 0.81 | 6.46 | 2.46 | 9.71 |
| BURBANK | NASN | 14.73 | 18.66 | 90.00 | 11.03 | 18.43 | 2.37 | 0.53 | 10.68 | 2.07 | 13.93 |
| GLENDALE | NASN | 10.12 | 7.70 | 71.00 | 8.39 | 11.86 | 2.08 | 0.47 | 8.02 | 1.99 | 10.16 |
| LOS ANGELES | NASN | 12.33 | 9.17 | 83.00 | 10.43 | 14.23 | 2.29 | 0.44 | 9.87 | 1.95 | 12.32 |
| LOS ANGELES | LAAPCD | 14.29 | 12.63 | 212.00 | 12.76 | 15.83 | 2.29 | 0.80 | 9.89 | 2.44 | 14.72 |
| PASADENA | LAAPCD | 10.94 | 10.73 | 214.00 | 9.64 | 12.23 | 1.94 | 0.99 | 6.93 | 2.71 | 11.38 |
| PASADENA | NASN | 12.00 | 8.97 | 79.00 | 10.09 | 13.91 | 2.24 | 0.50 | 9.43 | 2.03 | 12.10 |
| GARDEN GROVE | CHESS | 11.08 | 7.53 | 898.00 | 10.80 | 11.37 | 2.19 | 0.47 | 8.97 | 1.98 | 11.32 |
| ANAHEIM | CHESS | 11.37 | 8.34 | 966.00 | 11.10 | 11.65 | 2.20 | 0.52 | 8.99 | 2.06 | 11.68 |
| ANAHEIM | NASN | 11.15 | 7.85 | 83.00 | 9.52 | 12.78 | 2.20 | 0.44 | 9.04 | 1.94 | 11.25 |
| SANTA ANA | NASN | 10.51 | 8.21 | 83.00 | 8.81 | 12.21 | 2.16 | 0.34 | 8.68 | 1.79 | 10.30 |
| AZUSA | LAAPCD | 12.55 | 11.37 | 215.00 | 11.18 | 13.91 | 2.12 | 0.92 | 8.35 | 2.61 | 13.22 |
| WEST COVINA | CHESS | 12.57 | 9.93 | 881.00 | 12.20 | 12.95 | 2.23 | 0.69 | 9.27 | 2.29 | 13.07 |
| GLENDORA | CHESS | 12.66 | 10.58 | 937.00 | 12.31 | 13.02 | 2.20 | 0.76 | 9.02 | 2.40 | 13.22 |
| ONTARIO | NASN | 10.99 | 7.86 | 64.00 | 9.12 | 12.87 | 2.16 | 0.49 | 8.64 | 2.02 | 11.06 |
| RIVERSIDE | NASN | 11.40 | 6.54 | 18.00 | 8.40 | 14.40 | 2.29 | 0.33 | 9.92 | 1.78 | 11.71 |
| SAN BERNARDINO | NASN | 12.80 | 10.70 | 75.00 | 10.46 | 15.14 | 2.25 | 0.64 | 9.47 | 2.22 | 13.04 |
| VISTA | CHESS | 9.45 | 7.06 | 1035.00 | 9.25 | 9.65 | 2.00 | 0.53 | 7.40 | 2.07 | 9.65 |

intervals on the three year arithmetic mean sulfate concentration at each monitoring station are given in Table 2.3. The confidence interval estimation procedure is detailed in Appendix B4.

The confidence intervals on the three year arithmetic mean sulfate concentrations overlap at most monitoring sites. For example, confidence intervals at fourteen of the twenty-five monitoring sites would contain the basin-wide mean value of 11.7 $\mu gm/m^3$. Of the remaining eleven stations, three miss containing that value by less than 0.3 $\mu gm/m^3$, which is probably less than the uncertainty introduced by the approximations made when calculating the confidence intervals. Average sulfate values at the margins of our study area, at Vista and Thousand Oaks, are significantly lower than those at stations in the central portion of the Los Angeles basin. Distinctly higher values than average are reported at Lennox in the immediate vicinity of some major $SO_2$ sources. High values are also found in the San Fernando and the eastern San Gabriel Valleys. Even these relative "hot spots" differ from the concentrations reported elsewhere in the central portion of the air basin by about the same amount as the differences between sulfate averages found by two different monitoring agencies at the same location, downtown Los Angeles.

These comparisons of long-term concentration averages plus the previous discussion of off-shore and desert sulfate air quality lead to three important physical generalizations:

Generalization 1: Long-run average sulfate concentrations are about the same at monitoring sites in the central portion of the South Coast

Air Basin (i.e. about 11.7 micrograms per cubic meter over our three base years).

Generalization 2: The lowest sulfate concentrations observed are systematically found at the margins of our study area (e.g. at San Nicolas Island, Lancaster, Thousand Oaks, and Vista).

Generalization 3: Los Angeles sulfate air quality is significantly elevated above background sulfate concentrations in incoming marine or desert air.

### 2.2.5 Seasonal Trends in Sulfate Concentration in the South Coast Air Basin

Sulfate concentrations observed at the downtown Los Angeles station of the LAAPCD during the past decade are shown in time series in Figure 2.8. Concentration fluctuations from day to day are quite large, with high values occurring at least occasionally in all seasons of the year. However, the data can be smoothed to reveal seasonal trends, as shown in Figure 2.9.

The graph in Figure 2.9 was generated by passing the time sequence of 24 hour average sulfate readings over the period of interest through a linear digital filter.[1] The effect of this processing is to reveal long-term air quality trends by suppressing fluctuations with frequency greater than four cycles per year, leaving seasonal variations intact.

---

[1] The filter's characteristics are such that it returns the low frequency signal with unit gain, half power cutoff set to remove disturbances with period shorter than three months, and roll off at the half power point of 20 db per octave. For a discussion of digital filtering methods see Bendat and Piersol (1971), Chapter 9.2.

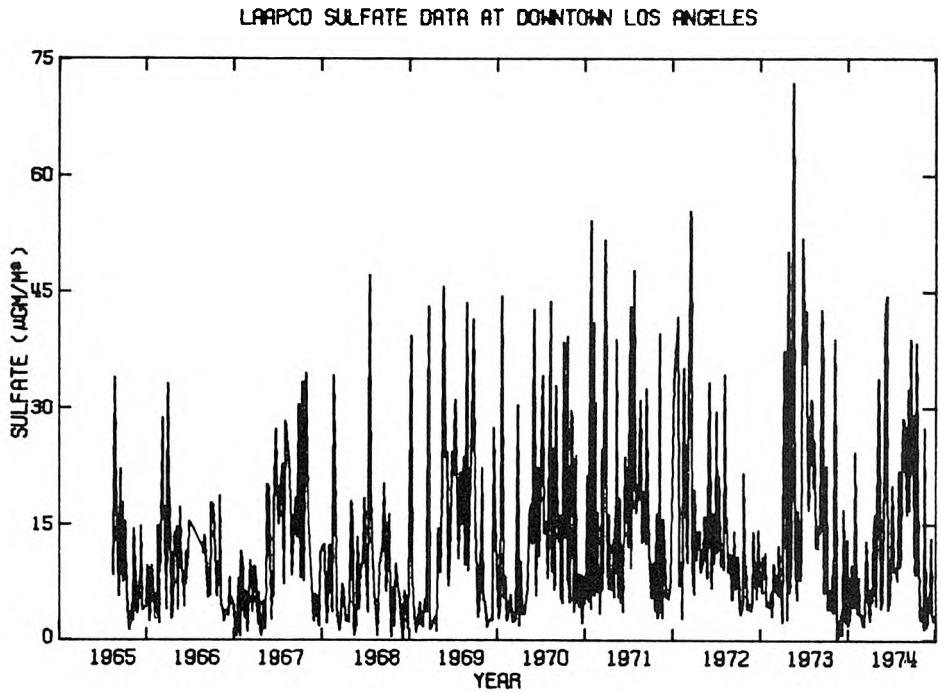


FIGURE 2.8

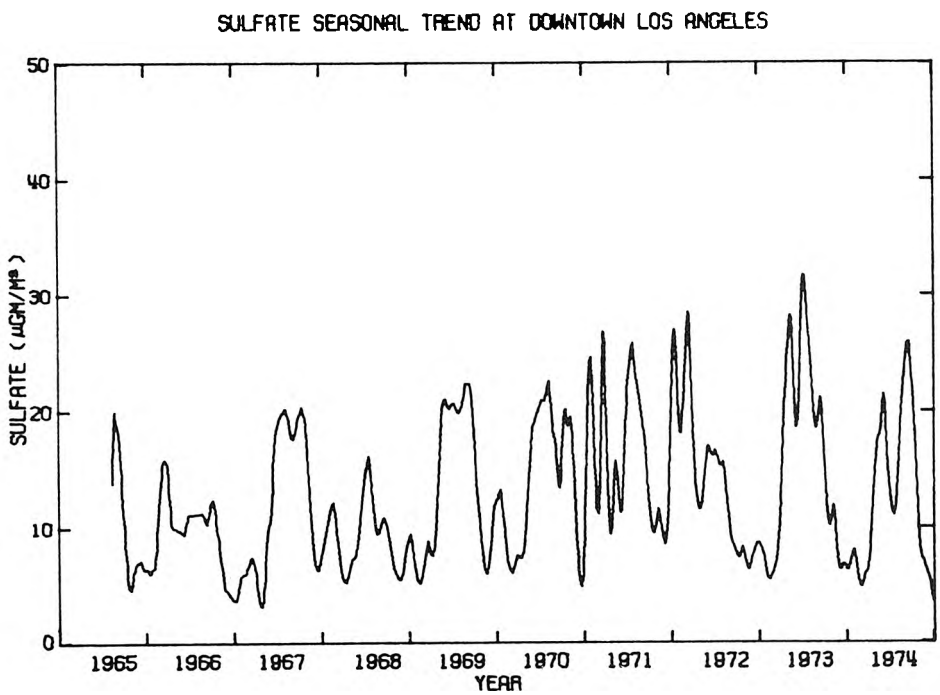


FIGURE 2.9
(From Cass, 1975)

It is apparent from Figure 2.9 that measured sulfate levels at downtown Los Angeles have risen over the past decade, reaching a relative peak in 1973. A small decline followed in 1974. Both the annual mean and upper bound of seasonal maxima follow this trend. There is a broad summer seasonal peak in sulfate levels apparent in most years of record. A wintertime peak is also apparent, but its magnitude varies greatly from year to year. In the winters of 1972-73 and 1973-74, for example, the winter peak was very small and confined to a few weeks around the first of the year, while in the winters of 1970-71 and 1971-72 the winter peak was characterized by isolated days of very high sulfate levels which led to elevated annual averages for those years.

In Figure 2.10, the same filtering process has been applied to the LAAPCD and CHESS sulfate data at all monitoring stations active during the period 1972 through 1974. The resulting graphs are positioned on a map of the South Coast Air Basin in close proximity to each station's physical location. National Air Surveillance Network data were not presented because their infrequent monitoring schedule provides insufficient data for this sort of treatment. The graphs in Figure 2.10 are small and thus difficult to read. They have been reproduced at a larger scale in Appendix B5.

The similarity of seasonal pollutant patterns at all monitoring stations is quite striking. The timing and relative magnitude of seasonal concentration peaks and troughs is apparently related from

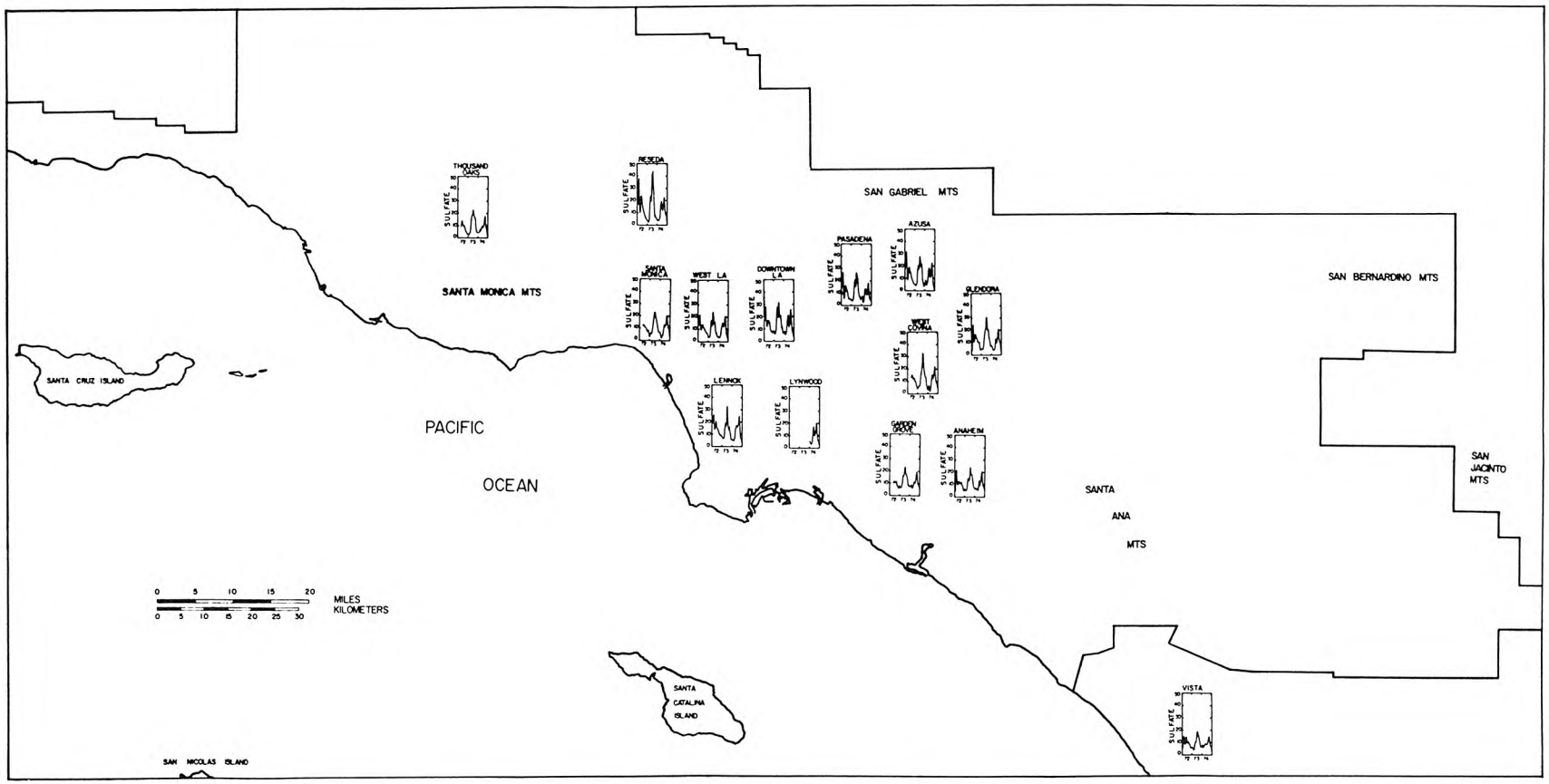


FIGURE 2.10

Seasonal Trends in Sulfate Air Quality 1972 through 1974

Thousand Oaks to the northwest to Vista on the south, a distance of nearly two hundred kilometers.

### 2.2.6 A Comparison of Simultaneous 24-Hour Average Sulfate Air Quality Measurements

Two features noted so far are that long-run average sulfate concentrations in the central portion of the air basin are fairly uniform, and similar seasonal modulation of those concentration levels appears to be applied basin-wide. We will now find something even more interesting. This organized behavior is manifested to a large degree on a day-to-day basis.

Figures 2.11 and 2.12 show the relationship between sulfate levels measured at Lennox, downtown Los Angeles, and Pasadena on the same days during the years 1972 through 1974. These three monitoring sites lie approximately along a resultant sea breeze wind trajectory stretching from a major $SO_2$ source area at the coast through the central business district and into inland valleys beyond, as shown by comparing Figure 2.3 with Figures 2.13 and 2.14. Sulfate values are approximately the same at all three locations on the same day, as shown by the unit slope and near zero intercept of the regression lines describing the best fit relationship between sulfate values at pairs of stations.

But how widespread is this tracking of daily sulfate concentration changes? Tables 2.4 and 2.5 show the log-linear correlation between sulfate concentrations reported at pairs of monitoring stations for the same day, plus the number of simultaneous observations available

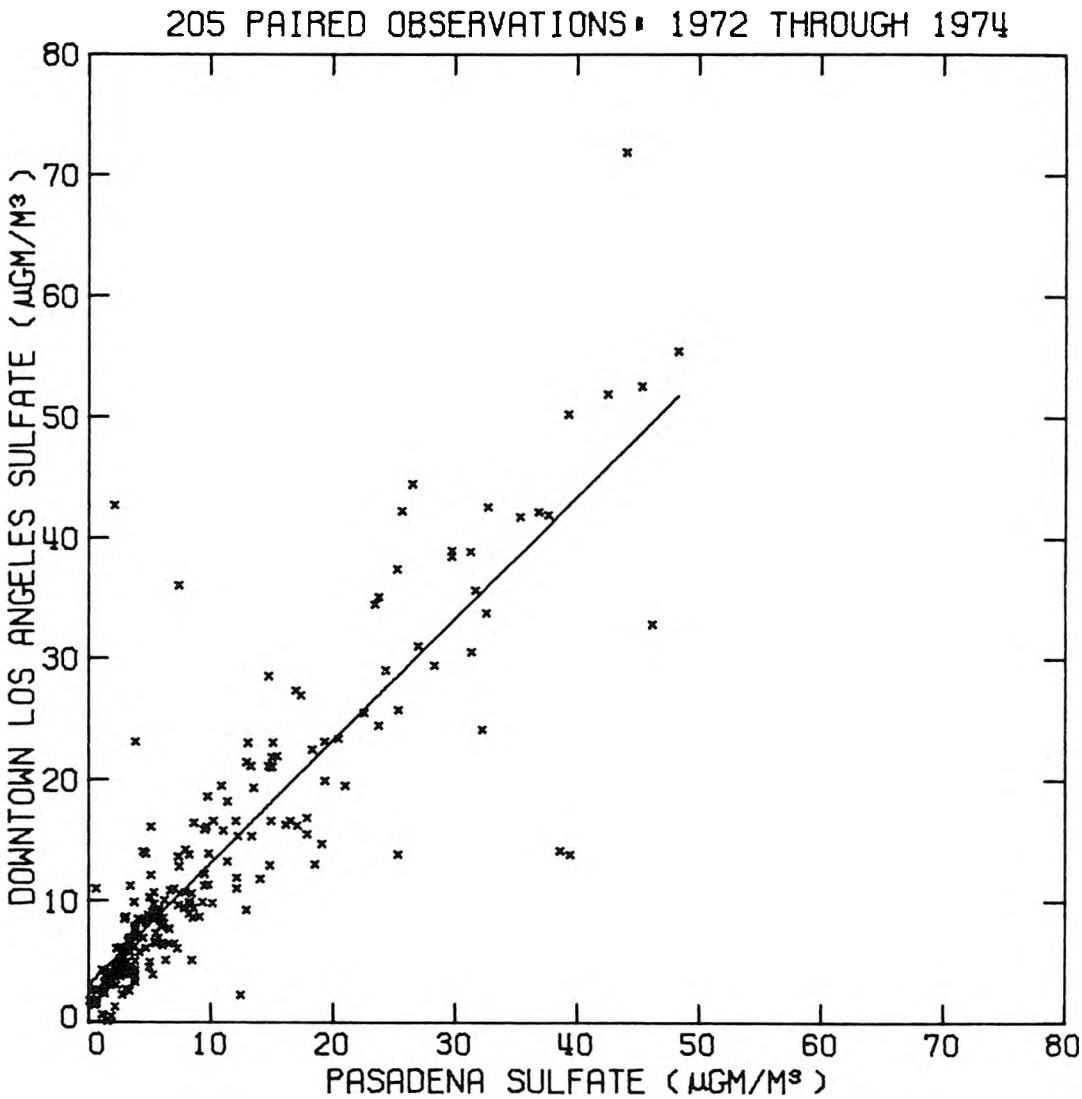
205 PAIRED OBSERVATIONS: 1972 THROUGH 1974
DOWNTOWN LOS ANGELES SULFATE (μGM/M³)
PASADENA SULFATE (μGM/M³)
0
10
20
30
40
50
60
70
80

FIGURE 2.11

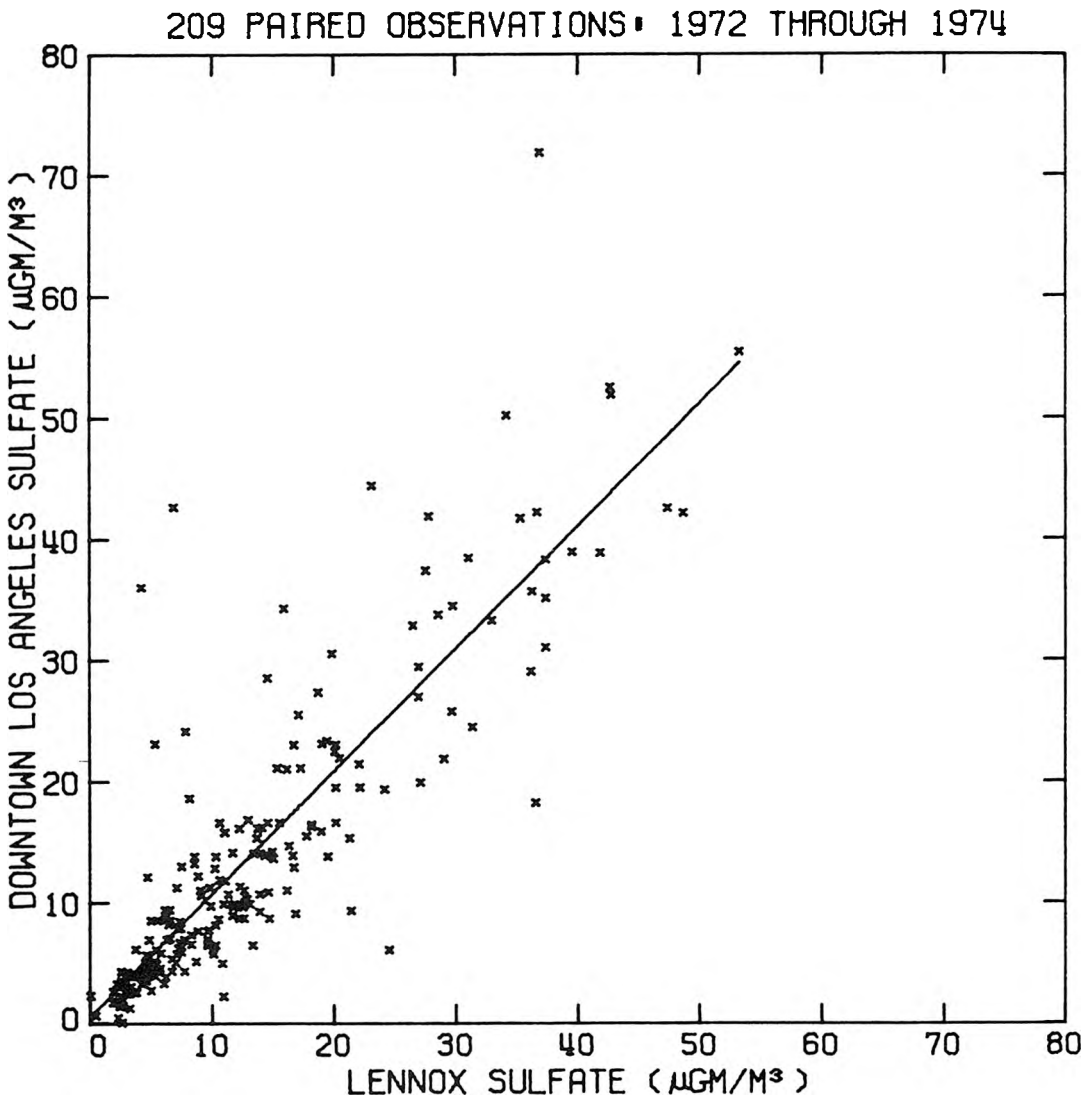
209 PAIRED OBSERVATIONS: 1972 THROUGH 1974
DOWNTOWN LOS ANGELES SULFATE (μGM/M³)
LENNOX SULFATE (μGM/M³)
0
10
20
30
40
50
60
70
80

FIGURE 2.12

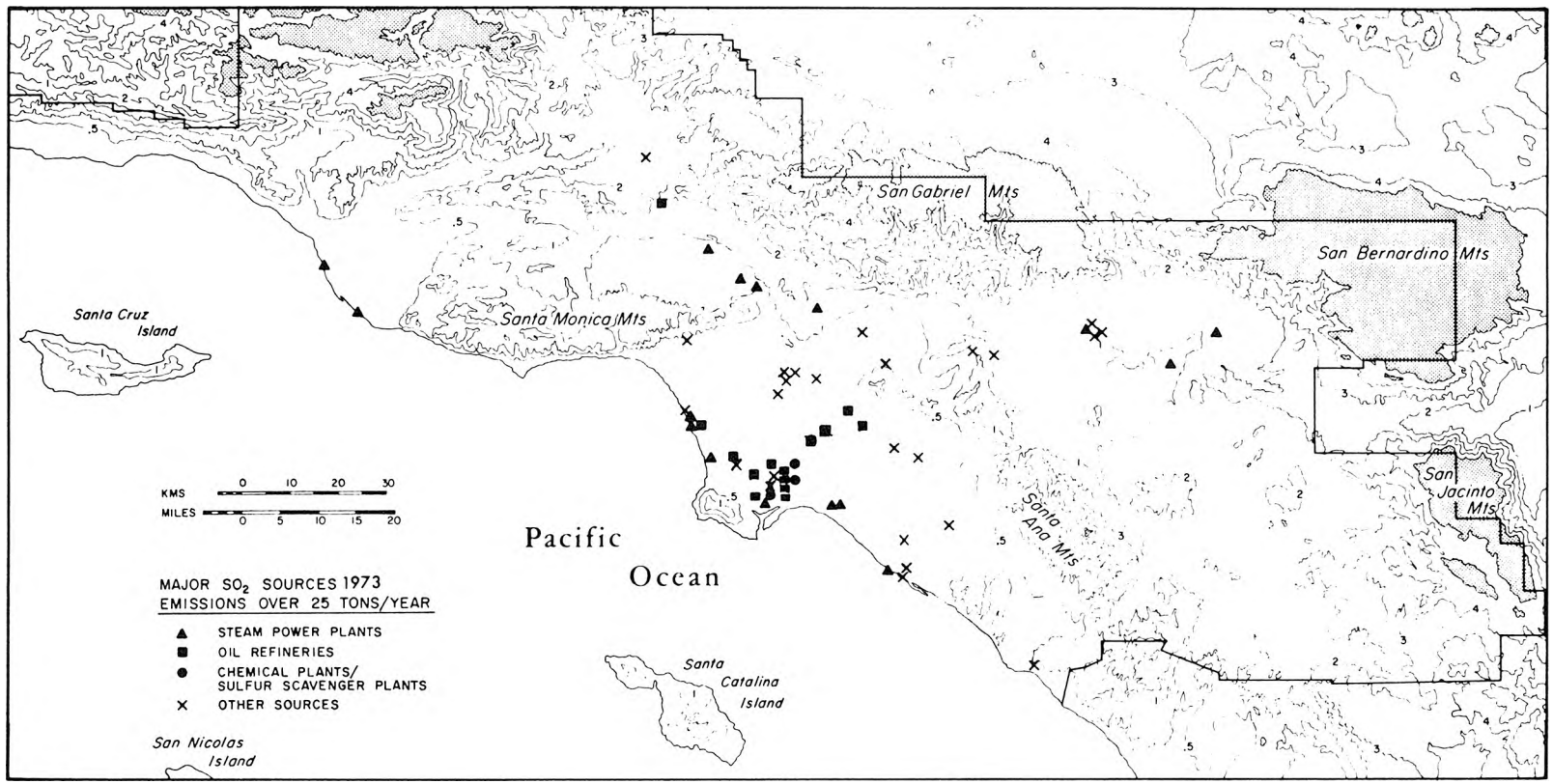
San Gabriel Mts
San Bernardino Mts
Santa Cruz Island
Santa Monica Mts
San Jacinto Mts
Santa Ana Mts
Pacific Ocean
Santa Catalina Island
San Nicolas Island
KMS 0 10 20 30
MILES 0 5 10 15 20
MAJOR $SO_2$ SOURCES 1973
EMISSIONS OVER 25 TONS/YEAR
STEAM POWER PLANTS
OIL REFINERIES
CHEMICAL PLANTS/ SULFUR SCAVENGER PLANTS
OTHER SOURCES

FIGURE 2.13

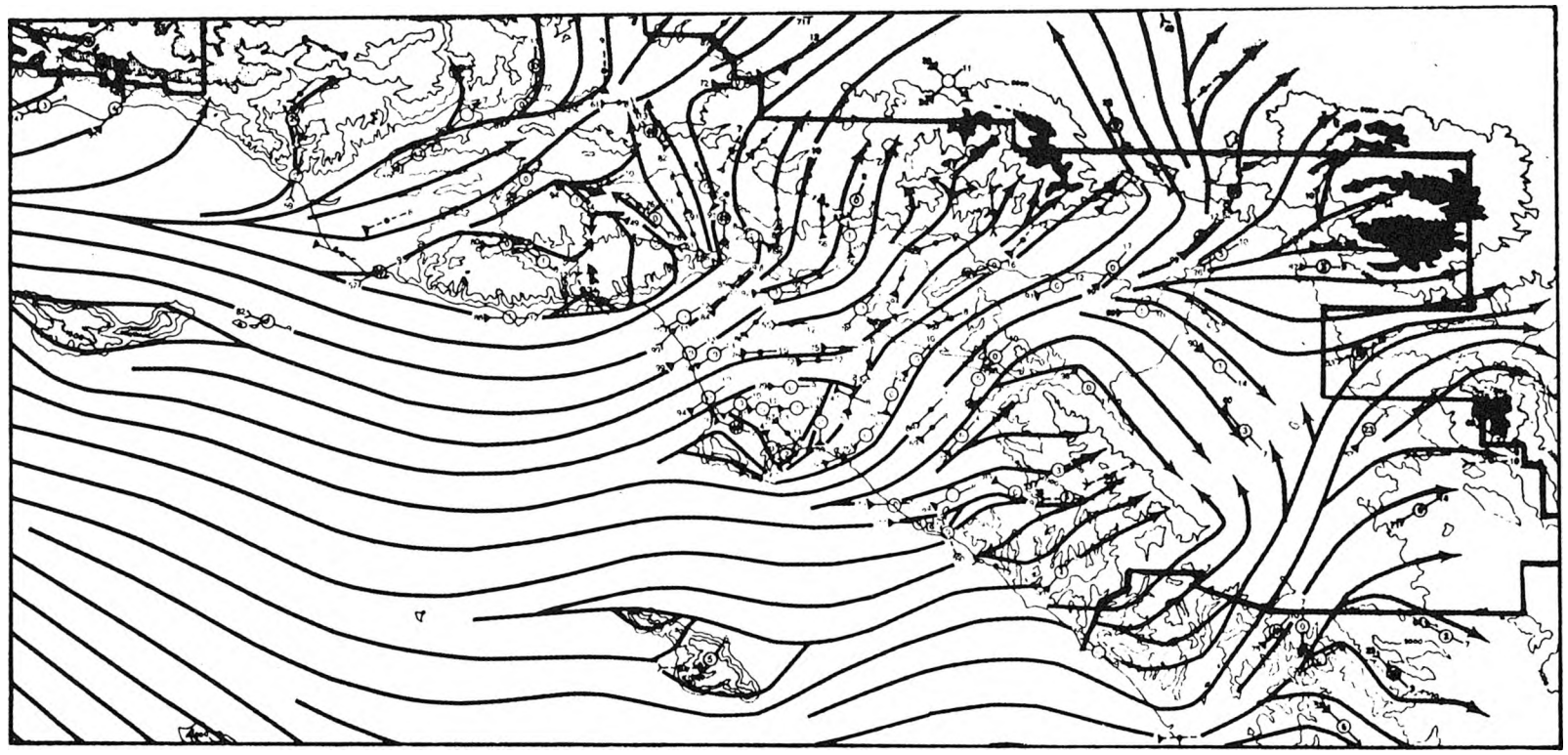

FIGURE 2.14

Typical Onshore Wind Flow Pattern
July 12:00-18:00 Hours PST
(From DeMarrais, Holzworth, and Hosler, 1965)

TABLE 2.4

Correlation Between Logs of Sulfate Observations at Pairs of Monitoring Stations: 1972-1974

| | | INLAND-WEST | | LOS ANGELES COUNTY-COASTAL | | | | | LOS ANGELES COUNTY-CENTRAL | | | | | | | ORANGE COUNTY | | | | EASTERN SAN GABRIEL VALLEY | | | EASTERN INLAND COUNTIES | | | ADJACENT BASINS |
|---|---|---|---|---|---|---|---|---|---|---|---|---|---|---|---|---|---|---|---|---|---|---|---|---|---|---|
| | | THOUSAND OAKS | RESEDA | SANTA MONICA | WEST LA | LENNOX | TORRANCE | LONG BEACH | LYNWOOD | BURBANK | GLENDALE | LOS ANGELES | LOS ANGELES | PASADENA | PASADENA | GARDEN GROVE | ANAHEIM | ANAHEIM | SANTA ANA | AZUSA | WEST COVINA | GLENDORA | ONTARIO | RIVER-SIDE | SAN B'DINO | VISTA |
| | | CHESS | LAAPCD | CHESS | LAAPCD | LAAPCD | NASN | NASN | LAAPCD | NASN | NASN | NASN | LAAPCD | LAAPCD | NASN | CHESS | CHESS | NASN | NASN | LAAPCD | CHESS | CHESS | NASN | NASN | NASN | CHESS |
| THOUSAND OAKS | CHESS | 1.00 | 0.81 | 0.80 | 0.79 | 0.74 | 0.61 | 0.67 | 0.70 | 0.71 | 0.66 | 0.76 | 0.80 | 0.80 | 0.79 | 0.66 | 0.65 | 0.50 | 0.62 | 0.84 | 0.73 | 0.77 | 0.48 | 0.27 | 0.74 | 0.61 |
| RESEDA | LAAPCD | 0.81 | 1.00 | 0.68 | 0.80 | 0.74 | 0.46 | 0.20 | 0.73 | 0.69 | 0.69 | 0.62 | 0.78 | 0.82 | 0.44 | 0.60 | 0.61 | 0.03 | 0.33 | 0.86 | 0.74 | 0.77 | 0.41 | 0.51 | 0.60 | 0.51 |
| SANTA MONICA | CHESS | 0.80 | 0.68 | 1.00 | 0.80 | 0.82 | 0.65 | 0.75 | 0.85 | 0.78 | 0.62 | 0.77 | 0.78 | 0.76 | 0.72 | 0.71 | 0.73 | 0.63 | 0.65 | 0.78 | 0.76 | 0.75 | 0.41 | 0.27 | 0.73 | 0.68 |
| WEST LA | LAAPCD | 0.79 | 0.80 | 0.80 | 1.00 | 0.88 | 0.70 | 0.50 | 0.82 | 0.65 | 0.67 | 0.58 | 0.90 | 0.82 | 0.63 | 0.66 | 0.67 | 0.50 | 0.57 | 0.87 | 0.73 | 0.72 | 0.04 | 0.75 | 0.51 | 0.58 |
| LENNOX | LAAPCD | 0.74 | 0.74 | 0.82 | 0.88 | 1.00 | 0.54 | 0.68 | 0.90 | 0.67 | 0.79 | 0.50 | 0.86 | 0.84 | 0.70 | 0.77 | 0.74 | 0.58 | 0.76 | 0.83 | 0.74 | 0.76 | 0.07 | 0.92 | 0.62 | 0.68 |
| TORRANCE | NASN | 0.61 | 0.46 | 0.65 | 0.70 | 0.54 | 1.00 | 0.63 | 0.50 | 0.64 | 0.72 | 0.63 | 0.54 | 0.24 | 0.66 | 0.57 | 0.61 | 0.63 | 0.62 | 0.56 | 0.58 | 0.62 | 0.49 | 0.13 | 0.69 | 0.46 |
| LONG BEACH | NASN | 0.67 | 0.20 | 0.75 | 0.50 | 0.68 | 0.63 | 1.00 | 0.93 | 0.80 | 0.71 | 0.77 | 0.86 | 0.78 | 0.82 | 0.72 | 0.78 | 0.88 | 0.91 | 0.74 | 0.77 | 0.74 | 0.51 | -0.11 | 0.74 | 0.66 |
| LYNWOOD | LAAPCD | 0.70 | 0.73 | 0.85 | 0.82 | 0.90 | 0.50 | 0.93 | 1.00 | 0.94 | 1.00 | 0.59 | 0.81 | 0.74 | 0.76 | 0.71 | 0.73 | 0.91 | 0.84 | 0.77 | 0.72 | 0.74 | 1.00 | * | 0.65 | 0.50 |
| BURBANK | NASN | 0.71 | 0.69 | 0.78 | 0.65 | 0.67 | 0.64 | 0.80 | 0.94 | 1.00 | 0.76 | 0.72 | 0.69 | 0.78 | 0.87 | 0.57 | 0.67 | 0.68 | 0.71 | 0.78 | 0.60 | 0.72 | 0.50 | -0.12 | 0.77 | 0.53 |
| GLENDALE | NASN | 0.66 | 0.69 | 0.62 | 0.67 | 0.79 | 0.72 | 0.71 | 1.00 | 0.76 | 1.00 | 0.62 | 0.74 | 0.74 | 0.84 | 0.53 | 0.52 | 0.61 | 0.73 | 0.65 | 0.59 | 0.65 | 0.54 | 0.58 | 0.81 | 0.40 |
| LOS ANGELES | NASN | 0.76 | 0.62 | 0.77 | 0.58 | 0.50 | 0.63 | 0.77 | 0.59 | 0.72 | 0.62 | 1.00 | 0.63 | 0.57 | 0.71 | 0.58 | 0.68 | 0.70 | 0.72 | 0.54 | 0.73 | 0.67 | 0.27 | 0.50 | 0.70 | 0.44 |
| LOS ANGELES | LAAPCD | 0.80 | 0.78 | 0.78 | 0.90 | 0.86 | 0.54 | 0.86 | 0.81 | 0.69 | 0.74 | 0.63 | 1.00 | 0.85 | 0.80 | 0.75 | 0.75 | 0.67 | 0.86 | 0.89 | 0.71 | 0.76 | 0.25 | 0.71 | 0.65 | 0.67 |
| PASADENA | LAAPCD | 0.80 | 0.82 | 0.76 | 0.82 | 0.84 | 0.24 | 0.78 | 0.74 | 0.78 | 0.74 | 0.57 | 0.85 | 1.00 | 0.80 | 0.71 | 0.71 | 0.68 | 0.86 | 0.91 | 0.77 | 0.80 | 0.19 | 0.62 | 0.82 | 0.63 |
| PASADENA | NASN | 0.79 | 0.44 | 0.72 | 0.63 | 0.70 | 0.66 | 0.82 | 0.76 | 0.87 | 0.84 | 0.71 | 0.80 | 0.80 | 1.00 | 0.60 | 0.64 | 0.71 | 0.73 | 0.79 | 0.74 | 0.75 | 0.65 | 0.53 | 0.86 | 0.54 |
| GARDEN GROVE | CHESS | 0.66 | 0.60 | 0.71 | 0.66 | 0.77 | 0.57 | 0.72 | 0.71 | 0.57 | 0.53 | 0.58 | 0.75 | 0.71 | 0.60 | 1.00 | 0.86 | 0.64 | 0.74 | 0.74 | 0.75 | 0.74 | 0.37 | 0.62 | 0.64 | 0.73 |
| ANAHEIM | CHESS | 0.65 | 0.61 | 0.73 | 0.67 | 0.74 | 0.61 | 0.78 | 0.73 | 0.67 | 0.52 | 0.68 | 0.75 | 0.71 | 0.64 | 0.86 | 1.00 | 0.74 | 0.79 | 0.73 | 0.75 | 0.74 | 0.46 | 0.57 | 0.75 | 0.73 |
| ANAHEIM | NASN | 0.50 | 0.03 | 0.63 | 0.50 | 0.58 | 0.63 | 0.88 | 0.91 | 0.68 | 0.61 | 0.70 | 0.67 | 0.68 | 0.71 | 0.64 | 0.74 | 1.00 | 0.90 | 0.72 | 0.64 | 0.67 | 0.32 | 0.39 | 0.81 | 0.62 |
| SANTA ANA | NASN | 0.62 | 0.33 | 0.65 | 0.57 | 0.76 | 0.62 | 0.91 | 0.84 | 0.71 | 0.73 | 0.72 | 0.86 | 0.86 | 0.73 | 0.74 | 0.79 | 0.90 | 1.00 | 0.84 | 0.74 | 0.75 | 0.47 | -0.10 | 0.73 | 0.71 |
| AZUSA | LAAPCD | 0.84 | 0.86 | 0.78 | 0.87 | 0.83 | 0.56 | 0.74 | 0.77 | 0.78 | 0.65 | 0.54 | 0.89 | 0.91 | 0.79 | 0.74 | 0.73 | 0.72 | 0.84 | 1.00 | 0.80 | 0.83 | 0.12 | 0.67 | 0.81 | 0.63 |
| WEST COVINA | CHESS | 0.73 | 0.74 | 0.76 | 0.73 | 0.74 | 0.58 | 0.77 | 0.72 | 0.60 | 0.59 | 0.73 | 0.71 | 0.77 | 0.74 | 0.75 | 0.75 | 0.64 | 0.74 | 0.80 | 1.00 | 0.87 | 0.44 | 0.49 | 0.77 | 0.68 |
| GLENDORA | CHESS | 0.77 | 0.77 | 0.75 | 0.72 | 0.76 | 0.62 | 0.74 | 0.74 | 0.72 | 0.65 | 0.67 | 0.76 | 0.80 | 0.75 | 0.74 | 0.74 | 0.67 | 0.75 | 0.83 | 0.87 | 1.00 | 0.47 | 0.29 | 0.82 | 0.67 |
| ONTARIO | NASN | 0.48 | 0.41 | 0.41 | 0.04 | 0.07 | 0.49 | 0.51 | 1.00 | 0.50 | 0.54 | 0.27 | 0.25 | 0.19 | 0.65 | 0.37 | 0.46 | 0.32 | 0.47 | 0.12 | 0.44 | 0.47 | 1.00 | -0.08 | 0.67 | 0.50 |
| RIVERSIDE | NASN | 0.27 | 0.51 | 0.27 | 0.75 | 0.92 | 0.13 | -0.11 | * | -0.12 | 0.58 | 0.50 | 0.71 | 0.62 | 0.53 | 0.62 | 0.57 | 0.39 | -0.10 | 0.67 | 0.49 | 0.29 | -0.08 | 1.00 | 0.54 | 0.33 |
| SAN BERNARDINO | NASN | 0.74 | 0.60 | 0.73 | 0.51 | 0.62 | 0.69 | 0.74 | 0.65 | 0.77 | 0.81 | 0.70 | 0.65 | 0.82 | 0.86 | 0.64 | 0.75 | 0.81 | 0.73 | 0.81 | 0.77 | 0.82 | 0.67 | 0.54 | 1.00 | 0.64 |
| VISTA | CHESS | 0.61 | 0.51 | 0.68 | 0.58 | 0.66 | 0.46 | 0.66 | 0.50 | 0.53 | 0.40 | 0.44 | 0.67 | 0.63 | 0.54 | 0.73 | 0.73 | 0.62 | 0.71 | 0.63 | 0.68 | 0.67 | 0.50 | 0.33 | 0.64 | 1.00 |

Sulfate observations below 2 $\mu gm/m^3$ disregarded.

TABLE 2.5

Number of Paired Observations with Sulfate Concentration Greater Than or Equal to 2 μgm/$m^3$: 1972-1974

| | | INLAND - WEST | | LOS ANGELES COUNTY - COASTAL | | | | | LOS ANGELES COUNTY - CENTRAL | | | | | | | ORANGE COUNTY | | | | EASTERN SAN GABRIEL VALLEY | | | | EASTERN INLAND COUNTIES | | | ADJACENT BASINS |
|---|---|---|---|---|---|---|---|---|---|---|---|---|---|---|---|---|---|---|---|---|---|---|---|---|---|---|---|
| | | THOUSAND OAKS | RESEDA | SANTA MONICA | WEST LA | LENNOX | TORRANCE | LONG BEACH | LYNWOOD | BURBANK | GLENDALE | LOS ANGELES | LOS ANGELES | PASADENA | PASADENA | GARDEN GROVE | ANAHEIM | ANAHEIM | SANTA ANA | AZUSA | WEST COVINA | GLENDORA | ONTARIO | RIVER-SIDE | SAN B'DINO | VISTA |
| | | CHESS | LAAPCD | CHESS | LAAPCD | LAAPCD | NASN | NASN | LAAPCD | NASN | NASN | NASN | LAAPCD | LAAPCD | NASN | CHESS | CHESS | NASN | NASN | LAAPCD | CHESS | CHESS | NASN | NASN | NASN | CHESS |
| THOUSAND OAKS | CHESS | 765. | 141. | 671. | 141. | 150. | 58. | 59. | 48. | 68. | 52. | 56. | 147. | 140. | 57. | 698. | 683. | 58. | 58. | 140. | 684. | 646. | 43. | 11. | 51. | 705. |
| RESEDA | LAAPCD | 141. | 192. | 143. | 182. | 191. | 14. | 14. | 53. | 14. | 11. | 11. | 181. | 180. | 14. | 152. | 167. | 16. | 14. | 178. | 154. | 155. | 12. | 4. | 13. | 174. |
| SANTA MONICA | CHESS | 671. | 143. | 800. | 146. | 159. | 61. | 57. | 45. | 67. | 52. | 60. | 154. | 141. | 56. | 733. | 728. | 59. | 61. | 141. | 747. | 710. | 43. | 11. | 51. | 727. |
| WEST LA | LAAPCD | 141. | 182. | 146. | 194. | 193. | 15. | 15. | 57. | 15. | 12. | 12. | 185. | 182. | 15. | 157. | 168. | 17. | 15. | 182. | 158. | 157. | 12. | 4. | 13. | 177. |
| LENNOX | LAAPCD | 150. | 191. | 159. | 193. | 217. | 15. | 16. | 63. | 16. | 14. | 13. | 199. | 191. | 16. | 172. | 185. | 18. | 16. | 192. | 167. | 172. | 13. | 4. | 14. | 191. |
| TORRANCE | NASN | 58. | 14. | 61. | 15. | 15. | 83. | 60. | 5. | 61. | 39. | 55. | 15. | 12. | 53. | 63. | 73. | 66. | 70. | 14. | 61. | 65. | 47. | 8. | 59. | 77. |
| LONG BEACH | NASN | 59. | 14. | 57. | 15. | 16. | 60. | 79. | 6. | 63. | 43. | 55. | 16. | 13. | 56. | 60. | 69. | 64. | 67. | 15. | 59. | 61. | 48. | 10. | 53. | 73. |
| LYNWOOD | LAAPCD | 48. | 53. | 45. | 57. | 63. | 5. | 6. | 63. | 5. | 2. | 3. | 59. | 52. | 5. | 54. | 50. | 6. | 6. | 54. | 52. | 45. | 2. | 0. | 4. | 60. |
| BURBANK | NASN | 68. | 14. | 67. | 15. | 16. | 61. | 63. | 5. | 90. | 43. | 64. | 16. | 14. | 57. | 79. | 80. | 66. | 67. | 15. | 67. | 74. | 51. | 8. | 61. | 81. |
| GLENDALE | NASN | 52. | 11. | 52. | 12. | 14. | 39. | 43. | 2. | 43. | 69. | 42. | 14. | 10. | 40. | 56. | 61. | 45. | 45. | 13. | 52. | 55. | 38. | 8. | 42. | 63. |
| LOS ANGELES | NASN | 56. | 11. | 60. | 12. | 13. | 55. | 55. | 3. | 64. | 42. | 82. | 13. | 11. | 51. | 61. | 74. | 65. | 62. | 13. | 60. | 66. | 46. | 9. | 58. | 74. |
| LOS ANGELES | LAAPCD | 147. | 181. | 154. | 185. | 199. | 15. | 16. | 59. | 16. | 14. | 13. | 203. | 183. | 16. | 164. | 177. | 18. | 16. | 185. | 163. | 163. | 13. | 4. | 14. | 182. |
| PASADENA | LAAPCD | 140. | 180. | 141. | 182. | 191. | 12. | 13. | 52. | 14. | 10. | 11. | 183. | 192. | 12. | 153. | 166. | 14. | 12. | 184. | 152. | 156. | 12. | 4. | 13. | 173. |
| PASADENA | NASN | 57. | 14. | 56. | 15. | 16. | 53. | 56. | 5. | 57. | 40. | 51. | 16. | 12. | 79. | 60. | 70. | 59. | 59. | 15. | 58. | 63. | 43. | 6. | 50. | 72. |
| GARDEN GROVE | CHESS | 698. | 152. | 733. | 157. | 172. | 63. | 60. | 54. | 70. | 56. | 61. | 164. | 153. | 60. | 854. | 744. | 62. | 64. | 153. | 750. | 698. | 47. | 11. | 57. | 769. |
| ANAHEIM | CHESS | 683. | 167. | 728. | 168. | 185. | 73. | 69. | 50. | 80. | 61. | 74. | 177. | 166. | 70. | 744. | 906. | 73. | 74. | 168. | 739. | 785. | 55. | 15. | 64. | 834. |
| ANAHEIM | NASN | 58. | 16. | 59. | 17. | 18. | 66. | 64. | 6. | 66. | 45. | 65. | 18. | 14. | 59. | 62. | 73. | 82. | 72. | 17. | 58. | 65. | 54. | 9. | 64. | 74. |
| SANTA ANA | NASN | 58. | 14. | 61. | 15. | 16. | 70. | 67. | 6. | 67. | 45. | 62. | 16. | 12. | 59. | 64. | 74. | 72. | 83. | 15. | 61. | 66. | 52. | 10. | 62. | 77. |
| AZUSA | LAAPCD | 140. | 178. | 141. | 182. | 192. | 14. | 15. | 54. | 15. | 13. | 13. | 185. | 184. | 15. | 153. | 168. | 17. | 15. | 193. | 154. | 156. | 13. | 4. | 13. | 174. |
| WEST COVINA | CHESS | 684. | 154. | 747. | 158. | 167. | 61. | 59. | 52. | 67. | 52. | 60. | 163. | 152. | 58. | 750. | 739. | 58. | 61. | 154. | 826. | 733. | 41. | 11. | 51. | 763. |
| GLENDORA | CHESS | 646. | 155. | 710. | 157. | 172. | 65. | 61. | 45. | 74. | 55. | 66. | 163. | 156. | 63. | 698. | 785. | 65. | 66. | 156. | 733. | 859. | 47. | 13. | 60. | 795. |
| ONTARIO | NASN | 43. | 12. | 43. | 12. | 13. | 47. | 48. | 2. | 51. | 38. | 46. | 13. | 12. | 43. | 47. | 55. | 54. | 52. | 13. | 41. | 47. | 63. | 10. | 48. | 56. |
| RIVERSIDE | NASN | 11. | 4. | 11. | 4. | 4. | 8. | 10. | 0. | 8. | 8. | 9. | 4. | 4. | 6. | 11. | 15. | 9. | 10. | 4. | 11. | 13. | 10. | 17. | 10. | 16. |
| SAN BERNARDINO | NASN | 51. | 13. | 51. | 13. | 14. | 59. | 53. | 4. | 61. | 42. | 58. | 14. | 13. | 50. | 57. | 64. | 64. | 62. | 13. | 51. | 60. | 48. | 10. | 74. | 68. |
| VISTA | CHESS | 705. | 174. | 727. | 177. | 191. | 77. | 73. | 60. | 81. | 63. | 74. | 182. | 173. | 72. | 769. | 834. | 74. | 77. | 174. | 763. | 795. | 56. | 16. | 68. | 955. |

from which to compute each correlation coefficient. For reasons explained previously, only those sulfate observations reported at or above 2 $\mu gm/m^3$ were considered.

Measurements taken on the same day at all of the LAAPCD stations are highly correlated (about 0.80 to 0.90) with each other. The correlation between pairs of CHESS stations is typically in the range of 0.80 to 0.70. The log-linear correlations between pairs of NASN stations typically lie in the range 0.80 to 0.60. The NASN station at Ontario, however, provides an exception to this pattern: it does not correlate well with observations at other monitoring sites. The distribution of correlation coefficients between station pairs involving more than one monitoring agency is similar to the distribution of correlation coefficients between pairs of stations operated solely by NASN. The distribution of correlation coefficients between monitoring programs is summarized in Table 2.6.

Examination of Table 2.4 shows that most of the highest correlation coefficients (above 0.80) involve pairings with LAAPCD stations. But if one examines the variance of the logs of the sulfate observations, $\beta^2$, in Table 2.3, they will note that it is data from the LAAPCD network that deviate most noticeably from long-run distributional equivalence with data from neighboring stations operated by other monitoring agencies. In contrast, the NASN and CHESS air monitoring results show more consistent statistical distributions, but lower cross-correlation between simultaneous individual samples. The explanation for that behavior is probably found in mismatches between the sampling schedules

TABLE 2.6

DISTRIBUTION OF CORRELATION COEFFICIENTS: 1972 through 1974

Correlation Coefficients taken from Table 2.4

| Correlation Between Logs of Simultaneous Observations | Number of Station Pairs Whose Cross Correlation Falls in the Range Stated: | | | |
|---|---|---|---|---|
| | Station Pairs within the Same Monitoring Program | | | Station Pairs in Two Different Monitoring Programs |
| | CHESS | LAAPCD | NASN | |
| 1.00 to 0.90 | | 3 | 2 | 4 |
| 0.89 to 0.80 | 3 | 13 | 8 | 20 |
| 0.79 to 0.70 | 12 | 5 | 16 | 66 |
| 0.69 to 0.60 | 6 | | 12 | 53 |
| 0.59 to 0.50 | | | 7 | 28 |
| 0.49 to 0.40 | | | 2 | 12 |
| 0.39 to 0.30 | | | 2 | 3 |
| 0.29 to 0.20 | | | 1 | 6 |
| 0.19 to 0.10 | | | 1 | 2 |
| 0.09 to 0.00 | | | 0 | 3 |
| -0.10 to -0.01 | | | 2 | |
| -0.20 to -0.11 | | | 2 | |
| Insufficient Data | | | | 3 |

maintained by different agencies as described in Appendix B1. The CHESS sampling period, for example, is offset by about a half day from that of the NASN and APCD samples reported for the same "day". Sample start and stop times may have differed at stations within the CHESS network itself. This cannot help but reduce the day-to-day correlation between CHESS and other agencies' data since fully comparable "events" have not been sampled. In the case of the NASN data, a review of the reported dates on which sulfate samples were taken indicates that the NASN volunteer operators often run their samples on days other than those assigned, especially when assigned days fall on a weekend. There is some doubt as to the exact date on which some of the NASN data were actually collected. In both of these instances, a mismatch in sampling schedules between monitoring agencies would reduce the apparent day-to-day correlation between stations. The long-run statistics and distribution of the data collected would be unaffected since all samples taken at a station would still be drawn from the underlying population of events at that location even if the information on the date of a given event was confused somewhat. Correlation coefficients given in Table 2.4 thus probably understate the true degree to which 24-hour average sulfate concentrations tracked each other at pairs of monitoring sites during the three years of interest.

Widespread similarity in seasonal sulfate concentration trends and a high positive correlation between samples taken on the same day at widely separated air monitoring stations leads to two more important physical generalizations.

Generalization 4: Major sulfate concentration trends appear to be determined by forcing functions which are felt over the entire South Coast Air Basin.

Generalization 5: Sulfate concentration changes are felt to a large degree on a basin-wide basis within the same 24-hour period.

This suggests that mesoscale and larger meteorological fluctuations may be the dominant determinants of sulfate concentration changes from day-to-day within this particular airshed. An extremely detailed *spatial* representation of meteorological inputs and chemical mechanisms within our air quality model might be unnecessary. A relatively uncomplicated emissions to air quality model should be attempted initially to test its explanatory power.

### 2.2.7 Selection of an Averaging Time for Air Quality Model Calculations

It is clear from Figures 2.4, 2.8, 2.9 and 2.10 that temporal trends in sulfate air quality are more pronounced than average spatial gradients. Thus for an air quality model to verify its explanatory power, relatively short time averaging of concentration predictions would be desired. The implications of averaging sulfate concentrations over shorter time intervals within our three year study period will be explored.

Tables 2.7, 2.8 and 2.9 present the results of the statistical methods of Appendix B4 applied separately to data from the years 1972, 1973 and 1974. As the number of samples being considered within a group declines, the confidence interval associated with the group mean

# TABLE 2.7

## Statistical Description of Sulfate Air Quality Data in the South Coast Air Basin: 1972

| | | ARITHMETIC STATISTICS | | | | | GEOMETRIC STATISTICS | | | | |
|---|---|---|---|---|---|---|---|---|---|---|---|
| | | SAMPLE ARITHMETIC MEAN $\bar{y}$ | SAMPLE ARITHMETIC STANDARD DEVIATION $\sigma$ | NUMBER OF SAMPLES $n$ | LOWER CONFIDENCE LIMIT ON $\bar{y}$ (2.5 %ile) | UPPER CONFIDENCE LIMIT ON $\bar{y}$ (97.5 %ile) | ESTIMATED MEAN LOG $\alpha$ | ESTIMATED VARIANCE OF LOGS $\beta^2$ | ESTIMATED GEOMETRIC MEAN $\mu_g$ | ESTIMATED GEOMETRIC STANDARD DEVIATION $\sigma_g$ | ARITHMETIC MEAN ESTIMATED FROM $\alpha$ and $\beta^2$ |
| THOUSAND OAKS | CHESS | 8.25 | 7.31 | 231.00 | 7.61 | 8.89 | 1.88 | 0.48 | 6.58 | 2.00 | 8.38 |
| RESEDA | LAAPCD | 15.99 | 15.75 | 72.00 | 12.71 | 19.26 | 2.37 | 0.82 | 10.65 | 2.47 | 16.05 |
| SANTA MONICA | CHESS | 9.40 | 5.84 | 238.00 | 8.87 | 9.92 | 2.09 | 0.32 | 8.05 | 1.76 | 9.44 |
| WEST LA | LAAPCD | 11.86 | 9.04 | 72.00 | 9.98 | 13.74 | 2.23 | 0.48 | 9.32 | 1.99 | 11.83 |
| LENNOX | LAAPCD | 15.37 | 9.78 | 73.00 | 13.35 | 17.39 | 2.56 | 0.33 | 13.00 | 1.77 | 15.31 |
| TORRANCE | NASN | 11.34 | 6.35 | 30.00 | 9.15 | 13.52 | 2.30 | 0.26 | 9.96 | 1.66 | 11.32 |
| LONG BEACH | NASN | 11.29 | 7.55 | 29.00 | 9.59 | 13.98 | 2.27 | 0.30 | 9.63 | 1.73 | 11.19 |
| LYNWOOD | LAAPCD | * | * | 0.0 | * | * | * | * | * | * | * |
| BURBANK | NASN | 11.18 | 7.87 | 29.00 | 8.42 | 13.94 | 2.18 | 0.52 | 8.85 | 2.06 | 11.50 |
| GLENDALE | NASN | 10.27 | 7.27 | 28.00 | 7.68 | 12.97 | 2.12 | 0.44 | 8.35 | 1.94 | 10.40 |
| LOS ANGELES | NASN | 11.07 | 8.19 | 32.00 | 8.35 | 13.79 | 2.22 | 0.35 | 9.16 | 1.81 | 10.91 |
| LOS ANGELES | LAAPCD | 14.38 | 11.60 | 68.00 | 11.88 | 16.88 | 2.41 | 0.48 | 11.17 | 2.00 | 14.19 |
| PASADENA | LAAPCD | 11.55 | 10.77 | 70.00 | 9.27 | 13.82 | 2.12 | 0.62 | 8.29 | 2.19 | 11.29 |
| PASADENA | NASN | 10.67 | 7.58 | 27.00 | 7.91 | 13.43 | 2.13 | 0.53 | 8.39 | 2.08 | 10.96 |
| GARDEN GROVE | CHESS | 9.20 | 5.39 | 239.00 | 8.72 | 9.69 | 2.08 | 0.33 | 8.01 | 1.78 | 9.47 |
| ANAHEIM | CHESS | 10.95 | 7.68 | 328.00 | 10.52 | 11.39 | 2.21 | 0.38 | 9.15 | 1.85 | 11.07 |
| ANAHEIM | NASN | 11.19 | 8.24 | 28.00 | 8.25 | 14.13 | 2.19 | 0.50 | 8.91 | 2.03 | 11.46 |
| SANTA ANA | NASN | 11.69 | 11.06 | 29.00 | 7.82 | 15.56 | 2.20 | 0.46 | 9.06 | 1.97 | 11.40 |
| AZUSA | LAAPCD | 13.98 | 11.91 | 71.00 | 11.48 | 16.48 | 2.33 | 0.63 | 10.30 | 2.21 | 14.12 |
| WEST COVINA | CHESS | 11.06 | 6.77 | 241.00 | 10.46 | 11.66 | 2.23 | 0.38 | 9.30 | 1.85 | 11.25 |
| GLENDORA | CHESS | 11.98 | 9.63 | 303.00 | 11.38 | 12.58 | 2.22 | 0.57 | 9.19 | 2.13 | 12.24 |
| ONTARIO | NASN | 10.03 | 8.29 | 28.00 | 7.07 | 12.99 | 2.01 | 0.59 | 7.43 | 2.16 | 9.99 |
| RIVERSIDE | NASN | 11.40 | 6.54 | 18.00 | 8.44 | 14.36 | 2.29 | 0.33 | 9.92 | 1.78 | 11.70 |
| SAN BERNARDINO | NASN | 11.06 | 7.90 | 30.00 | 8.34 | 13.78 | 2.15 | 0.59 | 8.57 | 2.16 | 11.52 |
| VISTA | CHESS | 9.66 | 6.82 | 336.00 | 9.29 | 10.03 | 2.09 | 0.36 | 8.07 | 1.83 | 9.67 |

AN ASTERISK (*) INDICATES DATA THAT ARE UNAVAILABLE

# TABLE 2.8

## Statistical Description of Sulfate Air Quality Data in the South Coast Air Basin: 1973

| | | ARITHMETIC STATISTICS | | | | | GEOMETRIC STATISTICS | | | | |
|---|---|---|---|---|---|---|---|---|---|---|---|
| | | SAMPLE ARITHMETIC MEAN $\bar{y}$ | SAMPLE ARITHMETIC STANDARD DEVIATION $\sigma$ | NUMBER OF SAMPLES $n$ | LOWER CONFIDENCE LIMIT ON $\bar{y}$ (2.5 %ile) | UPPER CONFIDENCE LIMIT ON $\bar{y}$ (97.5 %ile) | ESTIMATED MEAN LOG $\alpha$ | ESTIMATED VARIANCE OF LOGS $\beta^2$ | ESTIMATED GEOMETRIC MEAN $\mu_g$ | ESTIMATED GEOMETRIC STANDARD DEVIATION $\sigma_g$ | ARITHMETIC MEAN ESTIMATED FROM $\alpha$ and $\beta^2$ |
| THOUSAND OAKS | CHESS | 11.03 | 10.96 | 352.00 | 10.58 | 11.49 | 1.95 | 1.02 | 7.06 | 2.75 | 11.77 |
| RESEDA | LAAPCD | 16.45 | 21.17 | 72.00 | 12.05 | 20.84 | 2.03 | 1.77 | 7.65 | 3.78 | 18.50 |
| SANTA MONICA | CHESS | 12.49 | 10.10 | 354.00 | 12.04 | 12.94 | 2.23 | 0.64 | 9.33 | 2.23 | 12.86 |
| WEST LA | LAAPCD | 10.63 | 10.47 | 71.00 | 8.44 | 12.83 | 1.89 | 1.05 | 6.59 | 2.79 | 11.14 |
| LENNOX | LAAPCD | 13.94 | 12.17 | 73.00 | 11.43 | 16.45 | 2.28 | 0.77 | 9.73 | 2.41 | 14.33 |
| TORRANCE | NASN | 11.21 | 7.43 | 25.00 | 8.39 | 14.03 | 2.23 | 0.38 | 9.32 | 1.86 | 11.28 |
| LONG BEACH | NASN | 10.59 | 5.58 | 25.00 | 8.47 | 12.70 | 2.25 | 0.21 | 9.50 | 1.58 | 10.54 |
| LYNWOOD | LAAPCD | * | * | 0.0 | * | * | * | * | * | * | * |
| BURBANK | NASN | 14.87 | 11.32 | 31.00 | 11.05 | 18.70 | 2.45 | 0.54 | 11.55 | 2.08 | 15.12 |
| GLENDALE | NASN | 10.46 | 7.82 | 30.00 | 7.77 | 13.15 | 2.14 | 0.41 | 8.47 | 1.90 | 10.42 |
| LOS ANGELES | NASN | 12.30 | 6.59 | 25.00 | 9.80 | 14.80 | 2.37 | 0.29 | 10.71 | 1.71 | 12.35 |
| LOS ANGELES | LAAPCD | 15.80 | 14.70 | 73.00 | 12.77 | 18.83 | 2.35 | 0.91 | 10.51 | 2.59 | 16.55 |
| PASADENA | LAAPCD | 12.66 | 12.33 | 73.00 | 10.12 | 15.20 | 2.02 | 1.15 | 7.56 | 2.93 | 13.47 |
| PASADENA | NASN | 13.59 | 9.93 | 30.00 | 10.16 | 17.00 | 2.36 | 0.55 | 10.63 | 2.10 | 14.00 |
| GARDEN GROVE | CHESS | 13.23 | 8.76 | 352.00 | 12.79 | 13.67 | 2.36 | 0.50 | 10.57 | 2.03 | 13.57 |
| ANAHEIM | CHESS | 12.31 | 9.18 | 352.00 | 11.89 | 12.75 | 2.25 | 0.62 | 9.44 | 2.20 | 12.89 |
| ANAHEIM | NASN | 9.48 | 5.40 | 25.00 | 7.43 | 11.54 | 2.09 | 0.33 | 8.12 | 1.78 | 9.60 |
| SANTA ANA | NASN | 8.02 | 3.64 | 25.00 | 6.64 | 9.41 | 1.99 | 0.19 | 7.31 | 1.56 | 8.06 |
| AZUSA | LAAPCD | 13.11 | 11.98 | 73.00 | 10.64 | 15.58 | 2.10 | 1.10 | 8.18 | 2.86 | 14.19 |
| WEST COVINA | CHESS | 14.54 | 12.00 | 347.00 | 13.98 | 15.09 | 2.29 | 0.90 | 9.91 | 2.58 | 15.55 |
| GLENDORA | CHESS | 14.43 | 12.10 | 356.00 | 13.91 | 14.95 | 2.28 | 0.91 | 9.77 | 2.59 | 15.40 |
| ONTARIO | NASN | 10.50 | 7.10 | 21.00 | 7.55 | 13.45 | 2.16 | 0.39 | 8.71 | 1.87 | 10.59 |
| RIVERSIDE | NASN | * | * | 0.0 | * | * | * | * | * | * | * |
| SAN BERNARDINO | NASN | 15.69 | 14.34 | 22.00 | 9.87 | 21.51 | 2.42 | 0.71 | 11.24 | 2.32 | 16.00 |
| VISTA | CHESS | 10.03 | 7.58 | 350.00 | 9.67 | 10.39 | 2.02 | 0.66 | 7.51 | 2.25 | 10.43 |

AN ASTERISK (*) INDICATES DATA THAT ARE UNAVAILABLE

# TABLE 2.9

## Statistical Description of Sulfate Air Quality Data in the South Coast Air Basin: 1974

| | | ARITHMETIC STATISTICS | | | | | GEOMETRIC STATISTICS | | | | |
|---|---|---|---|---|---|---|---|---|---|---|---|
| | | SAMPLE ARITHMETIC MEAN $\bar{y}$ | SAMPLE ARITHMETIC STANDARD DEVIATION $\sigma$ | NUMBER OF SAMPLES $n$ | LOWER CONFIDENCE LIMIT ON $\bar{y}$ (2.5 %ile) | UPPER CONFIDENCE LIMIT ON $\bar{y}$ (97.5 %ile) | ESTIMATED MEAN LOG $\alpha$ | ESTIMATED VARIANCE OF LOGS $\beta^2$ | ESTIMATED GEOMETRIC MEAN $\mu_g$ | ESTIMATED GEOMETRIC STANDARD DEVIATION $\sigma_g$ | ARITHMETIC MEAN ESTIMATED FROM $\alpha$ and $\beta^2$ |
| THOUSAND OAKS | CHESS | 8.42 | 7.54 | 307.00 | 7.97 | 8.86 | 1.77 | 0.81 | 5.86 | 2.46 | 8.80 |
| RESEDA | LAAPCD | 11.05 | 10.72 | 70.00 | 8.78 | 13.32 | 1.86 | 1.29 | 6.41 | 3.11 | 12.20 |
| SANTA MONICA | CHESS | 11.32 | 8.95 | 248.00 | 10.59 | 12.05 | 2.12 | 0.67 | 8.33 | 2.27 | 11.67 |
| WEST LA | LAAPCD | 9.42 | 8.92 | 72.00 | 7.57 | 11.28 | 1.76 | 1.09 | 5.81 | 2.85 | 10.03 |
| LENNOX | LAAPCD | 11.82 | 10.01 | 73.00 | 9.76 | 13.89 | 2.13 | 0.71 | 8.38 | 2.32 | 11.93 |
| TORRANCE | NASN | 11.65 | 6.29 | 28.00 | 9.40 | 13.89 | 2.32 | 0.28 | 10.21 | 1.70 | 11.75 |
| LONG BEACH | NASN | 13.95 | 9.21 | 26.00 | 10.53 | 17.37 | 2.48 | 0.30 | 11.89 | 1.73 | 13.81 |
| LYNWOOD | LAAPCD | 9.47 | 8.55 | 68.00 | 7.63 | 11.31 | 1.87 | 0.81 | 6.46 | 2.46 | 9.70 |
| BURBANK | NASN | 18.02 | 29.20 | 30.00 | 7.98 | 28.05 | 2.47 | 0.45 | 11.81 | 1.96 | 14.83 |
| GLENDALE | NASN | 9.02 | 8.80 | 13.00 | 4.31 | 13.72 | 1.89 | 0.63 | 6.64 | 2.22 | 9.12 |
| LOS ANGELES | NASN | 13.92 | 12.09 | 26.00 | 9.43 | 18.41 | 2.30 | 0.75 | 9.95 | 2.38 | 14.47 |
| LOS ANGELES | LAAPCD | 12.66 | 11.19 | 71.00 | 10.31 | 15.00 | 2.10 | 0.98 | 8.20 | 2.69 | 13.36 |
| PASADENA | LAAPCD | 8.56 | 8.41 | 71.00 | 6.80 | 10.32 | 1.67 | 1.11 | 5.31 | 2.87 | 9.24 |
| PASADENA | NASN | 11.47 | 9.23 | 22.00 | 7.72 | 15.22 | 2.22 | 0.39 | 9.24 | 1.87 | 11.26 |
| GARDEN GROVE | CHESS | 10.09 | 6.82 | 307.00 | 9.65 | 10.52 | 2.10 | 0.45 | 8.18 | 1.96 | 10.24 |
| ANAHEIM | CHESS | 10.69 | 7.89 | 286.00 | 10.15 | 11.24 | 2.12 | 0.52 | 8.36 | 2.06 | 10.87 |
| ANAHEIM | NASN | 12.51 | 9.10 | 30.00 | 9.39 | 15.63 | 2.31 | 0.44 | 10.09 | 1.95 | 12.60 |
| SANTA ANA | NASN | 11.47 | 7.48 | 29.00 | 8.85 | 14.09 | 2.27 | 0.34 | 9.65 | 1.79 | 11.44 |
| AZUSA | LAAPCD | 10.54 | 9.96 | 71.00 | 8.45 | 12.62 | 1.92 | 1.00 | 6.85 | 2.71 | 11.26 |
| WEST COVINA | CHESS | 11.49 | 9.00 | 293.00 | 10.90 | 12.09 | 2.14 | 0.66 | 8.53 | 2.26 | 11.89 |
| GLENDORA | CHESS | 11.13 | 9.08 | 278.00 | 10.49 | 11.77 | 2.08 | 0.73 | 8.02 | 2.35 | 11.58 |
| ONTARIO | NASN | 13.49 | 8.05 | 15.00 | 9.49 | 17.49 | 2.42 | 0.42 | 11.25 | 1.91 | 13.86 |
| RIVERSIDE | NASN | * | * | 0.0 | * | * | * | * | * | * | * |
| SAN BERNARDINO | NASN | 12.32 | 9.68 | 23.00 | 8.48 | 16.16 | 2.23 | 0.62 | 9.27 | 2.20 | 12.67 |
| VISTA | CHESS | 8.66 | 6.68 | 349.00 | 8.34 | 8.97 | 1.90 | 0.55 | 6.70 | 2.10 | 8.82 |

AN ASTERISK (*) INDICATES DATA THAT ARE UNAVAILABLE

value of course widens. When attention is turned to even shorter time periods, such as a month, the result is well illustrated by Figures 2.15 and 2.16. These figures show the monthly arithmetic means of all sulfate samples taken at typical CHESS and LAAPCD stations during the period 1972 through 1974. The o's indicate the magnitude of the monthly averages of the raw sulfate data, $\bar{y}$, while the +'s indicate an estimate of the arithmetic mean of the underlying population of events, $\mu$, calculated from a log-normality assumption applied to those sulfate values above 2 $\mu gm/m^3$ by the methods outlined in Appendix B4. In general, correspondence between $\bar{y}$ and $\mu$ is still close, even for the LAAPCD stations which average only 6 samples per month. The important feature of these graphs, however, is that the 95% confidence intervals on the monthly means of the LAAPCD data have become quite large due to the small number of samples taken each month. The NASN data have not been plotted at all since the insufficiency of data is even more extreme (only one or two samples per month). A graphical description of the monthly arithmetic means of the CHESS and LAAPCD sulfate data at all monitoring stations is given at the end of Appendix B4.

These confidence interval estimates hold important implications for a long-term air quality modeling study. It is clear from the previous discussion plus Appendix B4 that rather long averaging times are needed to reduce the uncertainty introduced into the NASN and LAAPCD data averages by their sparse sampling schedules. A compromise must be struck between the desire for short averaging times and the

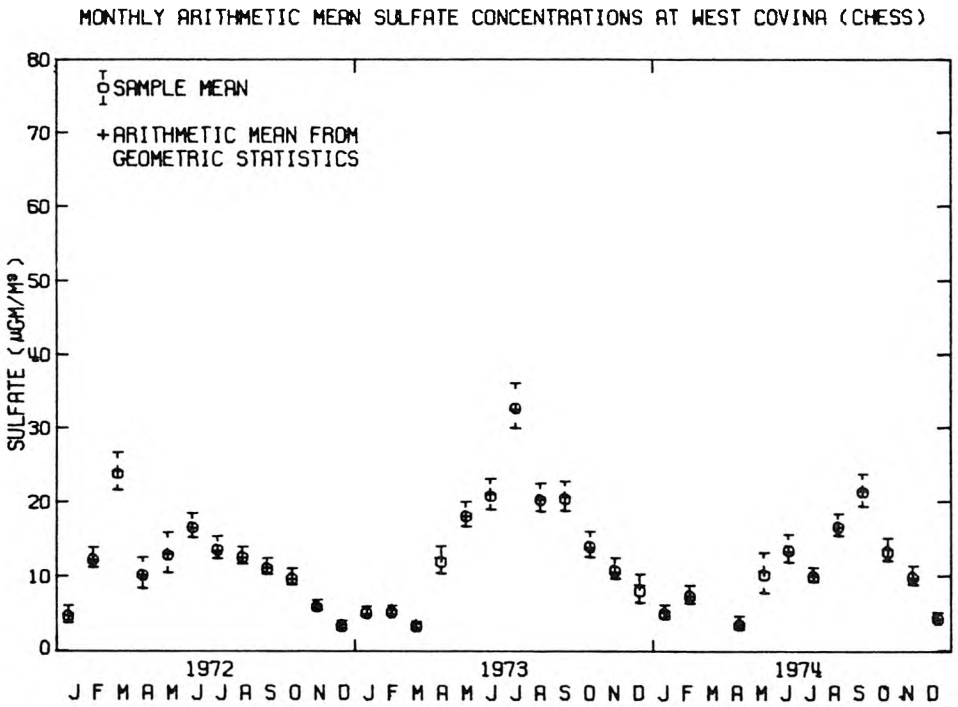


FIGURE 2.15

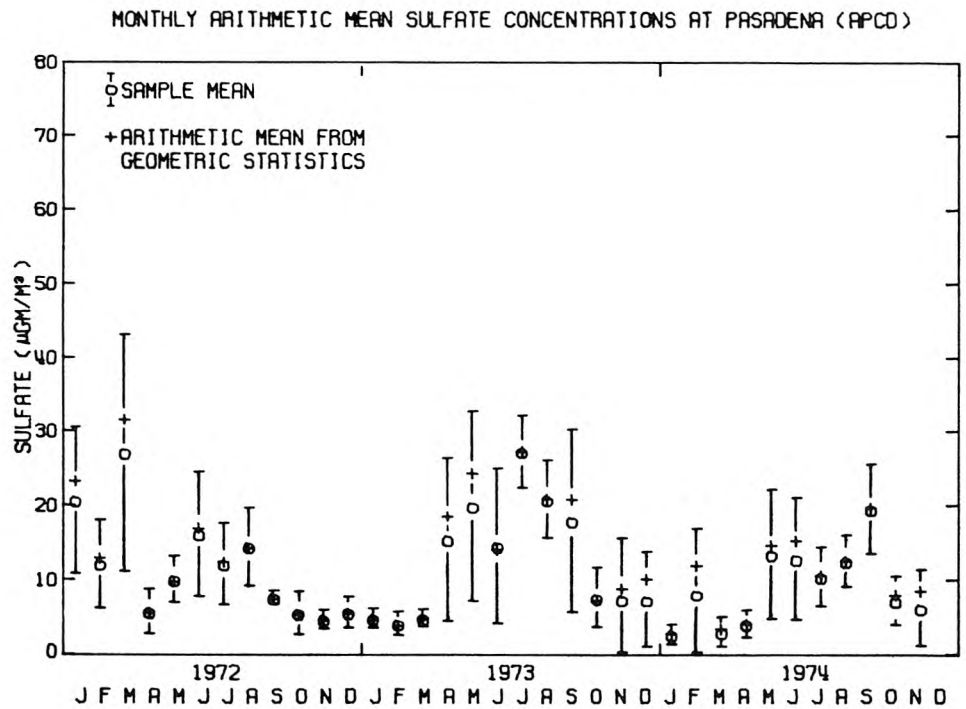


FIGURE 2.16

desire for tight confidence intervals on the ambient concentration averages used to validate air quality model predictions.

Monthly average sulfate concentrations will be modeled with the understanding that only the CHESS data and certain portions of the LAAPCD data strings will provide an exacting test of model performance on a monthly basis. These monthly predictions can then be combined to form annual average predictions for comparison to annual average air quality measurements which are known to ± a few micrograms per cubic meter at a larger number of monitoring sites.

## 2.3 Sulfate Air Quality in Relation to the Total Sulfur Content of the Atmosphere

The reason for the localized sulfate enrichment of the air over metropolitan Los Angeles is likely to be found in emissions of sulfur oxides from fuel burning and industrial activities. Roberts (1975) has outlined the atmospheric sulfur budget of the Los Angeles area, as shown in Figure 2.17. His calculations indicate that while only about thirty percent of the global sulfur emissions are due to man's activities, ninety-eight percent of the sulfur emissions within the Los Angeles Basin are attributable to man-made pollution sources. Most of these emissions are in the form of sulfur dioxide gas.

Sulfur dioxide emissions undergo transport, dilution, and removal processes in the atmosphere. Chemical reactions proceed which can oxidize sulfur dioxide gas to form particulate sulfates downwind from $SO_2$ emission sources. With the exception of trace amounts of other sulfur compounds, such as $H_2S$, sulfur dioxide and particulate

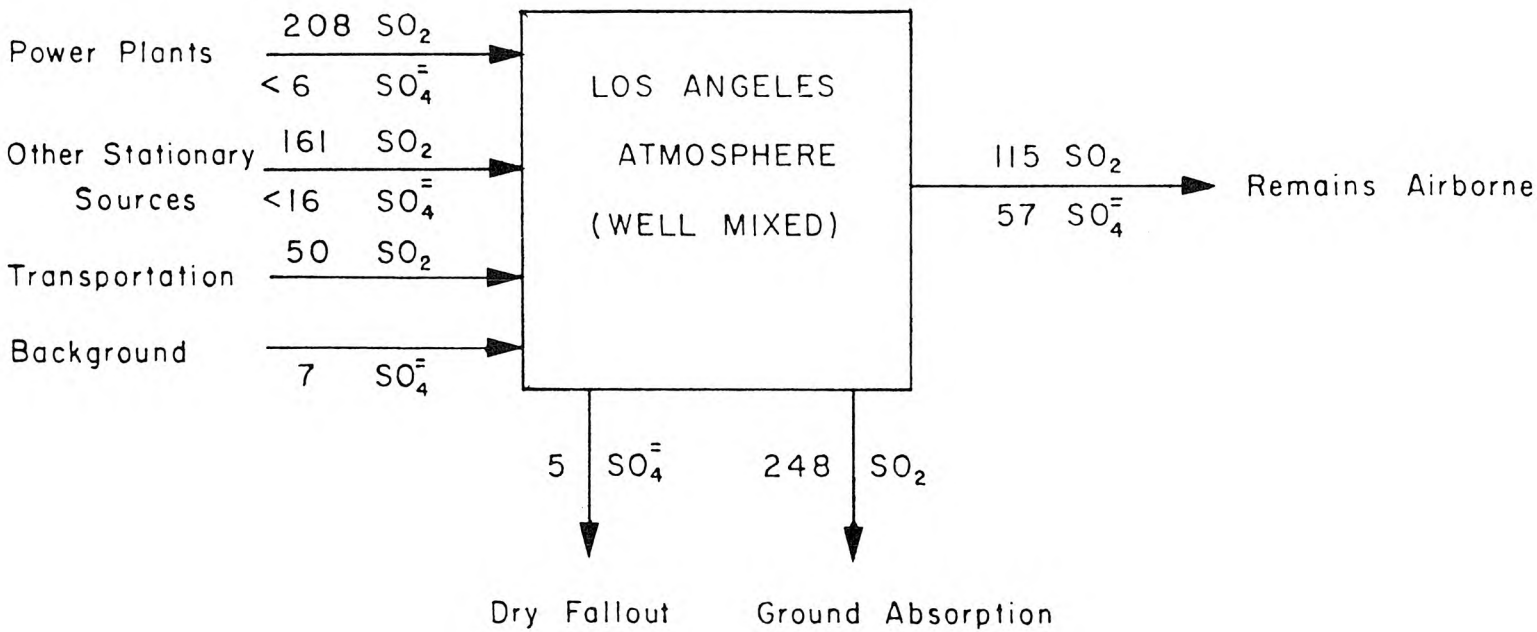


FIGURE 2.17

The Los Angeles Basin Atmospheric Sulfur Balance for July 25, 1973 (from Roberts 1975)

sulfur oxides (measured as sulfates) together make up the total sulfur burden of the Los Angeles area atmosphere. The atmospheric ratio of particulate sulfur to total sulfur, $f_s$, is a convenient indicator of the extent to which the reaction of $SO_2$ to form "sulfates" has reached completion. This ratio can be computed in the course of our air quality modeling study, and provides a check on the computed rate of removal of $SO_2$ from the gas phase.

Sulfur oxides emissions within the South Coast Air Basin are generated primarily by activities at power plants, oil refineries, chemical plants and metallurgical operations. Figure 2.13 shows the location of major sulfur oxides emission sources in that air basin. According to 1974 emission inventory information (Hunter and Helgeson, 1976), about eighty percent of the stationary source sulfur oxides emissions in the South Coast Air Basin originate from sources adjacent to the coast. Prevailing winds transport these coastal emissions inland along resultant sea-breeze wind trajectories as indicated in Figure 2.14, (De Marrais, Holzworth, and Hosler, 1965). At locations upwind or to the side of major $SO_2$ emission sources, a large percentage of the observed sulfate will be of the background variety, and the value of $f_s$ could be relatively high. At distances close to major $SO_2$ emission sources, most of the sulfur in the atmosphere will appear as $SO_2$, and the value of $f_s$ will be relatively low. Then at distances further downwind, conversion of $SO_2$ to form sulfates, plus removal of $SO_2$ at the earth's surface should act to raise the value of $f_s$. Let us

examine the available air quality data to see if these hypotheses are supported.

In the absence of direct air monitoring data for total sulfur, as would be revealed by a flame photometric total sulfur analyzer, a close approximation to $f_s$ should be obtainable from:

$$f_s = \frac{S_p}{S_T} \approx \frac{S_{SO_4}}{S_{SO_2} + S_{SO_4}} \qquad (2.1)$$

where

$S_p$ is particulate sulfur concentration.

$S_T$ is total sulfur concentration.

$S_{SO_4}$ is particulate sulfur oxides concentration measured as sulfates and restated in $\mu gm/m^3$ as elemental sulfur.

$S_{SO_2}$ is sulfur dioxide concentration in $\mu gm/m^3$ as elemental sulfur.

Both $S_p$ and $S_T$ could be considered as air pollutants. If they were mutually independent and log-normally distributed, then $f_s$ should also be log-normally distributed. Stochastic independence of $S_p$ and $S_T$ is rather doubtful, however, in light of the way in which they are estimated in equation (2.1). The distribution of $f_s$ is therefore uncertain. In Figures 2.18, 2.19 and 2.20, the cumulative distribution of $f_s$ is displayed for typical CHESS, NASN, and LAAPCD stations. Similar graphs for the remaining stations are presented in Appendix B6. The rapid fall-off at the lower tails of the CHESS and LAAPCD distributions again probably is due to the problems with measurement of very low sulfate concentrations. At the upper tails of the CHESS and NASN

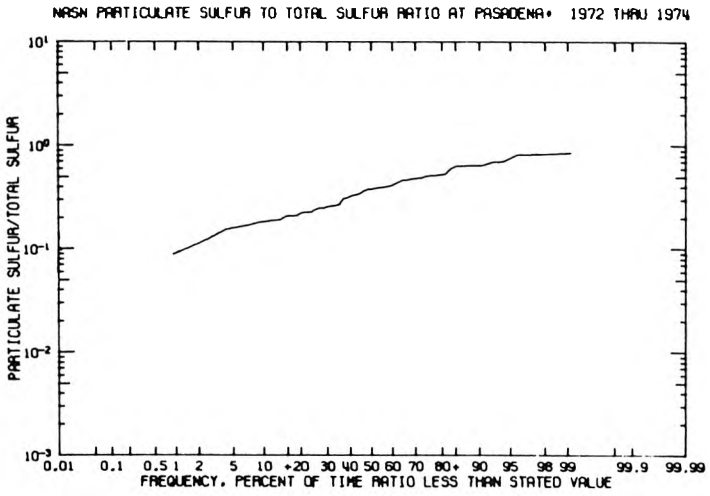


FIGURE 2.18

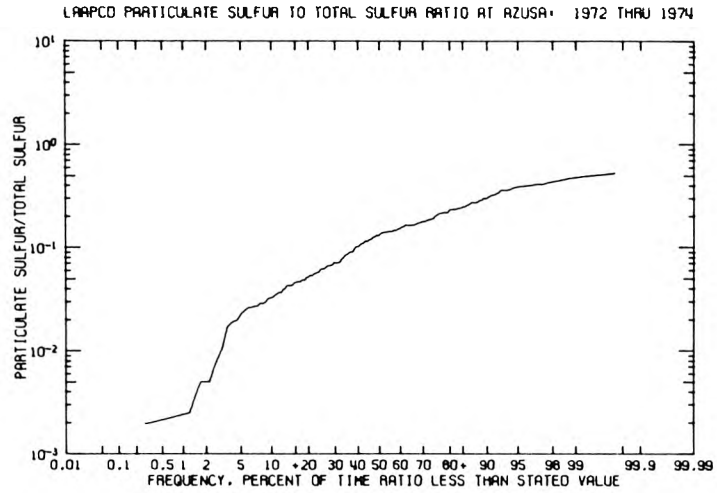


FIGURE 2.19

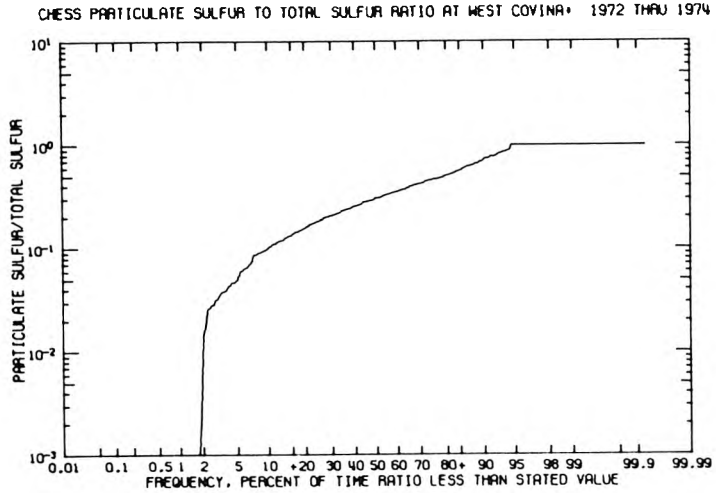


FIGURE 2.20

distributions, a flattening of the curve at $f_s = 1$ is caused by reported zero concentrations of sulfur dioxide.

In Table 2.10 the three year arithmetic mean values of $f_s$ are shown, labeled by geographic location and monitoring agency. It is seen that the CHESS and NASN stations located in close proximity display roughly the same values of $f_s$, while values of $f_s$ at the LAAPCD stations are systematically lower. We already know that the sulfate observations are not the cause of such large differences between monitoring agencies. Therefore, it follows that the lower values of $f_s$ at the APCD stations are due to systematically higher $SO_2$ measurements as would be expected from the discussions in Appendix B1.

It is not possible on the basis of these differences alone to state that any particular $SO_2$ data base is "correct". A good case can be made for the assertion that the true $SO_2$ values should lie somewhere between the results obtained by the APCD's conductometric technique and the West-Gaeke technique employed by CHESS and NASN. The minimum detection limit of the LAAPCD $SO_2$ monitoring instruments is 26 $\mu gm/m^3$. All $SO_2$ concentrations below that value would also be reported as 26 $\mu gm/m^3$. The APCD instruments encounter $SO_2$ concentrations at or below their minimum detection limit much of the time. Twenty-four hour average $SO_2$ concentrations constructed from APCD data thus often will be biased high. In contrast CHESS and NASN data possibly underestimate $SO_2$ levels due to sample collection efficiency problems, and due to lack of control of the time-temperature history of samples

TABLE 2.10

Particulate Sulfur to Total Sulfur Ratio
Mean Value for the Years 1972 through 1974
Grouped by Monitoring Agency and Location

| Region | Monitoring Site (Mean Value of $f_s$) | | | | | |
|---|---|---|---|---|---|---|
| | NASN | | CHESS | | LAAPCD | |
| Los Angeles County Central | | | | | Lynwood* | 0.10 |
| | Los Angeles | 0.36 | | | Los Angeles | 0.15 |
| | Pasadena | 0.39 | | | Pasadena | 0.14 |
| | Glendale | 0.39 | | | | |
| Orange County | | | Garden Grove | 0.39 | | |
| | Anaheim | 0.39 | Anaheim | 0.50 | | |
| | Santa Ana | 0.42 | | | | |
| Eastern San Gabriel Valley | | | West Covina | 0.35 | Azusa | 0.15 |
| | | | Glendora | 0.40 | | |
| Los Angeles County Coastal | | | Santa Monica | 0.43 | West L.A. | 0.15 |
| | | | | | Lennox | 0.13 |
| | Torrance | 0.48 | | | | |
| | Long Beach | 0.28 | | | | |
| Inland-West | | | | | Reseda | 0.20 |
| | | | Thousand Oaks | 0.53 | | |
| Inland-East | San Bernardino | 0.59 | | | | |
| Adjacent Air Basin | | | Vista | 0.60 | | |

*1974 only

between time of collection and later analysis (see Appendix B1). CHESS and NASN values of $f_s$ should be considered as upper bounds to the true value of $f_s$.

Because of the likelihood that all available $SO_2$ data sets are systematically biased to an unknown degree, no attempt will be made to place confidence intervals on the $f_s$ data through ordinary statistical techniques. Instead, a limited amount of statistical information on each data set will be given in Table 2.11 for the entire three year period, and in Tables 2.12, 2.13, and 2.14 for the individual years 1972, 1973 and 1974, respectively. Then qualitative conclusions will be drawn from the temporal and spatial gradients in $f_s$ values apparent from within groups of stations using the same monitoring methods.

In Figure 2.21, average values of $f_s$ at the NASN and CHESS stations during the years 1972 through 1974 are shown in relation to monitoring site location. At Long Beach near major coastal point sources in the Los Angeles Harbor area, the three year average value of $f_s$ is seen to be in the range of 0.20 to 0.30. Intermediate locations in the center of the Los Angeles Basin, like Glendale, Los Angeles, and Pasadena, show values of $f_s$ which are higher, in the range of 0.30 to 0.40. Further downwind at Glendora, $f_s$ increases to above 0.40. By the time that air masses reach inland locations as distant as San Bernardino most of the sulfur is in the particulate phase. Our expectation that $f_s$ should increase with distance downwind from major $SO_2$ sources in the harbor area seems supported. Values of $f_s$ at Vista, Thousand Oaks, Santa Monica and central Orange County are more difficult to interpret

TABLE 2.11

Particulate Sulfur to Total Sulfur Ratio, $f_s$
for the Period 1972 through 1974

| | | SAMPLE ARITHMETIC MEAN VALUE OF $f_s$ | SAMPLE ARITHMETIC STANDARD DEVIATION | NUMBER OF SAMPLES |
|---|---|---|---|---|
| LOS ANGELES | LAAPCD | 0.15 | 0.10 | 209.00 |
| AZUSA | LAAPCD | 0.15 | 0.11 | 210.00 |
| WEST LA | LAAPCD | 0.15 | 0.10 | 214.00 |
| RESEDA | LAAPCD | 0.20 | 0.15 | 214.00 |
| LENNOX | LAAPCD | 0.13 | 0.08 | 217.00 |
| PASADENA | LAAPCD | 0.14 | 0.11 | 213.00 |
| LYNWOOD | LAAPCD | 0.10(b) | 0.07(b) | 68.00(b) |
| VISTA | CHESS | 0.60 | 0.30 | 954.00 |
| SANTA MONICA | CHESS | 0.43 | 0.28 | 756.00 |
| THOUSAND OAKS | CHESS | 0.53 | 0.32 | 780.00 |
| ANAHEIM | CHESS | 0.50 | 0.31 | 841.00 |
| GARDEN GROVE | CHESS | 0.39 | 0.29 | 812.00 |
| GLENDORA | CHESS | 0.41 | 0.25 | 833.00 |
| WEST COVINA | CHESS | 0.35 | 0.24 | 772.00 |
| TORRANCE | NASN | 0.48 | 0.25 | 65.00 |
| LONG BEACH | NASN | 0.28 | 0.19 | 61.00 |
| LOS ANGELES | NASN | 0.36 | 0.22 | 60.00 |
| BURBANK | NASN | (a) | (a) | 0.0 |
| GLENDALE | NASN | 0.39 | 0.24 | 53.00 |
| PASADENA | NASN | 0.39 | 0.19 | 61.00 |
| ANAHEIM | NASN | 0.39 | 0.21 | 78.00 |
| SANTA ANA | NASN | 0.42 | 0.21 | 72.00 |
| ONTARIO | NASN | (a) | (a) | 0.0 |
| RIVERSIDE | NASN | (a) | (a) | 0.0 |
| SAN BERNARDINO | NASN | 0.59 | 0.26 | 62.00 |

Notes: (a) Data unavailable.

(b) 1974 only.

TABLE 2.12

Particulate Sulfur to Total Sulfur Ratio, $f_s$
for the Year 1972

| | | SAMPLE ARITHMETIC MEAN VALUE OF $f_s$ | SAMPLE ARITHMETIC STANDARD DEVIATION | NUMBER OF SAMPLES |
|---|---|---|---|---|
| LOS ANGELES | LAAPCD | 0.15 | 0.08 | 66.00 |
| AZUSA | LAAPCD | 0.16 | 0.10 | 67.00 |
| WEST LA | LAAPCD | 0.17 | 0.09 | 71.00 |
| RESEDA | LAAPCD | 0.22 | 0.13 | 72.00 |
| LENNOX | LAAPCD | 0.13 | 0.07 | 73.00 |
| PASADENA | LAAPCD | 0.16 | 0.10 | 70.00 |
| LYNWOOD | LAAPCD | (a) | (a) | 0.0 |
| VISTA | CHESS | 0.60 | 0.26 | 304.00 |
| SANTA MONICA | CHESS | 0.44 | 0.25 | 215.00 |
| THOUSAND OAKS | CHESS | 0.53 | 0.25 | 196.00 |
| ANAHEIM | CHESS | 0.40 | 0.25 | 297.00 |
| GARDEN GROVE | CHESS | 0.37 | 0.26 | 214.00 |
| GLENDORA | CHESS | 0.36 | 0.19 | 274.00 |
| WEST COVINA | CHESS | 0.34 | 0.18 | 219.00 |
| TORRANCE | NASN | 0.42 | 0.22 | 22.00 |
| LONG BEACH | NASN | 0.31 | 0.22 | 21.00 |
| LOS ANGELES | NASN | 0.27 | 0.13 | 24.00 |
| BURBANK | NASN | (a) | (a) | 0.0 |
| GLENDALE | NASN | 0.34 | 0.20 | 23.00 |
| PASADENA | NASN | 0.38 | 0.18 | 21.00 |
| ANAHEIM | NASN | 0.37 | 0.17 | 27.00 |
| SANTA ANA | NASN | 0.47 | 0.19 | 27.00 |
| ONTARIO | NASN | (a) | (a) | 0.0 |
| RIVERSIDE | NASN | (a) | (a) | 0.0 |
| SAN BERNARDINO | NASN | 0.54 | 0.24 | 24.00 |

Note: (a) Data unavailable.

TABLE 2.13

Particulate Sulfur to Total Sulfur Ratio, $f_s$ for the Year 1973

| | | SAMPLE ARITHMETIC MEAN VALUE OF $f_s$ | SAMPLE ARITHMETIC STANDARD DEVIATION | NUMBER OF SAMPLES |
|---|---|---|---|---|
| LOS ANGELES | LAAPCD | 0.17 | 0.11 | 72.00 |
| AZUSA | LAAPCD | 0.14 | 0.11 | 72.00 |
| WEST LA | LAAPCD | 0.13 | 0.10 | 71.00 |
| RESEDA | LAAPCD | 0.21 | 0.18 | 72.00 |
| LENNOX | LAAPCD | 0.11 | 0.07 | 72.00 |
| PASADENA | LAAPCD | 0.16 | 0.12 | 72.00 |
| LYNWOOD | LAAPCD | (a) | (a) | 0.0 |
| VISTA | CHESS | 0.51 | 0.26 | 315.00 |
| SANTA MONICA | CHESS | 0.35 | 0.23 | 312.00 |
| THOUSAND OAKS | CHESS | 0.43 | 0.27 | 308.00 |
| ANAHEIM | CHESS | 0.68 | 0.30 | 314.00 |
| GARDEN GROVE | CHESS | 0.35 | 0.22 | 315.00 |
| GLENDORA | CHESS | 0.38 | 0.24 | 308.00 |
| WEST COVINA | CHESS | 0.29 | 0.19 | 304.00 |
| TORRANCE | NASN | 0.38 | 0.19 | 18.00 |
| LONG BEACH | NASN | 0.33 | 0.17 | 18.00 |
| LOS ANGELES | NASN | 0.35 | 0.15 | 18.00 |
| BURBANK | NASN | (a) | (a) | 0.0 |
| GLENDALE | NASN | 0.35 | 0.15 | 18.00 |
| PASADENA | NASN | 0.39 | 0.20 | 19.00 |
| ANAHEIM | NASN | 0.33 | 0.13 | 22.00 |
| SANTA ANA | NASN | 0.31 | 0.14 | 19.00 |
| ONTARIO | NASN | (a) | (a) | 0.0 |
| RIVERSIDE | NASN | (a) | (a) | 0.0 |
| SAN BERNARDINO | NASN | 0.52 | 0.20 | 17.00 |

Note: (a) Data unavailable.

TABLE 2.14

Particulate Sulfur to Total Sulfur Ratio, $f_s$ for the Year 1974

| | | SAMPLE ARITHMETIC MEAN VALUE OF $f_s$ | SAMPLE ARITHMETIC STANDARD DEVIATION | NUMBER OF SAMPLES |
|---|---|---|---|---|
| LOS ANGELES | LAAPCD | 0.15 | 0.11 | 71.00 |
| AZUSA | LAAPCD | 0.14 | 0.12 | 71.00 |
| WEST LA | LAAPCD | 0.14 | 0.11 | 72.00 |
| RESEDA | LAAPCD | 0.18 | 0.14 | 70.00 |
| LENNOX | LAAPCD | 0.13 | 0.09 | 72.00 |
| PASADENA | LAAPCD | 0.11 | 0.09 | 71.00 |
| LYNWOOD | LAAPCD | 0.10 | 0.07 | 68.00 |
| VISTA | CHESS | 0.68 | 0.33 | 335.00 |
| SANTA MONICA | CHESS | 0.55 | 0.34 | 229.00 |
| THOUSAND OAKS | CHESS | 0.65 | 0.36 | 276.00 |
| ANAHEIM | CHESS | 0.40 | 0.30 | 230.00 |
| GARDEN GROVE | CHESS | 0.46 | 0.35 | 283.00 |
| GLENDORA | CHESS | 0.49 | 0.31 | 251.00 |
| WEST COVINA | CHESS | 0.45 | 0.31 | 249.00 |
| TORRANCE | NASN | 0.60 | 0.27 | 25.00 |
| LONG BEACH | NASN | 0.21 | 0.17 | 22.00 |
| LOS ANGELES | NASN | 0.48 | 0.32 | 18.00 |
| BURBANK | NASN | (a) | (a) | 0.0 |
| GLENDALE | NASN | 0.52 | 0.35 | 12.00 |
| PASADENA | NASN | 0.41 | 0.19 | 21.00 |
| ANAHEIM | NASN | 0.45 | 0.27 | 29.00 |
| SANTA ANA | NASN | 0.44 | 0.24 | 26.00 |
| ONTARIO | NASN | (a) | (a) | 0.0 |
| RIVERSIDE | NASN | (a) | (a) | 0.0 |
| SAN BERNARDINO | NASN | 0.72 | 0.28 | 21.00 |

Note: (a) Data unavailable.

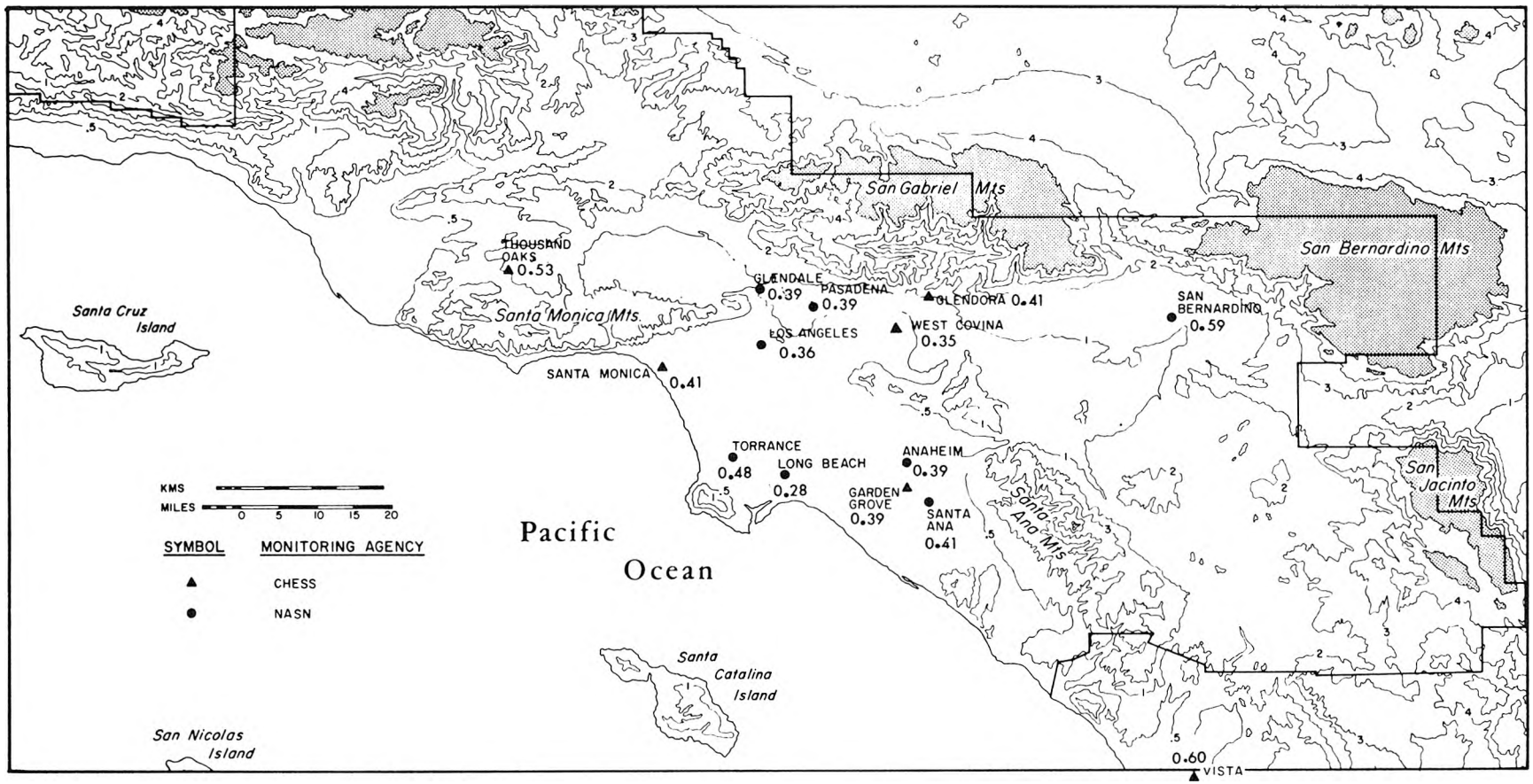


FIGURE 2.21

Average Values of $f_s$ During the Years 1972 through 1974 at CHESS and NASN Monitoring Stations

because those locations lie to the side of the predominant direction of transport of sulfur oxides from Los Angeles harbor area emission sources. The Torrance station appears to be "upwind" of the harbor industrial complex. Comparable values of $f_s$ in the San Fernando Valley are unavailable, but the LAAPCD data indicate that $f_s$ at Reseda is high in relation to downtown Los Angeles.

Appendix B7 displays the seasonal trends in $f_s$ values computed from data of the CHESS and LAAPCD networks. Also shown is the seasonal trend in a second statistic, $\bar{f}_s$, which is the ratio of *monthly average* particulate sulfur oxides concentration to *monthly average* total sulfur oxides concentration. This second statistic is more readily computed from the results of a long-term average air quality model than is the average value of $f_s$ itself. It therefore will become convenient to compare air quality model results to trends in $\bar{f}_s$ as one means of assessing air quality model performance.

While sulfate concentration trends were found to be very similar over widespread areas of the South Coast Air Basin, there are some distinct, and often puzzling differences between $f_s$ observations at nearby monitoring stations. The most obvious differences are still between monitoring networks using different measurement techniques. The LAAPCD and CHESS networks both show relative peaks in $f_s$ during the summer months, but as with the annual averages, the LAAPCD $f_s$ values are consistently roughly half the magnitude of those obtained by CHESS. Even internally to the CHESS program, there are some noteworthy differences between results at nearby monitoring stations. At the start of

1973, CHESS $f_s$ measurements at Anaheim begin to climb sharply above those calculated at the Garden Grove station located less than two miles away. Then during 1974, some uncharacteristically high $f_s$ values are apparent periodically at a larger number of CHESS monitoring sites. One is led to speculate that the CHESS network may have encountered sample collection problems at about the same time that they changed the volume of West-Gaeke reagent in their bubblers and reduced sampler air flow rate in order to match the Federal reference sampling method for $SO_2$ employed by NASN (see Appendix B1).

In summary, data on the fraction of atmospheric sulfur present as sulfates are not as reliable as one would like. These problems arise from difficulties in measurement of very low sulfur dioxide levels by the methods used at the stations under study. In spite of these problems, relative spatial variations in three year average $f_s$ values from CHESS and NASN stations using similar $SO_2$ measurement procedures are consistent with our prior expectations. The lowest values of $f_s$ are found near major $SO_2$ source areas, and $f_s$ values increase with distance downwind as $SO_2$ is removed at the ground or is oxidized in the atmosphere to form sulfates. Actual use of numerical values of $f_s$ in our modeling study should proceed with caution. About all that can be said is that model results should fall at or below the long-term average $f_s$ values reported by CHESS and NASN stations, but above values calculated from LAAPCD data.

## 2.4 Atmospheric Oxidation of $SO_2$ to Form Sulfates

The observed uniformity of average sulfate levels is in marked contrast to the highly localized nature of the major sources of precursor sulfur dioxide. For a conserved or slowly decaying pollutant emitted from coastal point sources, one expects pollutant concentration to drop greatly with distance downwind as atmospheric dispersion and removal processes come into effect. Sulfur dioxide concentrations do decline, as expected, with distance inland from the coast. The contrasting constant sulfate levels with distance inland from major sulfur oxide sources is probably explained by a competition between dispersion which tends to lower pollutant concentrations and additional gas-to-particle conversion involving $SO_2$ which tends to build up sulfate concentrations. An additional possibility is that some sulfate formation occurs aloft or offshore during late night land breezes and early morning stagnation periods. This well-aged aerosol might then be swept across the Basin during the day by the advancing sea breeze, contributing roughly equal amounts of sulfate to successive air monitoring stations in passing. In either case, the rate at which $SO_2$ is oxidized to form sulfates will influence the magnitude of the sulfate concentrations observed.

### 2.4.1 An Overview of Atmospheric Sulfur Chemistry

The relative importance of various $SO_2$ to sulfate conversion mechanisms is poorly understood at present. $SO_2$ oxidation rates have been measured in the Los Angeles atmosphere and found to vary from one

percent to 15 percent per hour under photochemically active, daylight sea breeze conditions (Roberts, 1975). At least three general classes of chemical reactions could oxidize $SO_2$ at rates fast enough to account for observed sulfate levels. These possibilities include:

1. Homogeneous gas-phase oxidation of $SO_2$ by free radicals generated in Los Angeles photochemical smog.
2. Heterogeneous phase processes involving absorption of $SO_2$ by aqueous particles in the atmosphere followed by oxidation in the liquid phase.
3. Heterogeneous phase processes involving surface adsorption of $SO_2$ by carbonaceous or metal oxide particles, followed by oxidation to sulfate.

The scientific literature supporting specific chemical reaction mechanisms within these three broad classes is voluminous. A number of review articles have been written which taken together provide a good summary of current knowledge (Urone and Schroeder, 1969; Bufalini, 1971; Calvert, 1973; Harrison, Larson and Hobbs, 1975; Sander and Seinfeld, 1976).

Homogeneous gas phase reactions considered to be important in explaining atmospheric sulfur dioxide oxidation include:

1. oxidation of $SO_2$ by hydroxyl (OH) radicals

$$SO_2 + OH + M \rightarrow HSO_3 + M \qquad (2.2)$$

2. oxidation of $SO_2$ by $HO_2$ radicals

$$HO_2 + SO_2 \rightarrow SO_3 + OH \quad (2.3a)$$

$$HO_2 + SO_2 \rightarrow SO_2HO_2 \quad (2.3b)$$

3. oxidation of $SO_2$ by other oxy-, peroxy-, and ozonide free radicals such as RO, $RO_2$, $RCO(O_2)$ (for example the ozone-olefin - $SO_2$ reactions studied by Cox and Penkett, 1972; and McNelis, 1974).

$$SO_2 + RO \rightarrow ROSO_2 \quad (2.4)$$

$$SO_2 + RO_2 \rightarrow SO_3 + RO \quad (2.5a)$$

$$SO_2 + RO_2 \rightarrow SO_2RO_2 \quad (2.5b)$$

$$SO_2 + RCO(O_2) \rightarrow RCO_2 + SO_3 \quad (2.6)$$

Rate constants for this latter group of reactions involving organic free radicals are poorly established at present, but they are thought to be fast enough to be important in a heavily polluted atmosphere.

Sander and Seinfeld (1976) embedded the first two of these $SO_2$ free radical reactions (i.e. OH and $HO_2$ reactions) within a basic hydrocarbon/$NO_x$ mechanism suitable for simulating smog photochemistry. They then tested the speed of that homogeneous reaction system against $SO_2$ oxidation rates observed in a wide variety of laboratory experiments. They conclude for a purely homogeneous system "...that known reactions involving $SO_2$ for which rate constants have been measured are insufficient in themselves to account for observed $SO_2$ oxidation rates

in $NO_x$/hydrocarbon/$SO_2$ systems." They speculate that reactions for which rate constants are currently unknown (e.g. organic peroxy radical reactions) may be important or that heterogeneous processes are responsible for accelerated $SO_2$ oxidation even in experimental systems in which heterogeneous processes were avoided to the greatest extent possible.

In a further simulation roughly approximating atmospheric photochemistry in Los Angeles, Sander and Seinfeld (1976) estimated a *maximum* $SO_2$ oxidation rate of 4.5% per hour due to purely homogeneous processes. That simulation included reactions and rate estimates for $SO_2$ oxidation by OH, $HO_2$, $RO_2$, $RCO_3$, and $O(^3P)$ radicals. Oxidation of $SO_2$ by OH and $HO_2$ radicals still dominated, and the maximum rate of sulfate formation was still slower than some of the atmospherically observed rates of $SO_2$ oxidation reported for Los Angeles by Roberts (1975).

Heterogeneous chemical reactions involving gaseous/liquid phase interactions have long been suspected as important routes for promoting $SO_2$ oxidation to form sulfates. Health related studies continually point out that increased mortality associated with $SO_x$ and particulate air pollution observed in the Muse Valley, Belgium (1930), Donora, Pennsylvania (1948), and London, England (1952) were all accompanied by fog. The supposition is that large amounts of acid aerosol may have been formed by fixation of sulfur oxides inside aqueous droplets. Data needed to prove or refute that conjecture are unavailable for those particular pollution episodes. But a large number of field and

laboratory experimental studies show that the following types of heterogeneous $SO_2$ oxidation processes involving aqueous particles can occur at a rapid enough rate to be important in the atmosphere:

1. Oxidation of $SO_2$ by $O_2$ in well buffered droplets (Scott and Hobbs, 1967). The overall reaction including gas transfer to the droplet is

$$2SO_2 + 2H_2O + O_2 \rightarrow 2H_2SO_4 \qquad (2.9)$$

2. Metal-ion catalyzed oxidation of $SO_2$ by $O_2$ in the liquid phase (Johnstone and Coughanowr, 1958; Junge and Ryan, 1958; Foster, 1968, and many others). The overall reaction including gas transfer to the droplet is

$$2SO_2 + 2H_2O + O_2 \xrightarrow{\text{catalyst}} 2H_2SO_4 \qquad (2.10)$$

3. Oxidation of $SO_2$ by photochemical oxidants dissolved in droplets (Penkett, 1972). One example of this class of reactions (including gaseous transfer to the droplet) presumably is

$$SO_2 + H_2O + O_3 \rightarrow H_2SO_4 + O_2 \qquad (2.11)$$

These liquid phase reactions are substantially affected by droplet acidity. As acid concentrations build up in a droplet, oxidation of dissolved $SO_2$ can slow to a negligible rate. But for clean clouds at a pH of about 5.6 these mechanisms proceed to oxidize $SO_2$ to form sulfate at a rate of from several percent per hour to over ten percent per hour. At high catalyst concentrations or high oxidant concentrations, reaction types (2.10) and (2.11) above are still significant

even for moderately acidic aerosols at pH 4.6 (ref. Harrison, Larson and Hobbs, 1975). Catalyst type would also be an important factor, with transition metal ions of manganese and vanadium noted for their promotion of rapid oxidation, and iron often considered to be an important catalyst because of its relative abundance.

High $SO_2$ oxidation rates due to these heterogeneous reactions are often associated with high ambient relative humidity for two reasons. First, as relative humidity increases, hygroscopic particles pick up liquid water and grow in size, providing an aqueous medium in which the reactions can take place. Secondly, as humidity increases further, additional condensation of water can dilute aerosol acidity and cause the reaction rate internal to the droplet to increase above what it would have been otherwise.

Heterogeneous phase reactions involving $SO_2$ adsorption on the surfaces of carbonaceous or metal oxide particles are not as well understood at present, but possibly are important. An investigation of $SO_2$ reactions on the surfaces of soot particles by Novakov, et al. (1974) showed rapid conversion to sulfate. The rate of reaction in that mechanism was also thought to increase sharply with increasing relative humidity.

### 2.4.2 An Empirical Investigation of Factors Affecting Sulfur Oxides Chemistry and Dispersion in the Los Angeles Atmosphere

The variety of chemical reactions *potentially* leading to oxidation of $SO_2$ to form sulfates at a rate of several percent per hour is readily apparent. Several practical questions now arise. Is any

single type of well-known reaction responsible for the bulk of the high sulfate episodes observed in Los Angeles? Is that reaction path simple enough to simulate from first principles in an air quality model which will be run for long periods of time, or must some approximations be made?

An empirical analysis of downtown Los Angeles air monitoring data was conducted by Cass(1975) to see if day-to-day fluctuations in sulfate level at downtown Los Angeles could be shown to depend on fluctuations in meteorological dispersion or on factors affecting $SO_2$ to sulfate conversion rates. Meteorological dispersion indicators studied include early morning and afternoon inversion heights plus daily average wind speed, solar radiation intensity, and temperature. While changes in gas-phase free radical reactions are unobservable from conventional air monitoring data, there are data on possible indicators of the intensity of daily photochemical smog activity, including oxidant concentrations, $NO_2$, and hydrocarbon level. Roberts (1975) showed that knowledge of ambient ozone levels improves the estimation of $SO_2$ oxidation rates in the Los Angeles atmosphere. If oxidation of $SO_2$ were occurring in the liquid phase on hydrated particles, then ambient relative humidity and suspended particulate concentrations would be important (along with such factors as ammonia concentration and catalytic metals levels, for which we do not have complete air monitoring data).

Data for over six hundred days of observation on air quality parameters and meteorological variables were reviewed, and 342 rainless

days with a complete set of observations on all variables of interest were located. A statistical description of the explanatory variables used is given in Appendix B8. This data set was matched to a step-wise regression model to determine which other atmospheric circumstances most closely track fluctuations in sulfate levels. Fluctuations in atmospheric variables generally have multiplicative effects on pollutant levels. For instance, halving the inversion height while doubling the reaction rate would quadruple expected sulfate concentrations, all other factors remaining equal. For this reason, the regression model was specified in multiplicative or log-linear form.

Results of these correlation studies are presented in Tables 2.15 and 2.16 for the entire data base of record and for those samples taken since the change in LAAPCD sampling schedule of September 1970. Sulfate concentrations appear to be strongly inversely proportional to changes in afternoon inversion height. Sulfate concentration is found to be strongly dependent on daily relative humidity (RH) levels. This dependence on relative humidity is consistent with the observation of numerous investigators that a variety of sulfate formation mechanisms accelerate at high humidity. Knowledge of total suspended particulate matter (TSP) concentration provides a significant improvement in model fit. This is interesting because the grouping $TSP \cdot (1-RH)^{-1}$ for a hygroscopic aerosol would provide a term very roughly proportional to

TABLE 2.15

Stepwise Regression of Log $SO_4^=$ on Logs of Other Pollutant and Meteorological Variables at Downtown Los Angeles (For Description of Data Base, See Appendix B8) (from Cass, 1975)

RESULTS: 1965-1974 — 342 Days of Observation

| First 8 Steps | | Multiple Correlation Coefficient |
|---|---|---|
| STEP 1 | $SO_4^= \propto \frac{1}{(\text{Inv Max})^{1.36}}$ | 0.60 |
| STEP 2 | $SO_4^= \propto \frac{1}{(1-RH)^{0.61}(\text{Inv Max})^{1.07}}$ | 0.65 |
| STEP 3 | $SO_4^= \propto \frac{(TSP)^{1.10}}{(1-RH)^{1.14}}$ | 0.66 |
| STEP 4 | $SO_4^= \propto \frac{(TSP)^{0.77}}{(1-RH)^{0.81}(\text{Inv Max})^{0.73}}$ | 0.70 |
| STEP 5 | $SO_4^= \propto \frac{(TSP)^{0.84}(\text{Inv Base})^{0.23}}{(\text{Inv Max})^{1.08}}$ | 0.71 |
| STEP 6 | $SO_4^= \propto \frac{(TSP)^{0.92}(\text{Inv Base})^{0.16}}{(1-RH)^{0.54}(\text{Inv Max})^{0.80}}$ | 0.73 |
| STEP 7 | $SO_4^= \propto \frac{(TSP)^{0.88}(\text{Inv Base})^{0.15}(\text{Avg O3})^{0.21}}{(1-RH)^{0.56}(\text{Inv Max})^{0.72}}$ | 0.74 |
| STEP 8 | $SO_4^= \propto \frac{(TSP)^{0.96}(\text{Inv Base})^{0.12}(\text{Avg O3})^{0.85}}{(1-RH)^{0.55}(\text{Inv Max})^{0.72}(\text{O3 Max})^{0.55}}$ | 0.75 |

| VARIABLE TYPE | SYMBOL | ESTIMATED EXPONENT AT STEP 8 | STANDARD ERROR OF THAT ESTIMATE |
|---|---|---|---|
| Total suspended particulate | TSP | 0.95 | 0.11 |
| $(1-\frac{\text{relative humidity \%}}{100})$ | (1-RH) | -0.55 | 0.10 |
| Afternoon inversion height | Inv Max | -0.72 | 0.10 |
| Morning inversion base height | Inv Base | 0.12 | 0.03 |
| 24 hour avg. oxidant | Avg. O3 | 0.85 | 0.18 |
| Daily instantaneous oxidant peak | O3 Max | -0.55 | 0.15 |

TABLE 2.16

Stepwise Regression of Log $SO_4^=$ on Logs of Other Pollutant and Meteorological Variables at Downtown Los Angeles (For Description of Data Base, See Appendix B8)
(from Cass, 1975)

RESULTS: September 1970-1974 — 186 Days of Observation

| First 5 Steps | | Multiple Correlation Coefficient |
|---|---|---|
| STEP 1 | $SO_4^= \propto \frac{1}{(1-RH)^{1.24}}$ | 0.66 |
| STEP 2 | $SO_4^= \propto \frac{(TSP)^{0.86}}{(1-RH)^{1.31}}$ | 0.78 |
| STEP 3 | $SO_4^= \propto \frac{(TSP)^{0.82}(Avg\ O3)^{0.44}}{(1-RH)^{1.28}}$ | 0.82 |
| STEP 4 | $SO_4^= \propto \frac{(TSP)^{0.65}(Avg\ O3)^{0.37}}{(1-RH)^{1.13}(Inv\ Max)^{0.39}}$ | 0.83 |
| STEP 5 | $SO_4^= \propto \frac{(TSP)^{0.75}(Inv\ Base)^{0.11}(Avg\ O3)^{0.39}}{(1-RH)^{0.92}(Inv\ Max)^{0.46}}$ | 0.85 |

| VARIABLE TYPE | SYMBOL | ESTIMATED EXPONENT AT STEP 5 | STANDARD ERROR OF THAT ESTIMATE |
|---|---|---|---|
| Total suspended particulate | TSP | 0.75 | 0.09 |
| $(1-\frac{\text{relative humidity}\ \%}{100})$ | 1-RH | -0.92 | 0.10 |
| Afternoon inversion height | Inv Max | -0.46 | 0.10 |
| Morning inversion base height | Inv Base | 0.11 | 0.03 |
| 24 hour avg. oxidant | Avg. O3 | 0.39 | 0.07 |

the volume of aqueous solution available in the atmosphere at a given time.[2]

Further improvement in model fit is provided by the inclusion of daily average oxidant concentration.

Beyond this point, improvements in model fit are provided mainly by attempts to better estimate the effects of the above phenomena through inclusion of oxidant peak data, for example, rather than by entry of new explanatory variables. The unexpected inclusion of morning inversion base in the numerator of these regression expressions indicates that very low morning inversion base heights are associated with low sulfate levels. That finding has since been confirmed by APCD analysts (Zeldin, Davidson, Brunelle and Dickenson, 1976), and by the California Air Resources Board (1976). The explanation seems to be that a relatively high morning inversion base (between 225 and 1100 meters above sea level) traps overnight emissions from elevated sources next to the ground within a thick moist marine layer, below an inversion which will be difficult to burn off during the next day. A very high sulfate day often has a 600 meter morning inversion base height with little or no rise in inversion base during the day, yielding a lower than average afternoon maximum mixing depth. Relatively little vertical

---

[2] Neiburger and Wurtele's (1949) discussion of water uptake by hygroscopic atmospheric particles develops the approximation that particle radius is roughly proportional to [particle solute mass/(1-RH)]$^{1/3}$. Particle volume is thus proportional to solute mass times (1-RH)$^{-1}$. If TSP is proportional to soluble particulate matter and the relative size distribution of dry solute mass per particle is preserved from day to day, then the above approximation follows.

dilution of pollutants is achieved. In the absence of much vertical inversion base movement, little down-mixing of dry air from aloft will occur, and relative humidity stays high throughout the day. In contrast, surface-based inversions overnight isolate the effluent from elevated emission sources well above ground level receptors for many hours. These overnight surface inversions often are rather weak, and may burn off completely by the following afternoon[3]. Separation of elevated emissions from ground level receptors at night, followed by high dilution of pollutants the next afternoon may explain why days with very low morning inversion base heights have less than average potential for creating high sulfate concentrations.

It is significant that changes in *scalar* average wind speed seem to bear little relation to sulfate concentrations. For primary pollutants linked to ground level area source emissions, such as total hydrocarbons or CO, scalar wind speed determines initial atmospheric dilution. When nearby sources dominate air quality for these pollutants, then scalar wind speed and measured pollutant concentration are significantly negatively correlated. For a secondary pollutant formed in the atmosphere, such as sulfate, extensive mixing occurs during pollutant formation. Initial dilution is thus less important to

---

[3] A spot survey of morning and afternoon inversion base data given by the Los Angeles Air Pollution Control District (1972, 1973) indicates that about 60% of the mornings with surface inversions are followed by afternoons with higher than usual (1219+ m; 4000+ ft) maximum mixing depths over downtown Los Angeles. Most of these days had afternoon mixing depths greater than the APCD's maximum recorded level of 1524 m (5000 ft).

observed concentrations than is the volume of the reactor (inversion height), the speed of the reaction, and total retention time in the airshed (which depends on vector-valued wind behavior).

A second approach to understanding the circumstances associated with high sulfate levels in Los Angeles is more subjective, but perhaps as instructive. Due to the typical time lag of several months between sulfate sample collection and analysis, few accounts of sulfate air quality contain any mention of the observer's description of the way the weather "looked" on days of abnormally high sulfate values. Of particular interest is whether weather conditions were conducive to high photochemical smog levels which might imply a gas-phase $SO_2$ to sulfate conversion mechanism, or whether conditions were typical of a London fog-type situation in which liquid-phase oxidation of $SO_2$ predominates. The LAAPCD sulfate data base was scanned to select all days of record through the end of 1974 for which 24-hour average sulfate levels exceeded 30 $\mu gm/m^3$ at downtown Los Angeles.[4] Sixty-two such days were found. The weather *forecast* printed for each day in the *Los Angeles Times* was then reviewed, and the question asked, "Was the word fog mentioned in the forecast for that day at locations within Los Angeles and Orange Counties?" Then the U.S. Weather Service data logs for each of these days at coastal airports were reviewed to see if fog was *observed* that day at those locations. Unfortunately, Weather Service fog observations are

[4] If duplicate samples were available, they were averaged to obtain the daily values used.

unavailable at downtown Los Angeles. Then, daily oxidant concentrations at downtown Los Angeles were recorded for both the daily instantaneous peak and 24-hour average corresponding to the period of each sulfate sample. The results of this sulfate episode survey are shown in Table 2.17 (from Cass, 1975).

Review of Table 2.17 shows that fog was forecast at some point in the Basin on all but 10 days of the 62 days of high sulfate values. Four of these remaining days contained forecasts for "drizzles" or "sprinkles", leaving only 6 days of high sulfate without a prior indication of high moisture concentrations. Of those 6 days, fog was observed on 3 days, even though not forecast; drizzle occurred on a fourth day, and a fifth day showed the highest average relative humidity of the entire 62-day sample population. On 29 days, fog was forecast for the immediate vicinity of the air monitoring station at downtown Los Angeles. Fog was observed at coastal airports near major $SO_2$ sources on 31 of the days in question, and other indicators of condensation such as trace precipitation or drizzles were observed on 10 additional days. In most cases the weather forecasts were for "late night and early morning low clouds and fog". While this is not a particularly uncommon forecast, high sulfate values are likewise common in the Los Angeles area. Oxidant levels on these days are quite variable: 9 days with instantaneous maximum over 0.20 ppm; 28 days between 0.20 and 0.10 ppm instantaneous maximum; 22 days when ozone levels never exceeded 0.10 ppm at any time at downtown Los Angeles. While higher oxidant concentrations in this air basin usually

TABLE 2.17

Atmospheric Humidification and Ozone on Days With
30 μgm/m$^3$ $SO_4^=$ or Greater at Downtown Los Angeles

| DATE | | | DOWNTOWN LOS ANGELES SULFATE | WAS FOG MENTIONED IN WEATHER FORECAST? | | | | | WAS FOG OBSERVED? | | APPROXIMATE 24 HOUR AVG RELATIVE | OZONE | |
|---|---|---|---|---|---|---|---|---|---|---|---|---|---|
| Month | Day(s) | Year | (μgm/m$^3$) | L. A. | Beaches | San Fernando Valley | San Gabriel Valley | Orange County | L. A. Airport | Long Beach Airport | HUMIDITY @LA | 24hr Avg | Inst Max (pphm) |
| 8 | 19/20 | 65 | 34.0 | | | | | b | | | 90.0 | 4.6 | 15 |
| 3 | 28/29 | 66 | 33.2 | "drizzles" | "drizzles" | "drizzles" | "drizzles" | b | | | b | 4.5 | 12 |
| 9 | 27/28 | 67 | 30.6 | | | Yes | Yes | Yes | T. Precip | b | 81.5 | 3.5 | 15 |
| 10 | 10/11 | 67 | 33.5 | Yes | Yes | Yes | Yes | Yes | Yes 2 | Yes 2ce | 72.4 | 5.8 | 24 |
| 10 | 25/26 | 67 | 34.6 | Yes | Yes | Yes | Yes | Yes | Yes | Yes 2e | 75.9 | 6.4 | 29 |
| 2 | 20/21 | 68 | 34.4 | Yes | Yes | Yes | Yes | Yes | b | Yes g | 85.0 | 1.6 | 5 |
| 7 | 17/18 | 68 | 47.2 | | | | | | Yes d | Yes f | 81.7 | 6.8 | 22 |
| 1 | 8/9 | 69 | 39.4 | Yes | Yes | Yes | Yes | Yes | | | 77.7 | 1.5 | 3 |
| 3 | 19/20 | 69 | 43.2 | Yes | Yes | Yes | Yes | Yes | b | b | 60.3 | 3.9 | 17 |
| 5 | 21/22 | 69 | 45.7 | Yes | | Yes | Yes | Yes | T. Precip c | | 77.3 | 5.1 | 12 |
| 7 | 9/10 | 69 | 31.2 | | | Yes | Yes | Yes | Yes | | 70.0 | 4.6 | 14 |
| 8 | 27/28 | 69 | 43.6 | | | Yes | Yes | Yes | Yes e | | 77.9 | 7.0 | 21 |
| 9 | 24/25 | 69 | 41.6 | Yes | | Yes | Yes | Yes | | | 78.5 | b | b |
| 1 | 21/22 | 70 | 44.5 | Yes | | | | | Yes 2 | Yes 2 | 89.6 | 1.3 | 3 |
| 3 | 25/26 | 70 | 30.4 | Yes | Yes | Yes | Yes | Yes | T. Precip c | | 67.1 | 4.0 | 13 |
| 6 | 3/4 | 70 | 42.8 | Yes | Yes | Yes a | Yes a | Yes | Yes e | Yes e | 63.5 | 3.8 | 17 |
| 7 | 8/9 | 70 | 34.3 | | | | | | | | 76.3 | 3.7 | 14 |
| 8 | 5/6 | 70 | 30.1 | Yes | | Yes | Yes | Yes | Yes c | Yes 2c | 72.2 | 4.0 | 13 |
| 8 | 10/11 | 70 | 43.8 | Yes | | | | Yes | Yes 2 | Yes 2e | 64.2 | 4.8 | 17 |
| 9 | 2 | 70 | 33.0 | Yes | Yes | | | Yes | | | 75.7 | 6.0 | 21 |
| 10 | 5 | 70 | 38.6 | Yes | Yes | Yes | Yes | Yes | T. Precip | T. Precip f | 87.2 | 2.3 | 6 |
| 10 | 19 | 70 | 39.3 | Yes | Yes | | | | | | 78.8 | 3.1 | 12 |
| 1 | 25 | 71 | 54.2 | Yes | | Yes | Yes | Yes | Yes | Yes | 65.8 | 2.8 | 9 |
| 2 | 1 | 71 | 30.1 | | Yes | | | Yes | | Yes 2 | 69.6 | 1.2 | 2 |
| 2 | 8 | 71 | 41.1 | Yes | Yes | Yes | Yes | Yes | Yes | Yes 2 | 69.1 | 2.0 | 10 |
| 2 | 15 | 71 | 30.7 | Yes | | Yes | Yes | Yes | Yes e | | 71.9 | 1.8 | 5 |
| 3 | 22 | 71 | 39.2 | | | | Yes | | | | 71.0 | b | b |
| 3 | 24 | 71 | 51.7 | | | "drizzle" | "drizzle" | | | | 73.3 | 1.9 | 6 |
| 5 | 12 | 71 | 39.0 | | | Yes | Yes | Yes | Yes | Yes | 84.5 | 1.9 | 9 |
| 7 | 7 | 71 | 43.2 | | | Yes | Yes | | | | 72.4 | 3.8 | 13 |
| 7 | 22 | 71 | 47.9 | | | "sprinkles" | "sprinkles" | | T. Precip | | 76.1 | 3.6 | 12 |
| 8 | 21 | 71 | 31.1 | | | | Yes | | | | 70.0 | 3.7 | 12 |
| 9 | 15 | 71 | 32.6 | Yes | Yes | Yes | Yes | Yes | | | 67.9 | 1.1 | 4 |
| 11 | 9 | 71 | 39.7 | Yes | Yes | Yes | Yes | Yes | Yes 2 | Yes 2 | 66.9 | 3.2 | 9 |
| 1 | 8 | 72 | 34.5 | Yes | Yes | | | Yes | Yes | Yes | 79.6 | 1.1 | 3 |
| 1 | 18 | 72 | 38.5 | Yes | Yes | Yes | Yes | Yes | Yes | Yes | 82.3 | 1.2 | 3 |
| 1 | 23 | 72 | 41.8 | Yes | | | Yes | Yes | | Yes | 83.0 | 1.3 | 4 |
| 2 | 17 | 72 | 35.2 | Yes | Yes | | | Yes | Yes 2 | Yes 2 | 73.5 | 2.0 | 7 |
| 3 | 8 | 72 | 32.9 | "drizzles" | Yes | Yes | Yes | "drizzles" | | | 84.5 | 2.6 | 7 |
| 3 | 13 | 72 | 55.5 | Yes | "drizzles" | Yes | Yes | Yes | Yes | | 87.7 | 2.2 | 9 |
| 3 | 18 | 72 | 52.6 | "drizzles" | | "drizzle" | Yes | "drizzle" | Yes f | | 83.7 | 4.2 | 13 |
| 6 | 1 | 72 | 33.3 | | | | | | Yes f | | 80.0 | 5.5 | 21 |
| 8 | 5 | 72 | 34.4 | | | Yes | Yes | | | | 60.9 | 4.2 | 13 |
| 4 | 12 | 73 | 37.5 | | Yes | Yes | Yes | Yes | | | 78.1 | 3.6 | 12 |
| 4 | 27 | 73 | 50.3 | | | | | | Yes | Yes | 78.6 | 2.0 | 8 |
| 5 | 12 | 73 | 42.0 | Yes | Yes | Yes | Yes | Yes | "drizzle" | "drizzle" | 80.0 | 3.4 | 8 |
| 5 | 17 | 73 | 72.0 | | Yes | Yes | Yes | Yes | Yes | "drizzle" | 75.6 | 3.5 | 13 |
| 6 | 26 | 73 | 52.0 | Yes | Yes | Yes | Yes | Yes | Yes | Yes | 68.6 | 4.6 | 24 |
| 7 | 1 | 73 | 42.2 | | | | Yes | | | | 74.5 | 4.3 | 14 |
| 7 | 6 | 73 | 35.7 | | | Yes | Yes | | | T. Precip | 80.8 | 1.8 | 6 |
| 7 | 11 | 73 | 42.6 | | | Yes | Yes | | | | 75.8 | 3.7 | 13 |
| 7 | 31 | 73 | 31.1 | | | Yes | Yes | | Yes f | | 75.9 | 3.7 | 12 |
| 8 | 5 | 73 | 30.6 | | | | | | T. Precip | T. Precip | 85.3 | 4.1 | 10 |
| 9 | 14 | 73 | 42.8 | "drizzle" | "drizzle" | "drizzle" | "drizzle" | "drizzle" | | "drizzle" | 86.8 | 4.2 | 11 |
| 9 | 19 | 73 | 36.1 | | | Yes | Yes | | | | 83.5 | 4.4 | 19 |
| 11 | 8 | 73 | 39.0 | | Yes | | | Yes | Yes | Yes 2 | 64.5 | 2.3 | 8 |
| 5 | 7 | 74 | 33.8 | | | Yes | Yes | | | | 84.3 | 5.3 | 11 |
| 6 | 6 | 74 | 42.3 | | Yes | Yes | Yes | Yes | T. Precip | | 78.1 | 3.9 | 12 |
| 6 | 11 | 74 | 44.5 | | | Yes | Yes | Yes | | | 78.9 | 4.8 | 11 |
| 9 | 10 | 74 | 32.4 | | Yes | Yes | Yes | Yes | Yes | Yes | 76.9 | 6.7 | 24 |
| 9 | 19 | 74 | 38.9 | Yes | Yes | Yes | Yes | Yes | Yes | | 78.8 | 4.8 | 21 |
| 10 | 14 | 74 | 38.4 | Yes | Yes | Yes | Yes | Yes | Yes 2 | Yes 2 | 75.1 | 4.9 | 18 |

Notes:

a Fog forecast for early part of second day on 8:00 am to 8:00 am sampling schedule
b Data not immediately available
c Observed during early part of second day on 8:00 am to 8:00 am sampling schedule
d Fog observed during second day segment of sample - no time of observation given
e Observed in hours prior to beginning of sample
f No time indicated for observation (possible internal inconsistency in records)
g Fog prior to sample, trace precipitation or "drizzle" during sample
2 Heavy Fog

Relative humidity and ozone averages are taken for the 24 hour period corresponding to sulfate samples. Missing hourly data were replaced by linear interpolation between adjacent data points prior to averaging. 24 hour average relative humidity values are approximate since observations are taken for 14 hours daily, thus necessitating extensive interpolation.

T. Precip. - Trace of precipitation

(Source: Cass, 1975)

occur inland from downtown Los Angeles, it must be remembered that the sulfate measurements studied here were taken at downtown Los Angeles and oxidant concentrations measured farther downwind may not be particularly relevant to explaining events at this location.

From the above discussion we wish to draw two more important physical generalizations.

Generalization 6: The most important phenomena explaining the large fluctuations in sulfate level from day to day are meteorological in nature. Low afternoon inversions concentrate sulfate pollutants near ground level. High relative humidity or fog seems to accelerate the conversion of $SO_2$ to form sulfate or to otherwise increase the total quantity of sulfate formed.

Generalization 7: A variety of sulfate formation mechanisms are probably important in the Los Angeles atmosphere.

From the order of entry of explanatory variables in the regression results of Tables 2.15 and 2.16, plus the persistence of fog associated with high sulfate levels in Table 2.17, one is led to speculate that heterogeneous reactions involving wetted particles are the dominant determinants of $SO_2$ oxidation rate on days of high sulfate levels in the Los Angeles Basin. However, apparent dependence of sulfate levels on both relative humidity, photochemical indicators (oxidant) and ambient particulate concentrations suggest that sulfate levels do respond to increases in nearly all the main ingredients of all of the competitive reaction processes (while not responding significantly

to largely unrelated pollutants like total hydrocarbons, which are mostly a measure of the extent to which ambient methane has been diluted on a given day).

Rate constants and catalyst concentration data needed to model the details of the chemical conversion of $SO_2$ to form sulfate in an atmosphere characterized by a competition between these many possible reaction paths are simply unavailable. Some approximations must be made if modeling is to proceed on the basis of currently available data.

One reason why so many competitive reaction paths are under consideration is that all of these reactions are likely to result in a relatively slow macroscopically observed rate of $SO_2$ oxidation on the average over long periods of time. Overall average $SO_2$ oxidation rates of a few percent per hour are expected. A useful approach at this point would seem to be to concentrate on calculating this overall average oxidation rate from the available monitoring data.

Slow chemical conversion processes often are approximated well by a pseudo-first order (exponential) decay. In the absence of $SO_2$ deposition at the ground, the reaction of $SO_2$ to form sulfate would be simplified and expressed as:

$$\frac{dS_{SO_2}}{dt} = -k[S_{SO_2}] \tag{2.7}$$

where k is the pseudo-first order rate "constant" for oxidation of $SO_2$ by all competing chemical mechanisms acting simultaneously. Sulfur dioxide removal is accompanied by sulfate formation:

$$\frac{dS_{SO_4}}{dt} = k[S_{SO_2}] \qquad (2.8)$$

Data on atmospheric sulfate concentrations and bounds on the fraction of sulfur present in the particulate phase are available. That means that in an air quality modeling exercise one can assume successive values for k, and check those assumptions against a fully determined system until the value of k is attained that best satisfies both the observed sulfate levels and the required relationships between sulfate and $SO_2$. No arbitrary assumptions are required.

Simply knowing whether the average $SO_2$ conversion rate, k, is 3% per hour or 10% per hour would make a great deal of difference to the further work that a theoretical chemist might need to undertake to satisfactorily come up with a mix of mechanisms that would yield plausible results. Furthermore, knowledge of whether or not a strong seasonal variation in reaction rate was needed to explain summer sulfate peaks would help one generate a credible mix of reaction mechanisms.

## 2.5 Summary of Implications for a Sulfate Air Quality Modeling Study

The availability of sulfur dioxide and sulfate air quality data in the South Coast Air Basin has been reviewed. The years 1972 through 1974 appear to form an attractive base time period for a sulfate air quality modeling study. During those years, the Los Angeles APCD, EPA's CHESS program and the National Air Surveillance Network air monitoring programs operated concurrently, yielding the widest available geographic coverage of sulfate air quality data.

Spatial gradients in sulfate concentration during those base years suggest that the atmosphere over metropolitan Los Angeles is enriched in sulfates when compared to surrounding areas in all directions. Over the Channel Islands and the Mojave Desert, to the southwest and northeast of the Basin, respectively, sulfate concentrations averaged 3 to 5 $\mu gm/m^3$. Onshore, to the northwest of Los Angeles County at Thousand Oaks, and to the southeast in San Diego County at Vista, sulfate concentrations averaged about 9 $\mu gm/m^3$. In contrast, average sulfate concentrations in the center of the South Coast Air Basin within metropolitan Los Angeles, Orange, San Bernardino and Riverside Counties ranged from 11 to 14 $\mu gm/m^3$. This localized sulfate enrichment makes the central portion of the South Coast Air Basin an ideal candidate for a sulfur oxides emissions to sulfate air quality modeling study. A distinct increment in sulfate levels above background has been found in an area where long-distance transport from sources outside the air basin is unlikely to be the entire explanation for observed sulfate concentrations.

Seasonal fluctuations in sulfate air quality have been shown to be similar throughout the entire South Coast Air Basin. A broad summer seasonal peak is apparent in all years of record, with occasional high values occurring in some winters of record. Observations taken at most stations on the same day are so highly correlated that they would be considered mutually dependent. The implication for our modeling study is that the major factors influencing 24-hour average sulfate air quality are felt basin-wide. Detailed

spatial representations of meteorological parameters and chemical reactions within our air quality model may be unnecessary. A relatively uncomplicated emissions to air quality model should be attempted initially to test its explanatory power.

The fraction of atmospheric sulfur present as particulate sulfur oxides, $f_s$, has been explored in relation to major $SO_x$ emission source locations and general air transport patterns in the South Coast Air Basin. Average values of $f_s$ were found to vary widely from one monitoring organization to another, and even varied substantially between nearby stations within the same monitoring program. This is due to inconsistencies in measured sulfur dioxide levels from one station to another. Nevertheless, it was found that the fraction of total sulfur present as sulfates increases with distance downwind from major $SO_2$ emission sources located in the Los Angeles harbor area. This behavior is consistent with the hypothesis that $SO_2$ is converted to form sulfates in the atmosphere downwind of these emission sources. That behavior is also consistent with preferential removal of $SO_2$ at the earth's surface as air parcels move downwind. These two $SO_2$ removal processes will have to be considered in our modeling study. The available data on the fraction of sulfur present in the particulate phase was judged to be less reliable than the sulfate data, and will hamper attempts to accurately confirm the rate at which $SO_2$ is oxidized to form sulfates in the Los Angeles atmosphere.

The availability of monitoring data on both sulfates and fraction sulfur present as sulfates restricts the geographic area over which air

quality model calculations may be compared to field observations. The Los Angeles County and Orange County coastal plains, plus the San Gabriel Valley are relatively well monitored. In contrast, the San Fernando Valley contains only one sulfate monitoring site in its interior (Reseda) and one site at its entrance (Burbank). The same circumstance occurs in the San Bernardino Valley, where useful sulfate and sulfur dioxide data are available simultaneously only at a single isolated monitoring site. Sulfate data are unavailable in the Oxnard, Ventura and Santa Barbara portions of the airshed. The area over which a sulfur oxides emissions to sulfate air quality model might be specified with the possibility of closely verifying its predictions is largely confined to coastal Los Angeles County south of the Santa Monica Mountains, plus Orange County and the San Gabriel Valley.

Fluctuations in measured sulfate values from day-to-day have been shown to track changes in inversion height, relative humidity, total suspended particulate levels and oxidant concentrations. From these relationships, it is suggested that day-to-day fluctuations in sulfate concentration are driven mainly by changes in factors affecting $SO_2$ to sulfate reaction rate and by changes in the effective volume of the reactor.

Meteorological parameters important to sulfate dilution and transport are inversion height movement and vector valued wind. Very low morning inversions permit pollutant emissions from elevated sources to be injected at least temporarily above the mixed layer. Low afternoon inversions determine the maximum vertical dilution of air parcels

residing below the inversion base. Scalar valued wind speed did not prove significant in explaining changes in sulfate level from one day to the next. It is therefore suggested that vector valued wind behavior, which determines air parcel retention time in the air basin, would be more important to sulfate concentrations than initial dilution at the source.

Sulfate levels have been shown to closely track changes in relative humidity and suspended particulate levels, with additional intrusion of fog on days of very high sulfate concentrations. On this basis one could speculate that heterogeneous oxidation of $SO_2$ on or within wetted particles is very important to high sulfate levels in Los Angeles. Sulfate concentrations are also slightly (but significantly) higher on days with elevated oxidant levels. Thus a variety of homogeneous gas-phase sulfate formation mechanisms may also be important.

In light of the complexity of the details of the chemical reactions possible, chemical conversion of $SO_2$ to form sulfate will be modeled as a slow pseudo-first order reaction. Emphasis should be placed initially on solving for the overall $SO_2$ oxidation rate and on identifying any seasonal trend in oxidation rate that may guide future theoretical investigations.

Two central questions to be answered by a study of the long-term relationship between sulfur oxides emissions and sulfate air quality are posed. Can the demonstrated sulfate enrichment above background in the Los Angeles metropolitan area be reasonably explained in terms

of local sulfur oxides emission sources? And if so, how do sulfur oxides emissions which are concentrated at a relative handful of locations along the coast become mapped into an average sulfate air quality pattern which is so nearly uniform over such a large geographical area?

# CHAPTER 3

# A SIMULATION MODEL FOR SULFATE FORMATION AND TRANSPORT UNDER UNSTEADY METEOROLOGICAL CONDITIONS

## 3.1 Introduction

An appropriate means must be constructed for relating sulfur oxides pollutant emissions to observed sulfate air quality over the central portion of the Los Angeles Basin. In the preceding chapter, it was decided that our understanding of emissions-air quality relationships would be verified by simulating monthly average sulfate concentrations observed during the years 1972 through 1974. For this reason, an air quality model capable of simulating long-term average sulfate concentrations must be selected.

Techniques in current use for modeling long-term average emissions-air quality relationships first will be reviewed. Commonly employed modeling methods lack the ability to calculate long-term average pollutant concentrations in a geographic region like Los Angeles which is characterized by unsteady meteorological conditions (e.g. light and variable winds). To resolve this problem, a simulation model will be constructed which calculates long-run average pollutant levels using a Lagrangian marked particle technique. The model will be derived for first-order chemical reaction and dry deposition of sulfur oxides dispersing in an airshed which experiences a temperature inversion aloft. Then a series of approximations will be made which permit the model

to be applied to simulation of long-run average sulfate concentrations in Los Angeles using readily available meteorological data.

## 3.2 An Overview of Long-Term Average Air Quality Models

Long-term average air quality models in current use are of two general types: empirical models based on statistical analysis of air quality data, and deterministic models based on the atmospheric diffusion equation.

### 3.2.1 Empirical Emissions to Air Quality Models

Statistical techniques have been widely applied as the primary means of developing empirical emissions-air quality relationships. The frequency distribution of existing air pollutant levels in the air basin of interest is first established from ambient air monitoring data by methods such as those of Larsen (1971). Then linear or non-linear rollback techniques are used to make air quality projections. Linear rollback models assume that current air quality levels are proportional to current basin-wide emissions levels, and that ambient pollutant concentrations will decline in proportion to emission reductions until background air quality is reached at zero emissions. Non-linear rollback models hold that air quality response to an emission change for a reactive contaminant is some stated non-linear function of current contaminant emissions or air quality levels. Examples of linear and non-linear rollback models recommended by the U.S. Environmental Protection Agency are found in the Federal Register, (36 F.R. 158, August 14, 1971, pp. 15489-15491 and Appendix J). The sulfate air

pollution control strategy study conducted by Trijonis, et al. (1975) depends on a linear rollback calculation.

Linear rollback models assume uniform proportionate response at all receptor points due to a change in emissions anywhere in the air basin. Thus linear rollback models are likely to be valid only under a very limited set of circumstances. Situations in which a simple rollback air quality projection is likely to fail include cases where

(a) the relative spatial distribution of emission source strength is to be changed;

(b) changes are made in source effective stack height;

(c) atmospheric chemical reactions introduce non-linear effects; and

(d) unsteady meteorological conditions require an explicit treatment of source to receptor transport.

Spatial homogeniety of emission reduction is seldom achieved in any real situation involving a stationary source emission control strategy. Simple linear rollback models are of questionable utility in these cases. Spatial homogeniety assumptions can be relaxed so that the effect of controlling geographically dissimilar source classes to different degrees of stringency may be deduced (provided that a long history of emissions and air quality data is available for model development; see Cass, 1975). However, as model complexity increases, the effort involved in constructing an empirical emissions-air quality model can quickly approach that required for a deterministic representation of the problem based on solution of the atmospheric diffusion equation.

### 3.2.2 Models Based on a Description of Atmospheric Transport and Chemistry

Deterministic emissions to air quality models are distinguished into two types based on the coordinate system employed: Lagrangian or Eulerian. In the Lagrangian approach, air pollutant dispersion is represented by the trajectories of representative fluid particles. The underlying coordinate system is tied to the moving fluid particle. Pollutant concentrations at downwind receptor locations are determined by the probability that a pollutant-laden fluid parcel emitted at a known time, t', and place, X', will occupy a given location, X, in the airshed at later time t.

A generalized expression for most Lagrangian air quality models in current use is of the form:

$$\langle c(X,t)\rangle = \int_{-\infty}^{\infty}\int_{-\infty}^{\infty}\int_{-\infty}^{\infty} Q(X,t|X_o,t_o)\langle c(X_o,t_o)\rangle R(t,t_o)dX_o + \int_{-\infty}^{\infty}\int_{-\infty}^{\infty}\int_{-\infty}^{\infty}\int_{t_o}^{t} Q(X,t|X',t')S(X',t')R(t,t')dt'dX' \quad (3.1)$$

where

| | |
|---|---|
| $\langle c(X,t)\rangle$ | is the ensemble mean pollutant concentration at point X at time t. |
| $Q(X,t\|X',t')$ | is the transition probability density that a fluid particle at location X' at time t' will undergo a displacement to location X at time t. |
| $R(t,t')$ | is the probability that a fluid particle will retain its chemical identity at time t' until time t. |

$S(X',t')$ is the spatial-temporal distribution of emission sources, in mass per location per unit time.

$X_o$ and $t_o$ establish initial conditions for location and time within the airshed.

The form in which equation (3.1) is expressed is largely as developed for air quality modeling by Lamb (see Lamb and Neiburger, 1971; Lamb, 1971; Lamb and Seinfeld, 1973).

The first integral term on the right hand side of equation (3.1) maps initial pollutant concentration in the airshed into its effect on air quality at time t. The second term on the right hand side of equation (3.1) computes the effect of fresh emissions on air quality over the time interval $t_o$ to t. The chemical reaction expressions $R(t,t_o)$ and $R(t,t')$ in equation (3.1) are valid for first-order chemistry. For first-order chemistry, each fluid particle's probability of undergoing chemical reaction is independent of the chemical conversion of other particles of that species elsewhere in the system. In that case, fluid transport and fluid chemistry are independent. The probability that the fluid particle is found at location X, at time t is thus simply the product of the transition probability $Q(X,t|X',t')$ that air parcel transport to that location will occur, times the probability $R(t,t')$ that the chemical status of that air parcel will not change in the interim.

Eulerian air quality models rely on a mass balance constructed for a volume element which is fixed in space. The instantaneous pollutant concentration for each species i, $c_i$, within that volume element must satisfy the following continuity equation:

$$\frac{\partial c_i}{\partial t} + \frac{\partial u_j c_i}{\partial x_j} = D_i \frac{\partial^2 c_i}{\partial x_j \partial x_j} + R_i(c_1,\ldots,c_N,T) + S_i(X,t) \qquad (3.2)$$

$$i = 1,2,\ldots,N$$
$$j = 1,2,3$$

where

$u_j$ is the fluid velocity in the $j^{th}$ coordinate direction at the location of interest.

$D_i$ is the molecular diffusivity of species i in the air within the control volume.

$R_i$ is the rate of formation of species i by chemical reaction (as a function of pollutant concentrations and temperature, $T$).

$S_i$ is source strength for species i within the volume element.

X is location, given as $(x_1, x_2, x_3)$.

t is time.

From this fundamental mass balance, one can derive an approximate relationship for the mean concentration of a pollutant species (see Lamb and Seinfeld, 1973).

$$\frac{\partial \langle c_i \rangle}{\partial t} + \frac{\partial}{\partial x_j}(\bar{u}_j \langle c_i \rangle) = \frac{\partial}{\partial x_j}\left(\bar{K}_{jk} \frac{\partial \langle c_i \rangle}{\partial x_k}\right)$$

$$+ R_i(\langle c_1 \rangle,\ldots,\langle c_N \rangle) + S_i(X,t) \qquad (3.3)$$

$$i = 1,2,\ldots,N$$
$$j = 1,2,3$$
$$k = 1,2,3$$

where

$\bar{u}_j$ is the average wind velocity in the $j^{th}$ coordinate direction.

$\bar{K}_{jk}$ is the atmospheric eddy diffusivity tensor.

Usually it is assumed for convenience that $\bar{K}_{jk} = 0$ for $j \neq k$.

For a discussion of the theoretical relationship between the modeling approaches of equations (3.1) and (3.3), see Lamb and Seinfeld (1973). For a discussion of some of the implications of the assumptions needed to introduce those equations into practical urban air quality models, see Liu and Seinfeld (1975).

### 3.2.3 Application of Deterministic Air Quality Models to the Calculation of Long-Term Average Air Quality

There are two methods in current use for modeling long-run average air pollutant concentrations. A dynamic model for short-term concentration predictions could be developed based on equations (3.1) or (3.3). Then the very large number of nearly instantaneous concentration predictions that result could be averaged. However, when a fully determined short-term urban air quality simulation is run over a period of several years, the computing resources required become enormous if the simulation is at all realistic. For that reason, long-term average air pollutant levels are usually calculated using pseudo-steady state models.

Pseudo-steady state air quality models are derived from a Lagrangian formulation of the atmospheric diffusion equation, such as given in (3.1). The objective of these models is to directly calculate a

long-term average concentration as a function of location within the airshed:

$$\overline{\langle c(X) \rangle} = \frac{1}{T} \int_0^T \langle c(X,t) \rangle dt \qquad (3.4)$$

where T, in our case, is a month or a year in duration.

Long-term average air quality models in current use view meteorological behavior as a sequence of steady state conditions. Steady meteorological conditions exist when constant wind speed, wind direction, and atmospheric stability persist for time periods longer than the characteristic time for which an air pollutant parcel's contribution to observed air quality remains significant. That time period would correspond to the shorter of either the characteristic time for advection to beyond the boundaries of the air basin, or the time needed for dilution to reduce pollutant concentration to insignificance. One can see that many locations affected by light and variable winds may not often encounter meteorological circumstances which satisfy this steady state definition. Therefore, for the sake of discussion, Seinfeld (1975) defines two meterological domains.

$\Omega_s$ = the collection of all time intervals during the long time period (0,T) in which wind speed exceeds a defined minimum value, and the meteorology is steady.

$\Omega_u$ = the collection of all time intervals during the long time period (0,T) in which either the wind speed does not exceed a defined threshold (stagnation conditions) or the meteorology is unsteady.

For the simple case of an inert pollutant with $\langle c(X,t_o) \rangle = 0$ and $t_o = 0$, substitution of equation (3.1) into (3.4) plus a separation

of meteorological conditions into domains $\Omega_s$ and $\Omega_u$, Seinfeld (1975) obtains an expression for long-term average pollutant concentration against which virtually all long-run average emissions-air quality models may be judged.

$$\overline{<c(X)>} = \int_{-\infty}^{\infty}\int_{-\infty}^{\infty}\int_{-\infty}^{\infty} \sum_{m=1}^{M} \sum_{i=1}^{N_1} \sum_{j=1}^{N_2} f_{ijm} g(X,X',U_i,\theta_j,\sigma(t_{ijm}))S(X',t_{ijm})\Delta t_{ijm} dX'$$

$$+ \int_{-\infty}^{\infty}\int_{-\infty}^{\infty}\int_{-\infty}^{\infty}\int_{\Omega_u} \overline{Q}(X,X',t';T)S(X',t')dt'dX' \qquad (3.5)$$

where the newly introduced terms are:

$f_{ijm}$ the joint frequency distribution of wind speed, wind direction, and atmospheric stability class during the m periods of steady meteorology which make up domain $\Omega_s$.

$g(X,X',U_i,\theta_j,\sigma(t_{ijm}))$
a diffusion kernel which gives the response at location X to a unit source at location X' which began emitting at time t' under *steady* meteorological conditions. Usually the form of $g(X,X',U_i,\theta_j,\sigma(t_{ijm}))$ is obtained from a Gaussian plume formula (see Turner, 1969).

$U_i$ scalar wind speed, expressed within speed class intervals $i = 1,\ldots,N_1$.

$\theta_j$ wind direction blowing into sector j.

$\sigma(t_{ijm})$ the standard deviation of plume spread about its centerline as a function of travel time.

$\Delta t_{ijm}$ the length of the $m^{th}$ steady meteorological time interval (with wind speed in class i and wind direction into sector j).

$\overline{Q}(X,X',t';T)$ an averaged source to receptor transport probability equal to

$$\frac{1}{T}\int_{t'}^{T} Q(X,t|X',t')dt \ .$$

Equation (3.5) is the complete expression for the long-run average concentration of an inert pollutant. Existing long-term average air quality models, however, commonly evaluate only the steady state joint Gaussian term [i.e. the first term on the right hand side of equation (3.5)]. Popular long-run average models which do not treat unsteady meteorological conditions include those of Martin and Tikvart (1968), Calder (1971) and Gifford and Hanna (1970). Seinfeld (1975) notes that the neglect of the unsteady meteorological domain $\Omega_u$ can be a serious problem with typical long-run average air quality models:

> "Because the form of $\overline{Q}$ under dynamic or stagnant conditions is very difficult to determine, most steady-state models based on (3.5) neglect the contribution to $\langle c(X) \rangle$ from $\Omega_u$. Unfortunately, during stagnation periods the contribution to the overall long-term average concentration $\langle c(X) \rangle$ is the most important. Thus, steady-state models based on $\Omega_s$ may underestimate the long-term average concentration."

## 3.3 A Long-Term Average Model for Sulfate Air Quality Under Unsteady Meteorological Conditions

Examination of Los Angeles meteorology indicates that the steady state assumptions inherent in conventional long-term average air quality models are regularly violated in this locale. The Los Angeles Basin is influenced by coastal meteorology characterized by a daily land breeze/sea breeze wind reversal. Differential solar heating of land and sea surfaces leads to a daytime wind pattern with transport inland across the coastline as shown in Figure 3.1. At night, the characteristic transport pattern reverses. Slow drainage winds and land breeze conditions cause flow out to sea, as shown in Figure 3.2. Early morning

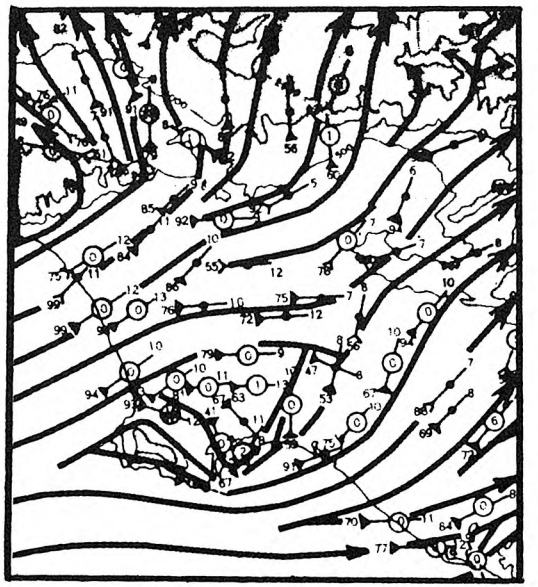

Typical Afternoon Onshore Flow Pattern
July 12:00-18:00 Hours PST

FIGURE 3.1

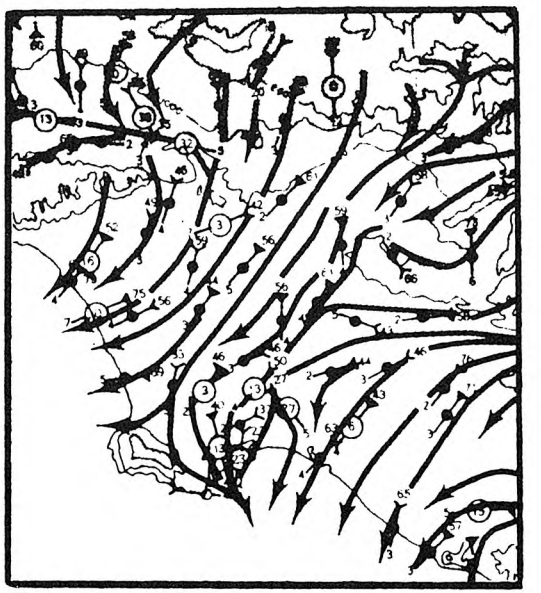

Typical Late Night
Offshore Flow Pattern
October 00:00-07:00 Hours PST

FIGURE 3.2

(from DeMarrais, Holzworth and Hosler, 1965)

and early evening wind stagnation periods occur as transition from one transport direction to another takes place.

Secondly, there is a strong diurnal variation in inversion base behavior over the Los Angeles Basin. Solar heating of the land surface causes the base of low overnight inversions to be eroded by warming of air from below during the day. Superimposed on this is a sinking motion induced by the Pacific Anticyclone which causes the inversion base to descend again at night after the strong solar input has ceased. Thus maximum air parcel dilution in the vertical direction changes drastically as a function of time during air parcel transport across the basin. This too violates steady state assumptions.

A pseudo-steady state model for ground level area source emission of a conserved pollutant might still function reasonably well in Los Angeles. That would be the case if relative pollutant dilution were so rapid as to shorten the time, $\Delta t_m$, over which steady state conditions had to be maintained in order to reasonably reproduce observed air quality. For carbon monoxide emissions from automotive traffic, observed air quality is often dominated by emissions from the immediate neighborhood of the receptor point. A succession of steady state conditions might still be used to represent transport over such short travel distances.

However, sulfate air quality is the result of atmospheric chemical reactions in which sulfates are formed with travel distance downwind. Dilution is not sufficiently rapid to overwhelm sulfate formation rates. For that reason, the time interval, $\Delta t_m$, over which steady state

transport conditions would have to be maintained in order to model sulfate concentrations is limited by the time necessary for an air parcel to clear the airshed. In Los Angeles, the characteristic times for wind reversal, inversion base change, and air stagnation periods are shorter than transport times out of the air basin. An air parcel may wander in the basin for more than a day until a high speed wind event clears it from the airshed. For that reason, a long-term average air quality model for sulfate formation in Los Angeles will have to cope with unsteady meterological conditions.

Lamb and Seinfeld (1973) suggest that the only feasible way of determining source to receptor transport probabilities under unsteady meterological conditions is by means of a simulation model. Analytical solutions are unavailable. Lamb (1971) has used Deardorff's (1970) planetary boundary layer model to explore such a simulation for a single point source release into an atmosphere with a steady wind but inhomogeneous non-stationary turbulence. In the following sections of this chapter, we will describe the formulation of a multiple source urban simulation model for long-term average sulfate concentrations. The model uses a Lagrangian marked particle technique to compute source to receptor transport and reaction probabilities in accordance with the time sequence of meteorological events. The model is derived for a geographic region characterized by unsteady meteorological conditions and an idealized persistent temperature inversion aloft. First order chemical reactions and pollutant dry deposition are incorporated.

At first, the progress of a single representative fluid particle containing sulfur oxides will be tracked through the airshed. Then by integrating over all such particles in the airshed, general expressions will be written for the average concentration of sulfur dioxide and sulfates within a ground level receptor cell. Finally, the meteorological data available for Los Angeles will be examined and the general approach to tracking fluid particle location and chemical status will be reduced to a specific computational procedure. Long-run average pollutant concentrations may then be resolved by simulating release of sulfur oxides-laden fluid particles from a multiplicity of urban source classes.

### 3.3.1 Single Particle Transport and Reaction Probabilities

Consider the history of a fluid particle containing a sulfur oxide molecule which was emitted from location $X'$ at time $t_o$. The fluid particle has several important attributes which determine its future importance to observed sulfate air quality. These attributes include:

(a) a time history of its trajectory across the air basin in the horizontal plane

(b) its position over time in the vertical dimension

(c) its initial chemical composition

(d) its chance of being absorbed by reaction with the earth's surface, and

(e) its chance of undergoing atmospheric chemical reactions.

We wish to know the likelihood that this representative fluid particle will be present as a sulfate molecule within the ground level air volume surrounding location $X(x_1,x_2,0)$ at future time $t = (t_o + n\Delta t)$.

The trajectory and chemical history of each fluid particle is determined by a sequence of meteorological events, and by the air parcel's retention time in the airshed. Let the fluid particle's history be broken down into n short time steps of $\Delta t$ in duration, each short enough that meteorological conditions were unchanging over the span of one time step. Since these time steps may be arbitrarily small, even unsteady meteorological conditions, as defined previously, may be represented easily.

A set of physical rules will be specified which allows one to calculate the air parcel's likely chemical status and location at the end of a single time step, $n_j$, given its initial starting conditions and its status at the end of the $n_{j-1}^{th}$ time step. Then the fluid particle's probable location over time can be modeled as the result of a stochastic chain of events.

The transition probabilities linking this chain of events are functions of meteorological conditions and chemical reaction paths. In order to specify one form of those functions, our air quality model will be derived for air pollution problems which may be approximated by the following idealized meteorological and chemical conditions:

(1) *The important chemical reactions and pollutant removal paths to be considered are confined to pseudo-first order reactions and ground level dry deposition.*

(2) *The geographic region of interest is characterized as having an idealized persistent temperature inversion.* An idealized temperature inversion is defined as a multi-layered system, with unstable air from ground level to height h(x',t'), and a stable layer of air from height h(x',t') upward. The function h(x',t') will be referred to as the inversion base height.

(3) *The case will be considered in which inversion base height above ground level may be taken as independent of location in the horizontal plane at any single time.* Inversion base height, however, varies with time throughout the airshed; h(x',t') equals h(t') alone.

(4) *Vertical mixing of air parcels within the unstable layer next to the ground is assumed to be quasi-instantaneous.* By that, we mean that the time scales used to integrate the transport equations may be made long compared to the time scales for vertical mixing.

(5) *Vertical diffusion will be neglected for air parcels located within the stable portion of the elevated temperature inversion.*

(6) *Vertical exchange between air parcels embedded within the inversion and those below the inversion base takes place as the inversion base height changes with time.* Air parcels located above the inversion base are fumigated downward as the inversion base height, h(t), rises during the day to intercept a previously stable air mass at height H within the inversion. At night the inversion base descends. Some of the

air parcels which were previously located in the mixed layer next to the ground are now trapped above the new lowered inversion base and are stabilized to prevent further vertical motion or contact with the ground. Air parcels remaining below the overnight inversion base are still free to mix vertically and maintain a uniform distribution between ground level and inversion base in the presence of ground level removal processes. The inversion thus described acts much like a diode in an electric circuit. It insures vertical transport and mixing as the inversion base rises but does not reconcentrate previously diluted pollutants as the inversion base is lowered.

The idealized physical setting hypothesized above will not necessarily be found in any particular airshed. The degree to which an air pollution problem in a given geographic region corresponds to that description of course can be tested on a case by case basis.[1]

Factors affecting vertical dilution within our idealized airshed are specified independently of air parcel location in the horizontal plane at any single time. In that case we find it convenient to separate calculation of horizontal source-to-receptor transport probability from vertical transport. The chemical status of each air parcel

---

[1]For example, the assumption of direct modulation of ground level sulfate concentrations by inversion base location is supported in the Los Angeles basin by the strong correlation between inversion base height and sulfate levels shown in the analysis of Cass (1975) presented in Chapter 2 of this study. (See correlation matrices of Appendix B8).

will depend on ground level deposition of sulfur oxides, which in turn depends on whether the fluid particle's likely vertical location is above or below the inversion base. Thus vertical motion and pollutant chemistry must be combined.

### 3.3.2 Vertical Motion and Pollutant Chemistry

We wish to construct a set of rules by which we may calculate the probability that a given fluid particle containing a sulfur oxides molecule is both in communication with ground level (i.e. below the inversion base within the fully-mixed layer) and is present as sulfates (rather than $SO_2$). These are the two obvious conditions which must be met if the pollutant emission is to contribute to ground level sulfate air quality. First the initial conditions present after parcel insertion into the atmosphere will be considered.

The following terms are defined:

$U_a(\phi)$ = a unit step function

$$U_a(\phi) = \begin{cases} 0 & \text{when } \phi \leq a \\ 1 & \text{when } \phi > a \end{cases}$$

$P_{SO_{2a}}(t|t_o,i)$ = the probability that a fluid particle is above the inversion base at time t, and that its chemical identity is as $SO_2$, given that it was emitted from source class i at time $t_o$.

$P_{SO_{4a}}(t|t_o,i)$ = the probability that a fluid particle is above the inversion base at time t, and that its chemical identity is as $SO_4^=$, given that it was emitted from source class i at time $t_o$.

$P_{SO_{2b}}(t|t_o,i)$ = the probability that a fluid particle is below the inversion base at time t, and that its chemical identity is as $SO_2$, given that it was emitted from source class i at time $t_o$.

$P_{SO_{4b}}(t|t_o,i)$ = the probability that a fluid particle is below the inversion base at time t, and that its chemical identity is as $SO_4^=$, given that it was emitted from source class i at time $t_o$.

$P_{SO_{2d}}(t|t_o,i)$ = the probability that a fluid particle emitted from source class i which resided below the inversion as $SO_2$ has deposited at the ground between time t and time $t_o$.

$P_{SO_{4d}}(t|t_o,i)$ = the probability that a fluid particle emitted from source class i which resided below the inversion as $SO_4^=$ has deposited at the ground between time t and time $t_o$.

At the time of fluid particle release, $t_o$, from source class i at effective stack height $H(t_o,i)$ the initial probability of finding the fluid particle in a given compartment depends only on exhaust gas composition and height of insertion into the atmosphere:

$$P_{SO_{2a}}(t_o,i) = U_{h(t_o)}(H(t_o,i)) \cdot [1 - f_{s_o}(i)] \quad (3.6)$$

$$P_{SO_{4a}}(t_o,i) = U_{h(t_o)}(H(t_o,i)) \cdot f_{s_o}(i) \quad (3.7)$$

$$P_{SO_{2b}}(t_o,i) = [1 - U_{h(t_o)}(H(t_o,i))] \cdot [1 - f_{s_o}(i)] \quad (3.8)$$

$$P_{SO_{4b}}(t_o,i) = [1 - U_{h(t_o)}(H(t_o,i))] \cdot f_{s_o}(i) \quad (3.9)$$

$$P_{SO_{2d}}(t_o,i) = 0 \quad (3.10)$$

$$P_{SO_{4d}}(t_o,i) = 0 \quad (3.11)$$

where

$f_{s_o}(i)$ is the initial fraction of the sulfur oxides from source class i which are present in the particulate phase (e.g. as sulfates or sulfuric acid mist).

Examining the arguments of the unit step functions in equations (3.6) through (3.11) we note that

$$P_{SO_{2a}}(t_o,i) + P_{SO_{4a}}(t_o,i) + P_{SO_{2b}}(t_o,i) + P_{SO_{4b}}(t_o,i) + P_{SO_{2d}}(t_o,i) + P_{SO_{4d}}(t_o,i) = 1 \qquad (3.12)$$

Schematically, we have two possible initial conditions as shown in Figure 3.3. The first case represents pollutant insertion below the inversion base with rapid vertical mixing. In the second case, the plume is inserted into the stable layer aloft and no fluid particles are found initially in the mixed layer below the inversion base.

Next, we must define a set of rules which will propagate the air parcel's probable status from that initial condition through each successive time step. First consider atmospheric chemistry and pollutant dry deposition.

Atmospheric chemical reactions compete with dry deposition for the removal of $SO_2$ molecules from the gas phase within the mixed layer. In Chapter 2, it was decided that chemical conversion of $SO_2$ to form sulfates would be modeled as a pseudo-first order chemical reaction. $SO_2$ dry deposition may also be represented as a simple first order process. Within our fully mixed layer next to the ground, a differential equation for $SO_2$ removal from the gas phase would be:

$$\frac{d\, S_{SO_{2b}}}{dt} = -k\, S_{SO_{2b}} - \frac{V_g}{h} S_{SO_{2b}} \qquad (3.13)$$

FIGURE 3.3

Air Parcel Insertion into the Atmosphere

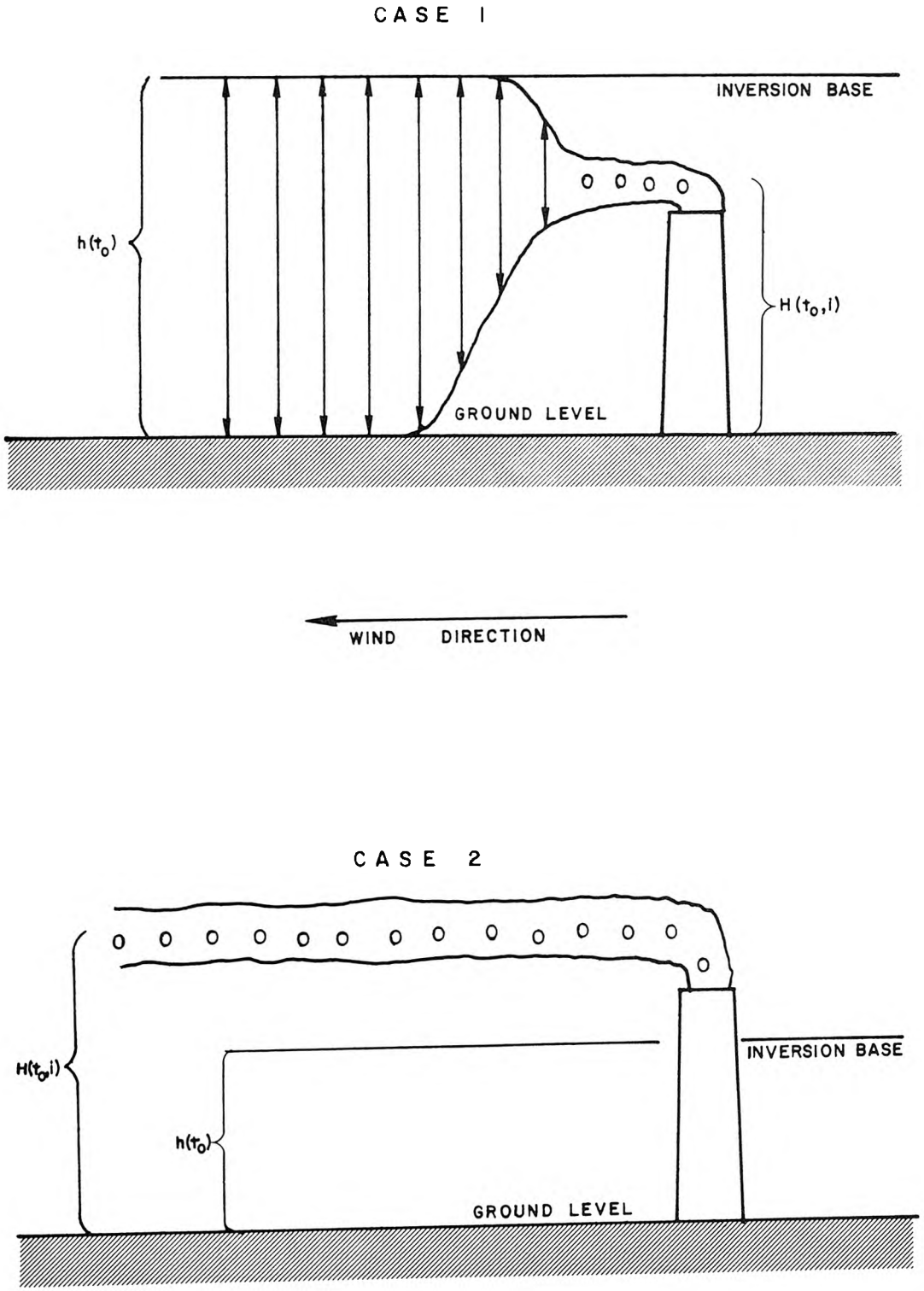

where

$S_{SO_{2b}}$ denotes sulfur atoms present as sulfur dioxide below the inversion base.

$k$ is the pseudo-first order rate constant for oxidation of $SO_2$ to form sulfates by all competing chemical paths.

$V_g$ is the "deposition velocity" for $SO_2$. This is not actually a settling velocity, but rather the ratio between pollutant flux to the ground and atmospheric concentration.

Solving this expression for $SO_2$ removal from the gas phase over a time interval t to $(t+\Delta t)$ which is short enough that $h(t) \approx h(t+\Delta t) \approx h$, we get

$$S_{SO_{2b}}(t+\Delta t) = S_{SO_{2b}}(t) \exp\{-[k + \frac{V_g}{h}]\Delta t\} \qquad (3.14)$$

The term $\exp\{-[k + V_g/h]\Delta t\}$ takes the form of a transition probability that an $SO_2$ molecule in the gas phase within the mixed layer will still be present in that state at the end of a time step of $\Delta t$ in duration.

The sulfur dioxide removed from the gas phase within the mixed layer appears as either sulfates or deposited material at the ground. Changes in sulfate concentration are affected by formation of new material out of the gas phase and by depletion of sulfates by dry deposition at the ground.

$$\frac{d\, S_{SO_{4b}}}{dt} = k\, S_{SO_{2b}} - \frac{V_p}{h} S_{SO_{4b}} \qquad (3.15)$$

where

$V_p$ is the deposition velocity for particulate sulfur oxides.

Ground level deposition of $SO_2$ and sulfates is represented by

$$\frac{d\, S_{SO_{2d}}}{dt} = \frac{V_g}{h} S_{SO_{2b}} \tag{3.16}$$

and

$$\frac{d\, S_{SO_{4d}}}{dt} = \frac{V_p}{h} S_{SO_{4b}} \tag{3.17}$$

Solving equation (3.15) over the time interval t to (t+Δt) in light of the $SO_2$ time history given in equation (3.14) we get

$$S_{SO_{4b}}(t+\Delta t) = S_{SO_{4b}}(t) \exp\{-\frac{V_p}{h} \Delta t\} + \frac{k\, S_{SO_{2b}}(t)}{k + \frac{V_g}{h} - \frac{V_p}{h}} \cdot \left\{ \exp\{-\frac{V_p}{h} \Delta t\} - \exp\{-[k + \frac{V_g}{h}]\Delta t\} \right\} \tag{3.18}$$

Substituting the $SO_2$ time history into equation (3.16) and integrating we get

$$S_{SO_{2d}}(t+\Delta t) = S_{SO_{2d}}(t) + \frac{\frac{V_g}{h}}{k + \frac{V_g}{h}} \cdot \left\{ 1 - \exp\{-[k + \frac{V_g}{h}]\Delta t\} \right\} S_{SO_{2b}}(t) \tag{3.19}$$

Substituting atmospheric concentrations for both $SO_2$ and sulfates into equation (3.17) and solving

$$S_{SO_{4d}}(t+\Delta t) = S_{SO_{4d}}(t) + S_{SO_{4b}}(t)\left\{1 - \exp\{-[V_p/h]\Delta t\}\right\}$$

$$+ \frac{k\, S_{SO_{2b}}(t)}{k + \frac{V_g}{h} - \frac{V_p}{h}} \left\{\left[1 - \exp\{-[V_p/h]\Delta t\}\right] - \left[\frac{(V_p/h)}{k + (V_g/h)}\right] \cdot \left[1 - \exp\{-[k + \frac{V_g}{h}]\Delta t\}\right]\right\} \tag{3.20}$$

The terms such as $\frac{[V_g/h]}{k + [V_g/h]} \left\{1 - \exp\{-[k + \frac{V_g}{h}]\Delta t\}\right\}$ in equation (3.19) can also be thought of as transition probabilities which determine the likely disposition of the $SO_2$ removed from the gas phase.

Above the mixed layer, the pollutants are stably stratified and are not in communication with the ground. Dry deposition does not affect such elevated air parcels. The transition probabilities affecting air parcels above the inversion base are due to chemical reaction alone.

$$S_{SO_{2a}}(t+\Delta t) = S_{SO_{2a}}(t) \exp\{-k\Delta t\} \tag{3.21}$$

$$S_{SO_{4a}}(t+\Delta t) = S_{SO_{4a}}(t) + S_{SO_{2a}}(t)\,[1 - \exp\{-k\Delta t\}] \tag{3.22}$$

Combining transport probabilities in the vertical direction with chemical reaction and deposition terms we see that the chain of coupled vertical transport and chemical reaction events is propagated by the following series of equations:

$$P_{SO_{2a}}(t+\Delta t|t_o,i) = \left\{P_{SO_{2a}}(t|t_o,i)\cdot[1-r(t+\Delta t|t_o,i)]+P_{SO_{2b}}(t|t_o,i)\cdot[d(t+\Delta t|t_o,i)]\right\}\cdot e^{-k\Delta t} \quad (3.23)$$

$$P_{SO_{4a}}(t+\Delta t|t_o,i) = \left\{P_{SO_{4a}}(t|t_o,i)\cdot[1-r(t+\Delta t|t_o,i)]+P_{SO_{4b}}(t|t_o,i)\cdot[d(t+\Delta t|t_o,i)]\right\}$$
$$+\left\{P_{SO_{2a}}(t|t_o,i)\cdot[1-r(t+\Delta t|t_o,i)]+P_{SO_{2b}}(t|t_o,i)\cdot[d(t+\Delta t|t_o,i)]\right\}\cdot\{1-e^{-k\Delta t}\} \quad (3.24)$$

$$P_{SO_{2b}}(t+\Delta t|t_o,i) = \left\{P_{SO_{2a}}(t|t_o,i)\cdot[r(t+\Delta t|t_o,i)]+P_{SO_{2b}}(t|t_o,i)\cdot[1-d(t+\Delta t|t_o,i)]\right\}$$
$$\cdot \exp\{-[k+\frac{V_g}{h(t+\Delta t)}]\Delta t\} \quad (3.25)$$

$$P_{SO_{2d}}(t+\Delta t|t_o,i) = P_{SO_{2d}}(t|t_o,i) + \left\{P_{SO_{2a}}(t|t_o,i)\cdot[r(t+\Delta t|t_o,i)]+P_{SO_{2b}}(t|t_o,i)\cdot[1-d(t+\Delta t|t_o,i)]\right\}$$
$$\cdot\left\{\frac{\frac{V_g}{h(t+\Delta t)}}{\frac{V_g}{h(t+\Delta t)}+k}\left[1-\exp\{-[k+\frac{V_g}{h(t+\Delta t)}]\Delta t\}\right]\right\} \quad (3.26)$$

$$P_{SO_{4b}}(t+\Delta t|t_o,i) = \left\{P_{SO_{4a}}(t|t_o,i)\cdot[r(t+\Delta t|t_o,i)]+P_{SO_{4b}}(t|t_o,i)\cdot[1-d(t+\Delta t|t_o,i)]\right\}\cdot \exp\{-\frac{V_p}{h(t+\Delta t)}\Delta t\}$$

$$+ \left\{P_{SO_{2a}}(t|t_o,i)\cdot[r(t+\Delta t|t_o,i)]+P_{SO_{2b}}(t|t_o,i)\cdot[1-d(t+\Delta t|t_o,i)]\right\}$$

$$\cdot\left\{\frac{k}{k+\frac{V_g}{h(t+\Delta t)}-\frac{V_p}{h(t+\Delta t)}}\left[\exp\{-\frac{V_p\ \Delta t}{h(t+\Delta t)}\} - \exp\{-[k+\frac{V_g}{h(t+\Delta t)}]\Delta t\}\right]\right\} \qquad (3.27)$$

$$P_{SO_{4d}}(t+\Delta t|t_o,i) = P_{SO_{4d}}(t|t_o,i) + \left\{P_{SO_{4a}}(t|t_o,i)\cdot[r(t+\Delta t|t_o,i)]+P_{SO_{4b}}(t|t_o,i)\cdot[1-d(t+\Delta t|t_o,i)]\right\}$$

$$\cdot\left\{1 - \exp\left\{-\frac{V_p}{h(t+\Delta t)}\Delta t\right\}\right\} + \left\{P_{SO_{2a}}(t|t_o,i)\cdot[r(t+\Delta t|t_o,i)]+P_{SO_{2b}}(t|t_o,i)\cdot[1-d(t+\Delta t|t_o,i)]\right\}$$

$$\cdot\left\{\frac{k}{k+\frac{V_g}{h(t+\Delta t)}-\frac{V_p}{h(t+\Delta t)}}\right\}\cdot\left\{\left[1 - \exp\{-\frac{V_p}{h(t+\Delta t)}\Delta t\}\right]-\left[\frac{\frac{V_p}{h(t+\Delta t)}}{k+\frac{V_g}{h(t+\Delta t)}}\right]\cdot\left[1 - \exp\{-[k+\frac{V_g}{h}]\Delta t\}\right]\right\}$$

(3.28)

where the newly introduced functions r and d are defined as follows:

$r(t+\Delta t|t_o,i)$ is the probability that the inversion base is rising and that a representative fluid particle emitted from source class i at time $t_o$ will be transferred from above the mixed layer to below the inversion base during the time interval t to $t+\Delta t$.

$d(t+\Delta t|t_o,i)$ is the probability that the inversion base is descending and that a representative fluid particle emitted from source class i at time $t_o$ will be transferred from below the inversion base to above the mixed layer during the time interval t to $t+\Delta t$.

Obviously, the inversion base cannot be both rising and descending at the same time in our spatially homogeneous system, so r and d never take on non-zero values simultaneously.

Stated simply, equation (3.23) says that the probability of finding an $SO_2$ molecule above the mixed layer at time $(t+\Delta t)$, given that it was emitted from source class i at time $t_o$, is equal to

(a) the probability that it was above the mixed layer at the start of the time step and was not mixed downward; plus

(b) the probability that it was below the inversion base at the start of the time interval and was mixed upward; both multiplied by

(c) the probability that it did not lose its chemical identity as $SO_2$ during the time interval.

The other expressions above have analogous meanings. Once the forms of the functions r and d have been specified, equations (3.23) through (3.28) form a series of recursion formulae which can be embedded in a simulation model. A means of estimating the upward and downward mixing

probabilities $r(t+\Delta t|t_o,i)$ and $d(t+\Delta t|t_o,i)$ from available meteorological data will be considered in section 3.4.1 of this chapter.

It should be noted that the scheme of equations (3.23) through (3.28) implies that transport precedes chemical reaction. The two processes could be considered simultaneously, but that would require input of new material into the chemical reactions as inversion base height changed within the course of a single time step. As will be seen in section 3.4 of this chapter, inversion base motion is not known accurately enough to justify such detail. Instead, time steps will be chosen which are short compared to the time scales of the chemical reactions and also short enough that inversion base height is known no better than to a single value over that time step. A further important feature of this scheme for propagating pollutant status between time steps is that it absolutely conserves sulfur mass.

$$
\begin{aligned}
&P_{SO_{2a}}(t+\Delta t|t_o,i) + P_{SO_{4a}}(t+\Delta t|t_o,i) + P_{SO_{2b}}(t+\Delta t|t_o,i) \\
&\qquad + P_{SO_{4b}}(t+\Delta t|t_o,i) + P_{SO_{2d}}(t+\Delta t|t_o,i) + P_{SO_{4d}}(t+\Delta t|t_o,i) \\
&= P_{SO_{2a}}(t|t_o,i) + P_{SO_{4a}}(t|t_o,i) + P_{SO_{2b}}(t|t_o,i) + P_{SO_{4b}}(t|t_o,i) \\
&\qquad + P_{SO_{2d}}(t|t_o,i) + P_{SO_{4d}}(t|t_o,i) \\
&= 1.0
\end{aligned}
\tag{3.29}
$$

### 3.3.3 Transport Probabilities in the Horizontal Plane

Having specified a chain of events which tracks both the vertical location and chemical composition of a single fluid particle over time, we now turn to advection in the horizontal plane. Particle motion in the horizontal plane is determined by all scales of atmospheric turbulence acting together. Large scale features of the atmospheric circulation are resolvable by hourly average measurements of wind speed and direction. Wind measurements along the air parcel's path can be integrated to yield an air parcel trajectory. In addition to the trajectory of the particle computed from hourly wind fields, small scale features of the atmospheric turbulence with period less than about one half hour act to randomize particle location beyond that computed from gross wind behavior alone. The cumulative effect of this small scale turbulence is usually referred to as eddy diffusion. It is seen, however, that separation of transport and diffusion into two categories merely reflects the observer's frame of reference. A single particle in the fluid is simply transported from one location to another by a variety of scales of motion in the atmosphere. Therefore, without loss of generality, we may write

$$X''(t|X_o,t_o) = \int_{t_o}^{t} U(X''(t'|X_o,t_o))dt' + X_o \qquad (3.30)$$

where

$X''(t|X_o,t_o)$ is fluid particle location at time t given starting location, $X_o$, and starting time, $t_o$.

$U(X''(t'|X_o,t_o))$ is instantaneous fluid velocity along the path followed by the particle.

The integration above is performed along the path of the particle.

If the above integration were performed exactly, then the probability of finding the particle within a given volume element $x_i - \frac{\Delta x_i}{2} < x_i < x_i + \frac{\Delta x_i}{2}$, i = 1,2,3, surrounding location X at time t, given that the particle originated at location $X_o$ at time $t_o$ would be

$$P(X,t|X_o,t_o) = \lambda(X'' - X) \tag{3.31}$$

where

$P(X,t|X_o,t_o)$ is the probability of finding the particle in the volume element surrounding location X at time t, given that it was emitted at location $X_o$ at time $t_o$.

$\lambda(X'' - X)$ is a proximity function

$$\lambda(X'' - X) = \begin{cases} 1 \text{ if } |(x_i'' - x_i)| < \frac{\Delta x_i}{2} & \text{for all } i = 1,2,3 \\ 0 \text{ otherwise} \end{cases}$$

Now take the following step: equations (3.30) and (3.31) are integrated over all possible locations in the vertical dimension (direction $x_3$). The above expressions may be rewritten as

$$\underset{\sim}{X}''(t|\underset{\sim}{X}_o,t_o) = \int_{t_o}^{t} \underset{\sim}{U}(\underset{\sim}{X}''(t'|\underset{\sim}{X}_o,t_o))dt' + \underset{\sim}{X}_o \tag{3.32}$$

and

$$\underset{\sim}{P}(\underset{\sim}{X},t|\underset{\sim}{X}_o,t) = \underset{\sim}{\lambda}(\underset{\sim}{X}'' - \underset{\sim}{X}) \tag{3.33}$$

where all terms have the same meaning as before, except that the underbar (~) refers to their projection on the $\underset{\sim}{X} = (x_1,x_2)$ horizontal plane only. For example, $P(\underset{\sim}{X},t|\underset{\sim}{X}_o,t_o)$ now denotes the probability of finding the particle of interest in the airspace over the surface area element $x_1 - \frac{\Delta x_1}{2} < x_1 < x_1 + \frac{\Delta x_1}{2}$ by $x_2 - \frac{\Delta x_2}{2} < x_2 < x_2 + \frac{\Delta x_2}{2}$.

Combining that transport probability in the horizontal plane with the vertical transport and chemical reaction expressions of equations (3.25) and (3.27), plus the ongoing assumption that the air mass next to ground level is vertically well mixed, we may write:

$$P_{SO_{4\tilde{}}}(X,t|\underset{\sim}{X}_o,t_o,i) = \underset{\sim}{P}(X,t|\underset{\sim}{X}_o,t_o)\cdot P_{SO_{4b}}(t|t_o,i)\cdot \frac{\Delta x_3}{h(t)} \qquad (3.34)$$

and

$$P_{SO_{2\tilde{}}}(X,t|\underset{\sim}{X}_o,t_o,i) = \underset{\sim}{P}(X,t|\underset{\sim}{X}_o,t_o)\cdot P_{SO_{2b}}(t|t_o,i)\cdot \frac{\Delta x_3}{h(t)} \qquad (3.35)$$

where the left sides of these expresssions have the following definition:

$P_{SO_{4\tilde{}}}(X,t|\underset{\sim}{X}_o,t_o,i)$ is the probability that a sulfur oxide molecule emitted from source class i at location $\underset{\sim}{X}_o$ at time $t_o$ resides as sulfate in the ground level volume element

$$x_i - \frac{\Delta x_i}{2} < x_i < x_i + \frac{\Delta x_i}{2} \; ; \; i = 1,2$$

by $0 < x_3 < \Delta x_3$ at later time t.

$P_{SO_{2\tilde{}}}(X,t|\underset{\sim}{X}_o,t_o,i)$ is the probability that a sulfur oxide molecule emitted from source class i at location $\underset{\sim}{X}_o$ at time $t_o$ resides as sulfur dioxide in the ground level volume element

$$x_i - \frac{\Delta x_i}{2} < x_i < x_i + \frac{\Delta x_i}{2} \; ; \; i = 1,2$$

by $0 < x_3 < \Delta x_3$ at later time t.

and $\Delta x_3/h(t)$ is the probability that a sulfur oxide molecule known to be within the mixed layer at time t will be found within the thin ground level layer of height $\Delta x_3$.

Recall that the initial vertical location of the air parcel, $x_{3_o}$, enters these expressions through the effective stack height $x_{3_o} = H(t_o,i)$ for the $i^{th}$ source class.

### 3.3.4 Ground Level Pollutant Concentrations

As stated so far, $P_{SO_4}(\underset{\sim}{X},t|\underset{\sim}{X}_o,t_o,i)$ is a transition probability representing transport and reaction of a single sulfur oxide molecule. If one now defines a source strength function over the airshed and integrates over all source classes and starting times, we acquire

$$\langle c_{SO_4}(\underset{\sim}{X},t)\rangle = \frac{1}{\Delta x_1 \Delta x_2 \Delta x_3} \sum_{i=1}^{N_4} \int_{-\infty}^{\infty}\int_{-\infty}^{\infty}\int_{-\infty}^{t} P_{SO_4}(\underset{\sim}{X},t|\underset{\sim}{X}_o,t_o,i) S(\underset{\sim}{X}_o,t_o,i)\, dt_o\, d\underset{\sim}{X}_o \tag{3.36}$$

and

$$\langle c_{SO_2}(\underset{\sim}{X},t)\rangle = \frac{1}{\Delta x_1 \Delta x_2 \Delta x_3} \sum_{i=1}^{N_4} \int_{-\infty}^{\infty}\int_{-\infty}^{\infty}\int_{-\infty}^{t} P_{SO_2}(\underset{\sim}{X},t|\underset{\sim}{X}_o,t_o,i) S(\underset{\sim}{X}_o,t_o,i)\, dt_o\, d\underset{\sim}{X}_o \tag{3.37}$$

where

$\langle c_{SO_4}(\underset{\sim}{X},t)\rangle$ is total sulfur concentration existing as sulfates in the ground level element of volume $\Delta x_1 \Delta x_2 \Delta x_3$ surrounding location $(x_1,x_2,0)$ at time t.

$\langle c_{SO_2}(\underset{\sim}{X},t)\rangle$ is total sulfur concentration existing as sulfur dioxide in the ground level element of volume $\Delta x_1 \Delta x_2 \Delta x_3$ surrounding location $(x_1,x_2,0)$ at time t.

$S(\underset{\sim}{X}_o,t_o,i)$ is the source strength for sulfur oxides molecules from source class i at horizontal location $\underset{\sim}{X}_o$ at release time $t_o$.

Equations (3.36) and (3.37) anticipate summation over a discrete number of source classes, i, within the airshed of interest.

As structured above, $\langle c_{SO_4}(\underset{\sim}{X},t)\rangle$ is computed by a Lagrangian marked particle technique. The source strength function, S, counts the number of sulfur oxide "particles" released from each source class and location. The transition probabilities $P_{SO_4}$ and $P_{SO_2}$ mark each particle

with a liklihood that it will appear as sulfate or as $SO_2$ within a given volume element at a later time. The concentration within that volume element is computed by adding up the probable number of particles with the desired chemical status in the volume element at time t, and then dividing by the volume of the cell.

### 3.3.5 Long-Term Average Sulfate and Sulfur Dioxide Air Quality

The concentration predictions of the model of equations (3.36) and (3.37) are instantaneous representations at time t. For long-term average sulfate concentrations at ground level over horizontal location $\underset{\sim}{x}$ we wish to obtain

$$\overline{\langle c_{SO_4}(\underset{\sim}{x};T,t_s)\rangle} = \frac{1}{T}\int_{t_s}^{T+t_s} \langle c_{SO_4}(\underset{\sim}{x},t)\rangle \, dt \tag{3.38}$$

and

$$\overline{\langle c_{SO_2}(\underset{\sim}{x};T,t_s)\rangle} = \frac{1}{T}\int_{t_s}^{T+t_s} \langle c_{SO_2}(\underset{\sim}{x},t)\rangle \, dt \tag{3.39}$$

where

$\overline{\langle c_{SO_4}(\underset{\sim}{x};T,t_s)\rangle}$ is the long-term average total sulfur concentration existing as sulfate at ground level at horizontal location $\underset{\sim}{x}$ over the time interval $(t_s, T+t_s)$.

$\overline{\langle c_{SO_2}(\underset{\sim}{x};T,t_s)\rangle}$ is the long-term average total sulfur concentration existing as sulfur dioxide at ground level at horizontal location $\underset{\sim}{x}$ over the time interval $(t_s, T+t_s)$.

$T$ is, for example, the length of a given month or year.

$t_s$ is the beginning of the time interval of interest.

Next, consider the case where the individual emission sources within a given source class have a common diurnal periodicity. An

example would be the diurnal pattern imposed by daily rush-hour traffic peaks, or the daily cycling of power plants between afternoon peak demand and late night off-peak periods. Then a point source distribution might be represented as

$$S(\underset{\sim}{x}_o, t_o, i) = \overline{S}(\underset{\sim}{x}_o, i)\ \omega(t_o, i) \tag{3.40}$$

where

$\overline{S}(\underset{\sim}{x}_o, i)$ = average emission source strength for sources of class i as a function of location in the horizontal plane of the air basin

$\omega(t_o, i)$ = a diurnal source strength cycle for sources of class i.

Two obvious properties of $\omega(t_o, i)$ are that

$$\overline{\omega} = \frac{1}{24}\ \text{hrs} \int_{t_s}^{t_s + 24\ \text{hours}} \omega(t_o, i)\ dt_o = 1$$

and

$$\omega(t, i) = \omega(t + 24\ \text{hours}, i).$$

Introduce the change of variable $t_o = t - \tau$. Then substituting equations (3.40), (3.36) and (3.37) into equations (3.38) and (3.39), and performing the indicated integrations over time, we get

$$\overline{\langle c_{SO_4}(\underset{\sim}{x}; T, t_s)\rangle} = \sum_{i=1}^{N_4} \int_{-\infty}^{\infty}\int_{-\infty}^{\infty} \overline{Q}_{SO_4}(\underset{\sim}{x}|\underset{\sim}{x}_o, i; T, t_s)\overline{S}(\underset{\sim}{x}_o, i)\ d\underset{\sim}{x}_o \tag{3.41}$$

and

$$\overline{\langle c_{SO_2}(\underset{\sim}{x}; T, t_s)\rangle} = \sum_{i=1}^{N_4} \int_{-\infty}^{\infty}\int_{-\infty}^{\infty} \overline{Q}_{SO_2}(\underset{\sim}{x}|\underset{\sim}{x}_o, i; T, t_s)\overline{S}(\underset{\sim}{x}_o, i)\ d\underset{\sim}{x}_o \tag{3.42}$$

where

$$\overline{Q}_{SO_4}(\underset{\sim}{x}|\underset{\sim}{x}_o,i;T,t_s) = \frac{1}{T\Delta x_1\Delta x_2\Delta x_3}\int_{t_s}^{T+t_s}\int_{0}^{\infty} P_{SO_4}(\underset{\sim}{x},t|\underset{\sim}{x}_o,t-\tau,i)\omega(t-\tau,i)d\tau dt$$

$$\overline{Q}_{SO_2}(\underset{\sim}{x}|\underset{\sim}{x}_o,i;T,t_s) = \frac{1}{T\Delta x_1\Delta x_2\Delta x_3}\int_{t_s}^{T+t_s}\int_{0}^{\infty} P_{SO_2}(\underset{\sim}{x},t|\underset{\sim}{x}_o,t-\tau,i)\omega(t-\tau,i)d\tau dt$$

In practice, one need not integrate air parcel starting times over all past history. Integration over $\tau$ from $\tau = 0$ to $\tau = \tau_c$ should be sufficient, where $\tau_c$ is the longest time for retention of an air parcel within the airshed of interest. When $T >> \tau_c$, the outer integral determines the length of the computation required.

Up to this point, we have discussed a general approach to calculating sulfate and sulfur dioxide concentrations in a region characterized as having an idealized persistent temperature inversion. A means for direct estimation of $\overline{Q}_{SO_4}$ and $\overline{Q}_{SO_2}$ from meteorological measurements made in a particular airshed now will be developed.

## 3.4 A Computational Procedure for Simulating Los Angeles Sulfate Air Quality

Analytical solutions for the source to receptor transition probabilities appearing in equations (3.41) and (3.42) are unlikely to be obtained for an arbitrary sequence of unsteady meteorological events. But the stochastic chain of events pictured in equations (3.23) through (3.28) plus trajectory equations (3.32) and (3.33) is ideally suited for inclusion in a numerical simulation model. The only additions to these equations needed to simulate the fate of representative fluid particles are a means of calculating the upward and downward mixing

probabilities $d(t+\Delta t|t_o,i)$ and $r(t+\Delta t|t_o,i)$, plus a means of obtaining particle trajectories, $X''(t|X_o,t_o)$, in the horizontal plane. By simulating the fate of a large number of representative fluid particles, and then averaging over their ultimate dispositions, one can estimate the desired source to receptor transition probability densities.

### 3.4.1 Calculating Exchange Between the Stable Inversion and the Mixed Layer Below from Available Monitoring Data

Historic data on inversion base movement have been regularly compiled by the Los Angeles Air Pollution Control District (LAAPCD) for many years. But while the extent of the data base is great, the detail is rather coarse. Each day's data base contains an early morning inversion base height sounding at a coastal location, nominally taken at Los Angeles International Airport at 6:00 am. Secondly, each afternoon's maximum mixing depth, $h_{max}$, is calculated from earlier soundings plus temperature conditions observed at downtown Los Angeles. Additional data on inversion base motion might be acquired from military installations on the fringes of the South Coast Air Basin or from an acoustic sounder operated at the California Air Resources Board laboratory in El Monte. However, only the LAAPCD meteorological records are available in a uniform format extending throughout our years of interest. For the long-term study that we intend to pursue, only the LAAPCD data are in a form suitable for practical use.

Inversion base motion must still be defined as a function of space and time if air parcel progress is to be tracked. In light of having only two point estimates of maximum and minimum inversion base height

daily, some further assumptions must be made. Regarding the spatial distribution of mixing depths above ground level at a given time, the assumption made is that inversion base height *above ground level* is spatially homogeneous at any single time over the central flatlands of the Los Angeles Basin. This approximation can be checked against the average cross-sectional inversion height diagram shown in Figure 3.4. Figure 3.4 was adapted from Neiburger, Beer and Leopold (1945) after having sketched a ground elevation profile. A second set of nearly instantaneous cross-sections through the air basin prepared by Edinger (1973) is shown in Figure 3.5. Over a long-term average (Figure 3.4), the mixing depth between the inversion base and ground level is roughly constant throughout the cross-section shown, while at any single time the assumption of a spatially homogeneous mixing depth holds only approximately. Note that Figure 3.5 shows ozone concentrations from aloft being fumigated downward as inversion base height rises into a previously stable layer, as would be modeled for sulfates by our vertical transport scheme.[2]

Mixing depth is thus taken as independent of location over the central portion of the air basin. The function $h(X',t')$ is roughly equal to $h(t')$ alone, and thus is compatible with our earlier model derivation.

Specification of short term temporal fluctuations in inversion base height must proceed by means of an interpolation scheme. Since the

---

[2]Ozone is not expected to be fully mixed in the vertical at all times (see Figure 3.5 c'). One reason is that strong spatial gradients exist in pollutant species (like NO) which scavenge ozone.

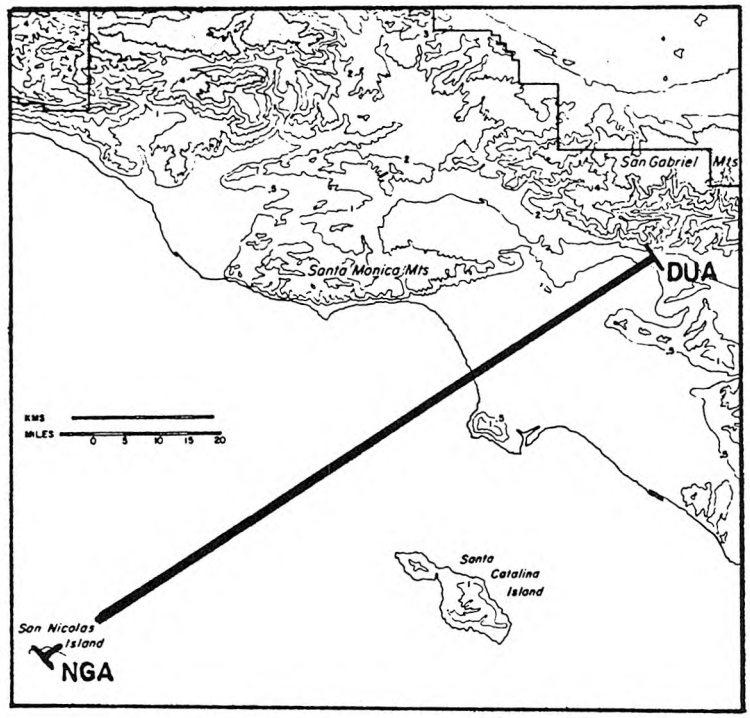


FIGURE 3.4

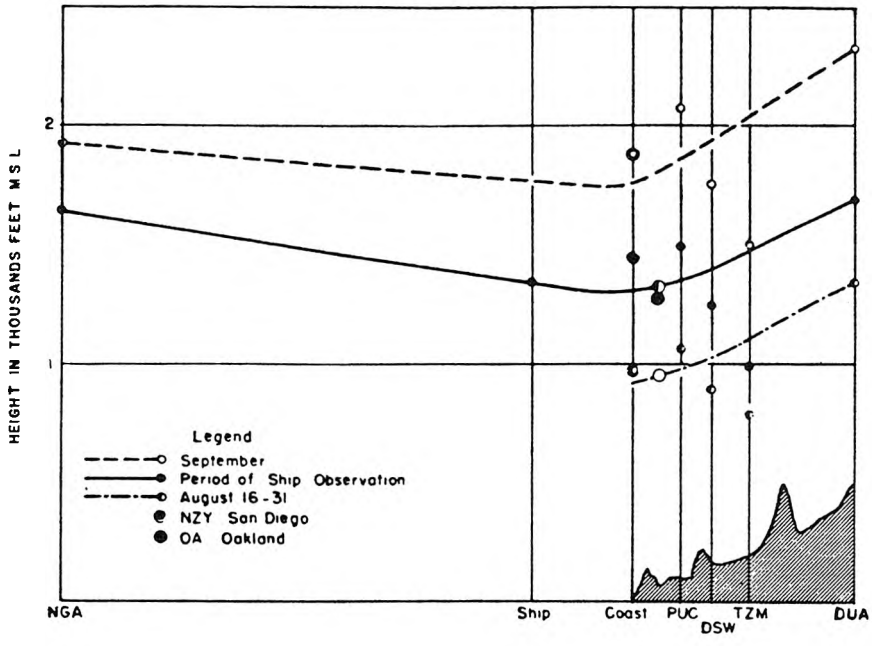


AVERAGE CROSS SECTION OF INVERSION BASE
NORMAL TO COAST
STATIONS ARE ARRANGED ACCORDING TO DISTANCE FROM SHORE
INDEPENDENTLY OF POSITION ALONG IT

Reference: Neiburger, Beer and Leopold (1945)

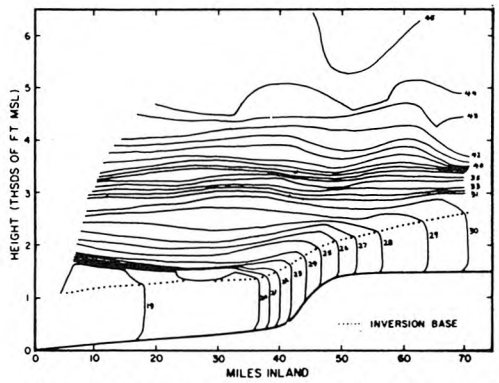


(a) Field of potential temperature (°C) in the vertical cross section from Santa Monica to Rialto-Miro, 9:00 am, June 20, 1970

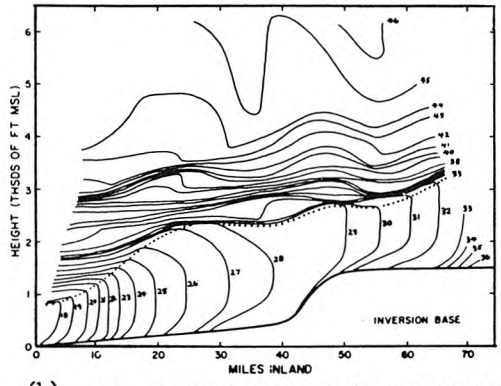


(b) Field of potential temperature (°C) in the vertical cross section from Santa Monica to Rialto-Miro, 12:00 noon, June 20, 1970

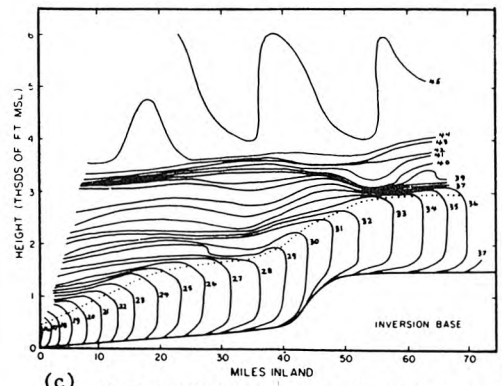


(c) Field of potehtial temperature (°C) in the vertical cross section from Santa Monica to Rialto-Miro, 4:30 pm, June 20, 1970

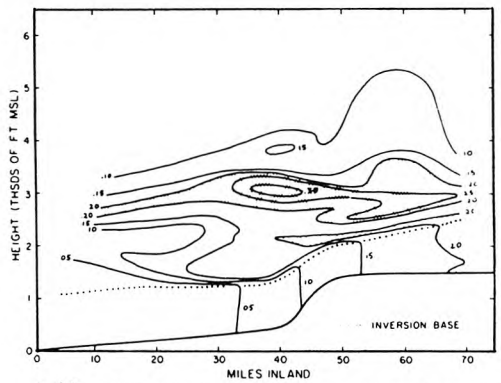


(a') Field of oxidant concentrations (ppm) in the vertical cross section from Santa Monica to Rialto-Miro. 9 00 am, June 20, 1970

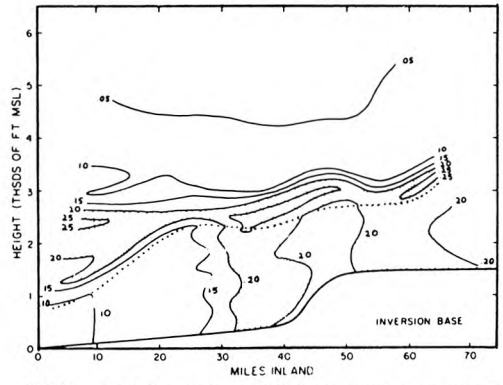


(b') Field of oxidant concentrations (ppm) in the vertical cross section from Santa Monica to Rialto-Miro. 12 00 noon June 20 1970

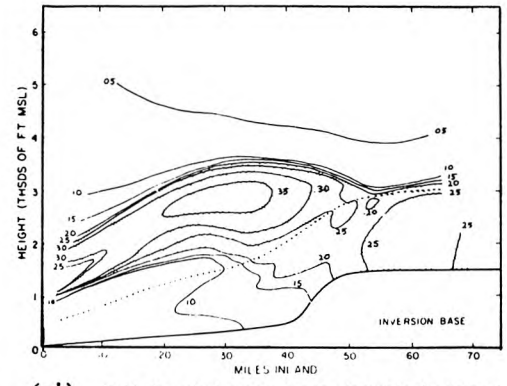


(c') Field of oxidant concentrations (ppm) in the vertical cross section from Santa Monica to Rialto-Miro, 4:30 pm, June 20, 1970

source: Edinger, 1973

FIGURE 3.5

Vertical Temperature Structure and Inversion Base Location in the Los Angeles Atmosphere at Three Times of the Day - June 20, 1970.

data only represent daily peaks and troughs, it is hard to argue about the merits of different ways to specify intermediate behavior. All interpolation schemes will substantially exceed the available data. The method chosen here is similar to that suggested by Goodin (1976). Overnight mixing depth above ground level is set equal to the mixing depth reported for Los Angeles International Airport (LAX) at 6:00 am according to the records of the LAAPCD. If a surface-based inversion existed, it was recorded by the LAAPCD as a mixing depth of 30.48 m (100 ft). At sunrise, ground level heating causes the base of the inversion to begin to lift. A linear rate of inversion base rise is maintained until the LAAPCD's reported maximum mixing depth over downtown Los Angeles for that day is achieved at solar noon. Substantial inland transport of cooler marine air in the afternoon halts further rise in inversion base height. The inversion base is held constant at the maximum mixing depth achieved until sunset. Then at sunset, stable layers begin to reform in the atmosphere beneath the level of that day's maximum mixing depth. The lowest of these new stable layers becomes the next overnight inversion base height. Thus at sunset, the mixing depth adjacent to ground level is set equal to the next measured overnight value at LAX and remains there until sunrise the following day.

As stated so far, the form of the downward and upward transport probabilities, r and d, is quite general. Let us consider a hypothetical time history of an inert individual fluid particle and note some of the possible interactions between it and the inversion base which could affect upward and downward transport. In Figure 3.6, a fluid particle

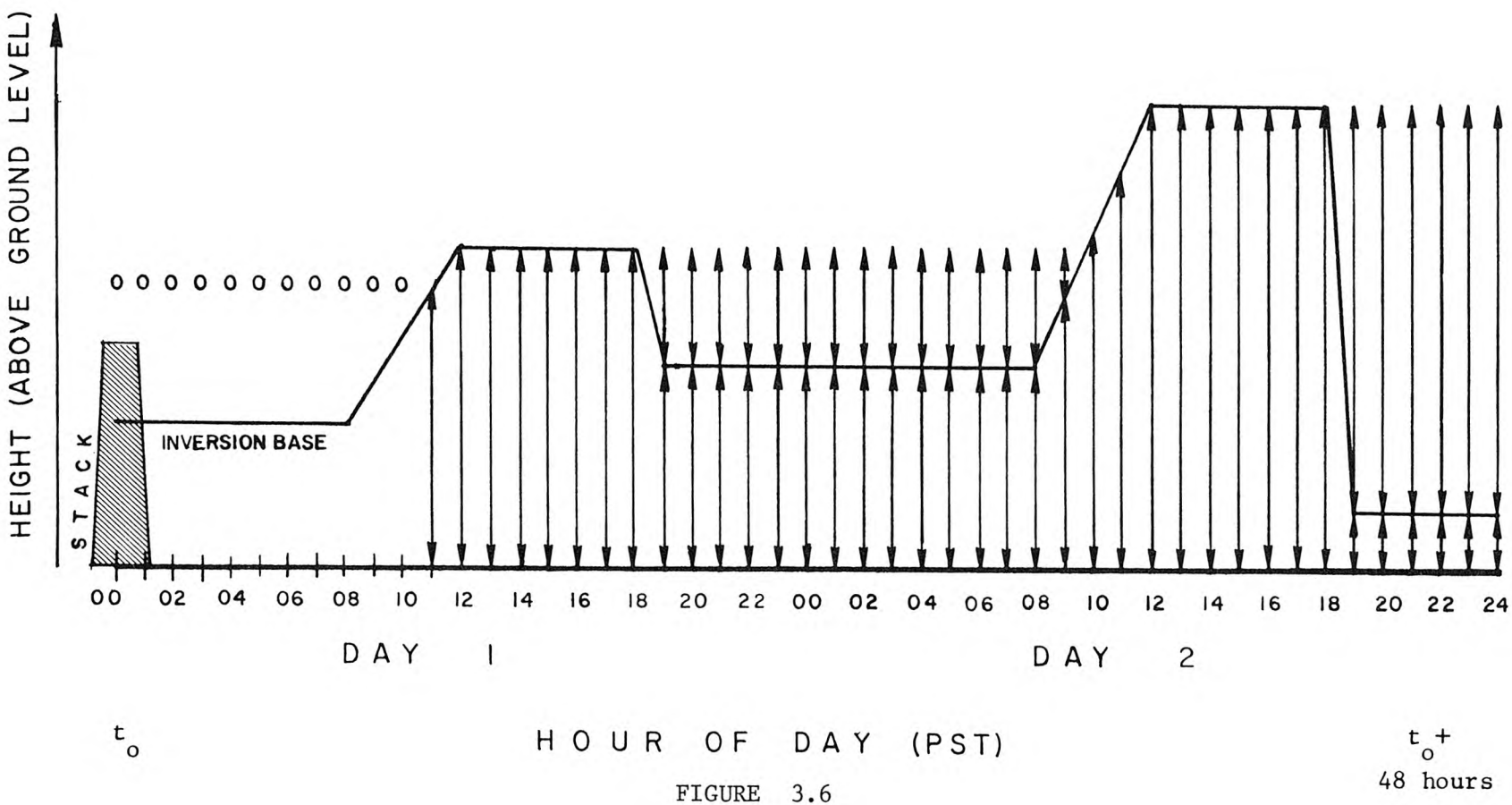


FIGURE 3.6

Hypothetical Time History of Interaction Between the Inversion Base and a Fluid Particle Released at Time $t_o$

is emitted from a source belonging to class i and enters the atmosphere at $t_o$ equals midnight at effective stack height $H(t_o,i)$. The height of emission is within the stable inversion and no vertical motion occurs. The early morning proceeds by time steps of $\Delta t$ equal to one hour, but nothing happens immediately to alter air parcel vertical location. By sunrise that morning, the inversion base begins to rise at a constant rate from its overnight low toward its maximum mixing height for the day. The fluid particle is still within what remains of the stable layer until 11:00 am. At that point, the inversion has passed the height of insertion of the particle into the stable layer and down-mixing occurs. The particle now has a uniform probability of being found anywhere within the unstable mixed layer.

The vertical space over which the particle is free to travel expands until the day's maximum mixing height is reached at solar noon. Then as the sun goes down, the inversion reforms and establishes itself at its overnight base height. A segment of the vertical space in which the particle might have resided previously is now found above the new inversion base. With some probability, the particle is either above or below the new overnight inversion base. If it is below the inversion base overnight, it is exposed to the possibility of undergoing deposition at the ground. Above the inversion base, the probability of finding the particle in any given vertical space remains unchanged overnight due to the extreme stability of the atmosphere within the inversion. Then as the inversion base rises the next day, this uniformly mixed layer aloft is progressively destabilized and entrained

downward, carrying with it some probability that the particle has been returned to the mixed layer below the inversion base.

Given the type of inversion base behavior pictured in Figure 3.6, two relatively simple algebraic expressions for the upward and downward transport transition probabilities are proposed:

$$r(t+\Delta t|t_o,i) = \frac{h(t+\Delta t) - h(t)}{\ell(t+\Delta t|t_o)-h(t)} \cdot U_{h(t)}(h(t+\Delta t)) \cdot U_{H(t_o,i)}(\ell(t+\Delta t|t_o)) \tag{3.43}$$

and

$$d(t+\Delta t|t_o,i) = \frac{h(t) - h(t+\Delta t)}{h(t)} \cdot U_{h(t+\Delta t)}(h(t)) \cdot U_{H(t_o,i)}(\ell(t+\Delta t|t_o)) \tag{3.44}$$

where the newly introduced function

$\ell(t+\Delta t|t_o)$ is a marker which tracks the maximum vertical dilution experienced by an air parcel located below the inversion base between time $t_o$ and time $(t+\Delta t)$. In our vertically mixed system, $\ell(t+\Delta t|t_o)$ tracks maximum mixing depth achieved over the life history of the particle:

$$\ell(t+\Delta t|t_o) = h(t+\Delta t) \cdot U_{\ell(t|t_o)}(h(t+\Delta t)) + \ell(t|t_o) \cdot [1-U_{\ell(t|t_o)}(h(t+\Delta t))] \tag{3.45}$$

Equation (3.45) merely says that the maximum mixing depth seen by an air parcel is the maximum depth seen in the past history of the air parcel or the current inversion base height, whichever is greater. Initial conditions for propagation of $\ell$ would be

$$\ell(t_o|t_o) = h(t_o) \tag{3.46}$$

Consider how the expression for $r(t+\Delta t|t_o,i)$ responds to the various interrelationships between air parcel location and a rising inversion base as shown in Figure 3.6. At hours prior to 11:00 am on the first day of travel, $H(t_o,i) > \ell(t+\Delta t|t_o)$ and the unit step function

on the right side of equation (3.43) yields zero probability of down-mixing. Between 11:00 am and noon on the first day $h(t+\Delta t)=\ell(t+\Delta t|t_o)$, the inversion base is rising, and $\ell(t+\Delta t|t_o) > H(t_o,i)$, giving unit probability that an air parcel above the mixed layer would be mixed downward. For the period just following noon, the inversion base is not moving, $U_{h(t)}(h(t+\Delta t))$ takes on value zero, and no vertical transport occurs. Until the inversion begins to reform near the ground at sunset, the function $d(t+\Delta t|t_o,i)$ has taken only zero values. As the inversion base height is lowered, a pollutant particle traveling within the mixed layer at time t has probability $d(t+\Delta t|t_o,i) = [h(t)-h(t+\Delta t)]/h(t)$ of being caught above the new inversion base height, and probability $[1-d(t+\Delta t|t_o,i)]$ of being caught below the overnight inversion base. Then as the inversion base rises on the second day, a particle which was caught above the inversion base is likely to be fumigated downward into the mixed layer with probability $r(t+\Delta t|t_o,i) = [h(t+\Delta t)-h(t)]/[\ell(t+\Delta t|t_o)-h(t)]$ in proportion to the fraction of the stable polluted layer aloft which has been mixed downward at each time step.

These simple expressions for r and d will not hold exactly for indefinitely long transport chains. In particular if an air parcel were mixed to a high altitude $h_{max_1}$, on the first day, then a second day followed with $h_{max_2} < h_{max_1}$, by the morning of the third day, the inversion base would be rising into a stable inversion which contained a non-uniform vertical distribution of the probability of finding the particle at a given altitude within the inversion. In that case, the probability of down-mixing of the particle would depend on the maximum

mixing depth achieved on both of the prior days, and the form of $r(t+\Delta t|t_o,i)$ becomes more complex. However, this problem is not of major concern in the application which we have in mind. The probability of finding the particle in the mixed layer is calculated as correctly as possible for more than a day and a half. By that time, the air parcel will typically have exited the study area surrounding the Los Angeles coastal plains and San Gabriel and San Fernando Valleys. If the particle has not yet been deposited at the ground or advected out of the study area, then its probable composition is likely to be as sulfate after over a day and a half of reaction time. Sulfates behave as a nearly inert pollutant in our model. Inversion base motion acts only in the direction toward reestablishing a uniform pollutant concentration in the vertical both above and below the inversion base for an inert pollutant. Any significant non-uniform distribution of $P_{SO_4}(t|t_o,i)$ with altitude is transitory when it does occur. Since this situation will be transitory by nature and will occur only under a special series of meteorological circumstances involving at least one day of relatively high dilution, (and thus low ground level impact in any case), modification of the form of $r(t+\Delta t|t_o,i)$ to cover this special case is not felt to be necessary for the application that we have in mind.

The form adopted for $r(t+\Delta t|t_o,i)$ and for $d(t+\Delta t|t_o,i)$ may be inserted into equations (3.23) through (3.28). Given the available ambient monitoring data, a time series of inversion base motion like that of Figure 3.6 can be constructed for any time period of interest in the Los Angeles Basin over the past decade. Thus the probability

that any representative fluid particle containing sulfur oxides is at ground level in a given chemical state can be estimated from ambient monitoring data, given that its initial chemical status, location, and time of origin were known.

### 3.4.2 Calculating Trajectories in the Horizontal Plane

Equation (3.32) calls for particle trajectories to be constructed by integration of the wind vector apparent along the path of each particle. Unfortunately, wind data are not available along such trajectories. Rather, wind speed and direction is measured by a network of Eulerian wind stations which are fixed to the earth's surface.

A variety of means may be used to compute particle trajectories from a network of Eulerian measurements. Perhaps the most realistic approach would be to interpolate wind data from the thirty or so available wind stations in the Los Angeles Basin to form a mass-consistent wind field at a closely spaced network of grid points. If data were available on winds aloft, then a vertical wind speed and direction profile reflecting the effects of wind shear could be included. A random number generator could be used to perturb particle position between time steps and thus simulate those scales of atmospheric motion which were too small to be resolved by conventional wind measurements. Then the fluid particle could be passed through a sequence of transport steps by a self-propagating stochastic chain similar in concept to the chains developed for vertical motion and pollutant chemistry.

Our air quality model derivation is compatible with a sophisticated trajectory calculation procedure. However, the application that we intend to pursue involves simulation of sulfate air quality over months covering a three year test period. The computer time needed to construct highly accurate wind fields hourly for three years is simply beyond our budget. It therefore becomes necessary to consider the merits of testing this model using an approximate trajectory calculation scheme. Since our interest lies in a particular air quality problem in Los Angeles, the following discussion will be placed in the context of that air basin.

The two main parameters of our sulfate air quality model which depend on horizontal trajectory calculations are air parcel retention time in the air basin, and the lateral location of various concentration peaks. From the standpoint of making most sulfate air quality control strategy decisions, a correct computation of air parcel retention time is probably the more critical of the two. That is because the retention time allowed for chemical reactions to proceed determines the total amount of sulfate formed within the study area. An air parcel trajectory calculation which differentiates between seaward and landward transport regimes and which distinguishes stagnation periods from times of high winds will probably track those features most important to determining air parcel retention time in Los Angeles.

Correct computation of the horizontal path of an air mass in the Los Angeles Basin is made difficult by complex terrain. Fluid flow lines are diverted around the obstructions posed by many hills and valleys.

If these obstructions are ignored, the calculated lateral location of air masses far downwind will be distorted. The main effect of ignoring streamline diversion around terrain features within the context of a sulfate model for the Los Angeles Basin is to sacrifice some information on exactly who is exposed to a peak pollutant concentration. Most air quality standards are aimed at protecting the general public from pollutant exposures above certain levels regardless of where they might live. Therefore a little uncertainty in the location of a predicted concentration peak can usually be tolerated in most practical decision-making processes.

Therefore, the following approximation is made: horizontal motion in the atmosphere over the Los Angeles Basin will be represented as if it were in uniform parallel flow at any single time. That approximation is certainly untrue for near stagnant conditions over the scale of a given time step. Over a long averaging time the approximation may not be too bad. That is because most net transport occurs during higher wind speed events at which time flow over the basin is quite organized. Returning to Figures 3.1 and 3.2 we note that the predominant wind flow directions during daytime and nighttime transport by and large do follow parallel paths to within the 22.5° of arc which are included within each sector of the 16 point compass into which wind direction measurements are resolved. Two exceptions to this behavior are apparent. There is a flow diversion around the Palos Verdes Hills at the center of the Los Angeles County coastline. That diversion however seems to pose only a local problem. Secondly, there is a distinct turning of

the wind flow at the entrance to the San Fernando Valley. As a result, calculation of pollutant transport into the San Fernando Valley definitely requires the use of a detailed windfield. Use of a parallel flow approximation in this locale at least restricts the validity of air quality model calculations to the central flatlands of the Los Angeles Basin and the adjoining San Gabriel Valley. Fortunately, the area over which model calculations still should perform well is substantially the same area identified in Chapter 2 as having air quality data sufficient to verify model predictions.

If the air mass over the basin were actually in uniform parallel flow, wind speed and direction at any location in the air basin should be represented well by observations at a single wind station. However, since this type of flow regime is only an approximation in our case, a representative wind station should be chosen carefully. To minimize discrepancies between the generally higher wind speeds at the coast versus the slower wind speeds in inland valleys, a wind station in the center of the air basin will be chosen. Secondly, to partially account for higher wind speeds aloft at the height of elevated sources, a wind station with a relatively high measurement height should be chosen. Finally, if average trajectories are to be calculated, then a LAAPCD wind station which reports integrated wind speed and direction over each hourly interval should be picked rather than a U.S. Weather Service airport wind station which reports only point measurements at a single instant once per hour. A wind station is available which satisfies these criteria at the downtown Los Angeles headquarters

monitoring site of the LAAPCD. It is located in the center of our study area on a mast above the top of a six story building with relatively unobstructed exposure. Its strip chart record is reduced to hourly average speed and direction. And because of its proximity to agency staff, its equipment probably receives superior maintenance.

Having selected a given wind station, trajectory calculation in the horizontal plane is straightforward. Breaking equation (3.32) into components in the $x_1$ and $x_2$ directions, we get

$$x_1''(t|x_{1_o},t_o) = \int_{t_o}^{t} U_1(t')dt' + x_{1_o} \tag{3.47}$$

$$x_2''(t|x_{2_o},t_o) = \int_{t_o}^{t} U_2(t')dt' + x_{2_o} \tag{3.48}$$

If wind measurements reduced from each hour's strip chart recording have previously been integrated over that hour, we may obtain the expected value of particle location at the end of each time step of the chemical chain of the previous section of this chapter by summing wind components in each coordinate direction.

$$x_1''(t|x_{1_o},t_o) = \sum_{n=0}^{N_5-1} U_1(t_o+n\Delta t)\Delta t + x_{1_o} \tag{3.49}$$

$$x_2''(t|x_{2_o},t_o) = \sum_{n=0}^{N_5-1} U_2(t_o+n\Delta t)\Delta t + x_{2_o} \tag{3.50}$$

where $N_5 = \dfrac{(t - t_o)}{\Delta t}$ .

If wind direction were known accurately, our trajectory integration procedure would be nearly complete. But reported wind direction measurements at downtown Los Angeles are resolved only to within the 22.5° of arc which make up the sectors of a 16 point compass. As far as can be discerned from available monitoring data, a given particle trajectory for an hour could have followed any path consistent with the compass sector and wind speed reported. In order to construct a specific trajectory at each hour from the family of wind directions within each sector, our calculations will employ several random number generators. In order to pick the mean wind direction used at each hour, a specific bearing is drawn from a uniform distribution of the possible directions contained within the sector of interest. The resulting mean wind vectors will be integrated in time series as in equations (3.49) and (3.50). But in addition to this mean displacement over time, small scale atmospheric fluctuations (measurable in terms of the standard deviation of the wind direction about its mean) impart small diffusive displacements to individual fluid particles. This process of eddy diffusion will be simulated by means of a two dimensional Gaussian random number generator. The standard deviation of fluid particle displacements from mean trajectory paths dispersing over urban areas can be estimated as a function of travel time downwind from experimental data available for Los Angeles and elsewhere (Drivas and Shair, 1975; Shair, 1977; McElroy and Pooler, 1968). Then mean trajectory end points can be perturbed by adding a pair of displacements, $\delta x_1$ and $\delta x_2$, drawn at random from the family of displacements having a

two dimensional normal distribution with mean zero and variance $(\sigma_1^2(t - t_o), \sigma_2^2(t - t_o))$.

At this point, it becomes evident why the instantaneous parallel flow assumption leads to large gains in computational efficiency which make it attractive in spite of certain limitations as to accuracy. First, given that assumption, the displacement of a particle from its release point ($x_1'' - x_{1_o}''$) is only a function of t and $t_o$ plus randomness. A single set of trajectories represents source to receptor transport from all starting locations in the airshed. Separate trajectory integrations for hundreds or thousands of possible source locations can be collapsed into one source to receptor transfer calculation which may then be adapted to any starting location, $\underset{\sim}{x}_o$, merely by subtracting starting location from all trajectory end points of interest. The useful result is that

$$P_{SO_4}(\underset{\sim}{x},t|\underset{\sim}{x}_o,t-\tau,i) = P_{SO_4}(\underset{\sim}{x}-\underset{\sim}{x}_o,t,t-\tau,i) \tag{3.51}$$

$$P_{SO_2}(\underset{\sim}{x},t|\underset{\sim}{x}_o,t-\tau,i) = P_{SO_2}(\underset{\sim}{x}-\underset{\sim}{x}_o,t,t-\tau,i) \tag{3.52}$$

and

$$\overline{Q}_{SO_4}(\underset{\sim}{x}|\underset{\sim}{x}_o,i;T,t_s) = \overline{Q}_{SO_4}(\underset{\sim}{x}-\underset{\sim}{x}_o,i;T,t_s) \tag{3.53}$$

$$\overline{Q}_{SO_2}(\underset{\sim}{x}|\underset{\sim}{x}_o,i;T,t_s) = \overline{Q}_{SO_2}(\underset{\sim}{x}-\underset{\sim}{x}_o,i;T,t_s) \tag{3.54}$$

### 3.4.3 Calculation of Monthly Average Pollutant Levels

Given the foregoing methods for calculating probable chemical status and air parcel location over time, a simulation may be conducted to evaluate $\overline{Q}_{SO_4}$ and $\overline{Q}_{SO_2}$ for a given month. The procedure adopted is to order the necessary integrations so that a monthly average of pollutant concentrations apparent at given times of the day is first computed for each source class of interest. Then the average concentrations at $n = \left( \frac{24 \text{ hours}}{\Delta t} \right)$ times of the day will be pooled to obtain total monthly average concentration estimates for each source class. Finally, the source classes will be superimposed to form the total air quality impact due to local sources. This concentration estimate is then added to background air quality levels to obtain a total pollutant concentration estimate over the airshed of interest. A step by step description of one means of carrying out this numerical integration follows.

First we wish to calculate the chemical status and vertical dilution of all air parcels present in the airshed at a known time of day on each day of the month. Consider a simplified case. Let $\Delta t$ equal one hour. Attention is focussed on the first source class. An initial time of day is chosen, for example 0:00 hrs (midnight) at the start of each of the $\eta$ days of the month. Then the wind and inversion base data are repacked into $\eta$ sequences of $\tau_c$ consecutive hours of data each, starting with the $\tau_c^{th}$ hour preceeding midnight of each day of the month, for example. At each hour represented in each string of

meteorological data, a marker particle is released with an associated magnitude $\omega(t_o,i)$ at a height $H(t_o, i)$. The probable chemical status and vertical progress of each particle is tracked by the methods outlined previously from its time of release until the midnight hour at the end of its parent data string. The first particle released for each of the $\eta$ data strings travels for $\tau_c$ hours the second particle for $\tau_c$-1 hours, and so forth. This process is illustrated in Figure 3.7. After $P_{SO_{4b}}$ and $P_{SO_{2b}}$ have been evaluated for each particle at the final hour of each data string, the probabilities $P_{SO_{2b}}$ and $P_{SO_{4b}}$ associated with each particle are stored in a location tagged with their initial starting time.

Next the $\eta$ sets of wind data of $\tau_c$ hours each are integrated backwards by time steps of $\Delta t$ from the ending midnight of interest. This generates a set of streaklines which contain the horizontal displacement at the hour of initiation of the backward integration (i.e. at the $\eta$ midnights of interest) of all of the individual particles for which $P_{SO_{4b}}$ and $P_{SO_{2b}}$ were just calculated. This cuts the number of operations required for trajectory integration substantially.[3] The point is illustrated schematically for $\tau_c$ equals 5 hours in Figure 3.8.

Streaklines ending at all "midnights" for the month are superimposed. Then the horizontal displacement of each particle is paired

[3]The suggestion that wind vectors be integrated backward in order to increase computational efficiency is due to R.C.Y. Koh.

FIGURE 3.7

OBJECTIVE: TO CALCULATE THE CHEMICAL STATUS AND VERTICAL DILUTION OF AIR PARCELS PRESENT IN THE AIRSHED AT A KNOWN TIME OF DAY ON EACH DAY OF A MONTH.

STEP 1: FOCUS ON A TIME OF DAY, FOR INSTANCE, MIDNIGHT AT THE START OF EACH DAY OF THE MONTH.


STEP 2: REPACK DATA INTO 31 STRINGS OF $t_c$ HOURS, EACH ENDING AT THE TIME OF DAY AT WHICH WE WISH TO COMPUTE AIR PARCEL STATUS.

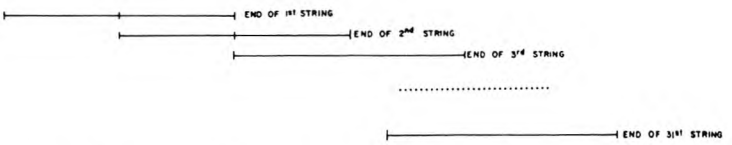


STEP 3: RELEASE ONE FLUID PARTICLE AT EACH TIME STEP SHOWN IN EACH DATA STRING. TRACK EACH PARTICLE'S CHEMICAL PROGRESS AND VERTICAL DILUTION UNTIL THE LAST HOUR APPEARING IN ITS PARENT DATA STRING.

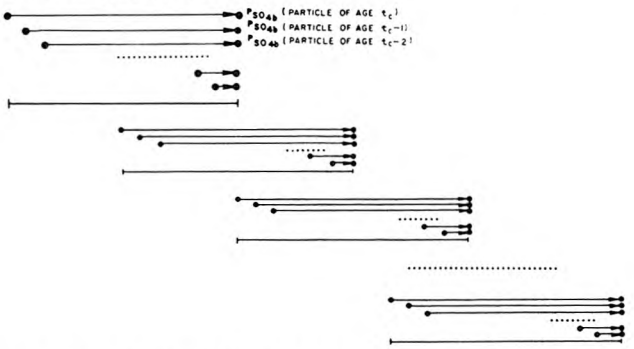


STEP 4: STORE RESULTS IN A LOCATION ASSOCIATED WITH EACH FLUID PARTICLE'S ORIGINAL RELEASE TIME.

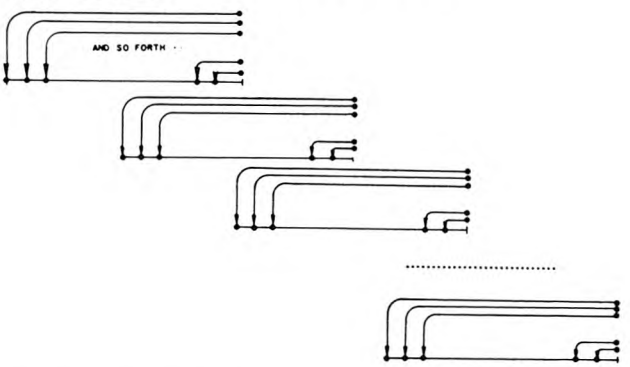


RESULT: THE CHEMICAL STATUS AND VERTICAL DILUTION OF REPRESENTATIVE AIR PARCELS OF ALL AGES PRESENT AT ALL MIDNIGHTS OF THE MONTH HAS BEEN DETERMINED. THE RESULTS ARE STORED IN A MANNER IN WHICH THEY ARE EASILY ASSOCIATED WITH TRAJECTORIES CALCULATED IN THE HORIZONTAL PLANE AND WITH THE DIURNAL SOURCE STRENGTH EVALUATED AT EACH PARTICLE'S TIME OF RELEASE.

FIGURE 3.8

OBJECTIVE: TO CALCULATE THE HORIZONTAL DISPLACEMENT FROM LOCATION $\underset{\sim}{X}_0$ AT A GIVEN MIDNIGHT FOR ALL PARTICLES RELEASED PRIOR TO THAT TIME.

STEP 1: TAKE A SERIES OF $\tau_c$ WIND VECTORS.

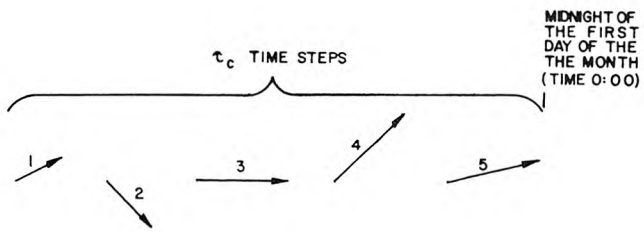


STEP 2: TO GET DISPLACEMENT FROM LOCATION $\underset{\sim}{X}_0$ AT TIME 0:00 FOR ALL PARTICLES RELEASED PREVIOUSLY:

(a) CALCULATE $\tau_c$ FOWARD TRAJECTORIES,

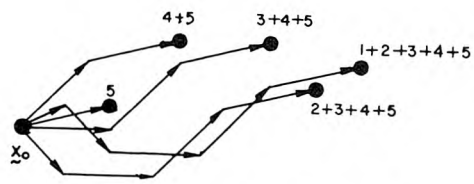


(b) OR ONE BACKWARD STREAKLINE INTEGRATION.

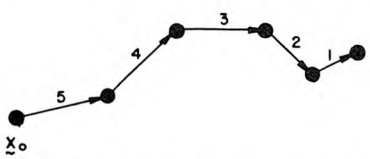


THINK OF THIS AS A SNAP-SHOT OF A CROOKED PLUME PHOTOGRAPHED AT MIDNIGHT

STEP 3: PERFORM STREAKLINE TRAJECTORY INTEGRATION ON THE SEQUENCE OF WIND VECTORS PRESENT IN EACH DATA STRING SHOWN IN FIGURE 3.7. THESE PARTICLE DISPLACEMENTS ARE THEN TO BE MATCHED WITH THE CHEMICAL STATUS OF EACH PARTICLE, PARTICLE VERTICAL DILUTION, AND THE DIURNAL SOURCE STRENGTH FUNCTION APPROPRIATE TO THE TIME OF PARTICLE RELEASE.

with the particle's probable chemical status and weighted by its diurnal source strength. The resulting magnitudes are accumulated to a matrix of receptor cells by summing magnitudes for all particles having displacements falling within the same receptor cell. Totals are accumulated separately for $SO_2$ and for sulfates. We divide the elements of these accumulation matrices by the size of the receptor cell and the number of "midnights" being superimposed. One quickly obtains a rough estimate of the spatial distribution of average $SO_2$ or sulfate concentrations appearing in the air at midnight due to a unit source of $SO_x$ of source class i located at the origin of our coordinate system. That averaging process is illustrated schematically in Figure 3.9.

Next, advance the starting time from midnight by increments of $\Delta t$ through the remainder of a day, repeating the above procedure and then averaging the set of source-receptor transfer relationships obtained. We finally arrive at the desired estimates of $\overline{Q}_{SO_4}$ and $\overline{Q}_{SO_2}$ in the form of matrices which were constructed from information on all trajectory starting and ending times for the month. Figure 3.10 shows this superposition of source to receptor transport matrices calculated at different trajectory ending times for the month.

If average source emission strength $\overline{S}(\underset{\sim}{x}_o, i)$ is given for each source location in class i as if the source were located in the center of a grid cell with the same spacing as the receptor cells, then the source to receptor transport probability matrices $\overline{Q}_{SO_2}$ and $\overline{Q}_{SO_4}$ just calculated may be used to map emissions into air quality by a process

FIGURE 3.9

OBJECTIVE: TO COMPUTE THE AVERAGE POLLUTANT CONCENTRATION OBSERVED AT MIDNIGHT RESULTING FROM A UNIT SOURCE LOCATED AT $\underset{\sim}{X}_0$.

STEP 1: SUPERIMPOSE STREAKLINES CONTAINING ALL FLUID PARTICLES OBSERVED TO BE PRESENT AT MIDNIGHT; ONE STREAKLINE FOR EACH MIDNIGHT IN THE MONTH.

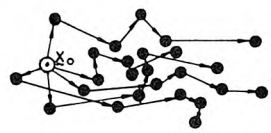


STEP 2: LOCATE PARTICLES WITHIN THE CELLS OF A RECEPTOR GRID

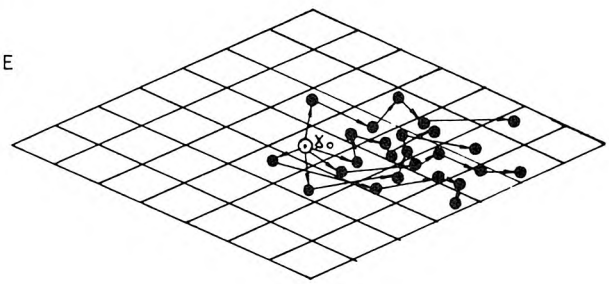


STEP 3: ACCUMULATE THE MAGNITUDES ASSOCIATED WITH THE PARTICLES FALLING WITHIN EACH GRID CELL

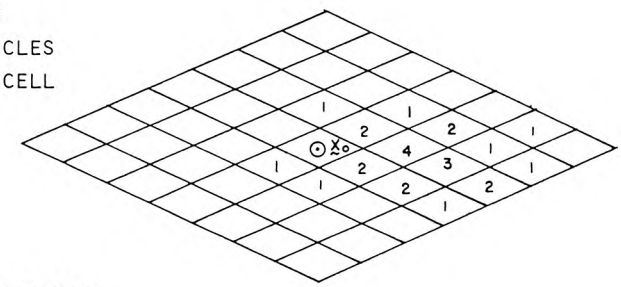


STEP 4: DIVIDE THE ACCUMULATED POLLUTANT MASS LOADINGS BY THE SIZE OF THE RECEPTOR CELL AND THE NUMBER OF "MIDNIGHTS" BEING SUPERIMPOSED

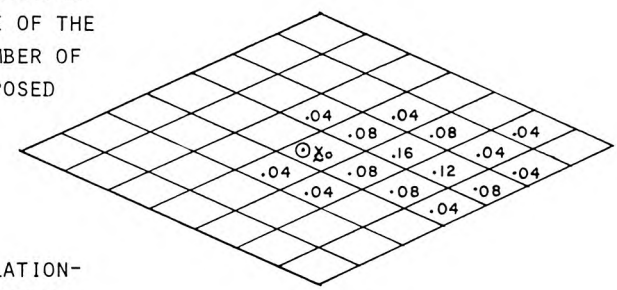


RESULT: THE SOURCE TO RECEPTOR RELATIONSHIP HAS BEEN CALCULATED WHICH MAPS EMISSIONS FROM A UNIT SOURCE AT LOCATION $\underset{\sim}{X}_0$ INTO AVERAGE POLLUTANT CONCENTRATION OBSERVED AT MIDNIGHT THROUGHOUT THE RECEPTOR GRID

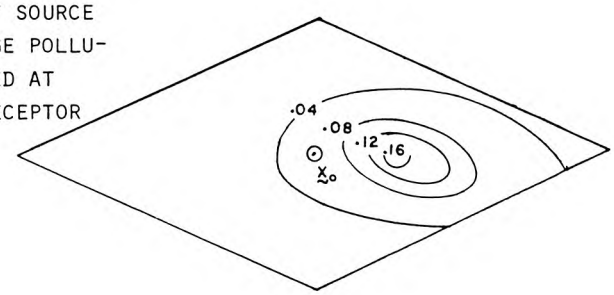

FIGURE 3.10

OBJECTIVE: TO CALCULATE THE MONTHLY AVERAGE SOURCE TO RECEPTOR TRANSFER RELATIONSHIP

PROCEDURE: SUPERIMPOSE THE RELATIONSHIPS CALCULATED FROM TRAJECTORIES ENDING AT EACH TIME OF DAY FOR THAT MONTH.

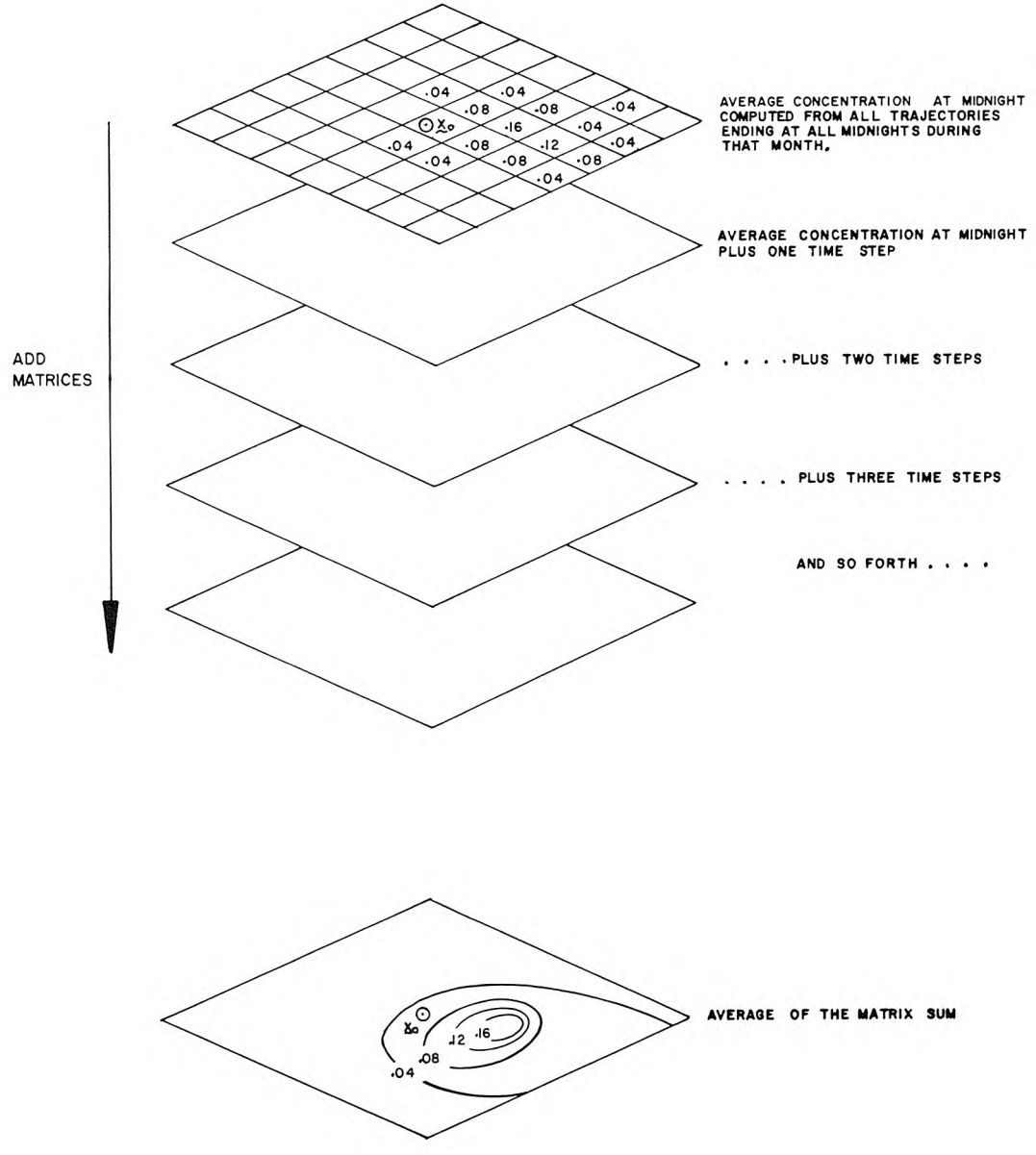

of superposition. The appropriate influence matrices $\overline{Q}_{SO_2}$ and $\overline{Q}_{SO_4}$ are merely centered on the origin of the source of interest and the emissions are scaled to incremental air quality impact at surrounding receptor sites.

The matrix of air quality increments defined at each receptor site due to emissions from the first source class is stored for future reference. Next the integration over fluid particle release, reaction and transport is repeated for each remaining source class of interest. Then all incremental impacts from all source classes are added to form a total air quality impact at each receptor point due to local pollution sources. Background air quality is added to the air quality impact predicted for local sources. The monthly average air quality calculations are now complete.

Superposition is permitted because the entire model is linear in $SO_x$ emissions. A multiple source urban air quality model for sulfate formation and dispersion is thus achieved which shows the contribution of each source class to air quality observed at each receptor site. That knowledge of source class influence is very valuable when searching for efficient emission control strategies. Control strategies can be aimed at source classes with the greatest air pollution impact per dollar spent on control.

Of course the order of integration could be changed in the above description. There is no necessity for accumulating intermediate concentration estimates at twenty-four hourly trajectory ending times per month. Source emission strength could be associated with individual

particles before the magnitudes of each particle are accumulated at each receptor site. No matter what the order of integration, evaluation of $\overline{<c_{SO_4}>}$ and $\overline{<c_{SO_2}>}$ by the equations presented previously simply results in estimation of long-run average pollutant concentrations from a distribution of sources by release of representative marker particles at intervals of $\Delta t$ followed by indexing of accumulating registers within each receptor cell at the end of each time step $\Delta t$.

## 3.5 Summary and Discussion

A simulation model has been described for calculating long-run average sulfate air quality levels in a multiple source urban setting. The model computes pollutant concentrations by a long-run average Lagrangian marked particle technique. First order chemical reactions and ground level dry deposition are incorporated. The model is capable of handling unsteady meteorological conditions in a region characterized as having an idealized persistent temperature inversion. This atmospheric temperature structure results in a well-mixed layer near ground level capped by a stable air mass aloft.

The *long-term average* air quality model thus formed has many of the merits and faults commonly associated with *short-term average* air quality models based on air parcel trajectory calculations. Potential sources of error in many of the most advanced trajectory models in use today include (Liu and Seinfeld, 1975):

1. neglect of horizontal diffusion (not neglected in our case)
2. neglect of the vertical component of the wind
3. neglect of wind shear.

Of these problems, neglect of wind shear and return flows aloft is probably the most serious. Due to a lack of wind data aloft, the wind shear problem would remain in practice in our intended application even if the computational procedure were designed to handle wind shear explicitly. Each of the above mentioned difficulties can be overcome in our marked particle simulation model given appropriate meteorological data and more computing resources.

In addition to these problems common to nearly all trajectory-based models, a series of approximations has been made in order to adapt a quite general concept for use in a particular application: sulfate air quality prediction in Los Angeles. The available meteorological data for Los Angeles were discussed. Then the following approximations were made which permit rapid calculation of the elements of the simulation model from existing monitoring records:

1. that inversion base height above ground level over the central Los Angeles Basin is spatially homogeneous at any given time
2. that inversion base motion over time may be represented by a stylized diurnal cycle which passes through the known daily maximum and minimum inversion base heights
3. that at any single time, the wind field over the Los Angeles Basin may be approximated as a uniform parallel flow.

Each of these approximations was made as a practical consideration aimed at conserving available computing resources, and not out of theoretical necessity. The accuracy of this air quality simulation depends on meteorological resolution, chemical resolution, and resolution obtained

by defining source class behavior more accurately. Within a fixed computing budget, contributions to model accuracy from treatment of each of these degrees of freedom must be balanced. Approximations (1) and (3) above permit isolation of chemical calculations and trajectory calculations from detailed dependence on a given starting location in the airshed. This results in a huge savings in computing time versus that which would be needed if either of these approximations were relaxed. That computational savings is necessary in our case if a reasonable number of source classes are to be defined. In short, a compromise has been struck between meteorological elegance and the number of separate source classes which may be entered into the model within a fixed computing budget.

Several of the particular merits of this simulation model also bear discussion at this point. First, the long-run average Lagrangian marked particle model need not compute pollutant concentrations as a real-time sequence of events. The order of integration over air parcel release and transport may be arranged to minimize computing time and intermediate data storage requirements. Secondly, the calculations required are very simple. The computational algorithm is completely stable over time. There are no artificial numerical diffusion problems associated with mixing a particle into a cell and then forgetting where it was located before mixing occurred. Pollutant mass is absolutely conserved.

The model builds its own initial conditions by integrating backward to connect all locally-emitted air parcels in the airshed at a given

time to their source. This is very important for solving our sulfate problem because instantaneous sulfate concentration data representing initial conditions at any time are completely unavailable. Even if measurements on pollutant initial conditions were available, one would prefer the chosen method because it permits deduction of the sources responsible for creating those initial conditions.

The chosen computational method also has advantages in the way that it treats behavior at the edges of the receptor grid. The model does not require that boundary conditions be specified at the edges of the grid system. Air parcels advected beyond the borders of the receptor grid are not lost to the model. Their position is remembered but their magnitudes are not accumulated to a receptor grid cell unless the air parcels are advected back into the region of the receptor grid. Receptor cells may thus be specified only over those areas where concentration estimates are desired without compromising model accuracy.

In the above discussion, the proposed long-term average air quality simulation has been discussed in light of features often sought in a dynamic model for short-term average air quality prediction. In a comparison with the pseudo-steady state models routinely used to predict *long-term average* air quality, the simulation model proposed here fares quite well. Pseudo-steady state models which employ a joint frequency distribution of wind speed, wind direction and atmospheric stability have no hope of correctly computing air parcel retention time in an air basin because they do not contain any information about the serial correlation of wind vectors. Without utilizing wind data in

time sequence to compute air parcel retention time, conventional pseudo-steady state air quality models cannot hope to track slow chemical reactions occurring in a recirculating air mass over the Los Angeles Basin.

# CHAPTER 4

# AN ENERGY AND SULFUR BALANCE ON THE SOUTH COAST AIR BASIN

## 4.1 Introduction

The most outstanding feature of sulfur oxides emissions in the Los Angeles area is that virtually all of the anthropogenic sulfur in this community's atmosphere originally entered the air basin in a barrel of crude oil. The questions of air pollutant emissions and energy use in Los Angeles are inseparably related.

In order to place the Los Angeles sulfur management problem in perspective, the origin of the sulfur itself will be sought. The sources of supply for crude oil used in the air basin in 1973 will be characterized by origin, quantity and sulfur content. *Potential* sulfur oxides emissions which could occur if all of that sulfur were released to the atmosphere during combustion will then become apparent.

The second problem at hand is to identify the sources from which sulfur oxides air pollutant emissions actually are released to the atmosphere within the Los Angeles area. Our immediate need is for the emissions data required as input to an air quality simulation model for sulfate formation in the Los Angeles atmosphere. But a broader goal is to achieve an understanding of the underlying demand for energy in various forms which brings with it the processing and combustion of sulfur-containing fuels. This understanding is important if one wishes

to control pollutant emissions to some desired level while at the same time meeting the fundamental demands for energy to run the economy of Southern California. Since our ultimate objective is to study possible air pollutant emissions control strategies, the effort needed to pursue this broader outlook is well justified.

The traditional approach to preparing emission inventories for Los Angeles is to locate the several hundred largest emission sources, measure their emissions, and then accumulate their emissions to form a total "from the bottom up". Examples of this sort of inventory have been compiled from time to time for Los Angeles sulfur oxides emissions by air pollution control agencies and by engineering consulting firms (Environmental Protection Agency, 1974; Trijonis, et al., 1975; Hunter and Helgeson, 1976; Southern California Air Pollution Control District, 1976b). In this report we will first collect and compile an inventory of stationary and mobile source $SO_x$ emissions for each month of the years 1972 through 1974. This inventory is based on a comparative appraisal of individual source emission estimates made possible by cooperation from the Southern California Air Pollution Control District, the California Air Resources Board, KVB Incorporated (a state ARB contractor), the Southern California Gas Company, the Southern California Edison Company, the California Department of Transportation, and conversations with a number of industrial source owners. Information will be presented on the spatial distribution of sources across the air basin, the seasonal and diurnal variation of source strength, the effective height of injection of emissions into the atmosphere, and

the distribution of emissions between gaseous and particulate sulfur oxides species. This data base will be specifically designed to meet the needs of an air quality modeling effort for monthly average sulfate concentrations.

Sulfur flows entering the air basin in crude oil then will be compared to estimates of atmospheric $SO_x$ emissions. It quickly becomes apparent that only a small fraction of the basin's sulfur supply is becoming airborne. In order to confirm that observation and to explain its occurrence, both mass balance and energy balance calculations will be performed on the flows of energy resources containing sulfur across a control surface drawn around the perimeter of the air basin. Petroleum resources will be tracked through the Los Angeles refinery complex, subdivided into refinery products, refinery fuel, recovered elemental sulfur and sulfuric acid. Then refinery products will be assigned to the consuming sectors of the air basin's economy, and to out-of-basin export markets. Natural gas and liquified petroleum gas use within the air basin will be detailed, as will be the importation of electric energy from outside the basin, and the generation of electricity within the airshed.

Sulfur flows accompanying each energy flow will be estimated. Points within the Los Angeles energy economy at which sulfur oxides emissions to the atmosphere occur thus will be identified.

In the following sections of this study, the crude oil supply characterization, the spatially resolved emission inventory and the energy and sulfur balance will be briefly introduced. Findings will

be summarized and discussed. The detailed basis for those discussions is described in a series of appendices which accompany this report.

## 4.2 The Quantity and Sulfur Content of Crude Oil Supplied to the South Coast Air Basin in 1973

In Appendix A1, the methods used to trace crude oil from its source to the South Coast Air Basin are described. The purpose of this study was to assure that the amount of sulfur entering the air basin via crude oil was fully determined. Therefore, a serious attempt was made to find the sulfur content as well as the quantity of the oil delivered. This survey was nominally conducted for the year 1973, although some of the data employed came from other recent years. In the following paragraphs, a brief description of the approach used in this study will be given.

### 4.2.1 Crude Oil Characterization -- Approach and Methods

Crude oil quality varies widely from one oil field to another. In order to obtain a quantitative description of crude oil properties entering the South Coast Air Basin, the oil must be tracked to its source. Oil-producing regions of the world were subdivided into three basic categories: California oil fields, other domestic sources, and foreign crude oil supplies. These categories are convenient because different data sources are needed to assess crude oil properties from each of these three producing territories.

Smaller geographic regions within each producing category were then defined. California oil fields were subdivided into five

producing regions based on geographic terrain and access to common transportation links. Previously reported surveys of California oil use (Nehring, 1975) showed that the only non-California domestic oil producing regions important to California oil consumption were in Alaska and the Four Corners area between Utah and New Mexico. Foreign crude oils first were considered by country of origin, and then grouped into ten major geographic zones (e.g. South Pacific, Persian Gulf, etc.).

Total oil production in each major field in each producing district was determined for a base year of interest. Then sulfur content information for crude oil from each field was used to compute the total quantity of associated sulfur produced along with the oil. Sulfur and oil production data were next pooled for all fields within the producing district of interest. The distribution of crude oil production within sulfur content intervals was determined. The fraction of oil production with a sulfur content between 0.26% and 0.50% sulfur, for example, was then apparent in any producing district. Finally, a weighted average sulfur content of crude oil was determined for each sulfur content interval in each producing district. In that manner, oil supplies at the wellhead around the world were organized and stratified by sulfur content.

Next, oil shipments to the South Coast Air Basin were estimated by investigating available transportation links. California crude oil shipments to the South Coast Air Basin were estimated from local production within the Los Angeles Basin, plus waterborne commerce data and pipeline capacities.

Crude oil transfers to the entire state of California from out-of-state domestic sources and from major foreign countries were obtained by producing district of origin for 1973. Total receipts of non-California crude oil at local harbors were determined. Unfortunately, the local harbor crude oil receipts are not resolved by state or by country of origin. Therefore the assumption was made that the distribution of crude oil by country of origin arriving at South Coast Air Basin ports was directly proportional to that estimated for all foreign and out-of-state domestic oils received by ship in California.

By combining crude oils from California fields, out-of-state domestic sources and foreign imports, both the total quantity of crude oil and the distribution of that oil between high sulfur and low sulfur crude oils was estimated. The details of this crude oil characterization study are given in Appendix A1. A discussion of this survey's implications for control of sulfur oxides emissions by manipulation of crude oil entering the South Coast Air Basin will now be presented.

### 4.2.2 Crude Oil Characterization -- Summary and Discussion

Table 4.1 and Figure 4.1 summarize the estimated crude oil and associated sulfur receipts by South Coast Air Basin customers in 1973. The result is that just over one million barrels of crude oil were received daily containing 3821 thousand pounds of sulfur per day. These crude oil receipts almost exactly match 1973 South Coast Air Basin refinery capacity of 1,006,200 bbls per stream day (Cantrell,

TABLE 4.1

Summary of 1973 South Coast Air Basin
Crude Oil Receipts plus Associated Sulfur Content

| Origin of Crude Oil | Average % Sulfur by Weight | 1973 Estimated Quantity Received in SCAB (1000's barrels/yr) | 1973 Approximate Quantity of Sulfur Contained (1000's lbs/year) |
|---|---|---|---|
| Los Angeles Basin | 1.49 | 128,207.9[a] | 613,878.5 |
| Ventura and Federal Offshore | 1.36 | 41,172.8[a] | 176,503.9 |
| Central California Coast | 3.35 | 8,648.9 | 99,808.8 |
| San Joaquin Valley | 0.81 | 39,055.4 | 102,912.4 |
| California subtotal | 1.42 | 217,085.0 | 993,103.6 |
| Alaska | 0.08 | 26,950.5 | 6,509.3 |
| Utah | 0.27 | 12,000.1 | 9,553.5 |
| Domestic Import subtotal | 0.14 | 38,950.6 | 16,062.8 |
| Group 1 (Persian Gulf) | 1.83 | 54,034.9 | 298,633.0 |
| Group 2 (Remainder of Middle East) | 1.64 | 644.1[b] | 3,243.3 |
| Group 3 (Africa, north and west coast) | 0.21 | 8,364.1[b] | 5,084.7 |
| Group 4 (South Pacific) | 0.14 | 30,357.0 | 12,633.5 |
| Group 5 (South America, Caribbean Coast) | 1.99 | 4,580.0 | 28,315.1 |
| Group 6 (Western South America) | 1.00 | 8,526.2[b] | 25,594.5 |
| Group 7 (Europe) | 1.38 | 454.6[b] | 1,887.6 |
| Group 8 (Mexico) | 2.56 | 762.3[b] | 6,099.0 |
| Group 9 (Canada) | 0.51 | 2,581.3[b] | 3,895.7 |
| Group 10 (Japan & Taiwan) | 0.13 | 24.6[b] | 9.6 |
| Foreign Import subtotal | 1.16 | 110,329.1 | 385,396.0 |
| TOTAL | 1.20 | 366,364.7 | 1,394,562.4 |

( = 3,821 thousand pounds per day)

Notes: (a) Local production less estimated net exports from the basin.

(b) Crude oil coming to the South Coast Air Basin from undesignated countries of origin was distributed amongst all producing regions whose exports to California were not known explicitly.

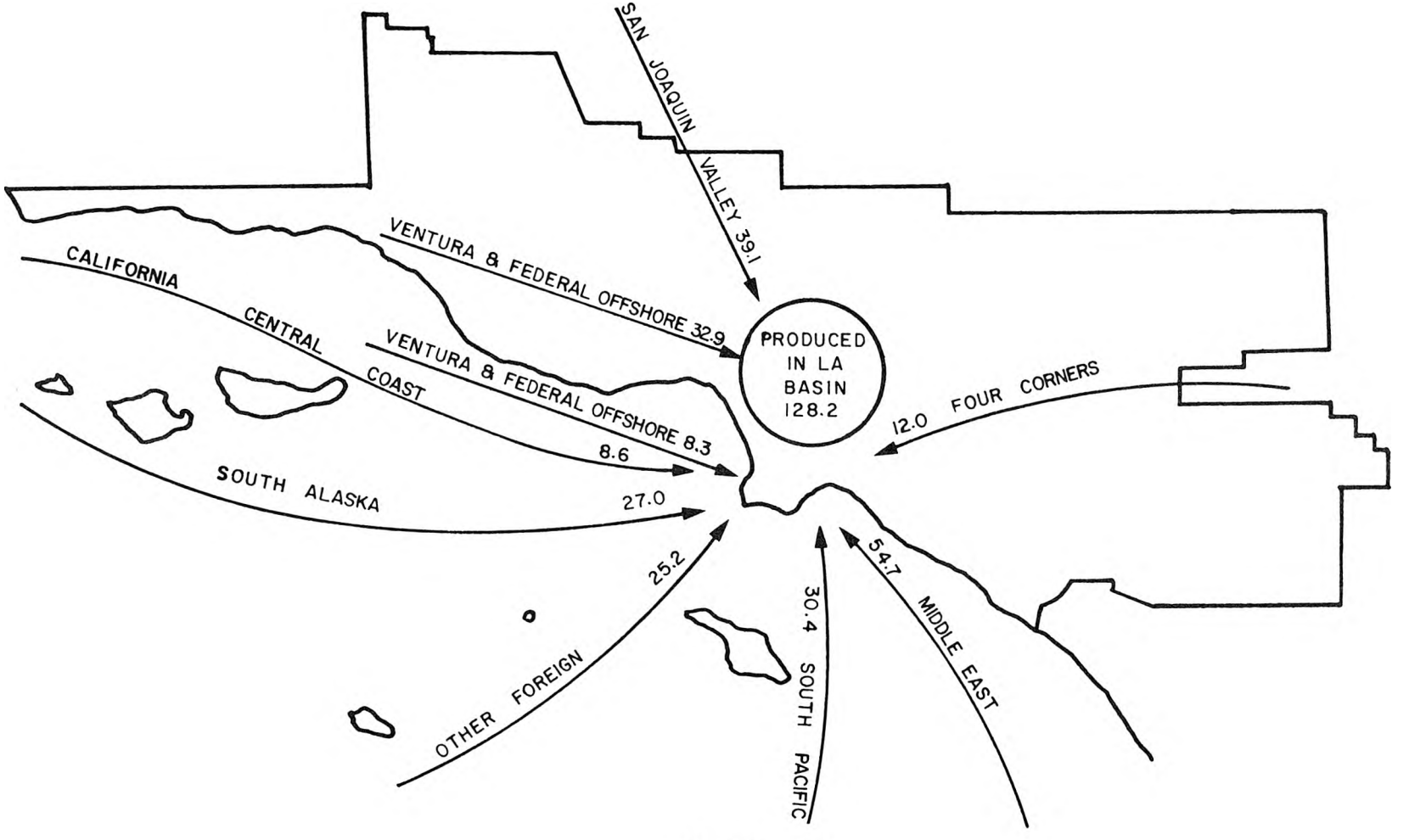


FIGURE 4.1

The Estimated Origin and Quantity of Crude Oils
Received by South Coast Air Basin Customers in 1973.
(Millions of Barrels per Year)

1973). Data on total 1973 crude oil sulfur intake by Los Angeles County refineries has been obtained by the Southern California Air Pollution Control District (1976a). Their data report that 3551.49 thousand pounds of sulfur arrived daily at Los Angeles County refineries in feedstocks (net of unfinished oils rerun) in that year. This agrees with our independent estimate to within about 7%. There are at least two small South Coast Air Basin refineries excluded from the APCD survey which, if included, would probably bring these two sulfur supply estimates into even closer agreement.

In spite of the high gasoline consumption in the Los Angeles area, the South Coast Air Basin uses only a very small portion of total world oil production. This fact is easily seen in Table 4.2. Most importantly, the basin uses but a small part of the very low sulfur (less than 0.25% S) crude oil produced in the world today. As seen in the trade maps of Figures 4.2 through 4.4, Japan is the major customer for South Pacific region (generally low sulfur) oil, buying more than ten times the amount delivered to the South Coast Air Basin from that producing region. An even smaller fraction of low sulfur African oils are imported to California. It is thus not physically impossible that sulfur input to the South Coast Air Basin could be sharply reduced by substitution of low sulfur crude oils for current high sulfur oil receipts.

However, the practical problems posed by such a fuel switching strategy look very formidable indeed. Figures 4.5 and 4.6 yield several important insights into the nature of the sulfur management

TABLE 4.2

Estimated South Coast Air Basin Crude Oil Receipts
As a Fraction of Oil Available at the Wellhead
in Various Producing Regions

| Origin of Crude Oil | Average Percent Sulfur by Weight | 1973 Estimated Quantity Consumed in SCAB (1000's barrels/yr) | Percent of total 1973 Production |
|---|---|---|---|
| Los Angeles Basin | 1.49 | 128,207.9 | 97.0% |
| Ventura and Federal Offshore | 1.36 | 41,172.8 | 87.4 |
| Central California Coast | 3.35 | 8,648.9 | 29.2 |
| San Joaquin Valley | 0.81 | 39,055.4 | 30.8 |
| California subtotal | 1.42 | 217,085.0 | 64.7% |
| Alaska (southern) | 0.08 | 26,950.5 | 36.9 |
| Utah | 0.27 | 12,000.1 | 46.2 |
| Domestic Import subtotal | 0.14 | 38,950.6 | |
| Group 1 (Persian Gulf) | 1.83 | 54,034.9 | 0.7 |
| Group 2 (Remainder of Middle East) | 1.64 | 644.1 | 0.4[a] |
| Group 3 (Africa, north and west coasts) | 0.21 | 8,364.1 | 0.4[a] |
| Group 4 (South Pacific) | 0.14 | 30,357.0 | 3.7 |
| Group 5 (South America, Caribbean Coast) | 1.99 | 4,580.0 | 0.3 |
| Group 6 (Western South America) | 1.00 | 8,526.2 | 3.0 |
| Group 7 (Europe) | 1.38 | 454.6 | 0.4[a] |
| Group 8 (Mexico) | 2.56 | 762.3 | 0.4[a] |
| Group 9 (Canada) | 0.51 | 2,581.3 | 0.4[a] |
| Group 10(Japan & Taiwan) | 0.13 | 24.6 | 0.4[a] |
| Foreign Import subtotal | 1.16 | 110,329.1 | |
| TOTAL | 1.20 | 366,364.7 | |

Note: (a) Crude oil coming to the South Coast Air Basin from undesignated countries of origin was distributed amongst all producing regions whose exports to California were not known explicitly.

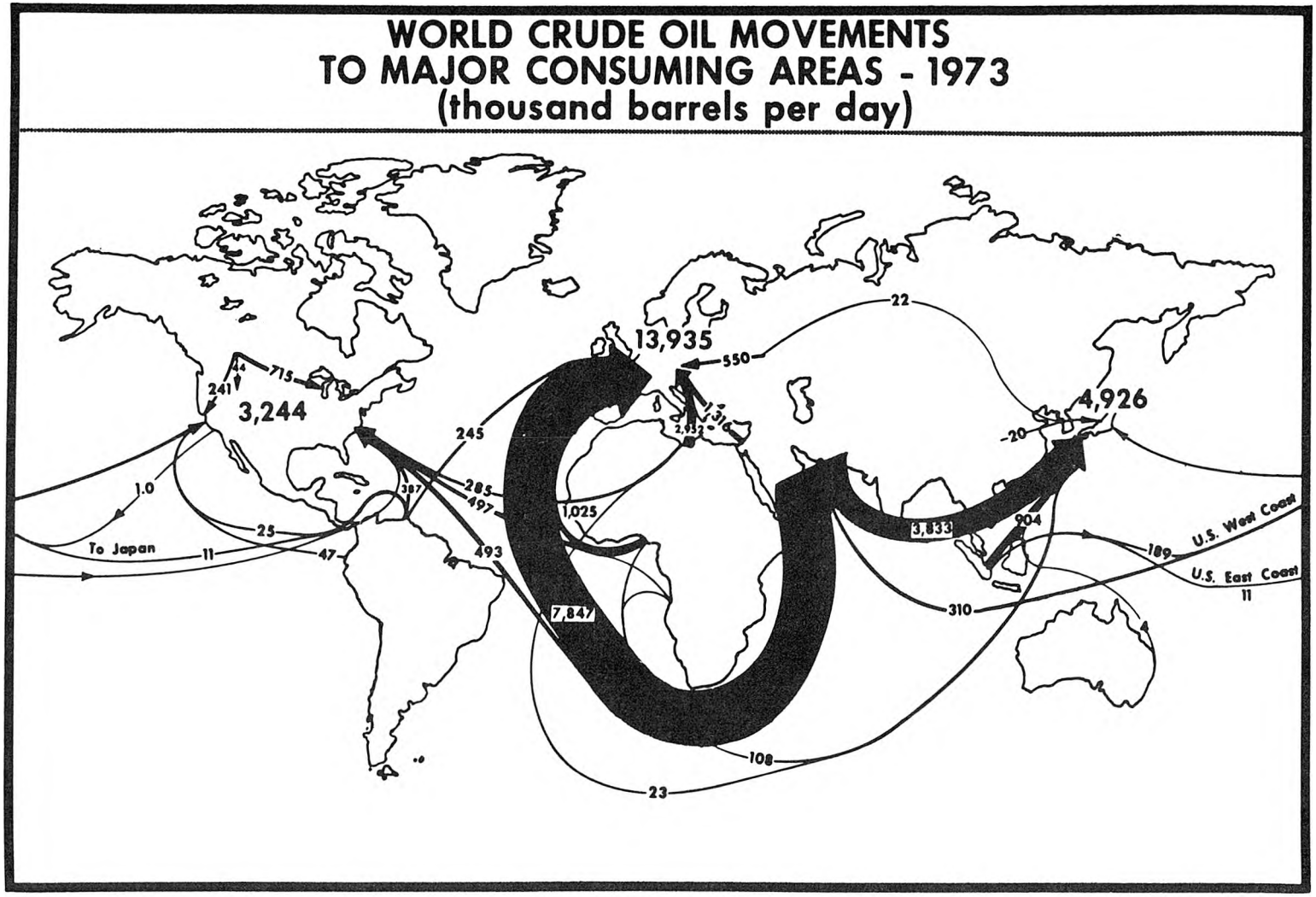


Source: Bureau of Mines (1975)

FIGURE 4.2

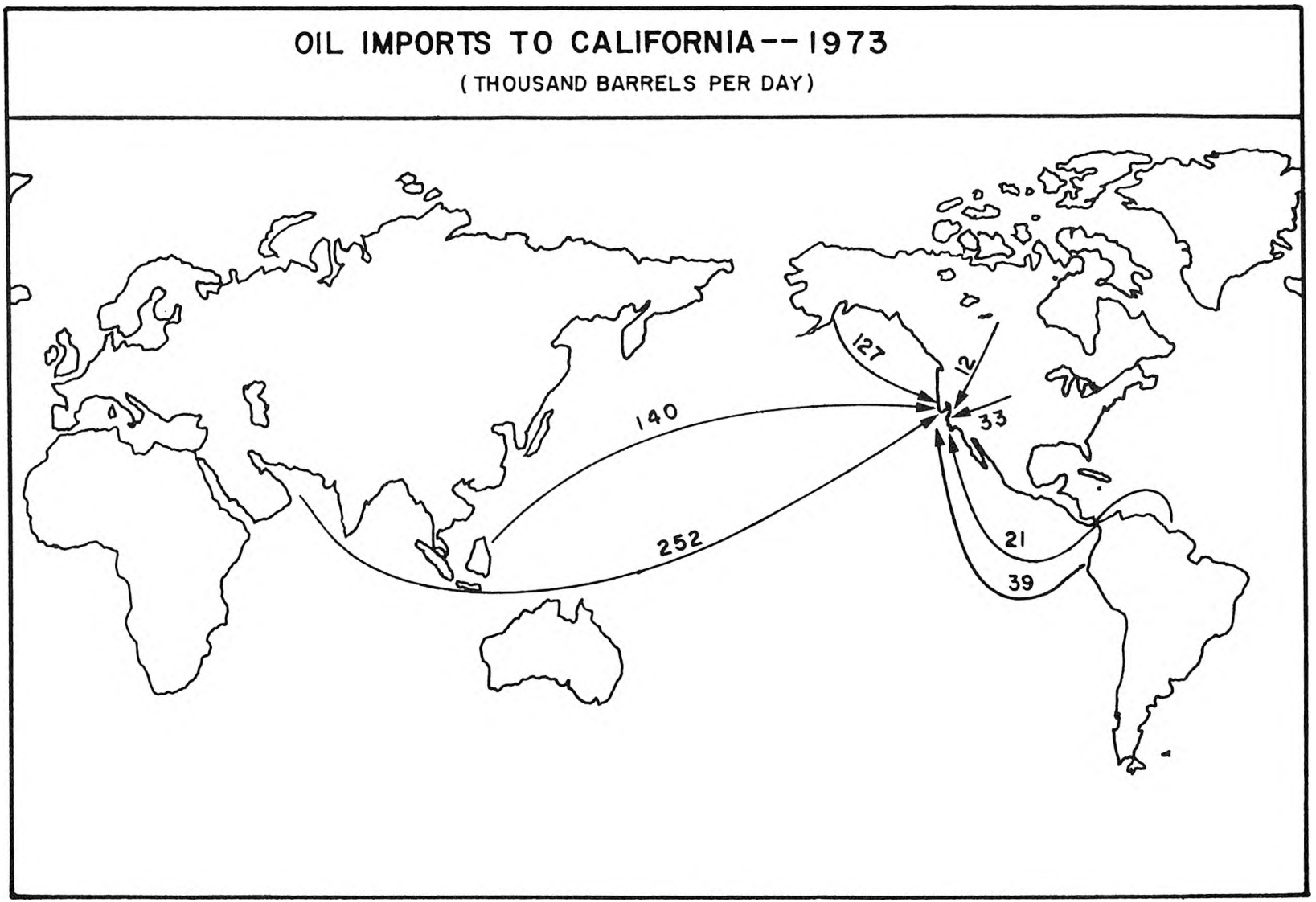
OIL IMPORTS TO CALIFORNIA -- 1973
(THOUSAND BARRELS PER DAY)
127
12
140
33
252
21
39

FIGURE 4.3

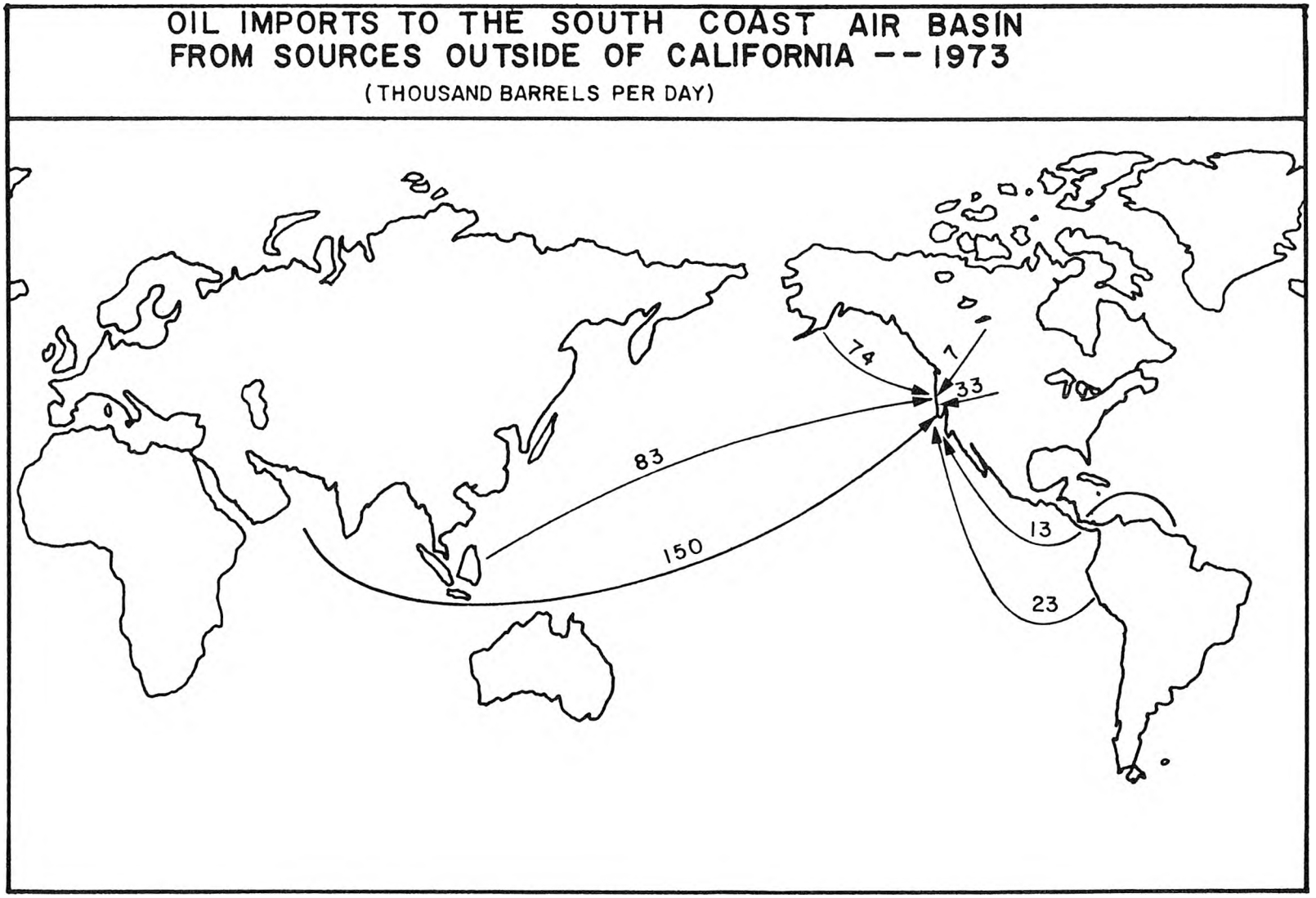
OIL IMPORTS TO THE SOUTH COAST AIR BASIN
FROM SOURCES OUTSIDE OF CALIFORNIA -- 1973
(THOUSAND BARRELS PER DAY)
74
1
33
83
150
13
23

FIGURE 4.4

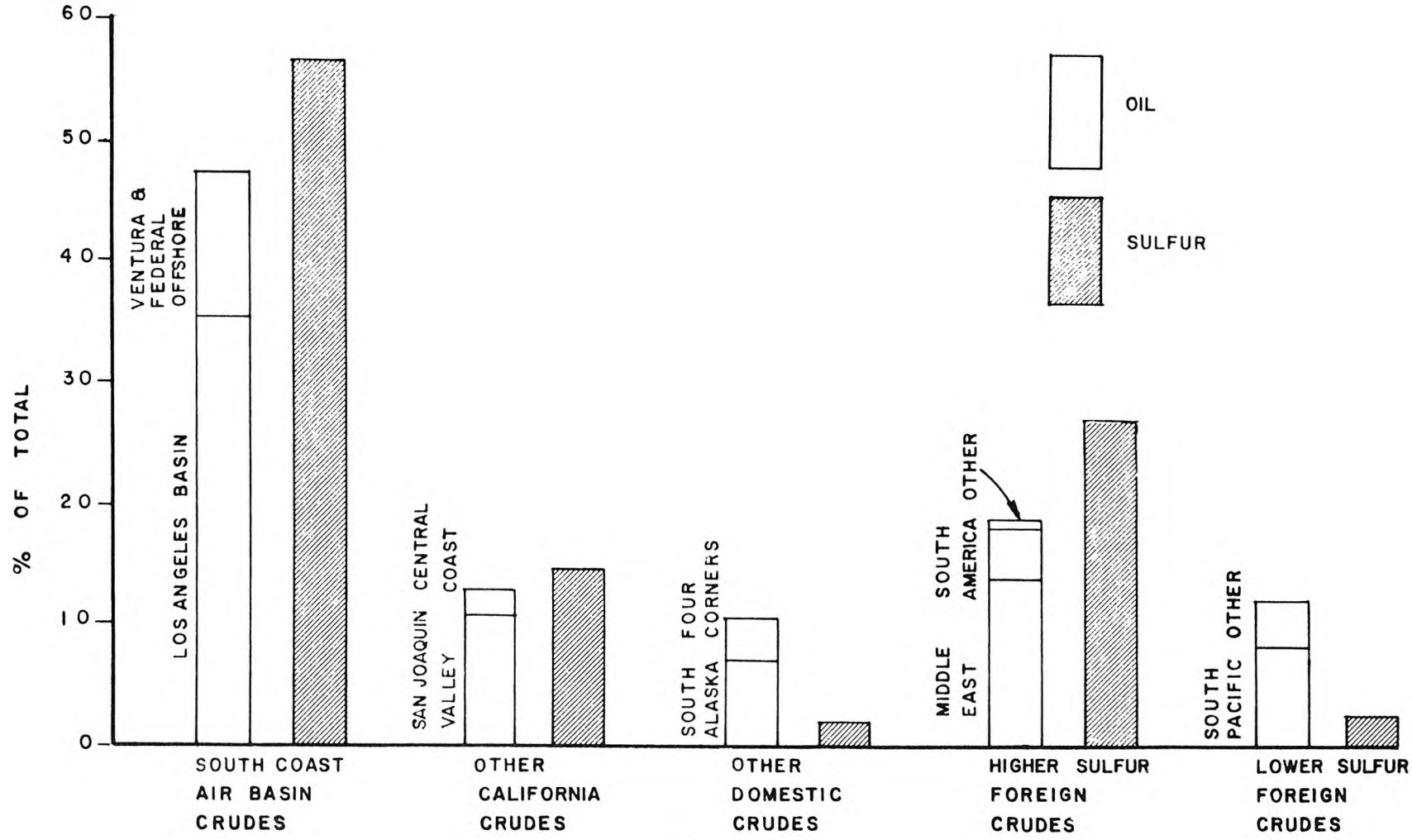


FIGURE 4.5

The Fraction of Crude Oil and Sulfur Received in the South Coast Air Basin from Various Producing Regions of the World - 1973.

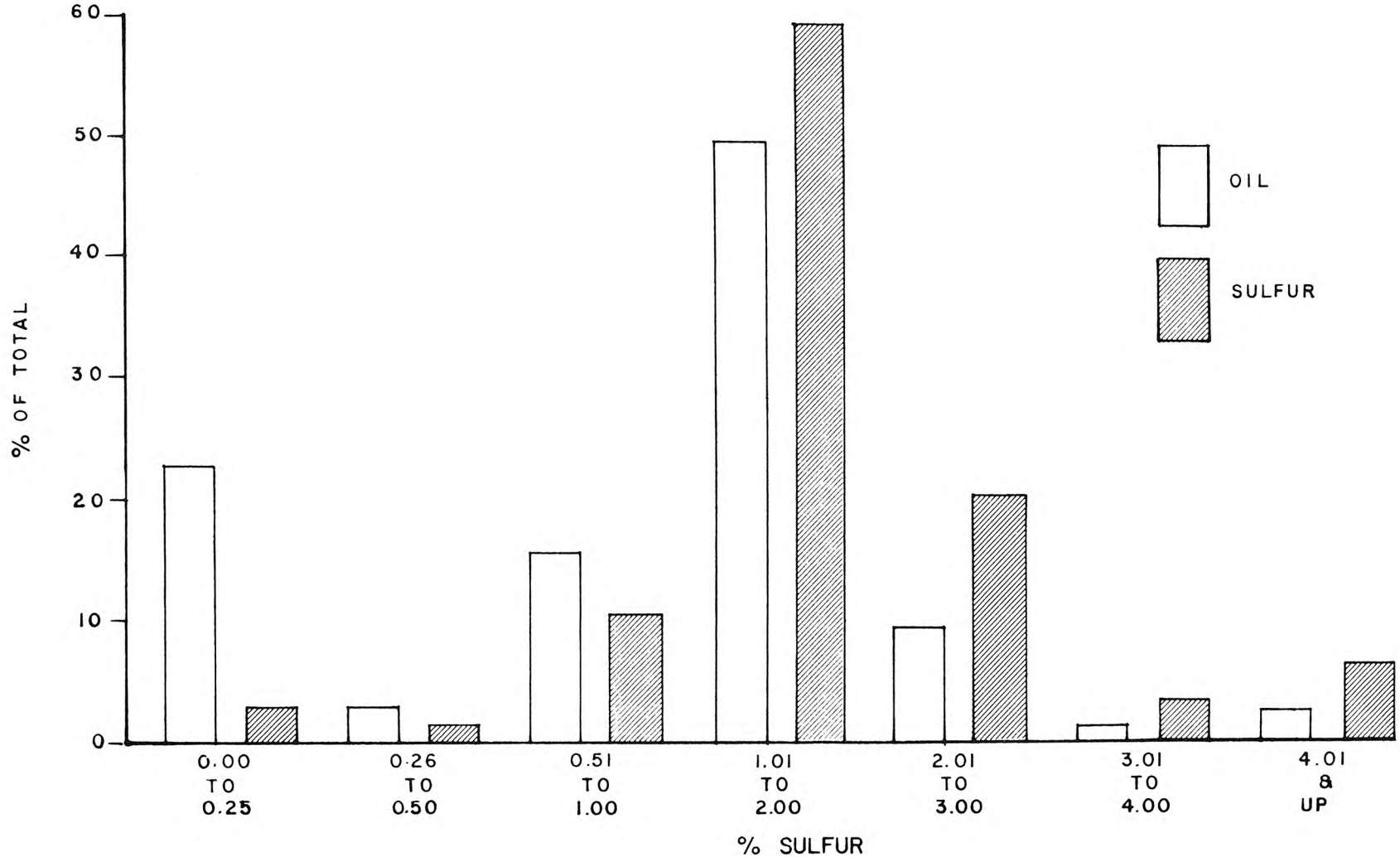


FIGURE 4.6

The Distribution of Crude Oils by Sulfur Content Received in the South Coast Air Basin in 1973.

problems facing Los Angeles area refineries. In the lowest sulfur category (< 0.25% S), 22% of the total oil contributes only 2% to the total sulfur burden on basin oil refineries, while in the 2.01% and higher sulfur categories, 12% of the total oil contributes 28.5% of the sulfur. Even so, the major portion of sulfur supply to the air basin comes from the 1.01 to 2.00% sulfur category where 49% of the total oil contributes 59% of the total sulfur. That 1.01% to 2.00% sulfur category is dominated by local crude oils produced in the Los Angeles and Ventura oil fields. One cannot easily divert this source of supply to other ports because the supply is already landed ashore. Substantial alteration of transfer and storage facilities would be needed if that oil were to be sold elsewhere. Thus, locally produced crude oil would be difficult to displace by importation of alternate low-sulfur oils. The South Coast Air Basin is apparently saddled with a sulfur management problem that is not likely to be exported elsewhere as long as local crude oils are processed in local refineries.

If converted completely into sulfur oxides air pollutant emissions, 3551 to 3821 thousand pounds of sulfur entering local refineries daily in feedstocks would result in 3551 to 3821 tons per day of $SO_x$ emissions (stated as $SO_2$). Actual atmospheric emissions within the South Coast Air Basin are thought to be far less than that, as explained in the following sections of this study.

## 4.3 A Spatially Resolved Sulfur Oxides Emission Inventory: 1972 Through 1974

In Figure 4.7, a square area 50 miles on each edge is shown superimposed over the central portion of the South Coast Air Basin. That square has been subdivided into a system of grid cells with a two mile spacing between adjacent cell boundaries. This grid system is suitable for use in displaying sulfate air quality model results since it substantially covers those areas of the air basin for which extensive air quality data are available for model validation. For historic reasons, the grid system is also convenient for compiling and displaying a detailed sulfur oxides source emission inventory. Each two mile by two mile grid cell corresponds to a combination of four one square mile areas used by the Southern California APCD to identify point source locations. Secondly, this grid system closely matches that used by Roth, et al. (1974) to display baseline traffic counts for Los Angeles for the year 1969 which are widely used by other air quality modeling groups. An attempt will be made here to develop inventory information which may assist the on-going efforts of these other investigators. The grid system employed does not cover the outlying areas of the airshed. An air quality model constructed to use this inventory should thus be capable of handling the few major off-grid sources that will be detailed later in this report.

### 4.3.1 Emission Inventory Methods and Approach

Appendix A2 describes the assembly of an inventory of sulfur oxides emissions for the central portion of the South Coast Air Basin.

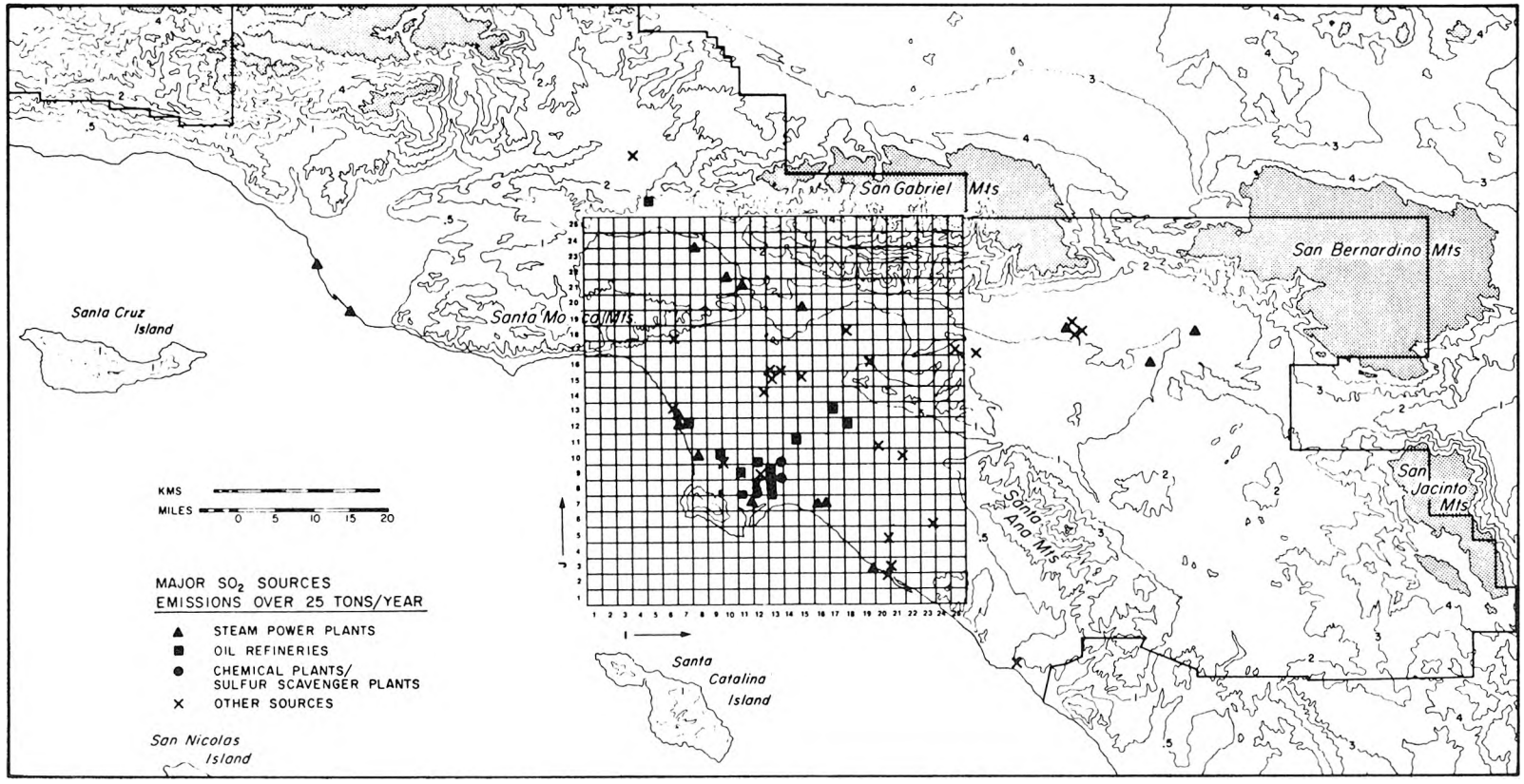


FIGURE 4.7

The Central Portion of the South Coast Air Basin
Showing the Grid System Used

Estimates were made of the emissions from over two thousand five hundred stationary sources and from seven classes of mobile sources for each month of the years 1972 through 1974. A general description of the approach used in assembling this inventory will be given here. Appendix A2 should be consulted for a detailed description of the emission estimation procedure for each source type.

Los Angeles Air Pollution Control District (1975) historical emission summaries were reviewed to obtain an idea of the relative magnitude of various classes of emission sources. The inventory was subdivided into mobile and stationary source categories, and the stationary sources were approached first. Los Angeles APCD permit files were consulted, and an APCD computerized data listing entitled "Emissions by ID Number" was selected for initial study. From this data base (hereafter referred to as the permit file) the location, ownership, equipment type and permit file emissions estimates were obtained for 2003 stationary source equipment items in Los Angeles County. Data on all equipment items listed as current sulfur oxides emitters were copied, as well as data on all boilers and all miscellaneous $NO_x$ emissions sources at premises with $NO_x$ emissions of greater than 50 pounds per week. Boilers and other $NO_x$ emission sources were considered as *potential* $SO_x$ emission sources in the event that their natural gas supply was curtailed.

While emission data were thus acquired for a large number of sources, it was quickly determined by conversation with APCD staff members that much of this permit file emission data was out-dated or

reflected source operation on only one type of fuel while fuel switching from oil to gas was known to be practiced on a seasonal basis. The permit file emission inventory is thus best suited to serve as an equipment list around which better emissions estimates might be organized.

The equipment list was therefore subdivided into fuel burning equipment, industrial process equipment, and incinerators. The permit file emissions data for fuel burning sources were discarded, and month by month emissions from fuel burning sources were estimated from actual fuel use data available for electric utilities, oil refineries, major industries and small natural gas users, as described in detail in Appendix A2. In the course of that investigation, several hundred additional fuel burning sources were located and added to the inventory.

Next, items of industrial process equipment emitting over one hundred pounds of $SO_x$ per week were isolated, and APCD staff engineers responsible for overseeing those sources were interviewed. As a result of this interview procedure, additional emission sources were located that were not yet a part of the computerized permit files, and better estimates were made of emissions from chemical plants, oil refineries, coke calcining kilns, glass furnaces and secondary lead smelters.

With the core of the stationary source emission data established, survey efforts were expanded beyond Los Angeles County. The source survey and staff interview procedures were repeated at the offices of the Southern California APCD-Southern Zone (formerly the Orange County

APCD). Fuel burning data on power plants located outside of Los Angeles County were acquired from the Southern California Edison Company. Major off-grid sources in San Bernardino and Riverside Counties were reviewed with the help of Southern California APCD staff. The operators of some emissions sources were contacted in order to firm-up data needed to make emission estimates.

Shortly after these emissions data from stationary sources were compiled, a detailed stationary source $SO_x$ emission inventory prepared independently by Hunter and Helgeson (1976) became available for 1974, one of our three years of interest. The two inventories were cross-checked for the year in which they overlap, with generally excellent agreement. Additions and corrections were made to our inventory to reflect certain cases in which Hunter and Helgeson's source test data were thought to present a more recent picture of source operation than was otherwise available. In most cases, however, the time sequence of emissions estimated from our fuel burning records and discussion with APCD staff were retained since they represented a longer historic period of observation, and were usually quite close to Hunter and Helgeson's estimates for the year in which both inventories overlap. Hunter and Helgeson's data for the fraction of each source's emissions evolved as $SO_3$ were adopted to supplement the APCD data base.

Finally, mobile source emissions categories for autos and light trucks, heavy duty vehicles, ships, railroads and aircraft were established. Freeway traffic counts were performed for each year of the three year period 1972 through 1974. A surface street traffic

growth survey was used to update existing 1969 surface street traffic data to the years of interest. Then the traffic count data were used to estimate motor vehicle $SO_x$ emissions for freeways and for surface streets on a spatially resolved basis. Shipping activities and railroad track mileage were assigned geographically to the grid system. Then fuel use by ships and railroads was scaled down to the grid system from the basin-wide fuel use data developed in the Energy and Sulfur Balance portion of this report (see Appendix A3). Aircraft emissions were estimated on the basis of the number of take-off and landing operations at each airport and military air base within our grid system.

### 4.3.2 Emission Inventory Summary and Discussion

Figure 4.8 summarizes sulfur oxides emissions within the 50 by 50 mile square for the years 1972 through 1974. The general source classes shown have been arranged to correspond to the traditional classification system of the Los Angeles Air Pollution Control District so that the reader may compare these results to historic emission trends given in Table 4.3. Historic data in Table 4.3 are available only for Los Angeles County, while the 50 by 50 mile grid covers the populated portions of both Los Angeles and Orange Counties. As will be seen, however, most major industrial emissions sources are confined to Los Angeles County.

From Figure 4.8, we note that the majority of sulfur oxides emissions arise from combustion-related sources, both stationary and mobile. Electric utility fuel combustion was the largest single $SO_x$

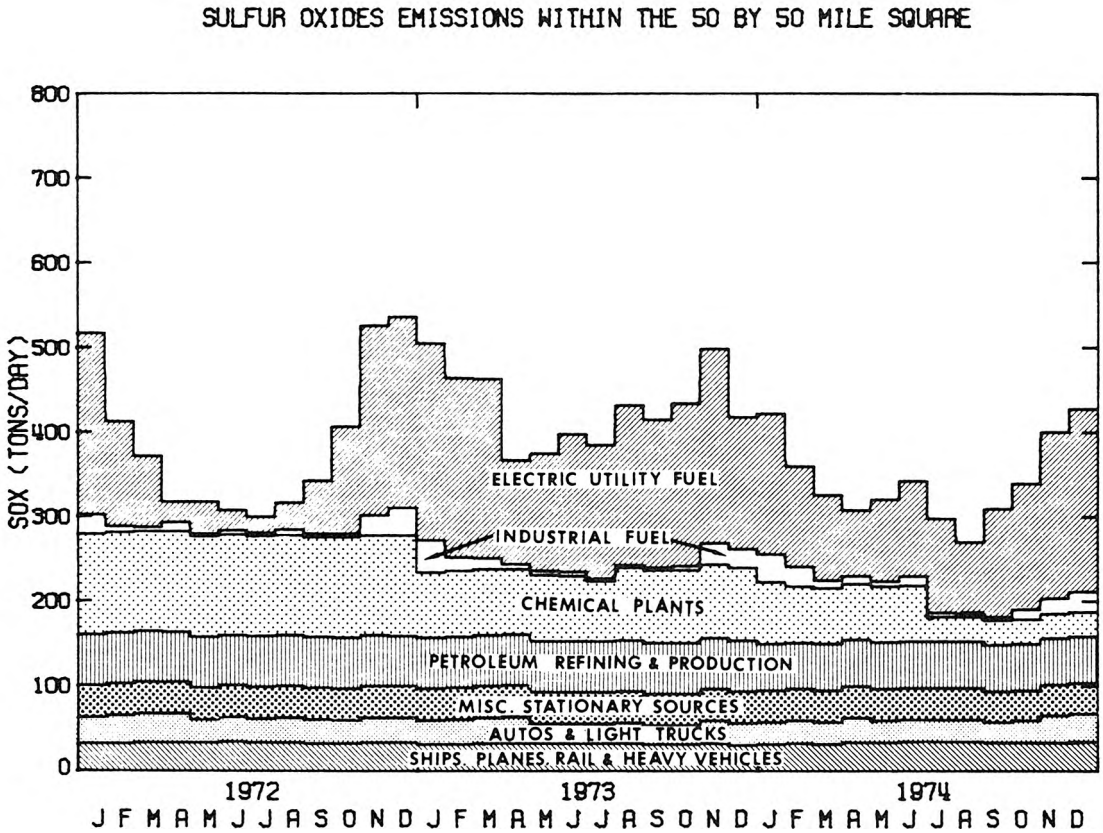
SULFUR OXIDES EMISSIONS WITHIN THE 50 BY 50 MILE SQUARE
SOX (TONS/DAY)
800
700
600
500
400
300
200
100
0
ELECTRIC UTILITY FUEL
INDUSTRIAL FUEL
CHEMICAL PLANTS
PETROLEUM REFINING & PRODUCTION
MISC. STATIONARY SOURCES
AUTOS & LIGHT TRUCKS
SHIPS, PLANES, RAIL & HEAVY VEHICLES
1972
1973
1974
J F M A M J J A S O N D J F M A M J J A S O N D J F M A M J J A S O N D

FIGURE 4.8

TABLE 4.3

Emissions of Sulfur Dioxide
in Los Angeles County
(tons per average day)

| Year | Steam Power Plants | Combustion of Fuels From Other Stationary Sources | Chemical Plants (a) | Petroleum Refining Producing and Marketing (b) | Misc. Sources | Gasoline Powered Vehicles | Aircraft, Ships, Railroads & Diesel Powered Vehicles | Total |
|---|---|---|---|---|---|---|---|---|
| 1955 | 182(47)[c] | 277 | 47 | 179 | 17 | 36 | 1 | 739 |
| 1956 | 187(47) | | | | | 35 | | |
| 1957 | 240(43) | 150 | 46 | 50 | | 35 | 14 | 545 |
| 1958 | 122(66) | 183 | 47 | 50 | 1 | 35 | 15 | 453 |
| 1959 | 150(63) | | | | | 30 | | |
| 1960 | 153(65) | 45 | 51 | 40 | 1 | 25 | 2 | 317 |
| 1961 | 132(71) | 44 | 52 | 36 | 1 | 25 | 2 | 292 |
| 1962 | 120(75) | | | | | 26 | | |
| 1963 | 108(78) | | | | | 25 | | |
| 1964 | 116(77) | 21 | 65 | 45 | 3 | 24 | 2 | 276 |
| 1965 | 136(76) | | | | | 23 | | |
| 1966 | 180(76) | 33 | 65 | 35 | 3 | 25 | 2 | 343 |
| 1967 | 138(83) | | | | | 26 | | |
| 1968 | 90(83) | 8 | 90 | 55 | 4 | 26 | 5 | 278 |
| 1969 | 57(79) | | | | | 27 | | |
| 1970 | 42(77) | 11 | 116 | 49 | 7 | 27 | 5 | 257 |
| 1971 | 76(60) | | | | | 28 | | |
| 1972 | 83(58) | | | | | 29 | | |
| 1973 | 161(30) | 14 | 60 | 55 | 30 | 30 | 15 | 365 |
| 1974 | 115(31) | 15 | 20 | 60 | 20 | 30 | 15 | 275 |

(a) Includes emissions from sulfur recovery plants and sulfuric acid plants.

(b) Includes only those emissions from refining, producing and marketing operations. Does not include emissions from the combustion of fuels, i.e., from fired heaters, boilers, etc.

(c) Parentheses indicate percent level of service of natural gas.

Source: Los Angeles Air Pollution Control District (1975)

emission source category during 1974. This represents a substantial change since 1972 when sulfur recovery and sulfuric acid plants in the chemical plant category constituted the largest group of $SO_x$ sources on an annual average basis. This shift in relative source contributions is attributed mainly to the installation of tail gas clean-up equipment at Los Angeles County chemical plants, combined with increased oil burning at power plants due to natural gas curtailment.

A second major shift in relative source contributions is seen to be seasonal in nature. Power plants historically have emitted greater quantities of $SO_x$ during the winter months. From Figure 4.8 one might quickly assume that electricity demand is vastly higher in the winter months than in the summer, but that conclusion would be wrong. Energy use within the 50 by 50 mile square grid is detailed in Figure 4.9 from information gathered while compiling Appendices A2 and A3 to this study. Total monthly electricity use within that study area is fairly constant throughout the year. Instead, what has happened is that residential, commercial and light industrial demands for fossil fuel rise sharply during the winter. These customers have a higher priority for receiving "firm" service from the relatively fixed supply of natural gas available throughout the year than do the basin's electric utilities. The result is that the gas supply to utilities and large industries has been curtailed during winter months. The wintertime increase in $SO_x$ emissions is due to substitution of sulfur-bearing fuel oil for natural gas by these curtailed gas customers. These major shifts in source emission strength from month to month will

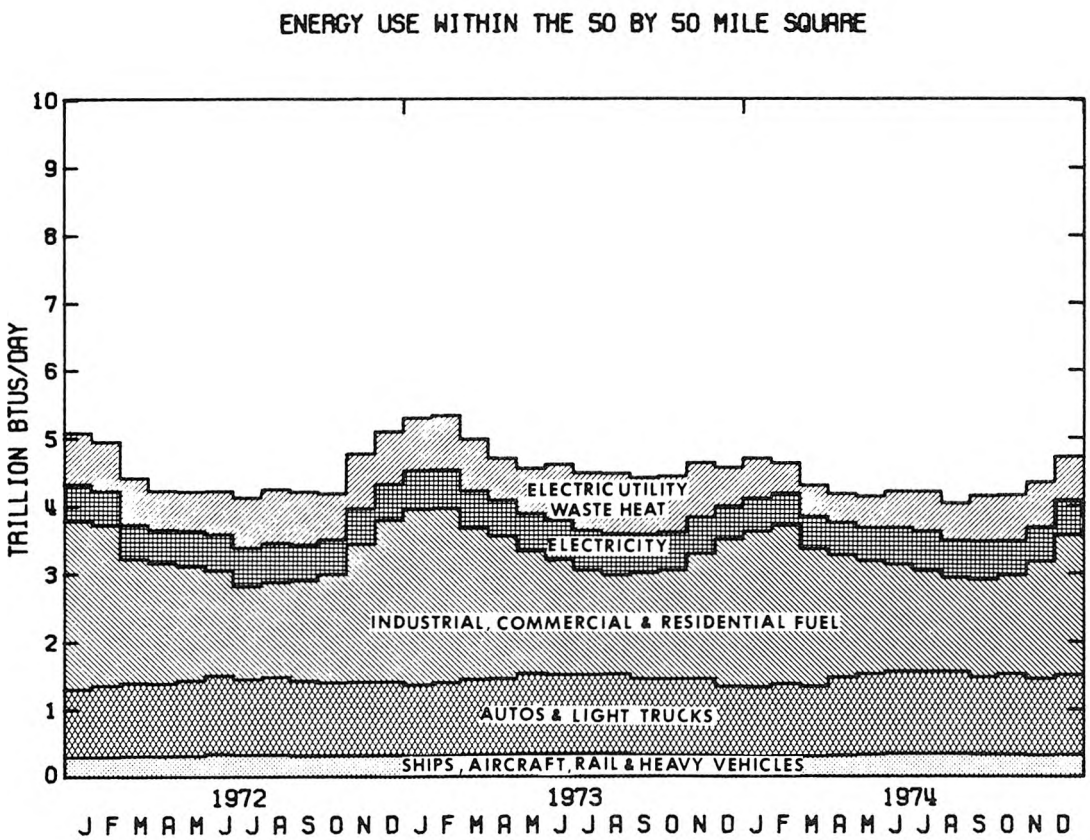
ENERGY USE WITHIN THE 50 BY 50 MILE SQUARE
TRILLION BTUS/DAY
10
9
8
7
6
5
4
3
2
1
0
ELECTRIC UTILITY WASTE HEAT
ELECTRICITY
INDUSTRIAL, COMMERCIAL & RESIDENTIAL FUEL
AUTOS & LIGHT TRUCKS
SHIPS, AIRCRAFT, RAIL & HEAVY VEHICLES
1972
1973
1974
J F M A M J J A S O N D J F M A M J J A S O N D J F M A M J J A S O N D

FIGURE 4.9

provide a tough test for any air quality model validation effort. This is particularly true for a sulfate air quality modeling study since sulfate concentration seasonal trends tend to buck the $SO_x$ emissions history shown here: Los Angeles sulfate concentrations generally peak in the summer months (for example, see Chapter 2).

It would be tempting to refer to these emission patterns as winter emissions and summer emissions, respectively. That may be misleading however, since only the availability of natural gas during the summer has prevented the higher emission pattern from appearing in the summer season. In fact, as can be seen in Figure 4.8, total $SO_x$ emissions for August 1973 were as high as any period of the winter 1973-74. By the year 1979 or 1980, natural gas supplies to electric utilities and large industries in Southern California are expected to be completely curtailed in all months of the year (1975 California Gas Report). The implication is that, in the absence of changes in 1974 emission control regulations, the summertime trough in electric utility $SO_x$ emissions would be "filled-in" to about the level of past winter emissions peaks. $SO_x$ emissions from industrial fuel burning would rise substantially.

Tables 4.4 through 4.6 show the monthly emissions history for individual source and equipment types within the general source categories of Figure 4.8. The emission inventory created for air quality model use contains spatially resolved source strength data defined on the 50 by 50 mile grid for each of the 26 source types shown in Tables 4.4 through 4.6 for each month of the years 1972

# TABLE 4.4a

1972 Sulfur Oxides Emissions Within the 50 by 50 Mile Square Grid
(in short tons per day as $SO_2$)

| STATIONARY SOURCES | JAN | FEB | MAR | APR | MAY | JUN | JUL | AUG | SEP | OCT | NOV | DEC | ANNUAL |
|---|---|---|---|---|---|---|---|---|---|---|---|---|---|
| Fuel Combustion | | | | | | | | | | | | | |
| Electric Utilities | 214.86 | 123.46 | 83.56 | 23.90 | 38.33 | 23.98 | 18.54 | 32.22 | 62.40 | 126.81 | 223.96 | 225.17 | 99.81 |
| Refinery Fuel | 17.69 | 5.78 | 3.66 | 9.55 | 2.50 | 3.62 | 3.42 | 5.86 | 3.38 | 3.85 | 20.95 | 19.69 | 8.33 |
| Other Interruptible Gas Customers | 5.56 | 1.37 | 0.61 | 0.75 | 0.64 | 0.67 | 0.39 | 0.63 | 0.51 | 0.59 | 2.74 | 13.29 | 2.33 |
| Firm Gas Customers | 0.46 | 0.43 | 0.29 | 0.27 | 0.24 | 0.20 | 0.17 | 0.15 | 0.16 | 0.18 | 0.30 | 0.40 | 0.27 |
| Chemical Plants | | | | | | | | | | | | | |
| Sulfur Recovery | 93.53 | 93.53 | 93.53 | 93.53 | 93.53 | 93.53 | 93.53 | 93.53 | 93.53 | 93.53 | 93.53 | 93.53 | 93.53 |
| Sulfuric Acid | 25.00 | 25.00 | 25.00 | 25.00 | 25.00 | 25.00 | 25.00 | 25.00 | 25.00 | 25.00 | 25.00 | 25.00 | 25.00 |
| Other Chemicals | 0.09 | 0.09 | 0.09 | 0.09 | 0.09 | 0.09 | 0.09 | 0.09 | 0.09 | 0.09 | 0.09 | 0.09 | 0.09 |
| Petroleum Refining and Production | | | | | | | | | | | | | |
| Fluid Catalytic Crackers | 52.07 | 52.07 | 52.07 | 52.07 | 52.07 | 52.07 | 52.07 | 52.07 | 52.07 | 52.07 | 52.07 | 52.07 | 52.07 |
| Sour Water Strippers | 0.13 | 0.13 | 0.13 | 0.13 | 0.13 | 0.13 | 0.13 | 0.13 | 0.13 | 0.13 | 0.13 | 0.13 | 0.13 |
| Delayed Cokers | 2.28 | 2.28 | 2.28 | 2.28 | 2.28 | 2.28 | 2.28 | 2.28 | 2.28 | 2.28 | 2.28 | 2.28 | 2.28 |
| Misc. Refinery Process | 1.02 | 1.02 | 1.02 | 1.02 | 1.02 | 1.02 | 1.02 | 1.02 | 1.02 | 1.02 | 1.02 | 1.02 | 1.02 |
| Oil Field Production | 4.00 | 4.00 | 4.00 | 4.00 | 4.00 | 4.00 | 4.00 | 4.00 | 4.00 | 4.00 | 4.00 | 4.00 | 4.00 |
| Misc. Stationary Sources | | | | | | | | | | | | | |
| Petroleum Coke Kilns | 25.52 | 25.52 | 25.52 | 25.52 | 25.52 | 25.52 | 25.52 | 25.52 | 25.52 | 25.52 | 25.52 | 25.52 | 25.52 |
| Glass Furnaces | 2.00 | 2.00 | 2.00 | 2.00 | 2.00 | 2.00 | 2.00 | 2.00 | 2.00 | 2.00 | 2.00 | 2.00 | 2.00 |
| Metals Industries | 8.78 | 8.78 | 8.78 | 8.78 | 8.78 | 8.78 | 8.78 | 8.78 | 8.78 | 8.78 | 8.78 | 8.78 | 8.78 |
| Mineral Products | 0.00 | 0.00 | 0.00 | 0.00 | 0.00 | 0.00 | 0.00 | 0.00 | 0.00 | 0.00 | 0.00 | 0.00 | 0.00 |
| Sewage Treatment Digesters | 0.64 | 0.64 | 0.64 | 0.64 | 0.64 | 0.64 | 0.64 | 0.64 | 0.64 | 0.64 | 0.64 | 0.64 | 0.64 |
| Other Industrial Processes | 0.02 | 0.02 | 0.02 | 0.02 | 0.02 | 0.02 | 0.02 | 0.02 | 0.02 | 0.02 | 0.02 | 0.02 | 0.02 |
| Permitted Incinerators | 0.07 | 0.07 | 0.07 | 0.07 | 0.07 | 0.07 | 0.07 | 0.07 | 0.07 | 0.07 | 0.07 | 0.07 | 0.07 |
| MOBILE SOURCES | | | | | | | | | | | | | |
| Autos and Lt. Trucks-Surface | 19.43 | 20.25 | 21.14 | 20.98 | 17.04 | 18.00 | 17.27 | 17.81 | 16.97 | 16.70 | 18.07 | 17.93 | 18.46 |
| Autos and Lt. Trucks-Freeway | 12.21 | 12.72 | 13.28 | 13.18 | 10.70 | 11.31 | 10.85 | 11.91 | 10.66 | 10.49 | 11.35 | 11.26 | 11.60 |
| Heavy Duty Vehicles-Surface | 9.71 | 10.14 | 10.44 | 10.35 | 10.29 | 10.85 | 10.40 | 10.68 | 10.17 | 10.00 | 10.25 | 10.20 | 10.29 |
| Heavy Duty Vehicles-Freeway | 6.10 | 6.37 | 6.56 | 6.50 | 6.46 | 6.81 | 6.53 | 6.71 | 6.39 | 6.28 | 6.44 | 6.41 | 6.46 |
| Airport Operations | 1.15 | 1.15 | 1.15 | 1.15 | 1.15 | 1.15 | 1.15 | 1.15 | 1.15 | 1.15 | 1.15 | 1.15 | 1.15 |
| Shipping Operations | 11.89 | 11.89 | 11.89 | 11.89 | 11.89 | 11.89 | 11.89 | 11.89 | 11.89 | 11.89 | 11.89 | 11.89 | 11.89 |
| Railroad Operations | 3.39 | 3.39 | 3.39 | 3.39 | 3.39 | 3.39 | 3.39 | 3.39 | 3.39 | 3.39 | 3.39 | 3.39 | 3.39 |
| TOTAL | 517.60 | 412.10 | 371.12 | 317.06 | 317.78 | 307.02 | 299.15 | 317.55 | 342.22 | 406.48 | 525.64 | 535.93 | 389.13 |

## TABLE 4.4b

Major Off-Grid Emission Sources Included within the 1972 South Coast Air Basin Sulfur Oxides Modeling Inventory
(in short tons per day as $SO_2$)

| STATIONARY SOURCES | JAN | FEB | MAR | APR | MAY | JUN | JUL | AUG | SEP | OCT | NOV | DEC | ANNUAL |
|---|---|---|---|---|---|---|---|---|---|---|---|---|---|
| Fuel Combustion | | | | | | | | | | | | | |
| Electric Utilities | 55.74 | 24.32 | 16.79 | 6.75 | 9.99 | 6.01 | 9.52 | 10.52 | 19.56 | 29.19 | 58.04 | 63.68 | 25.89 |
| Refinery Fuel | --- | --- | --- | --- | --- | --- | --- | --- | --- | --- | --- | --- | --- |
| Other Interruptible Gas Customers | --- | --- | --- | --- | --- | --- | --- | --- | --- | --- | --- | --- | --- |
| Firm Gas Customers | --- | --- | --- | --- | --- | --- | --- | --- | --- | --- | --- | --- | --- |
| Chemical Plants | | | | | | | | | | | | | |
| Sulfur Recovery | --- | --- | --- | --- | --- | --- | --- | --- | --- | --- | --- | --- | --- |
| Sulfuric Acid | --- | --- | --- | --- | --- | --- | --- | --- | --- | --- | --- | --- | --- |
| Other Chemicals | --- | --- | --- | --- | --- | --- | --- | --- | --- | --- | --- | --- | --- |
| Petroleum Refining and Production | | | | | | | | | | | | | |
| Fluid Catalytic Crackers | --- | --- | --- | --- | --- | --- | --- | --- | --- | --- | --- | --- | --- |
| Sour Water Strippers | --- | --- | --- | --- | --- | --- | --- | --- | --- | --- | --- | --- | --- |
| Delayed Cokers | --- | --- | --- | --- | --- | --- | --- | --- | --- | --- | --- | --- | --- |
| Misc. Refinery Processes | --- | --- | --- | --- | --- | --- | --- | --- | --- | --- | --- | --- | --- |
| Oil Field Production | --- | --- | --- | --- | --- | --- | --- | --- | --- | --- | --- | --- | --- |
| Misc. Stationary Sources | | | | | | | | | | | | | |
| Petroleum Coke Kilns | --- | --- | --- | --- | --- | --- | --- | --- | --- | --- | --- | --- | --- |
| Glass Furnaces | 0.23 | 0.23 | 0.23 | 0.23 | 0.23 | 0.23 | 0.23 | 0.23 | 0.23 | 0.23 | 0.23 | 0.23 | 0.23 |
| Metals Industries | 35.20 | 35.20 | 35.20 | 35.20 | 35.20 | 35.20 | 35.20 | 35.20 | 35.20 | 35.20 | 35.20 | 35.20 | 35.20 |
| Mineral Products | 2.30 | 2.30 | 2.30 | 2.30 | 2.30 | 2.30 | 2.30 | 2.30 | 2.30 | 2.30 | 2.30 | 2.30 | 2.30 |
| Sewage Treatment Digesters | --- | --- | --- | --- | --- | --- | --- | --- | --- | --- | --- | --- | --- |
| Other Industrial Processes | --- | --- | --- | --- | --- | --- | --- | --- | --- | --- | --- | --- | --- |
| Permitted Incinerators | --- | --- | --- | --- | --- | --- | --- | --- | --- | --- | --- | --- | --- |
| TOTAL | 93.47 | 62.05 | 54.52 | 44.48 | 47.72 | 43.74 | 47.25 | 48.25 | 57.29 | 66.92 | 95.77 | 101.41 | 63.62 |

# TABLE 4.5a

1973 Sulfur Oxides Emissions Within the 50 by 50 Mile Square Grid
(in short tons per day as $SO_2$)

| STATIONARY SOURCES | JAN | FEB | MAR | APR | MAY | JUN | JUL | AUG | SEP | OCT | NOV | DEC | ANNUAL |
|---|---|---|---|---|---|---|---|---|---|---|---|---|---|
| Fuel Combustion | | | | | | | | | | | | | |
| Electric Utilities | 232.77 | 212.31 | 212.13 | 123.36 | 139.48 | 163.87 | 157.77 | 189.23 | 174.16 | 192.05 | 229.72 | 155.48 | 181.71 |
| Refinery Fuel | 25.07 | 13.50 | 10.61 | 4.26 | 3.99 | 3.73 | 2.91 | 2.14 | 2.37 | 4.01 | 21.69 | 18.96 | 9.42 |
| Other Interruptible Gas Customers | 12.78 | 2.24 | 2.07 | 0.98 | 0.81 | 0.39 | 0.39 | 0.40 | 0.43 | 0.76 | 3.58 | 2.57 | 2.29 |
| Firm Gas Customers | 0.46 | 0.46 | 0.37 | 0.33 | 0.26 | 0.21 | 0.17 | 0.16 | 0.19 | 0.20 | 0.26 | 0.36 | 0.29 |
| Chemical Plants | | | | | | | | | | | | | |
| Sulfur Recovery | 57.18 | 57.18 | 57.18 | 57.18 | 57.08 | 57.08 | 50.70 | 66.20 | 66.20 | 66.20 | 66.20 | 66.20 | 60.40 |
| Sulfuric Acid | 20.00 | 20.00 | 20.00 | 20.00 | 20.00 | 20.00 | 20.00 | 20.00 | 20.00 | 20.00 | 20.00 | 20.00 | 20.00 |
| Other Chemicals | 0.09 | 0.09 | 0.09 | 0.09 | 0.09 | 0.09 | 0.09 | 0.09 | 0.09 | 0.09 | 0.09 | 0.09 | 0.09 |
| Petroleum Refining and Production | | | | | | | | | | | | | |
| Fluid Catalytic Crackers | 52.07 | 52.07 | 52.07 | 52.07 | 52.07 | 52.07 | 52.07 | 52.07 | 52.07 | 52.07 | 52.07 | 52.07 | 52.07 |
| Sour Water Strippers | 0.13 | 0.13 | 0.13 | 0.13 | 0.13 | 0.13 | 0.13 | 0.13 | 0.13 | 0.13 | 0.13 | 0.13 | 0.13 |
| Delayed Cokers | 2.28 | 2.28 | 2.28 | 2.28 | 2.28 | 2.28 | 2.28 | 2.28 | 2.28 | 2.28 | 2.28 | 2.28 | 2.28 |
| Misc. Refinery Process | 1.02 | 1.02 | 1.02 | 1.02 | 1.02 | 1.02 | 1.02 | 1.02 | 1.02 | 1.02 | 1.02 | 1.02 | 1.02 |
| Oil Field Production | 4.50 | 4.50 | 4.50 | 4.50 | 4.50 | 4.50 | 4.50 | 4.50 | 4.50 | 4.50 | 4.50 | 4.50 | 4.50 |
| Misc. Stationary Sources | | | | | | | | | | | | | |
| Petroleum Coke Kilns | 25.52 | 25.52 | 25.52 | 25.52 | 25.52 | 25.52 | 25.52 | 25.52 | 25.52 | 25.52 | 25.52 | 25.52 | 25.52 |
| Glass Furnaces | 2.00 | 2.00 | 2.00 | 2.00 | 2.00 | 2.00 | 2.00 | 2.00 | 2.00 | 2.00 | 2.00 | 2.00 | 2.00 |
| Metals Industries | 8.78 | 8.78 | 8.78 | 8.78 | 8.78 | 8.78 | 8.78 | 8.78 | 8.78 | 8.78 | 8.78 | 8.78 | 8.78 |
| Mineral Products | 0.00 | 0.00 | 0.00 | 0.00 | 0.00 | 0.00 | 0.00 | 0.00 | 0.00 | 0.00 | 0.00 | 0.00 | 0.00 |
| Sewage Treatment Digesters | 0.64 | 0.64 | 0.64 | 0.64 | 0.64 | 0.64 | 0.64 | 0.64 | 0.64 | 0.64 | 0.64 | 0.64 | 0.64 |
| Other Industrial Processes | 0.02 | 0.02 | 0.02 | 0.02 | 0.02 | 0.02 | 0.02 | 0.02 | 0.02 | 0.02 | 0.02 | 0.02 | 0.02 |
| Permitted Incinerators | 0.07 | 0.07 | 0.07 | 0.07 | 0.07 | 0.07 | 0.07 | 0.07 | 0.07 | 0.07 | 0.07 | 0.07 | 0.07 |
| MOBILE SOURCES | | | | | | | | | | | | | |
| Autos and Lt. Trucks-Surface | 17.17 | 17.75 | 18.56 | 18.76 | 14.27 | 14.15 | 14.05 | 14.36 | 13.51 | 13.51 | 16.95 | 15.70 | 15.71 |
| Autos and Lt. Trucks-Freeway | 10.98 | 11.35 | 11.87 | 12.01 | 9.13 | 9.05 | 8.99 | 9.19 | 8.64 | 8.64 | 10.85 | 10.05 | 10.05 |
| Heavy Duty Vehicles-Surface | 10.18 | 10.50 | 10.94 | 11.05 | 10.99 | 10.88 | 10.80 | 10.99 | 10.35 | 10.34 | 10.71 | 9.90 | 10.64 |
| Heavy Duty Vehicles-Freeway | 6.51 | 6.72 | 7.00 | 7.07 | 7.03 | 6.96 | 6.91 | 7.03 | 6.62 | 6.61 | 6.85 | 6.33 | 6.80 |
| Airport Operations | 1.06 | 1.06 | 1.06 | 1.06 | 1.06 | 1.06 | 1.06 | 1.06 | 1.06 | 1.06 | 1.06 | 1.06 | 1.06 |
| Shipping Operations | 10.13 | 10.13 | 10.13 | 10.13 | 10.13 | 10.13 | 10.13 | 10.13 | 10.13 | 10.13 | 10.13 | 10.13 | 10.13 |
| Railroad Operations | 3.32 | 3.32 | 3.32 | 3.32 | 3.32 | 3.32 | 3.32 | 3.32 | 3.32 | 3.32 | 3.32 | 3.32 | 3.32 |
| TOTAL | 504.73 | 463.64 | 462.36 | 366.63 | 374.67 | 397.95 | 384.27 | 431.33 | 414.10 | 433.95 | 498.44 | 417.18 | 428.94 |

## TABLE 4.5b

Major Off-Grid Emission Sources Included within the 1973 South Coast Air Basin Sulfur Oxides Modeling Inventory
(in short tons per day as $SO_2$)

| STATIONARY SOURCES | JAN | FEB | MAR | APR | MAY | JUN | JUL | AUG | SEP | OCT | NOV | DEC | ANNUAL |
|---|---|---|---|---|---|---|---|---|---|---|---|---|---|
| Fuel Combustion | | | | | | | | | | | | | |
| Electric Utilities | 60.19 | 45.46 | 57.94 | 39.18 | 53.62 | 64.68 | 54.07 | 58.97 | 45.38 | 59.69 | 91.75 | 66.46 | 58.20 |
| Refinery Fuel | --- | --- | --- | --- | --- | --- | --- | --- | --- | --- | --- | --- | --- |
| Other Interruptible Gas Customers | --- | --- | --- | --- | --- | --- | --- | --- | --- | --- | --- | --- | --- |
| Firm Gas Customers | --- | --- | --- | --- | --- | --- | --- | --- | --- | --- | --- | --- | --- |
| Chemical Plants | | | | | | | | | | | | | |
| Sulfur Recovery | --- | --- | --- | --- | --- | --- | --- | --- | --- | --- | --- | --- | --- |
| Sulfuric Acid | --- | --- | --- | --- | --- | --- | --- | --- | --- | --- | --- | --- | --- |
| Other Chemicals | --- | --- | --- | --- | --- | --- | --- | --- | --- | --- | --- | --- | --- |
| Petroleum Refining and Production | | | | | | | | | | | | | |
| Fluid Catalytic Crackers | --- | --- | --- | --- | --- | --- | --- | --- | --- | --- | --- | --- | --- |
| Sour Water Strippers | --- | --- | --- | --- | --- | --- | --- | --- | --- | --- | --- | --- | --- |
| Delayed Cokers | --- | --- | --- | --- | --- | --- | --- | --- | --- | --- | --- | --- | --- |
| Misc. Refinery Processes | --- | --- | --- | --- | --- | --- | --- | --- | --- | --- | --- | --- | --- |
| Oil Field Production | --- | --- | --- | --- | --- | --- | --- | --- | --- | --- | --- | --- | --- |
| Misc. Stationary Sources | | | | | | | | | | | | | |
| Petroleum Coke Kilns | --- | --- | --- | --- | --- | --- | --- | --- | --- | --- | --- | --- | --- |
| Glass Furnaces | 0.23 | 0.23 | 0.23 | 0.23 | 0.23 | 0.23 | 0.23 | 0.23 | 0.23 | 0.23 | 0.23 | 0.23 | 0.23 |
| Metals Industries | 41.46 | 41.46 | 41.46 | 41.46 | 41.46 | 41.46 | 41.46 | 41.46 | 41.46 | 41.46 | 41.46 | 41.46 | 41.46 |
| Mineral Products | 1.90 | 1.90 | 1.90 | 1.90 | 1.90 | 1.90 | 1.90 | 1.90 | 1.90 | 1.90 | 1.90 | 1.90 | 1.90 |
| Sewage Treatment Digesters | --- | --- | --- | --- | --- | --- | --- | --- | --- | --- | --- | --- | --- |
| Other Industrial Processes | --- | --- | --- | --- | --- | --- | --- | --- | --- | --- | --- | --- | --- |
| Permitted Incinerators | --- | --- | --- | --- | --- | --- | --- | --- | --- | --- | --- | --- | --- |
| TOTAL | 103.78 | 89.05 | 101.53 | 82.77 | 97.21 | 108.27 | 97.66 | 102.56 | 88.97 | 103.28 | 135.34 | 110.05 | 101.79 |

# TABLE 4.6a

1974 Sulfur Oxides Emissions Within the 50 by 50 Mile Square Grid
(in short tons per day as $SO_2$)

| STATIONARY SOURCES | JAN | FEB | MAR | APR | MAY | JUN | JUL | AUG | SEP | OCT | NOV | DEC | ANNUAL |
|---|---|---|---|---|---|---|---|---|---|---|---|---|---|
| Fuel Combustion | | | | | | | | | | | | | |
| Electric Utilities | 166.24 | 119.19 | 101.05 | 77.73 | 97.16 | 113.19 | 111.03 | 84.23 | 127.98 | 148.83 | 197.60 | 215.11 | 130.04 |
| Refinery Fuel | 23.69 | 20.91 | 7.61 | 7.59 | 5.18 | 9.27 | 4.35 | 3.22 | 3.78 | 10.44 | 15.53 | 20.32 | 10.93 |
| Other Interruptible Gas Customers | 8.30 | 1.61 | 0.94 | 0.71 | 0.69 | 1.05 | 0.64 | 0.59 | 0.54 | 1.12 | 2.04 | 3.72 | 1.84 |
| Firm Gas Customers | 0.41 | 0.41 | 0.35 | 0.27 | 0.23 | 0.21 | 0.17 | 0.15 | 0.16 | 0.17 | 0.25 | 0.35 | 0.26 |
| Chemical Plants | | | | | | | | | | | | | |
| Sulfur Recovery | 63.22 | 63.22 | 63.22 | 63.22 | 63.22 | 63.22 | 25.84 | 25.84 | 25.84 | 25.84 | 25.84 | 25.84 | 44.37 |
| Sulfuric Acid | 10.20 | 3.12 | 3.12 | 3.12 | 3.12 | 3.12 | 3.12 | 3.12 | 3.12 | 3.12 | 3.12 | 3.12 | 3.72 |
| Other Chemicals | 0.09 | 0.09 | 0.09 | 0.09 | 0.09 | 0.09 | 0.09 | 0.09 | 0.09 | 0.09 | 0.09 | 0.09 | 0.09 |
| Petroleum Refining and Production | | | | | | | | | | | | | |
| Fluid Catalytic Crackers | 45.48 | 45.48 | 45.48 | 45.48 | 45.48 | 45.48 | 45.48 | 45.48 | 45.48 | 45.48 | 45.48 | 45.48 | 45.48 |
| Sour Water Strippers | 1.03 | 1.03 | 1.03 | 1.03 | 1.03 | 1.03 | 1.03 | 1.03 | 1.03 | 1.03 | 1.03 | 1.03 | 1.03 |
| Delayed Cokers | 2.28 | 2.28 | 2.28 | 2.28 | 2.28 | 2.28 | 2.28 | 2.28 | 2.28 | 2.28 | 2.28 | 2.28 | 2.28 |
| Misc. Refinery Processes | 0.86 | 0.86 | 0.86 | 0.86 | 0.86 | 0.86 | 0.86 | 0.86 | 0.86 | 0.86 | 0.86 | 0.86 | 0.86 |
| Oil Field Production | 5.17 | 5.17 | 5.17 | 5.17 | 5.17 | 5.17 | 5.17 | 5.17 | 5.17 | 5.17 | 5.17 | 5.17 | 5.17 |
| Misc. Stationary Sources | | | | | | | | | | | | | |
| Petroleum Coke Kilns | 25.52 | 25.52 | 25.52 | 25.52 | 25.52 | 25.52 | 25.52 | 25.52 | 25.52 | 25.52 | 25.52 | 25.52 | 25.52 |
| Glass Furnaces | 2.00 | 2.00 | 2.00 | 2.00 | 2.00 | 2.00 | 2.00 | 2.00 | 2.00 | 2.00 | 2.00 | 2.00 | 2.00 |
| Metals Industries | 8.76 | 8.76 | 8.76 | 8.76 | 8.76 | 8.76 | 8.76 | 8.76 | 7.40 | 7.40 | 7.40 | 7.40 | 8.31 |
| Mineral Products | 0.00 | 0.00 | 0.00 | 0.00 | 0.00 | 0.00 | 0.00 | 0.00 | 0.00 | 0.00 | 0.00 | 0.00 | 0.00 |
| Sewage Treatment Digesters | 0.64 | 0.64 | 0.64 | 0.64 | 0.64 | 0.64 | 0.64 | 0.64 | 0.64 | 0.64 | 0.64 | 0.64 | 0.64 |
| Other Industrial Processes | 0.02 | 0.02 | 0.02 | 0.02 | 0.02 | 0.02 | 0.02 | 0.02 | 0.02 | 0.02 | 0.02 | 0.02 | 0.02 |
| Permitted Incinerators | 0.07 | 0.07 | 0.07 | 0.07 | 0.07 | 0.07 | 0.07 | 0.07 | 0.07 | 0.07 | 0.07 | 0.07 | 0.07 |
| MOBILE SOURCES | | | | | | | | | | | | | |
| Autos and Lt. Trucks-Surface | 15.84 | 16.84 | 15.88 | 17.71 | 15.63 | 15.94 | 16.00 | 15.86 | 15.02 | 15.44 | 19.65 | 20.50 | 16.66 |
| Autos and Lt. Trucks-Freeway | 9.88 | 10.27 | 9.91 | 11.05 | 9.75 | 9.94 | 9.98 | 9.89 | 9.37 | 9.63 | 12.26 | 12.79 | 10.39 |
| Heavy Duty Vehicles-Surface | 11.20 | 11.65 | 11.25 | 12.49 | 12.65 | 12.95 | 13.03 | 12.95 | 12.27 | 12.66 | 12.53 | 13.11 | 12.40 |
| Heavy Duty Vehicles-Freeway | 6.99 | 7.27 | 7.02 | 7.79 | 7.89 | 8.08 | 8.13 | 8.08 | 7.65 | 7.90 | 7.81 | 8.18 | 7.74 |
| Airport Operations | 1.17 | 1.17 | 1.17 | 1.17 | 1.17 | 1.17 | 1.17 | 1.17 | 1.17 | 1.17 | 1.17 | 1.17 | 1.17 |
| Shipping Operations | 9.38 | 9.38 | 9.38 | 9.38 | 9.38 | 9.38 | 9.38 | 9.38 | 9.38 | 9.38 | 9.38 | 9.38 | 9.38 |
| Railroad Operations | 2.87 | 2.87 | 2.87 | 2.87 | 2.87 | 2.87 | 2.87 | 2.87 | 2.87 | 2.87 | 2.87 | 2.87 | 2.87 |
| TOTAL | 421.31 | 359.83 | 325.69 | 307.02 | 320.86 | 342.31 | 297.63 | 269.27 | 309.71 | 339.13 | 400.61 | 427.02 | 343.24 |

TABLE 4.6b

Major Off-Grid Emission Sources Included within the 1974 South Coast Air Basin Sulfur Oxides Modeling Inventory
(in short tons per day as $SO_2$)

| STATIONARY SOURCES | JAN | FEB | MAR | APR | MAY | JUN | JUL | AUG | SEP | OCT | NOV | DEC | ANNUAL |
|---|---|---|---|---|---|---|---|---|---|---|---|---|---|
| Fuel Combustion | | | | | | | | | | | | | |
| Electric Utilities | 67.54 | 65.53 | 39.48 | 26.51 | 34.32 | 47.56 | 49.39 | 51.69 | 51.22 | 46.91 | 56.15 | 68.58 | 50.34 |
| Refinery Fuel | --- | --- | --- | --- | --- | --- | --- | --- | --- | --- | --- | --- | --- |
| Other Interruptible Gas Customers | --- | --- | --- | --- | --- | --- | --- | --- | --- | --- | --- | --- | --- |
| Firm Gas Customers | --- | --- | --- | --- | --- | --- | --- | --- | --- | --- | --- | --- | --- |
| Chemical Plants | | | | | | | | | | | | | |
| Sulfur Recovery | --- | --- | --- | --- | --- | --- | --- | --- | --- | --- | --- | --- | --- |
| Sulfuric Acid | --- | --- | --- | --- | --- | --- | --- | --- | --- | --- | --- | --- | --- |
| Other Chemicals | --- | --- | --- | --- | --- | --- | --- | --- | --- | --- | --- | --- | --- |
| Petroleum Refining and Production | | | | | | | | | | | | | |
| Fluid Catalytic Crackers | --- | --- | --- | --- | --- | --- | --- | --- | --- | --- | --- | --- | --- |
| Sour Water Strippers | --- | --- | --- | --- | --- | --- | --- | --- | --- | --- | --- | --- | --- |
| Delayed Cokers | --- | --- | --- | --- | --- | --- | --- | --- | --- | --- | --- | --- | --- |
| Misc. Refinery Processes | --- | --- | --- | --- | --- | --- | --- | --- | --- | --- | --- | --- | --- |
| Oil Field Production | --- | --- | --- | --- | --- | --- | --- | --- | --- | --- | -- | --- | --- |
| Misc. Stationary Sources | | | | | | | | | | | | | |
| Petroleum Coke Kilns | --- | --- | --- | --- | --- | --- | --- | --- | --- | --- | --- | --- | --- |
| Glass Furnaces | 0.23 | 0.23 | 0.23 | 0.23 | 0.23 | 0.23 | 0.23 | 0.23 | 0.23 | 0.23 | 0.23 | 0.23 | 0.23 |
| Metals Industries | 38.12 | 38.12 | 38.12 | 38.12 | 38.12 | 38.12 | 38.12 | 38.12 | 38.12 | 38.12 | 38.12 | 38.12 | 38.12 |
| Mineral Products | 1.90 | 1.90 | 1.90 | 1.90 | 1.90 | 1.90 | 1.90 | 1.90 | 1.90 | 1.90 | 1.90 | 1.90 | 1.90 |
| Sewage Treatment Digesters | --- | --- | --- | --- | --- | --- | --- | --- | --- | --- | --- | --- | --- |
| Other Industrial Processes | --- | --- | --- | --- | --- | --- | --- | --- | --- | --- | --- | --- | --- |
| Permitted Incinerators | --- | --- | --- | --- | --- | --- | --- | --- | --- | --- | --- | --- | --- |
| TOTAL | 107.79 | 105.78 | 79.73 | 67.76 | 74.57 | 87.81 | 89.64 | 91.94 | 91.47 | 87.16 | 96.40 | 108.83 | 90.59 |

through 1974. An itemization of large off-grid sources is also included. Details of the emission estimation procedures for each source type and further information on the spatial distribution of emissions from individual source classes are given in Appendix A2.

In order to introduce the emission inventory of Appendix A2 into an air quality model for sulfate formation and dispersion, additional information is needed. One needs to know the fraction of the emissions from each source type which originate as particulate sulfur oxides rather than $SO_2$. The diurnal variation of source emission strength is also important.

Table 4.7 lists a compilation of data on $f_{s_o}$, the fraction of total sulfur oxides emissions from various source classes which originate as sulfates or sulfuric acid mist rather than as gaseous $SO_2$. Using these data, a sulfur trioxide or "sulfates" emission inventory can be estimated from Tables 4.4 through 4.6 for each month of the years 1972 through 1974. An example $SO_4^=$ inventory for 1973 is presented in Table 4.7. On an emissions-weighted average basis, about 2.7% of the $SO_x$ emissions in the basin are evolved directly from their sources as $SO_3$ or sulfates. The principal source of direct sulfate or sulfuric acid mist emissions in the basin is seen to be the electric utility industry, followed by petroleum coke calcining kilns, refinery fluid catalytic crackers and an off-grid steel mill.

Daily average emission strength is often modulated by a strong diurnal variation in source utilization patterns. Two of the strongest diurnal source fluctuations affect power plants and motor

# TABLE 4.7

## Particulate Sulfur Oxides as a Fraction of Total $SO_x$ Emissions from Each Source Class

| Stationary Sources | Fraction Sulfates in Exhaust: Range of Test Results (% S atoms as $SO_3$ or $SO_4^=$) | Fraction Sulfates in Exhaust: Value Adopted for 1972-1974 Base Period (% S atoms as $SO_3$ or $SO_4^=$) | Reference | 1973 Sulfate Emissions (Tons/day as $SO_4^=$): On-Grid Sources | 1973 Sulfate Emissions (Tons/day as $SO_4^=$): Off-Grid Sources | Fraction Sulfates for Major Source Class Groups (1973 Emissions Weighted Average): On-Grid Sources | Fraction Sulfates for Major Source Class Groups (1973 Emissions Weighted Average): Off-Grid Sources |
|---|---|---|---|---|---|---|---|
| Fuel Combustion | | (h) | | | | | |
| Electric Utilities | <1.0% - 4.0% | 3.0% | (a) | 8.18 | 2.62 | 3.0% | 3.0% |
| Refinery Fuel Burning | | 3.0% | (d) | 0.42 | ---- | | |
| Other Interruptible Gas Customers | | 3.0% | (d) | 0.10 | ---- | 3.0% | |
| Firm Gas Customers | | 3.0% | (d) | 0.01 | ---- | | |
| Chemical Plants | | | | | | | |
| Sulfur Recovery Plants {Without Tail Gas Units} | 0.2% | 0.4%(i) | (a) | 0.40 | ---- | | |
| Sulfur Recovery Plants {With Tail Gas Units} | 2.8% - 29.1% | | | | | | |
| Sulfuric Acid Plants | 0.2% - 1.2% | 0.9% | (a) | 0.27 | ---- | 0.55% | |
| Other Chemicals | | 1.0% | (e) | 0.00 | ---- | | |
| Petroleum Refining and Production | | | | | | | |
| Fluid Catalytic Crackers | 0.0% - 7.9% | 2.8% | (a) | 2.19 | ---- | 2.8% | |
| Sour Water Strippers | | 1.0% | (e) | 0.00 | ---- | | |
| Delayed Cokers | | 4.3% | (f) | 0.15 | ---- | | |
| Miscellaneous Refinery Processes | | 1.0% | (e) | 0.02 | ---- | | |
| Oil Field Production | 1.7% - 1.8% | 1.8% | (a) | 0.12 | ---- | | |
| Miscellaneous Stationary Sources | | | | | | | |
| Petroleum Coke Calcining Kilns | 5.4% - 9.7% | 8.4% | (a) | 3.22 | ---- | 8.4% | |
| Glass Furnaces | 3.0% - 29.5% | 18.0% | (a) | 0.54 | 0.06 | 18.0% | 18.0% |
| Secondary Metals Industries (On-Grid) | 0.6% - 1.4% | 1.0% | (a) | 0.13 | ---- | 1.0% | |
| Primary Metals (off-Grid Steel Mill) | 0.0% - 5.5% | 2.5% | (a) | ---- | 1.55 | | 2.5% |
| Minerals Products | | 2.8% | (a) | ---- | 0.08 | | |
| Sewage Treatment Digesters | | 3.0% | (d) | 0.03 | ---- | | |
| Other Industrial Processes | | 3.0% | (e) | 0.00 | ---- | 2.8% | |
| Permitted Incinerators | | 3.0% | (d) | 0.00 | ---- | | |
| Mobile Sources | | | | | | | |
| Autos and Lt. Trucks - Surface | | 0.3% | (c) | 0.07 | ---- | 0.3% | |
| Autos and Lt. Trucks - Freeway | | 0.3% | (c) | 0.05 | ---- | | |
| Heavy Duty Vehicles - Surface | 2.0% - 3.0% | 2.3% | (b),(c) | 0.37 | ---- | | |
| Heavy Duty Vehicles - Freeway | 2.0% - 3.0% | 2.3% | (b),(c) | 0.23 | ---- | 2.5% | |
| Airport Operations | | 3.0% | (d) | 0.05 | ---- | | |
| Shipping Operations | | 3.0% | (d) | 0.46 | ---- | | |
| Railroad Operations | | 2.3% | (g) | 0.11 | ---- | | |
| TOTAL $SO_4^=$ EMISSIONS | | | | 17.12 | 4.31 | | |

Key to References and Notes

(a) Hunter and Helgeson (1976)

(b) Pierson and Brachaczek (1976)

(c) Personal Communication, Pierson (1977)

(d) Assumed for all other fuel combustion sources as was done by Hunter and Helgeson (1976)

(e) No data; value assumed.

(f) Taken from Hunter and Helgeson's (1976) refinery flare (odor incinerator) source test.

(g) Exhaust % sulfate assumed similar to highway diesel engines.

(h) For 0.5% sulfur oil.

(i) Most $SO_x$ emissions from this source class during the years 1972-1974 were from sulfur plants without tail gas units. Once tail gas units are applied to source, total $SO_x$ levels become so low that the higher $SO_4/SO_x$ ratio does not affect the source class average very much.

vehicle traffic. As shown in Figure 4.10, South Coast Air Basin power plants typically reach peak load in the late afternoon. Motor vehicle traffic peaks twice daily (at morning and afternoon rush hours), as shown in Figure 4.11. From discussions with APCD personnel and from information presented by Hunter and Helgeson (1976), it is estimated that most large industrial process sources of $SO_x$ in the South Coast Air Basin operate at a constant level throughout the day (although not always at full capacity). In view of the extremely small contribution to local $SO_x$ emissions made by light industry and commercial establishments, no attempt will be made to modify emission rates to reflect a typical work day, or a five day per week work schedule. All sources other than power plants and motor vehicles will be assumed to contribute their $SO_x$ emissions at an average rate independent of time of day. The fraction of daily emissions from power plants and motor vehicles assigned to each hour of the day by Figures 4.10 and 4.11 has been summarized in Table 4.8.

One principal reason for compiling emissions on a source by source basis is to be able to display the spatial distribution of $SO_x$ emission strength. Figures 4.12 through 4.14 show annual average $SO_x$ emissions density for the years 1972, 1973 and 1974 respectively. It is seen that the largest $SO_x$ emission source densities are located in a narrow strip along the coastline stretching from Los Angeles International Airport (near Lennox) on the north to Huntington Beach (opposite Santa Ana) on the south.

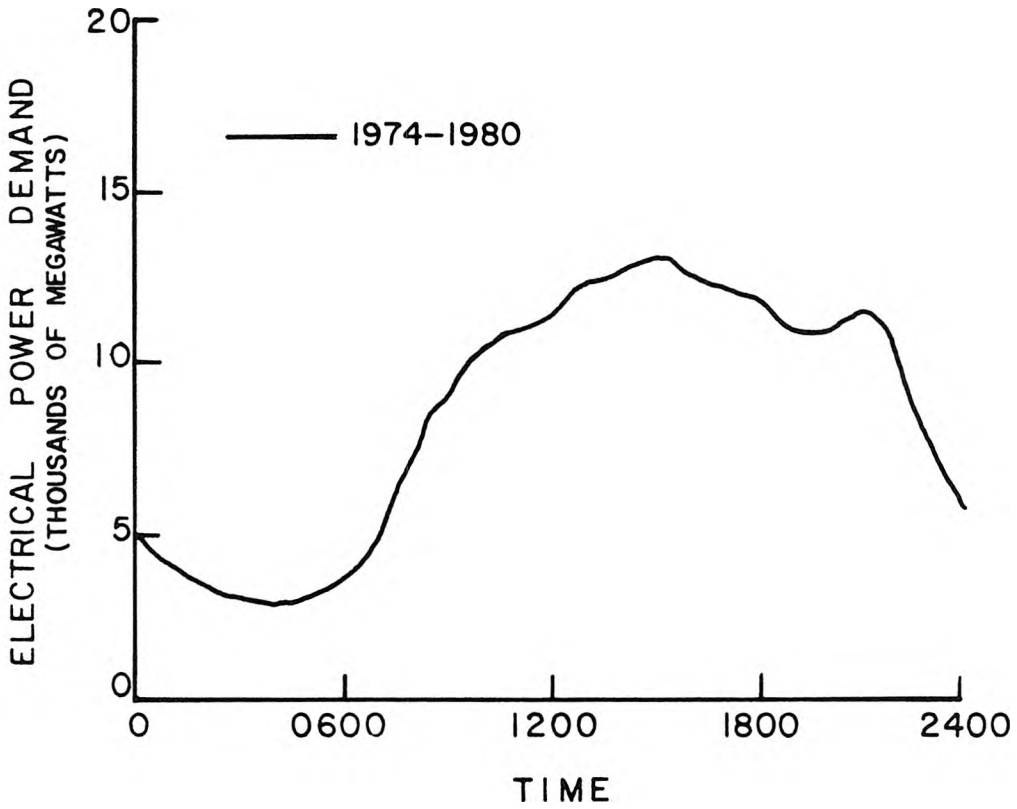


Projected Baseline Diurnal Power Demand on Oil Fired Power Plants in the South Coast Air Basin (From Sjovold, 1973).

FIGURE 4.10

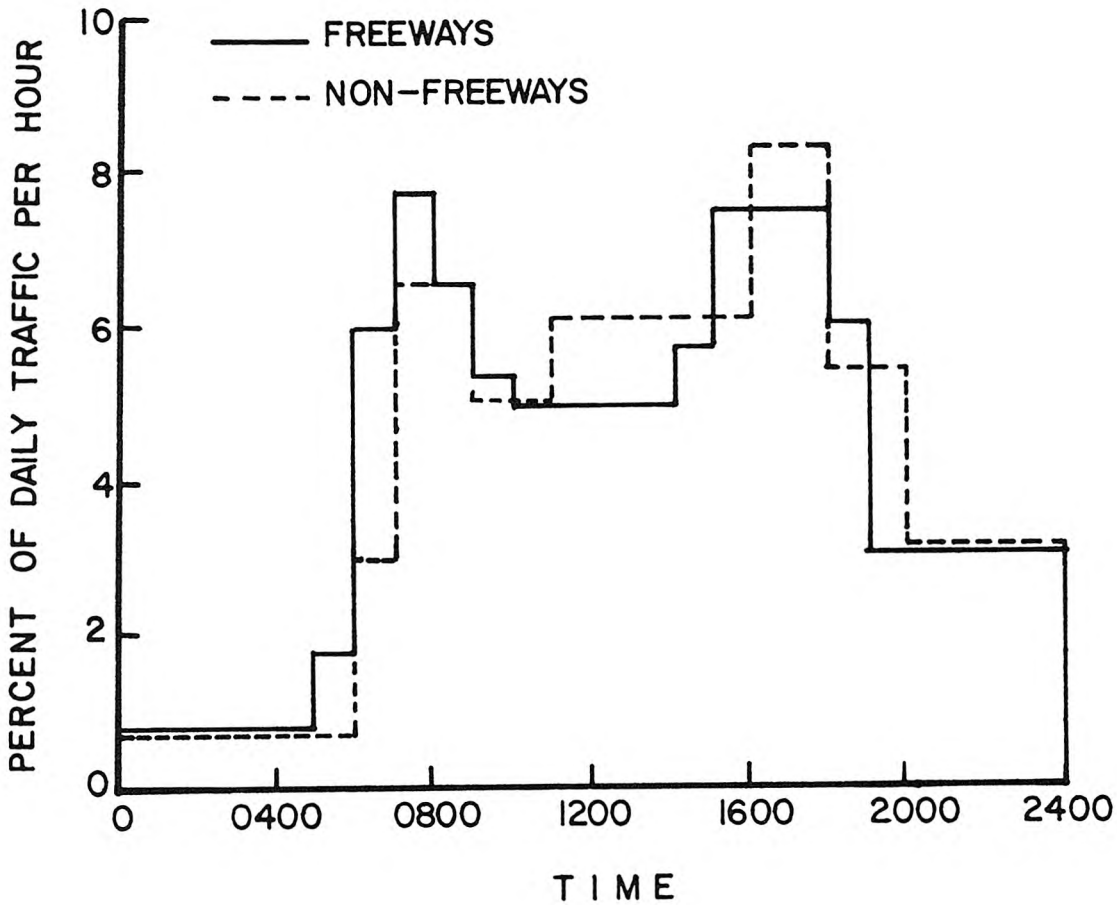


FIGURE 4.11

Diurnal Variation of Los Angeles Traffic Flow
(from Nordsieck, 1974)

TABLE 4.8

Diurnal Variations of Source Activities (1974)

(Fraction of Daily Total Assignable to a 1 Hour Period)

| Local Time | | Motor Vehicle Traffic | | | Power Plants |
|---|---|---|---|---|---|
| | | Freeways | Surface Streets | Weighted Average (0.39 Freeways + 0.61 Surface) | |
| (Midnight) | 2400-100 | 0.00776 | 0.00677 | .00716 | 0.02756 |
| | 100-200 | 0.00776 | 0.00677 | .00716 | 0.01911 |
| | 200-300 | 0.00776 | 0.00677 | .00716 | 0.01695 |
| | 300-400 | 0.00776 | 0.00677 | .00716 | 0.01484 |
| | 400-500 | 0.00776 | 0.00677 | .00716 | 0.01381 |
| | 500-600 | 0.0178 | 0.00677 | .01107 | 0.01484 |
| A.M. | 600-700 | 0.0591 | 0.0293 | .0409 | 0.01695 |
| | 700-800 | 0.0768 | 0.0651 | .0697 | 0.02334 |
| | 800-900 | 0.0648 | 0.0651 | .0650 | 0.03709 |
| | 900-1000 | 0.0536 | 0.0502 | .0515 | 0.04451 |
| | 1000-1100 | 0.0494 | 0.0502 | .0499 | 0.05095 |
| | 1100-1200 | 0.0494 | 0.06088 | .0564 | 0.05404 |
| Noon | 1200-1300 | 0.0494 | 0.06088 | .0564 | 0.05616 |
| | 1300-1400 | 0.0494 | 0.06088 | .0564 | 0.06043 |
| | 1400-1500 | 0.0569 | 0.06088 | .0593 | 0.06146 |
| | 1500-1600 | 0.0746 | 0.06088 | .0662 | 0.06387 |
| | 1600-1700 | 0.0746 | 0.0820 | .0791 | 0.06043 |
| | 1700-1800 | 0.0746 | 0.0820 | .0791 | 0.05940 |
| P.M. | 1800-1900 | 0.0598 | 0.0540 | .0563 | 0.05724 |
| | 1900-2000 | 0.0302 | 0.0540 | .0447 | 0.05306 |
| | 2000-2100 | 0.0302 | 0.03077 | .0306 | 0.05404 |
| | 2100-2200 | 0.0302 | 0.03077 | .0306 | 0.05616 |
| | 2200-2300 | 0.0302 | 0.03077 | .0306 | 0.04771 |
| (Midnight) | 2300-2400 | 0.0302 | 0.03077 | .0306 | 0.03606 |

Reference: Nordsieck (1974)

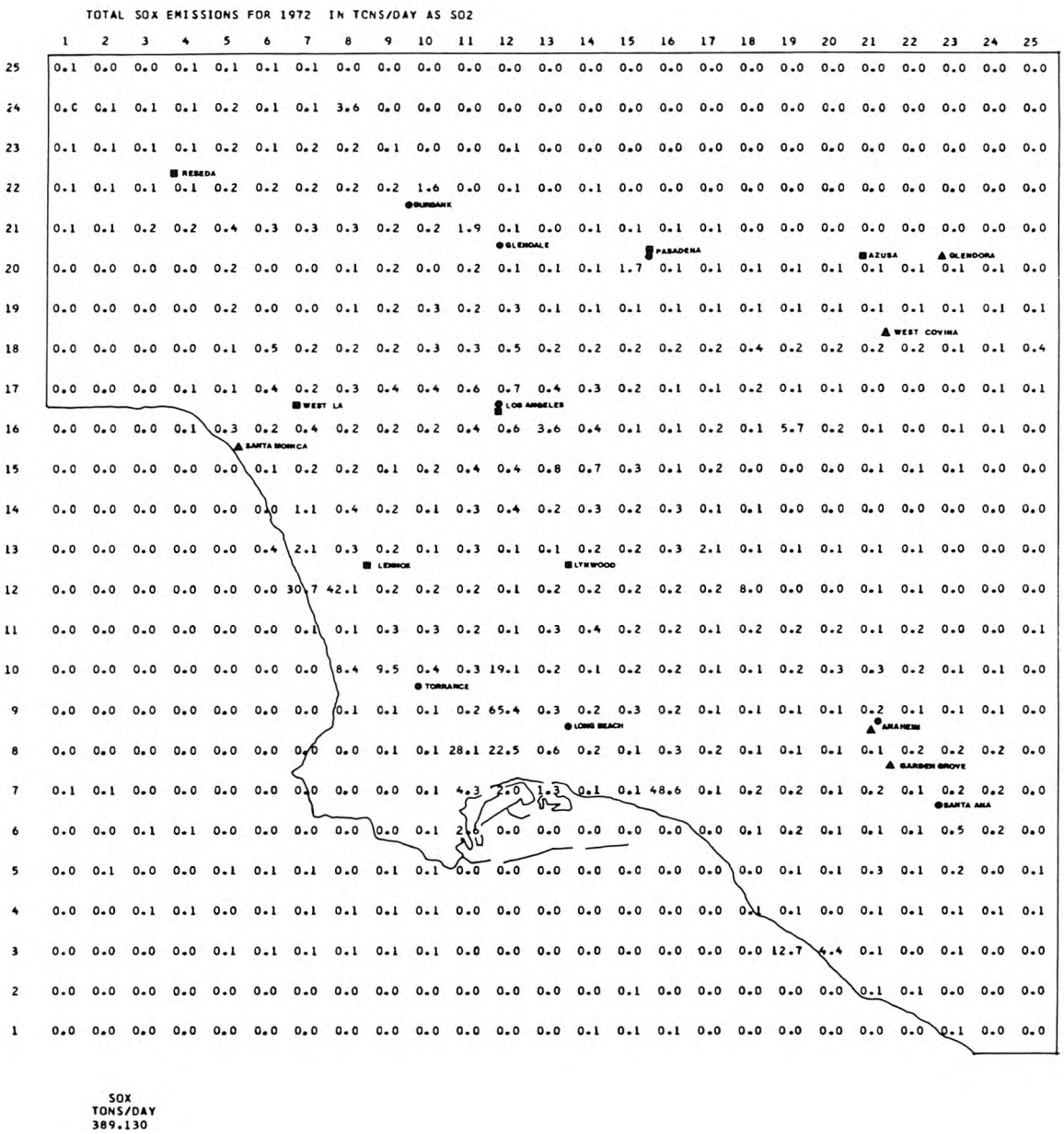
TOTAL SOX EMISSIONS FOR 1972 IN TONS/DAY AS SO2
1 2 3 4 5 6 7 8 9 10 11 12 13 14 15 16 17 18 19 20 21 22 23 24 25
25 0.1 0.0 0.0 0.1 0.1 0.1 0.1 0.0 0.0 0.0 0.0 0.0 0.0 0.0 0.0 0.0 0.0 0.0 0.0 0.0 0.0 0.0 0.0 0.0 0.0
24 0.0 0.1 0.1 0.1 0.2 0.1 0.1 3.6 0.0 0.0 0.0 0.0 0.0 0.0 0.0 0.0 0.0 0.0 0.0 0.0 0.0 0.0 0.0 0.0 0.0
23 0.1 0.1 0.1 0.1 0.2 0.1 0.2 0.2 0.1 0.0 0.0 0.1 0.0 0.0 0.0 0.0 0.0 0.0 0.0 0.0 0.0 0.0 0.0 0.0 0.0
22 0.1 0.1 0.1 0.1 0.2 0.2 0.2 0.2 0.2 1.6 0.0 0.1 0.0 0.1 0.0 0.0 0.0 0.0 0.0 0.0 0.0 0.0 0.0 0.0 0.0
21 0.1 0.1 0.2 0.2 0.4 0.3 0.3 0.3 0.2 0.2 1.9 0.1 0.0 0.1 0.1 0.1 0.1 0.0 0.0 0.0 0.0 0.0 0.0 0.0 0.0
20 0.0 0.0 0.0 0.0 0.2 0.0 0.0 0.1 0.2 0.0 0.2 0.1 0.1 0.1 1.7 0.1 0.1 0.1 0.1 0.1 0.1 0.1 0.1 0.1 0.0
19 0.0 0.0 0.0 0.0 0.2 0.0 0.0 0.1 0.2 0.3 0.2 0.3 0.1 0.1 0.1 0.1 0.1 0.1 0.1 0.1 0.1 0.1 0.1 0.1 0.1
18 0.0 0.0 0.0 0.0 0.1 0.5 0.2 0.2 0.2 0.3 0.3 0.5 0.2 0.2 0.2 0.2 0.2 0.4 0.2 0.2 0.2 0.2 0.1 0.1 0.4
17 0.0 0.0 0.0 0.1 0.1 0.4 0.2 0.3 0.4 0.4 0.6 0.7 0.4 0.3 0.2 0.1 0.1 0.2 0.1 0.1 0.0 0.0 0.0 0.1 0.1
16 0.0 0.0 0.0 0.1 0.3 0.2 0.4 0.2 0.2 0.2 0.4 0.6 3.6 0.4 0.1 0.1 0.2 0.1 5.7 0.2 0.1 0.0 0.1 0.1 0.0
15 0.0 0.0 0.0 0.0 0.0 0.1 0.2 0.2 0.1 0.2 0.4 0.4 0.8 0.7 0.3 0.1 0.2 0.0 0.0 0.0 0.1 0.1 0.1 0.0 0.0
14 0.0 0.0 0.0 0.0 0.0 0.0 1.1 0.4 0.2 0.1 0.3 0.4 0.2 0.3 0.2 0.3 0.1 0.1 0.0 0.0 0.0 0.0 0.0 0.0 0.0
13 0.0 0.0 0.0 0.0 0.0 0.4 2.1 0.3 0.2 0.1 0.3 0.1 0.1 0.2 0.2 0.3 2.1 0.1 0.1 0.1 0.1 0.1 0.0 0.0 0.0
12 0.0 0.0 0.0 0.0 0.0 0.0 30.7 42.1 0.2 0.2 0.2 0.1 0.2 0.2 0.2 0.2 0.2 8.0 0.0 0.0 0.1 0.1 0.0 0.0 0.0
11 0.0 0.0 0.0 0.0 0.0 0.0 0.1 0.1 0.3 0.3 0.2 0.1 0.3 0.4 0.2 0.2 0.1 0.2 0.2 0.2 0.1 0.2 0.0 0.0 0.1
10 0.0 0.0 0.0 0.0 0.0 0.0 0.0 8.4 9.5 0.4 0.3 19.1 0.2 0.1 0.2 0.2 0.1 0.1 0.2 0.3 0.3 0.2 0.1 0.1 0.0
9 0.0 0.0 0.0 0.0 0.0 0.0 0.0 0.1 0.1 0.1 0.2 65.4 0.3 0.2 0.3 0.2 0.1 0.1 0.1 0.1 0.2 0.1 0.1 0.1 0.0
8 0.0 0.0 0.0 0.0 0.0 0.0 0.0 0.0 0.1 0.1 28.1 22.5 0.6 0.2 0.1 0.3 0.2 0.1 0.1 0.1 0.1 0.2 0.2 0.2 0.0
7 0.1 0.1 0.0 0.0 0.0 0.0 0.0 0.0 0.0 0.1 4.3 2.0 1.3 0.1 0.1 48.6 0.1 0.2 0.2 0.1 0.2 0.1 0.2 0.2 0.0
6 0.0 0.0 0.1 0.1 0.0 0.0 0.0 0.0 0.0 0.1 2.6 0.0 0.0 0.0 0.0 0.0 0.0 0.1 0.2 0.1 0.1 0.1 0.5 0.2 0.0
5 0.0 0.1 0.0 0.0 0.1 0.1 0.1 0.0 0.1 0.1 0.0 0.0 0.0 0.0 0.0 0.0 0.0 0.0 0.1 0.1 0.3 0.1 0.2 0.0 0.1
4 0.0 0.0 0.1 0.1 0.0 0.1 0.1 0.1 0.1 0.1 0.0 0.0 0.0 0.0 0.0 0.0 0.0 0.1 0.1 0.0 0.1 0.1 0.1 0.1 0.1
3 0.0 0.0 0.0 0.0 0.1 0.1 0.1 0.1 0.1 0.1 0.0 0.0 0.0 0.0 0.0 0.0 0.0 0.0 12.7 4.4 0.1 0.0 0.1 0.0 0.0
2 0.0 0.0 0.0 0.0 0.0 0.0 0.0 0.0 0.0 0.0 0.0 0.0 0.0 0.0 0.1 0.0 0.0 0.0 0.0 0.0 0.1 0.1 0.0 0.0 0.0
1 0.0 0.0 0.0 0.0 0.0 0.0 0.0 0.0 0.0 0.0 0.0 0.0 0.0 0.0 0.1 0.1 0.1 0.0 0.0 0.0 0.0 0.0 0.0 0.1 0.0 0.0
RESEDA
BURBANK
GLENDALE
PASADENA
AZUSA
GLENDORA
WEST COVINA
WEST LA
LOS ANGELES
SANTA MONICA
LENNOX
LYNWOOD
TORRANCE
LONG BEACH
ANAHEIM
GARDEN GROVE
SANTA ANA
SOX
TONS/DAY
389.130

FIGURE 4.12

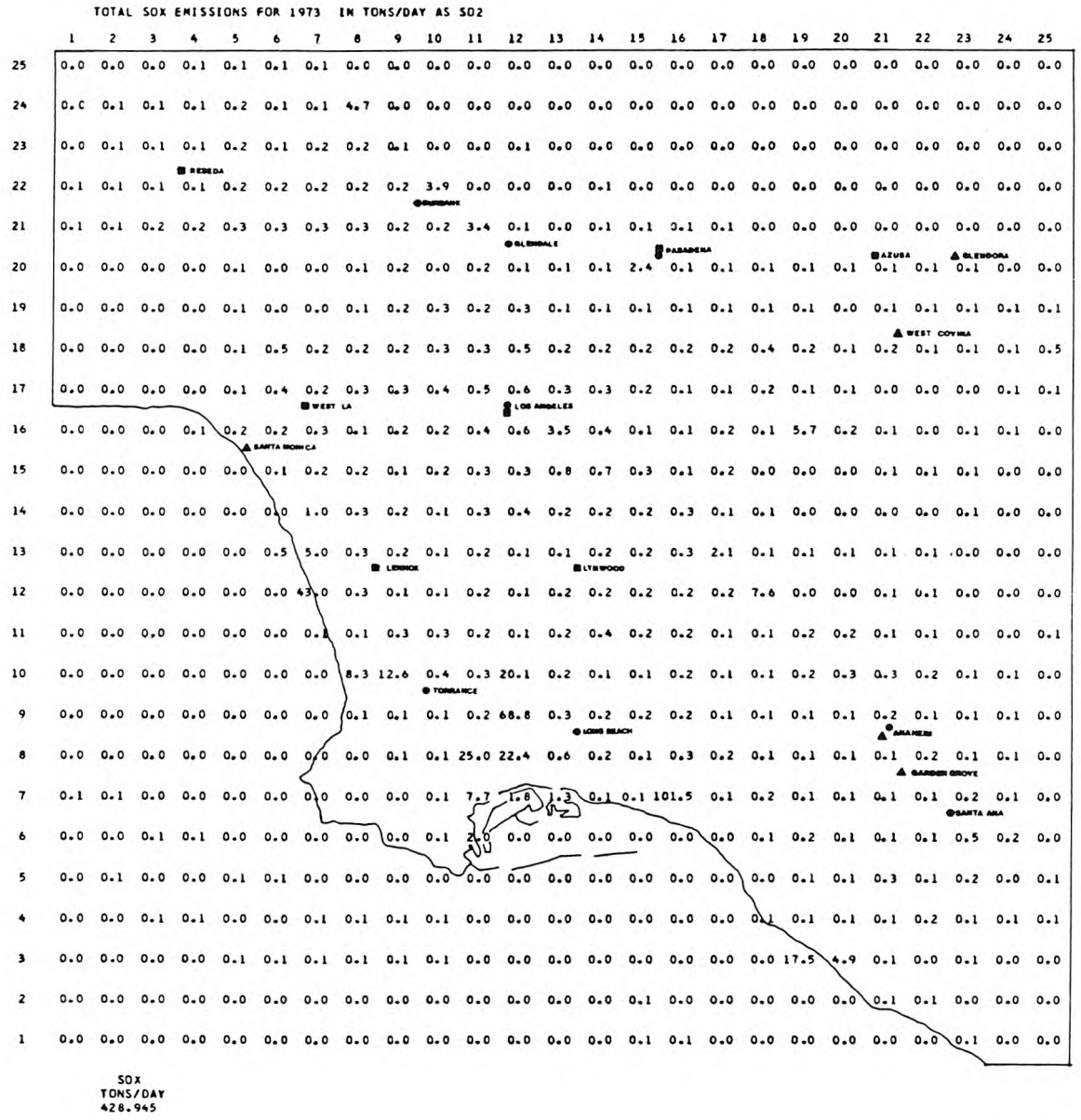
TOTAL SOX EMISSIONS FOR 1973 IN TONS/DAY AS SO2
SOX TONS/DAY 428.945
RESEDA
BURBANK
GLENDALE
PASADENA
AZUSA
GLENDORA
WEST COVINA
WEST LA
LOS ANGELES
SANTA MONICA
LENNOX
LYNWOOD
TORRANCE
LONG BEACH
ANAHEIM
GARDEN GROVE
SANTA ANA

FIGURE 4.13

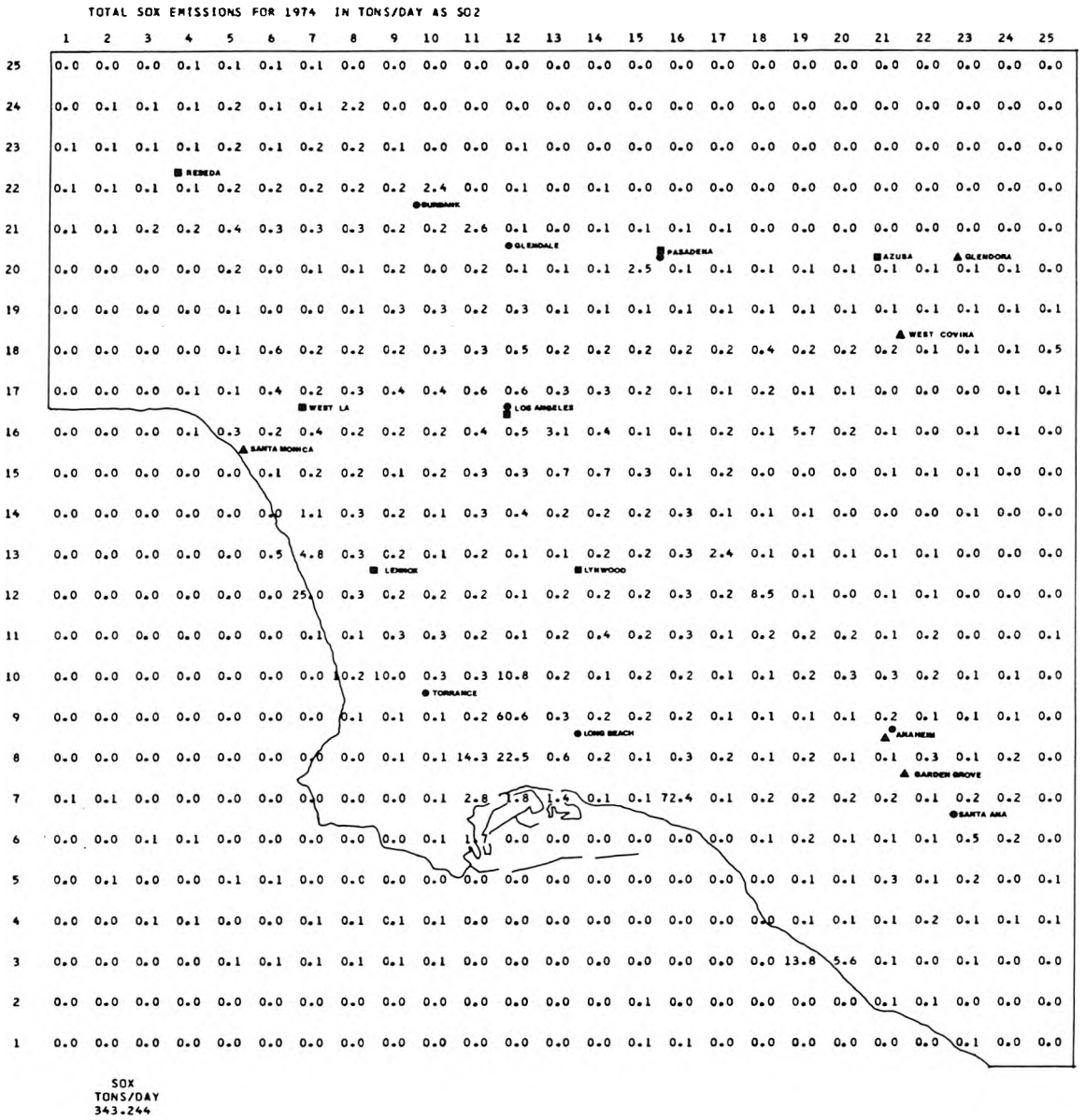
TOTAL SOX EMISSIONS FOR 1974 IN TONS/DAY AS SO2
1 2 3 4 5 6 7 8 9 10 11 12 13 14 15 16 17 18 19 20 21 22 23 24 25
25 0.0 0.0 0.0 0.1 0.1 0.1 0.1 0.0 0.0 0.0 0.0 0.0 0.0 0.0 0.0 0.0 0.0 0.0 0.0 0.0 0.0 0.0 0.0 0.0 0.0
24 0.0 0.1 0.1 0.1 0.2 0.1 0.1 2.2 0.0 0.0 0.0 0.0 0.0 0.0 0.0 0.0 0.0 0.0 0.0 0.0 0.0 0.0 0.0 0.0 0.0
23 0.1 0.1 0.1 0.1 0.2 0.1 0.2 0.2 0.1 0.0 0.0 0.1 0.0 0.0 0.0 0.0 0.0 0.0 0.0 0.0 0.0 0.0 0.0 0.0 0.0
22 0.1 0.1 0.1 0.1 0.2 0.2 0.2 0.2 0.2 2.4 0.0 0.1 0.0 0.1 0.0 0.0 0.0 0.0 0.0 0.0 0.0 0.0 0.0 0.0 0.0
21 0.1 0.1 0.2 0.2 0.4 0.3 0.3 0.3 0.2 0.2 2.6 0.1 0.0 0.1 0.1 0.1 0.1 0.0 0.0 0.0 0.0 0.0 0.0 0.0 0.0
20 0.0 0.0 0.0 0.0 0.2 0.0 0.1 0.1 0.2 0.0 0.2 0.1 0.1 0.1 2.5 0.1 0.1 0.1 0.1 0.1 0.1 0.1 0.1 0.1 0.0
19 0.0 0.0 0.0 0.0 0.1 0.0 0.0 0.1 0.3 0.3 0.2 0.3 0.1 0.1 0.1 0.1 0.1 0.1 0.1 0.1 0.1 0.1 0.1 0.1 0.1
18 0.0 0.0 0.0 0.0 0.1 0.6 0.2 0.2 0.2 0.3 0.3 0.5 0.2 0.2 0.2 0.2 0.2 0.4 0.2 0.2 0.2 0.1 0.1 0.1 0.5
17 0.0 0.0 0.0 0.1 0.1 0.4 0.2 0.3 0.4 0.4 0.6 0.6 0.3 0.3 0.2 0.1 0.1 0.2 0.1 0.1 0.0 0.0 0.0 0.1 0.1
16 0.0 0.0 0.0 0.1 0.3 0.2 0.4 0.2 0.2 0.2 0.4 0.5 3.1 0.4 0.1 0.1 0.2 0.1 5.7 0.2 0.1 0.0 0.1 0.1 0.0
15 0.0 0.0 0.0 0.0 0.0 0.1 0.2 0.2 0.1 0.2 0.3 0.3 0.7 0.7 0.3 0.1 0.2 0.0 0.0 0.0 0.1 0.1 0.1 0.0 0.0
14 0.0 0.0 0.0 0.0 0.0 0.0 1.1 0.3 0.2 0.1 0.3 0.4 0.2 0.2 0.2 0.3 0.1 0.1 0.1 0.0 0.0 0.0 0.1 0.0 0.0
13 0.0 0.0 0.0 0.0 0.0 0.5 4.8 0.3 0.2 0.1 0.2 0.1 0.1 0.2 0.2 0.3 2.4 0.1 0.1 0.1 0.1 0.1 0.0 0.0 0.0
12 0.0 0.0 0.0 0.0 0.0 0.0 25.0 0.3 0.2 0.2 0.2 0.1 0.2 0.2 0.2 0.3 0.2 8.5 0.1 0.0 0.1 0.1 0.0 0.0 0.0
11 0.0 0.0 0.0 0.0 0.0 0.0 0.1 0.1 0.3 0.3 0.2 0.1 0.2 0.4 0.2 0.3 0.1 0.2 0.2 0.2 0.1 0.2 0.0 0.0 0.1
10 0.0 0.0 0.0 0.0 0.0 0.0 0.0 10.2 10.0 0.3 0.3 10.8 0.2 0.1 0.2 0.2 0.1 0.1 0.2 0.3 0.3 0.2 0.1 0.1 0.0
9 0.0 0.0 0.0 0.0 0.0 0.0 0.0 0.1 0.1 0.1 0.2 60.6 0.3 0.2 0.2 0.2 0.1 0.1 0.1 0.1 0.2 0.1 0.1 0.1 0.0
8 0.0 0.0 0.0 0.0 0.0 0.0 0.0 0.0 0.1 0.1 14.3 22.5 0.6 0.2 0.1 0.3 0.2 0.1 0.2 0.1 0.1 0.3 0.1 0.2 0.0
7 0.1 0.1 0.0 0.0 0.0 0.0 0.0 0.0 0.0 0.1 2.8 1.8 1.4 0.1 0.1 72.4 0.1 0.2 0.2 0.2 0.2 0.1 0.2 0.2 0.0
6 0.0 0.0 0.1 0.1 0.0 0.0 0.0 0.0 0.0 0.1 1.7 0.0 0.0 0.0 0.0 0.0 0.1 0.2 0.1 0.1 0.1 0.5 0.2 0.0
5 0.0 0.1 0.0 0.0 0.1 0.1 0.0 0.0 0.0 0.0 0.0 0.0 0.0 0.0 0.0 0.0 0.0 0.0 0.1 0.1 0.3 0.1 0.2 0.0 0.1
4 0.0 0.0 0.1 0.1 0.0 0.0 0.1 0.1 0.1 0.1 0.0 0.0 0.0 0.0 0.0 0.0 0.0 0.0 0.1 0.1 0.1 0.2 0.1 0.1 0.1
3 0.0 0.0 0.0 0.0 0.1 0.1 0.1 0.1 0.1 0.1 0.0 0.0 0.0 0.0 0.0 0.0 0.0 0.0 13.8 5.6 0.1 0.0 0.1 0.0 0.0
2 0.0 0.0 0.0 0.0 0.0 0.0 0.0 0.0 0.0 0.0 0.0 0.0 0.0 0.0 0.1 0.0 0.0 0.0 0.0 0.0 0.1 0.1 0.0 0.0 0.0
1 0.0 0.0 0.0 0.0 0.0 0.0 0.0 0.0 0.0 0.0 0.0 0.0 0.0 0.0 0.1 0.1 0.0 0.0 0.0 0.0 0.0 0.0 0.1 0.0 0.0
RESEDA
BURBANK
GLENDALE
PASADENA
AZUSA
GLENDORA
WEST COVINA
WEST LA
LOS ANGELES
SANTA MONICA
LENNOX
LYNWOOD
TORRANCE
LONG BEACH
ANAHEIM
GARDEN GROVE
SANTA ANA
SOX
TONS/DAY
343.244

FIGURE 4.14

In Figures 4.15 through 4.20, the spatial distribution of $SO_x$ emissions for the year 1973 has been broken down into several broad source categories. When this is done, it is seen that the high emission levels in the coastal zone are due largely to a high concentration of power plants, oil refineries and chemical plants.

An ability to add spatial resolution to the emission inventory in the vertical dimension is also important. In order to characterize the local air quality impact of emissions from a particular source, it is often necessary to estimate the source's effective stack height. Source effective stack height is the elevation above ground level at which a bouyant plume ceases to rise further into the atmosphere and instead equilibrates with its surroundings. Effective stack height can be thought of as having two components. An elevation is imparted to the emissions by the physical height of the stack or chimney. Then a further increment to effective source height is contributed by plume rise above the physical stack.

Typical values for physical stack height and plume rise for members of each source class of our emission inventory are given in Table 4.9. Plume rise estimates were first calculated for nearly one hundred major $SO_x$ emission points in the South Coast Air Basin at a single set of reference meteorological conditions. Physical stack height and plume rise estimates for members of each source class were then averaged to obtain the typical values shown in Table 4.9. When data on stack parameters for a particular source class were unavailable,

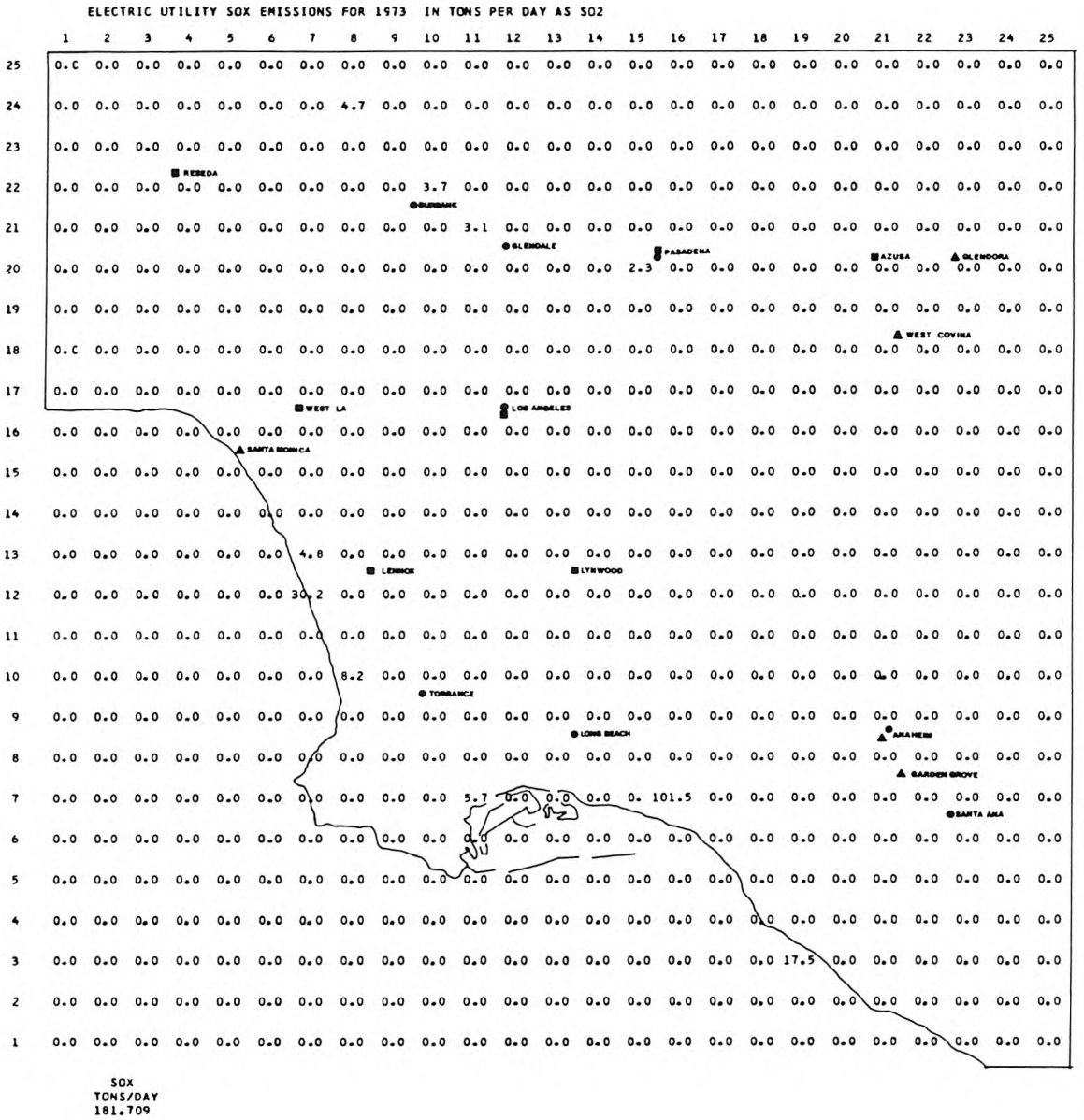
ELECTRIC UTILITY SOX EMISSIONS FOR 1973 IN TONS PER DAY AS SO2
1 2 3 4 5 6 7 8 9 10 11 12 13 14 15 16 17 18 19 20 21 22 23 24 25
25 0.0 0.0 0.0 0.0 0.0 0.0 0.0 0.0 0.0 0.0 0.0 0.0 0.0 0.0 0.0 0.0 0.0 0.0 0.0 0.0 0.0 0.0 0.0 0.0 0.0
24 0.0 0.0 0.0 0.0 0.0 0.0 0.0 4.7 0.0 0.0 0.0 0.0 0.0 0.0 0.0 0.0 0.0 0.0 0.0 0.0 0.0 0.0 0.0 0.0 0.0
23 0.0 0.0 0.0 0.0 0.0 0.0 0.0 0.0 0.0 0.0 0.0 0.0 0.0 0.0 0.0 0.0 0.0 0.0 0.0 0.0 0.0 0.0 0.0 0.0 0.0
22 0.0 0.0 0.0 0.0 0.0 0.0 0.0 0.0 0.0 3.7 0.0 0.0 0.0 0.0 0.0 0.0 0.0 0.0 0.0 0.0 0.0 0.0 0.0 0.0 0.0
21 0.0 0.0 0.0 0.0 0.0 0.0 0.0 0.0 0.0 0.0 3.1 0.0 0.0 0.0 0.0 0.0 0.0 0.0 0.0 0.0 0.0 0.0 0.0 0.0 0.0
20 0.0 0.0 0.0 0.0 0.0 0.0 0.0 0.0 0.0 0.0 0.0 0.0 0.0 0.0 2.3 0.0 0.0 0.0 0.0 0.0 0.0 0.0 0.0 0.0 0.0
19 0.0 0.0 0.0 0.0 0.0 0.0 0.0 0.0 0.0 0.0 0.0 0.0 0.0 0.0 0.0 0.0 0.0 0.0 0.0 0.0 0.0 0.0 0.0 0.0 0.0
18 0.0 0.0 0.0 0.0 0.0 0.0 0.0 0.0 0.0 0.0 0.0 0.0 0.0 0.0 0.0 0.0 0.0 0.0 0.0 0.0 0.0 0.0 0.0 0.0 0.0
17 0.0 0.0 0.0 0.0 0.0 0.0 0.0 0.0 0.0 0.0 0.0 0.0 0.0 0.0 0.0 0.0 0.0 0.0 0.0 0.0 0.0 0.0 0.0 0.0 0.0
16 0.0 0.0 0.0 0.0 0.0 0.0 0.0 0.0 0.0 0.0 0.0 0.0 0.0 0.0 0.0 0.0 0.0 0.0 0.0 0.0 0.0 0.0 0.0 0.0 0.0
15 0.0 0.0 0.0 0.0 0.0 0.0 0.0 0.0 0.0 0.0 0.0 0.0 0.0 0.0 0.0 0.0 0.0 0.0 0.0 0.0 0.0 0.0 0.0 0.0 0.0
14 0.0 0.0 0.0 0.0 0.0 0.0 0.0 0.0 0.0 0.0 0.0 0.0 0.0 0.0 0.0 0.0 0.0 0.0 0.0 0.0 0.0 0.0 0.0 0.0 0.0
13 0.0 0.0 0.0 0.0 0.0 0.0 4.8 0.0 0.0 0.0 0.0 0.0 0.0 0.0 0.0 0.0 0.0 0.0 0.0 0.0 0.0 0.0 0.0 0.0 0.0
12 0.0 0.0 0.0 0.0 0.0 0.0 30.2 0.0 0.0 0.0 0.0 0.0 0.0 0.0 0.0 0.0 0.0 0.0 0.0 0.0 0.0 0.0 0.0 0.0 0.0
11 0.0 0.0 0.0 0.0 0.0 0.0 0.0 0.0 0.0 0.0 0.0 0.0 0.0 0.0 0.0 0.0 0.0 0.0 0.0 0.0 0.0 0.0 0.0 0.0 0.0
10 0.0 0.0 0.0 0.0 0.0 0.0 0.0 8.2 0.0 0.0 0.0 0.0 0.0 0.0 0.0 0.0 0.0 0.0 0.0 0.0 0.0 0.0 0.0 0.0 0.0
9 0.0 0.0 0.0 0.0 0.0 0.0 0.0 0.0 0.0 0.0 0.0 0.0 0.0 0.0 0.0 0.0 0.0 0.0 0.0 0.0 0.0 0.0 0.0 0.0 0.0
8 0.0 0.0 0.0 0.0 0.0 0.0 0.0 0.0 0.0 0.0 0.0 0.0 0.0 0.0 0.0 0.0 0.0 0.0 0.0 0.0 0.0 0.0 0.0 0.0 0.0
7 0.0 0.0 0.0 0.0 0.0 0.0 0.0 0.0 0.0 0.0 5.7 0.0 0.0 0. 101.5 0.0 0.0 0.0 0.0 0.0 0.0 0.0 0.0 0.0 0.0
6 0.0 0.0 0.0 0.0 0.0 0.0 0.0 0.0 0.0 0.0 0.0 0.0 0.0 0.0 0.0 0.0 0.0 0.0 0.0 0.0 0.0 0.0 0.0 0.0 0.0
5 0.0 0.0 0.0 0.0 0.0 0.0 0.0 0.0 0.0 0.0 0.0 0.0 0.0 0.0 0.0 0.0 0.0 0.0 0.0 0.0 0.0 0.0 0.0 0.0 0.0
4 0.0 0.0 0.0 0.0 0.0 0.0 0.0 0.0 0.0 0.0 0.0 0.0 0.0 0.0 0.0 0.0 0.0 0.0 0.0 0.0 0.0 0.0 0.0 0.0 0.0
3 0.0 0.0 0.0 0.0 0.0 0.0 0.0 0.0 0.0 0.0 0.0 0.0 0.0 0.0 0.0 0.0 0.0 0.0 17.5 0.0 0.0 0.0 0.0 0.0 0.0
2 0.0 0.0 0.0 0.0 0.0 0.0 0.0 0.0 0.0 0.0 0.0 0.0 0.0 0.0 0.0 0.0 0.0 0.0 0.0 0.0 0.0 0.0 0.0 0.0 0.0
1 0.0 0.0 0.0 0.0 0.0 0.0 0.0 0.0 0.0 0.0 0.0 0.0 0.0 0.0 0.0 0.0 0.0 0.0 0.0 0.0 0.0 0.0 0.0 0.0 0.0
RESEDA
BURBANK
GLENDALE
PASADENA
AZUSA
GLENDORA
WEST COVINA
WEST LA
LOS ANGELES
SANTA MONICA
LENNOX
LYNWOOD
TORRANCE
LONG BEACH
ANAHEIM
GARDEN GROVE
SANTA ANA
SOX
TONS/DAY
181.709

FIGURE 4.15


1973 INDUSTRIAL, COMMERCIAL & RESIDENTIAL FUEL BURNING SOX EMISSIONS (TONS/DAY)
RESEDA
BURBANK
GLENDALE
PASADENA
AZUSA
GLENDORA
WEST COVINA
WEST LA
LOS ANGELES
SANTA MONICA
LENNOX
LYNWOOD
TORRANCE
LONG BEACH
ANAHEIM
GARDEN GROVE
SANTA ANA
SOX
TONS/DAY
11.997

FIGURE 4.16

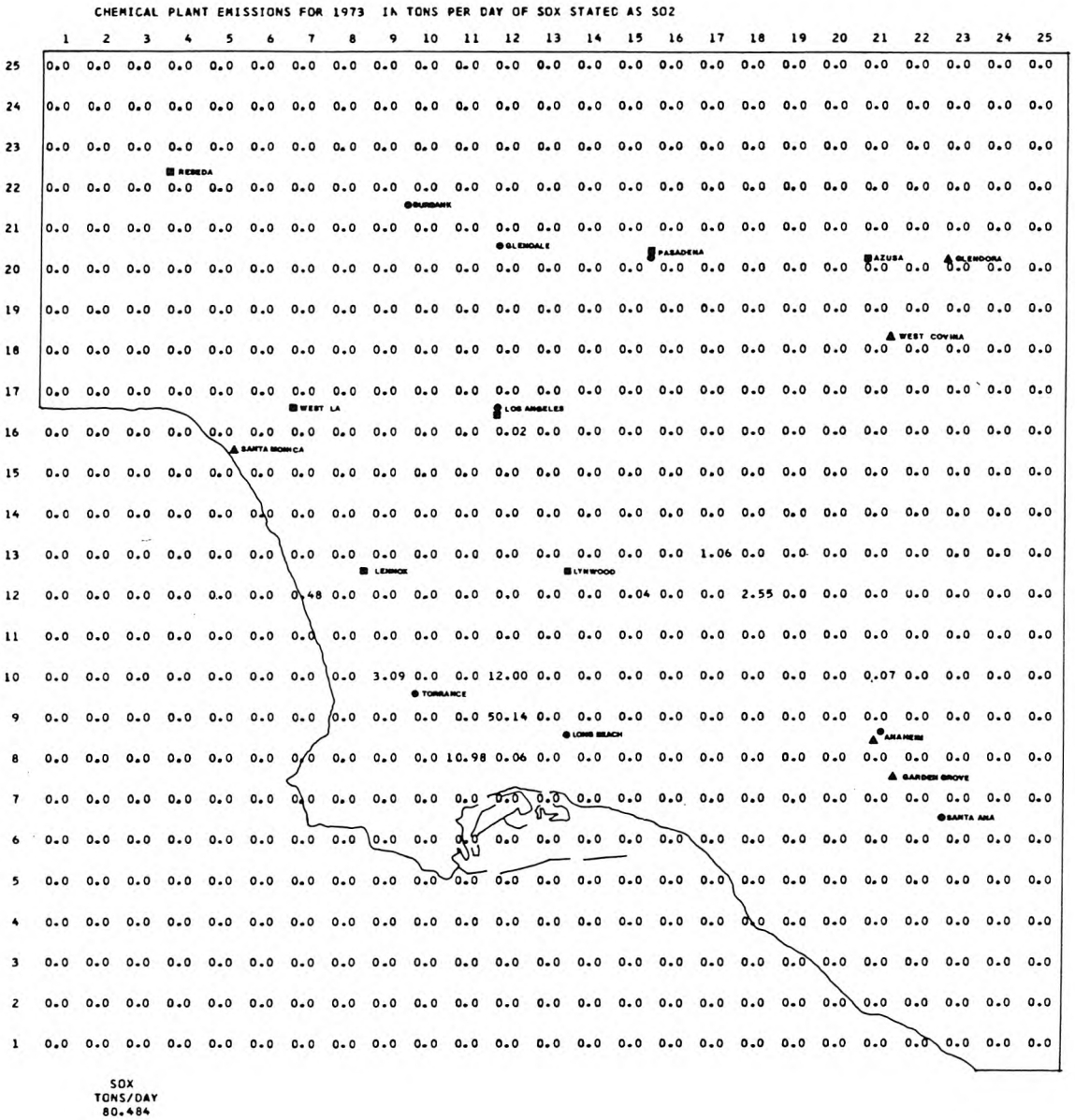
CHEMICAL PLANT EMISSIONS FOR 1973 IN TONS PER DAY OF SOX STATED AS SO2
1 2 3 4 5 6 7 8 9 10 11 12 13 14 15 16 17 18 19 20 21 22 23 24 25
25 0.0 0.0 0.0 0.0 0.0 0.0 0.0 0.0 0.0 0.0 0.0 0.0 0.0 0.0 0.0 0.0 0.0 0.0 0.0 0.0 0.0 0.0 0.0 0.0 0.0
24 0.0 0.0 0.0 0.0 0.0 0.0 0.0 0.0 0.0 0.0 0.0 0.0 0.0 0.0 0.0 0.0 0.0 0.0 0.0 0.0 0.0 0.0 0.0 0.0 0.0
23 0.0 0.0 0.0 0.0 0.0 0.0 0.0 0.0 0.0 0.0 0.0 0.0 0.0 0.0 0.0 0.0 0.0 0.0 0.0 0.0 0.0 0.0 0.0 0.0 0.0
22 0.0 0.0 0.0 0.0 0.0 0.0 0.0 0.0 0.0 0.0 0.0 0.0 0.0 0.0 0.0 0.0 0.0 0.0 0.0 0.0 0.0 0.0 0.0 0.0 0.0
21 0.0 0.0 0.0 0.0 0.0 0.0 0.0 0.0 0.0 0.0 0.0 0.0 0.0 0.0 0.0 0.0 0.0 0.0 0.0 0.0 0.0 0.0 0.0 0.0 0.0
20 0.0 0.0 0.0 0.0 0.0 0.0 0.0 0.0 0.0 0.0 0.0 0.0 0.0 0.0 0.0 0.0 0.0 0.0 0.0 0.0 0.0 0.0 0.0 0.0 0.0
19 0.0 0.0 0.0 0.0 0.0 0.0 0.0 0.0 0.0 0.0 0.0 0.0 0.0 0.0 0.0 0.0 0.0 0.0 0.0 0.0 0.0 0.0 0.0 0.0 0.0
18 0.0 0.0 0.0 0.0 0.0 0.0 0.0 0.0 0.0 0.0 0.0 0.0 0.0 0.0 0.0 0.0 0.0 0.0 0.0 0.0 0.0 0.0 0.0 0.0 0.0
17 0.0 0.0 0.0 0.0 0.0 0.0 0.0 0.0 0.0 0.0 0.0 0.0 0.0 0.0 0.0 0.0 0.0 0.0 0.0 0.0 0.0 0.0 0.0 0.0 0.0
16 0.0 0.0 0.0 0.0 0.0 0.0 0.0 0.0 0.0 0.0 0.0 0.02 0.0 0.0 0.0 0.0 0.0 0.0 0.0 0.0 0.0 0.0 0.0 0.0 0.0
15 0.0 0.0 0.0 0.0 0.0 0.0 0.0 0.0 0.0 0.0 0.0 0.0 0.0 0.0 0.0 0.0 0.0 0.0 0.0 0.0 0.0 0.0 0.0 0.0 0.0
14 0.0 0.0 0.0 0.0 0.0 0.0 0.0 0.0 0.0 0.0 0.0 0.0 0.0 0.0 0.0 0.0 0.0 0.0 0.0 0.0 0.0 0.0 0.0 0.0 0.0
13 0.0 0.0 0.0 0.0 0.0 0.0 0.0 0.0 0.0 0.0 0.0 0.0 0.0 0.0 0.0 0.0 1.06 0.0 0.0 0.0 0.0 0.0 0.0 0.0 0.0
12 0.0 0.0 0.0 0.0 0.0 0.0 0.48 0.0 0.0 0.0 0.0 0.0 0.0 0.0 0.04 0.0 0.0 2.55 0.0 0.0 0.0 0.0 0.0 0.0 0.0
11 0.0 0.0 0.0 0.0 0.0 0.0 0.0 0.0 0.0 0.0 0.0 0.0 0.0 0.0 0.0 0.0 0.0 0.0 0.0 0.0 0.0 0.0 0.0 0.0 0.0
10 0.0 0.0 0.0 0.0 0.0 0.0 0.0 0.0 3.09 0.0 0.0 12.00 0.0 0.0 0.0 0.0 0.0 0.0 0.0 0.0 0.07 0.0 0.0 0.0 0.0
9 0.0 0.0 0.0 0.0 0.0 0.0 0.0 0.0 0.0 0.0 0.0 50.14 0.0 0.0 0.0 0.0 0.0 0.0 0.0 0.0 0.0 0.0 0.0 0.0 0.0
8 0.0 0.0 0.0 0.0 0.0 0.0 0.0 0.0 0.0 0.0 10.98 0.06 0.0 0.0 0.0 0.0 0.0 0.0 0.0 0.0 0.0 0.0 0.0 0.0 0.0
7 0.0 0.0 0.0 0.0 0.0 0.0 0.0 0.0 0.0 0.0 0.0 0.0 0.0 0.0 0.0 0.0 0.0 0.0 0.0 0.0 0.0 0.0 0.0 0.0 0.0
6 0.0 0.0 0.0 0.0 0.0 0.0 0.0 0.0 0.0 0.0 0.0 0.0 0.0 0.0 0.0 0.0 0.0 0.0 0.0 0.0 0.0 0.0 0.0 0.0 0.0
5 0.0 0.0 0.0 0.0 0.0 0.0 0.0 0.0 0.0 0.0 0.0 0.0 0.0 0.0 0.0 0.0 0.0 0.0 0.0 0.0 0.0 0.0 0.0 0.0 0.0
4 0.0 0.0 0.0 0.0 0.0 0.0 0.0 0.0 0.0 0.0 0.0 0.0 0.0 0.0 0.0 0.0 0.0 0.0 0.0 0.0 0.0 0.0 0.0 0.0 0.0
3 0.0 0.0 0.0 0.0 0.0 0.0 0.0 0.0 0.0 0.0 0.0 0.0 0.0 0.0 0.0 0.0 0.0 0.0 0.0 0.0 0.0 0.0 0.0 0.0 0.0
2 0.0 0.0 0.0 0.0 0.0 0.0 0.0 0.0 0.0 0.0 0.0 0.0 0.0 0.0 0.0 0.0 0.0 0.0 0.0 0.0 0.0 0.0 0.0 0.0 0.0
1 0.0 0.0 0.0 0.0 0.0 0.0 0.0 0.0 0.0 0.0 0.0 0.0 0.0 0.0 0.0 0.0 0.0 0.0 0.0 0.0 0.0 0.0 0.0 0.0 0.0
REDEDA
BURBANK
GLENDALE
PASADENA
AZUSA
GLENDORA
WEST COVINA
WEST LA
LOS ANGELES
SANTA MONICA
LENNOX
LYNWOOD
TORRANCE
LONG BEACH
ANAHEIM
GARDEN GROVE
SANTA ANA
SOX
TONS/DAY
80.484

FIGURE 4.17


PETROLEUM PROCESSING EMISSIONS FOR 1973 IN TONS PER DAY OF SOX STATED AS SO2
1 2 3 4 5 6 7 8 9 10 11 12 13 14 15 16 17 18 19 20 21 22 23 24 25
25 0.0 0.0 0.0 0.0 0.0 0.0 0.0 0.0 0.0 0.0 0.0 0.0 0.0 0.0 0.0 0.0 0.0 0.0 0.0 0.0 0.0 0.0 0.0 0.0 0.0
24 0.0 0.0 0.0 0.0 0.0 0.0 0.0 0.0 0.0 0.0 0.0 0.0 0.0 0.0 0.0 0.0 0.0 0.0 0.0 0.0 0.0 0.0 0.0 0.0 0.0
23 0.0 0.0 0.0 0.0 0.0 0.0 0.0 0.0 0.0 0.0 0.0 0.0 0.0 0.0 0.0 0.0 0.0 0.0 0.0 0.0 0.0 0.0 0.0 0.0 0.0
22 0.0 0.0 0.0 0.0 0.0 0.0 0.0 0.0 0.0 0.0 0.0 0.0 0.0 0.0 0.0 0.0 0.0 0.0 0.0 0.0 0.0 0.0 0.0 0.0 0.0
21 0.0 0.0 0.0 0.0 0.0 0.0 0.0 0.0 0.0 0.0 0.0 0.0 0.0 0.0 0.0 0.0 0.0 0.0 0.0 0.0 0.0 0.0 0.0 0.0 0.0
20 0.0 0.0 0.0 0.0 0.0 0.0 0.0 0.0 0.0 0.0 0.0 0.0 0.0 0.0 0.0 0.0 0.0 0.0 0.0 0.0 0.0 0.0 0.0 0.0 0.0
19 0.0 0.0 0.0 0.0 0.0 0.0 0.0 0.0 0.0 0.0 0.0 0.0 0.0 0.0 0.0 0.0 0.0 0.0 0.0 0.0 0.0 0.0 0.0 0.0 0.0
18 0.0 0.0 0.0 0.0 0.0 0.0 0.0 0.0 0.0 0.0 0.0 0.0 0.0 0.0 0.0 0.0 0.0 0.0 0.0 0.0 0.0 0.0 0.0 0.0 0.0
17 0.0 0.0 0.0 0.0 0.0 0.0 0.0 0.0 0.0 0.0 0.0 0.0 0.0 0.0 0.0 0.0 0.0 0.0 0.0 0.0 0.0 0.0 0.0 0.0 0.0
16 0.0 0.0 0.0 0.0 0.0 0.0 0.0 0.0 0.0 0.0 0.0 0.0 0.0 0.0 0.0 0.0 0.06 0.0 0.0 0.0 0.0 0.0 0.0 0.0 0.0
15 0.0 0.0 0.0 0.0 0.0 0.0 0.0 0.0 0.0 0.0 0.0 0.0 0.0 0.0 0.0 0.0 0.0 0.0 0.0 0.0 0.0 0.0 0.0 0.0 0.0
14 0.0 0.0 0.0 0.0 0.0 0.0 0.0 0.0 0.0 0.0 0.0 0.0 0.0 0.03 0.0 0.0 0.0 0.0 0.0 0.0 0.0 0.0 0.0 0.0 0.0
13 0.0 0.0 0.0 0.0 0.0 0.0 0.0 0.0 0.0 0.0 0.0 0.0 0.0 0.0 0.0 0.0 0.90 0.0 0.0 0.0 0.0 0.0 0.0 0.0 0.0
12 0.0 0.0 0.0 0.0 0.0 0.0 11.14 0.0 0.0 0.0 0.0 0.0 0.0 0.0 0.0 0.0 4.70 0.0 0.0 0.0 0.0 0.0 0.0 0.0 0.0
11 0.0 0.0 0.0 0.0 0.0 0.0 0.0 0.0 0.0 0.0 0.0 0.0 0.0 0.11 0.0 0.0 0.0 0.0 0.0 0.0 0.0 0.0 0.0 0.0 0.0
10 0.0 0.0 0.0 0.0 0.0 0.0 0.0 0.0 8.70 0.0 0.0 5.52 0.0 0.0 0.0 0.0 0.0 0.0 0.0 0.0 0.0 0.0 0.0 0.0 0.0
9 0.0 0.0 0.0 0.0 0.0 0.0 0.0 0.0 0.0 0.0 0.01 8.32 0.0 0.0 0.0 0.0 0.0 0.0 0.0 0.0 0.0 0.0 0.0 0.0 0.0
8 0.0 0.0 0.0 0.0 0.0 0.0 0.0 0.0 0.0 0.0 13.00 3.00 0.0 0.0 0.0 0.0 0.0 0.0 0.0 0.0 0.0 0.0 0.0 0.0 0.0
7 0.0 0.0 0.0 0.0 0.0 0.0 0.0 0.0 0.0 0.0 0.0 0.0 0.0 0.0 0.0 0.0 0.0 0.0 0.0 0.0 0.0 0.0 0.0 0.0 0.0
6 0.0 0.0 0.0 0.0 0.0 0.0 0.0 0.0 0.0 0.0 0.0 0.0 0.0 0.0 0.0 0.0 0.0 0.0 0.0 0.0 0.0 0.0 0.0 0.0 0.0
5 0.0 0.0 0.0 0.0 0.0 0.0 0.0 0.0 0.0 0.0 0.0 0.0 0.0 0.0 0.0 0.0 0.0 0.0 0.0 0.0 0.0 0.0 0.0 0.0 0.0
4 0.0 0.0 0.0 0.0 0.0 0.0 0.0 0.0 0.0 0.0 0.0 0.0 0.0 0.0 0.0 0.0 0.0 0.0 0.0 0.0 0.0 0.0 0.0 0.0 0.0
3 0.0 0.0 0.0 0.0 0.0 0.0 0.0 0.0 0.0 0.0 0.0 0.0 0.0 0.0 0.0 0.0 0.0 0.0 4.50 0.0 0.0 0.0 0.0 0.0 0.0
2 0.0 0.0 0.0 0.0 0.0 0.0 0.0 0.0 0.0 0.0 0.0 0.0 0.0 0.0 0.0 0.0 0.0 0.0 0.0 0.0 0.0 0.0 0.0 0.0 0.0
1 0.0 0.0 0.0 0.0 0.0 0.0 0.0 0.0 0.0 0.0 0.0 0.0 0.0 0.0 0.0 0.0 0.0 0.0 0.0 0.0 0.0 0.0 0.0 0.0 0.0
RESEDA
BURBANK
GLENDALE
PASADENA
AZUSA
GLENDORA
WEST COVINA
WEST LA
LOS ANGELES
SANTA MONICA
LENNOX
LYNWOOD
TORRANCE
LONG BEACH
ANAHEIM
GARDEN GROVE
SANTA ANA
SOX
TONS/DAY
59.999

FIGURE 4.18


MISC INDUSTRIAL PROCESS EMISSIONS FOR 1973 IN TONS PER DAY OF SOX STATED AS SO2
1 2 3 4 5 6 7 8 9 10 11 12 13 14 15 16 17 18 19 20 21 22 23 24 25
25 0.0 0.0 0.0 0.0 0.0 0.0 0.0 0.0 0.0 0.0 0.0 0.0 0.0 0.0 0.0 0.0 0.0 0.0 0.0 0.0 0.0 0.0 0.0 0.0 0.0
24 0.0 0.0 0.0 0.0 0.0 0.0 0.0 0.0 0.0 0.0 0.0 0.0 0.0 0.0 0.0 0.0 0.0 0.0 0.0 0.0 0.0 0.0 0.0 0.0 0.0
23 0.0 0.0 0.0 0.0 0.0 0.0 0.00 0.0 0.0 0.0 0.0 0.0 0.0 0.0 0.0 0.0 0.0 0.0 0.0 0.0 0.0 0.0 0.0 0.0 0.0
RESEDA
22 0.0 0.0 0.0 0.0 0.0 0.0 0.0 0.0 0.0 0.0 0.0 0.0 0.0 0.0 0.0 0.0 0.0 0.0 0.0 0.0 0.0 0.0 0.0 0.0 0.0
BURBANK
21 0.0 0.0 0.0 0.00 0.0 0.0 0.0 0.0 0.0 0.0 0.0 0.00 0.0 0.0 0.0 0.0 0.0 0.0 0.0 0.0 0.0 0.0 0.0 0.0 0.0
GLENDALE
PASADENA
AZUSA
GLENDORA
20 0.0 0.0 0.0 0.0 0.0 0.0 0.0 0.0 0.0 0.0 0.0 0.0 0.0 0.0 0.0 0.0 0.0 0.00 0.0 0.0 0.02 0.0 0.0 0.0 0.0
19 0.0 0.0 0.0 0.0 0.0 0.0 0.0 0.0 0.0 0.00 0.02 0.0 0.0 0.0 0.00 0.0 0.0 0.0 0.0 0.0 0.0 0.00 0.0 0.0 0.0
WEST COVINA
18 0.0 0.0 0.0 0.0 0.0 0.0 0.0 0.0 0.0 0.0 0.00 0.06 0.00 0.0 0.0 0.0 0.0 0.19 0.0 0.00 0.0 0.0 0.0 0.0 0.00
17 0.0 0.0 0.0 0.0 0.0 0.0 0.0 0.0 0.0 0.00 0.00 0.0 0.0 0.0 0.0 0.0 0.00 0.0 0.0 0.0 0.0 0.0 0.0 0.0 0.04
WEST LA
LOS ANGELES
16 0.0 0.0 0.0 0.0 0.0 0.0 0.0 0.00 0.0 0.0 0.0 0.09 3.06 0.0 0.0 0.00 0.0 0.0 5.61 0.0 0.0 0.0 0.02 0.0 0.0
SANTA MONICA
15 0.0 0.0 0.0 0.0 0.0 0.0 0.0 0.0 0.0 0.0 0.0 0.00 0.51 0.39 0.0 0.00 0.0 0.0 0.0 0.0 0.0 0.0 0.0 0.0 0.0
14 0.0 0.0 0.0 0.0 0.0 0.00 0.0 0.00 0.02 0.0 0.0 0.22 0.00 0.00 0.0 0.0 0.00 0.0 0.0 0.0 0.0 0.0 0.0 0.0 0.0
13 0.0 0.0 0.0 0.0 0.0 0.0 0.10 0.0 0.00 0.0 0.0 0.0 0.0 0.0 0.02 0.0 0.00 0.00 0.02 0.0 0.0 0.0 0.0 0.0 0.0
LENNOX
LYNWOOD
12 0.0 0.0 0.0 0.0 0.0 0.0 0.0 0.00 0.00 0.01 0.00 0.0 0.00 0.00 0.0 0.0 0.00 0.0 0.0 0.0 0.0 0.0 0.0 0.0 0.0
11 0.0 0.0 0.0 0.0 0.0 0.0 0.0 0.0 0.0 0.0 0.00 0.0 0.00 0.00 0.0 0.0 0.00 0.0 0.0 0.13 0.0 0.0 0.0 0.0 0.0
10 0.0 0.0 0.0 0.0 0.0 0.0 0.0 0.0 0.0 0.0 0.0 0.0 0.0 0.0 0.0 0.0 0.00 0.0 0.0 0.0 0.0 0.0 0.0 0.0 0.0
TORRANCE
9 0.0 0.0 0.0 0.0 0.0 0.0 0.0 0.0 0.0 0.0 0.01 7.49 0.0 0.0 0.0 0.0 0.0 0.0 0.0 0.0 0.0 0.0 0.0 0.0 0.0
LONG BEACH
ANAHEIM
8 0.0 0.0 0.0 0.0 0.0 0.0 0.0 0.0 0.0 0.0 0.0 18.03 0.00 0.0 0.0 0.0 0.0 0.0 0.0 0.0 0.0 0.0 0.0 0.0 0.0
GARDEN GROVE
7 0.0 0.0 0.0 0.0 0.0 0.0 0.0 0.0 0.0 0.0 0.00 0.00 0.0 0.00 0.0 0.0 0.0 0.0 0.0 0.0 0.0 0.0 0.0 0.0 0.0
SANTA ANA
6 0.0 0.0 0.0 0.0 0.0 0.0 0.0 0.0 0.0 0.0 0.0 0.0 0.0 0.0 0.0 0.0 0.0 0.0 0.0 0.0 0.0 0.0 0.42 0.0 0.0
5 0.0 0.0 0.0 0.0 0.0 0.0 0.0 0.0 0.0 0.0 0.0 0.0 0.0 0.0 0.0 0.0 0.0 0.0 0.0 0.0 0.18 0.0 0.0 0.0 0.0
4 0.0 0.0 0.0 0.0 0.0 0.0 0.0 0.0 0.0 0.0 0.0 0.0 0.0 0.0 0.0 0.0 0.0 0.0 0.0 0.0 0.0 0.0 0.0 0.0 0.0
3 0.0 0.0 0.0 0.0 0.0 0.0 0.0 0.0 0.0 0.0 0.0 0.0 0.0 0.0 0.0 0.0 0.0 0.0 0.0 0.35 0.0 0.0 0.0 0.0 0.0
2 0.0 0.0 0.0 0.0 0.0 0.0 0.0 0.0 0.0 0.0 0.0 0.0 0.0 0.0 0.0 0.0 0.0 0.0 0.0 0.0 0.0 0.0 0.0 0.0 0.0
1 0.0 0.0 0.0 0.0 0.0 0.0 0.0 0.0 0.0 0.0 0.0 0.0 0.0 0.0 0.0 0.0 0.0 0.0 0.0 0.0 0.0 0.0 0.0 0.0 0.0
SOX
TONS/DAY
37.040

FIGURE 4.19


MOBILE SOURCE EMISSIONS FOR 1973 IN TONS PER DAY OF SOX STATED AS SO2
1 2 3 4 5 6 7 8 9 10 11 12 13 14 15 16 17 18 19 20 21 22 23 24 25
25 0.05 0.02 0.01 0.05 0.10 0.13 0.05 0.02 0.01 0.01 0.00 0.0 0.0 0.00 0.00 0.00 0.00 0.00 0.00 0.0 0.0 0.0 0.00 0.0 0.0
24 0.03 0.06 0.07 0.08 0.15 0.11 0.14 0.03 0.03 0.03 0.03 0.00 0.00 0.0 0.0 0.00 0.0 0.0 0.0 0.0 0.0 0.0 0.00 0.0 0.0
23 0.05 0.10 0.09 0.09 0.19 0.13 0.16 0.17 0.08 0.01 0.01 0.07 0.03 0.00 0.0 0.0 0.00 0.0 0.0 0.0 0.0 0.0 0.00 0.0 0.0
22 0.08 0.10 0.09 0.09 0.21 0.17 0.19 0.16 0.17 0.16 0.00 0.05 0.03 0.05 0.04 0.01 0.00 0.00 0.0 0.0 0.0 0.00 0.00 0.0 0.0
21 0.10 0.13 0.15 0.20 0.34 0.29 0.25 0.30 0.18 0.21 0.22 0.12 0.02 0.09 0.09 0.06 0.07 0.04 0.02 0.00 0.00 0.00 0.00 0.0 0.0
20 0.01 0.01 0.01 0.00 0.14 0.02 0.05 0.10 0.16 0.01 0.21 0.09 0.08 0.11 0.13 0.11 0.09 0.10 0.13 0.09 0.09 0.07 0.07 0.05 0.01
19 0.00 0.01 0.0 0.00 0.14 0.03 0.01 0.10 0.23 0.26 0.14 0.29 0.12 0.09 0.08 0.08 0.08 0.06 0.11 0.05 0.06 0.09 0.06 0.05 0.09
18 0.0 0.01 0.0 0.00 0.09 0.19 0.16 0.22 0.20 0.27 0.31 0.44 0.15 0.17 0.22 0.19 0.19 0.17 0.20 0.14 0.17 0.14 0.08 0.09 0.13
17 0.02 0.03 0.04 0.05 0.09 0.36 0.20 0.29 0.34 0.36 0.52 0.57 0.33 0.25 0.16 0.12 0.12 0.19 0.07 0.07 0.04 0.01 0.01 0.05 0.08
16 0.0 0.0 0.0 0.05 0.23 0.20 0.35 0.15 0.17 0.17 0.35 0.40 0.43 0.36 0.11 0.07 0.15 0.08 0.10 0.15 0.05 0.02 0.04 0.10 0.03
15 0.0 0.0 0.0 0.0 0.00 0.12 0.22 0.17 0.13 0.19 0.30 0.21 0.15 0.24 0.25 0.09 0.17 0.03 0.01 0.03 0.07 0.09 0.07 0.00 0.0
14 0.0 0.0 0.0 0.0 0.0 0.04 0.99 0.31 0.15 0.13 0.26 0.13 0.13 0.20 0.15 0.25 0.11 0.12 0.05 0.02 0.01 0.00 0.05 0.00 0.00
13 0.0 0.0 0.0 0.0 0.0 0.52 0.10 0.25 0.16 0.12 0.23 0.10 0.12 0.19 0.14 0.31 0.11 0.09 0.08 0.10 0.06 0.07 0.01 0.00 0.00
12 0.0 0.0 0.0 0.0 0.0 0.0 0.09 0.24 0.14 0.14 0.17 0.10 0.15 0.16 0.11 0.22 0.21 0.10 0.04 0.02 0.05 0.08 0.04 0.03 0.00
11 0.0 0.0 0.0 0.0 0.0 0.0 0.06 0.08 0.31 0.25 0.17 0.05 0.24 0.23 0.21 0.23 0.13 0.14 0.22 0.09 0.12 0.14 0.03 0.02 0.07
10 0.0 0.0 0.0 0.0 0.0 0.0 0.00 0.13 0.12 0.10 0.28 0.05 0.20 0.10 0.14 0.17 0.06 0.12 0.20 0.28 0.22 0.18 0.10 0.12 0.02
9 0.0 0.0 0.0 0.0 0.0 0.0 0.00 0.09 0.11 0.10 0.12 0.19 0.30 0.21 0.23 0.15 0.06 0.08 0.11 0.09 0.20 0.11 0.06 0.10 0.00
8 0.03 0.0 0.0 0.0 0.0 0.0 0.02 0.04 0.07 0.10 0.13 0.14 0.57 0.13 0.10 0.28 0.17 0.13 0.13 0.09 0.10 0.22 0.14 0.14 0.01
7 0.07 0.10 0.02 0.0 0.0 0.0 0.01 0.02 0.01 0.05 1.98 1.78 1.29 0.05 0.05 0.09 0.12 0.16 0.13 0.13 0.14 0.09 0.21 0.14 0.01
6 0.03 0.01 0.08 0.09 0.01 0.0 0.00 0.00 0.01 0.06 1.93 0.02 0.02 0.02 0.02 0.04 0.05 0.06 0.16 0.08 0.06 0.07 0.10 0.16 0.05
5 0.04 0.07 0.02 0.03 0.10 0.06 0.04 0.03 0.04 0.04 0.02 0.02 0.02 0.02 0.02 0.02 0.03 0.01 0.07 0.13 0.14 0.10 0.15 0.03 0.06
4 0.0 0.00 0.05 0.07 0.01 0.04 0.06 0.06 0.06 0.06 0.02 0.02 0.02 0.02 0.02 0.02 0.01 0.06 0.07 0.05 0.11 0.15 0.10 0.06 0.06
3 0.0 0.0 0.0 0.01 0.06 0.07 0.06 0.07 0.07 0.06 0.02 0.02 0.02 0.02 0.02 0.01 0.0 0.0 0.02 0.05 0.13 0.04 0.05 0.00 0.01
2 0.0 0.0 0.0 0.0 0.0 0.0 0.0 0.0 0.0 0.0 0.0 0.0 0.02 0.01 0.07 0.01 0.0 0.0 0.0 0.00 0.10 0.09 0.02 0.0 0.01
1 0.0 0.0 0.0 0.0 0.0 0.0 0.0 0.0 0.0 0.0 0.0 0.0 0.01 0.05 0.06 0.06 0.0 0.0 0.0 0.0 0.0 0.00 0.05 0.01 0.01
REDEDA
BURBANK
GLENDALE
PASADENA
AZUSA
GLENDORA
WEST COVINA
WEST LA
LOS ANGELES
SANTA MONICA
LENNOX
LYNWOOD
TORRANCE
LONG BEACH
ANAHEIM
GARDEN GROVE
SANTA ANA
SOX
TONS/DAY
57.715

FIGURE 4.20

# TABLE 4.9

## Stack Height and Plume Rise for Individual Source Classes

(estimated at reference conditions: neutral stability; ambient temperature 64.4°F; wind speed 6.2 mph)

| Stationary Sources | Number of Cases Examined in Table A4.1 | Notes | Range of Physical Stack Heights (ft) | Typical Physical Stack Height Adopted $H_s$ (ft) | Range of Plume Rise Calculated at Reference Conditions (ft) | Typical Plume Rise Adopted at Reference Conditions $\Delta H$ (ft) | Effective Stack Height Adopted at Reference Conditions $H_s + \Delta H$ (ft) |
|---|---|---|---|---|---|---|---|
| Fuel Combustion | | | | | | | |
| Electric Utilities at 75% of Full Load | | | | | | | |
| Large Generating Units (H > 150 ft) | 28 | | 176-300 | 225 | 409-1411 | 822 | 1047 |
| Small Generating Units (H ≤ 150 ft) | 16 | | 60-150 | 102 | 58 - 342 | 189 | 291 |
| Refinery Fuel Burning | -- | (b) | | 100 | | 180 | 280 |
| Other Interruptible Gas Customers (Large) | 2 | | 45 | 45 | 166 - 199 | 182 | 227 |
| Firm Gas Customers | -- | (c) | | 12 | | 24 | 36 |
| Chemical Plants | | | | | | | |
| Sulfur Recovery Plants | 9 | | 50-200 | 127 | 61 - 578 | 181 | 308 |
| Sulfuric Acid Plants | 3 | | 80-200 | 143 | 30 - 74 | 58 | 201 |
| Other Chemicals | -- | (c) | | 35 | | 70 | 105 |
| Petroleum Refining and Production | | | | | | | |
| Fluid Catalytic Crackers | 9 | | 89-181 | 122 | 282 - 794 | 540 | 662 |
| Sour Water Strippers | -- | (d) | | 130 | | 367 | 497 |
| Delayed Cokers | -- | (d) | | 130 | | 367 | 497 |
| Miscellaneous Refinery Processes | -- | (d) | | 130 | | 367 | 497 |
| Oil Field Production | -- | (c) | | 20 | | 72 | 92 |
| Miscellaneous Stationary Sources | | | | | | | |
| Petroleum Coke Calcining Kilns | 1 | | 150 | 150 | 1261 | 1261 | 1411 |
| Glass Furnaces | 17 | | 40-120 | 75 | 50 - 204 | 147 | 222 |
| Secondary Metals Industries (On-Grid) | 4 | (a) | 50 - 60 | 55 | | 110 | 165 |
| Sewage Treatment Plant Digesters | 1 | | 35 | 35 | 62 | 62 | 97 |
| Other Industrial Processes | -- | (c) | | 35 | | 70 | 105 |
| Permitted Incinerators | -- | (c) | | 35 | | 70 | 105 |
| Primary Metals Industries (Off-Grid Steel Mill) | 4 | | 175-300 | 238 | 341 - 548 | 426 | 664 |
| Mineral Products Industries (Off-Grid) | 1 | | 25 | 25 | 122 | 122 | 147 |
| **Mobile Sources** | | | | | | | |
| Autos and Light Duty Trucks | -- | (b) | | 1 | | 2 | 3 |
| Heavy Duty Vehicles | -- | (b) | | 12 | | 24 | 36 |
| Airport Operations | -- | (b) | | 20 | | 40 | 60 |
| Shipping Operations | -- | (b) | | 90 | | 180 | 270 |
| Railroad Operations | -- | (b) | | 18 | | 36 | 54 |

Notes: (a) Physical stack height known; plume rise assumed.

(b) Physical stack height estimated by observation of members of that source class; plume rise assumed.

(c) Physical stack height and plume rise assumed.

(d) Based on data for one refinery flare given in Table A4.1.

an assumed value has been noted in Table 4.9 based on a qualitative impression of the size of the sources involved.

The typical plume rise characteristics given in Table 4.9 provide a basis for visualizing the relative buoyancy of plumes from various source types. Petroleum coke calcining kilns and power plants are predicted to have by far the highest effective stack heights in the basin. Fluid catalytic crackers and a local steel mill display relatively tall effective stack heights. In contrast, sulfuric acid plants have non-buoyant plumes whose effective height of emission is due principally to their physical stack. Most small fuel burning sources and miscellaneous industrial processes display effective stack heights of between 100 and 300 feet above ground level at our reference conditions.

The brief discussion of effective stack height given here is supported in detail in Appendix A4. That appendix explains the calculation methods used. Stack parameters relevant to plume rise estimation for individual sources under a variety of meteorological conditions are tabulated. A method for dynamically allocating effective stack height as a function of wind speed within a simple air quality model is also described.

From the emissions estimates of Tables 4.5a and 4.5b, it is clear that at least 531 tons of sulfur oxides were emitted to the atmosphere on an average day in the South Coast Air Basin in 1973. That total, however, accounts for less than 15% of the sulfur thought to be entering local refineries in crude oil in that year. In order to account for

the rest of the sulfur, and thus to assess the accuracy of our emission inventory, an energy and sulfur balance was constructed for the South Coast Air Basin for the year 1973.

## 4.4 Energy and Sulfur Balance

### 4.4.1 Energy and Sulfur Balance -- Approach and Methods

The area under consideration is the entire South Coast Air Basin, which includes (using its 1973 boundaries) all of Orange and Ventura Counties, and portions of Los Angeles, Riverside, San Bernardino, and Santa Barbara Counties as shown in Figure 4.21. By determining the flows of energy resources across the boundaries of the basin, and by examining the transformations and uses of energy within the basin, an energy balance for this area can be derived. Similarly, by considering the sulfur content of these energy resources, flows of sulfur into and out of the basin, and points where sulfur is transformed or released to the atmosphere, a sulfur balance can also be determined. To the extent that energy intake can be balanced with energy consumption, one can build confidence that closure has been achieved over the fate of the sulfur accompanying those energy flows. Sulfur flows which were captured prior to becoming airborne can be identified. One can easily see what the potential emissions might be if one form of energy use were substituted for another.

The format of the energy balance is similar to that established by the Stanford Research Institute (1973). However in many cases our data sources, definitions and accounting conventions will differ significantly

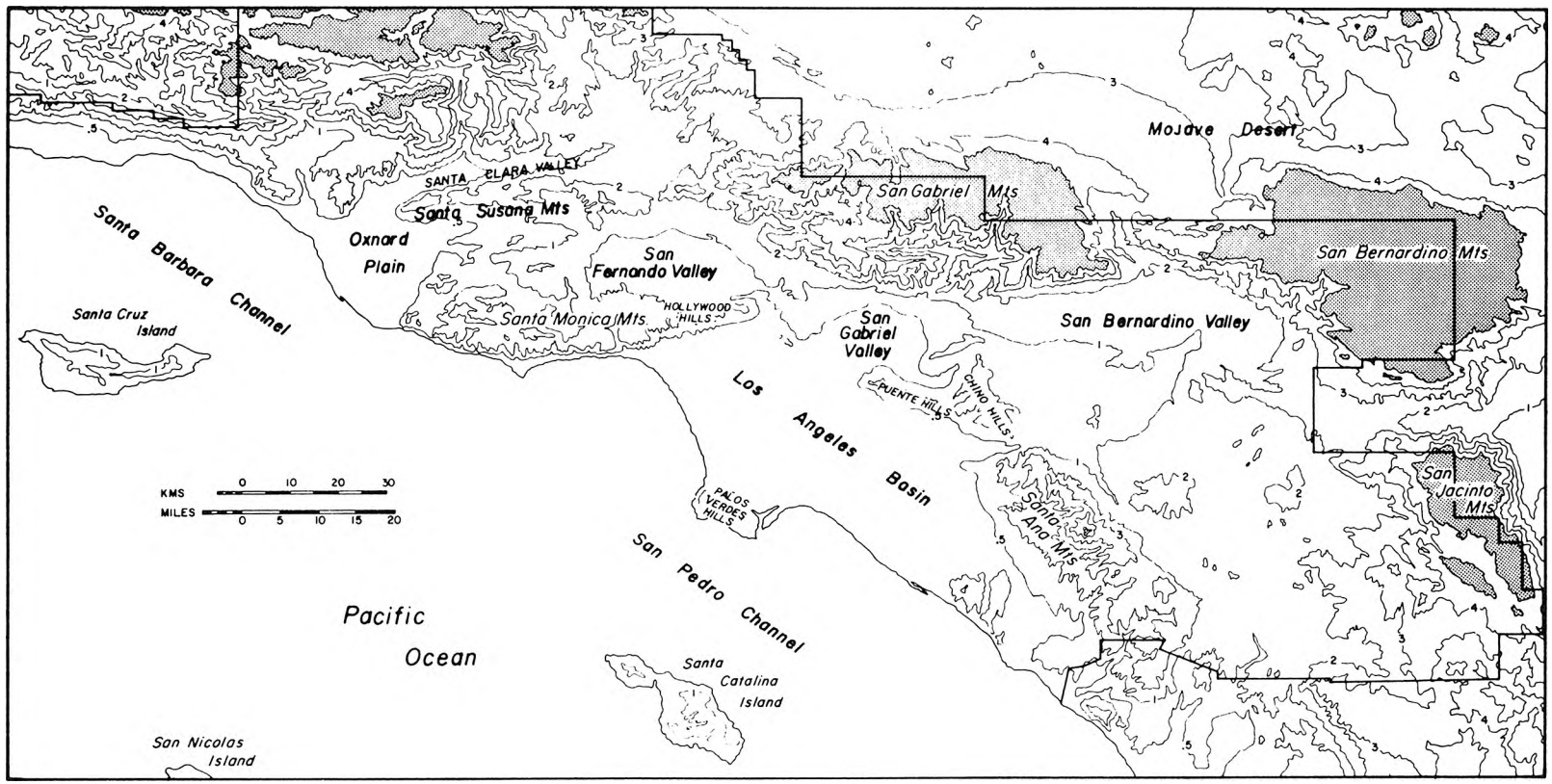


FIGURE 4.21

The South Coast Air Basin
(1973 Boundaries Shown by Heavy Outline)

from that prior survey of energy use in California. The energy balance is divided into four "sectors": sources, energy transformations, consumption, and exports. Energy sources include both local sources (i.e. those originating within the basin from crude oil and natural gas fields) and "imports" coming from outside the basin boundaries. These imports (the term will be used regardless of foreign or domestic origin) include items such as crude oil, refined petroleum products and other fuels, and electricity. In the transformation sector, two processes occur: crude oil is refined into a variety of petroleum products, and oil and natural gas are burned to generate electrical power. The consuming sector can be conveniently subdivided into six categories: raw materials use (e.g. use of natural gas in chemical fertilizer production), and five traditional energy use areas including residential/commercial, industrial, transportation, military, and miscellaneous energy consumption. Finally, energy can be exported from the basin in almost any form by pipeline or other overland transportation mode, by ship, or in the fuel tanks of various transportation media.

In each of the four sectors of the energy economy, a variety of energy forms are considered: natural gas, digester and refinery gas, LPG, natural gas liquids, crude oil, residual and distillate fuel oils, gasoline, jet fuel, petroleum coke, coal, and electricity. With such a wide variety of fuels to consider, and the need to study the sources, transformations, uses in a number of sectors, and exports for each fuel type, it has been necessary to employ a large number of data

sources. A complete discussion of the data sources used and the methods involved in their use is given in Appendix A3. In this section, only some general remarks about the types of information available and the treatment applied to them will be made. Appendix A3 should be consulted for a more detailed description of the methods and data sources employed.

The flow of natural gas through all four sectors of the energy balance was established from reports published jointly by the gas utilities serving the basin, and from additional information supplied to the California Air Resources Board by the Southern California Gas Company. Similarly, information on electrical energy within the basin was easily obtained from the annual reports of the utilities involved, and from the Federal Power Commission.

For other types of energy use, information had to come from a larger variety of sources. The U.S. Bureau of Mines publishes annual statistics on shipments of fuels, uses of various fuel types in different consuming sectors, and input and output at refineries. However, most of these data are reported on a state or district basis (California is a part of the West Coast district along with six other states). Thus, scaling factors must be developed, based on such statistics as refinery capacities, population, or industrial employment, to relate fuel sources and sinks at the basin level to those at the state or district levels.

For some items in the energy balance, state publications provided information on a county-by-county basis. Such data could be scaled

to the basin fairly easily, after making allowances for the out-of-basin portions of some counties. Some information was available on a point-by-point basis, e.g. operations at airports and fuel shipments received at various ports. In these cases, data for the basin were easily obtained by summation.

The purpose of the above discussion has been to give an introduction to the types of data sources and methods used to create the energy balance. Details on data, references, scaling factors, and assumptions made can be found in Appendix A3.

Much of the sulfur balance follows directly from the energy balance once the sulfur content of various fuels is known. The Bureau of Mines publishes yearly sulfur analyses for most of the fuels considered (see Appendix A3, Table A3.10). In some cases, local data on fuel sulfur content offer a better estimate of local fuel quality than do the regional analyses reported by the Bureau of Mines. These improved estimates of Los Angeles area fuel sulfur content have been used whenever possible. Data on the sulfur content of crude oils was adapted from the crude oil characterization study of Appendix A1.

In addition to fuel sulfur data, information is needed on sulfur flows occurring within certain industrial processes. Sulfur balance information on Los Angeles County refineries and chemical plants was obtained from the Southern California Air Pollution Control District (1976a). The refinery sulfur balance was used to confirm the quantity of sulfur received in crude oil by local refineries in 1973. That APCD refinery sulfur balance also permits comparison of sulfur flows leaving

the refineries in products to estimates of sulfur received in fuels by the consuming and export sectors of the Los Angeles energy economy. The APCD sulfur balance on local chemical plants was employed to gauge the amount of elemental sulfur and sulfuric acid produced in the basin from refinery wastes. Data on $SO_x$ emissions from other industrial processes were adapted to the sulfur balance from information given in Appendix A2.

A major strength of the energy and sulfur balance calculations is that independent estimates usually can be made of the amounts supplied and the amounts consumed of any given energy resource. Virtually every data point is estimated independently or has some degree of independence. Thus a summation of energy or sulfur sources and sinks, either for the entire system or for an individual fuel type, provides an assessment of the completeness and consistency of the information available.

### 4.4.2 Caveat

A variety of conventions could have been adopted at many points within the energy and sulfur balance that would have yielded seemingly different numbers within the summary Tables 4.10 and 4.11 which follow. If the reader wishes to compare this energy and sulfur balance summary to other data at his or her disposal, it is absolutely necessary to digest Appendix A3 first.

The terms to be used in the energy and sulfur balance are defined in Appendix A3. As an incentive to the reader to consult that appendix,

consider the following examples in which detailed knowledge is necessary to a correct interpretation of the energy and sulfur balance summary.

It is often possible to account for energy flows (or for that matter cash flows) on either a gross or net basis.[1] Sometimes one method is more convenient than another. In this energy balance, gross imports and exports are given for most refined petroleum products and for natural gas. From the descriptions given in Appendix A3, the reader can tell whether an import or export figure is stated on a gross or net basis.

As a second example, consider the definition of transportation fuel "consumption" as distinguished from fuel sales in the basin. Large quantities of petroleum sold as fuel to long range transportation vehicles (ships and aircraft) are not "consumed" (burned) in the air basin within the definitions used in this study. Only a small fraction of that fuel is burned within the South Coast Air Basin as those vehicles exit the area. Instead, the bulk of these fuels are "exported"

---

[1] Crude oil flows from Ventura area oil fields provide an illustration of the accounting choices available. This oil first enters the air basin when produced from local wells. Then some of the Ventura area crude oil is exported to sea by ship. Part of those Ventura area crude oil shipments later reappear as domestic oil receipts at other South Coast Air Basin ports. In Appendix A1, all crude oil flows were counted as part of the air basin's crude oil supply only if they remained in the air basin on a net basis. In the following energy balance, all crude oils will be considered as part of the energy balance's "source" category if they ever resided in the basin. Then net shipments to sea of locally produced oil will be shown as an "export". The net crude oil supply remaining in the basin as developed in Appendix A1 may thus be determined by difference between crude oil sources and exports.

from the basin in the fuel tanks of transportation media. That distinction is built into the energy and sulfur balance as it is important to a correct computation of local air pollutant emissions from the results of the sulfur balance.

### 4.4.3 The Energy Balance

Table 4.10 summarizes the energy balance on the South Coast Air Basin for the year 1973. A total of nearly 3700 x $10^{12}$ BTU's of energy resources entered the air basin's economy in that year. The ultimate fate of that energy supply is also apparent from Table 4.10:

- 15% of the energy supply is lost in transformation processes such as petroleum refining and electricity generation;
- 48% is expended for its heating value within the air basin by a final consumer of energy products;
- 4% of the energy content of the basin's energy resource base is tied-up in products that are used as industrial raw materials; and
- 33% of the gross energy supply passing through the air basin's economy is subsequently exported.

If the absolute value of all discrepancies between sources and sinks for various energy products appearing in Table 4.10 are added together, the total of all discrepancies is less than 5% of the gross energy input to the basin. On an aggregate basis, the energy balance actually balances with less than a 1% net surplus.

# TABLE 4.10

## South Coast Air Basin Energy Balance--1973
## ($10^{12}$ BTUs per year)

| | Electricity | Natural Gas | Crude and Unfinished Oils | NGL | LPG | Still Gas for Fuel | Gasoline | Jet Fuel | Light and Middle Distillate Fuel Oil | Residual and Heavy Distillate Fuel Oil | Petroleum Coke | Lubri-cants | Asphalt and Road Oil | Other Hydro-carbons | Coal | Digester Gas | TOTAL |
|---|---|---|---|---|---|---|---|---|---|---|---|---|---|---|---|---|---|
| SOURCES | | | | | | | | | | | | | | | | | |
| Resource base: imports plus local crude oil and natural gas production | 97.3 | 1050.3 | 2182.3 | 20.9 | 14.4 | | 69.6 | 4.4 | 83.6 | 127.6 | 5.5 | 12.3 | 0.1 | 4.6 | 57.4 | 2.6 | 3732.9 |
| Adjustments: change in gas storage; out-of-basin electric use | -13.1 | -25.2 | | | | | | | | | | | | | | | -38.3 |
| Subtotal | 84.2 | 1025.1 | 2182.3 | 20.9 | 14.4 | | 69.6 | 4.4 | 83.6 | 127.6 | 5.5 | 12.3 | 0.1 | 4.6 | 57.4 | 2.6 | 3694.6 |
| TRANSFORMATION SECTOR | | | | | | | | | | | | | | | | | |
| Refinery feedstock (-) | | | -2124.8[a] | -23.9 | -8.7 | | | | | | | | | -16.9[b] | | | -2174.3 |
| Refinery fuels (-) | -9.8 | -48.5 | | | | -149.8 | | | | -11.8 | | | | | | | -219.9 |
| Refinery production (+) | | | | | 36.1 | 108.4 | 863.0 | 224.3 | 126.9 | 581.2 | 112.0 | 18.5 | 88.0 | 60.3 | | | 2218.7 |
| Utility fuels (-) | | -160.9 | | | | | | | -2.7 | -386.3 | | | | | | -0.3 | -550.2 |
| Utility production (+) | 179.9 | | | | | | | | | | | | | | | | 179.9 |
| Subtotal | 170.1 | -209.4 | -2124.8 | -23.9 | | -14.0 | 863.0 | 224.3 | 124.2 | 183.1 | 112.0 | 18.5 | 88.0 | 43.4 | | -0.3 | -545.8 |
| CONSUMED IN BASIN AS ENERGY RESOURCE | | | | | | | | | | | | | | | | | |
| System uses; losses | -28.8 | -20.5 | | | | | | | | | | | | | | | -49.3 |
| Residential/commercial | -133.8 | -431.4 | | | -6.6 | | | | -8.1 | -8.1 | | | | | -0.2 | | -588.2 |
| Industrial (other than refinery) | -71.2 | -153.9 | | | -1.0 | | | | -15.6 | -19.5 | | | | | -57.2 | -2.3[a] | -320.7 |
| Transportation (civilian) | | | | | -1.9 | | -650.3 | -17.3 | -59.9 | -9.1 | | | | | | | -738.5 |
| Military | | | | | | | -2.2 | -6.1 | -6.5 | -0.1 | | | | | | | -14.9 |
| Miscellaneous | -21.9 | -8.7 | | | -3.0 | | | | -14.5 | -0.6 | | | | | | | -48.7 |
| Subtotal | -255.7 | -614.5 | | | -12.5 | | -652.5 | -23.4 | -104.6 | -37.4 | | | | | -57.4 | -2.3 | -1760.3 |
| CONSUMED AS A RAW MATERIAL[c] | | -18.6 | | | -8.4 | | | | | | pass through | -10.8[a] | -71.6[a] | -42.9[a] | | | -152.3 |
| EXPORTS | | | | | | | | | | | | | | | | | |
| As a commodity (by ship) | | | -57.5 | | -0.2 | | -47.9 | -17.4 | -89.7 | -155.1 | -109.4 | -20.0 | -16.5 | -5.1 | | | -518.8 |
| As a commodity (overland) | | -186.8[d] | | | | | -194.7 | -21.8 | -52.9 | -27.9 | | | | | | | -484.1 |
| In transport mode fuel tanks | | | | | | | -3.8 | -111.5 | -2.7 | -86.0 | | | | | | | -204.0 |
| Subtotal | | -186.8 | -57.5 | | -0.2 | | -246.4 | -150.7 | -145.3 | -269.0 | -109.4 | -20.0 | -16.5 | -5.1 | | | -1206.9 |
| SUMMARY | | | | | | | | | | | | | | | | | |
| Total sources (+ flows) | 277.2 | 1050.3 | 2182.3 | 20.9 | | 158.9 | 932.6 | 228.7 | 210.5 | 708.8 | 117.5 | 30.8 | 88.1 | 64.9 | 57.4 | 2.6 | |
| Total sinks (- flows) | -278.6 | -1054.5 | -2182.3 | -23.9 | | -179.6 | -898.9 | -174.1 | -252.6 | -704.5 | -109.4 | -30.8 | -88.1 | -64.9 | -57.4 | -2.6 | |
| Absolute difference | -1.4 | -4.2 | (a) | -3.0 | | -20.7 | 33.7 | 54.6 | -42.1 | 4.3 | 8.1 | (a) | (a) | (a) | | (a) | 29.3 |
| Difference as % of sources | -0.51% | -0.40% | (a) | -14.35% | | -13.03% | 3.61% | 23.87% | 20.0% | 0.61% | 6.89% | (a) | (a) | (a) | | (a) | |
| Difference as % of total energy resources | -0.04% | -0.11% | | -0.08% | | -0.56% | 0.91% | 1.48% | -1.14% | 0.12% | 0.22% | | | | | | 0.79% |

Notes: (a) Obtained by difference
(b) May include some natural gas
(c) Or put to other non-energy resource use
(d) Includes exchange with out-of-basin utility

The degree to which the energy balance balances for individual product types is more variable, but still is considered to be acceptable. Three of the five largest energy flows in the system (i.e. natural gas, electricity and heavy fuel oil) balance to within less than a 1% discrepancy between sources and sinks. The gasoline summary balances to within 4%, and the crude oil supply balances by virtue of the fact that refinery input was determined by difference between crude oil supply and exports. In addition, the petroleum coke summary balances with only a 7% surplus. That is considered to be good agreement given that petroleum coke production had to be scaled in two stages from a West Coast refinery total. The unaccounted for petroleum coke may well have been lost in coke calcining processes which have not been investigated for their effect on product "shrinkage".

Major percentage discrepancies between individual product sources and sinks occur in the light and middle distillate fuel oil categories including both jet fuel and light fuel oil. These two product lines share overlapping hydrocarbon boiling ranges. Kerosene heating oil has much the same composition as certain jet and turbine fuels. Our estimated surpluses of jet fuel and deficiency of light and middle distillate heating oil are of corresponding magnitude and opposite sign. These two discrepancies could well be self-cancelling. The source of the estimation error is not readily apparent from the highly aggregated data on refinery output which are at our disposal. For the purposes of the forthcoming sulfur balance, jet fuel and light fuel oils must be merged because available data on refinery sulfur output are given only

for both product streams combined. If the source of the jet fuel surplus and light fuel oil deficit lies in the refinery output estimate made for each fuel, that problem alone will not affect the forthcoming sulfur balance's accuracy.

The energy balance also shows an excess of LPG and NGL consumption above known supply. This problem is felt to arise from an inadequate knowledge of the sources of supply for these materials. LPG is the product of natural gas processing plants and refinery processes. Harbor receipts show that very small quantities of liquified gases were imported into the South Coast Air Basin in 1973 by waterborne commerce. Refinery gas consumption for fuel appears to include virtually all potential local refinery LPG production. Therefore, it seems likely that LPG sufficient to meet residential, commercial, industrial, and feedstock demand may have been imported into the basin by intrastate overland transportation modes (e.g. tank trucks). If that were the case, a significant source of LPG supply would not be identifiable in our commerce statistics and would have been omitted from the energy balance. A similar situation is thought to mask NGL supply: it is either included within crude oil statistics, lumped with unidentified hydrocarbons or moved overland within California in a way that does not easily stand out in the interstate commerce records. Since the sulfur content of LPG and NGL is very low, this discrepancy between LPG and NGL supply and consumption will not jeopardize the forthcoming sulfur balance.

Turning our attention to product supplies and uses, it is seen that crude oil is the principal energy input to the basin, accounting for 59% of the original energy supply. Natural gas is in second place with about 28% of the total energy supply. Imported refined petroleum products and imported electricity follow in order of importance to the gross energy resource base of the basin.

From Table 4.10 it is seen that estimated refinery feedstocks and gross product yield are in good agreement on a net energy content basis. However, in order to obtain this transformation of feedstocks into products, fuels were consumed with an energy content equal to about 10% of gross refinery product output. The ratio of fuel use to product energy content is about the same for the South Coast Air Basin and for all refineries located in the Western United States. However, South Coast Air Basin refineries appear to depend much more heavily on refinery gases for fuel than is typical of West Coast Region (PAD District V) refineries as a whole.

The principal refinery product in the South Coast Air Basin is gasoline, which accounts for 39% of total refinery product output on an energy content basis. The next largest refinery product stream consists of heavy fuel oil. The principal customer for this heavy fuel oil is a second stage of the energy transformation sector: the electric utility industry.

Electric utilities consumed $550.2 \times 10^{12}$ BTU's of fossil fuel within the South Coast Air Basin in 1973. Electricity generated from that fuel consumption amounted to $179.9 \times 10^{12}$ BTU's for an overall

conversion efficiency of about 33%. Seventy percent of that electricity was generated by combustion of heavy fuel oil. If a typical refinery energy loss of 10% is associated with preparation of the fuel oils used by utilities, then the overall efficiency of generating electricity using liquid petroleum products falls even further.

The largest energy demand in the end use consumption sector is for transportation fuels, principally gasoline. Gasoline accounts for roughly one third of the total energy used in the air basin by final product customers. Residential and commercial customer demand for natural gas is second in magnitude, followed by industrial natural gas use and residential/commercial electricity demand.

Energy exports from the basin consist almost entirely of refinery products, plus natural gas in transit to other parts of the state. Net refinery product exports (i.e. exports less imports) have an energy content equal to about 30% of that of the initial crude oil runs to local refineries. That raises an interesting observation about the nature of trade patterns in the Southwest. For many years, persons living in areas outside of Los Angeles have complained that Los Angeles is exporting air pollution by locating some electric generating stations serving Los Angeles in desert areas to the east of the basin. As can be seen from Table 4.10, 33% of the electricity supply for the South Coast Air Basin comes from sources outside of the basin. From Table A3.2 in Appendix A3, it is seen that about half of that imported electricity is generated by fossil fuel fired steam plants located outside the air basin. However, it is also now apparent that a fairly

large fraction of the emissions caused by petroleum refining in Los Angeles are incurred within the South Coast Air Basin for the benefit of final product customers located elsewhere, principally in San Diego, Arizona and Nevada. It is obvious that the energy economies of all of Southern California, Arizona and Southern Nevada are so closely intertied that the question of "exporting pollution" when siting a major energy transformation facility such as a power plant or refinery becomes nearly meaningless.

### 4.4.4 The Sulfur Balance

Table 4.11 summarizes the sulfur balance on the South Coast Air Basin for the year 1973. An estimated total of 4.2 million pounds of sulfur per day was tracked through the basin's economy. Over ninety percent of that sulfur input accompanied crude oil.

The estimated fate of that sulfur supply is also given in Table 4.11:

- Nearly half of the sulfur was captured at sulfur recovery and sulfuric acid plants;
- Approximately one quarter of the sulfur was exported from the basin in finished petroleum products;
- 4.4% of the sulfur supply found its way into solid or liquid wastes;
- At least 14% of the sulfur was emitted to the atmosphere in the form of 586.51 tons per day of sulfur oxides air pollutants (stated as $SO_2$); and
- The fate of 9.4% of the sulfur supply remains undetermined.

# TABLE 4.11

## South Coast Air Basin Sulfur Balance-1973
## (1000's lbs sulfur per day)

| | Natural Gas | Crude Oil; Unfinished Oils & Other Refinery Feedstocks | LPG and Still Gas for Fuel | Gasoline | Light and Middle Distillates & Jet Fuel | Residual and Heavy Distillate Fuel Oil | Petroleum Coke | Misc. Petroleum Products | Coal | Digester Gas | Hydrogen Sulfide | Sulfur | Acid Sludge | Sulfuric Acid | Misc. Indus. Raw Materials Sufficient to Balance Process Losses | Solid or Liquid Waste | Atmospheric Emissions: Industrial Process | Atmospheric Emissions: Fuel Burning | TOTAL |
|---|---|---|---|---|---|---|---|---|---|---|---|---|---|---|---|---|---|---|---|
| **SOURCES** | | | | | | | | | | | | | | | | | | | |
| Resource base: imports plus local crude oil and natural gas production | 0.81 | 3942.5 | 0.01 | 4.40 | 29.76 | 77.70 | 16.11 | small | 91.73 | 0.63 | | 0.06 | | | 17.69 | | | | |
| Adjustments: change in gas storage | -0.02 | | | | | | | | | | | | | | | | | | |
| Subtotal | 0.79 | 3942.5 | 0.01 | 4.40 | 29.76 | 77.70 | 16.11 | | 91.73 | 0.63 | | 0.06 | | | 17.69 | | | | 4181.38 |
| **TRANSFORMATION SECTOR** | | | | | | | | | | | | | | | | | | | |
| Refinery | | | | | | | | | | | | | | | | | | | |
| Feedstock sulfur | | -3551.5 | | | | | | | | | | | | | | | | | |
| Fuel sulfur | -0.04 | | -2.45 | | | -9.19 | | | | | | | | | | | | | |
| Products and wastes | | | 2.65 | 81.88 | 135.65 | 761.31 | 332.11 | 67.49 | | | 1980.4 | | 363.4 | -363.4 | | 134.95 | 53.77 | 11.68 | |
| Sulfur Recovery and Sulfuric Acid | | | | | | | | | | | | | | | | | | | |
| Feedstock sulfur | | | | | | | | | | | -1980.4 | -420.8 | -363.4 | | | | | | |
| Products and wastes | | | | | | | | 5.80 | | | | 1720.7 | | 959.4 | | | 81.46 | | |
| Electric Utilities | | | | | | | | | | | | | | | | | | | |
| Fuel sulfur | -0.12 | | | | -0.18 | -235.22 | | | | -0.07 | | | | | | | | 235.59 | |
| Subtotal | -0.16 | -3551.5 | 0.20 | 81.88 | 135.47 | 516.90 | 332.11 | 73.29 | | -0.07 | 0 | 1299.90 | 0 | 959.0 | | 134.95 | 135.23 | 247.27 | 1.47 |
| **END USE CONSUMPTION SECTOR** | | | | | | | | | | | | | | | | | | | |
| (Fuel Combustion in Basin) | | | | | | | | | | | | | | | | | | | |
| System uses; losses | -0.02 | | | | | | | | | | | | | | | | | 0.02 | |
| Residential/commercial | -0.33 | | -0.005 | | -2.80 | -4.64 | | | -0.32 | | | | | | | | | 8.10 | |
| Industrial (other than refinery) | -0.12 | | -0.001 | | -5.40 | -11.18 | | | -91.41 | -0.56 | | | | | | 50.05 | | 58.62[a] | |
| Transportation (civilian) | | | -0.001 | -41.15 | -23.03 | -21.84 | | | | | | | | | | | | 85.82 | |
| Military | | | | -0.14 | -2.88 | -0.24 | | | | | | | | | | | | 3.26 | |
| Miscellaneous | -0.01 | | -0.002 | | -4.63 | -0.34 | | | | | | | | | | | | 4.98 | |
| Subtotal | -0.48 | | -0.01 | -41.29 | -38.74 | -38.04 | | | -91.73 | -0.56 | | | | | | 50.05 | | 160.80 | 0.00 |
| **ADJUSTMENT FOR EFFECT OF RAW MATERIALS PROCESSING INDUSTRIES** | -0.01 | | -0.01 | | | | -25.52 | | | | | | | | -17.69 | | 43.21[b] | | -0.02 |
| **EXPORTS** | | | | | | | | | | | | | | | | | | | |
| As a commodity (by ship) | -0.07 | -121.8 | ~0 | -3.03 | -32.83 | -302.57 | -320.44 | | | | | -1.67 | | | | | | | |
| As a commodity (overland) | -0.07 | | | -12.32 | -20.18 | -16.99 | | | | | | unknown | | | | | | | |
| In transport mode fuel tanks | | | | -0.24 | -8.88 | -206.24 | | | | | | | | | | | | | |
| Subtotal | -0.14 | -121.8 | ~0 | -15.59 | -61.89 | -525.80 | -320.44 | | | | | -1.67 | | | | | | | -1047.33 |
| **SINK FOR MISC. NON-FUEL RESOURCES WHOSE ULTIMATE CUSTOMER WILL NOT BE SOUGHT** | | | | | | | | -73.29 | | | | -1298.29 | | -596.0 | | | | | -1967.58 |
| **SUMMARY** | | | | | | | | | | | | | | | | | | | |
| Total sources (+ flows) | 0.81 | 3942.5 | 2.66 | 86.28 | 165.41 | 839.01 | 348.22 | 73.29 | 91.73 | 0.63 | 1980.4 | 1720.76 | 363.4 | 959.4 | 17.69 | 185.00 | 586.51 | | |
| Total sinks (- flows) | -0.81 | -3673.3 | -2.47 | -56.88 | -100.81 | -808.25 | -345.96 | -73.29 | -91.73 | -0.63 | -1980.4 | -1720.76 | -363.4 | -959.4 | -17.69 | | | | |
| Absolute difference | 0 | 269.2 | 0.19 | 29.40 | 64.60 | 30.76 | 2.26 | | | | | | 0 | | | | | | 393.41 |
| Difference as % of sources | 0 | +6.8% | +7.1% | 34.1% | 39.1% | 3.7% | 0.65% | | | | | | | | | | | | |
| Difference as % of total sulfur input of 4181.38 thousand lbs/day | 0 | 6.4% | ~0% | 0.70% | 1.54% | 0.74% | 0.05% | | | | | | | | | | 14.0% | | |

Notes: (a) This fuel burning total includes 41.36 thousand pounds of sulfur per day from combined fuel burning and industrial processes activities at Kaiser Steel.

(b) These industrial process emissions include

| | |
|---|---|
| misc. chemical industries | 0.09 |
| oil field production | 4.50 |
| petroleum coke kilns | 25.52 |
| glass furnaces | 2.23 |
| metals industries | 8.88 |
| minerals industries | 1.90 |
| other industrial processes | 0.02 |
| incinerators | 0.07 |

In contrast to the energy balance, the sulfur balance at first glance does not appear to balance closely. The explanation for that problem, however, seems fairly straightforward.

The largest discrepancy between sulfur supply and consumption lies in the crude oil and refinery feedstocks column of Table 4.11. While sulfur supplied in that category exceeds known refinery feedstock sulfur intake plus exports by only 6.8%, that 6.8% difference is applied to two very large sulfur flows. One reason for this gap between estimated supply and demand lies in the fact that the APCD survey used to estimate sulfur intake by refineries did not include at least two small refineries which accounted for about 1% of the basin's daily crude oil demand in 1973. Refinery sulfur intake and products should be at least 1% higher than shown if more complete data were available on those small refineries. The remaining five to six percent surplus of sulfur in crude and unfinished oils probably represents an overestimate of either crude oil intake or crude oil sulfur content as part of the study conducted in Appendix A1 to this report. Considering the difficulty in estimating the origin of some of the crude oils received in the basin, that small percentage disagreement will be considered nearly unavoidable. Provided that the APCD refinery sulfur balance is correct, any overestimate of crude oil sulfur supply from Appendix A1 will not affect the rest of the sulfur flows shown in Table 4.11, nor will it inflate any atmospheric emissions estimates. With the crude oil sulfur discrepancy set aside, the remainder of the sulfur balance balances to within about 3%.

Turning to individual product streams, we note that the sulfur balances on the heavy petroleum products appear reasonable. Petroleum coke sulfur balances to within less than 1%, and heavy fuel oil balances to within 3.7%. Those two products account for about 28% of the total sulfur in the system. Heavy fuel oil combustion in the basin is the largest single source of sulfur oxides air pollutant emissions, accounting for just under half of the total $SO_x$ emissions to the atmosphere. It is therefore reassuring to obtain a fairly close sulfur balance on supply and use for this product.

Petroleum coke is produced almost exclusively for export from the basin. However, a close balance on petroleum coke sulfur is still important because significant emissions to the atmosphere come from the petroleum coke calcining industry (25.22 tons/day as $SO_2$; see adjustment for raw materials processing).

At the lightest product end of the sulfur balance, results also seem acceptable. Natural gas and refinery gases (LPG + still gas) contributed practically no sulfur oxides emissions even though they accounted for a third of the basin's total energy supply in 1973. Even a significant percentage error in estimating the sulfur content of either product would not change that conclusion.

In spite of the fact that the energy balance on gasoline closed almost exactly, the fate of 34% of the sulfur distributed in gasoline in 1973 remains undetermined. The apparent explanation is that the Bureau of Mines gasoline grab samples for that year were not

representative of a production-weighted average of local refinery products. Consider the following evidence to that effect.

Table 4.12 shows refinery sulfur output in gasoline for the years 1973 and 1974 as reported by refineries to the local air pollution control district. An estimate of the weight percent sulfur in gasoline implied by those refinery reports has been made for comparison with Bureau of Mines data. As can be seen, the refinery reports to the APCD closely follow the Bureau of Mines sulfur samples in 1974. But for 1973, either the Bureau of Mines samples are far too low, or the APCD sulfur balance is too high.

Since local refineries would be unlikely to overstate the total tonnage of sulfur distributed in gasoline by 47%, one tends to suspect the Bureau of Mines data. The Bureau of Mines appears to take grab samples of gasoline from a large number of refiners. These samples are first averaged for each refiner and then each refiner is weighted equally when computing the Southern California average gasoline sulfur content. But two of the eighteen refineries in the South Coast Air Basin accounted for about 40% of local refinery capacity in 1973. Unless the sulfur content of gasoline from the basin's large refineries is weighted by their market share, the Bureau of Mines would not compute a gasoline pool average sulfur content with any accuracy unless all gasoline samples were of about the same sulfur content. Bureau of Mines test results show wide variance in gasoline sulfur content between refineries. One therefore suspects that their average sulfur content

TABLE 4.12

Comparison of Bureau of Mines Gasoline Sulfur Content Data to the Sulfur Content of Gasoline Estimated from Refinery Reports to the Southern California APCD

| Calendar Year | Sulfur distributed in gasoline (1000's lbs/day)[a] | Sulfur distributed as weight percent of gasoline production (approximate)[b] | Average weight percent sulfur in gasoline as implied by Bureau of Mines[c] |
|---|---|---|---|
| 1973 | 81.88 | 0.070% | 0.047% |
| 1974 | 55.89 | 0.048% | 0.049% |

Notes: (a) Based on refinery reports to the Southern California Air Pollution Control District (1976a).

(b) Based on an approximate gasoline production rate for local refineries of 450 thousand barrels per day in both years (estimated from Table A3.3).

(c) See Table A3.10.

values could be quite a bit in error if used to represent a gasoline pool average.

Unlike the discrepancy in the crude oil sulfur balance, the gasoline sulfur surplus probably represents a real uncertainty in the basin's atmospheric emissions estimates for 1973. Most gasoline produced in local refineries is actually burned in the basin. If the 1973 gasoline sulfur content were 47% higher than reported by the Bureau of Mines, then atmospheric emissions from gasoline combustion would have been close to 60 tons per day (as $SO_2$) instead of the 41 tons per day calculated in Table 4.11.

A similar problem may have occurred with estimation of light and middle distillate fuel oil sulfur content in 1973. The average sulfur content of distillate oil products shown in Table A3.10 was given by the Bureau of Mines for the entire Western Region of the United States. Since several Southern California refineries handled very high sulfur crude oil, it would not be too surprising if Southern California distillate oil sulfur content were above the Western Region average. However, given the large variety of distillate oil products and the fact that our energy balance on these oils did not close exactly, it is not possible to pinpoint the nature of the imbalance in the distillate oil sulfur pool.

One of the most striking features of the sulfur balance is the relatively high degree of desulfurization of petroleum products that is already occurring at Los Angeles area refineries. Roughly half

of the sulfur entering those refineries is being captured as elemental sulfur or sulfuric acid, rather than leaving the refinery in products or waste discharges.

## 4.5 Comparison of the Air Quality Modeling Emission Inventory to the Results of the Sulfur Balance

In Table 4.13, atmospheric emissions calculated from the sulfur balance on the South Coast Air Basin are compared to emissions identified in the air quality modeling inventory of Appendix A2. Emissions from electric utilities compare closely in both surveys even though one emissions total was calculated from utility annual reports while the other came from monthly data on each generating plant's fuel use. Refinery fuel burning estimates are in reasonable agreement, as are industrial process $SO_x$ emissions levels. That is not too surprising since refinery and industrial process figures in both surveys were ultimately derived from local APCD records, with an independent check supplied by reference to Hunter and Helgeson (1976).

A comparison of mobile source emissions in Table 4.13 shows that about 36 tons per day of $SO_x$ emissions were found by the sulfur balance beyond those identified in the modeling inventory. Most of that discrepancy represents emissions occurring within the air basin but located outside of the 50 by 50 mile square grid. However, most of these off-grid emissions may never be advected into the modeling region. They thus pose less of a hazard to air quality model results than would neglect of on-grid emissions of comparable size.

TABLE 4.13

Comparison of the Air Quality Modeling Inventory of Appendix A2 to Emissions Implied by the 1973 Sulfur Balance on the South Coast Air Basin

| Category | $SO_x$ Emissions from the Spatially Resolved Modeling Inventory -1973- (Tons/day as $SO_2$) | | | $SO_x$ Emissions Implied by Sulfur Balance -1973- (Tons/day as $SO_2$) |
|---|---|---|---|---|
| | On-Grid Sources | Off-Grid Sources | Total | |
| Stationary Sources | | | | |
| Electric Utility Fuel | 181.71 | 58.20 | 239.91 | 235.59 |
| Refinery Fuel | 9.42 | (c) | 9.42 | 11.68 |
| Residential, Commercial and Industrial Fuel (*excluding Off-grid Steel Mill Fuel Use) | 2.58 | (c) | 2.58 | 25.36* |
| Gas Utility System Fuel Use | | | | 0.02 |
| Industrial Processes (including Off-Grid Steel Mill Fuel Burned) | 177.52 | 43.59 | 221.11 | 219.80 |
| Mobile Sources | | | | |
| Civilian Transportation | 57.71 | (c) | 57.71 | 85.82 |
| Military Fuel(a) | --- | (c) | --- | 3.26 |
| Miscellaneous(b) | --- | (c) | --- | 4.98 |
| Total Emissions | 428.94 | 101.79 | 530.73 | 586.51 |

Notes: (a) Military fuel is mostly for mobile sources.

(b) Miscellaneous uses are largely devoted to off-highway diesel fuel.

(c) Off-grid emissions in this category not inventoried.

In addition to the nearly certain 36 ton per day difference between the modeling inventory and actual basin-wide emissions, there are two uncertainties which are difficult to evaluate. The first is the 23 tons per day difference between residential, commercial and industrial fuel use $SO_x$ emissions identified in the two competitive inventories. The second uncertainty involves approximately 20 tons per day of additional $SO_x$ emissions which could have been missed by both survey techniques if the Bureau of Mines gasoline sulfur content data were too low.

The nature of the gasoline sulfur content issue has been explored previously and will not be pursued further at this time. However, the disagreement between survey methods in the area of residential, commercial and industrial stationary source fuel burning can be clarified somewhat.

Small stationary source fuel burning $SO_x$ emissions estimated from Bureau of Mines fuel oil sales data are a full order of magnitude greater than emissions estimated from fuel burning records reported to the local air pollution control district. List (1971) also noted a similar discrepancy, and concluded that the APCD records must be wrong. In Appendix A2, however, a simulation model was constructed which calculated $SO_x$ emissions within the 50 by 50 mile square grid from a combination of APCD reports and a knowledge of interruptible gas customers' sizes and locations in the basin. Natural gas use predicted by that simulation closely matched separate reports of total gas company dispatches to those customers. It is therefore concluded

that interruptible gas customers within the 50 by 50 mile grid have been correctly identified. Oil use estimates made for interruptible gas customers in Appendix A2 are known to be consistent with their gas curtailment status. Therefore oil burning $SO_x$ emissions from those customers within the 50 by 50 mile square are thought to be calculated correctly in the modeling inventory. If the Bureau of Mines oil sales data are also correct, then the additional fuel burning sources involved are either located beyond our 50 by 50 mile square grid, or burn oil without regard for the level of gas service available to interruptible gas customers.

While neither the gasoline sulfur content nor the small stationary source fuel use uncertainties may be laid to rest completely, the absolute values of these uncertainties are fairly small. If only one of these two possible additional emission sources were actually to have existed in 1973, the modeling inventory would still reproduce total basin-wide emissions to within about 10.5%. Emissions within the 50 by 50 mile grid would be simulated much more closely. Reasonable assurance has been obtained that the modeling emission inventory reproduces average 1973 $SO_x$ emissions to within a few percent error.

## 4.6 In Conclusion

Most of the sulfur entering the South Coast Air Basin's energy economy in 1973 arrived in a barrel of crude oil. Crude oils supplied to the basin in that year were characterized by origin, quantity and sulfur content. In the lowest sulfur category (< 0.25% S), 22% of the

total crude oil received contributed only 2% of the total sulfur input to local refineries. In contrast,12% of the oil with the highest sulfur content accounted for 28.5% of the basin's sulfur supply. Well over 50% of the sulfur input to local refineries came from crude oils produced from oil fields located within the South Coast Air Basin. The South Coast Air Basin is saddled with a sulfur management problem which is likely to command considerable attention as long as local crude oils are processed in local refineries.

A spatially resolved sulfur oxides emission inventory has been constructed to advance an emissions-air quality modeling study of sulfate formation in the Los Angeles atmosphere. Emissions estimates were developed for each of 26 classes of mobile and stationary sources for each month of the years 1972 through 1974. The spatial distribution of total $SO_x$ emissions from each source class in each month was determined within a 50 by 50 mile square laid over metropolitan Los Angeles and Orange Counties. Major off-grid stationary sources in the South Coast Air Basin were also inventoried. Information was presented on the fraction of each source class's $SO_x$ emissions which are evolved as $SO_3$ or sulfates rather than as gaseous $SO_2$. The diurnal variation of power plant and motor vehicle emissions was specified. The effective height of injection of emissions into the atmosphere has been investigated.

In the year 1973, for example, 82.6% of that $SO_x$ emissions inventory was concentrated in a small number of point source classes, as shown in Table 4.14. Electric utility generating plants constituted

TABLE 4.14

$SO_x$ Emissions from Point Source Classes Emitting over 20 tons/day in 1973 within the South Coast Air Basin

| Equipment Type | Number of Plant Sites | 1973 $SO_x$ Emissions tons/day | Percent of Total Modeling Inventory $SO_x$ Emissions* 1973 |
|---|---|---|---|
| Electric Utility Generating Stations | 18 | 239.91 | 45.2% |
| Sulfur Recovery Plants | 9 | 60.40 | 11.4% |
| Refinery Fluid Catalytic Crackers | 8 | 52.07 | 9.8% |
| Integrated Steel Mill | 1 | 41.46 | 7.8% |
| Petroleum Coke Calcining Kilns | 2 | 25.52 | 4.8% |
| Sulfuric Acid Plants | 3 | 20.00 | 3.8% |

Note: *Based on modeling inventory total of 530.73 tons/day $SO_x$

the largest source of total sulfur oxides emissions in the basin in recent years. Other major source classes emitting over 20 tons of $SO_x$ per day in 1973 included refinery fluid catalytic crackers, chemical plants involved in recovering sulfur and sulfuric acid from refinery wastes, a local steel mill, and petroleum coke calcining kilns. All other stationary sources combined totaled only 6% of the modeling emission inventory in 1973. Mobile sources accounted for the remaining $SO_x$ emissions surveyed.

From the results of the detailed emission inventory, it was estimated that less than 15% of the sulfur supplied to the basin daily in crude oil was being emitted to the atmosphere in the form of sulfur oxides air pollutants. In order to confirm that finding, an energy and sulfur balance was constructed for flows of energy and sulfur crossing a control surface drawn around the perimeter of the air basin. The findings of that sulfur balance indicated that about half of the sulfur arriving in crude oil in 1973 was recovered at the refinery level as elemental sulfur or sulfuric acid. Only 14% of the basin's original sulfur supply reached the atmosphere as sulfur oxides air pollutant emissions. Most of the remaining sulfur was diverted into solid materials like petroleum coke and asphalt that will not be burned within the basin for fuel, or was exported from the basin in heavy fuel oil or other petroleum products. The 1973 sulfur oxides emission control strategy for the South Coast Air Basin was found to entail about a 50% efficient overall desulfurization of products at local refineries,

followed by segregation of most of the remaining sulfur within products that will not be burned locally.

# CHAPTER 5

# APPLICATION OF THE SIMULATION MODEL TO LOS ANGELES SULFATE AIR QUALITY

## 5.1 Introduction

In order to verify our understanding of emissions-air quality relationships, we wish to simulate the succession of sulfate air quality patterns observed in the Los Angeles Basin over a period of several years. In Chapter 2, it was decided that the available air quality data would best support a simulation of monthly average sulfate air quality during the years 1972 through 1974.

An air quality model suited to this task has been derived. Sulfur oxides emissions in the South Coast Air Basin have been defined for each month of that three year test period. In this chapter, the remaining data requirements of the simulation model will be explained and satisfied. Then the air quality model will be applied to analysis of the Los Angeles sulfate problem, and comparisons will be drawn between observed and predicted sulfate concentrations.

## 5.2 The Data Required for Model Validation

Given the long-term average air quality model derived in Chapter 3, a simulation may be conducted to estimate the sulfate concentration patterns appearing in the Los Angeles Basin during each month of the years 1972 through 1974. The input data and data preparation steps required for this simulation are:

1. Consolidation of the $SO_x$ emissions inventory into $i = 1,2,\ldots,N_4$ source classes. A source class is composed of a group of j sources whose emissions behavior is similar except for geographic location $\underset{\sim}{X}_{o_j}$ and average emissions strength, $\overline{S}(\underset{\sim}{X}_{o_j},i)$ of each of the j members of that class.
2. Specification of effective stack height for each source class as a function of time of pollutant release.
3. Specification of the diurnal variation in source emission strength, $\omega(i,t_o)$, for each source class.
4. Specification of the initial fraction of the $SO_x$ emissions which originated as $SO_3$ or sulfates, $f_{s_o}(i)$, from each source class.
5. An estimate of the maximum retention time for an air parcel in the air basin, $\tau_c$.
6. A continuous record of hourly wind speed and direction data for each month of interest, plus the $\tau_c$ hours preceding the start of each month.
7. A sequence of hourly estimates for inversion base height for each month of interest plus the $\tau_c$ hours preceding the start of each month.
8. A function for estimating the rate of horizontal eddy diffusion in the form $(\sigma_1(t-t_o), \sigma_2(t-t_o))$.

9. Estimates of $SO_2$ deposition velocity, $V_g$; sulfate deposition velocity, $V_p$, and sulfate formation rate, k.

10. An estimate of the seasonal variation in sulfate background concentrations.

11. A choice of receptor cell size $\Delta x_1$, $\Delta x_2$. A review of our model derivation shows that the product of $\Delta x_3 \cdot \frac{h(t)}{\Delta x_3}$ cancels the need for specification of a vertical cell dimension.

12. Choice of a time step, $\Delta t$.

Acquisition or preparation of each of these data bases will be discussed in turn.

### 5.2.1 Emission Source Related Data

The spatially resolved $SO_x$ emissions estimates of Chapter 4 and Appendix A2 will be used as the basis for this air quality simulation. In that emissions inventory, separate source classes were defined for nineteen classes of stationary sources and seven types of mobile sources. For air quality modeling purposes, all members of a given source class residing within a single cell of the emissions grid displayed in Chapter 4 will be summed and then treated as a single virtual source located at the center of that cell. Emissions from major off-grid sources will be located at the center of the cells that they would occupy if the grid system of Chapter 4 was extended to cover the entire South Coast Air Basin.

To further speed the air quality model calculations, it is desirable to combine as many of the small source classes as possible in order to achieve a reduced number of virtual emission points. There are, however, two constraints on this process of source class aggregation. The first constraint is purely technical. All members of each of these larger source groupings must share a similar source effective stack height, fraction sulfates originating in their exhaust, and diurnal modulation of source emission strength. The second constraint on source class recombination is largely strategic in nature. If all source classes were lumped together for air quality model calculation purposes, no information would be gained on source class contribution to air pollutant increments observed at various air monitoring stations. This latter information on source class contribution to downwind air quality is absolutely vital if emission control strategy analysis is to proceed by a means other than trial and error.

Within this air quality model application, the decision has been made to preserve the major source classification system in use for many years by the Los Angeles Air Pollution Control District. Separate $SO_x$ source categories will be maintained for power plants, other stationary fuel combustion sources, chemical plants, petroleum industry processes, miscellaneous stationary sources, automobiles and light trucks, and other mobile sources.

In most cases, the equipment types grouped within these major headings do display similar stack heights, fraction sulfates in their

exhaust, and diurnal emissions patterns. However, the miscellaneous stationary source category is composed of a variety of disparate industrial processes, many of which have unique characteristics. Petroleum coke calcining kilns have very high effective stack heights, and a high fraction of their sulfur oxides emissions are released directly as $SO_3$ or sulfates. Glass furnaces have much lower stack heights, but a high fraction sulfates in their exhaust. The off-grid steel mill has a high effective stack height and a normal amount of $SO_3$ in its exhaust, while most remaining metals furnaces have lower effective stack heights and a lower fraction $SO_3$ in their effluent. Therefore, to avoid potential distortion of our results, the air quality impact of coke calcining kilns, glass furnaces, the steel mill, and metals melting furnaces each will be calculated as from a separate source class. The emissions from all remaining miscellaneous stationary sources will be lumped to form an additional source class. Then the air quality impact of these components of the miscellaneous stationary source category may be summed at each air quality receptor point in order to recover the pollutant contribution from the miscellaneous source category as a whole. A key to this source class aggregation procedure is provided in Table 5.1.

Table 4.7 in Chapter 4 was constructed in anticipation of this source class recombination scheme. It shows the weighted-average fraction sulfates in the exhaust of each of the major source class groupings that will be used for air quality model calculations. Those weighted-average values of $f_{s_o}$ are summarized in Table 5.1.

TABLE 5.1

Source Class Aggregation Scheme
Used to Reduce the Number of Virtual Emissions Sources
within the Air Quality Simulation Model

| Source Classes Inventoried | Aggregated Source Classes (Supplied to Air Quality Model) | Stack Parameters at Reference Conditions[a] | | Fraction $SO_3$ in Exhaust[b] |
|---|---|---|---|---|
| | | Stack Height H meters | Plume Rise ΔH meters | $f_{S_o}$ percent |
| **Stationary Sources** | | | | |
| Fuel Combustion | | | | |
| Electric Utilities | Electric Utilities | 68.6 | 250.6 | 3.0% |
| Refinery Fuel Burning<br>Other Interruptible Gas Customers<br>Firm Gas Customers | Other Stationary Fuel Combustion Sources | 30.5 | 54.9 | 3.0% |
| Chemical Plants | | | | |
| Sulfur Recovery Plants<br>Sulfuric Acid Plants<br>Other Chemicals | Chemical Plants | 41.2 | 36.6 | 0.6% |
| Petroleum Refining and Production | | | | |
| Fluid Catalytic Crackers<br>Sour Water Strippers<br>Delayed Cokers<br>Miscellaneous Refinery Processes<br>Oil Field Production | Petroleum Refining and Production | 37.2 | 164.6 | 2.8% |
| Miscellaneous Stationary Sources | Miscellaneous Stationary Sources | | | |
| Petroleum Coke Calcining Kilns | Petroleum Coke Calcining Kilns | 45.7 | 384.4 | 8.4% |
| Glass Furnaces | Glass Furnaces | 22.9 | 44.8 | 18.0% |
| Secondary Metals Industries (On-Grid) | Secondary Metals Industries (On-Grid) | 16.8 | 33.5 | 1.0% |
| Primary Metals (Off-Grid Steel Mill) | Primary Metals (Off-Grid Steel Mill) | 72.5 | 129.8 | 2.5% |
| Minerals Products<br>Sewage Treatment Digesters<br>Other Industrial Processes<br>Permitted Incinerators | Other Miscellaneous Stationary Sources | 10.7 | 21.3 | 2.8% |
| **Mobile Sources** | | | | |
| Autos and Lt. Trucks - Surface<br>Autos and Lt. Trucks - Freeway<br>Heavy Duty Vehicles - Surface<br>Heavy Duty Vehicles - Freeway | Autos and Light Trucks | Surface mixed layer | | 0.3% |
| Airport Operations<br>Shipping Operations<br>Railroad Operations | Other Mobile Sources | Surface mixed layer | | 2.5% |

Notes: (a) Reference Conditions: neutral stability, ambient temperature = 18°C, wind speed = 2.77 m/sec.

(b) 1973 emissions weighted average within each source grouping shown.

In a similar fashion, Table 5.1 assigns a typical physical stack height and plume rise at reference conditions to each of these major source class groupings, based on the more detailed analysis of Table 4.9 in Chapter 4. Emphasis has been placed on most closely reproducing the stack parameters of the dominant equipment type within each of these aggregated source classes. For example, since fluid catalytic cracking units totally dominate $SO_x$ emissions from petroleum refinery processes, the refinery process source class grouping as a whole was assigned stack parameters appropriate to fluid catalytic cracking units. These plume rise estimates at reference conditions will be adjusted hourly within the air quality model calculation in order to better reflect observed wind speed at each time step, as outlined in Appendix A4. Mobile sources are assumed to emit within the surface mixed layer of our model.

The diurnal variation of emissions from source class groupings must also be addressed. Automotive emission strength is taken to follow the weighted average of freeway and surface street traffic flows as given in Table 4.8. Power plants still occupy a single source class with diurnal variation in emission strength as given in Table 4.8. All other source groupings will be assumed to emit at an average rate independent of time of day.

### 5.2.2 Meteorological Data

From meteorological records, we need to prepare a time history of wind speed, wind direction and inversion base motion. The maximum

retention time, $\tau_c$, for an air parcel within our study area must also be estimated from available records on resultant air mass transport in the Los Angeles Basin.

In Chapter 3, section 3.4.2, it was decided that transport calculations would be based on wind data acquired at the downtown Los Angeles monitoring station of the Los Angeles Air Pollution Control District. A detailed justification for that selection is contained in Chapter 3. Wind records from that monitoring site were acquired on magnetic tape from the Los Angeles Air Pollution Control District (1975a).

In Chapter 3, it was also decided that inversion base motion would be represented by a stylized diurnal cycle which passes through the measured early morning and calculated afternoon maximum mixing depths in the Los Angeles area. These two point estimates of mixing depth in the Los Angeles Basin were again obtained on magnetic tape for each day of our three year period from the files of the Los Angeles Air Pollution Control District (1975b). The data were then interpolated to form an estimated mixing depth above ground level at each hour of each day in the manner described in Chapter 3 (see Figure 3.6). In those instances where inversion base height was stated only as greater than the LAAPCD's maximum reported altitude of 1524 m (5000 ft), a mixing depth of 2032 m (6667 ft) was assumed. That value was estimated by graphing sulfate concentration against $h_{max}^{-1}$ and then visually estimating a single mixing depth for all such events which

best preserved the already strong negative correlation between sulfate concentration and afternoon maximum mixing depth.

The National Oceanic and Atmospheric Administration (NOAA) of the U. S. Department of Commerce (1972a through 1974a) has published local climatological data summaries for their weather station located in Long Beach, California. Wind data at that station have been reduced by NOAA to form comparative summaries of scalar average and vector average wind speed. The vector average wind speeds, called resultant winds, reflect the net displacement of air masses passing that station during each month of the year. The scalar average wind speed is the average of the wind velocities computed without regard for reversals in the direction of air parcel transport. These data form an interesting preface to our discussion of $\tau_c$, the length of time needed for trajectory integration in order to transport air parcels emitted from local sources to beyond the boundaries of our study area.

Table 5.2 shows this comparison of vector averaged and scalar averaged wind speeds at Long Beach for each month of the years 1972 through 1974. Vector averaged wind speed at that location is typically less than half of the average scalar wind speed. This circumstance results from the daily sea breeze/land breeze reversal in wind direction which causes air parcel transport to recirculate within the Los Angeles Basin. The most extreme examples of the disparity between apparent average wind speed and actual vector displacement of air parcels from their points of origin occur in the winter months. Vector averaged wind speeds are often a factor of five to ten times slower than average

Table 5.2

Monthly Resultant Wind Data
For Long Beach During the
Years 1972 through 1974

| Month | Resultant Wind Speed Computed after Progressive Vector Addition of Successive Wind Observations for Each Month (miles per hour) | | | Scalar Average of Wind Velocity Observations (miles per hour) | | |
|---|---|---|---|---|---|---|
| | 1972 | 1973 | 1974 | 1972 | 1973 | 1974 |
| January | 0.4 | 1.0 | 1.0 | 5.6 | 6.4 | 4.8 |
| February | 0.9 | 1.4 | 1.2 | 5.2 | 6.5 | 5.4 |
| March | 2.5 | 4.3 | 2.5 | 6.0 | 8.2 | 5.2 |
| April | 2.7 | 2.8 | 3.5 | 6.2 | 8.1 | 5.7 |
| May | 3.4 | 3.2 | 3.1 | 6.9 | 6.4 | 5.7 |
| June | 3.8 | 3.1 | 2.7 | 7.3 | 6.4 | 5.3 |
| July | 3.0 | 2.9 | 2.7 | 7.1 | 5.8 | 5.4 |
| August | 2.8 | 2.8 | 2.6 | 6.7 | 6.1 | 5.4 |
| September | 3.2 | 2.6 | 1.6 | 6.8 | 6.2 | 3.3 |
| October | 2.0 | 2.1 | 2.6 | 5.7 | 5.6 | 5.4 |
| November | 1.3 | 1.5 | 1.9 | 5.5 | 5.1 | 4.9 |
| December | 2.1 | 0.6 | 0.6 | 6.2 | 3.0 | 5.3 |

Source: U.S. Department of Commerce (1972a through 1974a)

To convert miles per hour to meters per second, multiply by 0.45.

scalar wind speeds during the winter. Such persistent disparity between scalar average and resultant wind speeds is a clear indication of the need for a long-term average air quality model which can handle unsteady meteorological conditions.

The area over which we wish to compute sulfate concentrations is contained within the grid system established in Chapter 4 for displaying emission inventory results. The characteristic dimensions of that grid are defined by a square fifty miles (80.47 km) along each edge. Air masses transiting our study area may pass in and out of the boundaries of that receptor zone several times before permanently exiting the study area. But the average resultant wind speed at Long Beach just in excess of 0.9 meters per second (2 miles per hour) suggests that the typical air parcel will receive a net displacement to beyond the borders of our receptor grid within one twenty-four hour period.

While typical trajectories will clear the study area within one 24-hour period, a selection of trajectory integration time, $\tau_c$, must be made with the intent of matching the maximum retention time for air parcels within the airshed. Therefore a simulation was constructed to estimate the fraction of trajectories computed within the assumptions of our model which would still have endpoints remaining within the 50 by 50 mile square at the end of various lengths of time.

Three critical trajectory starting locations representing major point source areas in the airshed were first isolated. The starting locations chosen were El Segundo (near two power plants and one

refinery), Los Alamitos (near two very large power plants), and a third location in the middle of the harbor refinery complex (near Stauffer Chemical). Next a trial value for $\tau_c$ was assumed, for example $\tau_c$ = 24 hours. Trajectories of duration $\tau_c$ starting from these locations and ending at each hour of each day of the years 1972 through 1974 were estimated from wind data apparent at the LAAPCD's downtown Los Angeles monitoring station. Then the fraction of trajectory end points remaining within the 50 by 50 mile square after $\tau_c$ hours of pollutant transport could be determined by inspection.

As this trajectory screening process is repeated for successively larger values of $\tau_c$, the progression of events is as illustrated in Figure 5.1. Within the first few hours of trajectory integration, large numbers of air parcels released during high speed wind events are advected out of our study area. True to our expectations, the centroid of the average air parcel released is out of the 50 by 50 mile square at the end of a 24 hour period.

As $\tau_c$ is extended further in an attempt to completely eliminate trajectory end points from our grid, we face the prospect of diminishing returns to increased computational effort. A truncation point for trajectory integration must be established unless unreasonable amounts of computing time are to be spent extending the integration of hundreds of off-grid trajectories in order to search for a few stagnating trajectories which are still within the receptor grid.

For the purposes of this study, a value of $\tau_c$ will be selected such that 95% of the end points of trajectories of age $\tau_c$ originating

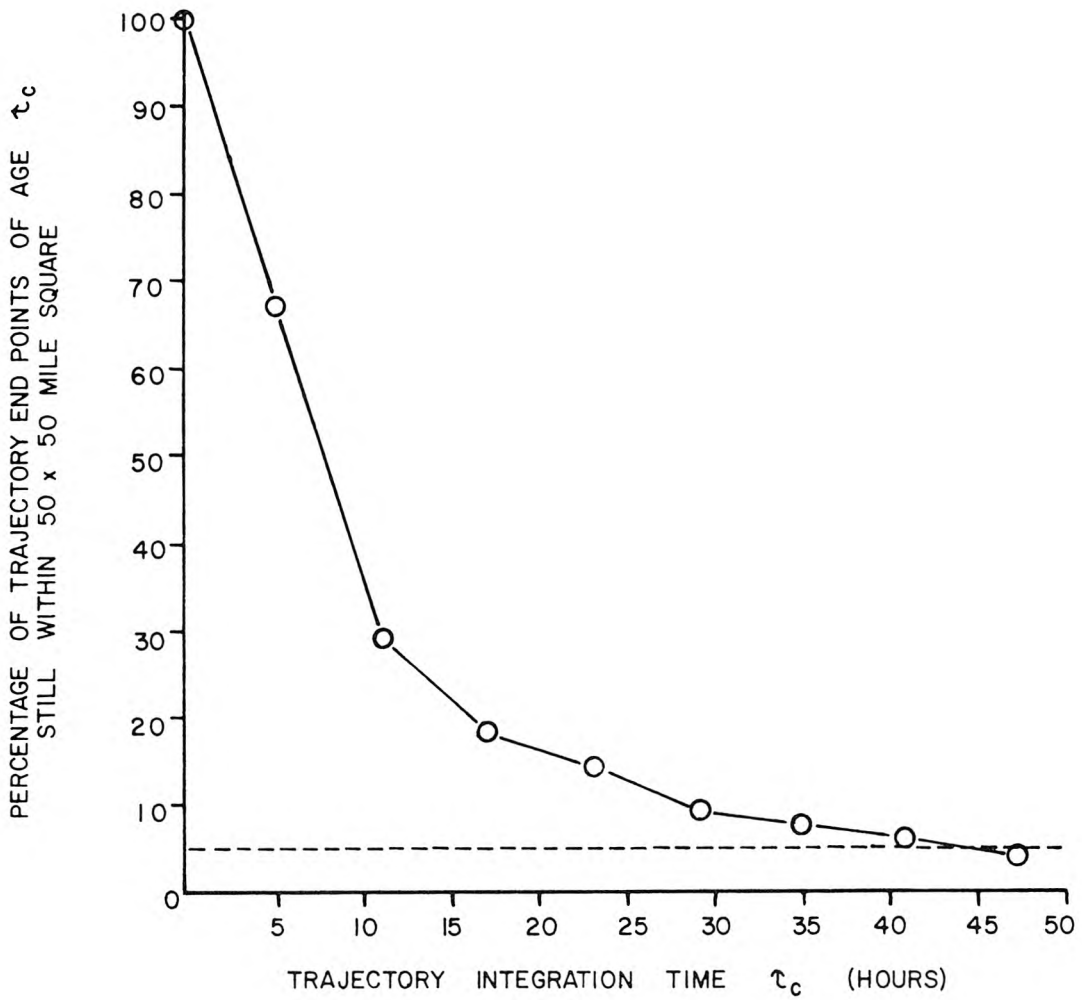


FIGURE 5.1

Retention of Air Parcels Released from Major Point Source Locations in the Los Angeles Basin.

from major point sources will be off-grid at the end of trajectory integration. From Figure 5.1 we find that that value of $\tau_{95\%} \simeq \tau_c$ corresponds to a trajectory integration time of two days for the major source locations and receptor grid of interest to us.

It should be noted that this selection does not mean that 5% of the material contributing to observed $SO_x$ concentrations has been neglected. That is because when selecting a value for $\tau_c$ we focused only on the oldest air parcels in the airshed for any assumed value of $\tau_c$. The retention of air parcels of all ages $\tau_c$ or less is given by the area under the curve of Figure 5.1. By truncating the trajectory integration at $\tau_{95\%} \simeq \tau_c$, we have removed an amount of pollutant mass approximately equal to the area of the tail of that declining curve beyond $\tau_{95\%}$ equals two days.

### 5.2.3 Estimation of Air Parcel Diffusive Displacement

Small scale turbulence in the atmosphere acts to influence fluid particle transport beyond that computed from trajectories based on mean wind speed and direction alone. We wish to estimate the rate at which this process of eddy diffusion occurs over the Los Angeles urban area so that diffusive displacements may be imparted to individual fluid particles within our simulation model.

The cross-wind standard deviation of a puff or plume, $\sigma_y$, is often used to specify the horizontal dispersion of pollutant material about its center of mass. A theoretically satisfactory way to predict the rate of plume spread in the atmosphere is still in its formative stages.

Therefore values of the growth in $\sigma_y$ with time or distance from the point of pollutant release are usually obtained from field measurement programs. Successive estimates of the dispersion parameter, $\sigma_y$, are calculated from experimental results and then organized in terms of simultaneously occurring indices of atmospheric turbulence. Plume dispersion experiments have been tabulated in terms of atmospheric "stability classes"; the rapidity of horizontal fluctuations in wind direction; the standard deviation of fluctuations in the angle of horizontal wind direction, and combinations of measured wind fluctuation and vertical atmospheric stability (McElroy and Pooler, 1968).

The most commonly encountered atmospheric dispersion estimates in use today rely on Pasquill-Gifford stability classes to predict plume spreading (see Pasquill (1961), Gifford (1961), Turner (1969)). The popularity of that system arises from the fact that it requires only readily available measurements of surface wind speed, solar radiation intensity and cloud cover in order to dictate selection of one of six stability classes. Each stability class is paired with expressions for estimation of the rate of plume spreading as a function of distance downwind from the source.

Turner (1969) summarizes some important background information on the experiments which form the basis for the Pasquill-Gifford dispersion estimates:

> "These methods will give representative indications of stability over open country or rural areas, but are less reliable for urban areas. This difference is due primarily to the influence of the city's larger surface roughness and heat island effects upon the stability regime over urban areas...."

Since our simulation model is to be applied to the atmosphere over one of the world's most extensive continuous urban areas, dispersion estimates specific to an urban airshed will be sought.

Figure 5.2 shows a series of experimental results for horizontal dispersion of inert tracer material over the urban area of St. Louis (McElroy and Pooler, 1968). The data are organized in terms of travel time downwind, which is particularly convenient for use in our simulation model. Dispersion data have been analyzed within four classes based on the standard deviation of wind direction fluctuations, $\sigma_\theta$, and bulk Richardson number, $Ri_B$. The actual separation of the data appears to fall into only two major classes. Dispersion under stable atmospheric conditions (the o's) is distinctly different from the grouping of all remaining observations on $\sigma_y$.

When the data of McElroy and Pooler (1968) are compared to estimates of $\sigma_y$ and $\sigma_z$[1] given by the Pasquill-Gifford curves, it is found that

> "...best-fit lines for $\sigma_y$ and $\sigma_z$ for the St. Louis data are everywhere larger than those for the open-country counterparts. When extrapolated to longer downwind distances, the best-fit lines for $\sigma_y$ approach their counterparts; those for $\sigma_z$ generally approach counterparts of stability one class higher." (McElroy and Pooler, 1968).

The need to extrapolate McElroy and Pooler's (1968) data to greater downwind distances should be emphasized. From Figure 5.2 it is seen

---

[1] $\sigma_z$ is the standard deviation of plume spread in the vertical dimension.

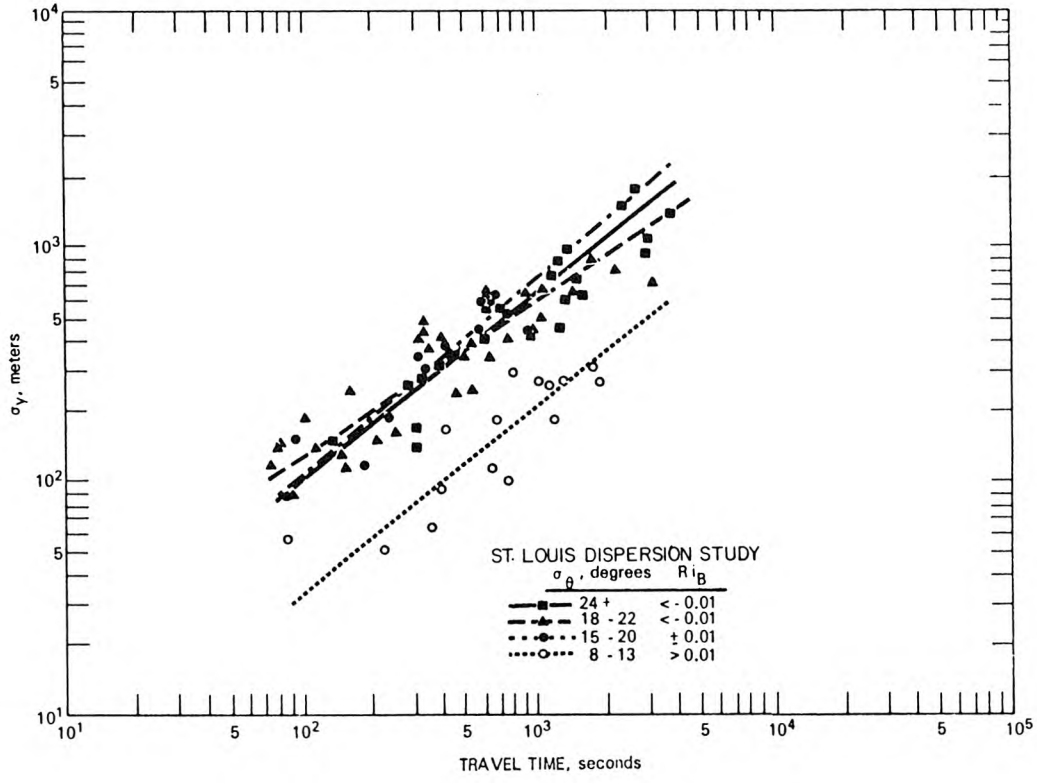


FIGURE 5.2

Cross-wind standard deviation of tracer meterial as a function of travel time in terms of standard deviation of wind direction fluctuations ($\sigma_\theta$) and bulk Richardson number ($Ri_B$). (From McElroy and Pooler, 1968)

that experimental results are available for only the first hour or so of downwind travel.

A limited amount of longer distance experimental data have been collected for dispersion over the Los Angeles Basin from the work of Drivas and Shair (1975) and Shair (1977). These data are displayed in Table 5.3, along with a few descriptive notes about the conditions of each experiment.

In Figure 5.3, the Los Angeles Basin data are plotted alongside the results of the St. Louis Dispersion Study. It is seen that the Los Angeles data fall within the envelope established by the extension of McElroy and Pooler's (1968) lines of best fit for their most turbulent and least turbulent atmospheric conditions.

A procedure for extending the results of McElroy and Pooler to include the Los Angeles data is sought. Two problems arise. First, if the data sets were pooled, the St. Louis data would dominate the statistics of the results as they are far more numerous. In contrast, we wish to emphasize the Los Angeles data because they represent transport over the scale of the particular urban air basin of interest to us rather than short distance transport downwind of sources in another city. Secondly, when the Los Angeles data are viewed in terms of the experimental conditions under which they were taken, there is no clear evidence that a separation of the data into groups of more or less "stable" atmospheric conditions (in the Pasquill-Gifford sense) would be supportable. About all that can be said is that the

TABLE 5.3

Values of the Dispersion Parameter, $\sigma_y$, Calculated from Experiments in the Los Angeles Basin

| Test Number | Date | Time of Day at which Traverse was taken PST | Wind velocity $\bar{u}$ m/sec | Downwind Distance at Point of Traverse x,km | Downwind Travel Time to Point of Traverse t sec | $\sigma_y$ m | Stability Class Estimated by Pasquill-Gifford Method | Remarks |
|---|---|---|---|---|---|---|---|---|
| Long Beach[a] No.2 | 10/11/74 | 3:23-3:45 PM | 2.5 | 15 | 6000 | 844 | B-C[c] | Trajectory Entirely Over Urban Area |
| Long Beach[a] No.3 | 10/17/74 | 3:14-3:35 PM | 3.0 | 15 | 5000 | 2460 | B-C[c] | Trajectory Entirely Over Urban Area |
| Long Beach[a] No.4 | 10/25/74 | 2:08-3:12 PM | 4.5 | 15 | 3333 | 769 | B-C[c] | Trajectory Entirely Over Urban Area |
| Long Beach[a] No.5 | 10/30/74 | 2:39-3:41 PM | 5.5 | 15 | 2727 | 864 | C-D[c] | Trajectory Entirely Over Urban Area |
| Long Beach[a] No.6 | 10/07/74 | 2:24-2:45 PM | 4.5 | 15 | 3333 | 1220 | B-C[c] | Trajectory Entirely Over Urban Area |
| Long Beach[a] No.6 | 11/07/74 | 2.53-3:11 PM | 6.0 | 15 | 2500 | 534 | C-D[c] | Trajectory Entirely Over Urban Area |
| Long Beach[a] No.6 | 11/07/74 | 3:50-4:10 PM | 5.0 | 15 | 3000 | 637 | C-D[c] | Trajectory Entirely Over Urban Area |
| Land-Sea Breeze[b] No.6 | 9/13/77 | 1:04-1:48 PM | 2.6 | 43 | 16800 | 3260 | Mixed[d] | Trajectory 90% Over water; 10% Over Urban Area |
| Land-Sea Breeze[b] No.6 | 9/13/77 | 2:26-3:12 PM | 2.6 | 43 | 16800 | 2062 | Mixed[d] | Trajectory 90% Over Water; 10% Over Urban Area |
| Land-Sea Breeze[b] No.6 | 9/13/77 | 3:30-4:27 PM | 3.4 | 67 | 19800 | 6205 | Mixed[d] | Trajectory 60% Over Water; 40% Over Urban Area |
| Land-Sea Breeze[b] No.6 | 9/13/77 | 4:02-4:38 PM | 3.4 | 88 | 26100 | 7064 | Mixed[d] | Trajectory 50% Over Water; 50% Over Urban Area |

(a) $SF_6$ Release from Power Plant Stack at Alamitos Bay; Reference Drivas and Shair (1975)
(b) $SF_6$ Release beginning at 9:00 AM, from Shipping Lanes at Sea; Reference Shair (1977)
(c) As estimated by Drivas and Shair (1975)
(d) Stability Class Could Have Ranged Between Class A and Class D During Different Parts of Trajectory; Release Made at Sea Under Cloudy Conditions, While Later Part of Trajectory Occurred Over Land Under Condtions of Strong Incoming Solar Radiation.

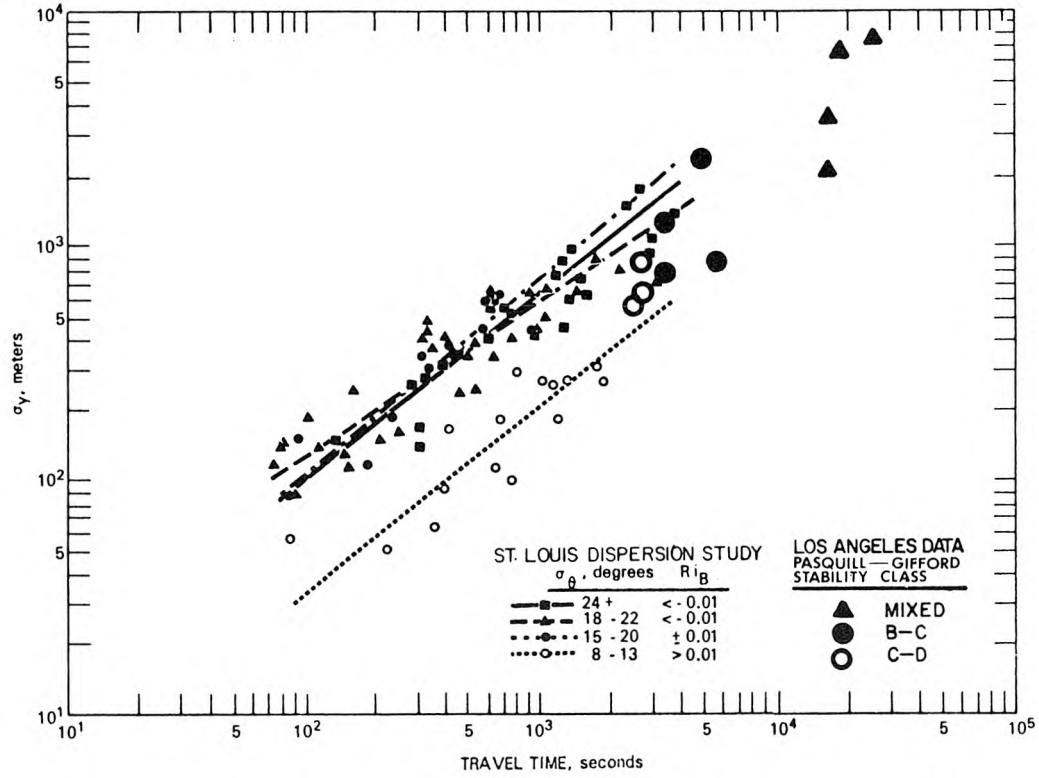


FIGURE 5.3

Cross-wind standard deviation of tracer material as a function of travel time in terms of standard deviation of wind direction fluctuations ($\sigma_\theta$) and bulk Richardson number ($Ri_B$), from McElroy and Pooler (1968), plus Los Angeles data from Drivas and Shair (1975) and Shair (1977), organized by Pasquill-Gifford stability classes.

Los Angeles results fall within the band formed by the extension of McElroy and Pooler's observations.

Therefore, the following approach was adopted. The Los Angeles data will be reduced to form a single function relating lateral plume spread to downwind travel time. That function will be expressed as a simple power law, similar to the curves in Figure 5.2, as follows:

(5.1)

where

| | |
|---|---|
| $\sigma_y$ | is the horizontal standard deviation of plume spread about its centerline. |
| t | is travel time downwind. |
| a and b | are fitted constants. |

The slope of the curve relating $\sigma_y$ to travel time ("a" in equation 5.1) will be estimated graphically from the slope of the band defined by McElroy and Pooler's most turbulent ($\sigma_\theta$ = 24°+) and least turbulent ($\sigma_\theta$ = 8°-13°) conditions. Then the constant b in expression (5.1) will be fitted to the Los Angeles data alone by least squares regression techniques. The following estimates for the rate of horizontal plume dispersion over Los Angeles result:

$$\sigma_y = 1.73\ t^{0.80} \tag{5.2}$$

for $\sigma_y$ in meters and time in seconds, or

$$\sigma_y = 0.75\ t^{0.80} \tag{5.3}$$

for $\sigma_y$ in miles and time in hours. Equation (5.2) is graphed alongside the available data in Figure 5.4.

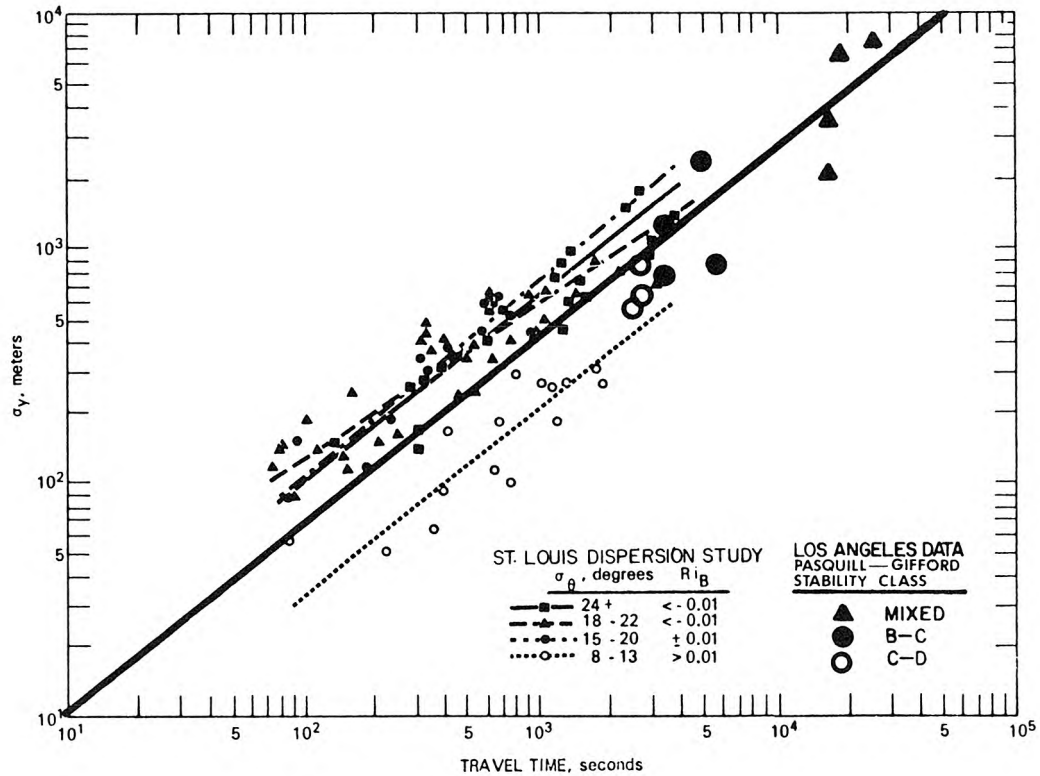


FIGURE 5.4

Cross-wind standard deviation of plume spread showing the function for $\sigma_y(t)$ fit to the Los Angeles data (heavy solid line). Function was estimated by linear regression after having transformed the time axis as $t^{0.8}$.
That explains why higher valued observations seem to dominate the result on this log-log plot.

Long distance trajectories will undoubtedly encounter changing atmospheric turbulence levels while in transit. The use of a single expression fitted to data from a variety of observational conditions in the field should help to yield results which do not stray greatly from a typical mixture of atmospheric conditions encountered by long distance trajectories in Los Angeles.

In order to introduce these estimates for horizontal dispersion into our simulation model, one further approximation must be made. It is assumed that an expanding puff in the atmosphere remains symmetric, with equal downwind and crosswind standard deviations at any single time. In that case, $\sigma_y = \sigma_1 = \sigma_2$, and the data on $(\sigma_1,\sigma_2)$ required by our air quality model derivation may be supplied by equations (5.2) or (5.3). In an open atmosphere characterized by both vertical and horizontal wind shear, this symmetry may not be preserved. Vertical wind shear could cause an air parcel shaped like an upright circular cylinder to bend over while vertical mixing acts to render the ground level profile of the air parcel into an ellipse. Horizontal wind shear could tear an expanding puff into separate fragments. But field data on long distance puff expansion upon which to base a more complex dispersion analysis are unavailable for Los Angeles.

### 5.2.4 Estimation of Pollutant Dry Deposition Velocities and Chemical Reaction Rates

From the mass balance calculations of Roberts (1975; see Figure 2.17) it is clear that estimation of pollutant deposition rates is critical to a correct simulation of Los Angeles sulfur oxides air

quality levels. Roberts estimated that dry deposition of $SO_2$ and sulfates removed half of the sulfur oxides emitted during his day of interest before those air parcels exited the Los Angeles area.

Dry deposition of sulfur dioxide has been studied under both laboratory and field conditions. From these studies and from theoretical considerations, it is found that the flux of sulfur dioxide to the earth's surface is limited by a resistance due to the rate of diffusion in the atmosphere plus a resistance due to the condition of the receiving surface material. This relationship is expressed as follows (Garland, 1974):

$$r = r_a + r_b + r_s \tag{5.4}$$

where

- $r$ is total resistance to $SO_2$ deposition in sec/cm.
- $r_a$ is aerodynamic resistance calculated from momentum transport considerations.
- $r_b$ is an aerodynamic resistance arising from the differences between mass transfer and momentum transfer processes.
- $r_s$ is surface resistance.

Deposition velocity is related to total resistance to deposition by

$$V_g = \frac{1}{r} \tag{5.5}$$

Large bodies of water may behave as a near perfect sink for $SO_2$ (Liss, 1971; Spedding, 1972), and gas phase resistance would control the rate of pollutant removal. But most measurements of $V_g$ show a reduced rate of $SO_2$ deposition that is significantly affected by surface conditions. Typical examples of sulfur dioxide deposition velocity onto natural surfaces are given in Table 5.4.

TABLE 5.4

SULFUR DIOXIDE DEPOSITION VELOCITY MEASURED OVER VARIOUS SURFACE TYPES

| Surface Material | Time of Year | Mean $SO_2$ Deposition Velocity $v_g$ (cm/sec) | References |
|---|---|---|---|
| Short Grass | March - June | 0.55 | Garland (1974) |
| Medium Grass (radioactive tracer) | June - November | 1.19 | Garland (1974) |
| Medium Grass (gradient method) | November - January | 0.77 | Garland (1974) |
| Bare Calcareous Soil | February - March | 1.1 | Garland (1974) |
| Fresh Water - pH 8 | April - June | 0.46 | Garland (1974) |
| Forest (Pine) | June | <2 | Garland (1974) |
| Grass | Summer | 0.8 | Shepherd (1974) |
| Grass | Autumn | 0.3 | Shepherd (1974) |
| Grassland (light wind) | | $0.7 \pm 0.1$ | Owers and Powell (1974) |
| Water (light wind) | | 0.9 | Owers and Powell (1974) |
| Grassland (windy conditions) | | $2.6 \pm 0.3$ | Owers and Powell (1974) |
| Grassland (low wind) | | $0.7 \pm 0.1$ | Owers and Powell (1974) |
| Water (low wind) | | $0.5 \pm 0.1$ | Owers and Powell (1974) |

Typical values for $SO_2$ deposition velocities recommended for mass balance calculations over grassland and water by Garland (1974) and by Owers and Powell (1974) range from 0.7 cm/sec to 0.9 cm/sec.

Studies of $SO_2$ deposition averaged over the surface of urban areas are quite rare. Laboratory studies of deposition to building materials and Los Angeles area soils have been conducted by Judeikis and Stewart (1976). These surveys show that concrete and stucco are excellent sinks for $SO_2$; that deposition rates to Los Angeles area soils are not greatly different from the average of results reported for other natural surfaces, while asphalt surfaces were found to show an extremely high resistance to $SO_2$ deposition. The only attempt to integrate deposition velocities over an entire urban area that we have found is due to Chamberlin (1960). He estimated a deposition rate of 0.7 cm/sec for $SO_2$ removal during a London pollution episode.

Following the mass balance work of Garland (1974) and Chamberlin (1960), it will be estimated that the deposition velocity for $SO_2$ to the surface of the Los Angeles Basin and coastal waters is about 0.7 cm/sec. However, it has been noted by Judeikis and Stewart (1976) that a surface's ability to take up $SO_2$ may become saturated, and that Los Angeles soils could become saturated within as little as eleven days under unfavorable conditions. Judeikis and Stewart (1976) also show that such saturated surfaces can be regenerated, for example, by a water wash or by exposure to ammonia. This process of saturation and regeneration could have a seasonal dependence. If so, that seasonal dependence would modulate both $SO_2$ removal rates, and (indirectly)

atmospheric sulfate concentrations. A field study to explore the question of possible seasonal dependence in Los Angeles area $SO_2$ deposition velocity should be a high priority for those seeking to understand the South Coast Air Basin sulfur cycle.

Dry deposition of atmospheric aerosols is controlled by the size distribution of the particulate matter and fluid mechanical considerations in the surface layer next to the ground. Large particles of an aerodynamic diameter greater than ten microns settle very rapidly under the influence of gravity or deposit by inertial impaction. Small particles of aerodynamic diameter less than 0.01 microns deposit rapidly by diffusing to the earth's surface. A minimum in the deposition rate for particulate matter exists in the size range 0.1 to 2.0 microns aerodynamic diameter. In that range, neither atmospheric process is efficient at removing aerosol particles. This dependence of particulate deposition rate on aerosol size is illustrated in Figure 5.5 from theoretical calculations performed by Davidson (1977).

The size distribution for Los Angeles area sulfate aerosols has been measured by Hidy et al. (1975). Those data show that sulfate mass in the Los Angeles atmosphere is strongly peaked in the accumulation mode with a mass median diameter of about 0.5 microns. From Figure 5.5 we see that particles of that size should have a dry deposition velocity of about 0.02 to 0.03 cm/sec. Integration over the entire sulfate size distribution gives approximately the same value. Davidson (1977) attempted to measure the rate of sulfate dry deposition in the Los Angeles area. In spite of measurement sensitivity problems, it was

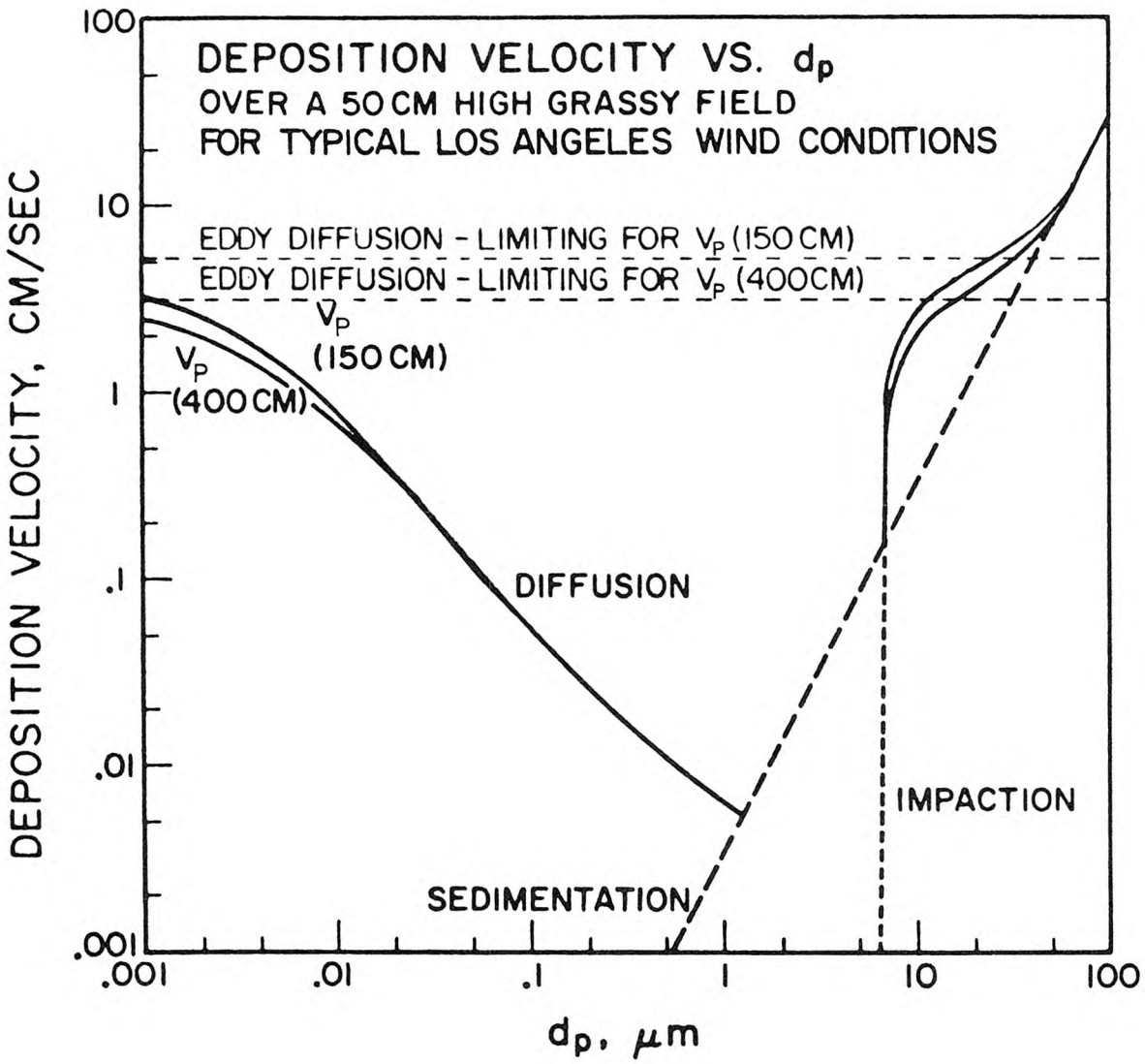


FIGURE 5.5

Calculated values of deposition velocity as a function of particle size for heights of 150 cm and 400 cm above the ground, for a field of Avena fatua, wild oat grass. Particle density is assumed to be 1 g/cm$^3$. (From Davidson,1977).

still possible to confirm that local sulfate deposition velocities lie in the range 0.01 to 0.1 cm/sec.

Following the practice of Garland (1974), a value for particulate sulfate dry deposition of 0.03 cm/sec will be assumed. That value implies a time scale for removal of sulfate particles by dry deposition which is on the order of several weeks. In contrast, our estimate for $SO_2$ dry deposition of 0.7 cm/sec is more than a factor of twenty higher, yielding a half life for $SO_2$ removal at the ground which is on the order of days. As a result, even a substantial percentage uncertainty in sulfate dry deposition velocity can be tolerated without expecting significant impact on the results of the atmospheric mass balance which is embedded within our air quality model calculations.

In light of the complexity of the chemical reactions possible, it was decided in Chapter 2 that chemical conversion of $SO_2$ to form sulfates will be modeled as a slow pseudo-first order reaction. Emphasis will be placed on solving for the overall $SO_2$ oxidation rate and on identifying any seasonal trend in oxidation rate that may guide future theoretical investigations.

Pseudo-first order rate constants for $SO_2$ oxidation to form sulfates in the Los Angeles atmosphere have been measured by Roberts (1975). It was found that $SO_2$ oxidation rates varied from 1% to 15% per hour under photochemically active daylight sea breeze conditions. These measurements provide the range within which an average conversion rate is likely to be found.

The summertime peak in the ratio of sulfate to total sulfur oxides established in Chapter 2 suggests that there is a seasonal dependence in $SO_2$ oxidation rate in the Los Angeles atmosphere. As was the case with Roberts' (1975) reaction rate experiments, it will be necessary to solve for the apparent average $SO_2$ oxidation rate within any averaging time by a process of iteration. A trial value of the reaction rate, k, will be assumed for a given month. Next the air quality model will be exercised to generate sulfate concentration predictions throughout the airshed. Then predictions at a large number of monitoring sites will be compared to observations, and a second trial value for k will be assumed.

Estimation of a seasonal trend in $SO_2$ oxidation rate is a tightly constrained process in spite of the fact that values of k must be obtained by iteration. That is because the system being simulated is highly over-determined. The value of k which solves the chemical reaction equations must result in sulfate air quality predictions which match observations at a large number of air monitoring sites. Certain relationships between sulfate and total sulfur concentrations must be satisfied within a model which conserves sulfur and which does not provide any means for adjustment of total sulfur concentration predictions. A prior estimate of the likely range of values for k exists. The only parameter in the model with any freedom of adjustment, k, must simultaneously satisfy a huge system of equations or inequalities. If the model is failing to deliver reasonable concentration predictions in both time and space, no small adjustment to the value of k is likely to hide that fact.

A further check on the accuracy of the chemical modeling approach is provided by reference to the details of Roberts' (1975) experiments. The bulk of Roberts' experiments were conducted during the month of July 1973, which is one of the months which will be included within our simulation. Roberts' pseudo-first order rate constant data for July 1973 are listed in Table 5.5. The average value of k from those experiments was just under 8% per hour. A value of k equal to 8% per hour will be used to test the air quality model without freedom of adjustment for the month of July 1973[2]. One warning concerning this test is in order, however. While the calculation methods for reduction of Roberts' data differ greatly from the concentration prediction scheme of our simulation model, the underlying physical assumptions of both this study and those experiments are the same. Air parcel trajectories containing sulfur oxides are transported in a well mixed layer beneath an inversion while first order chemistry and pollutant dry deposition processes proceed to alter sulfate and total sulfur concentrations. The deposition velocity assumptions used in both studies are similar (although not identical). It is therefore possible that confirming conclusions could be reached by the process of committing identical conceptual errors. In spite of that possibility, the use of measured

[2]As in any iterative process, a tolerance limit must be set within which the solution being sought will be accepted as having been achieved. Within this air quality simulation, we hope to solve for monthly average values of k to within the nearest 1% per hour or twenty-five percent of full scale, whichever is less (e.g. at reaction rates below 2% per hour we will work in 0.5% per hour increments; below 1% per hour we would work in 0.25% per hour increments). For that reason, the average of Roberts' data is rounded to the nearest whole percentage point.

TABLE 5.5

Pseudo-First Order Rate Constants for $SO_2$ Oxidation in the Los Angeles Atmosphere[2] Measured from Trajectories Terminating at Pasadena During July 1973

| Date (1973) | Trajectory Starting Location | Time of Trajectory Arrival at Pasadena (PST) | k ($\%\ hr^{-1}$) |
|---|---|---|---|
| July 10 | El Segundo | 1300 | 1.2 ± 0.9 |
| | El Segundo | 1400 | 3.0 ± 1.7 |
| | El Segundo | 1500 | 10.0 ± 5.7 |
| | El Segundo | 1600 | 14.6 ± 8.9 |
| July 25 | Alamitos Bay | 1400 | 12.1 ± 2.0 |
| | El Segundo | 1500 | 8.6 ± 3.4 |
| | El Segundo | 1600 | 10.3 ± 2.9 |
| July 26 | Alamitos Bay | 1200 | 5.2 ± 4.2 |
| | Alamitos Bay | 1300 | 5.1 ± 3.0 |
| | Alamitos Bay | 1400 | 8.1 ± 8.1 |
| | Alamitos Bay | 1500 | 4.6 ± 1.7 |
| Range for Month of July 1973 | | | 1 to 15 |
| Average | | | 7.53 |

Source: Roberts (1975)

values of k in the simulation for July 1973 provides as stringent a test as possible for most aspects of our simulation model.

July represented the peak month for the ratio of sulfate to total sulfur at most monitoring sites during the year 1973. Therefore it is expected that our estimate of an 8% per hour average conversion rate for that month will be among the highest average rates determined as a result of model calculations.

### 5.2.5 Estimation of the Seasonal Variation in Sulfate Background Air Quality

In Chapter 2 it was shown that Los Angeles sulfate air quality is elevated above background sulfate concentrations observed at remote locations in all surrounding directions. Since most new air masses entering the South Coast Air Basin are of marine origin, assumptions concerning background concentrations supplied to air quality model calculations should reflect the marine air monitoring data.

Observations on sulfate concentrations at San Nicolas Island were examined in Table 2.1 and Figure 2.2. These data show that sulfate concentrations do fluctuate in the marine environment off the Southern California Coast. Unfortunately, data sufficient to dictate the seasonal pattern in sulfate concentrations in incoming marine air for each month of the period 1972 through 1974 are unavailable to us. Instead, all that is available is a set of data at San Nicolas Island which is representative of the summer and fall of the year 1970.

However, from Figure 2.10 it is seen that every monitoring station for which we have a continuous record of sulfate air quality over the period 1972 through 1974 shows a similar seasonal trend in sulfate concentrations. That is even true of the CHESS station at Vista, located outside of the South Coast Air Basin in Northern San Diego County. While the Vista monitoring station is affected by local $SO_x$ emissions sources to a certain degree, its concentration measurements more closely approach background levels than at any other site offering comparable data on seasonal trends.

The approach adopted in this study for estimation of sulfate background concentrations on a month by month basis is as follows. The San Nicolas Island data of Hidy, et al. (1974) will be used to set the magnitude of the average sulfate background concentrations encountered during the summer and fall of the year. Then that average will be modulated by the seasonal trend in sulfate concentrations observed at Vista.

The constant of proportionality between Vista and San Nicolas Island was estimated by examining all sulfate concentration measurements taken at both locations during the period July through October of each year of record. That time interval was set by the extent of Hidy, et al.'s (1974) sampling program. The data falling within those time periods were averaged separately at each location. The seasonally adjusted mean at San Nicolas Island was found to be 40% of the average value observed at Vista. Therefore the sulfate background concentration estimates for each month of our three year period will be based

on 40% of the average sulfate concentrations observed at Vista for that month. This time sequence of background sulfate concentration estimates is listed in Table 5.6.

### 5.2.6 Selection of Time Step and a Receptor Cell Size

Selection of time step and receptor cell size should be considered simultaneously. The fundamental question at hand is: "Will enough particles per cell be introduced into the model to obtain a smooth stable estimate of pollutant concentrations?"

For economic reasons, one wishes to take relatively large time steps in order to speed the process of trajectory and chemical integration. In an opposing fashion, one prefers small receptor cells in order to more closely define the shape of pollutant pattern contours. If these two goals are pursued to the extreme, computed voids will appear in the middle of zones of significant pollutant concentration. This is due to the presence of receptor cells which are too small to have acquired a statistically significant number of pollutant particles.

The largest time step that can be taken in our simulation model without discarding useful data is a time step of one hour in duration. That is the fundamental time scale of the wind data which are available to us. Any shorter time step would have to be supported by additional synthetic wind data gained from an interpolation scheme. Therefore the implications of using a time step of one hour will be explored.

The time horizon for trajectory integration, $\tau_c$, has already been set at 48 hours. For the case of a one hour time step, 34560 trajectory

TABLE 5.6

Tabulation of Estimated Sulfate
Background Concentrations
for the South Coast Air Basin
(in $\mu gm/m^3$ as $SO_4^=$)

| Month | 1972 | | 1973 | | 1974 | |
|---|---|---|---|---|---|---|
| | Vista | Background Estimate at 40% of Vista | Vista | Background Estimate at 40% of Vista | Vista | Background Estimate at 40% of Vista |
| January | 6.03 | 2.41 | 5.87 | 2.35 | 6.78 | 2.71 |
| February | 11.07 | 4.43 | 4.98 | 1.99 | 6.50 | 2.60 |
| March | 14.12 | 5.65 | 3.28 | 1.31 | 7.21 | 2.88 |
| April | 8.03 | 3.21 | 6.54 | 2.62 | 6.43 | 2.57 |
| May | 9.78 | 3.91 | 10.32 | 4.13 | 9.84 | 3.94 |
| June | 16.12 | 6.45 | 11.39 | 4.56 | 8.55 | 3.42 |
| July | 8.14 | 3.26 | 19.25 | 7.70 | 7.76 | 3.10 |
| August | 11.73 | 4.69 | 17.71 | 7.08 | 12.35 | 4.94 |
| September | 9.16 | 3.66 | 14.02 | 5.61 | 13.98 | 5.59 |
| October | 7.91 | 3.16 | 11.03 | 4.41 | 12.17 | 4.87 |
| November | 4.90 | 1.96 | 6.66 | 2.66 | 7.40 | 2.96 |
| December | 5.75 | 2.30 | 7.93 | 3.17 | 4.87 | 1.95 |
| Unweighted Mean | | 3.76 | | 3.97 | | 3.46 |

Note: Background sulfate concentrations are estimated from the seasonal trend in sulfates observed at Vista, scaled to the level of the average sulfate concentrations measured at San Nicolas Island. Sulfates at Vista during the months of July through October averaged 12.15 $\mu gm/m^3$ (3 year mean) versus an average of 4.9 $\mu gm/m^3$ at San Nicolas Island in that season of the year (see Table 2.1). Background sulfate concentrations at San Nicolas Island are approximately 40% of those at Vista, our most remote site with enough data to estimate seasonal trends in background concentrations.

end points would be counted per source as separate particles by the model when computing a monthly average pollutant concentration.[3] The area under the air parcel retention probability curve of Figure 5.1 can be integrated graphically and used to estimate the fraction of the particles released which would be likely to be counted within the 50 by 50 mile square emissions grid. It is found that about 25.5% of the 34,560 particles associated with a source at one of these major point source locations would contribute to particle counts within that 50 by 50 mile square. That translates into 8813 particle counts per source per month on the average within the 50 by 50 mile square for those critical release points.

Choice of a receptor cell size with the same dimensions as the 2 mile by 2 mile (3.22 km by 3.22 km) squares which form the emissions grid would be convenient, although not necessary. Within the 50 by 50 mile square, 625 such receptor cells would be defined. At 8813 particle counts within that zone of 625 receptor cells, an average density of 14.1 particles per source per cell would result from a monthly average sulfate concentration computation centered on one of our critical release points. If all particles were weighted equally, that particle density would be sufficient to avoid serious concentration estimation errors.

---

[3] That value is computed as follows: at each of 24 times of the day for each of (nominally) 30 days of the month, 48 particles are located in the horizontal plane (24 x 48 x 30 = 34560 particles per month). Because of the random number generators built into the model, each of these trajectory end points is unique.

However, each particle carries a magnitude which reflects its source's emission strength and diurnal cycle. That magnitude changes while in transit based on its probable chemical status and probable vertical dilution. Therefore we should be somewhat reserved about our judgement that enough particles have been defined. It seems reasonable to try a one hour time step with 2 mile by 2 mile (3.22 km by 3.22 km) receptor grid spacing, and then check to see that the computed results are free of serious defects.

## 5.3 Application of the Simulation Model to the Years 1972 through 1974

The air quality model described in Chapter 3 was programmed using the universal data handling package MAGIC maintained on the Caltech IBM 370/158 computer by R. C. Y. Koh. User supplied subroutines were constructed at those points in the program where computational efficiency is critical. These special routines cover trajectory integration, the model's pollutant chemistry, and particle counting in order to produce concentration estimates. A summary of program execution characteristics is given in Table 5.7.

In order to conserve computing resources, the model was instructed to compute source to receptor transport relationships only from source cells with noticeable emissions. If a source cell contributed less than 0.01 tons per day of $SO_x$ emissions at the end of the source class aggregation process, the cell was treated as being vacant.

Model tests of the use of the one hour time step and 2 mile by 2 mile receptor cells revealed that the downwind sulfate concentration

TABLE 5.7

Execution Characteristics of
the Air Quality Simulation Model
Computer Program

Example Application: Computation of Sulfate Air Quality averaged over the month of July 1974 at one value of the rate of $SO_2$ oxidation, k.

Input: (a) 845 virtual emissions sources divided among 11 source classes.

(b) Meteorological data in time series for each hour of the month.

Output: (a) Sulfate concentration predictions within each of 625 receptor cells. It is required that air quality increments due to each source class be identified within each receptor cell. In effect that means that the model must repeat concentration calculations for each of eleven source classes.

(b) Predicted values of the ratio of average sulfate to average total sulfur oxides concentrations within each of 625 receptor cells.

(c) Mass balance calculations on the fate of sulfur released.

(d) Comparison of observed to predicted concentrations.

(e) Fifteen contour or x-y plots.

Computational Characteristics of that Application:

(a) Execution time: 25 minutes of CPU time on an IBM 370/158 computer with MVS operating system.

(b) Core storage used: 576 K bytes.

(c) Direct cost at Caltech Computing Center including contour plots: $40.48 at low priority large-user discount rate; about $80 otherwise. Charges at other computing centers will vary according to accounting system.

(d) Program utilizes some installation dependent features.

predictions were of acceptable quality. The concentration fields were generally free of spurious voids. Most features of the sulfate concentration patterns rise or fall in sequence across relative peaks and valleys which span the dimensions of several adjacent receptor cells.

The major drawback to the use of such a large time step occurs close to the source within the first hour of pollutant transport. An insufficient number of particles are present to define the shape of a plume with dimensions less than that of one of our receptor cells. To compound this problem, the assumption of instantaneous vertical mixing breaks down for some of those particles standing immediately above their release point from an elevated source at $(t-t_o)$ equals zero. For an illustration of that problem, see the early part of the plume in Case (1) of Figure 3.3.

Fortunately, this situation is easily resolved by one of a number of means. The first hour of pollutant transport is the only time period in the model in which unsteady meteorological conditions could be represented by a steady-state solution of the diffusion equation out to the distance of one time step downwind of the source. If we were interested mainly in concentrations of a primary contaminant from isolated low-level sources, that is the approach that would be taken. But because most observed sulfates are secondary pollutants formed by chemical reactions downwind of their source, highly accurate ground-level concentration estimates within the first few hundred meters from the stack are not as critical as they would be in many other

applications. If we resolve the singularity in the instantaneous vertical mixing assumption at the source, most of our other problems will vanish. That is because the definition of the shape of the plume is not important to ground level pollutant concentrations if the plume has not yet mixed to ground level.

Therefore, the following approach was adopted for this application of the model within the existing framework of the model derivation. The probabilities $P_{SO_4}$ and $P_{SO_2}$ that a pollutant particle contributes to ground level air quality are set equal to zero for the case $\underset{\sim}{X} = \underset{\sim}{X}_o$ and $t = t_o$ for all source classes, i, with elevated stack heights $H(t_o,i)$. That merely says that a fresh pollutant particle just released from an elevated source takes some non-zero time to mix to ground level. In practice, particles of age $\tau = 0$ from stationary source stacks will not be counted, while fresh emissions from ground-level mobile sources will still contribute immediately to observed air quality. This treatment was tested within the context of several monthly simulations. It was found to perform well enough that other corrective actions such as decreasing the time step, altering the receptor cell size or replacing the first hour of transport by an analytical solution to the diffusion equation will be deferred until an application arises which requires such attention.

The air quality model was applied to the task of predicting sulfate concentrations within the relatively level portion of the Los Angeles Basin and the San Gabriel Valley. That receptor zone is identical to our emissions grid of Figure 4.7, less the San Fernando

Valley (squares I 1-10 by J 20-25). Receptor zone selection was discussed in Chapters 2 and 3 on the basis of terrain considerations, coverage of air monitoring stations and inclusion of major source locations.

Convergence to a final estimate of the value of the rate constant, k, within the tolerance limits previously described (see footnote 2, section 5.2 of this chapter) was attained within an average of 2.25 iterations per month. An initial trial value of k for each month was obtained by scanning the measured values of $f_s$ appearing in various months of the year in relation to values of $f_s$ observed during July 1973, the month for which we had measured values for k. A subsequent selection of k for a second iteration on each month was usually necessary. That process was aided by evaluating the following linearized expression at each air monitoring site.

$$\frac{k_{new}}{k_{old}} \simeq \frac{\overline{\langle c_{SO_4} \rangle}_{observed} - \overline{\langle c_{SO_4} \rangle}_{background}}{\overline{\langle c_{SO_4} \rangle}_{predicted} - \overline{\langle c_{SO_4} \rangle}_{background}} \qquad (5.6)$$

where

$k_{old}$ is the value of k from the most recent iteration.

$k_{new}$ is the next guess for an improved value of k.

$\overline{\langle c_{SO_4} \rangle}_{observed}$ is average sulfate concentration measured at that air monitoring station for the month of interest.

$\overline{\langle c_{SO_4} \rangle}_{predicted}$ is the average sulfate concentration predicted at that monitoring site at the last model iteration.

$\overline{<c_{SO_4}>}_{background}$ is that month's average background sulfate concentration estimate.

These values of $k_{new}$ from ten to eleven monitoring sites in each month were usually averaged and then rounded to the nearest whole percent per hour, or appropriate fraction thereof in accordance with our tolerance limits on k. The iteration procedure would stop when all values of $k_{new}$ were within the same tolerance limit interval on $k_{old}$, or when a value of k is attained which was straddled by groups of monitoring sites demanding that iterations proceed in opposing directions. This latter circumstance can occur even when all values of $\overline{<c_{SO_4}>}_{predicted}$ are within the error bounds on $\overline{<c_{SO_4}>}_{observed}$. That is because values of $\overline{<c_{SO_4}>}_{observed}$ are known only to within large error bounds at some stations in some months.

## 5.4 Air Quality Model Results

### 5.4.1 Predicted Versus Observed Sulfate Concentrations

Figures 5.6(a) through 5.16(a) present the results of the air quality simulation model in time series at each of the LAAPCD and CHESS air monitoring stations located within our receptor zone. Model results are represented by a horizontal solid line which rises and falls in the form of a bar graph. The open symbols represent the arithmetic mean of all sulfate measurements at each monitoring site in each month. The error bounds shown reflect 95% confidence intervals on the mean value of the air quality observations (see Appendix B4). Any model

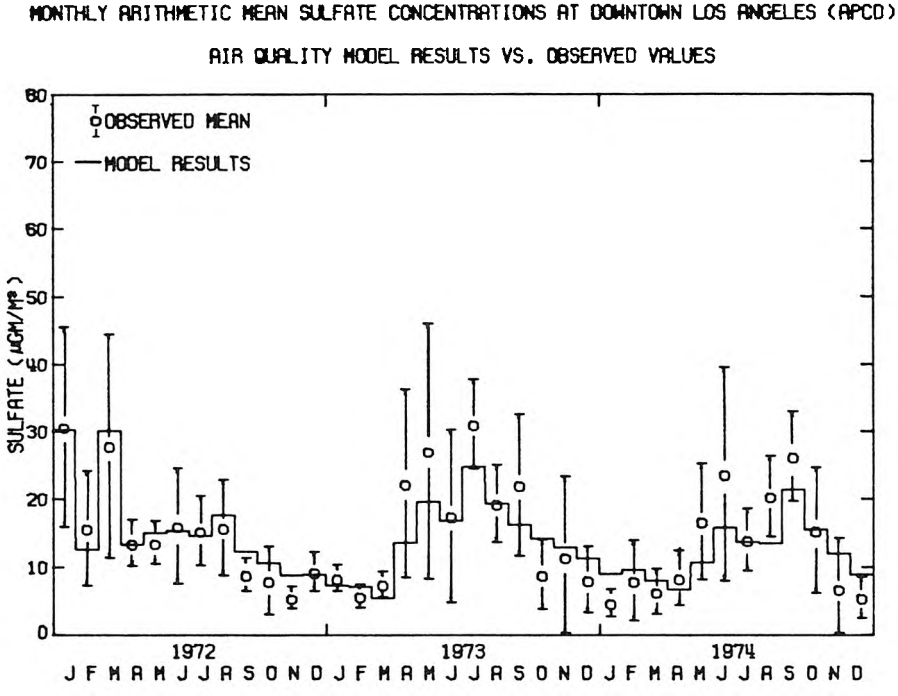


FIGURE 5.6(a)

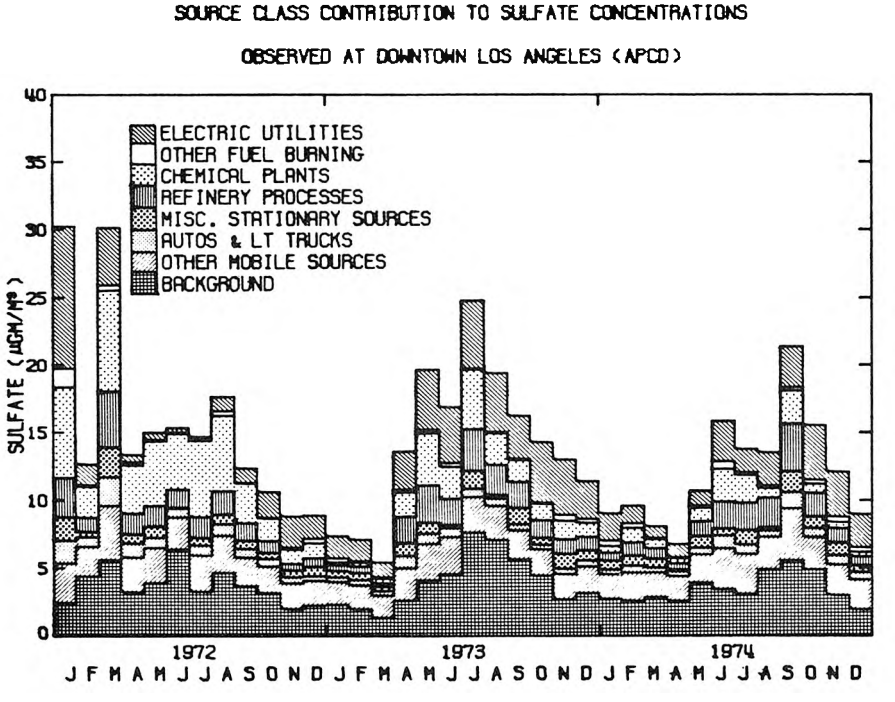


FIGURE 5.6(b)

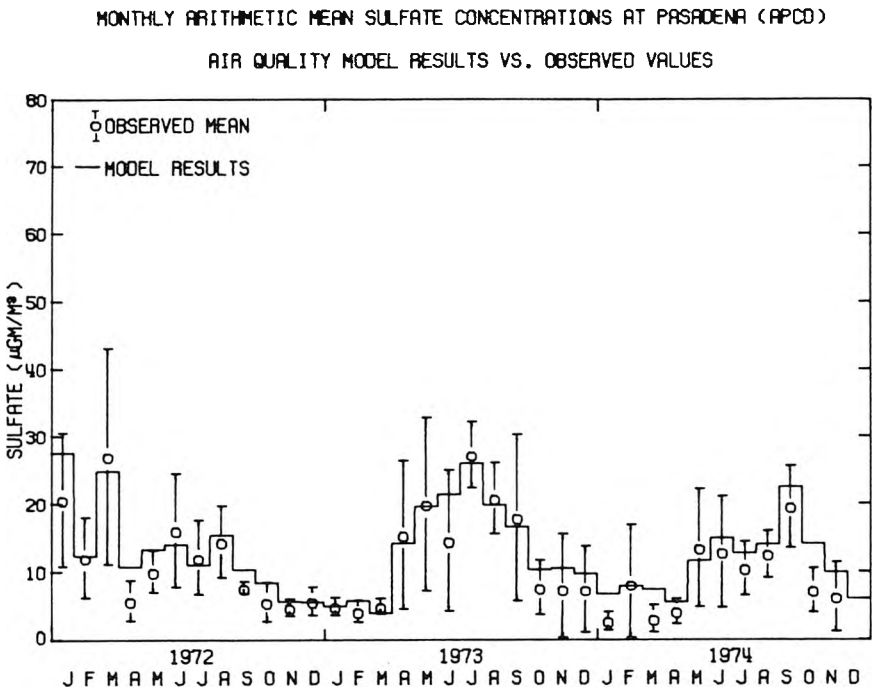


FIGURE 5.7(a)

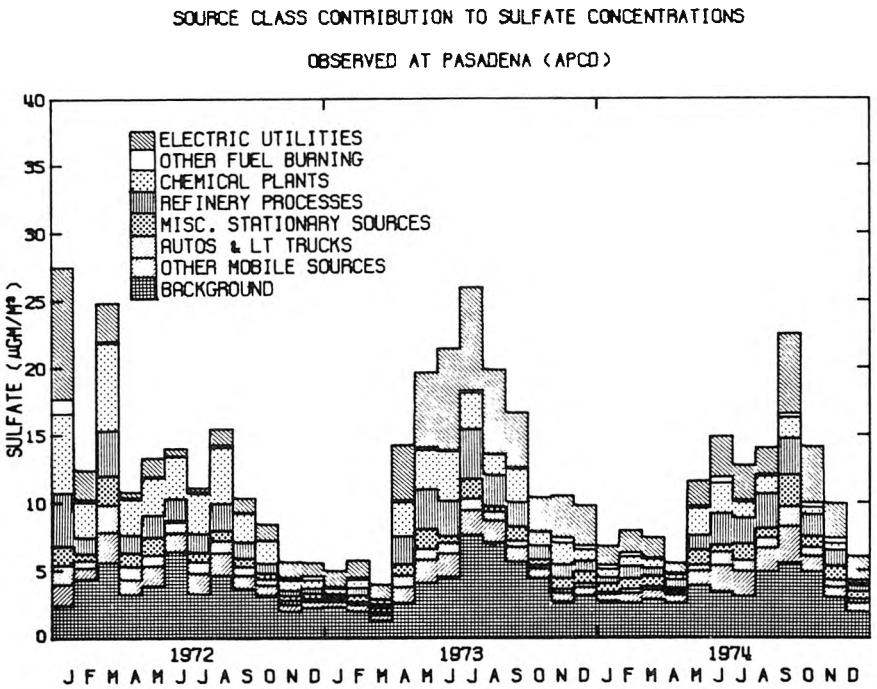


FIGURE 5.7(b)

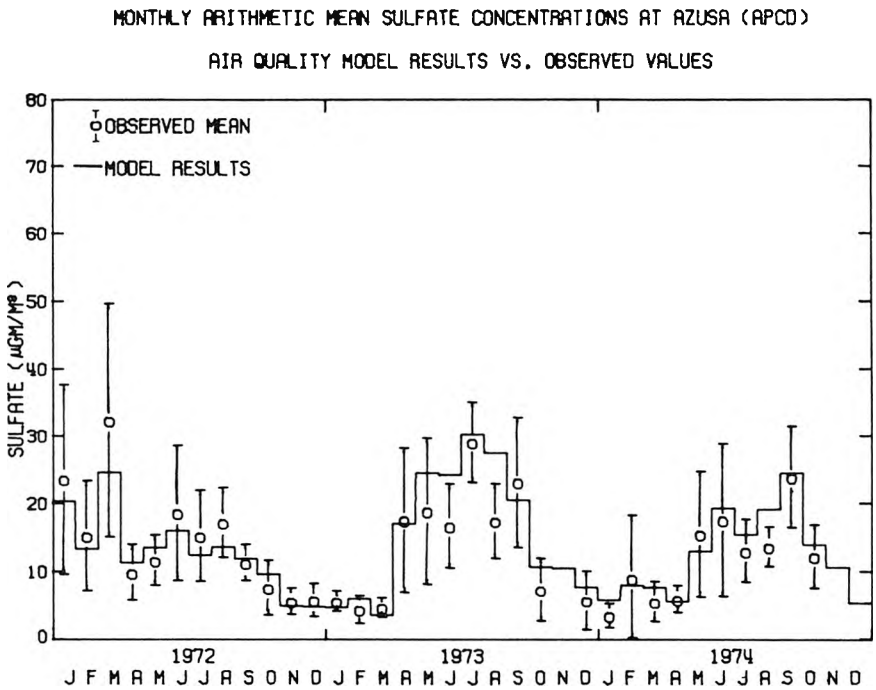


FIGURE 5.8(a)

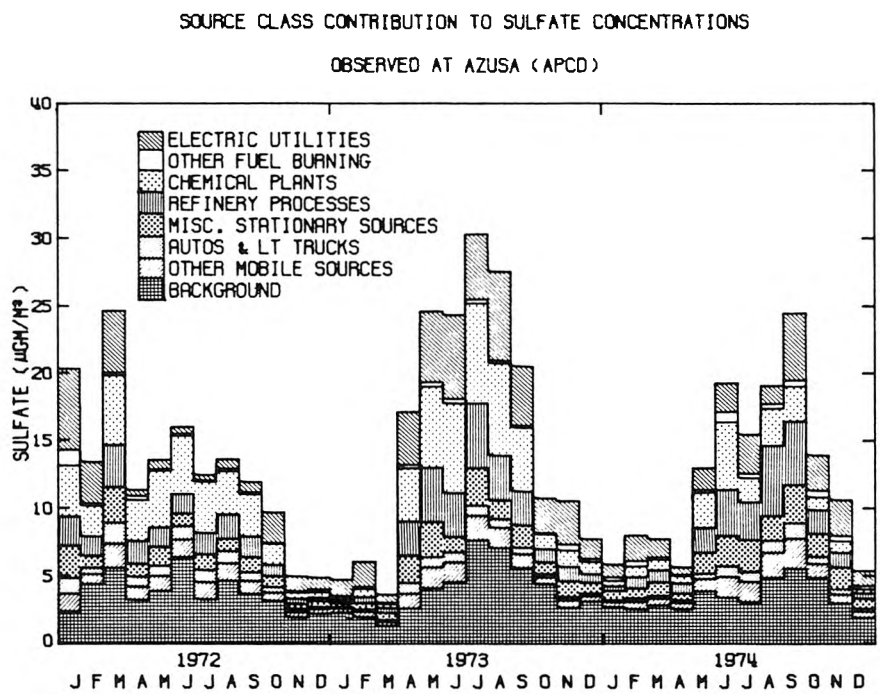


FIGURE 5.8(b)

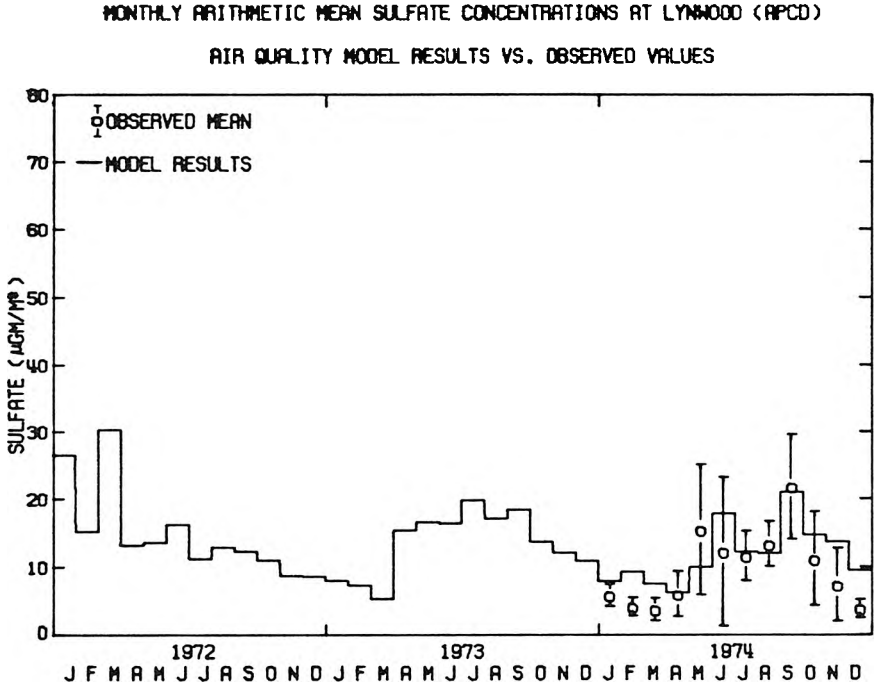


FIGURE 5.9(a)

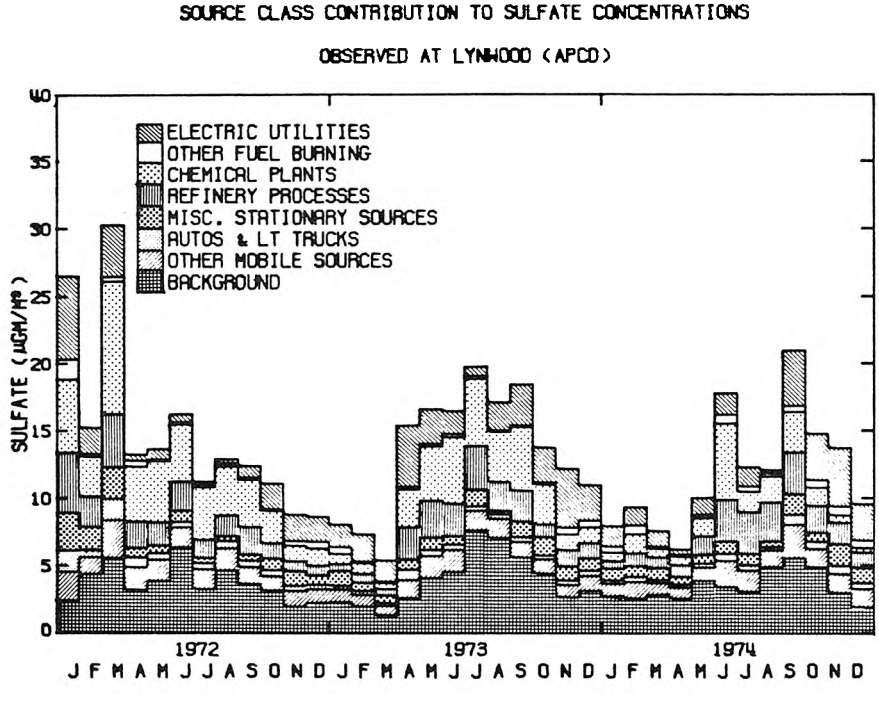


FIGURE 5.9(b)

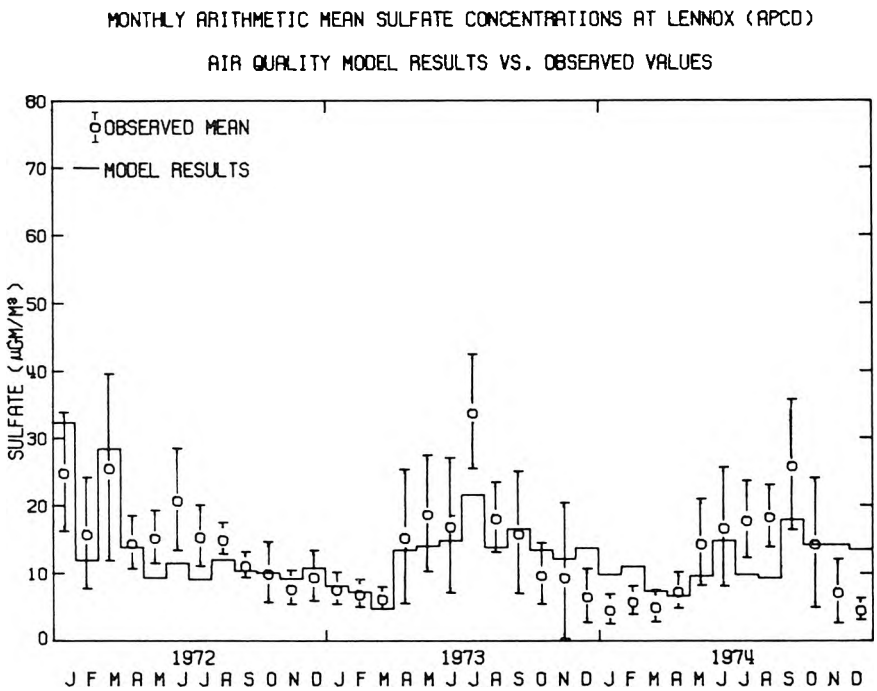


FIGURE 5.10(a)

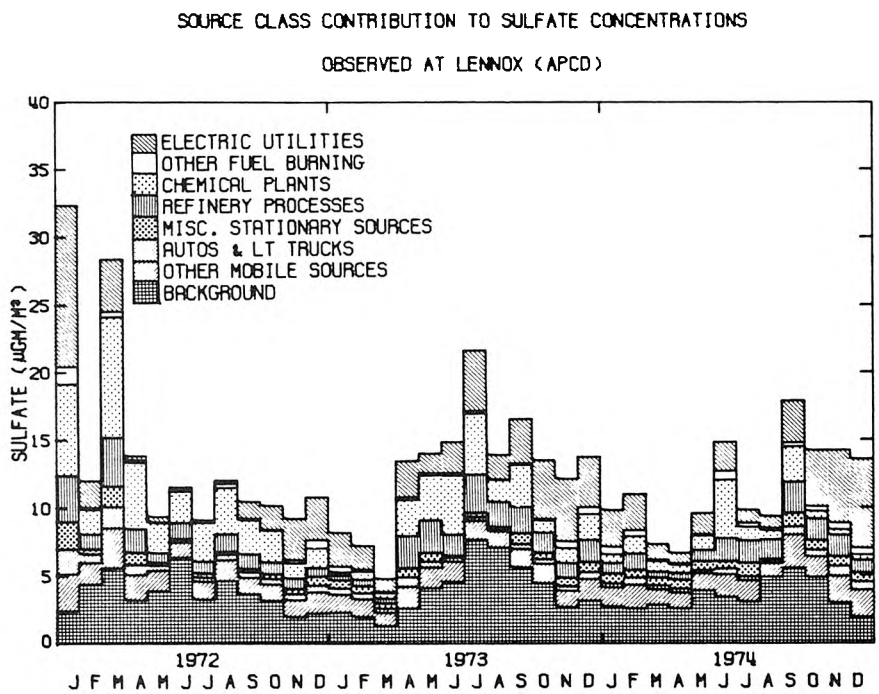


FIGURE 5.10(b)

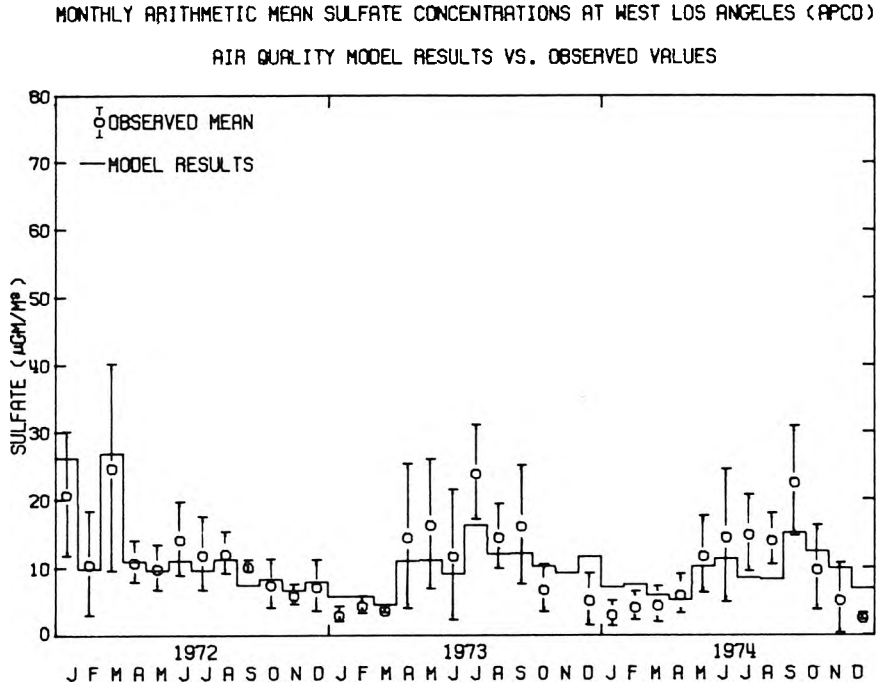


FIGURE 5.11(a)

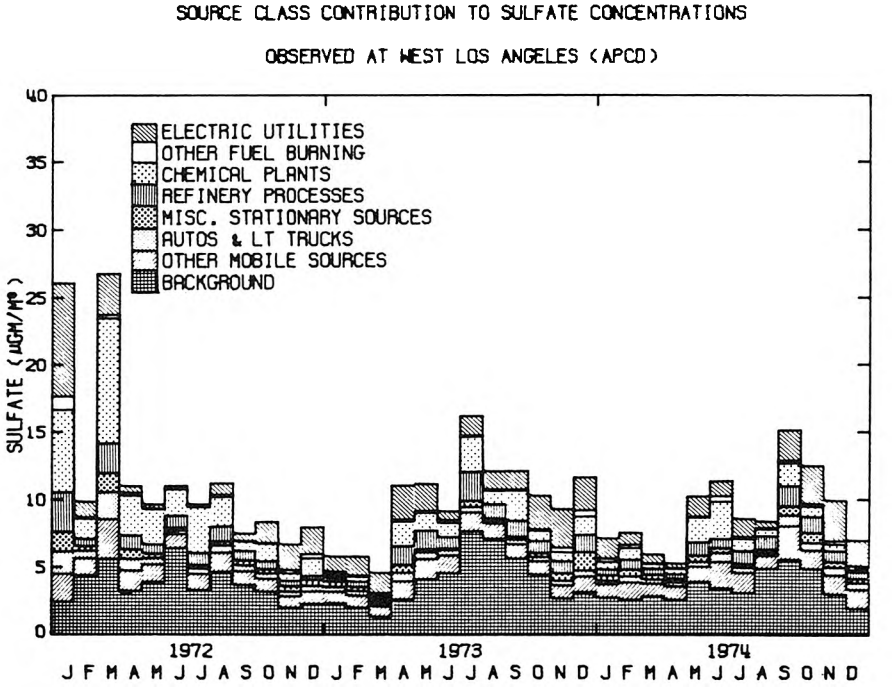


FIGURE 5.11(b)

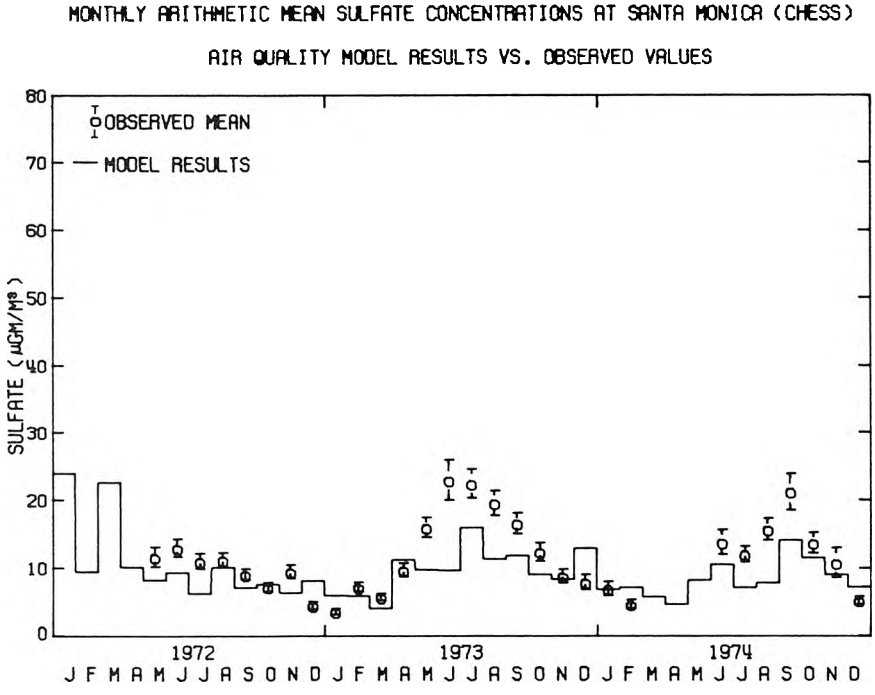


FIGURE 5.12(a)

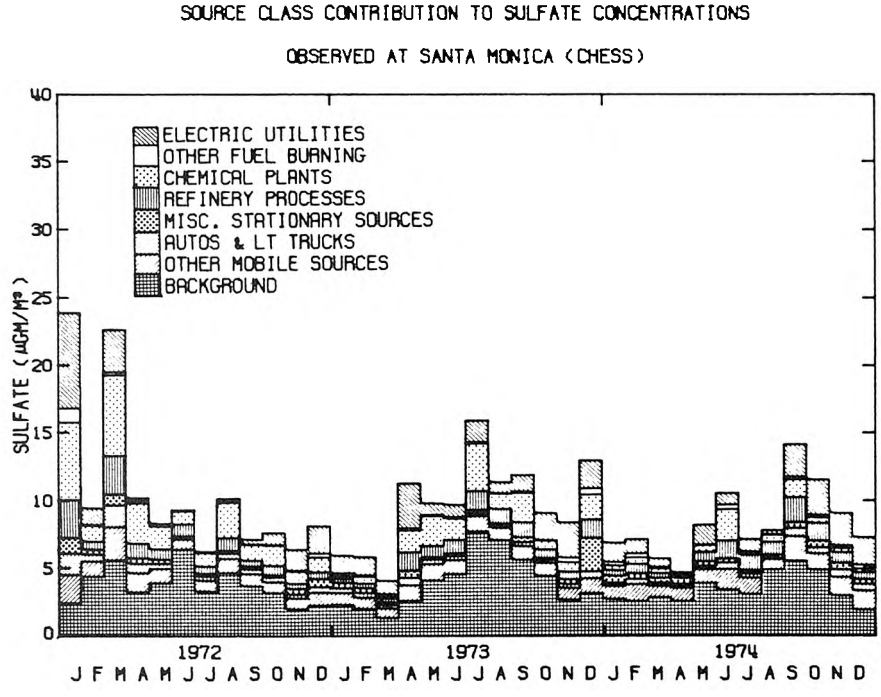


FIGURE 5.12(b)

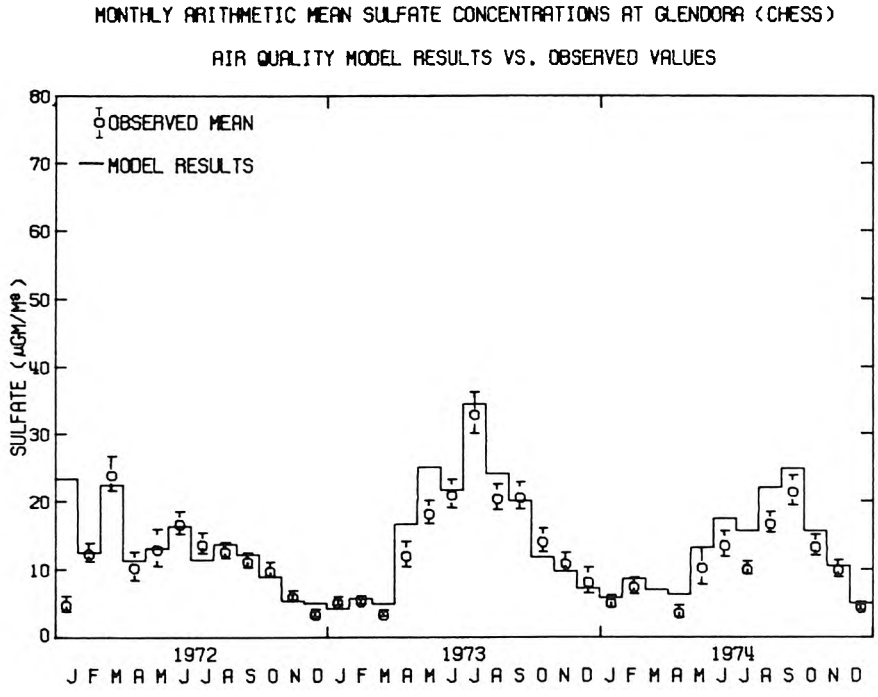


FIGURE 5.13(a)

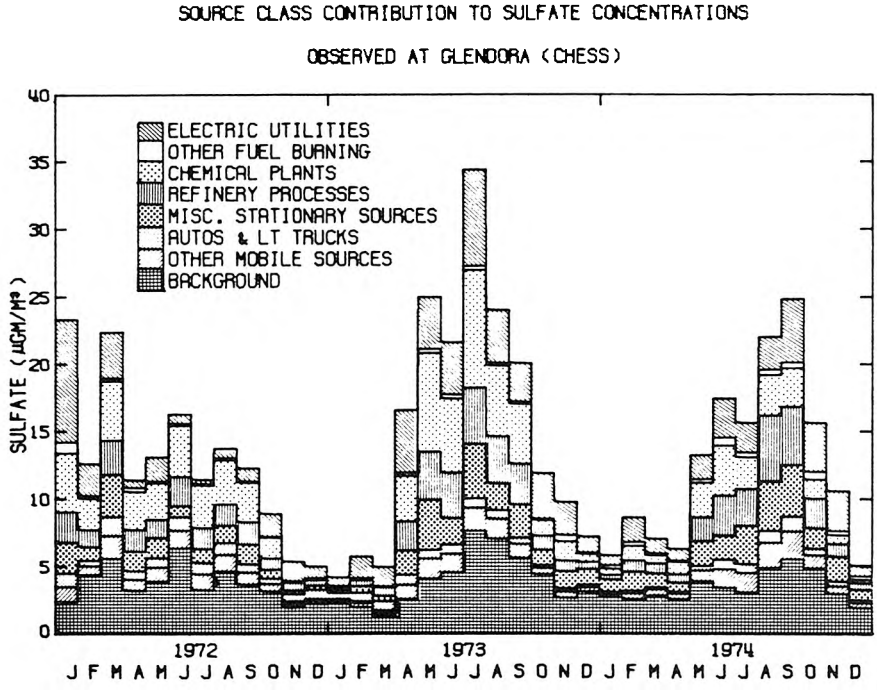


FIGURE 5.13(b)

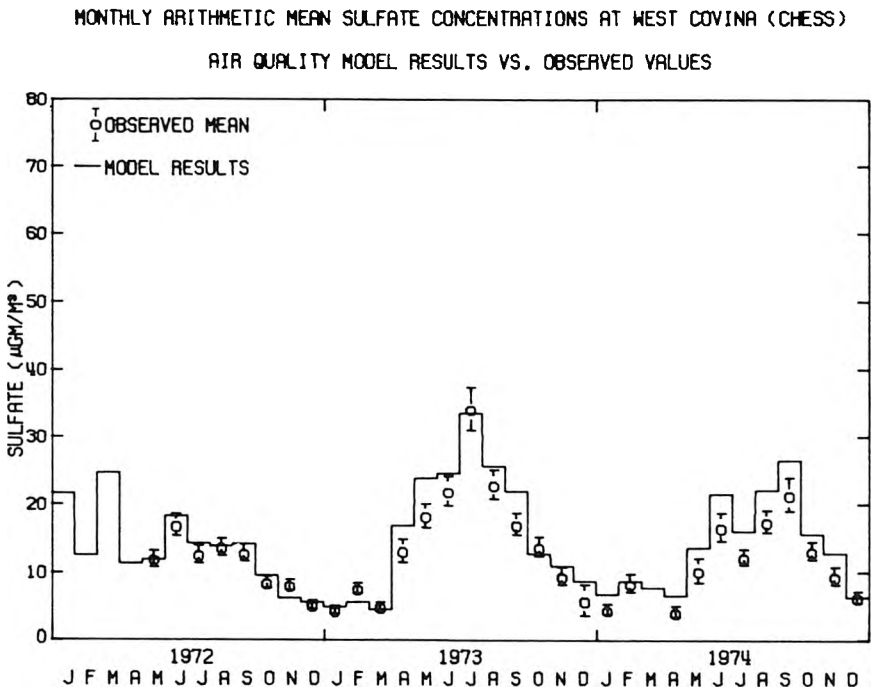


FIGURE 5.14(a)

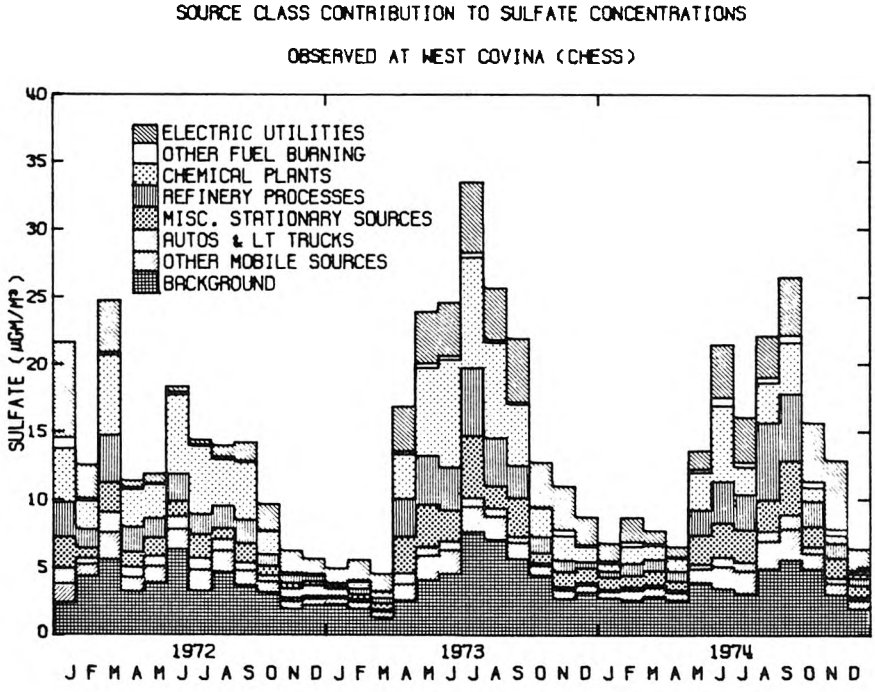


FIGURE 5.14(b)

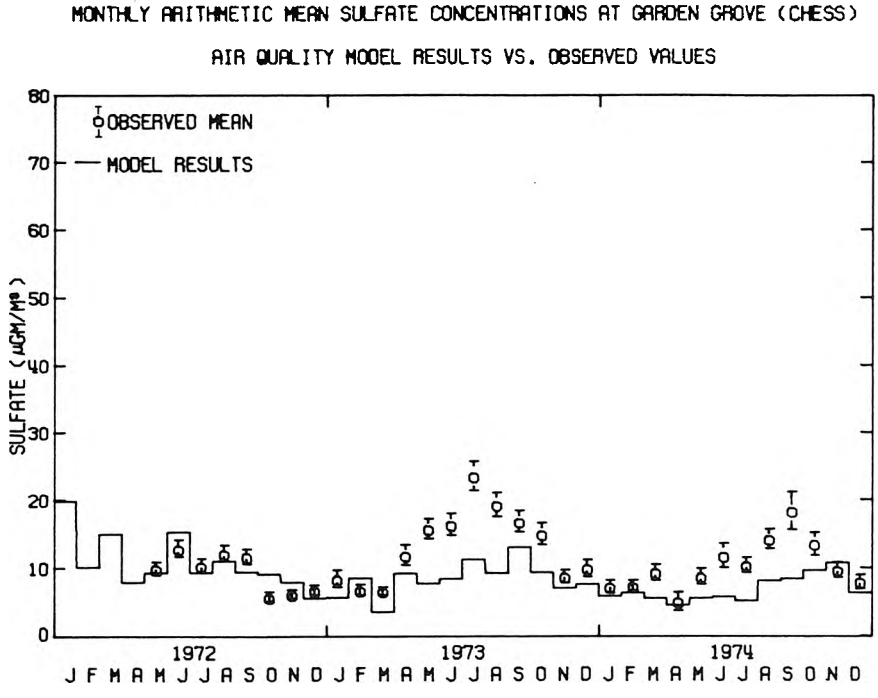


FIGURE 5.15(a)

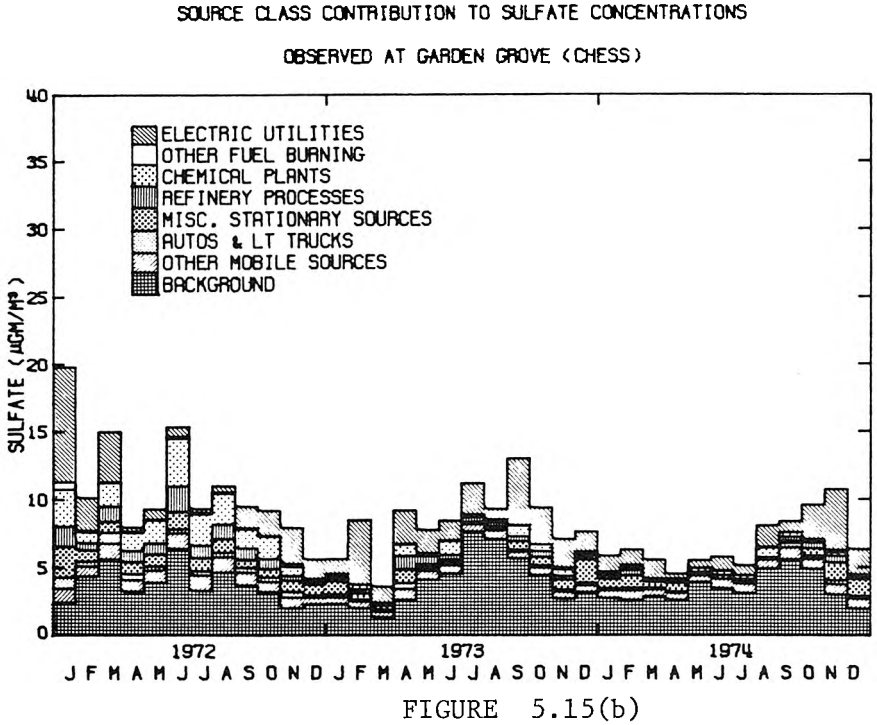


FIGURE 5.15(b)

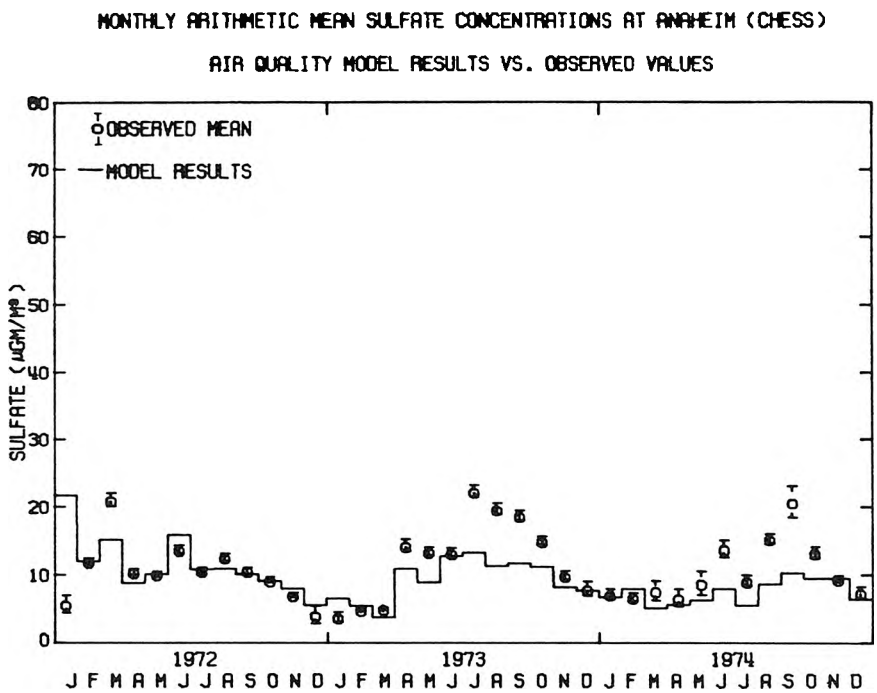


FIGURE 5.16(a)

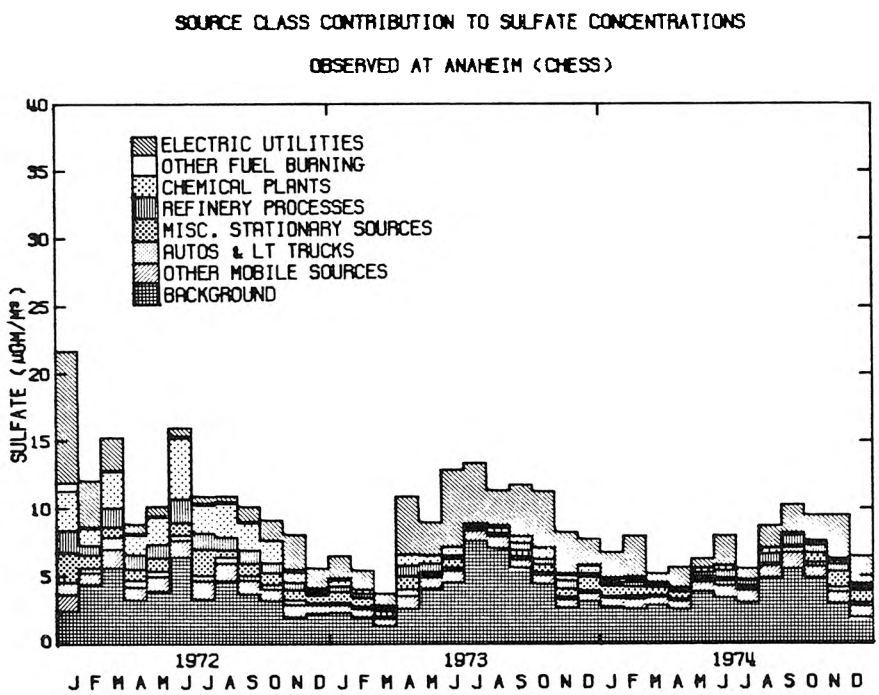


FIGURE 5.16(b)

prediction which threads those error bounds is indistinguishable from the field measurements.[4]

Approximately eighty percent of the sulfate concentration predictions at the LAAPCD stations are within the error bounds on the ambient monitoring results. At the CHESS stations the error bounds on the ambient data are much tighter due to the increased sampling schedule, and fewer predictions fall within the error bounds on the field observations. Model predictions still track observed sulfate levels closely at the critical CHESS stations in the Eastern San Gabriel Valley at Glendora and West Covina. A tendency to underpredict the summer peaks observed near the up-coast and down-coast edges of our receptor area at Santa Monica and at Garden Grove and Anaheim during 1973 and 1974 is noted.

Monthly concentration predictions can be pooled to form annual arithmetic mean sulfate estimates throughout the airshed. These annual average sulfate concentration predictions can be compared to observations at a larger number of air monitoring stations, as shown in Tables 5.8, 5.9 and 5.10. Sixty-four percent of the annual mean sulfate concentration predictions which can be compared to air quality

---

[4] An assessment of air quality model results against the criterion that they be indistinguishable from the ambient monitoring data is both the most severe and also the most appropriate test of model performance that this author has encountered. Most air quality model validation studies compare the correlation between observations and predictions or some measure of the ratio of observed to predicted air quality levels. Some of these more customary statistical measures of model performance will be presented shortly.

TABLE 5.8

OBSERVED VERSUS PREDICTED ANNUAL AVERAGE SULFATE AIR QUALITY
FOR THE YEAR 1972

(CONCENTRATIONS STATED IN $\mu GM/M^3$ AS $SO_4^=$)

| | | SULFATE AIR QUALITY OBSERVATIONS | | | | | SULFATE AIR QUALITY MODEL RESULTS | | |
|---|---|---|---|---|---|---|---|---|---|
| | | SAMPLE ARITHMETIC MEAN $\bar{y}$ | SAMPLE ARITHMETIC STANDARD DEVIATION $\sigma$ | NUMBER OF DAYS SAMPLED n | LOWER CONFIDENCE LIMIT ON $\bar{y}$ (2.5 %ile) | UPPER CONFIDENCE LIMIT ON $\bar{y}$ (97.5 %ile) | ARITHMETIC MEAN FROM AIR QUALITY MODEL | PREDICTION IS WITHIN CONFIDENCE INTERVAL ON OBSERVATIONS | DIFFERENCE BETWEEN OBSERVED AND PREDICTED MEANS |
| SANTA MONICA | CHESS | 9.40 | 5.84 | 238.00 | 8.87 | 9.92 | 10.82 | NOTE (b) | NOTE (b) |
| WEST LA | LAAPCD | 11.86 | 9.04 | 72.00 | 9.98 | 13.74 | 12.20 | YES | -0.34 |
| LENNOX | LAAPCD | 15.37 | 9.78 | 73.00 | 13.35 | 17.39 | 14.16 | YES | 1.21 |
| TORRANCE | NASN | 11.34 | 6.35 | 30.00 | 9.15 | 13.52 | 13.81 | NO | -2.47 |
| LONG BEACH | NASN | 11.29 | 7.55 | 28.00 | 8.59 | 13.98 | 15.06 | NO | -3.77 |
| LYNWOOD | LAAPCD | * | * | 0.0 | * | * | 15.05 | NOTE (a) | NOTE (a) |
| GLENDALE | NASN | 10.27 | 7.27 | 28.00 | 7.68 | 12.87 | 12.39 | YES | -2.12 |
| LOS ANGELES | NASN | 11.07 | 8.19 | 32.00 | 8.35 | 13.79 | 15.88 | NO | -4.81 |
| LOS ANGELES | LAAPCD | 14.38 | 11.60 | 68.00 | 11.88 | 16.88 | 15.88 | YES | -1.50 |
| PASADENA | LAAPCD | 11.55 | 10.77 | 70.00 | 9.27 | 13.82 | 13.32 | YES | -1.77 |
| PASADENA | NASN | 10.67 | 7.58 | 27.00 | 7.91 | 13.43 | 13.32 | YES | -2.65 |
| GARDEN GROVE | CHESS | 9.20 | 5.39 | 239.00 | 8.72 | 9.69 | 10.86 | NOTE (b) | NOTE (b) |
| ANAHEIM | CHESS | 10.95 | 7.68 | 328.00 | 10.52 | 11.39 | 11.57 | NOTE (b) | NOTE (b) |
| ANAHEIM | NASN | 11.19 | 8.24 | 28.00 | 8.25 | 14.13 | 11.57 | YES | -0.38 |
| SANTA ANA | NASN | 11.69 | 11.06 | 29.00 | 7.82 | 15.56 | 9.56 | YES | 2.13 |
| AZUSA | LAAPCD | 13.98 | 11.91 | 71.00 | 11.48 | 16.48 | 13.09 | YES | 0.89 |
| WEST COVINA | CHESS | 11.06 | 6.77 | 241.00 | 10.46 | 11.66 | 13.57 | NOTE (b) | NOTE (b) |
| GLENDORA | CHESS | 11.98 | 9.63 | 303.00 | 11.38 | 12.58 | 13.02 | NOTE (b) | NOTE (b) |

NOTES: (a) AN ASTERISK (*) INDICATES DATA THAT ARE UNAVAILABLE.

(b) ANNUAL MEANS CALCULATED AT THESE AIR MONITORING SITES ARE BIASED BEYOND THE ASSUMPTIONS OF THE CONFIDENCE INTERVAL CALCULATIONS. SAMPLING AT SANTA MONICA, GARDEN GROVE AND WEST COVINA DID NOT BEGIN UNTIL MAY 1972. SAMPLING AT ANAHEIM AND GLENDORA DID NOT BEGIN UNTIL THE LAST FEW DAYS OF JANUARY 1972. ALL CHESS MONITORING SITES WERE OUT OF OPERATION DURING THE EARLY JANUARY 1972 SULFATE EPISODES, AND MOST CHESS STATIONS MISSED THE MARCH 1972 SULFATE EPISODES AS WELL.

TABLE 5.9

OBSERVED VERSUS PREDICTED ANNUAL AVERAGE SULFATE AIR QUALITY
FOR THE YEAR 1973

(CONCENTRATIONS STATED IN $\mu GM/M^3$ AS $SO_4^=$)

| | | SULFATE AIR QUALITY OBSERVATIONS | | | | | SULFATE AIR QUALITY MODEL RESULTS | | |
|---|---|---|---|---|---|---|---|---|---|
| | | SAMPLE ARITHMETIC MEAN $\bar{y}$ | SAMPLE ARITHMETIC STANDARD DEVIATION $\sigma$ | NUMBER OF DAYS SAMPLED n | LOWER CONFIDENCE LIMIT ON $\bar{y}$ (2.5 %ile) | UPPER CONFIDENCE LIMIT ON $\bar{y}$ (97.5 %ile) | ARITHMETIC MEAN FROM AIR QUALITY MODEL | PREDICTION IS WITHIN CONFIDENCE INTERVAL ON OBSERVATIONS | DIFFERENCE BETWEEN OBSERVED AND PREDICTED MEANS |
| SANTA MONICA | CHESS | 12.49 | 10.10 | 354.00 | 12.04 | 12.94 | 9.71 | NO | 2.78 |
| WEST LA | LAAPCD | 10.63 | 10.47 | 71.00 | 8.44 | 12.83 | 9.96 | YES | 0.67 |
| LENNOX | LAAPCD | 13.94 | 12.17 | 73.00 | 11.43 | 16.45 | 12.87 | YES | 1.07 |
| TORRANCE | NASN | 11.21 | 7.43 | 25.00 | 8.39 | 14.03 | 12.16 | YES | -0.95 |
| LONG BEACH | NASN | 10.59 | 5.58 | 25.00 | 8.47 | 12.70 | 13.65 | NO | -3.06 |
| LYNWOOD | LAAPCD | * | * | 0.0 | * | * | 13.49 | NOTE (a) | NOTE (a) |
| GLENDALE | NASN | 10.46 | 7.82 | 30.00 | 7.77 | 13.15 | 10.55 | YES | -0.09 |
| LOS ANGELES | NASN | 12.30 | 6.59 | 25.00 | 9.80 | 14.80 | 14.14 | YES | -1.84 |
| LOS ANGELES | LAAPCD | 15.80 | 14.70 | 73.00 | 12.77 | 18.83 | 14.14 | YES | -1.66 |
| PASADENA | LAAPCD | 12.66 | 12.33 | 73.00 | 10.12 | 15.20 | 13.65 | YES | -0.99 |
| PASADENA | NASN | 13.59 | 9.93 | 30.00 | 10.18 | 17.00 | 13.65 | YES | -0.06 |
| GARDEN GROVE | CHESS | 13.23 | 8.76 | 352.00 | 12.79 | 13.67 | 8.39 | NO | 4.84 |
| ANAHEIM | CHESS | 12.31 | 9.18 | 352.00 | 11.88 | 12.75 | 9.37 | NO | 2.94 |
| ANAHEIM | NASN | 9.48 | 5.40 | 25.00 | 7.43 | 11.54 | 9.37 | YES | 0.11 |
| SANTA ANA | NASN | 8.02 | 3.64 | 25.00 | 6.64 | 9.41 | 7.98 | YES | 0.04 |
| AZUSA | LAAPCD | 13.11 | 11.98 | 73.00 | 10.64 | 15.58 | 15.72 | NO | -2.61 |
| WEST COVINA | CHESS | 14.54 | 12.00 | 347.00 | 13.98 | 15.09 | 16.26 | NO | -1.72 |
| GLENDORA | CHESS | 14.43 | 12.10 | 356.00 | 13.91 | 14.95 | 15.53 | NO | -1.10 |

NOTE: (a) AN ASTERISK (*) INDICATES DATA THAT ARE UNAVAILABLE.

TABLE 5.10

OBSERVED VERSUS PREDICTED ANNUAL AVERAGE SULFATE AIR QUALITY
FOR THE YEAR 1974

(CONCENTRATIONS STATED IN $\mu GM/M^3$ AS $SO_4^=$)

| | | SULFATE AIR QUALITY OBSERVATIONS | | | | | SULFATE AIR QUALITY MODEL RESULTS | | |
|---|---|---|---|---|---|---|---|---|---|
| | | SAMPLE ARITHMETIC MEAN $\bar{y}$ | SAMPLE ARITHMETIC STANDARD DEVIATION $\sigma$ | NUMBER OF DAYS SAMPLED n | LOWER CONFIDENCE LIMIT ON $\bar{y}$ (2.5 %ile) | UPPER CONFIDENCE LIMIT ON $\bar{y}$ (97.5 %ile) | ARITHMETIC MEAN FROM AIR QUALITY MODEL | PREDICTION IS WITHIN CONFIDENCE INTERVAL ON OBSERVATIONS | DIFFERENCE BETWEEN OBSERVED AND PREDICTED MEANS |
| SANTA MONICA | CHESS | 11.32 | 8.95 | 248.00 | 10.59 | 12.05 | 8.35 | NOTE (b) | NOTE (b) |
| WEST LA | LAAPCD | 9.42 | 8.92 | 72.00 | 7.57 | 11.28 | 9.08 | YES | 0.34 |
| LENNOX | LAAPCD | 11.82 | 10.01 | 73.00 | 9.76 | 13.89 | 11.53 | YES | 0.29 |
| TORRANCE | NASN | 11.65 | 6.29 | 28.00 | 9.40 | 13.89 | 11.24 | YES | 0.41 |
| LONG BEACH | NASN | 13.95 | 9.21 | 26.00 | 10.53 | 17.37 | 12.24 | YES | 1.71 |
| LYNWOOD | LAAPCD | 9.47 | 8.55 | 68.00 | 7.63 | 11.31 | 11.86 | NO | -2.39 |
| GLENDALE | NASN | 9.02 | 8.80 | 13.00 | 4.31 | 13.72 | 9.40 | YES | -0.38 |
| LOS ANGELES | NASN | 13.92 | 12.09 | 26.00 | 9.43 | 18.41 | 12.12 | YES | 1.80 |
| LOS ANGELES | LAAPCD | 12.66 | 11.19 | 71.00 | 10.31 | 15.00 | 12.12 | YES | 0.54 |
| PASADENA | LAAPCD | 8.56 | 8.41 | 71.00 | 6.80 | 10.32 | 11.15 | NO | -2.59 |
| PASADENA | NASN | 11.47 | 9.23 | 22.00 | 7.72 | 15.22 | 11.15 | YES | 0.32 |
| GARDEN GROVE | CHESS | 10.09 | 6.82 | 307.00 | 9.65 | 10.52 | 6.82 | NO | 3.27 |
| ANAHEIM | CHESS | 10.69 | 7.89 | 286.00 | 10.15 | 11.24 | 7.51 | NO | 3.18 |
| ANAHEIM | NASN | 12.51 | 9.10 | 30.00 | 9.38 | 15.63 | 7.51 | NO | 5.00 |
| SANTA ANA | NASN | 11.47 | 7.48 | 29.00 | 8.85 | 14.09 | 6.83 | NO | 4.64 |
| AZUSA | LAAPCD | 10.54 | 9.96 | 71.00 | 8.45 | 12.62 | 12.41 | YES | 1.87 |
| WEST COVINA | CHESS | 11.49 | 9.00 | 293.00 | 10.90 | 12.09 | 13.73 | NOTE (b) | NOTE (b) |
| GLENDORA | CHESS | 11.13 | 9.08 | 278.00 | 10.49 | 11.77 | 12.72 | NOTE (b) | NOTE (b) |

NOTE: (b) ANNUAL MEANS CALCULATED FROM OBSERVATIONS AT THESE AIR MONITORING SITES ARE BIASED BEYOND THE ASSUMPTIONS OF THE CONFIDENCE INTERVAL CALCULATIONS. THE CHESS STATION AT SANTA MONICA DID NOT FUNCTION DURING THE MONTHS OF MARCH, APRIL AND MAY, 1974. OBSERVATIONS AT WEST COVINA AND GLENDORA ARE ABSENT DURING MARCH 1974, AND ARE INFREQUENT DURING APRIL AND MAY. ANAHEIM AND GARDEN GROVE CHESS STATIONS SHOW ACTIVITY IN ALL MONTHS, BUT SAMPLING RATE FALLS DURING THE SAME PERIOD OF TIME.

measurements fall within the 95% confidence intervals on the sulfate air quality measurements.

### 5.4.2 The Spatial-Temporal Correlation between Observed and Predicted Sulfate Concentrations

Figures 5.17 through 5.19 show the correspondence between observed and predicted sulfate concentrations at all CHESS and LAAPCD stations for all months with useful observations within each of the years 1972, 1973 and 1974. A summary of the statistics of those data sets is given in Table 5.11. Model performance is particularly good during 1972 and 1973, and is felt to be acceptable during 1974.

The correlation between observed and predicted sulfate levels is 0.82 in both 1972 and 1973. From a visual comparison of Figures 5.17 and 5.18, most observers would hold that the 1972 model results represent a far better fit to the observations than was obtained in 1973. The statistics of the 1972 data set are degraded by two outlying data points with sulfate predictions of about 20 $\mu gm/m^3$ and observed values near 5 $\mu gm/m^3$. Those two data points were examined more closely. It was found that they are an artifact of the start-up of the CHESS air monitoring network. The CHESS air monitoring stations at Anaheim and Glendora initiated sampling during the closing days of January 1972. They thus missed sampling the high sulfate episodes which occurred earlier in that month. With those two observations discarded as biased, the remaining data for 1972 show a 0.89 correlation between observations and model predictions.

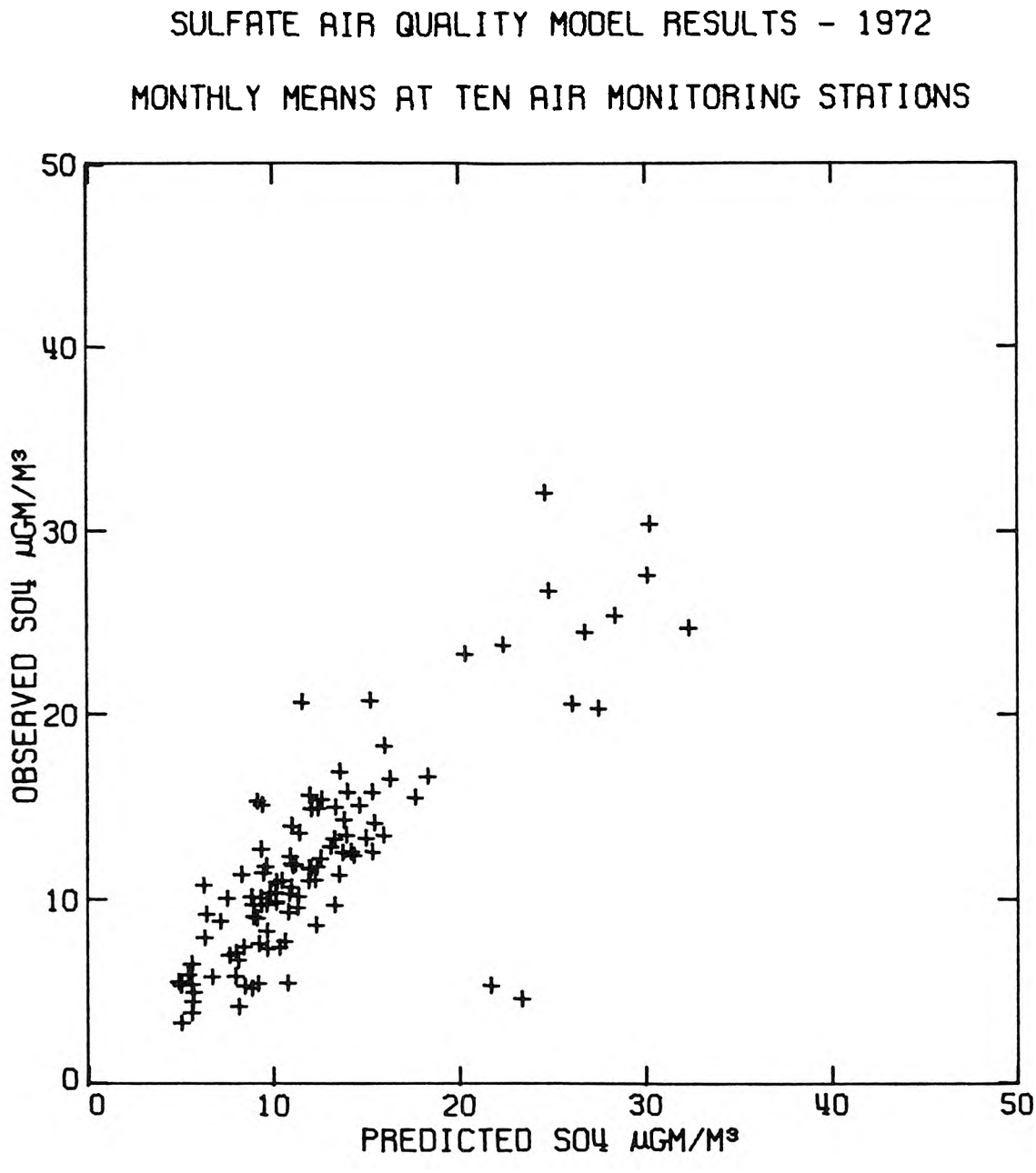
SULFATE AIR QUALITY MODEL RESULTS - 1972
MONTHLY MEANS AT TEN AIR MONITORING STATIONS
OBSERVED SO4 µGM/M³
PREDICTED SO4 µGM/M³
0
10
20
30
40
50

FIGURE 5.17

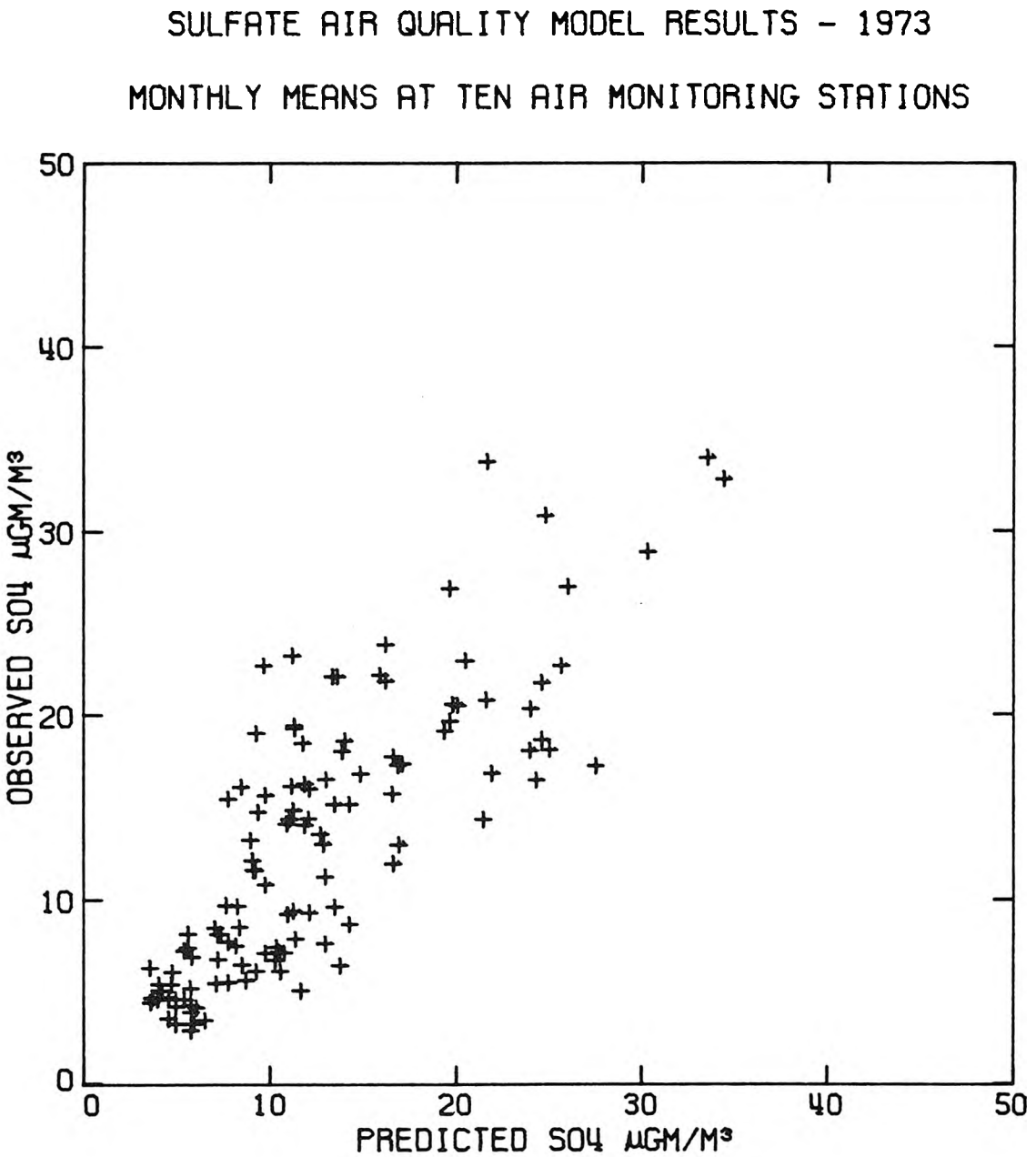
SULFATE AIR QUALITY MODEL RESULTS - 1973
MONTHLY MEANS AT TEN AIR MONITORING STATIONS
OBSERVED SO4 µGM/M³
PREDICTED SO4 µGM/M³
0
10
20
30
40
50

FIGURE 5.18

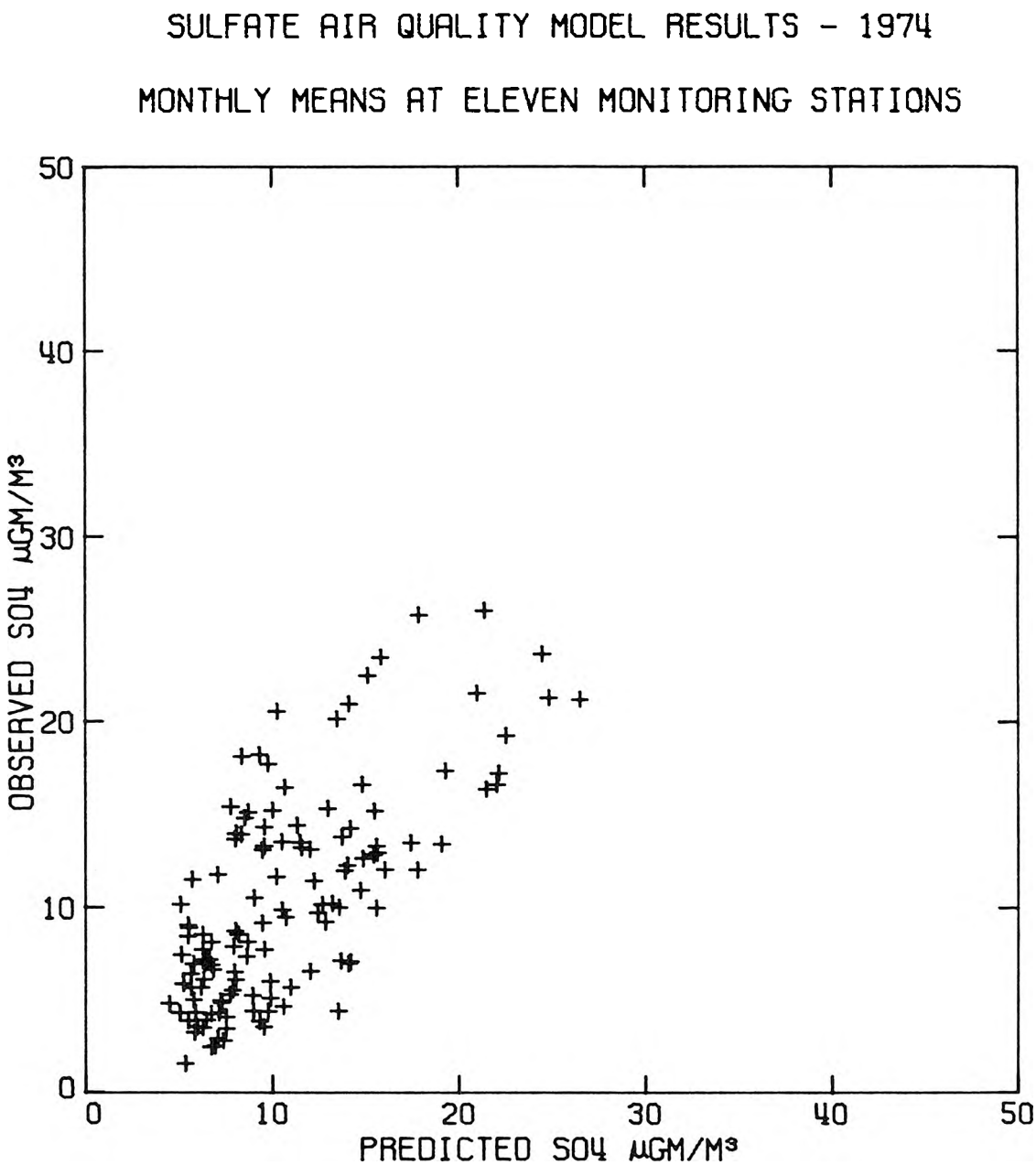
SULFATE AIR QUALITY MODEL RESULTS - 1974
MONTHLY MEANS AT ELEVEN MONITORING STATIONS
OBSERVED SO4 µGM/M³
PREDICTED SO4 µGM/M³
0
10
20
30
40
50

FIGURE 5.19

TABLE 5.11

Statistical Comparison of Monthly Average Sulfate Concentrations:
Observations vs. Air Quality Model Results
At Eleven Air Monitoring Sites.

| Year | Number of Pairs of Monthly Average Observations and Predictions | Observations | | Predictions | | Correlation: Observed vs. Predicted |
|---|---|---|---|---|---|---|
| | | Mean[(b)] $\mu gm/m^3$ | Standard Deviation $\mu gm/m^3$ | Mean[(b)] $\mu gm/m^3$ | Standard Deviation $\mu gm/m^3$ | |
| 1972 | 108 | 12.18 | 5.87 | 12.51 | 5.92 | 0.82 |
| 1972[(a)] | 106 | 12.31 | 5.84 | 12.32 | 5.81 | 0.89 |
| 1973 | 120 | 13.12 | 7.38 | 12.52 | 6.80 | 0.82 |
| 1974 | 128 | 10.45 | 5.65 | 10.80 | 4.86 | 0.70 |

Notes: (a) Biased observations at two CHESS stations discarded for January 1972. These stations did not begin operation until the last four days of that month and thus missed the early January 1972 sulfate episodes. Days sampled were thus not representative of that month.

(b) Unweighted average of available data pairs; because of changing number of days per month and absence of observations at some locations in some months this does not represent an annual mean value.

Correlation analysis alone is a poor measure of model performance. Many air quality models which track temporal trends well fail to accurately reproduce the absolute value of the pollutant concentrations. However, in our case, not only are the observations and predictions highly correlated, but the average values of the predictions and observations are quite close. In addition, the distribution of high and low values throughout the year is closely matched, as shown by the comparison of the standard deviations of the observed and predicted sulfate concentrations given in Table 5.11.

### 5.4.3 The Seasonal Variation in the Rate of Oxidation of $SO_2$ to Form Sulfates

Table 5.12 shows the values of the rate of $SO_2$ oxidation, k, which result from the air quality model application. Each of the entries in that table represents an overall average conversion rate for a particular month. The conversion rates estimated range from a high of 8% per hour to a low of 0.5% per hour.

When $SO_2$ oxidation rates are averaged horizontally across the columns of Table 5.12, a rather consistent seasonal pattern emerges. Three year average $SO_2$ oxidation rates are almost exactly 6% per hour from May through September of the year, with no single month in that group more than $\pm$2% per hour above or below the seasonal trend. $SO_2$ oxidation rates drop sharply in the wintertime. Estimated conversion rates of between 0.5% per hour to 3.0% per hour prevail from October through February.

TABLE 5.12

Calculated Rate of $SO_2$ Oxidation to Form Sulfates in the Los Angeles Atmosphere, in Percent per Hour (Overall Average Values of k for the Month Shown)

| Month | 1972 | 1973 | 1974 | Three year mean |
|---|---|---|---|---|
| January | 3% | 1% | 0.5% | 1.5% |
| February | 1% | 1.5% | 1% | 1.2% |
| March | 8% | 1% | 1% | 3.3% |
| April | 3% | 5% | 1% | 3.0% |
| May | 6% | 8% | 5% | 6.3% |
| June | 6% | 7% | 6% | 6.3% |
| July | 4% | 8%(a) | 5% | 5.7% |
| August | 5% | 5% | 8% | 6.0% |
| September | 4% | 5% | 8% | 5.7% |
| October | 2% | 1% | 3% | 2.0% |
| November | 1% | 0.75% | 1% | 0.9% |
| December | 1% | 1% | 0.5% | 0.8% |

Notes: (a) Average value from field measurement program in that month. (Roberts, 1975)

The 8% per hour conversion rate estimated for March 1972 is more than double the seasonally adjusted average for the month of March. At k equals 3% per hour, January 1972 also shows a conversion rate which is double the seasonally adjusted trend for a January month. Very high sulfate values were observed in early 1972 throughout the air basin. Weather records at Los Angeles International Airport (U.S. Department of Commerce, 1972b) indicate that half of the days of each of those two months were foggy or showed just enough condensation to yield trace precipitation without a general washout of the atmosphere. In January 1972, extreme resultant wind stagnation occurred during a period of high $SO_x$ emissions. That accounts for the very high sulfate concentrations observed during January 1972 in spite of the modest (by comparison to summertime) $SO_2$ oxidation rate.

The 8% per hour $SO_2$ oxidation rate estimated from Roberts' (1975) experiments in July 1973 was treated as a predetermined value for that month. Figure 5.7a shows that a very close fit to observed sulfate concentrations was obtained at the site of Roberts' experiments in Pasadena for that month. Such close agreement is probably fortuitous. But the fact remains that model results are clearly within the range of observed sulfate concentrations for the only occasion in which estimates for all parameters in the model are supported by experimental data.

### 5.4.4 Spatial Variations in Sulfate Air Quality

Figures 5.20 through 5.22 show contour plots of the annual mean sulfate air quality predictions throughout our study area for each of the years 1972, 1973 and 1974. A large zone of sulfate-enriched air is seen to influence most of Los Angeles and northern Orange Counties, extending from the coastline inland to the San Gabriel Mountains. Long-term average sulfate concentrations are lower over the ocean and over the southern portion of Orange County.

In Chapter 2, long-term average sulfate concentrations observed at local air monitoring stations were found to be rather uniform. From Figures 5.20 through 5.22 we see that concentration estimates at most air monitoring stations fall within or near the same contour interval. However, the simulation model suggests that additional structure to the sulfate concentration patterns in 1972 and 1973 would have been revealed if a closely spaced network of monitoring sites had been located downwind of the harbor industrial complex. In 1972, the highest mean sulfate levels are predicted over South Central Los Angeles. That pattern was influenced by unusually high sulfate concentrations in the winter and early spring of 1972 when inland transport of pollutants was relatively weak. In contrast, peak sulfate concentrations in 1973 are predicted downwind of the harbor industrial complex in a long corridor which stretches from Carson on the southwest to beyond the boundaries of our grid system at a point near Pomona on the northeast. That pattern is due to summertime peak sulfate values in 1973 which were accompanied by high speed inland transport during the

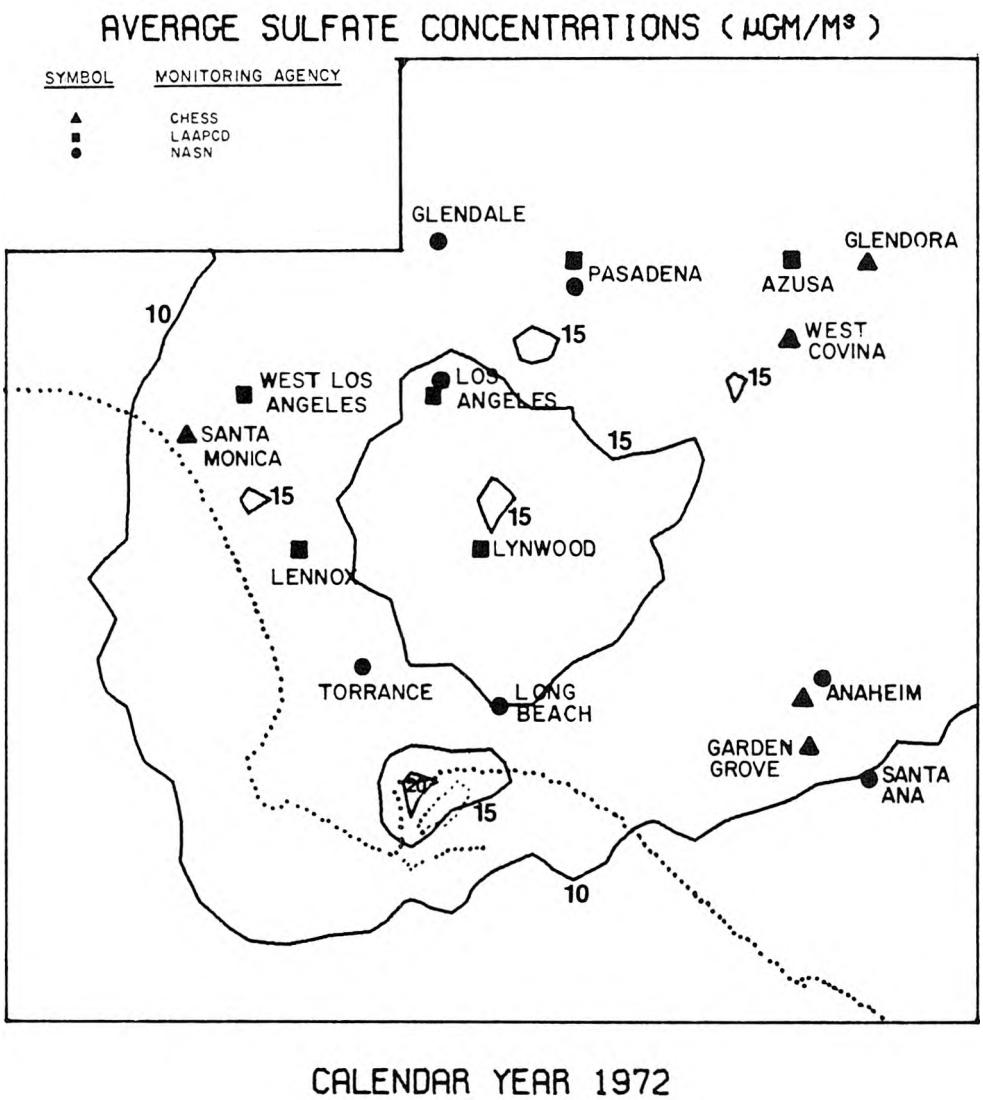


FIGURE 5.20

Annual Mean Sulfate Concentration Isopleths Calculated by the Air Quality Simulation Model - 1972

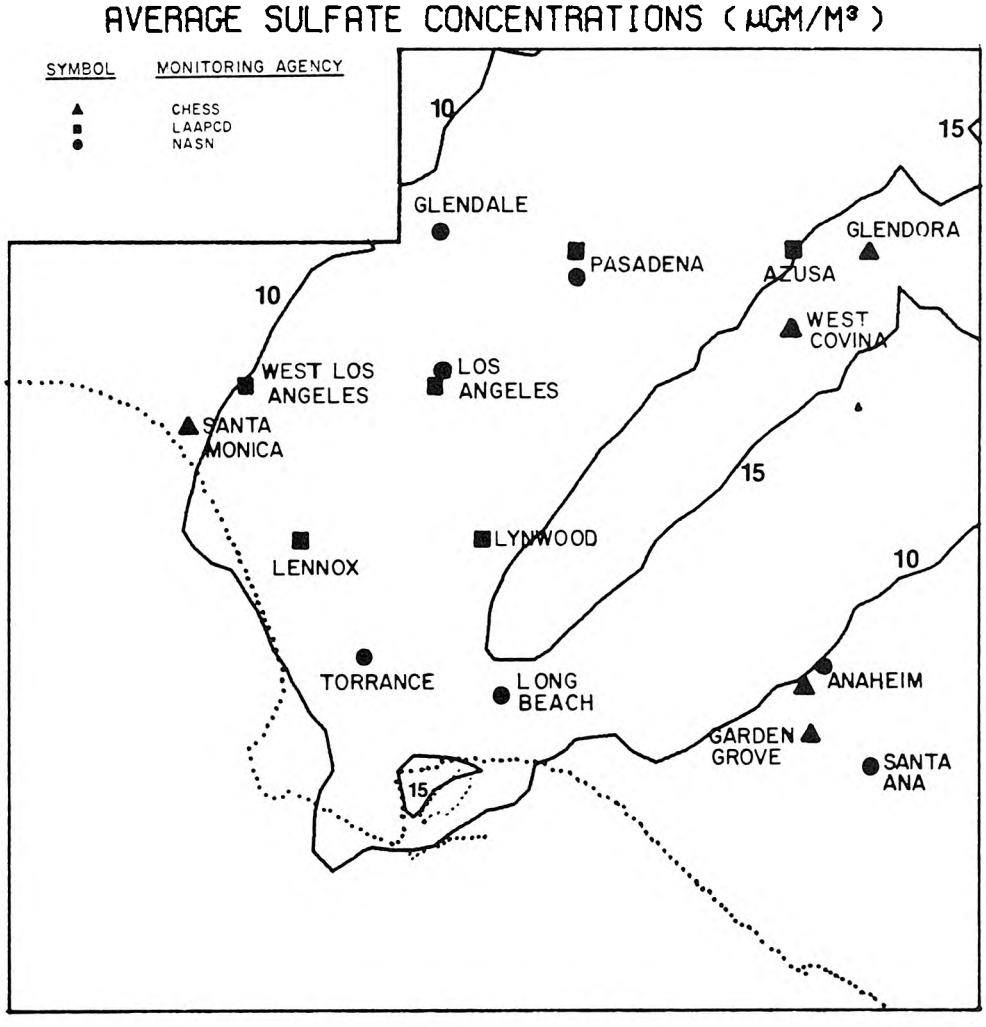


FIGURE 5.21

Annual Mean Sulfate Concentration Isopleths Calculated by the Air Quality Sumulation Model - 1973

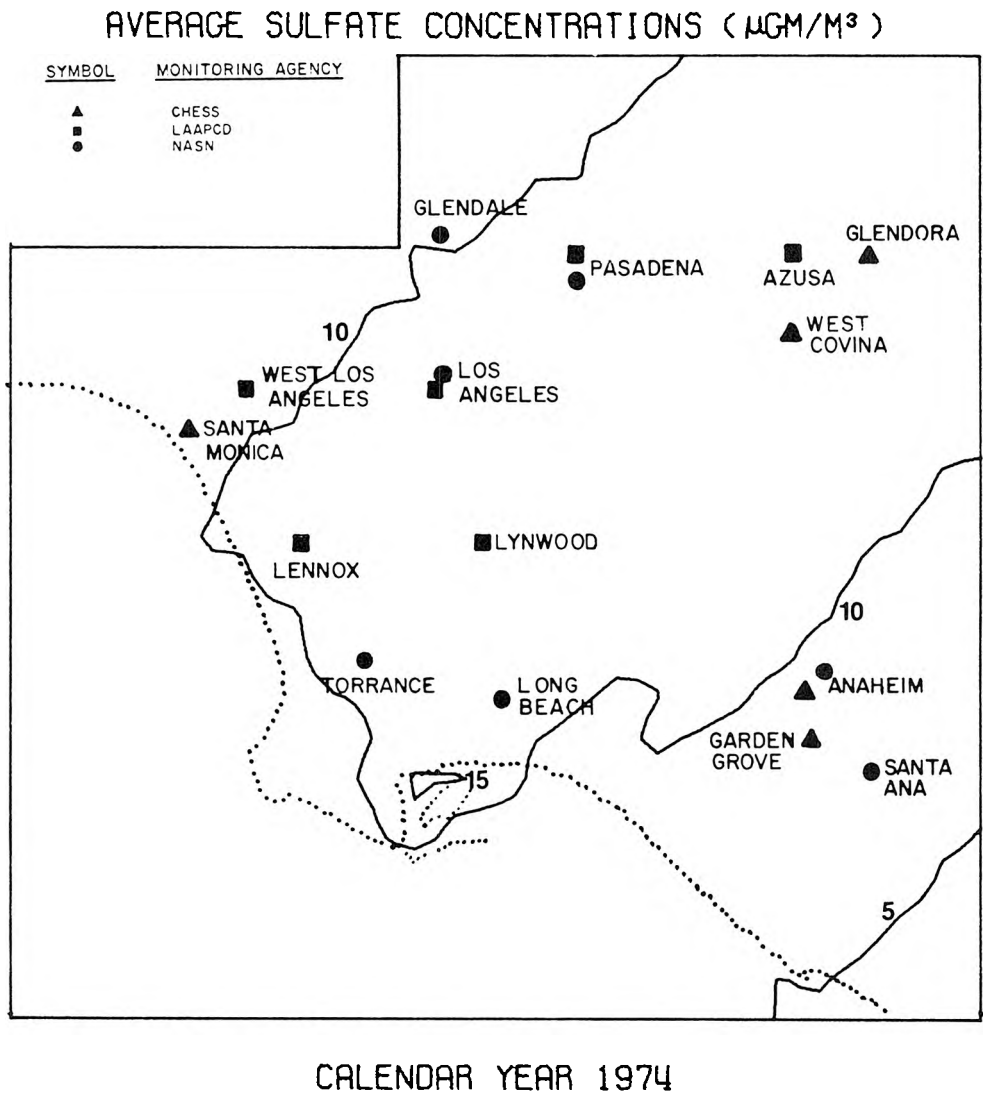


FIGURE 5.22

Annual Mean Sulfate Concentration Isopleths Calculated by the Air Quality Simulation Model - 1974

afternoon sea breeze regime. This central corridor of highest sulfate values is absent in 1974, largely because of the control of sulfur dioxide emissions from some very large chemical plants located just to the southwest of the start of the 15 $\mu gm/m^3$ sulfate isopleth calculated in 1973 (see Figure 5.23 and Figure 1.6 in Chapter 1, Section 1.6.1).

In addition, each of our three years of interest shows a small peak in sulfate concentrations located within the Los Angeles-Long Beach harbor at Terminal Island. That peak is influenced by fuel burning by ships in the harbor, as well as by local industries in the harbor area. To the extent that ships are involved, that peak may be an artifact of our source class aggregation scheme. All mobile sources were assigned low effective stack heights when source classes were recombined for modeling purposes. A ship underway at sea would have a bent-over plume influenced by the relative velocity between the atmosphere and the moving ship, while a ship sitting motionless at the dock would have stack characteristics more closely resembling a small industrial boiler. Both of these conditions cannot be simulated simultaneously unless our source classes are subdivided further. An overprediction of the impact of dockside emissions from ships may have resulted from an underestimation of their effective stack height. Sulfate air quality data within the harbor are unavailable, so the presence or absence of that local enrichment in sulfate levels cannot be confirmed or denied.

Contour plots showing sulfate concentration predictions for each month of our three year test period are given in Appendix C1. At the outset, in January and March of 1972, a large sulfate concentration

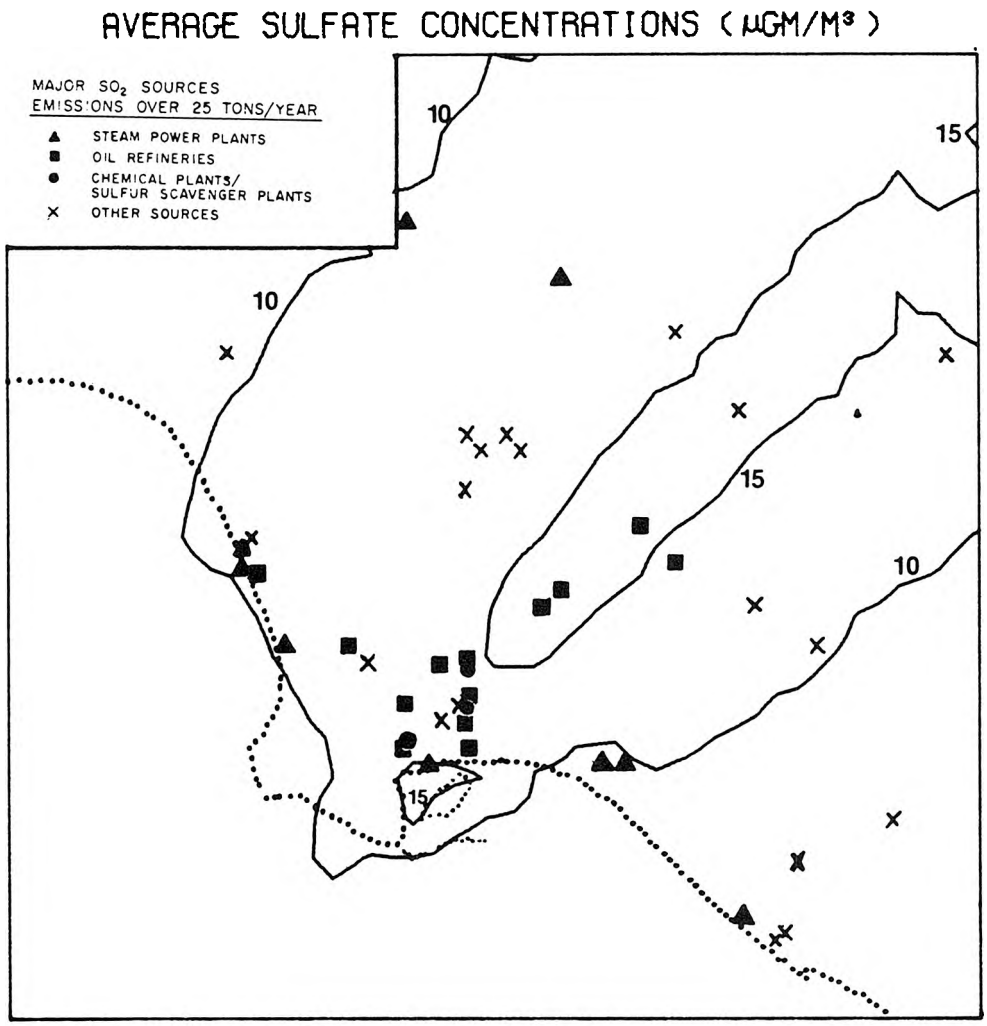


FIGURE 5.23

Annual Mean Sulfate Concentrations in Relation to Major Point Source Locations - 1973

buildup is noted in the southwest and central portions of Los Angeles County. Our highest sulfate concentration predictions for any month of the three year study period occur during January 1972, with values in several locations in excess of 40 $\mu gm/m^3$ average for the month. That situation occurred because of extended air stagnation in the presence of high $SO_2$ emissions and a moderate $SO_2$ oxidation rate estimated at about 3% per hour or less.[5] *While such extended stagnation is unusual, the fact that it can occur means that sulfate air quality control strategy design must consider avoidance of wintertime as well as summertime pollution episodes in Los Angeles.*

The late spring and summer of 1972 are seen to be uneventful. Sulfate concentrations are spread in large dilute air masses, and inland transport causes contours to extend off-grid to the northeast of the major sources in the harbor area. By October 1972, inland transport is stagnating and the $SO_2$ to sulfate conversion rate is slower. The area affected by sulfate concentrations greater than 10 $\mu gm/m^3$ declines in size and begins to move southwest back toward the harbor area. By December 1972 and January 1973, effective transport is to the seaward side of the air basin, and the inland valleys are nearly drained of their usual pollutant burden.

By April 1973, the cycle has reversed and transport is occurring inland toward Pomona and the Eastern San Gabriel Valley from the coastal

---

[5] Under extended stagnation conditions, $\tau_c = 48$ hours may not be long enough to capture all of the particles contributing to observed air quality. In that case our estimate of k equals 3% per hour would be raised artificially in order to capture the difference.

industrial complex. This year, the $SO_2$ to sulfate conversion rate is a few percent per hour faster than in the summer of 1972, and noticeable areas of elevated sulfate concentrations extend downwind from major source locations at the coast. Monthly mean sulfate concentrations in excess of 30 $\mu gm/m^3$ appear in the Eastern San Gabriel and Pomona-Walnut Valleys in mid-summer. In October 1973, the $SO_2$ oxidation rate drops and sulfate concentrations decline. By December 1973, the Eastern San Gabriel Valley is largely free of sulfates, and transport appears to have shifted pollutants to the south and west. During 1974, the seasonal cycle observed in 1973 largely repeats itself.

The relatively uniform upwind/downwind annual mean sulfate concentration patterns observed over our three years of interest result in part from a seasonal cycle in which peak sulfate concentrations appeared far inland during the summer and near the coast during the winter.

### 5.4.5 The Relationship Between Sulfate Air Quality and Total Sulfur Oxides Concentrations

In Chapter 2 it was shown that measured values of the ratio of particulate sulfur oxides to total sulfur oxides, $f_s$, varied widely from one monitoring network to another. Systematic errors were found to arise from difficulties in measurement of very low sulfur dioxide levels. From a discussion of the nature of those sampling problems, it was suggested that $SO_2$ data sets at CHESS and LAAPCD stations are likely to be biased *in opposite directions*. Thus all that could be said is that model results for the ratio of sulfates to total sulfur

oxides should fall below the average $f_s$ values from the CHESS and NASN networks, but at or above the typical $f_s$ values calculated from LAAPCD data.

Simulation model results for the ratio of average sulfate to average total sulfur are analyzed in Appendix C2. The air quality simulation tracks the observed seasonal trends in $\bar{f}_s$. Model results fall between the bounds established by the CHESS and LAAPCD monitoring data, as expected.

A search was conducted for monitoring sites in the vicinity of major $SO_2$ sources. The intent was to find locations impacted by high enough $SO_2$ levels that $SO_2$ instrument detection limit problems would be minimized. The only such site with both $SO_2$ and sulfate data is the LAAPCD station at Lennox. Agreement between model results for $\bar{f}_s$ and observations at Lennox are excellent. On a few occasions during 1973, sulfur ratio predictions can be compared to high quality field data from the ACHEX study (Hidy, et al., 1975). Again, reasonable agreement is obtained.

Total $SO_x$ concentrations at downtown Los Angeles appear to be overestimated by the model. That problem is thought to arise from mobile source emissions from within the grid cell containing the monitoring site, particularly from an imprecisely inventoried railroad switching yard. With that exception, predicted values of the ratio of particulate sulfur oxides to total sulfur oxides are found to closely reproduce those monitoring results which are free of minimum detection

limit problems, and to fall to the expected side of measurements at stations with significant monitoring biases.

### 5.4.6 Atmospheric Sulfur Balance Calculations

One advantage of our simulation model is that it maintains a mass balance on the fate of pollutant emissions from each source class. Sulfur oxides are present as $SO_2$ or as sulfates either within the mixed layer next to the ground or within the elevated inversion, until they have deposited at the ground. By averaging over the pollutant mass balances on emissions from various source types, we may study the long-range effect of source characteristics such as an elevated stack height or a high fraction sulfates in a source's exhaust.

Tables 5.13 through 5.15 show mass balance calculations on $SO_x$ emissions from each source class during one month drawn from each of our three years of interest. A variety of $SO_2$ oxidation rates and meteorological conditions are represented. The mass balance results summarize a moving average over the outstanding status of all $SO_x$ containing air parcels released from each source during the past 48 hours. The result is similar to examining a flow reactor with a retention time of 48 hours and then averaging over its contents. These calculations differ from those of Roberts (1975, see Figure 2.17) because he established fluxes entering and leaving the boundaries of the airshed over a shorter period of time.

One of the most interesting features revealed by Tables 5.13 through 5.15 is that source effective stack height makes little

TABLE 5.13

Sulfur Balance on Emissions from Each Major Source Class
for January 1972

| Source Class | Stack Parameters at Reference Conditions | | Fraction $SO_3$ in Exhaust | Fate of $SO_x$ Emissions Averaged over All On-Grid and Off-Grid Air Parcels Aged Two Days or Less (Percent in Category Shown) | | | | | |
|---|---|---|---|---|---|---|---|---|---|
| | Stack Height H m | Plume Rise ΔH m | $f_{S_o}$ (Percent) | $SO_2$ within mixed layer | $SO_4$ within mixed layer | $SO_2$ above mixed layer | $SO_4$ above mixed layer | $SO_2$ deposited at ground level | $SO_4$ deposited at ground level |
| Electric Utilities | 68.6 | 250.6 | 3% | 18.5 | 19.1 | 22.7 | 21.2 | 17.7 | 0.6 |
| Other Fuel Burning Sources | 30.5 | 54.9 | 3% | 20.9 | 19.5 | 16.2 | 17.5 | 24.9 | 0.7 |
| Chemical Plants | 41.2 | 36.6 | 0.6% | 21.4 | 18.5 | 16.4 | 16.8 | 26.0 | 0.6 |
| Refinery Processes | 37.2 | 164.6 | 2.8% | 20.4 | 19.9 | 18.4 | 18.4 | 22.0 | 0.7 |
| Petroleum Coke Kilns | 45.7 | 384.4 | 8.4% | 14.0 | 17.1 | 28.1 | 28.7 | 11.5 | 0.5 |
| Glass Furnaces | 22.9 | 44.8 | 18% | 17.7 | 25.1 | 13.5 | 21.0 | 21.4 | 1.0 |
| Metals Furnaces | 16.8 | 33.5 | 1% | 21.3 | 18.5 | 16.0 | 16.7 | 26.6 | 0.6 |
| Off-Grid Steel Mill | 72.5 | 129.8 | 2.5% | 20.7 | 19.8 | 17.9 | 18.0 | 22.6 | 0.7 |
| Misc. Stationary Sources | 10.7 | 21.3 | 2.8% | 20.8 | 19.0 | 15.3 | 16.9 | 27.2 | 0.7 |
| Autos and Light Trucks | Surface mixed layer | | 0.3% | 19.9 | 15.9 | 13.6 | 14.9 | 34.8 | 0.6 |
| Other Mobile Sources | Surface mixed layer | | 2.5% | 18.3 | 15.4 | 10.0 | 12.8 | 42.4 | 0.8 |

Important Characteristics of that Month:

(a) Average $SO_2$ Oxidation Rate = 3% per hour

(b) Average $SO_4^=$ Concentration = 25 $\mu gm/m^3$

TABLE 5.14

Sulfur Balance on Emissions from Each Major Source Class
for July 1973

| Source Class | Stack Parameters at Reference Conditions | | Fraction $SO_3$ in Exhaust | Fate of $SO_x$ Emissions Averaged over All On-Grid and Off-Grid Air Parcels Aged Two Days or Less (Percent in Category Shown) | | | | | |
|---|---|---|---|---|---|---|---|---|---|
| | Stack Height H m | Plume Rise ΔH m | $f_{S_O}$ (Percent) | $SO_2$ within mixed layer | $SO_4$ within mixed layer | $SO_2$ above mixed layer | $SO_4$ above mixed layer | $SO_2$ deposited at ground level | $SO_4$ deposited at ground level |
| Electric Utilities | 68.6 | 250.6 | 3% | 14.5 | 42.1 | 5.2 | 16.6 | 19.9 | 1.5 |
| Other Fuel Burning Sources | 30.5 | 54.9 | 3% | 15.7 | 41.3 | 2.9 | 14.4 | 23.9 | 1.5 |
| Chemical Plants | 41.2 | 36.6 | 0.6% | 16.1 | 40.4 | 2.9 | 14.1 | 24.8 | 1.5 |
| Refinery Processes | 37.2 | 164.6 | 2.8% | 15.4 | 41.8 | 3.8 | 15.3 | 22.0 | 1.5 |
| Petroleum Coke Kilns | 45.7 | 384.4 | 8.4% | 11.6 | 40.4 | 8.1 | 23.3 | 15.1 | 1.4 |
| Glass Furnaces | 22.9 | 44.8 | 18% | 13.3 | 46.4 | 2.4 | 15.4 | 20.5 | 1.8 |
| Metals Furnaces | 16.8 | 33.5 | 1% | 16.1 | 40.3 | 2.7 | 13.9 | 25.1 | 1.5 |
| Off-Grid Steel Mill | 72.5 | 129.8 | 2.5% | 15.5 | 41.6 | 3.6 | 15.0 | 22.5 | 1.5 |
| Misc. Stationary Sources | 10.7 | 21.3 | 2.8% | 15.8 | 40.9 | 2.6 | 14.0 | 24.9 | 1.5 |
| Autos and Light Trucks | Surface mixed layer | | 0.3% | 15.8 | 40.3 | 3.5 | 14.9 | 23.7 | 1.5 |
| Other Mobile Sources | Surface mixed layer | | 2.5% | 15.8 | 40.7 | 2.6 | 13.9 | 25.1 | 1.5 |

Important Characteristics of that Month:

(a) Average $SO_2$ Oxidation Rate = 8% per hour

(b) Average $SO_4^=$ Concentration = 29 $\mu gm/m^3$

TABLE 5.15

Sulfur Balance on Emissions from Each Major Source Class
for July 1974

| Source Class | Stack Parameters at Reference Conditions | | Fraction $SO_3$ in Exhaust | Fate of $SO_x$ Emissions Averaged over All On-Grid and Off-Grid Air Parcels Aged Two Days or Less (Percent in Category Shown) | | | | | |
|---|---|---|---|---|---|---|---|---|---|
| | Stack Height H m | Plume Rise ΔH m | $f_{s_o}$ (Percent) | $SO_2$ within mixed layer | $SO_4$ within mixed layer | $SO_2$ above mixed layer | $SO_4$ above mixed layer | $SO_2$ deposited at ground level | $SO_4$ deposited at ground level |
| Electric Utilities | 68.6 | 250.6 | 3% | 15.8 | 28.4 | 12.2 | 21.0 | 21.3 | 1.1 |
| Other Fuel Burning Sources | 30.5 | 54.9 | 3% | 17.5 | 27.1 | 7.4 | 17.3 | 29.3 | 1.1 |
| Chemical Plants | 41.2 | 36.6 | 0.6% | 18.0 | 25.8 | 7.1 | 16.5 | 31.2 | 1.1 |
| Refinery Processes | 37.2 | 164.6 | 2.8% | 16.8 | 28.0 | 10.2 | 19.5 | 24.1 | 1.1 |
| Petroleum Coke Kilns | 45.7 | 384.4 | 8.4% | 12.4 | 26.4 | 16.3 | 28.6 | 15.2 | 0.9 |
| Glass Furnaces | 22.9 | 44.8 | 18% | 14.8 | 32.5 | 5.9 | 19.2 | 25.7 | 1.5 |
| Metals Furnaces | 16.8 | 33.5 | 1% | 17.9 | 25.6 | 6.7 | 16.2 | 32.3 | 1.1 |
| Off-Grid Steel Mill | 72.5 | 129.8 | 2.5% | 17.0 | 28.1 | 9.9 | 19.1 | 24.5 | 1.1 |
| Misc. Stationary Sources | 10.7 | 21.3 | 2.8% | 17.6 | 26.2 | 6.5 | 16.4 | 31.9 | 1.1 |
| Autos and Light Trucks | Surface mixed layer | | 0.3% | 17.6 | 25.5 | 8.1 | 17.5 | 29.9 | 1.1 |
| Other Mobile Sources | Surface mixed layer | | 2.5% | 17.5 | 25.7 | 6.1 | 15.9 | 33.4 | 1.1 |

Important Characteristics of that Month:

(a) Average $SO_2$ Oxidation Rate = 5% per hour

(b) Average $SO_4^=$ Concentration = 12 $\mu gm/m^3$

difference to the amount of sulfate appearing in the ground level mixed layer during a two day period. Petroleum coke kilns with their very high effective stack heights succeed in forcing an unusually large amount of their emissions above the mixed layer into the elevated inversion. While this shields emissions from ground level temporarily, it also suppresses $SO_2$ deposition at the ground by a compensating amount. Receptor points close to the source will benefit from this treatment while those farther downwind will not.

Ground level mobile $SO_2$ sources ultimately achieve slightly lower sulfates mass loadings during the winter through enhanced $SO_2$ deposition under conditions of surface-based inversion. Since $SO_2$ concentration is the driving force for $SO_2$ dry deposition, this slight reduction in airborne sulfate mass over the long-term is being achieved at the expense of creating higher than usual $SO_2$ concentrations per ton of emissions. Ground level release of pollutants is not an acceptable route to sulfate air quality control. It does not result in much of a sulfate mass reduction and is likely to create an $SO_2$ or primary $SO_3$ concentration problem close to the source.

The effect of a high fraction sulfates in an elevated source's exhaust can be examined by comparing glass furnaces to metals furnaces. The plume rise characteristics of these source classes are similar, but the glass furnaces release about 18% of their $SO_x$ emissions as $SO_3$ or sulfates. The result is a definite enrichment in sulfates within the mixed layer as compared with a source with lower primary sulfates emissions. This discussion is not intended to single out glass furnaces

as being particularly offensive, since glass furnaces represent a very small fraction of the basin's $SO_x$ emission inventory. The objective is to show that primary $SO_3$ or sulfates emissions from any source should be avoided if possible.

It is concluded that for the historic cases examined here, source specific characteristics such as plume rise or fraction $SO_3$ in a source's exhaust have played a relatively minor role in determining differences between the mass of sulfate contributed by various source classes. The amount of sulfate residing in the mixed layer is most directly related to $SO_x$ emission strength and $SO_2$ oxidation rate. In addition, the concentration of sulfate observed in the air basin depends as much on transport patterns and source location as on reaction rate. The total amount of sulfate found during July 1973 at k = 8% per hour within our hypothetical flow reactor is about double the amount formed in January 1972 at k = 3% per hour. The average sulfate concentrations observed in those two months were comparable because a higher fraction of total $SO_x$ emissions stagnated close to their source in January than in July.

### 5.4.7 Source Class Contributions to Sulfate Air Quality

Contour plots of individual source class contributions to sulfate air quality can help to explain how the air basin becomes so nearly filled by sulfate concentrations of the same general magnitude while emissions remain concentrated in a handful of locations. In many months with a pronounced daily sea breeze/land breeze wind reversal,

air parcel trajectories wander widely over the basin. Sulfur oxides are dispersed within the airshed by the rotation of the wind vectors over time, much as a person stands in the center of his garden and waters the lawn by spraying a hose from side to side. Contours of average sulfate concentration from even the largest point sources can become an amorphous blob under such circumstances as shown in Figures 5.24 through 5.31. It is therefore not surprising that superposition of many such shapeless air quality impacts centered on different source locations leads to a nondescript average sulfate loading of the airshed in such months.

In contrast during the summer, onshore wind flow persists for most of the day. Similar air parcel trajectories are repeated from day to day. Distinct zones of major source influence stretch inland from the coast.

The impact of the power plant complexes at El Segundo and at Alamitos Bay is clearly evident in Figure 5.32. The El Segundo area generating stations lie at the head of a sulfate enrichment which typically passes over downtown Los Angeles and continues inland toward Pasadena in the summer. Emissions from the Alamitos Bay area are predicted to typically pass along the Los Angeles County-Orange County border, through La Mirada, La Habra, and Diamond Bar, and then out the Pomona-Walnut Valley.

Upwind-downwind sulfate concentration gradients along the transport paths downwind of these power plants are fairly small. Lateral

SULFATE AIR QUAILTY INCREMENT DUE TO
ELECTRIC UTILITY BOILERS (μGM/M³)

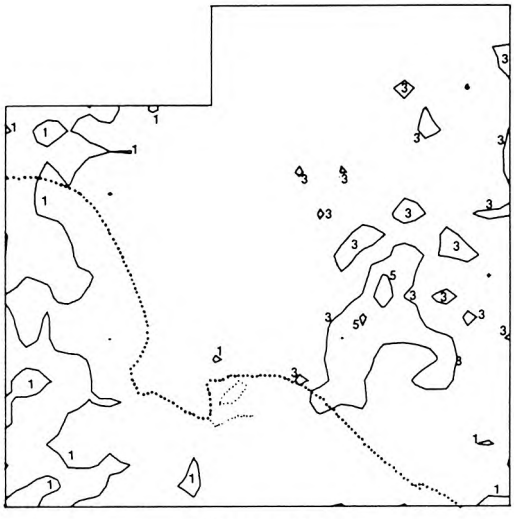

FEBRUARY 1972

FIGURE 5.24

SULFATE AIR QUAILTY INCREMENT DUE TO
OTHER FUEL BURNING SOURCES (μGM/M³)

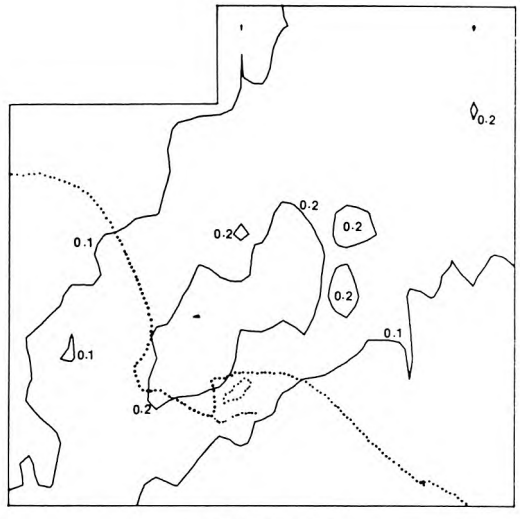


FEBRUARY 1972

FIGURE 5.25

SULFATE AIR QUAILTY INCREMENT DUE TO
CHEMICAL PLANTS (μGM/M³)

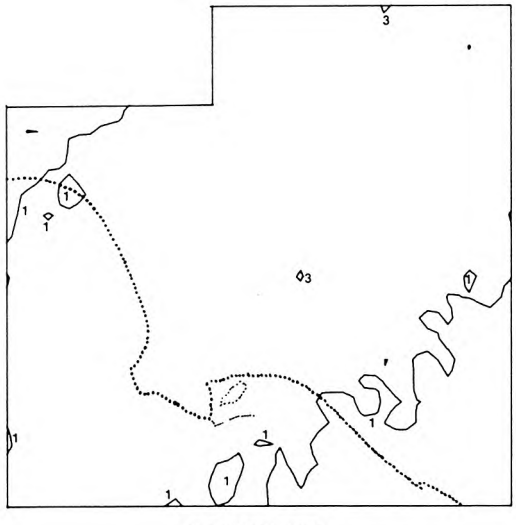

FEBRUARY 1972

FIGURE 5.26

SULFATE AIR QUAILTY INCREMENT DUE TO
PETROLEUM INDUSTRY PROCESSES (μGM/M³)

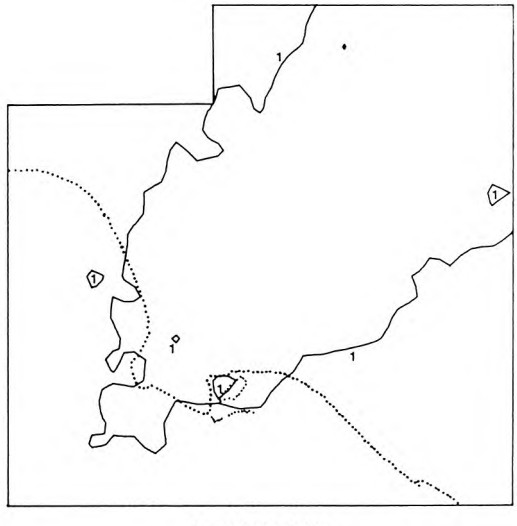

FEBRUARY 1972

FIGURE 5.27

SULFATE AIR QUAILTY INCREMENT DUE TO
MISCELLANEOUS STATIONARY SOURCES (μGM/M³)

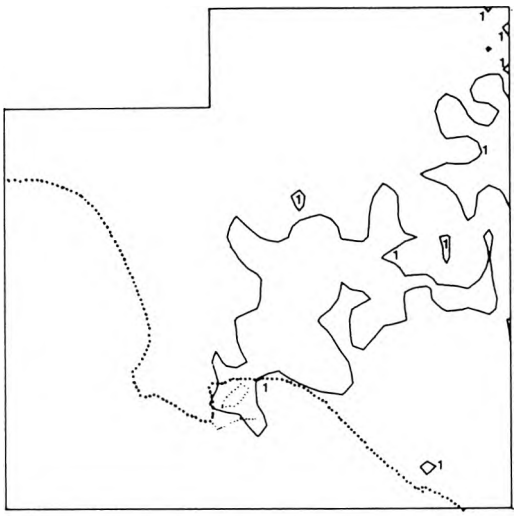

FEBRUARY 1972

FIGURE 5.28

SULFATE AIR QUAILTY INCREMENT DUE TO
AUTOS AND LIGHT TRUCKS (μGM/M³)

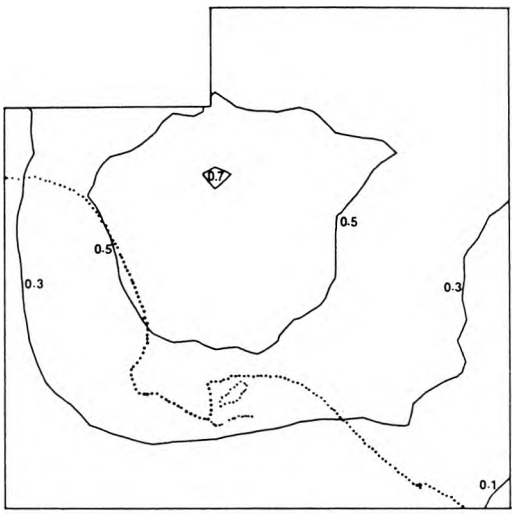


FEBRUARY 1972

FIGURE 5.29

SULFATE AIR QUAILTY INCREMENT DUE TO
OTHER MOBILE SOURCES (μGM/M³)

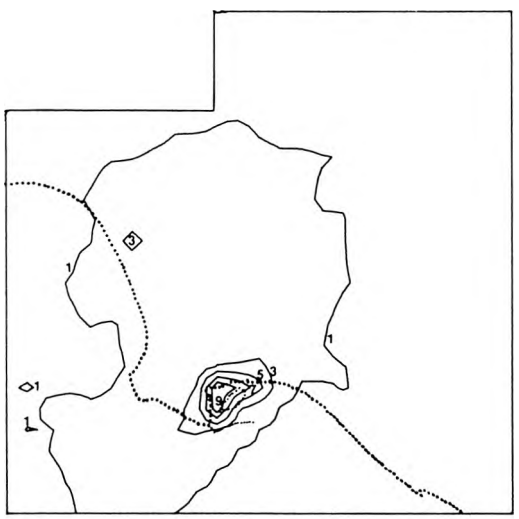

FEBRUARY 1972

FIGURE 5.30

SULFATE AIR QUAILTY INCREMENT DUE TO
ALL SOURCES PLUS BACKGROUND (μGM/M³)

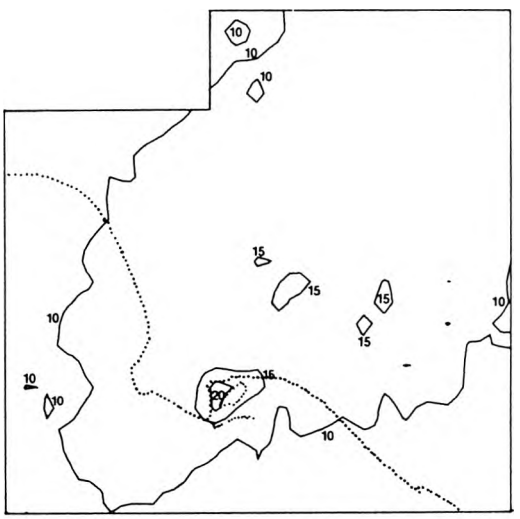

FEBRUARY 1972

FIGURE 5.31

SULFATE AIR QUAILTY INCREMENT DUE TO

ELECTRIC UTILITY BOILERS (μGM/M³)

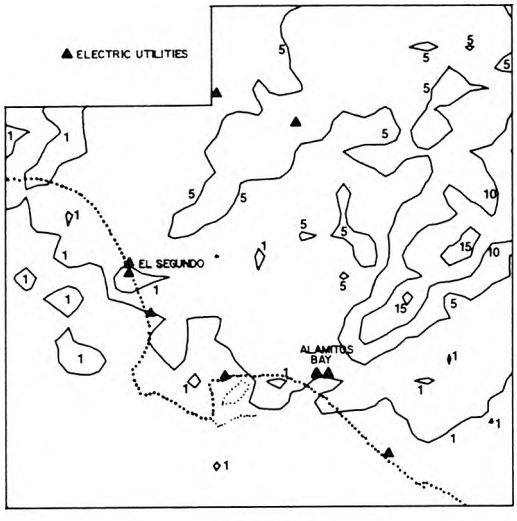


JULY 1973

FIGURE 5.32

SULFATE AIR QUAILTY INCREMENT DUE TO

OTHER FUEL BURNING SOURCES (μGM/M³)

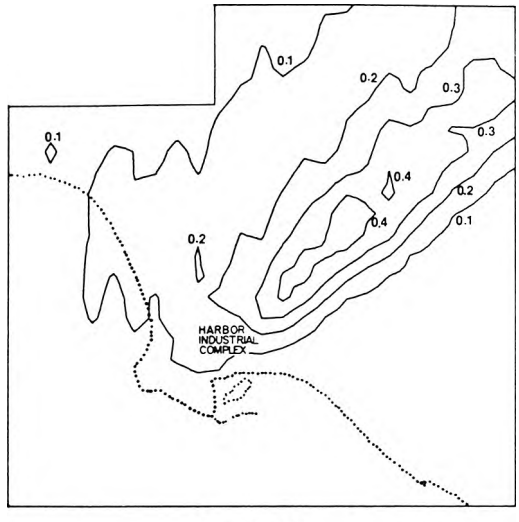


JULY 1973

FIGURE 5.33

SULFATE AIR QUAILTY INCREMENT DUE TO

CHEMICAL PLANTS (μGM/M³)

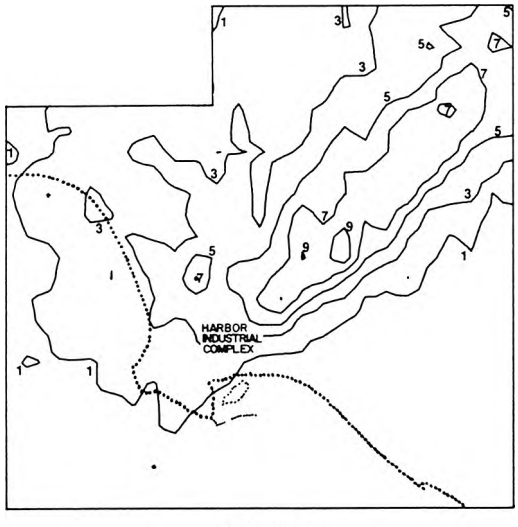


JULY 1973

FIGURE 5.34

SULFATE AIR QUAILTY INCREMENT DUE TO

PETROLEUM INDUSTRY PROCESSES (μGM/M³)

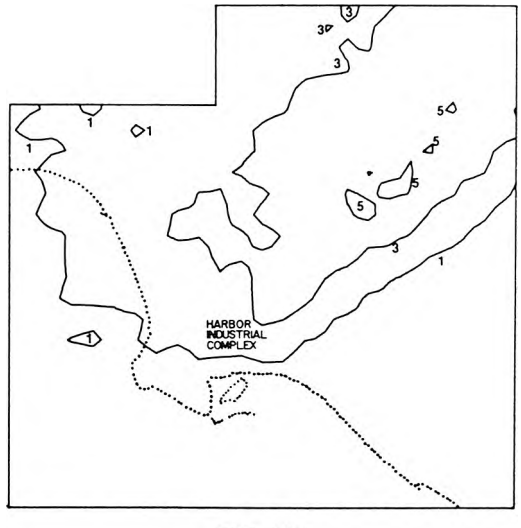


JULY 1973

FIGURE 5.35

SULFATE AIR QUAILTY INCREMENT DUE TO

MISCELLANEOUS STATIONARY SOURCES ( μGM/M³ )

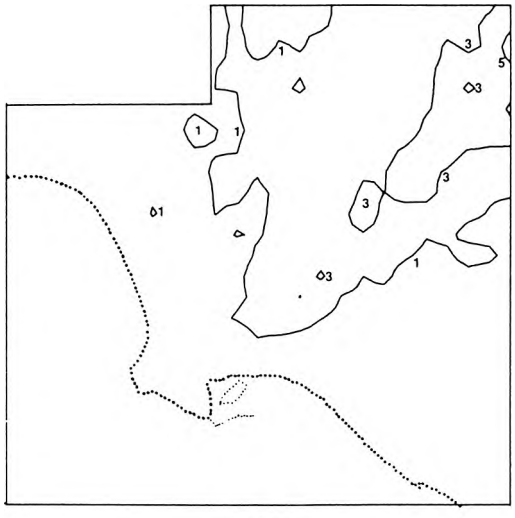


JULY 1973

FIGURE 5.36

SULFATE AIR QUAILTY INCREMENT DUE TO

AUTOS AND LIGHT TRUCKS ( μGM/M³ )

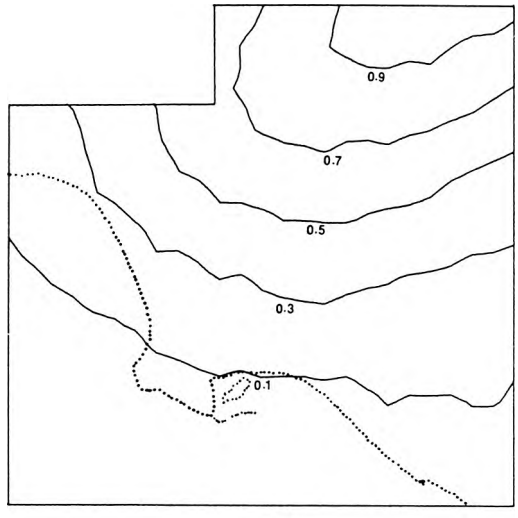


JULY 1973

FIGURE 5.37

SULFATE AIR QUAILTY INCREMENT DUE TO

OTHER MOBILE SOURCES ( μGM/M³ )

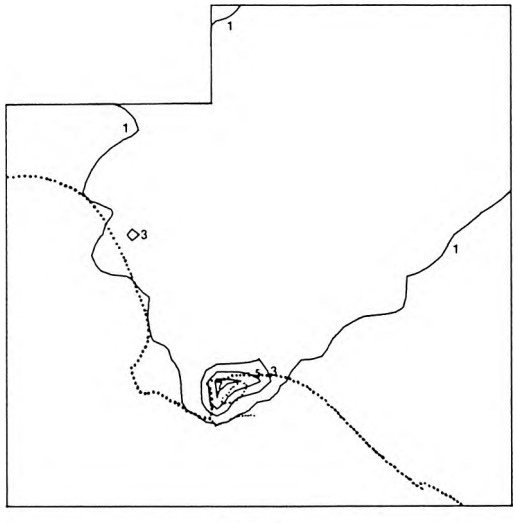


JULY 1973

FIGURE 5.38

SULFATE AIR QUAILTY INCREMENT DUE TO

ALL SOURCES PLUS BACKGROUND ( μGM/M³ )

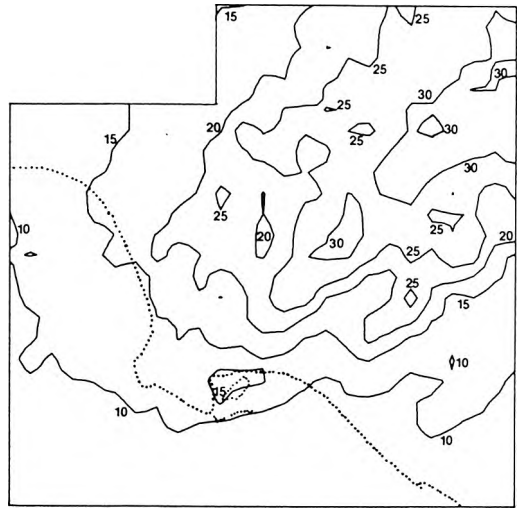


JULY 1973

FIGURE 5.39

spreading acts to reduce sulfate concentrations at a rate nearly sufficient to counteract sulfate formation.

The sulfate enrichment zones downwind of major point sources in July of 1973 are predicted to have a shape which resembles a plume over the long-term average. It should be noted however that the model does not presuppose a plume-like structure, and that in fact the existence of a definite plume from these sources is probably intermittent. Long-term average concentration patterns which resemble a plume trace can be achieved by permitting stagnation of pollutants in the morning, followed by transport of a well-aged air mass across the basin during the day in a way that passes over successive receptor points downwind in a relatively straight line.

The air parcel trajectory calculations within our simulation model were performed by a very approximate method. It is highly possible that source to receptor transport pairs could be misaligned somewhat as a result. However, power plant pollutant transport patterns like those of Figure 5.32 can be checked against the more detailed transport calculations of others with some success. Mid-day and afternoon pollutant transport patterns are heavily weighted when computing the air quality impact of power plant emissions. That is because the diurnal variation of power plant emissions peaks strongly at that time. Drivas and Shair (1975) marked an Alamitos Bay power plant plume with a conserved tracer on numerous mornings and afternoons during October 1973. In nearly every case sampled, Drivas and Shair located that plume within the area indicated by our simulation model.

The gap between the Alamitos Bay and El Segundo area power plant impacts during the summer is filled by the effluent from industries in the harbor area. The major point sources in that area are chemical plants, refinery process operations and petroleum coke calcining kilns.

Automotive emissions are distributed throughout the airshed. As a result, there is little opportunity for effective lateral dispersion of emissions from the source class as a whole. The sulfate air quality impact of automotive emissions becomes more intensive downwind as chemical reactions cause sulfate concentrations to increase within a large dilute air mass. The net transport differences between summer and winter are clearly evident when comparing Figure 5.29 to Figure 5.37. In summer the sulfate peak from downtown traffic is pushed far inland, while in winter, peak concentrations from automobiles occur in west central Los Angeles.

Figures 5.6(b) through 5.16(b) show the source class increments to sulfate air quality calculated at all CHESS and LAAPCD monitoring stations in time series. Those graphs were purposely presented alongside of the comparison of model results to observed sulfate concentrations. This was done so that the reader can easily identify situations where model predictions fall short of observations and thus where sulfate contributions from other unspecified sources are indicated. Source class increments to sulfate levels at NASN monitoring sites are shown in Figures 5.40 through 5.43. NASN stations at downtown Los Angeles, Pasadena and Anaheim are not presented since predictions at

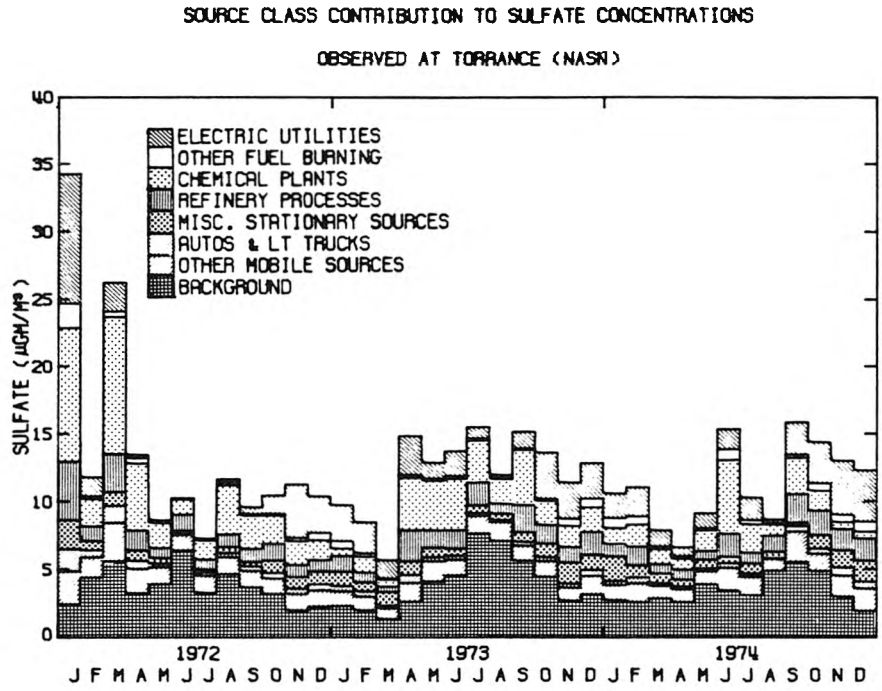


FIGURE 5.40

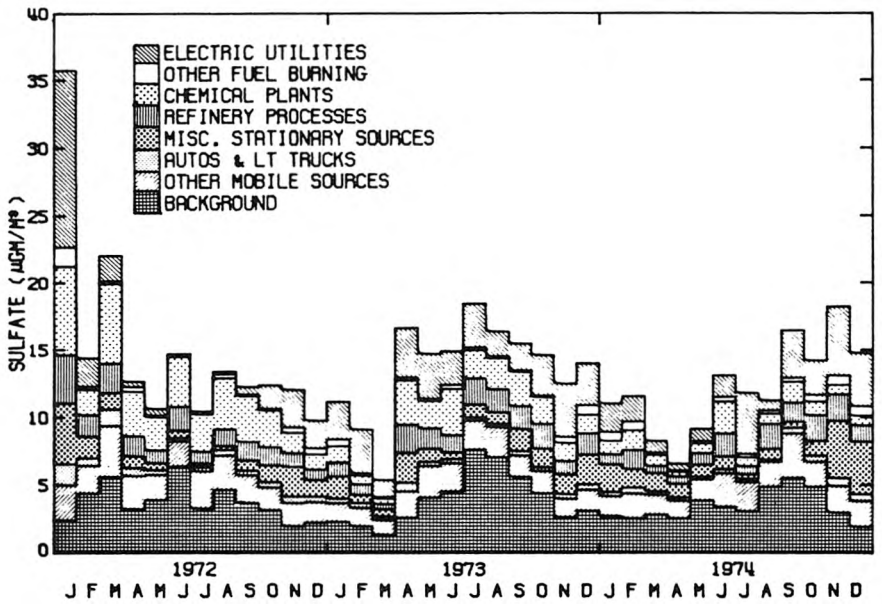


FIGUFE 5.41

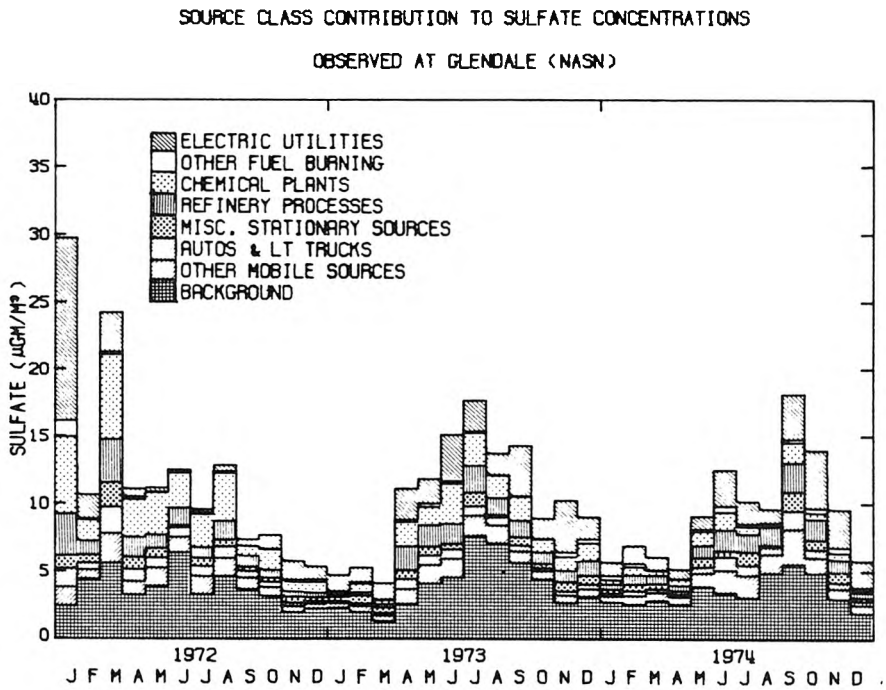


FIGURE 5.42

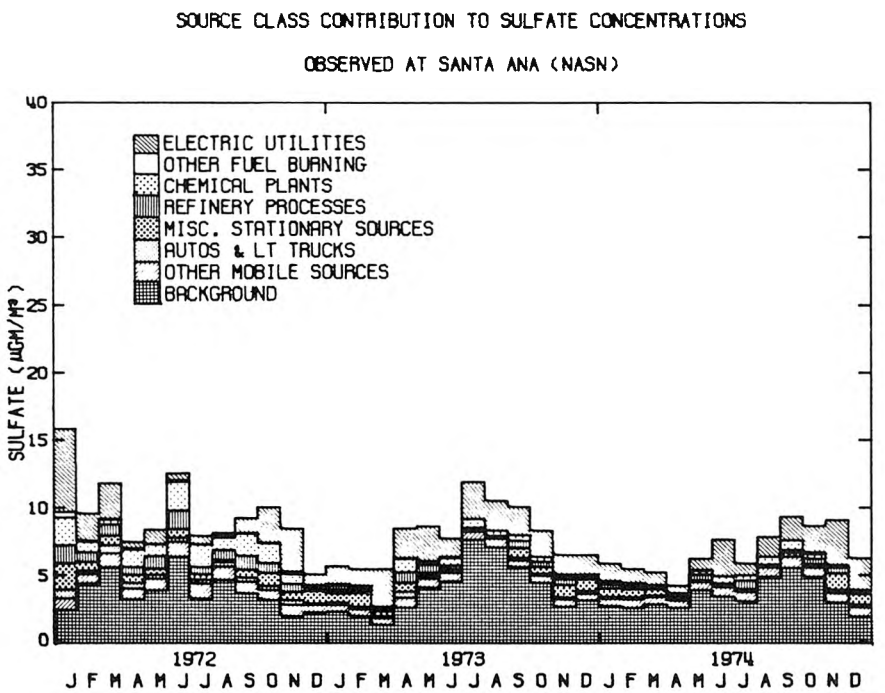


FIGURE 5.43

those locations are substantially the same as at the CHESS or LAAPCD monitoring sites of the same name.

Three to five source classes of about equal impact, plus background sulfates, must be considered simultaneously in order to come close to explaining observed sulfate levels at most locations. The main lesson drawn from these source class contribution estimates is that no single source class dominated sulfate air quality in the Los Angeles Basin during our study period.

Within the last few years, a number of investigators of Los Angeles sulfate air quality have attempted to deduce source to receptor influence relationships for sulfates by regression analysis of emissions and air quality data (Heisler, 1976; Joint Project 1977; White, et al., 1978). Great difficulty was encountered in formulating and validating empirical emissions-air quality relationships that would assist sulfate pollution control strategy analysis. The reason is now fairly clear. Referring to Figure 4.8, we see that most of the source classes responsible for observed sulfate levels have so little variance in their emissions patterns over time that it would be impossible to explain the wide variance in observed air quality on the basis of variance in emissions alone.

The only sources with large well-defined short-term fluctuations in emissions are power plants, and they do not account for enough of the total sulfate burden to dominate the variance in ambient sulfate air quality. However, using statistical techniques plus the lack of a strong correlation between power plant emissions and observed air

quality, White, et al. (1978) derived an upper limit estimate for the contribution of power plant emissions to sulfate air quality at West Covina. They determined that power plant emissions accounted for no more than 17% of the sulfate burden at that location. Our model results at West Covina do not conflict with that estimate. The power plant impact calculated from our simulation model accounts for 17.4% of the total sulfate loading at West Covina, averaged over three years.[6] Power plant impact is proportionately higher elsewhere, however.

It may seem discouraging that no clear cut "cure" for the sulfate problem can be obtained by attacking $SO_x$ emissions from a single source class. However, the situation depicted by the simulation model is not without its positive points. The condition of roughly equal impact from a wide variety of source types leaves the control strategy analyst with the flexibility to generate a wide variety of possibly acceptable emission control strategies. Decision-makers may then choose from among those options on the basis of minimization of emission control costs, flexibility of the control strategy to deal with changing circumstances, or compatibility of the strategy with other simultaneous objectives such as minimization of $NO_x$ emissions or conservation of energy resources.

---

[6] The extremely close agreement of these two estimates is again probably fortuitous. The air quality simulation model is sufficiently complex that we could not have hit a target that closely if we had tried, which we did not.

## 5.5 Summary

The data requirements of the sulfate air quality simulation model were examined. It was found that the number of virtual emissions sources supplied to the air quality model could be greatly reduced through recombination of sources into eleven broad source classes, and through aggregation of point sources located within a common grid square.

The retention time within the 50 by 50 mile square grid for air parcels released from major point source locations was investigated. It was estimated that 95% of those air parcels would be cleared from the grid system within two days (on an annual average basis). Fluctuations above and below that value will occur from month to month, with generally longer than average retention times in some winter months, and shorter than average retention times in most summer months.

The problem of estimating the rate of horizontal eddy diffusion over urban areas was addressed. Estimates for the standard deviation of horizontal plume spread as a function of travel time downwind, $\sigma_y(t)$, were made based on experimental data taken over the urban areas of St. Louis and Los Angeles.

The seasonal variation of sulfate background air quality in the South Coast Air Basin was examined. It was found that data sufficient to dictate the seasonal pattern in sulfate concentrations in incoming marine air for each month of the period 1972 through 1974 are unavailable. The best estimate that could be made of South Coast Air Basin sulfate background levels was obtained by scaling the seasonal

variation in sulfate air quality observed at the most rural air quality station influenced by coastal meteorology (at Vista) to the average magnitude of sulfate concentrations observed at San Nicolas Island.

The remaining data requirements of the model also were satisfied. These include selection of deposition velocities for $SO_2$ and for sulfates, selection of data on wind speed and direction, and specification of inversion base motion over time. It was determined that the overall rate of $SO_2$ oxidation to form sulfates would have to be determined by iteration, and a procedure was outlined for performing those calculations within a highly over-determined system of equations. Finally, a time step for trajectory integration and a receptor cell size were selected.

The air quality dispersion model was applied to Los Angeles sulfate air quality over each month of the years 1972 through 1974. It was found that model results closely reproduced observed sulfate concentration patterns within the central portion of the Los Angeles Basin, particularly during the years 1972 and 1973. The correlation between observed and predicted sulfate levels is 0.82 in both 1972 and 1973, and rises to 0.89 in 1972 if two biased observations are discarded.

A seasonal variation in the overall rate of $SO_2$ oxidation to form sulfates in the Los Angeles atmosphere was inferred from the results of the air quality modeling study. Monthly mean $SO_2$ oxidation rates

of between 0.5% per hour and 3% per hour prevail from October through February of our test years. During the late spring, summer and early fall, $SO_2$ oxidation rates were estimated to jump to an average of about 6% per hour, with individual months ranging ± 2% per hour about that mean value. Those numerical results must be qualified since a better understanding of seasonal trends in background sulfate concentrations or $SO_2$ deposition velocity might alter the outcome somewhat.[7]

Examination of individual source class contributions to sulfate air quality can help to explain how the air basin becomes so nearly filled by sulfate concentrations of the same general magnitude while emissions sources remain clustered in a handful of locations. In winter months with a pronounced daily sea breeze/land breeze wind reversal, sulfur oxides are dispersed within the airshed by the rotation of the wind vectors. In contrast, during mid-summer, onshore flow persists for most of the day. Similar air parcel trajectories are repeated from day to day. However, the sequential siting of major $SO_x$ sources along the coast means that the central portion of the air basin is downwind of one major source group or another at most times. Lateral dispersion of emissions is just about sufficient to balance sulfate formation, with the result that downwind and crosswind pollutant gradients are rather small in spite of the direct inland

---

[7] For a sensitivity study of conversion rate calculation dependence on other airshed parameters, see Roberts (1975).

transport from sources to receptors. Annual mean sulfate concentrations are further smoothed by seasonal transport cycles in which peak sulfate concentrations appeared far inland during the summer and near to the coast during the winter.

In January 1972, extreme resultant wind stagnation occurred during a period of high $SO_x$ emissions. The highest localized sulfate concentration predictions for any month of our three year period occurred at that time. While such extended stagnation is unusual, the fact that it can occur means that sulfate air quality control strategy design must consider avoidance of wintertime as well as summertime pollution episodes in Los Angeles.

Source class increments to predicted sulfate air quality were examined in time series at each air monitoring station. It was found that three to five source classes of roughly equal impact, plus background sulfates, must be considered simultaneously in order to come close to explaining sulfate levels observed at most locations. The implication is that a mixed strategy targeted at a combination of source types will be needed if significant sulfate air quality improvements are to be achieved in this airshed through precursor $SO_x$ control.

# CHAPTER 6

# THE RELATIONSHIP BETWEEN SULFATE AIR QUALITY AND VISIBILITY AT LOS ANGELES

## 6.1 Introduction

The problem at hand is to determine the relationship between atmospheric sulfate concentrations and visibility reduction at downtown Los Angeles over the past decade. Severe visibility deterioration is one of the most readily apparent features of the Los Angeles smog syndrome. During the 25-year period since 1950, prevailing visibilities of less than three miles at relative humidities below 70 percent have been observed at downtown Los Angeles on an average of 100 days per year (Birakos, 1974). Recently completed short-term studies of particulate air quality in relation to visibility (Hidy, et al., 1975; White and Roberts, 1975) indicate that sulfates in the Los Angeles atmosphere are much more effective light scatterers per unit mass than other particulate components, and that sulfates may be responsible for over half of the light scattering at downtown Los Angeles.

The findings of White and Roberts have important implications for a strategy aimed at improving visibility in Los Angeles. A particulate control strategy for the Los Angeles basin proposed by Trijonis, et al. (1975), involving reduction of sulfates and nitrates from annual average levels of 14 micrograms per cubic meter $SO_4^=$ and 12 micrograms per cubic meter $NO_3^-$ to levels of 6.1 and 10 micrograms per cubic meter annual mean, respectively, was estimated to cost

approximately 156 million dollars annually. If such pollution control measures were to be proposed in part on the basis of visibility improvement, it is important to determine if the relationship observed by White and Roberts (1975) is persistent, and not simply an anomaly of the few days on which their samples were taken.

A brief discussion of the causes of light extinction in the atmosphere will serve as the basis for structuring a statistical model for visibility at Los Angeles. The model will then be applied to the routine air monitoring data base of the Los Angeles Air Pollution Control District over the historic period August 1965 through December 1974. Empirical results will be compared to theory and to the more detailed observations of others where possible. Then the model will be used to estimate the impact of reduced levels of particulate sulfates in the atmosphere on the cumulative distribution of daily visibilities at Los Angeles.

## 6.2 Visibility in Theory and by Observation

Attenuation of light intensity, I, by a column of air over distance, x, can be used to define an extinction coefficient, b, for that air parcel in accordance with the Beer-Lambert law:

$$\frac{dI}{I} = -b\, dx \tag{6.1}$$

In his classical visibility theory, Koschmieder (1924) proposed a relationship between this extinction coefficient b (which is a property measurable by instrumental methods) and the maximum distance at which an average individual could distinguish an ideal black object

silhouetted against the horizon sky. By assuming that a contrast level of 0.02 was the lower limit distinguishable to the human eye, Koschmieder was able to define a theoretical maximum visual distance, now known as "meteorological range", $L_v$, by:

$$L_v = \frac{-\ln 0.02}{b} = \frac{3.912}{b} \quad \text{in consistent units.} \tag{6.2}$$

Visibility apparent to an individual observer can differ from Koschmieder's theoretical result due to a number of factors including variation in the observer's visual acuteness and the inhomogeneous illumination of the atmosphere. Thus it is useful to consider a more personal measure of visibility, called "visual range", which is defined as the actual distance at which an ideal black object can just be seen against the horizon sky. To partially account for spatial variation in the optical properties of the atmosphere, daylight visual range observations made in accordance with National Weather Service standards are stated in terms of a "prevailing visibility". Prevailing visibility is defined as the greatest visibility which is attained or surpassed around at least half of the horizon circle, but not necessarily in continuous sectors (Williamson, 1973). A discussion of the possible errors involved in using Koschmieder's formula to estimate visibility apparent to a human observer is given by Horvath (1971). He suggests that by proper selection of visibility markers it should be possible to use the Koschmieder formula to calculate the extinction coefficient from observed visibilities with an error of less than about ten percent.

## 6.3 Relating Visibility to Atmospheric Composition

From expression (6.2), it is seen that the larger the extinction coefficient, b, the lower the expected visibility. This extinction coefficient is depicted by Charlson (1969) as the sum of several components:

$$b = b_{scat} + b_{Rayleigh} + b_{abs\text{-}gas} + b_{abs\text{-}aerosol} \qquad (6.3)$$

where $b_{scat}$ is the contribution due to light scattering by aerosol particles, $b_{Rayleigh}$ is scattering due to air molecules, $b_{abs\text{-}gas}$ is light absorption due to gases like $NO_2$, and $b_{abs\text{-}aerosol}$ represents absorption due to particles such as carbon black. Charlson, et al. (1972) observed that scattering usually dominates light extinction in the Los Angeles area atmosphere, with wavelength-dependent absorption by $NO_2$ being significant about 20 percent of the time.

While the theory of light scattering by aerosols is well advanced, there are practical difficulties in computing the effect of multi-component smog aerosols on visibility from first principles in an urban situation. Extensive information would be needed on the size distribution of the aerosol, its refractive index, particle shape, illumination, humidification of the atmosphere, and the spatial distribution of aerosol mass concentration. However, there is a growing body of empirical evidence suggesting that total suspended particulate mass concentration, TSP, alone is very highly correlated with scattering coefficient measurements and inversely correlated with prevailing visibility. From simultaneous measurements of light scattering and aerosol mass at a variety of locations, Charlson, Ahlquist and Horvath

(1968) reported that:

$$L_v \cdot TSP \equiv \frac{3.9\ TSP}{b} \cong 1.2\ \frac{gm}{m^2} \tag{6.4}$$

or restated in units which we will use later:

$$b \equiv 0.0325 \cdot (TSP) \tag{6.5}$$

where

b is the atmospheric extinction coefficient in units of $[10^4\ m]^{-1}$.

TSP is the total suspended particulate mass in $\mu gm/m^3$.

Visual range observations were correlated with aerosol mass loadings by Noll, Mueller and Imada (1968) and a similar proportionality was found.

Figure 6.1 shows a plot of the ratio of atmospheric light scattering coefficient to mass concentration for a monodisperse aerosol of unit density spherical particles of refractive index 1.5 and diameter $D_p$ (White, Roberts and Friedlander, 1975). Much of the total suspended particulate mass in the atmosphere resides in a large particle mode ($D_p > 1\mu$) whose contribution to light scattering per unit mass concentration is well below that typically observed for the atmosphere as a whole; smaller particles of diameter equal to that of the wavelength of incoming solar radiation in the visible spectrum are the most effective light scatterers. This relatively small fraction of the particulate mass residing in the region around $D_p \cong 0.5$ microns is responsible for the bulk of the light scattering. *If these particles have an identifiable origin, then perhaps a relatively efficient strategy might be proposed for improving visibility in Los Angeles.*

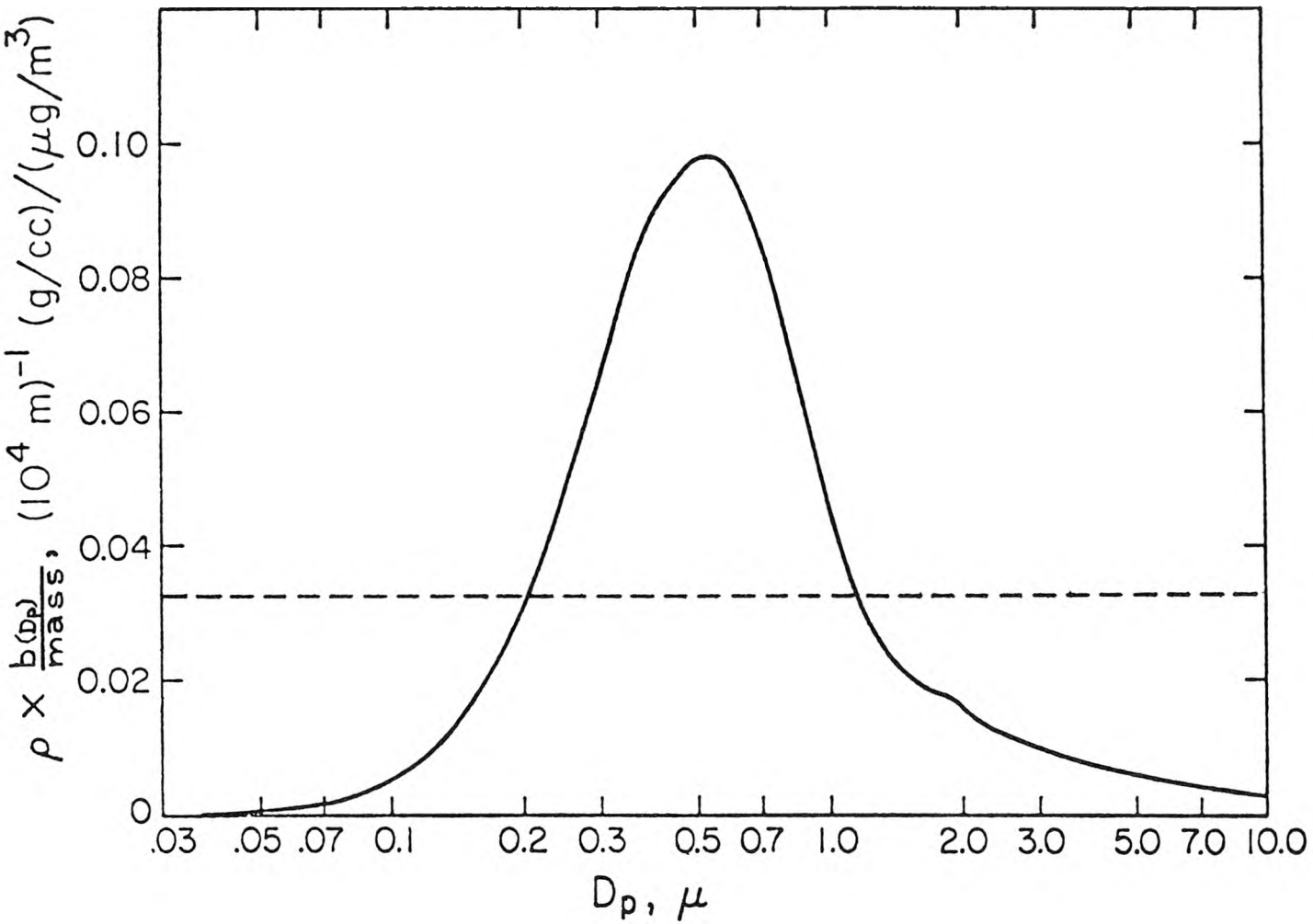


FIGURE 6.1

Normalized light scattering by aerosols as a function of particle diameter, $D_p$. Computed for unit density spherical particles of refractive index 1.5 (White, Roberts and Friedlander, 1975).

In a series of papers, Hidy and Friedlander and their co-workers (Hidy and Friedlander, 1971; Miller, Friedlander and Hidy, 1972; Heisler, Friedlander and Husar, 1973; Gartrell and Friedlander, 1975; Hidy et al., 1975) have examined the chemical composition of Los Angeles area atmospheric aerosols. These studies show that in Los Angeles the bulk of the particulate material in the effective light scattering size range (between one-tenth and one micron particle diameter) consists of sulfate, nitrate and ammonium ion, plus condensed organics. These portions of the atmospheric aerosol are known as secondary particulates because they originate predominantly from the conversion of pollutant gases to particulate matter in the atmosphere rather than from direct emission of dust or fume from natural or man-made sources.

The results of a variety of field investigations of visibility reduction support the proposition that such secondary particulates are largely responsible for atmospheric light extinction. Early studies of visibility reduction at Los Angeles, briefly outlined in Appendix D1, make it clear that such a relationship has been understood at least qualitatively for a long time. The importance of secondary particulates to light scattering is hardly unique to downtown Los Angeles. Eggleton (1969), for example, found a close inverse relationship between ammonium sulfate concentration and visibility in England. Investigations by Lundgren (1970) demonstrated a strong inverse correlation between atmospheric nitrates and visibility at Riverside, California.

In an attempt to isolate the relative importance of various particulate species to light extinction, White and Roberts (1975) examined nine days of simultaneous observations on light scattering in relation to aerosol chemical composition in the Los Angeles area. Their data consisted of 60 two-hour aerosol samples taken by the ACHEX II study (Hidy, et al., 1975) distributed among several locations in the Los Angeles basin along with nephelometer measurements of $b_{scat}$, plus relative humidity readings. They split the aerosol mass into four components: sulfates, nitrates, organics, and total mass less these three distinct chemical fractions. Postulating an additive relationship similar to expression (6.3), they were able to estimate the following dependence of $b_{scat}$ on aerosol mass composition by linear regression techniques:

$$\frac{b_{scat}}{TSP} = 0.032 \pm 0.009 \qquad (6.6)$$

and

$$b_{scat} = 0.025\ (TSP-SULFATES-NITRATES) + 0.074\ SULFATES + (0.025 + 0.049\ RH^2)\ NITRATES - 1.1 \qquad (6.7)$$

$$R = 0.97 = \text{Multiple correlation coefficient}$$

where

| | |
|---|---|
| $b_{scat}$ | is in units of $[10^4\ m]^{-1}$. |
| RH | is relative humidity in (%/100). |
| TSP | is total suspended particulate matter in micrograms per cubic meter. |

SULFATES and NITRATES are taken as $1.3 \cdot SO_4^=$ and $1.3 \cdot NO_3^-$ concentrations (in $\mu gm/m^3$) in order to account for the mass of associated cations (thought to be ammonium ion).

(TSP-SULFATES-NITRATES) thus denotes the non-sulfate, non-nitrate fraction of the total suspended particulate matter.

White and Roberts (1975) concluded that sulfates in the Los Angeles atmosphere are more effective light scatterers per unit mass than other suspended particulate components. Changes in relative humidity seemed to affect only light scattering by nitrates to a statistically significant degree. Furthermore, light scattering by organics could not be distinguished statistically from the relatively ineffective scattering provided by the rest of the non-sulfate, non-nitrate, aerosol components, even though large amounts of organics were found to be present. The relative abundance of the various components of the atmospheric aerosols studied by White and Roberts is shown in Figure 6.2, while the estimated fraction of light scattering due to each component is shown in Figure 6.3 (White, Roberts and Friedlander, 1975).

From a knowledge of aerosol chemical composition, the emission source classes responsible for particulate concentrations at an air monitoring station may be inferred (Friedlander, 1973). Using trace metal concentrations at their monitoring sites as an indicator of pollutant origin, White, Roberts and Friedlander (1975) estimated that half of the light scattering at downtown Los Angeles was due to combustion of fuel oil and refining of crude oil. All but a few percent of the remaining light scattering at that location was attributed to pollutant emissions from automobiles.

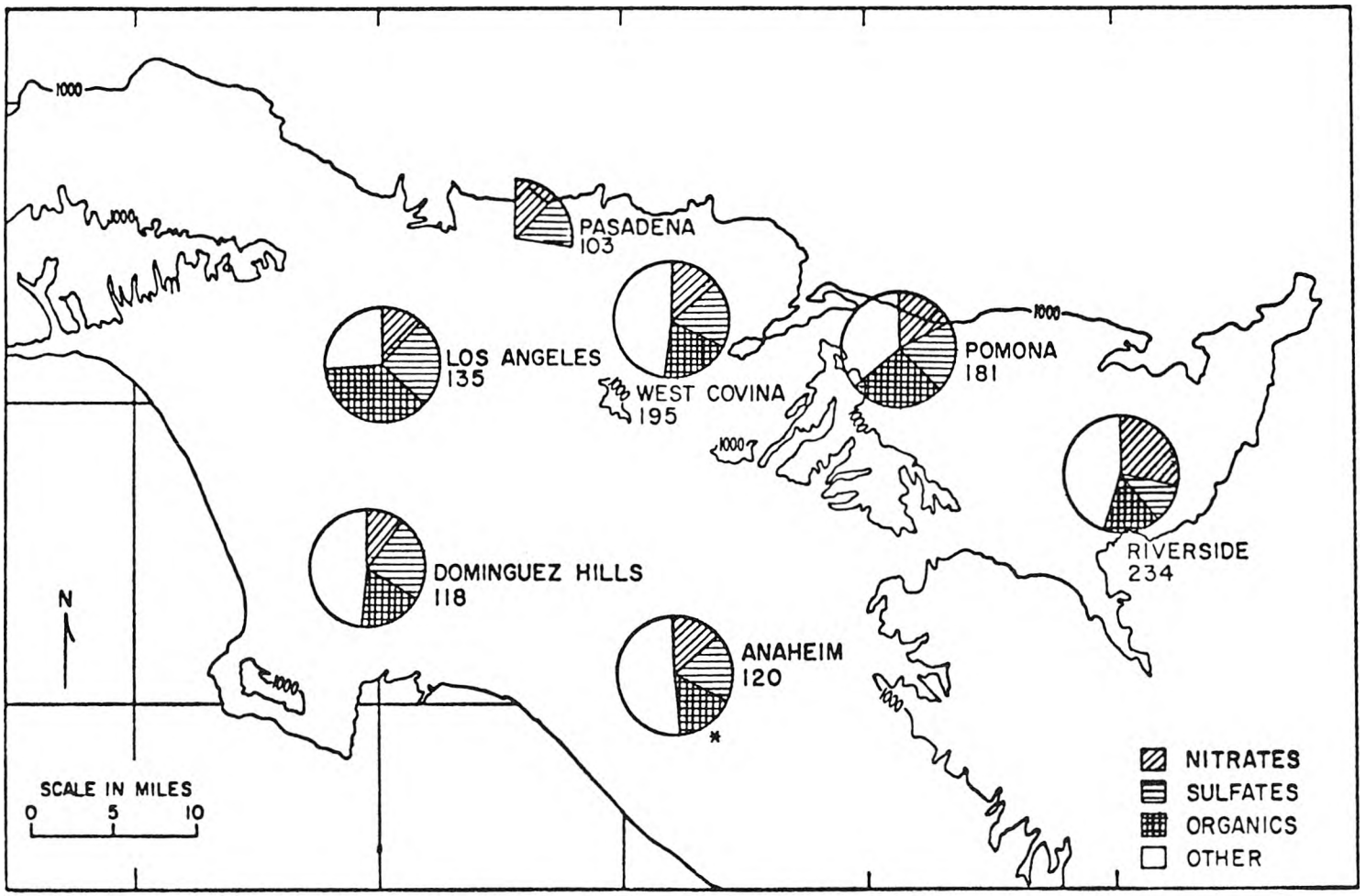


FIGURE 6.2

Division of total suspended particulate mass into its major chemical components on days and at locations covered by the ACHEX 1973 study. Numbers below locations give total suspended particulate mass in micrograms per cubic meter (from White, Roberts, and Friedlander, 1975).

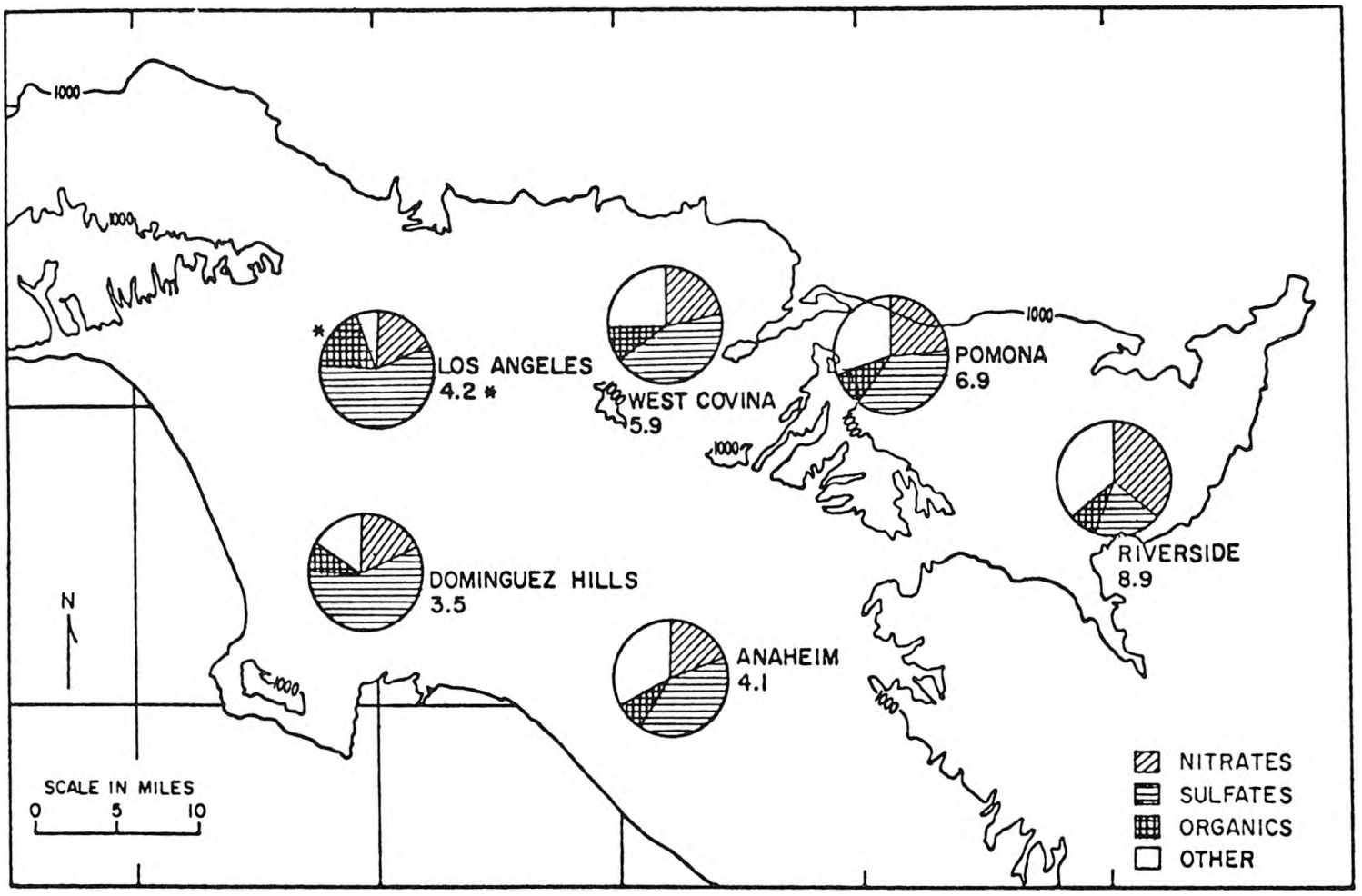


FIGURE 6.3

Attribution of $b_{scat}$ to major components of the atmospheric aerosol at locations covered by the ACHEX 1973 study. Numbers below locations give average $b_{scat}$ in units of $[10^4\ m]^{-1}$. Note the dominance of sulfates at downtown Los Angeles (from White, Roberts, and Friedlander, 1975).

## 6.4 An Investigation of Visibility in Relation to Atmospheric Composition at Downtown Los Angeles: 1965 through 1974

Our first objective is to determine whether the findings of White, Roberts and Friedlander are supported by the long-term historical particulate data base accumulated by the Los Angeles Air Pollution Control District (LAAPCD). Ideally, one would like to be able to make comparisons between continuous records of particulate composition and visibility observations. A high degree of chemical and temporal resolution in the data base would be desired. The historical data base, however, was not designed with this particular experiment in mind. Total suspended particulate matter samples have been collected by the LAAPCD at downtown Los Angeles by high volume sampling on a regular basis since August 1965. The sampling period is 24 hours in duration. Duplicate samples are taken simultaneously on a pair of matched Staplex Hi Vols. Gravimetric determination of total suspended particulate matter collected is made after filter equilibration at low relative humidity. At least one sample taken from each pair of filters is analyzed for sulfates, nitrates, and seven metals. Sulfates are determined by the turbidimetric method and nitrates by the xylenol method. At various times during the history of the sampling program, sampling frequency has ranged from weekly, to twice weekly, to every fifth day. From August 1965 through August 1970, samples were taken from 8:00 am to 8:00 am. Since that time, all samples were taken from midnight to midnight. The Air Pollution Control District's particulate sampling program is more fully described in a series of papers by MacPhee and Wadley (1972 through 1975).

Since July 1964, prevailing visibility observations have been taken at the downtown headquarters of the LAAPCD. Observations are made from the roof of a building at 80 feet above ground level, at the same location and elevation as the high volume samplers. A typical daily record consists of nine consecutive hourly observations beginning at 8:00 am civil time and ending at 4:00 pm civil time. Weekend observations often are not taken. Relative humidity data are available, usually for 14 daylight hours. Hourly observations on $NO_2$ concentrations (which could reduce visibility by absorption) have been taken at the same location by the automated continuous Saltzman method (Mills, Holland and Cherniack, 1974).

The temporal relationship between available useful observations is shown in Figure 6.4. There is clearly no way to adjust the historical data base to place 24-hour integrated particulate concentrations into exactly the same time frame as the daylight visibility observations. The best that can be done is to integrate the visibility observations for the longest period of time available within each particulate sampling event. Our mathematical treatment must take the available data into account. Suppose that we return to expression (6.3):

$$b = b_{scat} + b_{Rayleigh} + b_{abs\text{-}gas} + b_{abs\text{-}aerosol} \qquad (6.8)$$

Making the assumption that $L_v$ equals prevailing visibility, V, at any instant, i, observations on the left hand side of (6.8) can be obtained from existing data by use of Koschmieder's formula as follows:

$$b_i \cong \frac{24.31}{V_i} \quad \text{for conversion of } V_i \text{ in miles to } b_i \text{ in } [10^4 \text{ meters}]^{-1} \qquad (6.9)$$

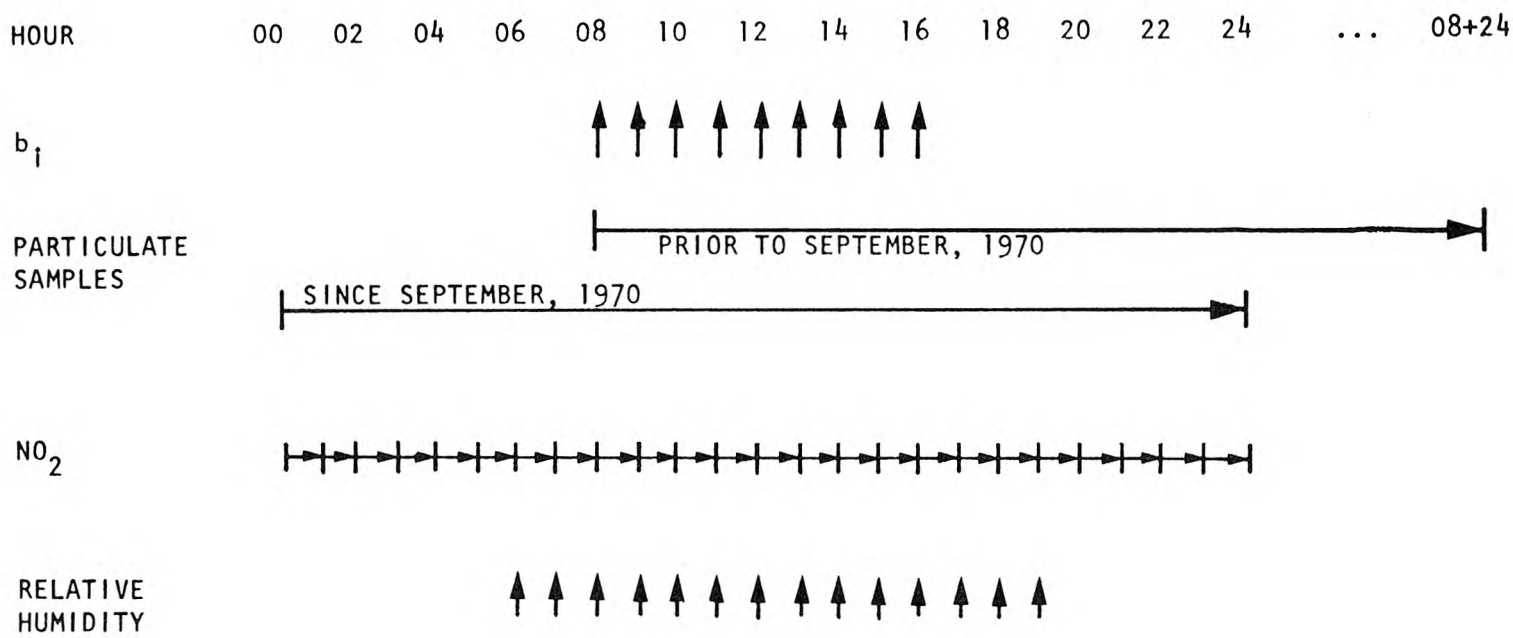


FIGURE 6.4

Temporal relationship between routine air monitoring observations. Averaging times indicated between arrows (⟶). Instantaneous readings indicated by (↑).

where i now refers to the $i^{th}$ hour of the day. After White and Roberts, we further assume that $b_{scat_i}$ can be represented as the sum of the extinction contributions of distinct chemical subfractions of the measured particulate, plus associated water. Since prevailing visibility takes into account aerosol light extinction due to both scattering and absorption, we assume:

$$b_{scat_i} + b_{abs\text{-}aerosol_i} = \sum_m \beta_{m_i} M_{m_i} \tag{6.10}$$

where

$\beta_{m_i}$ = the extinction coefficient per unit mass of the $m^{th}$ particulate chemical species at time i.

$M_{m_i}$ = the mass concentration of the $m^{th}$ particulate chemical species at time i.

And similarly for light absorption by gases

$$b_{abs\text{-}gas_i} = \sum_n \gamma_{n_i} C_{n_i} \tag{6.11}$$

where

$\gamma_{n_i}$ = the extinction coefficient per unit volumetric concentration of the $n^{th}$ gaseous chemical species at time i.

$C_{n_i}$ = the volumetric concentration of the $n^{th}$ gaseous chemical species at time i.

Averaging over the t hours of visibility observations in a day, we obtain:

$$\frac{1}{t}\sum_{i=1}^{t} b_i = \frac{1}{t}\sum_{i=1}^{t}\sum_m \beta_{m_i} M_{m_i} + \frac{1}{t}\sum_{i=1}^{t}\sum_n \gamma_{n_i} C_{n_i} + b_{Rayleigh} \tag{6.12}$$

where $b_{Rayleigh}$ is taken as constant. Let $\bar{M}_m$ be the available 24-hour average concentration of particulate species m. Let $M_{m_i}$ be decomposed into the sum of a 24-hour mean value plus a fluctuating component:

$$\beta_{m_i} M_{m_i} = \beta_{m_i} (\bar{M}_m + M'_{m_i}) \tag{6.13}$$

Forming a t hour daylight average corresponding to our period of visibility observations, and rearranging:

$$\frac{1}{t} \sum_{i=1}^{t} \beta_{m_i} M_{m_i} = \frac{1}{t} \sum_{i=1}^{t} \beta_{m_i} \bar{M}_m + \frac{1}{t} \sum_{i=1}^{t} \beta_{m_i} M'_{m_i} \tag{6.14}$$

For ease of notation, the last term on the right side of expression (6.14) will be referred to as $\delta_m$, the daily residual difference between the average of $\beta_m M_m$ and the product of the separate averages of $\beta_m$ and $M_m$. Summing (6.14) over the particulate species and assuming that light absorption per unit concentration by pollutant gases is unchanging over time, we may substitute into (6.12) and rearrange to get

$$\bar{b} = \frac{1}{t} \sum_{i=1}^{t} b_i = \sum_m \frac{1}{t} \sum_{i=1}^{t} \beta_{m_i} \bar{M}_m + \sum_n \gamma_n \frac{1}{t} \sum_{i=1}^{t} C_{n_i} + b_{Rayleigh} + \sum_m \delta_m \tag{6.15}$$

## 6.5 The Models Estimated

Following the practice of previous investigators, and as a rough check on the visibility and total suspended particulate data (TSP), a purely linear relationship will be fit between undifferentiated aerosol mass and light extinction similar to equation (6.6):

$$\bar{b}_j = \beta_{TSP} \cdot TSP_j + \alpha \cdot DUMMY_j + A + \varepsilon_j \tag{6.16}$$

As used above, $\bar{b}_j$ is the average extinction coefficient for t hours of visibility data (nominally t = 9) on any day, j, as estimated from prevailing visibility by Koschmieder's formula. Only a single particulate species is considered, and light extinction per unit particulate

concentration, $\beta_{TSP}$, is taken as an undetermined constant. Light absorption by gases is neglected. In this model and those that follow, a dummy variable, $DUMMY_j$, has been introduced to capture any effect on equation fit due to the change in particulate sampling schedule previously noted to have occurred beginning in September 1970. $DUMMY_j$ will be taken as unity for all samples prior to September 1970, and zero for all samples taken thereafter. The term $b_{Rayleigh}$ is absorbed into the regression constant, A, in equation (6.16). For the time being we will assume that the residual difference term $\sum_m \delta_m$ from equation (6.15) has mean zero and random fluctuation about its mean, and thus will be absorbed into the daily residual, $\varepsilon_j$. This assumption is not likely to be strictly correct, as will be discussed later.

Results of the regression of extinction coefficient on total suspended particulate concentration alone are shown in Table 6.1.[1] Referring to the second entry of Table 6.1, we see that the estimated light scattering coefficient per unit total suspended particulate concentration is virtually identical to that found by the short-term study of White and Roberts (1975), as shown in equation (6.6). The coefficient $\beta_{TSP}$ is significantly different from zero with greater than 99 percent confidence, while the constant term, A, was <u>not</u> significantly different from zero at any reasonable confidence level. However, the

---

[1] All computations shown in Tables 6.1 and 6.2 were performed using the double precision ordinary test squares stepwise regression package of the MAGIC data handling program maintained on the Caltech IBM 370/158 computer by R. C. Y. Koh. Data base preparation is detailed in Appendix D2 along with a statistical description of the data used.

TABLE 6.1

Linear Regression Model Used to Test the Relationship Between Total Suspended Particulate Matter Concentrations and Light Extinction in the Los Angeles Atmosphere

Model Estimated: $\bar{b}_j = \beta_{TSP} \cdot TSP_j + \alpha \cdot DUMMY_j + A + \varepsilon_j$

| Entry Number | Time Period | Number of Observations | $\bar{b}_j$ ($\bar{b}_j$ Average Variance) | $\beta_{TSP}$ | Coefficients (Standard Error) $\alpha$ | A | Correlation Coefficient (Variance of Residual) |
|---|---|---|---|---|---|---|---|
| 1. | 8/65 thru 12/74 | 413 | 6.62 (30.52) | 0.037 (0.0043) | 1.023 (0.498) | 0.154 NS | 0.40 (25.53) |
| 2. | 9/70 thru 12/74 | 199 | 6.01 (18.19) | 0.032 (0.0044) | N/A | 1.034 NS | 0.45 (14.41) |

Legend: N/A means that the dummy variable is not applicable in a regression involving only data taken after the change in particulate sampling schedule.

NS means not significantly different from zero at a 95% confidence level.

total fit of the model, as judged by the reduction in residual variance, is unimpressive. Twenty-four hour total suspended particulate concentration values alone are not a very precise estimator of daylight visibility reduction in the Los Angeles area.

Next, by analogy to equation (6.15), a series of regression models are proposed to explain the average light extinction coefficient, $\overline{b}_j$, on any day j at downtown Los Angeles as a detailed function of atmospheric composition. These models differ only in the means of incorporating relative humidity effects into the structure of the model.

Of necessity, in light of the available data, it is assumed that division of the particulate samples into SULFATES, NITRATES, and (TSP -SULFATES-NITRATES) is sufficient to capture the major light scattering differences among these particulate components which can be resolved on the basis of chemical analysis. It is further assumed that $NO_2$ is the only light absorbing gas of major significance to light extinction in the Los Angeles Basin.

Incorporation of relative humidity into our model poses several potentially serious problems. As relative humidity rises, hygroscopic and deliquescent particles pick up associated water and grow in size. Usually, this humidity-induced growth of an atmospheric aerosol is accompanied by an increase in light scattering which is not necessarily linear in relative humidity.[2] Three different approaches will be tried in an attempt to deal with the relative humidity effect.

---

[2]Growth associated with increased humidification may also affect atmospheric chemistry, for example, by providing a larger volume of the solution phase as a site for liquid phase reactions.

In the first case, a baseline for comparison of relative humidity-dependent models is established. The suspected non-linearity is disregarded, and a purely linear model is proposed:

$$\overline{b}_j = \beta_{SULFATES} \cdot SULFATES_j + \beta_{NITRATES} \cdot NITRATES_j + \beta_{(TSP-SULFATES-NITRATES)} \cdot (TSP-SULFATES-NITRATES)_j + \gamma_{NO_2} \cdot \overline{NO_2}_j + \Delta_{RH} \cdot \overline{RH}_j + \alpha \cdot DUMMY_j + A + \varepsilon_j. \quad (6.17)$$

In this simple model, the light scattering coefficients per unit concentration, $\beta_m$ and $\gamma_{NO_2}$, are taken to be undetermined constants, and the difference between light extinction on a high vs. low humidity day is captured by the undetermined coefficient, $\Delta_{RH}$, applied to the daytime average relative humidity.

When the chemically resolved linear model of equation (6.17) is estimated for the entire range of available average relative humidities (Table 6.2, entries 1 and 2), a substantial improvement in explanatory power is achieved over the total suspended particulate model of equation (6.16). Sulfates and $NO_2$ are implicated as major contributors to visibility reduction at downtown Los Angeles. As expected, increasing relative humidity is related to increasing light extinction, as shown by the significant t test on the coefficient $\Delta_{RH}$. The estimated light extinction coefficients per unit concentration for NITRATES and (TSP -SULFATES-NITRATES) are at least an order of magnitude lower than that for SULFATES. In the case of NITRATES, the coefficient is not significantly different from zero at any reasonable confidence level for either time grouping tested. The constant term, A, is significantly

# TABLE 6.2

## Chemically Resolved Linear Regression Model
## Relating Pollutant Concentrations to Light Extinction in the Los Angeles Atmosphere

MODEL ESTIMATED:

$$\bar{b}_j = \beta_{SULFATES} \cdot SULFATES_j + \beta_{NITRATES} \cdot NITRATES_j + \beta_{(TSP-SULFATES-NITRATES)} \cdot (TSP-SULFATES-NITRATES)_j + \gamma_{NO_2} \cdot \overline{NO}_{2_j} + \Delta_{RH} \cdot \overline{RH}_j + \alpha \cdot DUMMY_j + A + \epsilon_j$$

| ENTRY NO. | TIME PERIOD | NUMBER OF USABLE OBSERVATIONS (Comments) | $\bar{b}_j$ Average ($\bar{b}_j$ Variance) | COEFFICIENTS (Standard Error) $\beta_{SULFATES}$ | $\beta_{NITRATES}$ | $\beta_{(TSP-SULFATES-NITRATES)}$ | $\gamma_{NO_2}$ | $\Delta_{RH}$ | $\alpha$ | A | Correlation Coef. (Variance of Residual) |
|---|---|---|---|---|---|---|---|---|---|---|---|
| 1. | 8/65 thru 12/74 | 413 | 6.62 (30.52) | 0.173 (0.015) | 0.014 (0.019) NS | 0.0080 (0.0043) $S_{90}$ | 38.30 (4.42) | 8.30 (1.27) | 2.89 (0.38) | -7.37 (0.93) | 0.76 (12.70) |
| 2. | 9/70 thru 12/74 | 199 | 6.01 (18.19) | 0.161 (0.012) | -0.016 (0.013) NS | 0.0080 (0.0034) | 29.79 (3.69) | 4.33 (1.22) | N/A | -3.53 (0.84) | 0.86 (4.62) |
| 3. | 8/65 thru 12/74 | 406 (seven observations with $\bar{b}_j$ > 20 removed) | 6.20 (15.84) | 0.157 (0.009) | -0.017 (0.011) NS | 0.0152 (0.0026) | 24.99 (2.66) | 6.36 (0.76) | 1.85 (0.23) | -4.98 (0.56) | 0.85 (4.35) |
| 4. | 8/65 thru 12/74 | 390 (visibility data used only when RH not > 70%) | 5.65 (14.68) | 0.134 (0.0096) | -0.0063 (0.0116) NS | 0.013 (0.0026) | 28.57 (2.63) | 6.14 (0.95) | 1.79 (0.24) | -4.84 (0.61) | 0.82 (4.63) |
| 5. | 9/70 thru 12/74 | 192 (visibility data used only when RH not > 70%) | 5.18 (13.08) | 0.139 (0.011) | -0.0098 (0.0115) NS | 0.0040 (0.0030) NS | 29.17 (3.05) | 2.78 (1.28) | N/A | -2.13 (0.76) | 0.86 (3.39) |

Legend: All coefficients are significantly different from zero with greater than 95% confidence unless otherwise indicated.

NS means not significantly different from zero at a 95% confidence level.

$S_{90}$ means significantly different from zero with greater than 90% confidence.

N/A means that the dummy variable is not applicable in a regression involving only data taken after the change in particulate sampling schedule.

less than zero in all years tested. This is not too surprising since an attempt to fit a linear function to a non-linear phenomenon will likely result in the numerous days of high light extinction at higher relative humidities dominating the location of the intercept, rather than the few days of extremely good visibility which should fall close to the origin of our coordinate system.

Upon examination of the extinction coefficient data, it was observed that roughly half of the variance of $\overline{b}_j$ was contributed by a few very high values from among the 413 available samples. For example, on January 21, 1970, prevailing visibility ranged from 0.2 miles to 0.8 miles during the day, while relative humidity for the daylight hours averaged 87 percent, indicating a high likelihood of stabilized fog. The effect of deleting such observations from the data base was investigated. Discarding the data for all seven days over the nine-year period for which $\overline{b}_j$ exceeded 20 x $[10^4 \text{ m}]^{-1}$, then re-estimating the previous model, the results shown in entry 3 of Table 6.2 are obtained. The coefficients in this model are similar to those of entry 2 of Table 6.2 which employed all of the data available since the change in sampling schedule in August of 1970. All coefficients except $\beta_{\text{NITRATES}}$ are significantly different from zero with greater than 99 percent confidence. The t statistic on $\beta_{\text{SULFATES}}$ is very large.

The second approach taken to dealing with the relative humidity effect is to attempt to remove the non-linearity by selecting only those observations which occur at low relative humidity. Equation (6.17) will again be the basis for the model, but this time daily

visibility, humidity, and $NO_2$ averages will be computed only for those hours in the day for which relative humidity was not greater than 70 percent. Data for days of persistent high humidity will be discarded.

When the chemically resolved linear model of equation (6.17) is applied to the low humidity data base, the relationships outlined in Table 6.2 entries 4 and 5 are found. The size of the relative humidity effect has been reduced, but not eliminated, as shown by comparison of $\Delta_{RH}$ between corresponding entries 1 and 4, as well as between entries 2 and 5 of Table 6.2. The size of the coefficient $\beta_{SULFATE}$ has been reduced to a lower value of between 0.139 and 0.134 $[10^4 \text{ m}]^{-1}$ per $\mu gm/m^3$ when the higher humidity observations are eliminated, a trend which was not unexpected. The fit of the low humidity model is comparable to that obtained in the regressions of entries 2 and 3 of Table 6.2.

A third model which attempts to deal directly with the physical basis of the relative humidity effect is proposed as follows. The radius of a hygroscopic particle in equilibrium with a surrounding humid atmosphere is determined by a competition between the vapor pressure raising effects of particle surface curvature and the vapor pressure lowering effect of dissolved substances in the particle. Neiburger and Wurtele (1949) used this fact to develop a model for correlating light scattering with relative humidity over a broad range of relative humidities. Their analysis shows that particle radius, $r_p$, should as a rough approximation be dependent on solute mass, $m_s$, and relative humidity as follows:

$$r_p = K[m_s/(1-RH)]^{1/3} \tag{6.18}$$

where K is a parameter of the dissolved substance which is approximately constant over a broad range of temperature and solute concentration. Approximation of changes in particle size by a hyperbolic function of relative humidity, though not strictly correct, provides a practical basis for non-linear regression analysis without introducing an excessive number of degrees of freedom into the curve-fitting processes. A brief summary of Neiburger and Wurtele's derivation is contained in Appendix D3.

Neiburger and Wurtele were concerned with large sea salt particles of several microns in diameter. They noted that for a given particle number concentration and solute mass per particle, light scattering by large particles should increase as the cross-sectional area of the aerosol, and thus light scattering should be correlated with relative humidity as $(1-RH)^{-2/3}$. Our case of interest is considerably more complicated than Neiburger and Wurtele's hypothetical behavior of uniform sea salt solution droplets. As previously mentioned, the bulk of the soluble salts in the atmosphere at downtown Los Angeles is thought to consist of sulfate and nitrate compounds. These particles are found predominantly in submicron size ranges where the Mie theory of light scattering would not predict a simple dependence of light scattering on particle cross-sectional area as was the case with Neiburger and Wurtele's larger sea salt nuclei. However, Hidy, et al. (1975) have shown empirically that light scattering by submicron aerosols is well correlated with total submicron aerosol volume. Thus

it is expected that light scattering by a hygroscopic submicron aerosol will correlate well with changes in particle radius cubed. If it is assumed that total suspended solute mass concentration changes from day to day are proportional to changes in total particle number concentration, with the relative shape of the size distribution of dry solute nuclei remaining unchanged from day to day, then light scattering by SULFATES and NITRATES might be fit by a regression model containing the terms $\beta_{SO_4} \cdot (1\text{-RH})^{-1} \cdot$SULFATES and $\beta_{NO_3} \cdot (1\text{-RH})^{-1} \cdot$NITRATES.

Treatment of the effect of relative humidity on the non-SULFATE, non-NITRATE portion of the total suspended particulate matter is complicated by lack of detailed information on its chemical composition. Much of the remaining particulate mass is thought to reside in larger size ranges where light scattering per particle should be proportional to particle cross-sectional area. If the particles were hygroscopic, then a dependence of light scattering on relative humidity of $(1\text{-RH})^{-2/3}$ would be indicated, similar to Neiburger and Wurtele's sea salt droplets. If the particles are hydrophobic, then no dependence on relative humidity is expected, and the term (1-RH) would be raised to the zero power. In all likelihood, the atmospheric aerosol contains a mix of both types of large particles, and thus some intermediate behavior would be found to represent the relative humidity dependence of best fit. Therefore, our third regression model will be formulated as:

$$\bar{b}_j = \beta_{SO_4} \cdot \left\{ \frac{1}{t} \sum_{i=1}^{t} (1-RH_i)^{\Delta_{SO_4}} \right\}_j \cdot SULFATES_j + \beta_{NO_3} \cdot \left\{ \frac{1}{t} \sum_{i=1}^{t} (1-RH_i)^{\Delta_{NO_3}} \right\}_j \cdot NITRATES_j$$

$$+ \beta_{(TSP-SULFATES-NITRATES)} \cdot \left\{ \frac{1}{t} \sum_{i=1}^{t} (1-RH_i)^{\Delta_P} \right\}_j \cdot (TSP-SULFATES-NITRATES)_j$$

$$+ \gamma_{NO_2} \cdot \overline{NO}_{2_j} + \alpha \cdot DUMMY_j + A + \varepsilon_j \qquad (6.19)$$

where each symbol is as previously defined, except that the $\Delta_m$ are now undetermined exponents applied to the relative humidity dependence of light scattering by aerosol species m.

The non-linear model of equation (6.19) is not suitable to fitting by ordinary least squares regression procedures. Therefore the results of Table 6.3 were obtained by minimizing the sum of the squared residuals by the algorithm suggested by Marquardt (1963) as implemented by the Caltech computing center subroutine LSQENP.

Entry 1 of Table 6.3 begins with a test of our prior beliefs about the relative humidity dependence of light scattering by various types of aerosol species. The exponents $\Delta_{SO_4}$ and $\Delta_{NO_3}$ are initially set equal to -1.0 reflecting the expected correlation between submicron aerosol volume and light scattering. The exponent $\Delta_p$ is first set equal to -0.667 as would be the case if total suspended particulate matter resided in large particles which could grow in size with increasing humidification. The fit achieved is comparable to that of the linear model of entry 1, Table 6.2 fitted to the same data base. The only coefficient which is not of the expected sign appears to be

TABLE 6.3

Non-linear Regression Model Incorporating the Relative Humidity Effect on Light Scattering by Hygroscopic Particulate Matter in the Los Angeles Atmosphere

MODEL ESTIMATED:

$$\bar{b}_j = \beta_{SO_4} \cdot \left(\frac{1}{t}\sum_{i=1}^{t}(1-RH_i)^{\Delta_{SO_4}}\right)_j \cdot SULFATES_j + \beta_{NO_3} \cdot \left(\frac{1}{t}\sum_{i=1}^{t}(1-RH_i)^{\Delta_{NO_3}}\right)_j \cdot NITRATES_j + \beta_{(TSP-SULFATES-NITRATES)} \cdot \left(\frac{1}{t}\sum_{i=1}^{t}(1-RH_i)^{\Delta_p}\right)_j \cdot (TSP-SULFATES-NITRATES)_j + \gamma_{NO_2} \cdot \overline{NO}_{2_j} + \alpha \cdot DUMMY_j + A + \epsilon_j$$

TIME PERIOD: August 1965 through December 1974

NUMBER OF USABLE OBSERVATIONS = 413

| ENTRY NO. | COMMENTS | $\bar{b}_j$ Average ($\bar{b}_j$ Variance) | COEFFICIENTS (Standard Error) $\beta_{SO_4}$ | $\Delta_{SO_4}$ | $\beta_{NO_3}$ | $\Delta_{NO_3}$ | $\beta_{(TSP-SULFATES-NITRATES)}$ | $\Delta_p$ | $\gamma_{NO_2}$ | $\alpha$ | A | CORRELATION COEF. (Variance of Residual) |
|---|---|---|---|---|---|---|---|---|---|---|---|---|
| 1. | $\Delta_{SO_4}$ and $\Delta_{NO_3}$ forced to equal -1.0 $\Delta_p$ forced to equal -0.667 | 6.62 (30.53) | 0.041 (0.003) | -1.0 Fixed | 0.025 (0.005) | -1.0 Fixed | -0.002 (0.002) NS | -0.667 Fixed | 41.80 (3.86) | 2.54 (0.38) | -1.76 (0.51) | 0.76 (13.03) |
| 2. | $\Delta_{SO_4}$ and $\Delta_{NO_3}$ forced to equal -1.0 | 6.62 (30.53) | 0.039 (0.004) | -1.0 Fixed | 0.022 (0.005) | -1.0 Fixed | 0.004 (0.005) NS | -0.24 (0.96) NS | 38.57 (4.43) | 2.31 (0.38) | -2.23 (0.56) | 0.76 (13.02) |
| 3. | $\Delta_{SO_4}$ forced to equal $\Delta_{NO_3}$ | 6.62 (30.53) | 0.089 (0.010) | -0.67 (0.077) | 0.040 (0.0095) | -0.67 (0.077) | 0.0038 (0.0047) NS | -0.35 (0.92) NS | 33.81 (4.14) | 2.87 (0.36) | -3.28 (0.54) | 0.80 (11.13) |
| 4. | All parameters free to seek local minimum | 6.62 (30.53) | 0.107 (0.015) | -0.53 (0.10) | 0.024 (0.008) | -1.09 (0.13) | 0.0033 (0.0046) NS | -0.28 (1.07) NS | 33.86 (4.07) | 2.82 (0.35) | -3.14 (0.53) | 0.81 (10.68) |

Legend: NS means not significantly different from zero at a 95% confidence level.

insignificantly different from zero. The principal species responsible for explaining visibility reduction are again SULFATES and $NO_2$. The light extinction coefficient estimated for $NO_2$ is similar to that of entry 1, Table 6.2, indicating that our change in humidity treatment has left estimated light attenuation by this gas phase component largely unaffected, as expected. Finally, we note that the change in relative humidity treatment has brought the intercept, A, closer to zero, and for the period prior to September 1970 the coefficient on the dummy variable, $\alpha$, almost cancels A, leaving a net intercept value which is indistinguishable from zero. In short, our model based on simple assumptions about the light scattering behavior of a hygroscopic aerosol as a function of relative humidity displays many nice properties.

In an attempt to improve model fit, constraints placed on the exponents describing the relative humidity dependence of light scattering by various aerosol components will be relaxed one at a time. Perturbation of the parameter values shows that there is roughly a one-to-one trade-off possible between the values of the coefficients $\beta_{SO_4}$ and $\Delta_{SO_4}$ without disturbing model fit very much. Similar compensating adjustments could be made between $\beta_{NO_3}$ and $\Delta_{NO_3}$ and between $\beta_{(TSP-SULFATES-NITRATES)}$ and $\Delta_p$. Total model fit continues to improve until all parameters $\Delta_m$ are freed to seek a local minimum in entry 4 of Table 6.3. In that case, the function of relative humidity associated with NITRATES almost exactly matches our prior expectation that $\Delta_{NO_3}$ would equal -1.0. Light scattering by SULFATES is also a fairly strong function of relative humidity. Coefficients estimating the

light scattering by non-sulfate non-nitrate particulates are now of the expected sign, but are still not known with great accuracy.

Figure 6.5 shows the historical cumulative distribution of visibilities at downtown Los Angeles as compared to model output of entry 4, Table 6.3. The comparison is quite close.

Theoretical calculations have been performed by Garland (1969) to determine the extinction coefficient per unit concentration for liquid phase atmospheric ammonium sulfate aerosols as a function of relative humidity. Garland's example calculation for light scattering by a monodisperse ammonium sulfate aerosol of dry particle diameter equal to 0.42μ is plotted in Figure 6.6 along with the values of the function $\beta_{SULFATES} = \beta_{SO_4}(1-RH)^{\Delta_{SO_4}}$ from entry 4 of Table 6.3. The regression results are of similar shape, but somewhat higher than Garland's extinction coefficient calculations. If the assumption were made that the sulfate aerosols in Los Angeles over the period 1965 through 1974 on days of high relative humidity were predominantly ammonium sulfate, then the comparison would be somewhat closer. That is because the molecular weight of ammonium sulfate is 1.38 times that of the $SO_4^=$ ion, instead of the 1.3 times greater proportionality assumed at our data preparation step.

The model of equation (6.19) has the great advantage that it is close to being physically realizable for a hygroscopic aerosol. However, many sulfate and nitrate species exhibit a pronounced deliquescence. For example, light scattering by ammonium sulfate particles is not a smooth, slowly increasing function of relative humidity over a

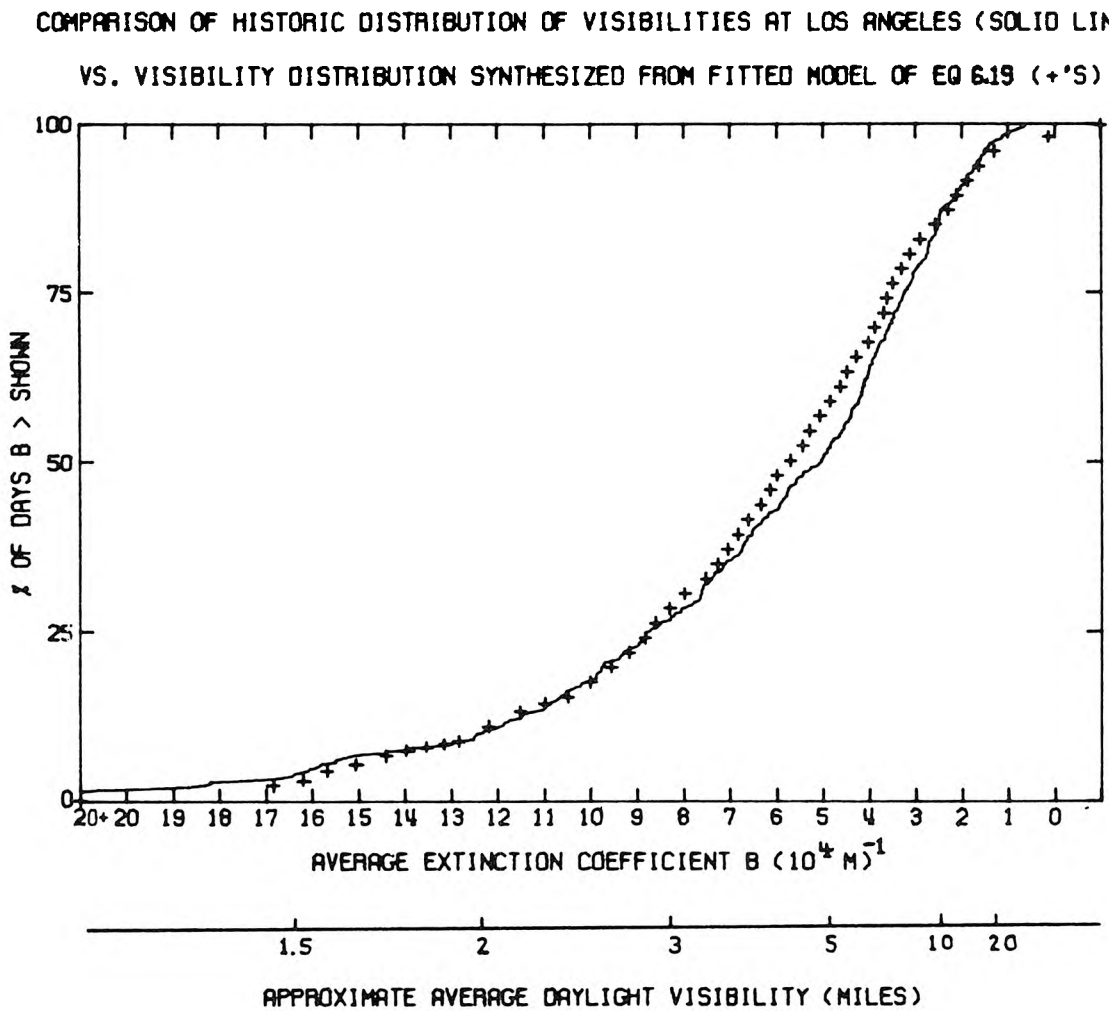


FIGURE 6.5

Results of model of entry 4, Table 6.3. Cumulative distribution of days on which the average extinction coefficient, $\overline{b}_j$, exceeded the stated values during the period August 1965 to December 1974 (413 days considered). Solid curve is historic data from LAAPCD visibility measurements. Broken curve is synthesized from regression model shown in entry 4 of Table 6.3.

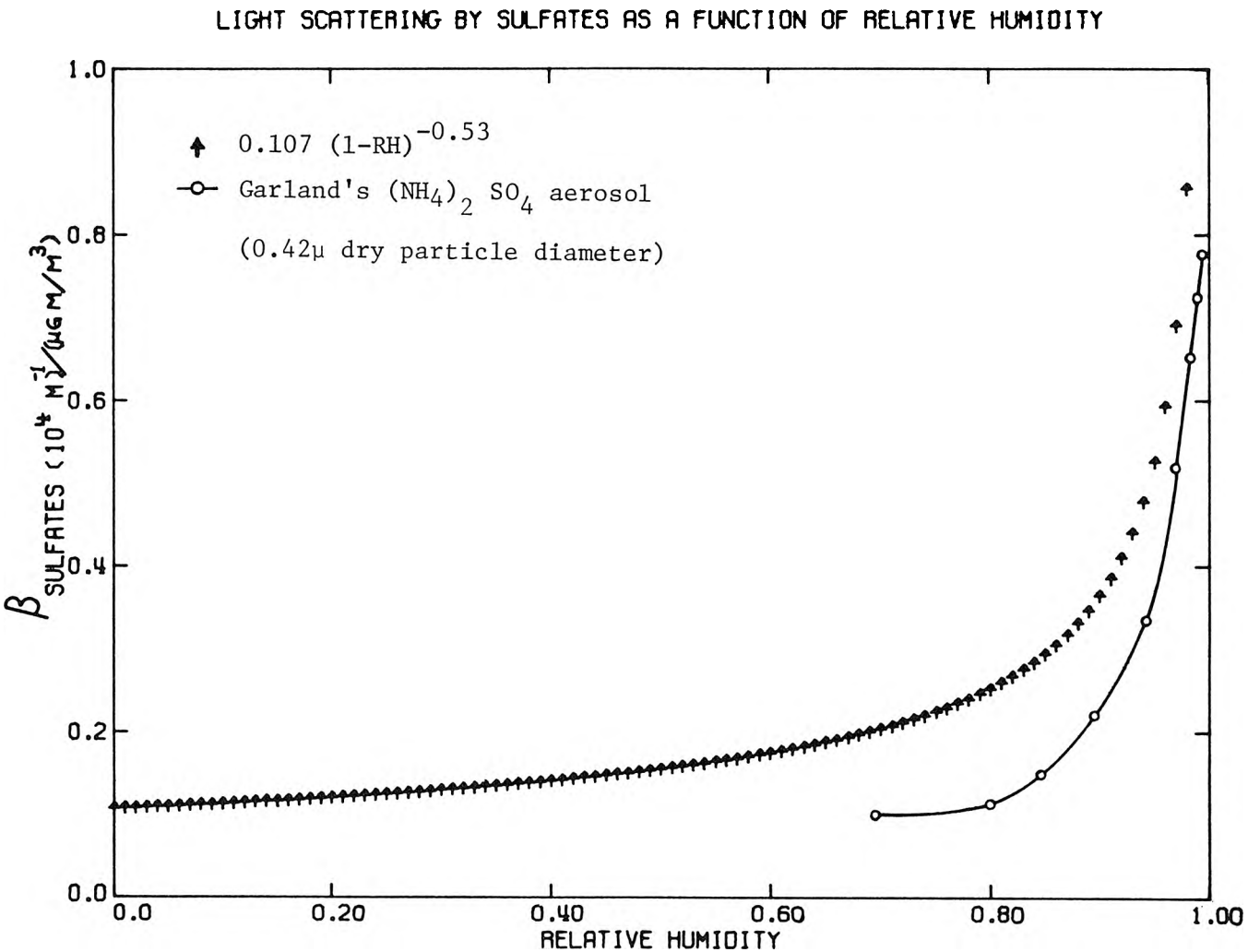
LIGHT SCATTERING BY SULFATES AS A FUNCTION OF RELATIVE HUMIDITY
0.107 (1-RH)^-0.53
Garland's (NH4)2 SO4 aerosol
(0.42μ dry particle diameter)
β SULFATES (10^-4 M^-1/μG M/M^3)
1.0
0.8
0.6
0.4
0.2
0.0
0.0
0.20
0.40
0.60
0.80
1.00
RELATIVE HUMIDITY

FIGURE 6.6

broad range of humidification. Instead, light scattering per unit mass for an ammonium sulfate aerosol remains fairly constant up to a relative humidity of ca. 80 percent, at which point the particle goes rapidly into solution with an attendant sharp rise in light scattering (Charlson, et al., 1974). Such complicated behavior would be difficult to incorporate theoretically into a simple regression model. Instead, an approach similar to that adopted by White and Roberts (1975) was tested in which an arbitrary relative humidity effect was to be approximated by fitting coefficients to series constructed from polynomials in relative humidity, pre-multiplying each aerosol mass concentration term. That approach was abandoned after discovering that only a slight improvement in model fit was achieved at the expense of creating estimated light scattering functions for each aerosol species which were ill-behaved at either the highest or lowest ends of the possible relative humidity range.

The function $\beta_{NITRATES} = \beta_{NO_3}(1\text{-}RH)^{\Delta_{NO_3}}$ describing light scattering by NITRATES as a function of relative humidity from entry 4 of Table 6.3 is plotted in Figure 6.7. Also plotted is the function $(0.025 + 0.049\ RH^2)$ from equation (6.7) describing White and Roberts' result for light scattering by NITRATES. At relative humidities below 60 percent, our estimate matches that of White and Roberts almost exactly.

In the regression models tested, the estimated light extinction coefficient per ppm for $NO_2$ has ranged between 41.80 $[10^4\ m]^{-1}$ and 24.99 $[10^4\ m]^{-1}$. In all but one case, the estimate of $\gamma_{NO_2}$ is within

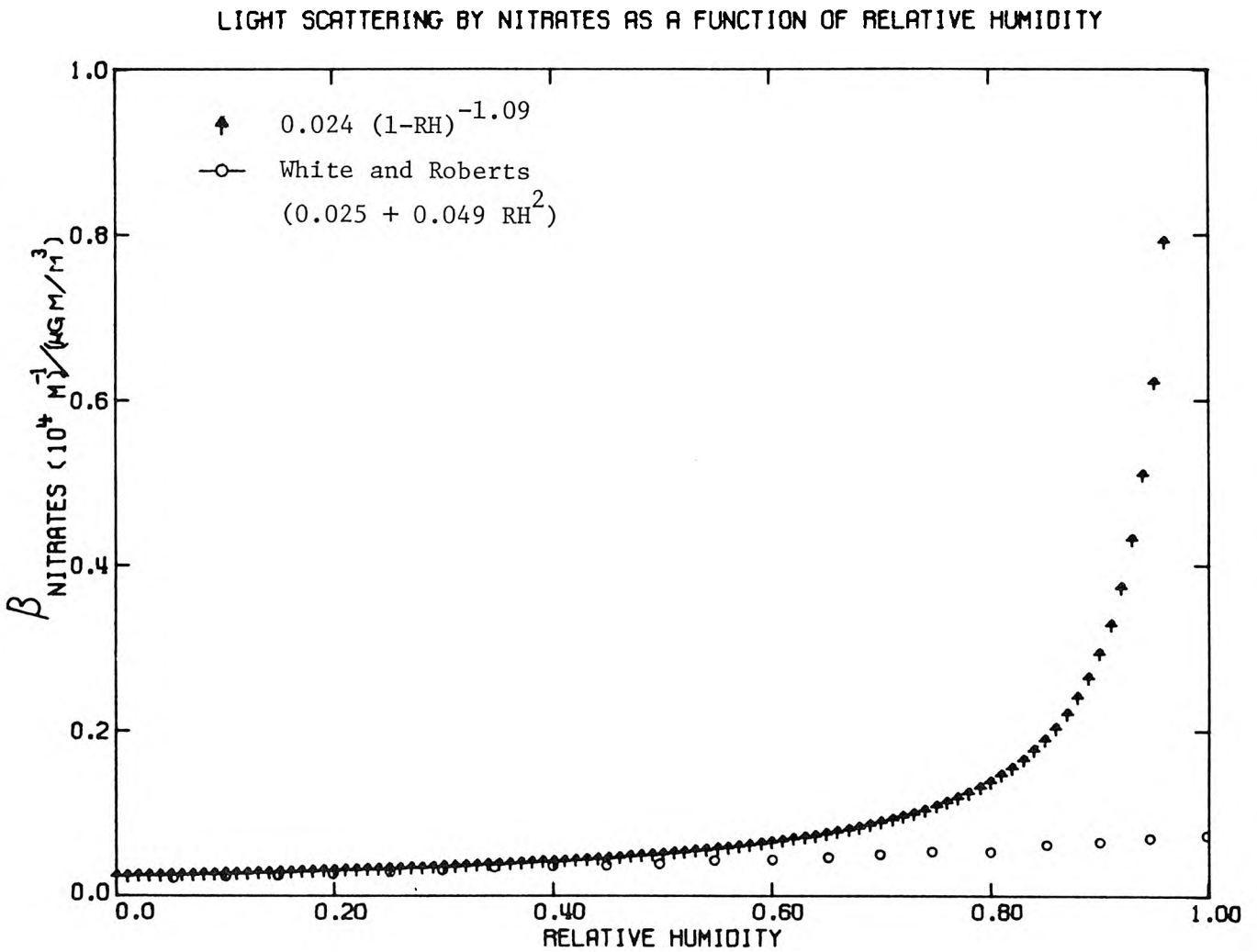
LIGHT SCATTERING BY NITRATES AS A FUNCTION OF RELATIVE HUMIDITY
0.024 (1-RH)^-1.09
White and Roberts
(0.025 + 0.049 RH^2)
β NITRATES (10^-4 M^-1/(μG M/M^3))
1.0
0.8
0.6
0.4
0.2
0.0
0.0
0.20
0.40
0.60
0.80
1.00
RELATIVE HUMIDITY

FIGURE 6.7

two standard errors of 30 $[10^4 \text{ m}]^{-1}$ per ppm. That value exceeds the literature estimates for light absorption by $NO_2$ as cited by Charlson and Ahlquist (1969) by roughly a factor of two to four, depending on the wavelength of light of interest. The discrepancy could be due in part to systematic underestimation of either $NO_2$ concentration or overestimation of the total atmospheric extinction coefficient. From the comments of previous investigators, it is not at all unlikely that less than ideal availability of visibility markers, plus the requirement that the markers be clearly recognized and not just seen could lead to a minimum contrast level for prevailing visibility observations in Los Angeles of 0.05 instead of Koschmieder's value of 0.02. Estimation of $\overline{b}_j$ from Koschmieder's formula would then be systematically high by about 25 percent, as would be the values of the coefficients estimated in our regression models. Experimental verification of the relationship between LAAPCD routine prevailing visibility observations and the atmospheric extinction coefficient, b, would be desirable. That still is unlikely to be a large enough source of error to account for the consistently high coefficient estimates for $NO_2$.

The coefficient on $NO_2$ might well be picking up some of the effects actually due to light scattering by its decay product, NITRATES. This seems quite likely in view of the difficulty in obtaining a significant contribution to light scattering by NITRATES in some of the linear regression models tested, even though most previous investigators have found a strong consistent NITRATE effect. The simple correlation between extinction coefficient and NITEATES is nearly zero, as shown

in Appendix D2. If light scattering were taken as an independent in situ check on the behavior of the nitrate air monitoring data, then the APCD might be well advised to check their nitrate collection and analysis techniques for possible interferences.

An additional interesting possibility is that $NO_2$ might be highly correlated with an important aerosol subfraction, perhaps submicron organics, for which explicit data were unavailable for inclusion in the model. The LAAPCD's historical tape sampler particulate data have been displayed by Phadke, et al. (1975). Their study notes that the diurnal variation of that particulate index is similar to the observed diurnal pattern for carbon monoxide at downtown Los Angeles, and they suggest that the automobile is a major source of particulate matter at that location. If particulate loadings closely follow automotive pollutant levels in general, then the coefficient on $NO_2$ in our regression models might be expected to be artificially high. If daylight $NO_2$ values are a better estimator of daylight particulate loadings than are our 24-hour average (TSP-SULFATES-NITRATES) values, then the difficulty in obtaining a significant estimate of light scattering by non-sulfate non-nitrate particulates in Table 6.3 may be explained.

The existence of a persistent daylight peak in Los Angeles particulate concentration would have other implications for this study. If there is a persistent daytime peak in particulate loading of the Los Angeles atmosphere, then the residual difference term $\sum_m \delta_m$ in equation (6.15), which we neglected, will not have mean zero and random fluctuation about that mean. Rather the 24-hour average particulate

measurements will be systematically lower than their 9-hour daytime counterpart corresponding to the period of visibility observations. The result will be that the extinction coefficients per unit concentration estimated from 24-hour averages of the particulate species exhibiting such a daytime peak will be artificially elevated in order to capture this discrepancy. Since aerosol sulfur (and for that matter its precursor, $SO_2$) is typically seen to exhibit a daytime peak at downtown Los Angeles (Hidy, et al., 1975; Phadke, et al., 1975; Thomas, 1962), the reason for the modest elevation of the estimated sulfate scattering coefficient per unit mass in the models estimated in this paper above those predicted by Garland (1969) and by White and Roberts (1975) may have been identified. In such a circumstance, the qualitative finding of an important sulfate effect on visibility shown by the regressions of Tables 6.2 and 6.3 would remain valid, while the use of numerical values from Tables 6.2 and 6.3 for correlation of light scattering with hourly average sulfate concentrations would not be recommended. Our regression equations would remain an unbiased predictor of the likely daylight visibility impact of a strategy aimed at control of 24-hour average particulate levels as long as the relative diurnal variation of pollutant concentrations remained unchanged. Since current State and Federal particulate standards and most historical particulate sampling data are stated in terms of 24-hour and longer concentration averages, the analysis contained in this study provides useful results in spite of the above potential problems.

## 6.6 Exploring the Visibility Impact of Reduced Sulfate Concentrations

We have seen that our statistical models are probably best behaved with respect to predicting the marginal impact of SULFATES on visibility. The test statistics on the $\beta_{SULFATES}$ coefficients are consistently significant, confidence intervals on these parameters are narrow, and the shape of the predicted non-linear humidity effect on light scattering by SULFATES is reasonable. The magnitude of the light scattering per unit mass predicted for SULFATES, while perhaps somewhat high, is still understood in relation to theory, the empirical findings of others, and several of the potential sources for error. Whatever problems may exist with estimating the light extinction behavior of other pollutant species, the behavior of light scattering by SULFATES is strong enough to stand out clearly from the background noise in the system. This is fortunate, because the motivation behind this study was to explore the impact of altered sulfate concentrations on the long-run distribution of prevailing visibilities at Los Angeles.

With this discussion in mind, the regression model of Table 6.3, entry 4, is used to "backcast" the impact on visibility of decreased sulfates levels at downtown Los Angeles. The sampling period of interest is again our data base of 413 rainless days distributed from August 1965 through December 1974.

Two cases will be considered. In the first instance, the daily average extinction coefficients, $b_j$, will be synthesized from the regression model using our historic air quality data after having reduced each day's SULFATES value by 50 percent. In the second case,

daily SULFATES values will be taken as 25 percent of their actual measured concentrations. This latter case approximates removal of virtually all of the non-background SULFATES in the Los Angeles atmosphere over the time period considered.[3] This is, of course, not to say that one knows how to achieve such a uniform proportionate reduction, but merely to estimate the visibility resulting should such an event have come to pass.

A comparison between the historic cumulative distribution of extinction coefficients and the distributions implied by the SULFATES reduction calculations is presented in Figures 6.8 and 6.9. The effect of sulfate reduction in those years is not uniform across the entire distribution of prevailing visibilities. Rather, as is most clearly shown in Figure 6.9, a 75 percent reduction in SULFATES levels on a daily basis would have reduced the number of days with worse than three-mile visibility by about two thirds, while improvement in the number of days of average visibility greater than ten miles (the California Air Resources Board's visibility target) would be much smaller, about 10 percent.

One likely explanation for this disproportionate SULFATES impact on the days of the very worst visibility is found in Table D2.1 of Appendix D2. As can be readily seen, suspended sulfate mass loadings are positively correlated with relative humidity. Thus days of high sulfate concentration often coincide with days of high light scattering

---

[3] Estimation of average $SO_4^=$ background concentrations in the Los Angeles basin is discussed by Trijonis, et al. (1975) and by Hidy, et al.(1975), and in Chapters 2 and 5 of this study.

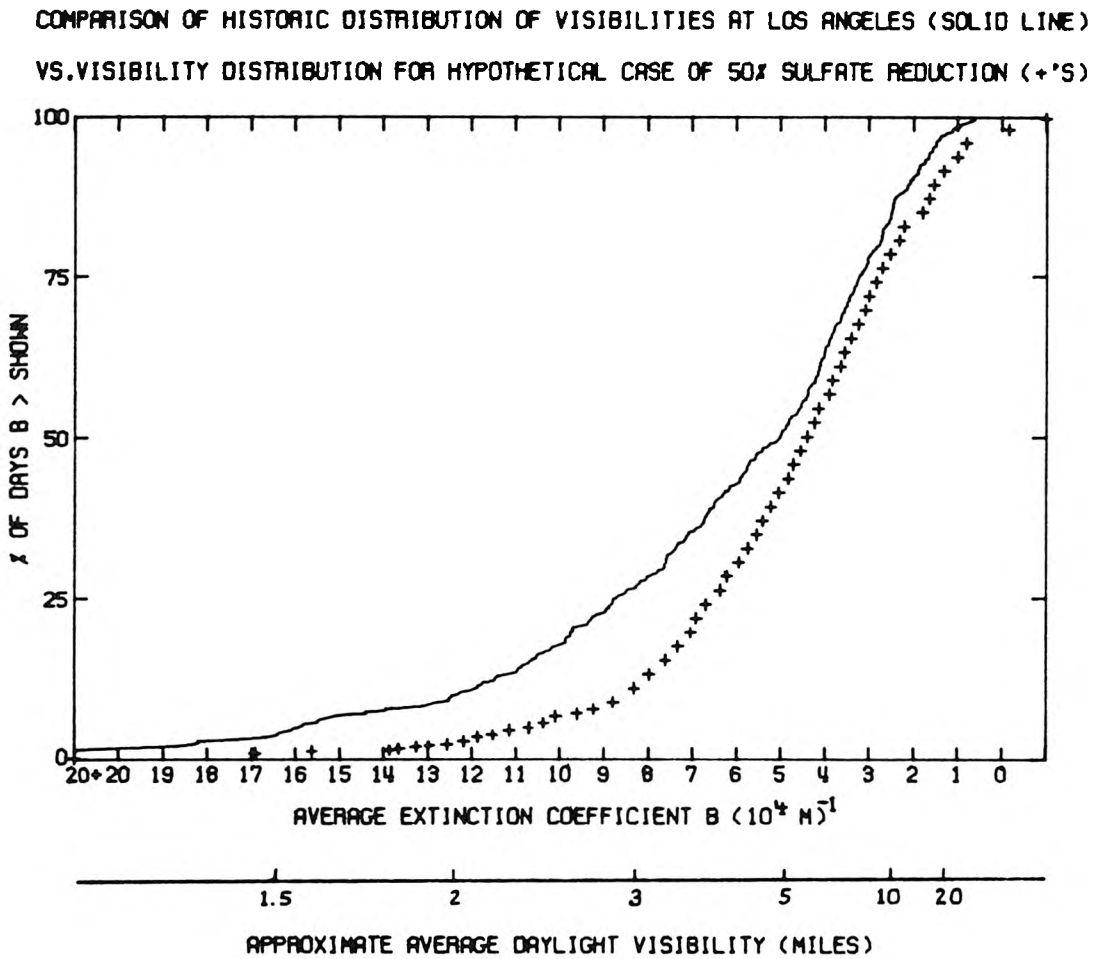


FIGURE 6.8

Impact of SULFATES reduction, Case I. Cumulative distribution of days on which the average extinction coefficient, $\bar{b}_j$, exceeded the stated values during the period August 1965 to December 1974 (413 days considered). Solid curve is historic data from LAAPCD visibility measurements. Broken curve is synthesized from regression model shown in entry 4, Table 6.3 after having reduced historic SULFATES levels by 50 percent on each day of observation.

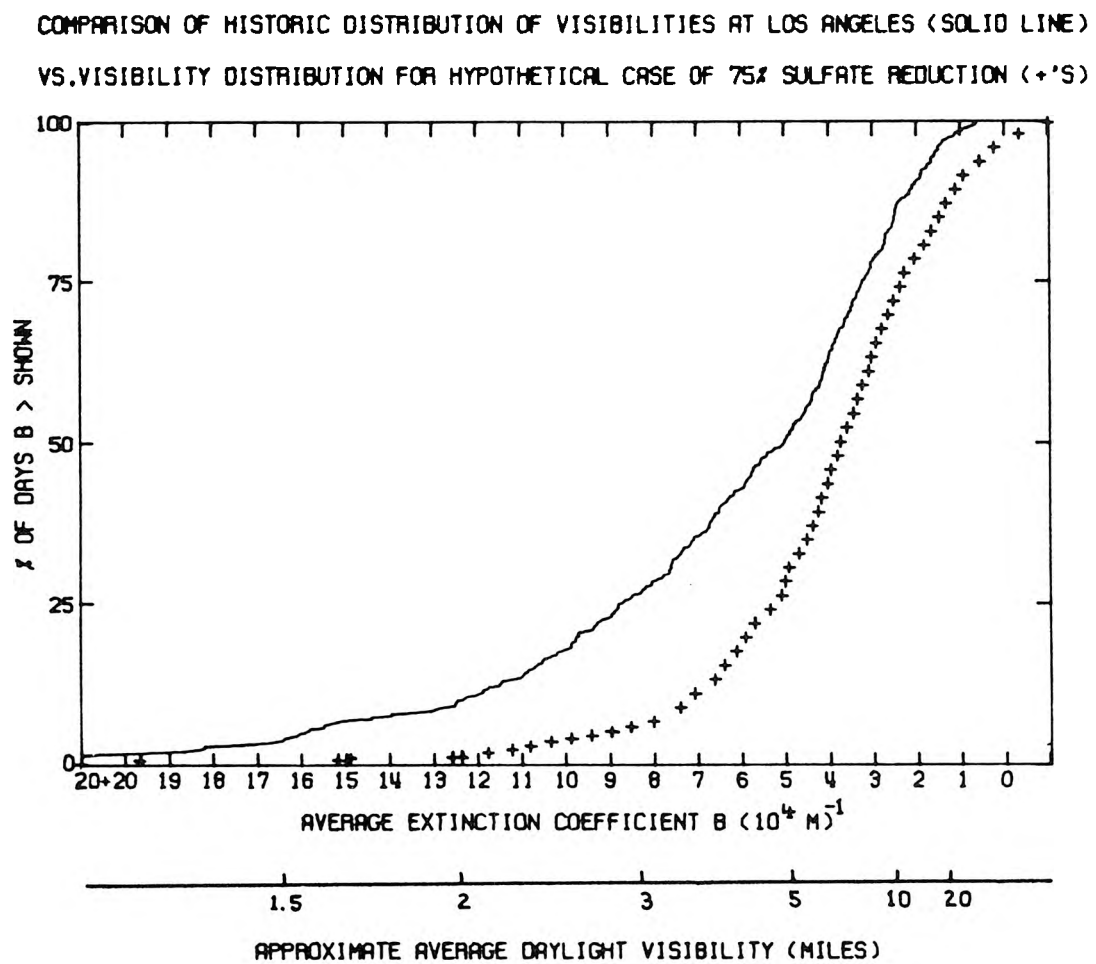


FIGURE 6.9

Impact of SULFATES reduction, Case II. Cumulative distribution of days on which the average extinction coefficient, $\bar{b}_j$, exceeded the stated values during the period August 1965 to December 1974 (413 days considered). Solid curve is historic data from LAAPCD visibility measurements. Broken curve is synthesized from regression model shown in entry 4, Table 6.3 after having reduced historic SULFATES levels by 75 percent on each day of observation.

per unit sulfate mass concentration. Conversely, fairly dry days on which visibility is relatively good were comparatively sulfate free.

## 6.7 In Conclusion

Techniques have been developed for relating air pollution control agency routine air monitoring data to prevailing visibility at downtown Los Angeles over the decade 1965 through 1974. It was shown that the apparent relationship between light extinction and total suspended particulate mass implied by the long-term historical data base is consistent with the findings of previous short-term special studies. However, total suspended particulate mass was found to be an imprecise estimator of daylight visibility reduction in the Los Angeles area.

When total suspended particulate samples are subdivided chemically, it becomes possible to more closely assess the effect of water-soluble submicron aerosol species, particularly sulfates, on light scattering at Los Angeles. A non-linear regression model for light extinction at Los Angeles was constructed which combines available aerosol chemical information with relative humidity and $NO_2$ data. Coefficients fitted to that model indicate that there is a pronounced increase in light scattering per unit sulfate mass on days of high relative humidity, as would be expected for a hygroscopic or deliquescent substance.

Having developed and fitted a model representing a decade of atmospheric events, it becomes possible to examine the likely long-run response of visibility in the Los Angeles basin to altered levels of particulate sulfates. It is estimated that the visibility impact of

reducing sulfates to a half or to a quarter of their measured historic values on each past day of record would be manifested most clearly in a reduction of the number of days per year of worse than three-mile visibility. The number of days of average visibility less than ten miles would be little affected. One reason for the disproportionate impact of the light scattering by sulfates on the days of the worst visibility is thought to result from a high positive correlation between sulfate mass loading and relative humidity. High values of light scattering per unit sulfate mass thus occur on days of high sulfate mass concentration.

---

Postscript. This chapter was previously distributed as:

Cass, G. R. (1976), The Relationship Between Sulfate Air Quality and Visibility at Los Angeles, Pasadena, California, California Institute of Technology, Environmental Quality Laboratory Memorandum Number 18, August 1976.

Since that time, excerpts from the working papers referenced to White and Roberts (1975), and White, Roberts, and Friedlander (1975) have been published as:

White, W. H. and P. T. Roberts (1977), "On the Nature and Origins of Visibility-Reducing Aerosols in the Los Angeles Air Basin," Atmospheric Environment, Vol. 11, pp. 803-812.

Some of the results shown in that journal article differ from the results attributed to White and Roberts (1975) in this chapter because only the subset of their previous work was reprinted in which the intercept ($\alpha$ in our regression equations) was suppressed. Either set of results may be referred to without material change in one's conclusions.

# CHAPTER 7

# PATHS TOWARD FUTURE RESEARCH

## 7.1 Introduction

Extensions of this research project can proceed along two general paths. First, tools developed in this study can be used to complete a public policy analysis of emission control strategy options. Secondly, the techniques developed for describing and modeling urban air quality problems may be further refined and improved. Points of departure along each of these paths will be suggested in turn.

## 7.2 Toward Improved Understanding of Airshed Physical Processes

Extension of the physical description of sulfate air quality problems developed in this study should proceed simultaneously by two mutually reinforcing routes. Physical measurement programs should be developed to relieve critical data deficiencies uncovered by this study. Development and testing of theoretical concepts also should be pursued in a way which makes further use of those data which already do exist.

Some of the most important data deficiencies facing a long-term average air quality study result from the short term nature of most special field measurement projects. Data on seasonal trends in sulfate background concentrations, $SO_2$ oxidation rates in the atmosphere, and $SO_2$ deposition velocity are virtually unavailable. Investigators with the skill to make such measurements should insist on obtaining a set of data which represents a year-round cycle. Sampling schedules should be sufficiently dense that narrow confidence

intervals will be obtained on such important statistics as the annual mean value of the phenomenon of interest.

Certain aspects of the routine monitoring networks which do supply year-round data also would benefit from systematic research. It should be clear by now that the attempt to use data obtained by three competitive air monitoring networks in the same locality within the same control strategy analysis has uncovered some serious problems with monitoring network design. While no one of these networks examined was without certain unique positive aspects, the sulfate and sulfur dioxide information system formed by the three networks operating concurrently could be improved greatly, possibly with a cost savings. Research into methods for coordinated design and operation of multiple air monitoring networks is needed.

Certain measurement technologies present prime candidates for further research. Since $SO_2$ has been measurable for many years by many methods, one would possibly assume that $SO_2$ concentration determination should be a dead issue. However, the analysis performed in this study shows that $SO_2$ monitoring instruments as they are currently operated suffer large *percentage* errors in their results, that different monitoring techniques are in conflict as to ambient concentrations, and that the inability to closely specify $SO_2$ concentrations is a serious handicap to control strategy formulation for sulfates. From the apparent erratic performance of the West-Gaeke $SO_2$ method when placed in the field in Los Angeles, one suspects that the Federal reference method for $SO_2$ will have to be revised.

If that is done, a researcher with a better method for $SO_2$ determination would be in a position to make a substantial contribution to national air pollution control efforts.

Additional suggestions for research projects which would improve the ability of routine air monitoring networks to support visibility control strategy studies are given in Appendix D4 to this thesis.

In addition to improvement of current field measurement practices, there is room for a number of pioneering approaches to unsolved measurement problems. Important questions for chemical research include: What is the relative abundance of the individual chemical species which make up the complex that we have referred to as particulate sulfur oxides or sulfates? How can one measure the relative rates of heterogeneous versus homogeneous phase $SO_2$ oxidation processes in an *open atmosphere*? Can those measurements lead to conclusions as to exactly which mechanisms are responsible for the bulk of the chemical conversion of $SO_2$ in the atmosphere (as opposed to smog chambers)? Does that answer vary from place to place and from time to time? Coastal fogs have been shown to co-occur with serious Los Angeles sulfate episodes. Can the role of these fogs in the Los Angeles sulfate problem be placed on a quantitative rather than phenomenological basis through a clever experimental program?

Opportunities exist for valuable contributions by persons interested in field measurements of transport and dispersion.

Extension of puff and plume dispersion measurements over long downwind travel times is important if $\sigma_y(t)$ is to be represented with reasonable accuracy over multi-day periods. It may even turn out that the concept of a Gaussian distribution of material about its centroid breaks down over very long travel times. Experimental determination of the distribution of air parcel retention times in the Los Angeles Basin would be of value. Validation of trajectory integration techniques used in air quality models could proceed if well defined data on instantaneous puff releases were available. Even more intriguing is the possibility that a long-term average physical (not mathematical) model for the airshed could be constructed based on the air quality simulation model derivation of Chapter 3. Sequential instantaneous $SF_6$ puff releases made at well-spaced periodic intervals from critical source locations, followed by automated integrated sampling at a grid-like network of receptor points could result in a direct estimate of source to receptor transport probabilities. Since the releases would be intermittent, the amount of $SF_6$ needed for a long-term study might be within the realm of economic reality when compared to the rather high cost of validating a mathematical air quality model applicable to very rough terrain. Assessment of especially complex transport situations, like the long-run impact of the Ormond Beach power plant located in Ventura County on Los Angeles air quality might well proceed by that means.

Statistical analysis of historic air quality data was shown to be a valuable technique for deducing the important physical

processes which must be incorporated within a successful sulfate air quality model for Los Angeles. Similar analyses should be performed in other geographic locations and for other pollutants. Great potential exists to expand the type and capability of data survey and screening techniques. Valuable contributions should be sought through the use of physical reasoning to improve the specification and structure of statistical models for air quality phenomena. An example of physical reasoning incorporated within the structure of a statistical model is found in the means for incorporating relative humidity effects within the non-linear visibility model of Chapter 6 to this study.

The air quality modeling approach of Chapter 3 of this study has considerable potential for improvement and adaptation to other problems. The dimensionality of that model can easily be increased to handle wind shear, trajectories computed from highly accurate wind fields, different averaging times, spatially inhomogeneous mixing depths over the airshed, changing atmospheric stability over time, finite vertical diffusion rates, and additional pollutant removal processes. A number of methods were identified in Chapter 5 for superimposing analytical solutions for the diffusion equation onto the simulation model in order to improve model accuracy within the first time step downwind of a source. The main barrier to these improvements is not technical knowledge, but rather the decision to pay for the added computing costs of a more realistic simulation. Therefore, research into the costs and benefits of increasing model capabilities should be pursued. A sensitivity study of model response

to simplifying assumptions would form a key part of that cost-benefit study.

The concept of computing long-term average source to receptor probabilities from Lagrangian marked particle statistics possesses great flexibility. In our application, each particle was tagged with magnitudes reflecting source emission strength, height of insertion into the atmosphere and chemical composition. There is no reason why the model could not be adapted to advecting marker particles labeled with certain moments of the aerosol size distribution function, or other pollutant properties of interest.

Several research questions are posed for those who seek to improve emissions inventory techniques. First, what battery of tests is appropriate for validating an emissions inventory? Can additional types of simulation models be developed, similar to our natural gas curtailment model of Appendix A2, Section A2.2.3, that will faithfully reproduce the behavior of area source classes whose members are too small to be inventoried individually (e.g., off-highway diesel vehicles)? Adaptation of energy and material balance techniques to support inventory estimates for pollutants other than $SO_x$ would be valuable.

Emissions inventory compilation requires enormous expenditure of time and effort. Means should be found to streamline the process without sacrificing accuracy. Extremely valuable uses for emissions inventory by-product data bases also can be identified. For example, our emission inventory is accompanied by a parallel energy dissipation

inventory which is spatially and temporally resolved over the Los Angeles Basin. Such a data base could be used in thermal modeling studies. Traffic count data can be used to validate transportation models.

## 7.3 Toward Emission Control Strategy Analysis

One intended use of this research is to advance the public policy analysis of sulfate air quality control strategy options. A procedure for emission control strategy analysis was briefly outlined at the bottom of Figure 1.2. Emissions forecasts first would be made. The air quality simulation model results then could be used to specify likely pollutant concentrations in the absence of further emissions controls. A wide variety of possible emission control techniques next should be identified. The air quality model would be used to project the air quality improvement likely to result from application of each control strategy option. At the same time, both the cost of the control technique and any quantifiable benefits (e.g., increased visibility) resulting from the air quality improvement would be estimated. Then control strategy options, their costs and some benefits could be arrayed in a manner that permits decision-makers to choose an economically attractive path toward any desired level of air quality improvement. Information on likely benefits is made available at that time in order to assist selection of an appropriate air quality goal if no firm prior objective exists.

Development of methods for performing each of these necessary steps toward a completed set of emission control strategies presents opportunities for advances in both decision theory and current engineering practice. In order to pose research questions for control strategy synthesis in concrete terms, a hypothetical example will be worked which illustrates the procedure, the data requirements, and some key dilemmas facing the control strategy designer.

For the moment, we will by-pass the question of making emissions and air quality forecasts. Attention is turned to the problems associated with identifying control options and choosing among them. Assume that the future status of some airshed of interest has been characterized and found to resemble the South Coast Air Basin as it existed in 1973. We wish to define attractive control strategy paths based on then-current knowledge. To confine the example to manageable proportions, we will further limit ourselves to those stationary source emissions control strategy options previously identified by Hunter and Helgeson (1976). Following Hunter and Helgeson, it is assumed that each control measure listed provides proportionately the same removal efficiency for both $SO_2$ and primary $SO_4^=$ emissions as is expected for total $SO_x$ (probably a poor assumption). It is further assumed that each emission control technique listed will be applied equally to all members of the source class for which it is specified. Each emission control option will be used continuously if adopted (i.e., we are not interested in emergency episode abatement but rather a proportionate reduction in $SO_x$ emissions on each day of record).

Technological emission control options identified by Hunter and Helgeson (1976) are listed in Table 7.1. Annual average $SO_x$ emissions for the year 1973 to which each control measure would apply were estimated from the on-grid plus off-grid portions of the emission inventory of Appendix A2 to this study. Emissions control removal efficiencies and control costs per ton of $SO_x$ emissions are as calculated from Hunter and Helgeson's examples.[1,2] The incremental sulfate air quality improvement at downtown Los Angeles shown in Table 7.1 is that which would have been realized in 1973 if each candidate control strategy option had been installed and in operation in that

---

[1]Costs given are for both recovery of capital investment and operation on an annual basis, stated in 1975-76 dollars. Control cost estimates given by Hunter and Helgeson (1976) were intended to represent actual "manufacturing costs" for each control technology in those cases where market price data were unavailable. These cost data are limited to Hunter and Helgeson's work because that study forms a single consistent set of cost estimates across a variety of South Coast Air Basin emission sources. They should not be interpreted as the only control measures available, nor are they necessarily the least costly.

[2]Fuel burning emissions sources have been observed to operate with a margin of safety below the maximum permissible level of emissions under past 0.5% sulfur in fuel regulations. When limited to 0.5% sulfur, utilities burned 0.45% sulfur residual oil while industry burned about 0.40% sulfur residual oil. Further tightening of fuel sulfur content limits will be viewed as generating similar percentage safety factor choices by fuel customers and fuel vendors. In constructing Table 7.1, each tightening of sulfur content in fuel regulations was assumed to generate a nominal percentage reduction in historic emissions levels in proportion to the nominal change in the maximum fuel sulfur content permitted, rather than strict conformance to the maximum permitted sulfur level. Hunter and Helgeson's cost estimation method per ton of $SO_x$ emissions reduced was not similarly adjusted, which results in a slight distortion of control cost effectiveness estimates (within the error bounds on their data).

TABLE 7.1

Annual Cost and Sulfate Air Quality Impact of Stationary Source $SO_x$ Emissions Control Technologies if Applied to $SO_x$ Emissions in the South Coast Air Basin As They Existed in 1973

(Control Techniques and Costs Identified by Hunter and Helgeson (1976); Air Quality Impact Estimated From Model Validation in Chapter 5 of This Report.)

| Emission Control Strategy Option | $SO_x$ Emissions Control Effectiveness When Applied to 1973 Emissions Inventory | | | | Incremental Cost of Emission Control Option (1975-76 Cost Basis) | | Annual Mean Sulfate Air Quality Improvement at Downtown Los Angeles | | Cost Effectiveness Index |
|---|---|---|---|---|---|---|---|---|---|
| | Degree of Control | Emissions from Source Class to Which Control Measure Would Apply (tons/day) | Emissions from Source Class After Application of that Control Measure (tons/day) | Total Reduction in Annual Average Emissions (tons/day) | Dollars Per Ton $SO_x$ Removed | Total Annual Cost ($10^6$ Dollars) | $\mu gm/m^3$ $SO_4^=$ Reduced per ton/day Emission Reduction | Total Incremental Sulfate Reduction ($\mu gm/m^3$) | $\mu gm/m^3$ $SO_4^=$ Reduced per $10^9$ Dollars Annual Cost |
| Electric Utility Residual Fuel Oil Desulfurization [a] | | | | | | | | | |
| (a) Reduction in fuel sulfur limit from 0.5% to 0.4% | -20% | 239.9 | 191.9 | 48.0 | 377[b] | 6.60 | 0.0138[e,f] | 0.662 | 100.3 |
| (b) Further reduction from 0.4% S to 0.3% S | -25% | 191.9 | 143.9 | 48.0 | 471[b] | 8.25 | 0.0138[e,f] | 0.662 | 80.2 |
| (c) Further reduction from 0.3% S to 0.2% S | -33% | 143.9 | 95.9 | 48.0 | 942[b] | 16.50 | 0.0138[e,f] | 0.662 | 40.1 |
| (d) Further Reduction from 0.2% S to 0.1% S | -50% | 95.9 | 47.9 | 48.0 | 1695[b] | 29.70 | 0.0138[e,f] | 0.662 | 22.3 |
| Industrial Residual Fuel Oil Desulfurization[a] | | | | | | | | | |
| (a) Reduction in fuel sulfur limit from 0.5% S to 0.4% S | -20% | 8.3 | 6.6 | 1.7 | 377[b] | 0.23 | 0.0158[f] | 0.027 | 117.4 |
| (b) Further reduction from 0.4% S to 0.3% S | -25% | 6.6 | 5.0 | 1.6 | 471[b] | 0.28 | 0.0158[f] | 0.025 | 89.3 |
| (c) Further reduction from 0.3% S to 0.2% S | -33% | 5.0 | 3.3 | 1.7 | 942[b] | 0.58 | 0.0158[f] | 0.027 | 46.6 |
| (d) Further reduction from 0.2% S to 0.1% S | -50% | 3.3 | 1.7 | 1.6 | 1695[b] | 0.99 | 0.0158[f] | 0.025 | 25.2 |
| Chemical Plant Emission Limit Met at 500 ppm $SO_x$ (or less) in exhaust (Rule 53.3)[g] | -93% | 80.0 | 5.5 | 74.5 | 235[c] | 6.39 | 0.0217[f] | 1.617 | 253.0 |
| (a) Claus tail gas clean-up units applied to sulfur plants | | | | | | | | | |
| (b) Additional absorption units, demisters, or plant derating applied to $H_2SO_4$ plants | | | | | | | | | |
| Petroleum Refining and Production | | | | | | | | | |
| (a) Caustic scrubber applied to refinery fluid catalytic crackers (FCC) | -95% | 52.1 | 2.6 | 49.5 | 1144 | 20.67 | 0.0257 | 1.272 | 61.5 |
| (b) Claus plant applied to oil field fire flooding operation exhaust | -90% | 4.5 | 0.5 | 4.0 | 312 | 0.46 | 0.0257[d] | 0.103 | 223.9 |
| Petroleum Coke Calcining Kiln Emissions Reduction Obtained From Scrubbing Coke Dust Prior to Combustion[g] | -80% | 25.5 | 5.1 | 20.4 | 600 | 4.47 | 0.0165 | 0.337 | 75.4 |
| Steel Mill | | | | | | | | | |
| (a) Desulfurization of coke oven gas | -90% | 21.2 | 2.1 | 19.1 | 122 | 0.85 | 0.0024 | 0.046 | 54.1 |
| (b) Scrubber applied to mill sinter plants | -80% | 4.8 | 1.0 | 3.8 | 470 | 0.65 | 0.0024 | 0.009 | 13.8 |

Notes

(a) Middle distillate fuel oil desulfurization was not addressed by Hunter and Helgeson (1976) and thus will be excluded from this example.

(b) The additional cost *beyond 0.5% sulfur fuel* was estimated by Hunter and Helgeson (1976) as $0.12, $0.27, $0.57, and $1.11 per barrel for fuel meeting 0.4% sulfur, 0.3% sulfur, 0.2% sulfur, and 0.1% sulfur rules respectively. Thus 0.3% sulfur fuel would cost ($0.27 - $0.12) = $0.15 more per barrel than 0.4% sulfur fuel. See Chapter 7 footnotes 1 and 2 for additional information and assumptions.

(c) No specific cost data for sulfuric acid plant control were given, but rules affecting both sulfur recovery and acid plants were adopted simultaneously and are assumed to be equally cost-effective.

(d) The air quality impact shown is proportional to the petroleum processing source class as a whole. This source is physically distant from downtown Los Angeles and this may not have an impact at downtown Los Angeles which is proportionately as large as from the FCC units which dominate that source class. However, the cost effectiveness of controlling that source is so high that control strategy conclusions would be distorted little even if the air quality impact estimate were reduced several fold.

(e) Based on emissions from both on-grid plus off-grid power plants located within the 1973 boundaries of the South Coast Air Basin. If only a subset of those power plants were to be considered for control, the impact per ton of $SO_x$ emissions reduced would be expected to vary depending on the group of generating stations chosen.

(f) Annual mean air quality impacts are sensitive to the seasonal variation in $SO_x$ emissions. Thus these values are specific to years with a seasonal emissions pattern like that of 1973.

(g) $SO_2$ reduction attributed to this technology seems to us to be a bit speculative. Other more costly alternatives, however, do exist with reasonable certainty.

year. That air quality impact estimate for each source class was obtained from the 1973 air quality model validation effort of Chapter 5, evaluated at downtown Los Angeles.[3]

The last column of Table 7.1 contains a measure of source emission control option effectiveness, in terms of sulfate concentration reduction at Los Angeles per dollar spent on $SO_x$ control. If these control measures were to have been implemented in 1973 in order of declining cost effectiveness index, the progression of air quality improvement versus cumulative control cost would have been as shown by the upper curve of Figure 7.1.

The points along the upper curve of Figure 7.1 form one possible emission control strategy. Up to 97 million dollars per year could have been spent in 1973 on these control measures, with up to 43% improvement expected in average sulfate air quality at downtown Los Angeles. Maximum obtainable visibility improvement would have been somewhat less than that illustrated in Figure 6.8. A decision could have been made to operate at any point along the upper control strategy curve of Figure 7.1 with fairly predictable results.

---

[3]The relative effectiveness of emissions controls applied to particular source classes would be somewhat different at different locations in the airshed. The relatively high impact of refinery FCC units per ton of $SO_x$ emitted when compared to the steel mill is due mainly to the distant siting of the steel mill versus downtown Los Angeles rather than to any design attribute of either source type. The fact that a source contributes weakly to sulfate levels at downtown Los Angeles of course says nothing about its influence elsewhere in the airshed.

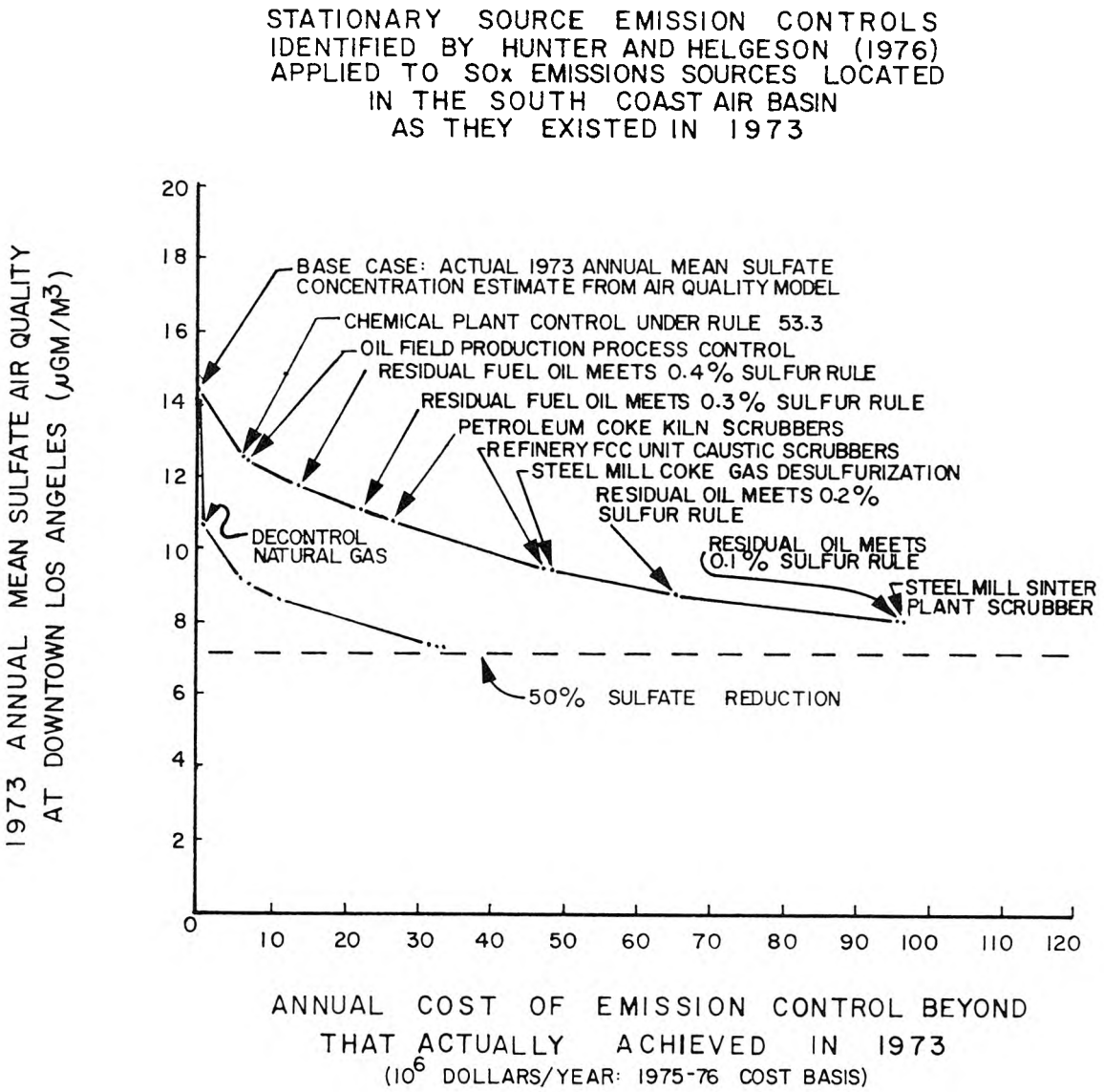


FIGURE 7.1

NOTE: This figure accompanies a sulfate air quality control strategy example calculation. It applies to conditions in that airshed *as they existed in 1973*. Further reductions in natural gas supply beyond the levels of service observed in 1973 will greatly increase the annual cost of the emissions control strategy pictured in the upper curve of this graph. Changes in assumptions about emissions control technology or clean fuel availability and price could significantly alter the cost effectiveness shown. This figure was constructed to *illustrate* the means by which the description of airshed physical processes developed in this study can be used almost immediately to formulate emission control strategies for sulfates in the South Coast Air Basin. It should not be interpreted as containing a control strategy recommendation. (Reproduction of this figure without this caption will not be authorized.)

A control strategy designer who identified the upper curve of Figure 7.1 as the least-cost means of obtaining a particular sulfate air quality improvement could have made a serious omission. An alternative emission control strategy could have been predicated upon releasing the institutional constraints which impede the free market allocation of clean fuels to those parts of the country with serious air quality problems.

For the past two decades, the Federal Power Commission (or its successor) has regulated the wellhead price of natural gas sold in interstate commerce. Natural gas sold within the state in which it was produced has remained free of Federal price controls. As prices for substitute fuels, such as residual oil, rose over the years, a two-tier pricing system developed. Controlled interstate gas sales were constrained to a price which was a small fraction of the energy content equivalent price of fuel oil, while intrastate gas prices followed oil prices upward.

The results of this two-tier price system were multi-fold. Many persons able to obtain price-controlled gas sought it solely because it was cheaper than oil. Demand was artifically stimulated. On the supply side, gas producers ceased to commit new gas reserves to the interstate market. The conflict between excess demand and decreased interstate supply lead to natural gas curtailments similar to those pictured in Figure 1.3 as old interstate supply contracts failed to be renewed or were otherwise voided. In areas like Los Angeles with serious air pollution problems, emission source

owners paid high prices for unusually high quality fuel oil to replace lost interstate natural gas supplies, and at the same time local pollutant emissions increased because no oil available today burns as cleanly as natural gas. Meanwhile, vast amounts of natural gas were committed to the intrastate markets in Texas and Louisiana at prices lower than oil but higher than the price ceiling on interstate natural gas sales. For a detailed account of the history and economic effects of FPC natural gas regulation efforts, see Breyer and Macavoy (1974).

If governmental policy makers were to rely on market forces to set the price of new natural gas sales to interruptible gas customers, an $SO_x$ emissions control strategy for Los Angeles like that of the lower curve of Figure 7.1 might well be achievable. Natural gas substitution at a small cost[4] over that of existing fuel oil prices would

---

[4]The actual free market price obtained as a result of deregulation of new gas sales to interruptible gas customers is, of course, uncertain. However, a large number of analysts, including the FPC's own staff (Seidel and Bryan, 1975) have contended that deregulated natural gas prices will not rise above the price currently paid for premium quality imported fuel oils. Considerable evidence lies behind that prediction. Free market natural gas sales in all available intrastate and international markets supplying the United States have consistently cleared at prices lower than that paid for 0.5% sulfur fuel oil on the West Coast (see Federal Energy Administration, 1973-1977). Even if natural gas prices rose above the intrastate market price in a fully competitive bidding environment, the group with the highest cost for substitutes other than natural gas still will be in a position to bid the most for gas supplies without experiencing a total cost increase. Los Angeles utilities currently pay among the nation's highest prices for fuel oil, and thus would be expected to fare well in an auction market for gas if motivated to do so. During the period of time around the year (continued)

eliminate the emissions from residual oil combustion. Then the remaining technological emissions controls of Table 7.1 directed at sources other than residual fuel oil combustion could be applied in sequence to achieve a 49% sulfate reduction at an annual cost of about 33.5 million dollars per year, with visibility benefits like those of Figure 6.8. This combination of technological controls and institutional changes is superior to a purely technological solution to the problem in two respects. It achieves a greater local air quality benefit at a far lower cost.[5]

By reference to the above example, many quite complex research needs can be identified.

It is clear that as the number of emissions control strategy options are expanded, the chance for an attractive combination of control measures can improve greatly. First, what methods can be devised for identifying greater numbers of existing control strategy options in a systematic manner? Technically, how does one cope with the flood of alternatives which must then be compared to one another? Some of these control options may be sufficiently complex that they

---

4 (continued)
1970, before price control induced shortages led to natural gas rationing, Los Angeles did choose to bid for natural gas instead of further desulfurizing fuel oil. They succeeded in that attempt while other regions of the country facing less dramatic pollution control problems chose less drastic approaches to emissions control.

[5]That strategy calculation also comes close to defining a possible future case since emissions forecasts for fuel oil are unnecessary if natural gas restoration occurs.

can only be understood if the control technology or approach is itself made the subject of a simulation model. Development of models for emission source modification should be pursued.

The control strategy design process should be adopted to assess apparent inefficiencies within the air basin that are prime candidates for innovative solutions which do not yet exist. Referring to Chapter 4, one can identify large numbers of source types for which no control measures have been found so far. From the control strategy example, several situations can be isolated in which control measures are available, but their cost-effectiveness is relatively unattractive. By quantifying the shape of the present least-cost paths to air quality improvement, one can identify those points along each curve where the law of diminishing returns begins to set in. At those points, a technological breakthrough should be sought which will cause one to transfer to another control strategy path. While no one could guarantee that such a breakthrough could be achieved, at least the search would focus on a place where the breakthrough would be adopted quickly if found.

The control strategy example given in Figure 7.1 was purely hypothetical. This is because it was constructed without reference to expected future conditions in the air basin. It would have been desirable to pursue the expected future case at that point, but technical advances in emissions forecasting should be developed first in order to support such an effort.

The track record with regard to forecasting $SO_x$ emissions levels several years in advance in the Los Angeles Basin is not very impressive (for example, see Cass, 1976). APCD ten-year emissions forecasts presented in Figures 1.4 through 1.7 of this thesis were rendered obsolete within three years (even before this thesis could reach publication). Similar surprises have befallen every other previous local $SO_x$ forecast known to this author. That situation results not from carelessness, but rather from the highly volatile nature of both emissions control policy and clean-fuel availability in the South Coast Air Basin. Development of techniques for making better emissions forecasts is needed if deliberate analysis is to contribute to public policy formation. That is because lead times for a deliberate solution are longer than the apparent half-life of most forecasts. By "better" forecasting techniques, one does not necessarily mean more "accurate" forecasts in the sense of being able to predict the unforeseeable, but rather forecasts which explicitly acknowledge and search for a <u>range</u> of likely outcomes. An energy and sulfur balance approach to making $SO_x$ emissions projections benefits from many built-in physical checks and balances. Potentially large perturbations in emissions behavior may be explored in that manner without creating a physically impossible forecast. Techniques for making energy and sulfur balance style $SO_x$ emissions forecasts should be developed and demonstrated. An empirical parameterization of the relationship between past emissions forecasts and eventual outcomes also might be useful in evaluating the confidence interval on a state of the art forecast system.

In Chapter 5, the sulfate air quality simulation model was validated against three years of historic sulfate air quality data. The measured meteorological and other input parameters used in that simulation exercise were appropriate to those validation years. When faced with making air quality forecasts, how does one choose an appropriate set of meteorological and other input data? One promising technique could result from the development of synthetic meteorological data which statistically resembled measurements made in the airshed of interest without representing any particular year. This would be particularly useful in airsheds where the measured record is too short to locate even the expected worst year in a decade. The meteorological data synthesizer could be used to generate many decades of sequences of probable weather patterns. Then the air quality model, operating on a selection of that data, could be used to assess both the most likely results of an emission control strategy option, and the frequency of control strategy failure to deliver expected results within some tolerance limit.

The natural gas deregulation example illustrates that a mix of institutional changes and technological control measures may be more effective than either approach pursued independently. What are the technical, economic and political properties of such mixed strategies? What other mixed strategies could be defined which incorporate taxation as an incentive to induce desired emissions reductions?

The control strategy design example given above illustrated two alternate paths to a roughly equal emissions reduction. In

principle, many such alternate paths should be defined. History shows that no single path will be adhered to over great lengths of time. How can an air quality strategist systematically identify combinations of technologies which preserve the flexibility of decision-makers to alter their course without rendering large prior capital investments prematurely obsolete?

The existence of a large number of potentially attractive, but possibly mutually exclusive, approaches to emissions control raises serious questions about the methods available to assist choices among those alternatives. A cost-minimizing decision-maker might well feel comfortable with one of the two strategies defined in our example. But as the possible objectives of the emission control program expand beyond the question of least total cost for an air quality improvement, the entire picture can become quite muddled. The simultaneous existence of important questions concerning who pays the related control costs, combined with a variety of pollutant reduction benefits which are not reducible to a common measure (e.g., improved visibility, and reduced materials damage and reduced health effects) leads quickly to two questions. How can one better define the nature of those cost distributions and benefits, and what methods can be used to sharpen choices between increased costs accompanied by packages of incommensurable benefits? Additional health and welfare effect studies are clearly useful if that information can be obtained at an acceptable cost. Demonstration of multi-objective mathematical programming techniques applied to air quality problems

should be attempted. A fully deterministic means for resolving the final choice between control strategy alternatives does not exist. But practical methods may be developed to isolate those options which are Pareto-superior.

In conclusion, it can be seen that the ability to characterize an air pollution problem as was done in this study will probably lead to questions which are made more difficult (in the short run) in the presence of good physical information than would seem to be the case without it. Conventional approaches taken in the past may seem ill-advised in the presence of the ability to generate many good answers to previously intractable problems. Air pollution control strategy development is truly a design process with an open-ended rather than unique outcome. The objective of the design process is to generate many new opportunities while at the same time advancing and testing the state of the description of physical principles. As the multiplicity of possible control strategy options increases, the chances for an acceptable outcome to the design process increases, but the decision as to which option to select may become more difficult.

# CHAPTER 8

# SUMMARY AND CONCLUSIONS

## 8.1 Overview

The objective of this study has been to develop the technical understanding needed for sulfate air quality control strategy design. A general approach to air pollution control strategy design was described in which mathematical models verified against historical environmental data are used to define the likely costs and effects of sulfur oxides emission control alternatives.

A new type of long-run average emissions to air quality model was derived which computes pollutant concentrations from Lagrangian marked particle statistics based on the time sequence of measured wind speed, wind direction, and inversion base motion. Physical assumptions drawn from analysis of existing air quality and meteorological data were used to adapt this model to a specific application -- sulfate air quality prediction in Los Angeles. An energy and sulfur balance on the fate of energy resources containing sulfur was developed to test the consistency of a sulfur oxides emissions inventory for that air basin. Then material balance arguments were used to trace sulfur flows within that regional energy economy through the air quality model which also conserves sulfur mass. Sulfate air quality model predictions were compared to historical observations over the years 1972 through 1974. The sulfate air quality impact of individual emission source classes was estimated at a large number of air monitoring sites.

A hybrid theoretical-empirical model was constructed which explains the relationship between sulfate air quality and prevailing visibility

at Los Angeles. An estimate was made of the visibility improvement which would have accrued if Los Angeles sulfate concentrations were reduced by 50 percent on each past day of record. Then two emissions control strategy example calculations were performed to illustrate the means by which the air quality model results could be used to evaluate the cost of attaining such an air quality improvement.

One self-imposed constraint on this project was that the data employed be of the type available from air pollution control agency historical data banks and other public records. The result is that while the procedures developed were tested in Los Angeles, the data base required is available in kind (if not in such quantity) throughout the United States. With relatively minor modifications, analytical techniques developed in this study could have general application to a wide variety of air pollution control strategy studies, both for sulfates and for other selected contaminants.

## 8.2 Conclusions

### 8.2.1 Characterization of Los Angeles Sulfate Air Quality

Los Angeles forms an ideal location for sulfate air quality model development.

- It possesses a long term historic sulfate air quality data base.
- From those data it can be shown that the Los Angeles atmosphere is enriched in sulfates due to local emission sources. Annual mean sulfate concentrations above 14 $\mu gm/m^3$ were measured over central Los Angeles County at a time when background concentrations in incoming marine or desert air averaged 3 to 4 $\mu gm/m^3$.

In contrast to the problems arising from long distance transport of sulfates in the eastern United States, a sulfate air quality model employing only local $SO_x$ emissions data could be validated in the Los Angeles Basin.

Seasonal trends in sulfate air quality are similar throughout the South Coast Air Basin which surrounds Los Angeles.

- A broad summer seasonal peak in sulfate concentration occurs in all years of record, with clusters of high values in only two of nine winters examined.
- Long-term average spatial gradients in Los Angeles sulfate air quality are small.
- Simultaneous 24-hour average sulfate concentration measurements taken at widely separated monitoring sites are highly correlated.

In the Los Angeles area, temporal trends in sulfate air quality are far more pronounced than average spatial gradients. When constructing an air quality model which must explain the dynamic nature of Los Angeles sulfate air quality, concentration predictions made in time series should be emphasized.

The ability of available field data to verify time series air quality predictions was investigated statistically. From analysis of measurement errors and sampling frequency it was found that sulfate air quality predictions made over monthly and longer averaging times could be closely verified. Therefore, an air quality model for monthly average sulfate concentrations was sought.

Sulfate concentration changes from day to day are driven mainly by factors affecting the rate of $SO_2$ oxidation to form sulfates, and by

changes in the effective mixing volume of the air basin. From analysis of pollutant concentration data and meteorological variables it was found that:

- Afternoon inversion base height determines the extent of vertical dilution for sulfates within this airshed.
- Changes in scalar average wind speed are uncorrelated with changes in sulfate concentrations, indicating that a successful air quality model should employ vector-valued wind data.
- Air parcel retention time within the air basin seems to be more important to explaining sulfate concentrations than is initial dilution at the source
- An air parcel trajectory integration time of two days would be needed to insure that 95 percent of the air parcels of that age are advected to beyond the borders of a 50 by 50 mile square modeling area laid over central Los Angeles and Orange Counties.

An air quality model is needed which can compute long term average sulfate concentrations from the time series of wind vectors and inversion base motion. Special attention must be paid to integrating the transport equations long enough that pollutants held over from the previous day are entered into the concentration predictions.

A mass balance on the fate of sulfur oxides emissions in Los Angeles conducted by Roberts (1975) shows that:

- Emissions of both primary sulfates and $SO_2$ must be considered.
- Ground level deposition of sulfur oxides is a significant removal mechanism.
- The atmospheric oxidation of $SO_2$ to form sulfates must be modeled in order to account for total observed sulfate concentrations.

In order to select a chemical modeling approach, atmospheric sulfur oxides air chemistry first was reviewed, then sulfate concentration changes from day to day were compared to fluctuations in the other observable components of the likely chemical oxidation processes.

- Sulfate concentration changes closely track changes in relative humidity and total suspended particulate levels, with intrusion of fog on days of very high sulfate concentration. This suggests that heterogeneous oxidation of $SO_2$ on or within wetted particles is important to days of high sulfate concentration in Los Angeles.
- Sulfate concentrations are significantly higher on days of elevated oxidant concentrations. Thus a variety of homogeneous gas-phase sulfate formation mechanisms may also be important.

Sulfate concentrations increase with increases in all of the major observable components of all of the likely $SO_2$ oxidation mechanisms. In light of the complexity of the details of these competitive chemical reactions, it was decided that chemical conversion of $SO_2$ to form sulfates should be modeled as a slow pseudo-first order overall reaction within the range of existing experimental data on the rate of $SO_2$ oxidation in the Los Angeles atmosphere.

### 8.2.2 Air Quality Model Development

Existing long-term average air quality models lack the ability to reproduce those conditions most important to sulfate air quality in a coastal region like Los Angeles. Pseudo-steady state models which employ a joint frequency distribution of wind speed, wind direction and atmospheric stability have no hope of correctly computing air parcel retention time in an air basin characterized by a daily sea breeze/

land breeze reversal in wind direction. That is because those models contain no information about the serial correlation of the wind vectors.

Therefore a new type of simulation model was derived for directly calculating long-run average sulfate air quality under unsteady meteorological conditions. The model computes pollutant concentrations from long-run average source to receptor transport and reaction probabilities. These transport and reaction probabilities were in turn estimated from Lagrangian marked particle statistics based on the time sequence of historical measured wind speed, wind direction, and inversion base height motion within the airshed of interest. First order chemical reactions and pollutant dry deposition were incorporated. The model was adapted to a multiple source urban setting in a way which permits retention of the air quality impact of each source class contributing to air quality predictions at each receptor site.

Potential sources of error in this model as well as the most advanced trajectory models in use today include:

- Neglect of the vertical component of the wind.
- Neglect of wind shear.

These problems can be overcome mathematically in our model at an increase in computing cost. However, lack of appropriate measurements on winds aloft prevents incorporation of these improvements at present.

The long-run average Lagrangian marked particle air quality model has several particular merits:

- The model need not compute concentration averages from a real-time sequence of events. The order of integration over air parcel

release and transport may be arranged to minimize computing time and intermediate data storage requirements.

- The calculations are very simple and completely stable over time.
- There are no artificial diffusion problems associated with the transport scheme employed.
- Pollutant mass is completely conserved.
- The model builds its own initial conditions by integrating backward to connect all locally-emitted air parcels in the airshed at a given time to their source.
- Air parcels advected beyond the edges of the receptor grid are not lost to the system. Their position is remembered but their magnitude is not accumulated to a receptor cell unless the air parcel is advected back into the region of interest.
- Receptor cells may be specified only over those areas where concentration estimates are desired.

When adapting the air quality model for use in Los Angeles, the following approximations were made as a practical consideration aimed at conserving available computing resources:

- That inversion base height above ground level over the central Los Angeles Basin is spatially homogeneous at any given time.
- That inversion base motion over time may be represented by a stylized diurnal cycle which passes through the known daily maximum and minimum inversion base heights.
- That at any single time, the wind field over our study area may be approximated as a uniform parallel flow.

The first and third approximations above result in a huge savings in computing time by permitting the separation of trajectory and chemical

calculations from detailed dependence on a given starting location in the airshed. Model validation results presented in Chapter 5 indicate that these approximations typically do not lead to errors in sulfate concentration predictions which would exceed the error bounds on the field air quality observations against which the model was tested.

### 8.2.3 An Energy and Sulfur Balance on the South Coast Air Basin

In order to test our modeling approach, a spatially resolved sulfur oxides emissions inventory was constructed for the South Coast Air Basin. Emissions estimates were developed for 26 classes of mobile and stationary sources for each month of the years 1972 through 1974. During 1973, for example,

- $SO_x$ emissions within that modeling inventory totaled nearly 531 tons per average day.
- Over 80 percent of that $SO_x$ emissions inventory was concentrated in a small number of point source classes: electric utility generating plants, refinery fluid catalytic crackers, chemical plants recovering sulfur and sulfuric acid from refinery wastes, one local steel mill, and petrolemm coke calcining kilns.
- All other stationary sources combined total only 6 percent of the modeling emissions inventory.
- Mobile sources account for the remaining $SO_x$ emissions surveyed.

Small distributed area sources lying outside of Los Angeles and Orange Counties were neglected for air quality modeling purposes.

Techniques were developed and tested for performing both energy balance and sulfur balance calculations on flows of energy resources

containing sulfur throughout the economy of the airshed of interest. This approach provides five valuable functions.

- It serves as a nearly independent check on the detailed modeling emissions inventory. A formal methodology for validating an $SO_x$ emissions inventory has been demonstrated.
- It establishes the true current emissions control strategy in the airshed by showing those points in the system where sulfur is captured or segregated into products which will not lead to pollutant emissions. That is important because emissions control may be occurring in ways not obvious from reading local emissions control regulations.
- It connects pollutant emissions to energy flows in a way that control strategy questions involving fuel or process substitution can be addressed.
- By forcing the emissions inventory to be energy consistent, prospects for making plausible emissions forecasts are improved.
- By examining the fate of anthropogenic sulfur prevented from entering the atmosphere, it extends the description of the global sulfur cycle as described by Friend (1973) or Robinson and Robbins (1968).

A material balance on sulfur supplied within energy resources entering the South Coast Air Basin in 1973 shows that:

- Virtually all of the sulfur entering the air basin in that year arrived in a barrel of crude oil.
- Nearly 50 percent of the sulfur arriving was recovered at the refinery level as elemental sulfur or sulfuric acid.

- Approximately 25% of the sulfur was segregated into products like petroleum coke, asphalt and exported high sulfur fuel oil which would not be burned locally.
- 4.4% of the sulfur supply found its way into solid or liquid wastes.
- At least 14% of the sulfur was emitted to the atmosphere.
- The fate of 9.4% of the sulfur supply was undetermined. Over 70% of that sulfur imbalance was due to small percentage differences between two independent estimates of total sulfur supplied in crude oil versus total sulfur reported processed by refiners. This discrepancy would not lead to a significant change in atmospheric $SO_x$ emissions estimates.

The air quality modeling emission inventory was confirmed to be within about 10% of the atmospheric emissions identified by the sulfur balance. It was further demonstrated that the Los Angeles Basin in 1973 was already achieving greater than 80% overall control of its potential $SO_x$ emissions. Any future emission control measures adopted must be consistent with maintaining control over all of the sulfur which could get into the air rather than just that portion which currently does become airborne.

### 8.2.4 Results of the Air Quality Simulation Model

The air quality dispersion model was applied to simulation of Los Angeles sulfate air quality over each month of the years 1972 through 1974. Model results closely reproduced observed sulfate concentration patterns within the central portion of the Los Angeles Basin, particularly during the years 1972 and 1973. The correlation between

observed and predicted sulfate levels is 0.82 in both 1972 and 1973, and rises to 0.89 in 1972 if two biased observations are discarded.

An appropriate test of air quality model performance is whether or not model predictions are statistically indistinguishable from the air quality observations.

- Approximately 80% of the sulfate concentration predictions at LAAPCD air monitoring stations are within the error bounds on the ambient monitoring results.
- Model predictions track observed sulfate levels closely at the critical CHESS stations in the eastern San Gabriel Valley at Glendora and West Covina.
- A tendency to underpredict the summer peaks observed near the up-coast and down-coast edges of our study area at Santa Monica and at Garden Grove and Anaheim during 1973 and 1974 was noted.

A seasonal variation in the overall rate of $SO_2$ oxidation in the Los Angeles atmosphere was inferred from simultaneous comparison of observations and model predictions at a large number of monitoring sites.

- Monthly mean $SO_2$ oxidation rates of between 0.5% per hour and 3% per hour prevail from October through February of our test years.
- During late spring, summer, and early fall, $SO_2$ oxidation rates were estimated to jump to an average of about 6% per hour, with individual months ranging ± 2% per hour about that mean value.

Those numerical results must be qualified since a better understanding of seasonal trends in background sulfate concentrations or $SO_2$ deposition velocity could alter the outcome somewhat.[1]

---

[1]For a sensitivity study of conversion rate calculation dependence on other airshed parameters, see Roberts (1975).

One striking feature of Los Angeles sulfate air quality is that average horizontal concentration gradients are rather small in spite of the highly localized nature of major $SO_x$ emission sources. Air quality model results showing individual source class contributions to observed sulfate air quality help to explain this phenomenon. In winter months with a pronounced daily sea breeze/land breeze wind reversal, air parcel trajectories wander widely over the basin. Sulfur oxides emitted from all source classes are dispersed widely within the airshed by the rotation of the wind vectors. In contrast, during mid-summer, onshore flow persists for most of the day. However, the sequential siting of major $SO_x$ sources along the coast means that the central portion of the air basin is downwind of one major source group or another at most times. Lateral dispersion of emissions is just about sufficient to balance sulfate formation, with the result that upwind/downwind pollutant gradients are rather small in spite of the direct inland transport from sources to receptors. Annual mean sulfate concentrations are further smoothed by seasonal transport cycles in which peak sulfate concentrations appeared far inland during the summer and near the coast during the winter.

In January 1972, extreme resultant wind stagnation occurred during a period of high $SO_x$ emissions. The highest localized sulfate concentration predictions for any month of our three year period occurred at that time. While such extended stagnation is unusual, the fact that it can occur means that sulfate air quality control strategy design must consider avoidance of wintertime as well as summertime pollution episodes in Los Angeles.

Source class increments to predicted sulfate air quality were examined in time series at each air monitoring station. It was found

that three to five source classes of roughly equal impact, plus background sulfates, must be considered simultaneously in order to come close to explaining sulfate levels observed at most locations. For example, during the year 1973 at downtown Los Angeles, contributors to the annual mean sulfate concentrations observed were estimated to be:

- Background sulfates - 28%
- Electric utility generating stations - 23%
- Heavy duty mobile sources - 15%
- Sulfur recovery and sulfuric acid plants - 12%
- Petroleum refining and production - 11%
- Autos and light trucks - 4%
- Petroleum coke calcining kilns - 3%
- All remaining sources - 4%

The relative importance of particular source classes varies from one monitoring site to another, but no single source class clearly dominates the observed sulfate concentrations. The implication is that a mixed strategy targeted at a combination of source types will be needed if significant sulfate air quality improvements are to be achieved in this airshed through precursor $SO_x$ control.

### 8.2.5 The Relationship Between Sulfate Air Quality and Visibility

Techniques were developed for analysis of the long-run impact of pollutant concentrations on visibility at downtown Los Angeles. Existing statistical models which use particle chemical composition as a key to particle size and solubility were reviewed. An analysis of vapor pressure lowering over solutions of electrolytes was used to add structure to these models so that the relative humidity dependence of light

scattering by hygroscopic aerosols could be represented in a more physically realistic manner. Light absorption by $NO_2$ was added to the analysis. Coefficients were fit to the model based on air pollution control agency routine air monitoring data taken at downtown Los Angeles over the decade 1965 through 1974. It was found that:

- The principal contributors to visibility reduction at downtown Los Angeles include sulfates and oxides of nitrogen ($NO_2$ and nitrates).
- There is a pronounced increase in light scattering per unit sulfate solute mass on days of high relative humidity, as would be expected for a hygroscopic or deliquescent substance. Light extinction by SULFATES was quantified as $0.107\ (1\text{-RH})^{-0.53}\ (10^4\text{m})^{-1}$ per $\mu gm/m^3$, where RH stands for relative humidity in (%/100) and SULFATES is taken as 1.3 times the measured $SO_4^=$ concentration in order to account for the mass of associated cations.
- That functional relationship between light extinction by sulfates and relative humidity was compared to theoretical calculations for light scattering by ammonium sulfate aerosols. Our results were found to be similar in shape but slightly higher than the theoretical calculation would indicate.

These small differences between theory and analysis of Los Angeles observations may be due to the deviation of an actual human observer's visual acuteness from that assumed by Koschmieder.

Having developed and fitted a model representing a decade of atmospheric events, it becomes possible to examine the likely long-run response of visibility in the Los Angeles basin to altered levels of particulate sulfates. It was estimated that the visibility impact of

reducing sulfates to a half or to a quarter of their measured historic values on each past day of record would be manifested most clearly in a reduction of the number of days per year with average visibility less than three miles. For example, a 75 percent reduction in sulfates levels on a daily basis would have reduced the number of days with worse than three-mile visibility by about two-thirds, while improvement in the number of days of average visibility greater than ten miles would be much smaller, about 10 percent.

### 8.2.6 Toward Emission Control Strategy Analysis

The results of the air quality and visibility models can be used to evaluate sulfate air quality control strategy options. Example calculations worked for the year 1973 show that a 43% reduction in annual mean sulfate concentrations at downtown Los Angeles could have been achieved in that year through application of the $SO_x$ emission control technologies suggested by Hunter and Helgeson (1976). A second strategy predicated in part on deregulation of the price and availability of new natural gas supplies to industry could have achieved about a 49% decrease in sulfate concentrations in 1973 at lower cost than a purely technological solution to the Los Angeles sulfate problem.

## REFERENCES FOR CHAPTER 1

Bendat, J.S., and A.G. Piersol (1971), Random Data: Analysis and Measurement Procedures, New York, John Wiley and Sons.

Bureau of Mines (1972 through 1975), Motor Gasolines, Winter 1971-1972 (also Summer 1972, Winter 1972-1973, Summer 1973, Winter 1973-1974 and Summer 1974), U.S. Department of the Interior, Mineral Industry Surveys, Petroleum Products Surveys No. 75, 78, 80, 83, 85, 88.

California Air Resources Board (1975), An Assessment of the Aerosol-Visibility Problem in the South Coast Air Basin, California Air Resources Board Staff Report 75-20-3. Emissions projections read from Figure V-4.

Clean Air Act (42 U.S.C. §§1857 et seq.). This act has recently been amended by addition of the "Clean Air Act Amendments of 1977" and is now classified to (42 U.S.C. 7401 et seq.).

Committee on Mineral Resources and the Environment (1975), Mineral Resources and the Environment, Washington D.C., National Academy of Sciences.

Friend, J.P. (1973), "The Global Sulfur Cycle," in Chemistry of the Lower Atmosphere, S.I. Rasool (editor), New York, Plenum Press.

Hidy, G.M. et al.(1972), Aerosols and Atmospheric Chemistry, New York, Academic Press.

Hidy, G.M. et al.(1975), Characterization of Aerosols in California, (ACHEX), Science Center, Rockwell International, prepared under California Air Resources Board Contract No. 358, report issued September 1974, revised April 1975.

Lemke, E. et al.(1969), Profile of Air Pollution Control in Los Angeles County, 1969 edition, Los Angeles Air Pollution Control District.

Los Angeles Air Pollution Control District (1975a), "History and Outlook of Emissions of Sulfur Dioxide in Los Angeles County," summary sheet dated 11-21-75.

Los Angeles Air Pollution Control District (1975b), personal communication. This historical account is abstracted from discussions with District personnel plus a District summary entitled, "Control of Sulfur Compounds in Los Angeles County," dated 12-19-74. Emission control regulations have since been renumbered, but their provisions are essentially as described herein.

Los Angeles Air Pollution Control District (1950), Technical and Administrative Report on Air Pollution Control in Los Angeles County, Annual Report 1949-1950.

Middleton, J.T., et al. (1970), Air Quality Criteria for Sulfur Oxides, Washington, D.C., National Air Pollution Control Administration, Publication Number AP-50, second printing.

Middleton, W.E.K. (1952), Vision Through the Atmosphere, Toronto, University Press.

National Research Council (1975), Air Quality and Stationary Source Emission Control, Washington, D.C., U.S. Government Printing Office, Senate Document No. 94-4.

Pacific Lighting Corporation (1974), "Facts of Gas Supply," distributed by Southern California Gas Company, a subsidiary of Pacific Lighting Corporation.

Renzetti, N.A. et al. (1955), An Aerometric Survey of the Los Angeles Basin: August-November 1954, Los Angeles, Air Pollution Foundation Report No. 9.

Roberts, P.T. (1975), Gas to Particle Conversion: Sulfur Dioxide in a Photochemically Reactive System, Ph.D. thesis, California Institute of Technology, Pasadena, California.

Task Group on Lung Dynamics (1966), "Deposition and Retention Models for Internal Dosimetry of the Human Respiratory Tract," Health Physics, Vol. 12, pp. 173-207.

Temple, Barker, and Sloan (1976), Economic and Financial Impacts of Federal Air and Water Pollution Controls on the Electric Utility Industry, Wellesley Hills, Massachusetts, Temple, Barker and Sloane, Inc., U.S. Environmental Protection Agency Publication Number EPA-230/3-76-013.

Trijonis, J. et al. (1975), An Implementation Plan for Suspended Particulate Matter in the Los Angeles Region, Redondo Beach, California, TRW Transportation and Environmental Engineering Operations.

U.S. Environmental Protection Agency (1975), Position Paper on Regulation of Atmospheric Sulfates, Research Triangle Park, North Carolina, Office of Air and Waste Management, Office of Air Quality Planning and Standards, U.S. Environmental Protection Agency Publication Number EPA-450/2-75-007.

Whitby, K.T. et al. (1971), Aerosol Measurements in Los Angeles Smog, Research Triangle Park, North Carolina, U.S. Environmental Protection Agency Publication APTD-0630.

## References for Chapter 2

Bendat, J. S., and A. G. Piersol (1971), Random Data: Analysis and Measurement Procedures, New York, John Wiley and Sons.

Bufalini, M. (1971), "Oxidation of Sulfur Dioxide in Polluted Atmospheres - A Review", Environmental Science and Technology, Vol. 5, No. 3, pp. 685-700.

California Air Resources Board (1976), California Air Quality Data, Vol. VIII, No. 2, April, May, June 1976.

Calvert, J. G. (1973), "Interactions of Air Pollutants", in Proceedings of the Conference on Health Effects of Air Pollutants, Washington, D.C., U.S. Government Printing Office, Stock No. 5270-02105. Proceedings of a National Academy of Sciences Conference, reprinted for the Committee on Public Works of the United States Senate.

Cass. G. R. (1975), Dimensions of the Los Angeles $SO_2$/Sulfate Problem, Pasadena, California, California Institute of Technology, Environmental Quality Laboratory Memorandum No. 15.

Cox, R. A., and S. A. Penkett (1972), "Aerosol Formation from Sulfur Dioxide in the Presence of Ozone and Olefinic Hydrocarbons," J. Chem. Soc., Faraday Trans, I., Vol. 68, p. 1735.

De Marrais, G. A, G. C. Holzworth and C. R. Hosler (1965), Meteorological Summaries Pertinent to Atmospheric Transport and Dispersion over Southern California, Washington, D. C., U. S. Weather Bureau Technical Paper No. 54.

Foster, P. M. (1968), "The Oxidation of Sulphur Dioxide in Power Station Plumes," Atmospheric Environment, Vol. 3, pp. 157-175.

Friend, J. P. (1973), "The Global Sulfur Cycle," in Chemistry of the Lower Atmosphere, S. I. Rasool (editor), New York, Plenum Press.

Gillette, D. A., and I. H. Blifford (1971), "Composition of Tropospheric Aerosols as a Function of Altitude," J. Atmos. Sci., Vol. 28, pp. 1199-1210.

Harrison, H., T. V. Larson and P. V. Hobbs (1975), "Oxidation of Sulfur Dioxide in the Atmosphere: A Review," International Conference on Environmental Sensing and Assessment, Vol. 2, New York, Institute of Electrical and Electronics Engineers, IEEE Catalogue No. 75-CH 1004-1 ICESA.

Hidy, G. M., et al. (1975), Characterization of Aerosols in California (ACHEX), Science Center, Rockwell International, prepared under California Air Resources Board Contract No. 358, report issued September (1974), revised April (1975).

Hidy, G. M., et al. (1974), "Observations of Aerosols over Southern California Coastal Waters," J. Appl. Meteor., Vol. 13, pp. 96-107.

Holzworth, G. C. (1959), "Atmospheric Contaminants at Remote California Coastal Sites," J. Meteorology, Vol. 16, No. 1, pp. 68-79.

Hunter, S. C. and N. L. Helgeson (1976), Control of Oxides of Sulfur from Stationary Sources in the South Coast Air Basin of California, Tustin, California, KVB Incorporated, Document Number KVB 5802-432, prepared under California Air Resources Board Contract Number ARB 4-421.

Johnstone, H. F., and D. R. Coughanowr (1958), "Absorption of Sulfur Dioxide from Air--Oxidation in Drops Containing Dissolved Catalysts," Ind. Engr. Chem., Vol. 50, No. 8, pp. 1169-1172.

Junge, C. E. (1957), "Chemical Analysis of Aerosol Particles and of Gas Traces on the Island of Hawaii," Tellus, Vol. 9, No. 4, pp. 528-537.

Junge, C. E., and T. G. Ryan (1958), "Study of the $SO_2$ Oxidation in Solution and its Role in Atmospheric Chemistry," Quart. J. Roy. Meteorol. Soc., Vol. 84, pp. 46-56.

Kurosaka, D. (1976), Sulfate Concentrations in the South Coast Air Basin, Division of Technical Services, State of California Air Resources Board, Publication No. DTS-76-1.

Larsen, R. I. (1971), A Mathematical Model for Relating Air Quality Measurements to Air Quality Standards, Research Triangle Park, North Carolina, U. S. Environmental Protection Agency Publication No. AP-89.

Los Angeles Air Pollution Control District (1972, 1973), Report of Meteorology, Air Pollution Effects and Contaminant Maxima of Los Angeles County (later issues titled Air Quality and Meteorology), Volumes XVII and XVIII, January 1972 through December 1973, monthly.

Lundgren, D. A. (1970), "Atmospheric Aerosol Composition and Concentration as a Function of Particle Size and of Time," J. Air Pollution Control Association, Vol. 20, No. 9, pp. 603-608.

MacPhee, R. D., and M. W. Wadley (1975a), Airborne Particulate Matter in Los Angeles County 1974, Technical Services Division, Los Angeles Air Pollution Control District, Air Quality Report No. 79.

MacPhee, R. D., and M. W. Wadley (1975b), Airborne Particulate Matter in Los Angeles County 1975, Technical Services Division, Los Angeles Air Pollution Control District, Air Quality Report No.81.

McNelis, D. N. (1974), Aerosol Formation from Gas-Phase Reactions of Ozone and Olefin in the Presence of Sulfur Dioxide, Research Triangle Park, North Carolina, Office of Research and Development, U. S. Environmental Protection Agency, Publication No. EPA-650/4-74-034.

Neiburger, M. and M. G. Wurtele (1949), "On the Nature and Size of Particles in Haze, Fog and Stratus of the Los Angeles Region," Chemical Reviews, Vol. 44, No. 2, pp. 321-335.

Novakov, T., et al. (1974), "Sulfates as Pollution Particulates: Catalytic Formation on Carbon (Soot) Particles," Science, Vol. 186, pp. 259-261.

Penkett, S. A. (1972), "Oxidation of $SO_2$ and Other Atmospheric Gases by Ozone in Aqueous Solution," Nature-Physical Science, Vol. 240, pp. 105-106.

Porter, M., et al. (1976), Statistical Comparison of Manual and Automated Methods for Analysis of Sulfate and Nitrate in Particulate Matter, Southern California Air Pollution Control District, Metropolitan Zone, a Technical Services Division Report, June 1976.

Renzetti, N. A., et al. (1955), An Aerometric Survey of the Los Angeles Basin, August-November, 1954, Los Angeles, California, Air Pollution Foundation Report No. 9.

Roberts, P. T. (1975), Gas to Particle Conversion: Sulfur Dioxide in a Photochemically Reactive System, Ph.D. thesis, California Institute of Technology, Pasadena, California.

Sander, S. P., and J. H. Seinfeld, "Chemical Kinetics of Homogeneous Oxidation of Sulfur Dioxide," Environmental Science and Technology, Vol. 10, pp. 1114-1123.

Scott, W. D., and P. V. Hobbs (1967), "The Formation of Sulfate in Water Droplets," J. Atmos. Sci.,Vol. 24, pp. 54-57.

Thomas, M. D. (1962), "Sulfur Dioxide, Sulfuric Acid Aerosol and Visibility in Los Angeles," Int. J. Air. Wat. Poll., Vol. 6, pp. 443-454.

Tokiwa, Y., et al. (1974), Evaluation of Sulfate Data in the Los Angeles Metropolitan Area, Berkeley, California, Air and Industrial Hygiene Laboratory, State of California, Department of Public Health, Prepared for Rockwell International Science Center under Contract No. 262-1951.

Trijonis, J., et al. (1975), An Implementation Plan for Suspended Particulate Matter in the Los Angeles Region, Redondo Beach, California, TRW Transportation and Environmental Engineering Operations.

Urone, P. and W. H. Schroeder (1969), "$SO_2$ in the Atmosphere: A Wealth of Monitoring Data, but Few Reaction Rate Studies," Environmental Science and Technology, Volume 3, No. 5, pp. 436-445.

Zeldin, M. D., A. Davidson, M. F. Brunelle and J. E. Dickenson (1976), A Meteorological Assessment of Ozone and Sulfate Concentrations in Southern California, Southern California Air Pollution Control District, Document No. E&P 76-1.

## References for Chapter 3

Calder, K. L. (1971), "A Climatological Model for Multiple Source Urban Air Pollution," presented at the First Meeting of the NATO/CCMS Panel on Modeling. This paper is conveniently reproduced in the User's Guide for the Climatological Dispersion Model by A. D. Busse and J. R. Zimmerman, Research Triangle Park, North Carolina, Office of Research and Development, U.S. Environmental Protection Agency Publication No. EPA-R4-73-024, December (1973).

Cass, G. R. (1975), Dimensions of the Los Angeles $SO_2$/ Sulfate Problem, Pasadena, California, California Institute of Technology, Environmental Quality Laboratory Memorandum No. 15.

Deardorff, J. W. (1970), "A Three-Dimensional Numerical Investigation of the Idealized Planetary Boundary Layer," Geophys. Fluid Dyn., Vol. 1, pp. 377-410.

De Marrais, G. A., G. C. Holzworth, and C. R. Hosler (1965), Meteorological Summaries Pertinent to Atmospheric Transport and Dispersion over Southern California, Washington, D.C., U.S. Weather Bureau Technical Paper No. 54.

Drivas, P. J., and F. H. Shair (1975), The Chemistry, Dispersion, and Transport of Air Pollutants Emitted from Fossil Fuel Power Plants in California--Transport of Plumes Associated with the Complex Coastal Meteorology, Division of Chemistry and Chemical Engineering, California Institute of Technology, performed under California Air Resources Board Contract No. ARB-915.

Edinger, J. G. (1973), "Vertical Distribution of Photochemical Smog in Los Angeles Basin," Environmental Science and Technology, Vol. 7, No. 3, pp. 247-252.

Gifford, F. A., Jr. and S. R. Hanna (1970), "Urban Air Pollution Modeling," presented at 1970 Meeting of the Int. Union of Air Poll. Prev. Assoc., Washington (1970). Reproduced in Proceedings of the Second International Clean Air Congress, H. M. Eglund and W. T. Berry, editors, New York, Academic Press (1971).

Goodin, W. R. (1976), "An Empirical Technique for Computing Mixing Depths in the Los Angeles Basin," unpublished working paper, Environmental Quality Laboratory, California Institute of Technology, Pasadena, California.

Lamb, R. G. (1971), "The Application of a Generalized Lagrangian Diffusion Model to Air Pollution Simulation Studies," in Proceedings of the Symposium on Air Pollution, Turbulence and Diffusion, H. W. Church and R. E. Luna, editors, Las Cruces, New Mexico, New Mexico State University, December 7-10, 1971.

Lamb, R. G. and M. Neiburger (1971), "An Interim Version of a Generalized Urban Air Pollution Model," Atmospheric Environment, Vol. 5, pp. 239-264.

Lamb, R. G. and J. H. Seinfeld (1973), "Mathematical Modeling of Urban Air Pollution--General Theory," Environmental Science and Technology, Vol. 7, No. 3, pp. 253-261.

Larsen, R. I. (1971), A Mathematical Model for Relating Air Quality Measurements to Air Quality Standards, Research Triangle Park, North Carolina, U.S. Environmental Protection Agency Publication No. AP-89.

Liu, M-K. and J. H. Seinfeld (1975), "On the Validity of Grid and Trajectory Models of Urban Air Pollution," Atmospheric Environment, Vol. 9, pp. 555-574.

Martin, D. O. and J. A. Tikvart (1968), "A General Atmospheric Diffusion Model for Estimating the Effects on Air Quality of One or More Sources," Air Pollution Control Association Paper 68-148. The widely used multiple source urban air quality model computer program AQDM (Air Quality Display Model) is based on this work.

McElroy, J. L.,and F. Pooler Jr. (1968), St. Louis Dispersion Study, Volume II--Analysis, Arlington, Virginia, U.S. Public Health Service, National Air Pollution Control Administration Publication No. AP-53.

Neiburger, M., C.G.P. Beer, and L.B. Leopold (1945), Report on the 1944 Investigation of California Stratus, Part I, AAF Research Weather Station, University of California at Los Angeles.

Seinfeld, J. H. (1975), Air Pollution: Physical and Chemical Fundamentals, New York, McGraw-Hill Book Company.

Shair, F. H. (1977), personal communication, September 30, 1977. Forwarded preliminary analyses of $SF_6$ tracer studies performed under California Air Resources Board Contract A6-202-30.

Trijonis, J. et al. (1975), An Implementation Plan for Suspended Particulate Matter in the Los Angeles Region, Redondo Beach, California, TRW Transportation and Environmental Engineering Operations.

Turner, D. B., (1969), Workbook of Atmospheric Dispersion Estimates, Cincinnati, Ohio, National Air Pollution Control Administration, U.S. Public Health Service Publication No. 999-AP-26.

## References for Chapter 4

Bureau of Mines (1975), Minerals Yearbook, 1973, Vol. 1, Metals, Minerals and Fuels, Washington D. C., U. S. Government Printing Office, U. S. Department of the Interior.

Cantrell, A. (1973), "Annual Refining Survey", The Oil and Gas Journal, Vol. 71, No. 14, April 2, 1973.

Environmental Protection Agency (1974), 1972 National Emissions Report, Research Triangle Park, North Carolina, Office of Air and Waste Management, Office of Air Quality Planning and Standards, U. S. Environmental Protection Agency publication number EPA-450/2-74-012.

Hunter, S. C., and N. L. Helgeson (1976), Control of Oxides of Sulfur from Stationary Sources in the South Coast Air Basin of California, Tustin, California, KVB Incorporated, Document Number KVB 5802-432, prepared under California Air Resources Board Contract Number ARB 4-421.

List, E. J. (1971), Energy Use in California: Implications for the Environment, Pasadena, California, California Institute of Technology, Environmental Quality Laboratory Report No. 3.

Los Angeles Air Pollution Control District (1975), "History and Outlook of Emissions of Sulfur Dioxide in Los Angeles County", table dated November 21, 1975.

Nehring, R. (1975), Oil and Gas Supplies for California: Past and Future, Santa Monica, California, The Rand Corporation, document R-1850-CSA/RF, December 1975.

1975 California Gas Report (1975), a report prepared by California utilities in response to California Public Utilities Commission Decision No. 62260; authorship and publisher are unknown, but copies are obtainable from the Southern California Gas Company.

Nordsieck, R. A. (1974), Air Quality Impacts of Electric Cars in Los Angeles, Appendix A, Pollutant Emissions Estimates and Projections for the South Coast Air Basin, Santa Barbara, California, General Research Corporation document RM-1905-A.

Pierson, W. R. (1977), Ford Motor Company, personal communication, August 3, 1977.

Pierson, W. R. and W. W. Brachaczek (1976), Particulate Matter Associated With Vehicles on the Road, Society of Automotive Engineers Paper 760039.

Roth, P. M., et al. (1974), "Mathematical Modeling of Photochemical Air Pollution--II. A Model and Inventory of Pollutant Emissions," Atmospheric Environment, Vol. 8, pp. 97-130.

Sjovold, A. R. (1973), Electric Energy Projections for the Los Angeles Region, 1980-2000, General Research Corporation, document RM-1859, November 1973 (as cited by Nordsieck (1974)).

Southern California Air Pollution Control District,(1976a), personal communication. The district furnished abbreviated versions of the following internal documents:

(1) "Sulfur Balance - Los Angeles County Refineries - 1973"
(2) "Sulfur Balance - Los Angeles County Refineries - 1974"
(3) "Sulfur Recovery and Sulfuric Acid Plant Operations - Los Angeles County - 1973"
(4) "Sulfur Recovery and Sulfuric Acid Plant Operations - Los Angeles County - 1974"

All documents were censored to conceal sulfur and acid production data for individual refineries and chemical plants while summarizing activities for the county as a whole. Atmospheric emissions were however apparent on a plant by plant basis.

Southern California Air Pollution Control District (1976b), "Major Point Sources of Air Pollution in the Four Counties Served by the Southern California APCD", El Monte, California, Southern California Air Pollution Control District list dated April, 1976.

Stanford Research Institute (1973), Meeting California's Energy Requirements, 1975-2000, Menlo Park, California, SRI Project ECC-2355.

Trijonis, J., et al. (1975), An Implementation Plan for Suspended Particulate Matter in the Los Angeles Region, Redondo Beach, California, TRW Transportation and Environmental Engineering Operations.

## References for Chapter 5

Chamberlin, A. C. (1960), "Aspects of the Deposition of Radioactive and Other Gases and Particles," Int. J. Air Pollut., Vol. 3, pp. 63-88.

Davidson, C. I. (1977), Deposition of Trace Metal-Containing Aerosols on Smooth, Flat Surfaces and on Wild Oat Grass (Avena fatua), Ph.D. thesis, California Institute of Technology, Pasadena, California.

Drivas, P. J., and F. H. Shair (1975), The Chemistry, Dispersion and Transport of Air Pollutants Emitted from Fossil Fuel Power Plants in California--Transport of Plumes Associated with the Complex Coastal Meteorology, Division of Chemistry and Chemical Engineering, California Institute of Technology, performed under California Air Resources Board Contract No. ARB-915.

Garland, J. A. (1974), "Dry Deposition of $SO_2$ and Other Gases," in Atmosphere-Surface Exchange of Particulate and Gaseous Pollutants, Proceedings of a symposium held at Richland, Washington, September 4-6, 1974, published by Technical Information Center, Office of Public Affairs, U.S. Energy Research and Development Administration, 1976.

Gifford, F. A. (1961), "Uses of Routine Meteorological Observations for Estimating Atmospheric Dispersion," Nuclear Safety, Vol. 2, pp. 47-51.

Heisler, S. L. (1976), Assessment of the Influence of Electric Generating Stations on Daily Sulfate Levels in the South Coast Air Basin, Westlake Village, California Environmental Research and Technology Document P-5088R4.

Hidy, G. M., et al. (1975), Characterization of Aerosols in California (ACHEX), Science Center, Rockwell International, prepared under California Air Resources Board Contract No. 358, report issued September (1974), revised April (1975).

Hidy, G. M., et al. (1974), "Observations of Aerosols over Southern California Coastal Waters," J. Appl. Meteor., Vol. 13, pp. 96-107.

Joint Project (1977), Joint Project for Relating Emissions of $SO_2$ to Air Quality--Interim Report, Westlake Village, California, Environmental Research and Technology Inc., Document P-5088.

Judeikis, H. S. and T. B. Stewart (1976), "Laboratory Measurements of $SO_2$ Deposition Velocities on Selected Building Materials and Soils," Atmospheric Environment, Vol. 10, pp. 769-776.

Liss, P. S. (1971), "Exchange of $SO_2$ Between the Atmosphere and Natural Waters," Nature, Vol. 233, pp. 327-329.

Los Angeles Air Pollution Control District (1975a), "Wind Data File, DSNAME WDMAST," Technical Services Division, Los Angeles Air Pollution Control District, magnetic tape of the District's wind data.

Los Angeles Air Pollution Control District (1975b), "Master VAR99 Disk File, DSNAME SYSAG.VAR99, " Technical Services Division, Los Angeles Air Pollution Control District, magnetic tape copy of disk file containing District's inversion base data.

McElroy, J. L., and F. Pooler Jr. (1968), St. Louis Dispersion Study, Volume II--Analysis, Arlington, Virginia, U.S. Public Health Service, National Air Pollution Control Administration Publication No. AP-53.

Owers, M. J., and A. W. Powell (1974), "Deposition Velocity of Sulphur Dioxide on Land and Water Surfaces Using a $^{35}S$ Tracer Method," Atmospheric Environment, Vol. 8, pp. 63-68.

Pasquill, F. (1961), "The Estimation of the Dispersion of Windborne Material," Meteorol. Mag., Vol. 90, pp. 33-49.

Roberts, P. T. (1975), Gas to Particle Conversion: Sulfur Dioxide in a Photochemically Reactive System, Ph. D. Thesis, California Institute of Technology.

Shair, F. H., (1977), personal communication, September 30, 1977. Forwarded preliminary analyses of $SF_6$ tracer studies performed under California Air Resources Board Contract A6-202-30.

Shepherd, J. G. (1974), "Measurements of the Direct Deposition of Sulfur Dioxide onto Grass and Water by the Profile Method," Atmospheric Environment, Vol. 8, pp. 69-74.

Spedding, D. J. (1972), "Sulfur Dioxide Absorption by Sea Water," Atmospheric Environment, Vol. 6, pp. 583-586.

Turner, D. B., (1969), Workbook of Atmospheric Dispersion Estimates, Cincinnati, Ohio, National Air Pollution Control Administration, U.S. Public Health Service Publication No. 999-AP-26.

U.S. Department of Commerce (1972a through 1974a), Local Climatological Data, Annual Summary with Comparative Data, Long Beach, California--1972 (1973, 1974), Asheville, North Carolina, National Climatic Center, National Oceanic and Atmospheric Administration, U.S. Department of Commerce.

U.S. Department of Commerce (1972b), "Local Climatological Data, Los Angeles California, International Airport, January 1972, (March 1972)" Asheville, North Carolina, National Climatic Center, National Oceanic and Atmospheric Administration, U.S. Department of Commerce.

White, W. et al. (1978), "The Same-Day Impact of Power Plant Emissions on Sulfate Levels in the Los Angeles Air Basin," Atmospheric Environment, in press, expected January 1978.

## References for Chapter 6

Birakos, J. N. (1974), 1974 Profile of Air Pollution Control, County of Los Angeles, Air Pollution Control District.

California Air Resources Board (1975), Bulletin, Vol. 6, July.

Charlson, R. J., N. C. Ahlquist and H. Horvath (1968), "On the Generality of Correlation of Atmospheric Aerosol Mass Concentration and Light Scatter," Atmospheric Environment, Vol. 2, pp. 455-464.

Charlson, R. J. (1969), "Atmospheric Visibility Related to Aerosol Mass Concentration - A Review," Environmental Science and Technology, Vol. 3, No. 10, p. 913.

Charlson, R. J. and N. C. Ahlquist (1969), "Brown Haze: $NO_2$ or Aerosol?" Atmospheric Environment, Vol. 3, pp. 653-656.

Charlson, R. J., et al. (1972), "Multiwavelength Nephelometer Measurements in Los Angeles Smog Aerosol III. Comparison to Light Extinction by $NO_2$," J. Colloid and Interface Science, Vol. 39, No. 1, p. 260.

Charlson, R. J., et al. (1974), "$H_2SO_4/(NH_4)_2SO_4$ Background Aerosol: Optical Detection in St. Louis Region," Atmospheric Environment, Vol. 8, pp. 1257-1267.

Eggleton, A. E. J. (1969), "The Chemical Composition of Atmospheric Aerosols on Tees-Side and its Relation to Visibility," Atmospheric Environment, Vol. 3, pp. 355-372.

Friedlander, S. K. (1973), "Chemical Element Balances and Identification of Air Pollution Sources," Environmental Science and Technology, Vol. 7, pp. 235-240.

Garland, J. A. (1969), "Condensation on Ammonium Sulphate Particles and its Effect on Visibility," Atmospheric Environment, Vol. 3, pp. 347-354.

Gartrell, G., Jr. and S. K. Friedlander (1975), "Relating Particulate Pollution to Sources: The 1972 California Aerosol Characterization Study," Atmospheric Environment, Vol. 9, pp. 279-299.

Heisler, S. L., S. K. Friedlander and R. B. Husar (1973), "The Relationship of Smog Aerosol Size and Chemical Element Distributions to Source Characteristics," Atmospheric Environment, Vol. 7, pp. 633-649.

Hidy, G. M., et al. (1975), Characterization of Aerosols in California (ACHEX), Science Center, Rockwell International, prepared under California Air Resources Board Contract No. 358, Revision of April (1975).

Hidy, G. M. and S. K. Friedlander (1971), "The Nature of the Los Angeles Aerosol," in H. M. Eglund and W. T. Berry, editors, Proceedings of the Second International Clean Air Congress, New York, Academic Press.

Horvath, H. (1971), "On the Applicability of the Koschmieder Visibility Formula," Atmospheric Environment, Vol. 5, pp. 177-184.

Koschmieder's (1924) visibility formula is conveniently reproduced in Middleton, W. E. K., Vision Through the Atmosphere, Toronto, University Press (1952).

Lundgren, D. A. (1970), "Atmospheric Aerosol Composition and Concentration as a Function of Particle Size and of Time," J. Air Pollution Control Association, Vol. 20, No. 9, pp. 603-608.

MacPhee, R. D. and M. W. Wadley (1972 through 1975), Airborne Particulate Matter in Los Angeles County, 1965 through 1974 editions, Los Angeles Air Pollution Control District, Technical Services Division, Air Quality Reports Nos. 69, 70, 71, 72, 73, 75, 76, 77, 79 and 81.

Marquardt, D. W. (1963), "An Algorithm for Least-Squares Estimation of Non-linear Parameters," Jour. Soc. Industrial and Applied Math., Vol. 11, No. 2, pp. 431-441.

Miller, M. S., S. K. Friedlander and G. M. Hidy (1972), "A Chemical Element Balance for the Pasadena Aerosol," J. Colloid and Interface Science, Vol. 39, pp. 165-176.

Mills, J., W. D. Holland, and I. Cherniack (1974), Air Quality Monitoring Instruments and Procedures, Los Angeles Air Pollution Control District.

Neiburger, M. and M. G. Wurtele (1949), "On the Nature and Size of Particles in Haze, Fog and Stratus of the Los Angeles Region," Chemical Reviews, Vol. 44, No. 2, pp. 321-335.

Noll, K. E., P. K. Mueller and M. Imada (1968), "Visibility and Aerosol Concentration in Urban Air," Atmospheric Environment, Vol. 2, pp. 465-475.

Phadke, M. S., et al. (1975), Los Angeles Aerometric Data on Sulfur Dioxide, Particulate Matter and Sulphate 1955-1972, Technical Report No. 410, Department of Statistics, University of Wisconsin, Madison.

Thomas, M. D. (1962), "Sulfur Dioxide, Sulfuric Acid Aerosol and Visibility in Los Angeles," Int. Journal of Air and Water Pollution, Vol. 6, pp. 446-454.

Trijonis, J., et al. (1975), An Implementation Plan for Suspended Particulate Matter in the Los Angeles Region, TRW Transportation and Environmental Engineering Operations, Redondo Beach, California, Edition of March 1975. Cost cited is for the sulfur dioxide and $NO_2$ reduction features of Strategy I.

White, W. H. and P. T. Roberts (1975), "The Nature and Origins of Visibility-Reducing Aerosols in Los Angeles," presented at the 68th annual meeting of the Air Pollution Control Association, June 15-20, 1975.

White, W. H., P. T. Roberts and S. K. Friedlander (1975), "On the Nature and Origins of Visibility-Reducing Aerosols in the Los Angeles Air Basin," working paper, W. M. Keck Laboratories of Environmental Health Engineering, California Institute of Technology, Pasadena, California. These figures also appear in the study referenced to Hidy, et al. (1975).

Williamson, S. J. (1973), Fundamentals of Air Pollution, Reading, Mass., Addison Wesley. Contains this definition, along with a straightforward discussion of visibility and Koschmieder's formula.

## References for Chapter 7

Breyer, S. G. and P. W. MacAvoy (1974), Energy Regulation by the Federal Power Commission, Washington, D.C., The Brookings Institution.

Cass, G. R. (1976), "Air Pollution Control Agency Behavior: Implementing Legal Mandates in an Uncertain World," presented at the CIT/IA Conference on Governmental Regulatory Policies, California Institute of Technology, Pasadena, California, May 6-7, 1976.

Hunter, S. C. and N. L. Helgeson (1976), Control of Oxides of Sulfur from Stationary Sources in the South Coast Air Basin of California, Tustin, California, KVB Incorporated, Document Number KVB-5802-432, prepared under California Air Resources Board Contract Number ARB 4-421.

Seidel, M. R. and H. G. Bryan (1975), The Consumer Costs of Deregulation of the Field Price of Natural Gas, Federal Power Commission, April 28, 1975.

## References for Chapter 8

Friend, J. P. (1973), "The Global Sulfur Cycle," in Chemistry of the Lower Atmosphere, S. I. Rasool (editor), New York, Plenum Press.

Hunter, S. C. and N. L. Helgeson (1976), Control of Oxides of Sulfur from Stationary Sources in the South Coast Air Basin of California, Tustin, California, KVB Incorporated, Document Number KVB-5802-432, prepared under California Air Resources Board Contract Number ARB 4-421.

Roberts, P. T. (1975), Gas-to-Particle Conversion: Sulfur Dioxide in a Photochemically Reactive System, Ph.D. thesis, California Institute of Technology, Pasadena, California.

Robinson, E. and R. C. Robins (1968), Sources, Abundance and Fate of Gaseous Atmospheric Pollutants, Menlo Park, California, Stanford Research Institute, SRI Project PR-6755.